

V/STOL TILT ROTOR AIRCRAFT STUDY MATHEMATICAL MODEL FOR A REAL TIME SIMULATION OF A TILT ROTOR AIRCRAFT (BOEING VERTOL MODEL 222)

VOLUME VIII

By: H. Rosenstein
M. A. McVeigh
P. A. Mollenkof

APRIL 1973

Distribution of this Report is provided in the interest of information exchange. Responsibility for the contents resides in the author or organization that prepared it.

Prepared Under Contract No. NAS2-6598 by

BOEING VERTOL COMPANY
A DIVISION OF THE BOEING COMPANY
P.O. BOX 16858
PHILADELPHIA, PENNSYLVANIA 19142

for

AMES RESEARCH CENTER
NATIONAL AERONAUTICS AND SPACE ADMINISTRATION

and

UNITED STATES ARMY AIR MOBILITY RESEARCH & DEVELOPMENT LABORATORY
AMES DIRECTORATE

NASA-CR-11460 V/STOL TILT ROTOR AIRCRAFT STUDY N73-31947
MATHEMATICAL MODEL FOR A REAL TIME SIMULATION
OF A TILT ROTOR AIRCRAFT BOEING VERTOL CO. PHILADELPHIA, PA.
570 P HC 30.50
63/02 18184
CSCL OIC

- Volume III -- Overall Research Aircraft Project Plan,
Schedules, and Estimated Cost, NASA
CR-114439
- Volume IV -- Wind Tunnel Investigation Plan for a
Full Scale Tilt Rotor Research Aircraft,
CR-114440
- Volume V -- Definition of Stowed Rotor Research
Aircraft, NASA CR-114598
- Volume VI -- Preliminary Design of a Composite Wing
for Tilt Rotor Aircraft, NASA CR-114599
- Volume VII -- Tilt Rotor Flight Control Program
Feedback Studies, NASA CR-114600
- Volume VIII -- Mathematical Model for a Real Time
Simulation of a Tilt Rotor Aircraft
(Boeing Vertol Model 222), NASA CR-114601
- Volume IX -- Piloted Simulator Evaluation of the
Boeing Vertol Model 222 Tilt Rotor
Aircraft, NASA CR-114602
- Volume X -- Performance and Stability Test of a
1/4.622 Froude Scaled Boeing Vertol
Model 222 Tilt Rotor Aircraft (Phase I),
NASA CR-114603

SUMMARY

This report documents the development of a real time mathematical model of a tilt rotor aircraft. This mathematical model is to be used in conjunction with the NASA Flight Simulator for Advanced Aircraft (FSAA) at Ames Research Center for evaluation of aircraft performance and handling qualities. In addition to developing the mathematical model, a parallel programming effort was conducted utilizing Boeing-Vertol's Hybrid Simulation Laboratory for the purpose of developing and evaluating model simplification.

The mathematical model is an eleven degree of freedom total force model. This model includes the basic six degree of freedom rigid body outer loop equations written about the instantaneous center of gravity with the inertial and aerodynamic terms included. The rotor is treated as a point source of forces and moments with appropriate response time lags and actuator dynamics. The wing has one vertical bending and one wing torsion degree of freedom. These structural degrees of freedom are treated on a "quasistatic" basis; i.e., the natural frequencies of vibration of the structure are much higher than the frequencies of the rigid body motion, and the coupling is in the aerodynamic terms. Each nacelle has an independent pitch degree of freedom about the wing pivot. The aerodynamics of the wing, tail, rotors, landing gear and fuselage are included. Wing and tail mutual interference effects and turbine engine performance and dynamic responses are represented.

The control system elements represented include pilot command (longitudinal and lateral stick, pedals, nacelle position and rate, power), three-axis stability augmentation systems (SAS), thrust management system (includes rotor constant speed governor) and a load alleviation system (LAS). The LAS system incorporates feedback to rotor cyclic and collective pitch for purposes of improving stability, blade load reduction, gust alleviation and increased damping of aeroelastic modes. Control system actuator dynamics are represented by appropriate second order systems.

The mathematical model was programmed on Boeing's hybrid computer. This program was real time and was used to evaluate model simplification and also to develop and optimize stability augmentation, control, and load alleviation systems.

The mathematical model was written to make it as flexible and as general as possible while still retaining the real time execution capability. This program is a valuable design tool for control system design, SAS optimization, and flying qualities evaluations and improvements. The model is capable of operating in all modes of V/STOL flight (forwards, backwards, and sideways) with no restrictions. This mathematical model represents the Model 222 tilt rotor configuration as proposed in Boeing's "Study of V/STOL Tilt Rotor Research Aircraft Program (Phase II)", dated January 1973.

TABLE OF CONTENTS

	<u>PAGE</u>
FOREWORD	iii
SUMMARY	v
LIST OF ILLUSTRATIONS	xi
NOMENCLATURE	xv
1.0 INTRODUCTION	1.0-1
2.0 GENERAL DESCRIPTION OF SIMULATION	2.0-1
3.0 SIGN CONVENTIONS	3.0-1
4.0 MODEL 222 TILT ROTOR AIRCRAFT DESCRIPTION	4.0-1
5.0 EQUATIONS OF MOTION	5.0-1
5.1 AXES SYSTEM	5.0-1
5.2 AIRCRAFT GROUND TRACK	5.0-3
5.3 FORCE EQUATIONS	5.0-4
5.4 MOMENT EQUATIONS	5.0-5
5.5 EQUATIONS OF MOTION FOR A MASS ELEMENT	5.0-5
5.6 EQUATIONS OF MOTION FOR NACELLES	5.0-10
5.7 DETERMINATION OF ROTOR GYROSCOPIC MOMENTS	5.0-13
6.0 AIRFRAME AERODYNAMICS	6.0-1
6.1 FUSELAGE	6.0-1
6.2 NACELLES	6.0-3
6.3 HORIZONTAL TAIL	6.0-4
6.4 VERTICAL TAIL	6.0-10
6.5 WING AERODYNAMICS	6.0-12
6.5.1 BASIC WING AERODYNAMICS	6.0-12
6.5.2 ROTOR SLIPSTREAM INTERFERENCE	6.10-13

TABLE OF CONTENTS

	<u>PAGE</u>
7.0 ROTOR AERODYNAMICS	7.0-1
7.1 FORMAT AND RANGE OF DATA	7.0-1
7.2 PROGRAMS USED TO COMPUTE ROTOR DATA	7.0-4
7.3 ROTOR SIGN CONVENTION	7.0-10
7.4 CURVE FIT FORMAT	7.0-10
7.5 EFFECT OF WING UPWASH ON ROTOR PERFORMANCE	7.0-12
7.6 ROTOR/ROTOR INTERFERENCE	7.0-12
7.7 ISOLATED ROTOR AERODYNAMICS	7.0-13
7.7.1 THRUST	7.0-13
7.7.2 POWER	7.0-14
7.7.3 NORMAL FORCE	7.0-14
7.7.4 SIDE FORCE	7.0-15
7.7.5 HUB PITCHING MOMENT	7.0-15
7.7.6 HUB YAWING MOMENT	7.0-16
7.8 CORRELATIONS OF ROTOR PREDICTION METHODS WITH TEST DATA	7.0-18
7.8.1 MODEL 213 FOUR BLADE HINGELESS ROTOR CORRELATION	7.0-18
7.8.2 CORRELATION WITH MODEL 222 26-FOOT DIAMETER ROTOR TEST IN NASA-AMES 40x80-FOOT TUNNEL	7.0-18
7.8.3 CORRELATION WITH MODEL 222 1/4.622 SCALE MODEL DATA	7.0-21
8.0 CONTROL SYSTEM DESCRIPTION	8.0-1
8.1 CONTROL AERODYNAMIC CONFIGURATION	8.0-1
8.2 LONGITUDINAL CONTROL	8.0-1
8.3 LATERAL CONTROL	8.0-3

TABLE OF CONTENTS

	<u>PAGE</u>
8.4 DIRECTIONAL CONTROL	8.0-5
8.5 THRUST/COLLECTIVE CONTROL	8.0-5
8.6 CONTROL FEEL	8.0-6
8.7 STABILITY AUGMENTATION SYSTEMS	8.0-7
8.8 LOAD ALLEVIATION SYSTEM (LAS)	8.0-8
8.9 THRUST MANAGEMENT SYSTEM	8.0-10
9.0 ENGINE REPRESENTATION	9.0-1
10.0 GROUND EFFECTS	10.0-1
11.0 AIRFRAME REPRESENTATION (PREPROCESSOR)	11.0-1
12.0 AEROELASTIC REPRESENTATION	12.0-1
13.0 CONCLUSIONS AND RECOMMENDATIONS	13.0-1
14.0 REFERENCES	14.0-1

APPENDICES

A. TREATMENT OF WING FLEXIBILITY	A-1
A.1 WING TWIST	A-1
A.2 WING VERTICAL BENDING	A-5
B. DERIVATION OF LANDING GEAR EQUATIONS	B-1
C. VELOCITY AND ACCELERATION TRANSFORMATION AND CENTER OF GRAVITY/INERTIA EQUATIONS	C-1
C.1 VELOCITY TRANSFORMATIONS	C-1
C.2 CENTER OF GRAVITY AND INERTIA EQUATIONS	C-5
C.3 PILOT STATION ACCELERATION-BODY AXES	C-8
C.4 AIRCRAFT INERTIAS	C-9

TABLE OF CONTENTS

	<u>PAGE</u>
D. CALCULATIONS OF SLIPSTREAM-IMMERSED WING AREAS	D-1
E. COMPUTER REPRESENTATION	E-1
F. MATHEMATICAL MODEL INPUT DATA	F-1
F.1 CONTROL SYSTEM INPUT DATA	F-11
F.2 ENGINE INPUT DATA	F-26
F.3 ROTOR AERODYNAMIC INPUT DATA	F-34
F.4 AIRFRAME AERODYNAMIC INPUT DATA	F-44
F.5 GEOMETRIC, WEIGHTS AND BALANCE DATA	F-50
F.6 SIMULATION INPUT DATA	F-53
G. IN-HOUSE HYBRID SIMULATION	G-1
G.1 SIMULATION ARCHITECTURE	G-3
G.2 TRIM LOOPS	G-160
G.3 SIMULATION PROGRAM OUTPUT	G-238
H. VALIDATION OF THE MODEL 222 SIMULATION AT AMES RESEARCH CENTER	H-1
H.1 VALIDATION PLAN AND CRITERIA	H-1
H.2 SIMULATION ACCEPTANCE	H-3
H.3 OPERATING INSTRUCTIONS AND LIMITATIONS	H-8

LIST OF ILLUSTRATIONS

<u>FIGURE NO.</u>	<u>TITLE</u>	<u>PAGE</u>
1.1	SUMMARY OF USES FOR PILOTED SIMULATION1.0-2
2.1	SALIENT FEATURES OF MATH MODEL2.0-5
4.1	MODEL 222 TILT ROTOR RESEARCH AIRCRAFT4.0-3
5.1	AXES SYSTEMS5.0-2
6.1	VARIATION OF HORIZONTAL TAIL DOWNWASH ANGLE WITH THRUST COEFFICIENT6.0-5
6.2	CORRELATION OF THEORY WITH TEST FOR PRE- DICTIONS OF SLIPSTREAM FORCES AND MOMENTS .	.6.0-20
7.1	ROTOR SIGN CONVENTIONS7.0-11
7.2	MODEL 213 1/9 SCALE CONVERSION MODEL - 85 FT/SEC DERIVATIVE VARIATION WITH RPM .	.7.0-19
7.3	26 FT. ROTOR TEST STAND IN NASA'S 40'x80' TUNNEL7.0-20
7.4	CORRELATION OF 26 FT ROTOR TEST DATA WITH VARIOUS ROTOR DERIVATIVE PROGRAMS7.0-22
7.5	CORRELATION OF 26 FT ROTOR TEST DATA WITH VARIOUS ROTOR DERIVATIVE PROGRAMS - CYCLIC MOMENT DERIVATIVES7.0-23
7.6	CORRELATION OF 26 FT ROTOR TEST DATA WITH VARIOUS ROTOR DERIVATIVE PROGRAMS - CYCLIC FORCE DERIVATIVES7.0-24
7.7	ROTOR MOMENT AND AZIMUTH ANGLE DUE TO ANGLE OF ATTACK - CORRELATION WITH 26 FT ROTOR DATA7.0-25
7.8	COMPARISON OF CALCULATED AND TEST ROTOR HUB FORCE AND MOMENT DERIVATIVES FOR M222 1/4.622 SCALE MODEL (YAW SWEEP) $\Omega=386$ RPM :	.7.0-27
7.9	COMPARISON OF CALCULATED AND TEST ROTOR HUB FORCE AND MOMENT DERIVATIVES FOR M222 1/4.622 SCALE MODEL (PITCH SWEEP) $\Omega=386$ RPM	.7.0-28
10.1	EFFECT OF ROTOR HEIGHT ON THRUST AUGMENTATION RATIO	10.0-3

LIST OF ILLUSTRATIONS

<u>FIGURE NO.</u>	<u>TITLE</u>	<u>PAGE</u>
A.1	WING GEOMETRY FOR DERIVATION OF FLEXIBILITY .	A-3
A.2	WING BENDING FUNCTIONS	A-10
B.1	GEOMETRY OF LANDING GEAR	B-2
C.1	REFERENCE AXES SYSTEMS	C-2
D.1	GEOMETRY OF ROTOR SLIPSTREAM/WING PLANFORM INTERACTION	D-4
E.1	BLOCK DIAGRAM ELEMENT INDEX NUMBERS	E-2
F.1	MASS PROPERTIES	F-7
F.2	C.G. LIMIT DIAGRAM	F-9
F.3	DIFFERENTIAL LONG. CYCLIC FOR YAW CONTROL VS NACELLE INCIDENCE	F-14
F.4	ROTOR ROLL CONTROL SCHEDULES IN TRANSITION .	F-15
F.5	LONGITUDINAL CYCLIC FOR PITCH CONTROL GAIN VS NACELLE INCIDENCE	F-16
F.6	LOAD ALLEVIATION SYSTEM GAIN SCHEDULE	F-17
F.7	PROGRAMMED CYCLIC, ELEVATOR, AND FLAP DEFLECTION VS NACELLE INCIDENCE	F-18
F.8	ROLL CONTROL DEFLECTION VS STICK DEFLECTION .	F-19
F.9	SPOILER ACTUATOR LIMIT VS AIRSPEED	F-20
F.10	ASSUMED THROTTLE TRAVEL MODEL 222 SIMULATION BOTH ENGINES	F-21
F.11	ENGINE CHARACTERISTICS LYCOMING T53-L13 ENGINE	F-22
F.12	ENGINE CHARACTERISTICS LYCOMING T53-L13 ENGINE	F-23
F.13	THRUST MANAGEMENT SYSTEM-SCHEDULED PARAMETERS	F-24
F.14	THRUST MANAGEMENT SYSTEM - SCHEDULED PARAMETERS	F-25

LIST OF ILLUSTRATIONS

<u>FIGURE NO.</u>	<u>TITLE</u>	<u>PAGE</u>
F.15	TURBINE ENGINE PERFORMANCE - ENGINE CYCLE 1.78	F-30
F.16	TURBINE ENGINE PERFORMANCE - ENGINE CYCLE 1.78	F-31
F.17	TURBINE ENGINE PERFORMANCE - ENGINE CYCLE 1.78	F-32
F.18	TURBINE ENGINE PERFORMANCE - ENGINE CYCLE 1.78	F-33
F.19	COEFFICIENTS OF CURVE FIT EQUATIONS FOR THRUST COEFFICIENT	F-35
F.20	COEFFICIENTS OF CURVE FIT EQUATIONS FOR POWER COEFFICIENT	F-36
F.21	COEFFICIENTS OF CURVE FIT EQUATIONS FOR NORMAL FORCE COEFFICIENT	F-37
F.22	COEFFICIENTS OF CURVE FIT EQUATIONS FOR SIDE FORCE COEFFICIENT	F-38
F.23	COEFFICIENTS OF CURVE FIT EQUATIONS FOR PITCHING MOMENT COEFFICIENT	F-39
F.24	COEFFICIENTS OF CURVE FIT EQUATIONS FOR YAWING MOMENT COEFFICIENT	F-40
F.25	CURVE FIT COEFFICIENTS FOR $\frac{\partial C_{PM}}{\partial \Omega}$	F-41
F.26	CURVE FIT COEFFICIENTS FOR $\frac{\partial C_{YM}}{\partial R}$	F-42
F.27	CONSTANTS FOR CYCLIC PITCH EFFECTIVENESS IN ROTOR EQUATIONS	F-43
F.28	MODEL 222 DOWNWASH FUNCTIONS @ $C_T=0$, $i_w=+2.0^\circ$	F-47
F.29	VARIATION OF LIFT CURVE SLOPE WITH GROUND HEIGHT	F-48
F.30	ROTOR/ROTOR AND WING/ROTOR INTERFERENCE	F-49
F.31	MODEL 222 PILOT STATION REQUIREMENTS	F-54

LIST OF ILLUSTRATIONS

<u>FIGURE NO.</u>	<u>TITLE</u>	<u>PAGE</u>
F.32	MODEL 222 CONTROL FORCE GRADIENTS AND BREAKOUT FORCES	F-55
G.1	UTILIZATION OF THE HYBRID LABORATORY FOR THE MODEL 222 MATH MODEL	G-5
G.2	FOREGROUND OPTIONS	G-8
G.3	GHP PHASE OVERLAY STRUCTURE (DIGITAL CORE ALLOCATIONS)	G-10
G.4	CONTENTS OF REAL TIME TASK - FAST LOOP	G-11
G.5	CONTENTS OF REAL TIME TASK - SLOW LOOP	G-13
G.6	MODEL 222 SIMULATION DIGITAL LISTING	F-15
G.7	ANALOG SYMBOLS	G-161
G.8	ANALOG DIAGRAMS FOR MODEL 222 SIMULATION	G-162
G.9	ANALOG STATIC CHECK ROUTINE (DIGITAL)	G-194
G.10	TYPICAL MODEL 222 TRIM SHEET	G-239
G.11	DEFINITION OF TRIM SHEET PARAMETERS	G-241
G.12	TYPICAL TIME HISTORY RESPONSE TO A .25 INCH LONGITUDINAL STICK PULSE AT 150 KNOTS	G-243

LIST OF TABLES

<u>TABLE NO.</u>	<u>TITLE</u>	<u>PAGE</u>
7.1	RANGE OF ROTOR DATA	7.0-5
8.1	FLIGHT CONTROL MIXING	8.0-2
9.1	ENGINE CYCLE DATA FORMAT	9.0-2
12.1	WING UNCOUPLED FREQUENCIES (BLADES OFF) CRUISE CONFIGURATION	12.0-2

NOMENCLATURE

<u>Symbol</u>	<u>Definition</u>	<u>Units</u>
A	Rotor disc area (per rotor)	ft ²
AR	Aspect ratio	N.D.
A _D (u+5v)	Coefficients of curve fit equation for wing drag coefficient as a function of angle of attack and surface deflection	--
A _{NF} (u+4v)	Coefficients of curve fit equation for normal force coefficient with zero cyclic pitch	--
A _P (u+4v)	Coefficients of curve fit equation for rotor power coefficient with zero cyclic pitch	--
A _{PM} (u+4v)	Coefficients of curve fit equation for rotor pitching moment coefficient with zero cyclic pitch	--
A _{SF} (u+4v)	Coefficients of curve fit equation for rotor side force coefficient with zero cyclic pitch	--
A _T (u+4v)	Coefficients of curve fit equation for rotor thrust coefficient with zero cyclic pitch	--
A _{YM} (u+4v)	Coefficients of curve fit equation for rotor yawing coefficient with zero cyclic pitch	--
A _{lc}	Lateral cyclic angle in rotor wind axes	deg
A' _{lc}	Lateral cyclic angle in swashplate axes	deg
A'' _{lc}	Lateral cyclic angle in swashplate axes resolved through swashplate phase angle	deg
\bar{a}	Speed of sound or acceleration	ft/sec or ft/sec ²
a	Acceleration	ft/sec ²
(a _g /a)	Ratio of lift curve slope in ground effect to lift curve slope out of ground effect	ND

NOMENCLATURE

<u>Symbol</u>	<u>Definition</u>	<u>Units</u>
B_G	Percent brake pedal deflection	N.D.
B.L.	Aircraft butt line	inches
B_{1c}	Longitudinal cyclic angle in rotor wind axes	deg
B'_{1c}	Longitudinal cyclic angle in swashplate axes	deg
B''_{1c}	Longitudinal cyclic angle in swashplate axes resolved through swashplate phase angle	deg
b	Span of lifting surface (wing, tail, etc.)	feet
c	Chord	ft.
C_D	Drag coefficient = $\frac{D}{qS}$	ND
C_{D_0}	Drag coefficient at zero lift	ND
ΔC_D	Drag coefficient increment	ND
C_{DS}	Drag coefficient referred to rotor slipstream dynamic pressure = $D/q_s S$	ND
C_L	Lift coefficient = L/qS	ND
C_{L_0}	Average lift coefficient	ND
ΔC_L	Lift coefficient increment	ND
C_{L_s}	Lift coefficient referred to rotor slipstream dynamic pressure = $L/q_s S$	ND
C_{L_α}	Lift curve slope	1/rad
C_{L_δ}	Lift increment due to flap deflection	1/deg
C_L	Rolling moment coefficient = $L/q bS$	ND
C_{L_s}	Rolling moment coefficient referred to rotor slipstream dynamic pressure = $L/q_s bS$	ND

NOMENCLATURE

<u>Symbol</u>	<u>Definition</u>	<u>Units</u>
C_M	Pitching moment coefficient = M/qSC	ND
C_{M_0}	Wing pitching moment coefficient as a function of flap deflection; pitching moment coefficient of fuselage or nacelles at zero angle of attack	ND
ΔC_M	Pitching moment coefficient increment	ND
C_{M_s}	Pitching moment coefficient referred to rotor slipstream dynamic pressure = $M/q_s SC$	
C_{M_δ}	Change in wing/body pitching moment coefficient as a function of flap/aileron deflection	ND
C_N	Yawing moment coefficient = N/qSb	ND
C_{N_0}	Yawing moment coefficient of fuselage or nacelles at zero angle of attack	ND
C_{n_s}	Yawing moment coefficient referred to rotor slipstream dynamic pressure = $N/q_s Sb$	ND
C_{NF}	Rotor normal force coefficient = $NF/\rho\pi\Omega^2 R^4$	ND
C_{NF_0}	Rotor normal force coefficient with zero cyclic pitch	ND
C_p	Rotor power coefficient = $\frac{550RHP}{\rho\pi\Omega^3 R^5}$	ND
C_{p_0}	Rotor power coefficient with zero cyclic pitch	ND
C_{PM}	Rotor hub pitching moment coefficient = $PM/\rho\pi\Omega^2 R^5$	ND
C_{PM_0}	Rotor hub pitching moment coefficient with zero cyclic pitch	ND
C_{SF}	Rotor side force coefficient = $SF/\rho\pi\Omega^2 R^4$	ND

NOMENCLATURE

<u>Symbol</u>	<u>Definition</u>	<u>Units</u>
C_{SF_0}	Rotor side force coefficient with zero cyclic pitch	ND
C_T	Rotor thrust coefficient = $T/\rho\pi\Omega^2R^4$	ND
C_{T_0}	Rotor thrust coefficient with zero cyclic pitch	ND
C_{T_s}	Rotor thrust coefficient referred to rotor slipstream dynamic pressure = T/q_sA	ND
C_Y	Side force coefficient = Y/q_s	ND
C_{YM}	Rotor yawing moment coefficient $\eta/\rho\pi\Omega^2R^5$	ND
C_{YM_0}	Rotor yawing moment coefficient with zero cyclic pitch	ND
C_{Y_α}	Lift curve slope of vertical tail	1/rad
C_0	Coefficient of equation that defines pitching moment coefficient as a function of flap deflection	ND
C_1	Coefficient of equation that defines pitching moment coefficient as a function of flap deflection	1/rad
C_2	Coefficient of equation that defines pitching moment coefficient as a function of flap deflection	1/rad ²
D	Rotor diameter	ft.
(D/T)	Aircraft download to thrust ratio	ND
$D_{NF_{1 \rightarrow 4}}$	Coefficients in the equation for the change in normal force coefficient with lateral cyclic angle	1/deg
$D_{PM_{1 \rightarrow 7}}$	Coefficients in the equation for the change in hub pitching moment coefficient with lateral cyclic angle	1/deg
$D_{SF_{1 \rightarrow 4}}$	Coefficients in the equation for the change in side force coefficient with lateral cyclic angle	1/deg

NOMENCLATURE

<u>Symbol</u>	<u>Definition</u>	<u>Units</u>
D_{ST_n}	Damping coefficients of the landing gear oleo struts	lb/ft/sec
$D_{Y_{M_{1 \rightarrow 7}}}$	Coefficients in the equation for the change in hub yawing moment coefficient with lateral cyclic angle	1/deg
dC_{NF}/dA_{1c}	Change in normal force coefficient with lateral cyclic angle	1/deg
dC_{NF}/dB_{1c}	Change in normal force coefficient with longitudinal cyclic angle	1/deg
dC_{PM}/dA_{1c}	Change in hub pitching moment coefficient with lateral cyclic angle	1/deg
dC_{PM}/dB_{1c}	Change in hub pitching moment coefficient with longitudinal cyclic angle	1/deg
dC_{PM}/dQ	Change in hub pitching moment coefficient with pitch rate	1/rad/sec
dC_{SF}/dA_{1c}	Change in side force coefficient with lateral cyclic angle	1/deg
dC_{SF}/dB_{1c}	Change in side force coefficient with longitudinal cyclic angle	1/deg
dC_{YM}/dA_{1c}	Change in hub yawing moment coefficient with lateral cyclic angle	1/deg
dC_{YM}/dB_{1c}	Change in hub yawing moment coefficient with longitudinal cyclic angle	1/deg
dC_{YM}/dR	Change in hub yawing moment coefficient with yaw rate	1/rad/sec
dC_M / dC_L	Change in wing pitching moment with lift coefficient	ND
$d\sigma/d\beta$	Change in fuselage sidewash angle with sideslip angle	ND
EI	Product of modulus of elasticity and moment of inertia	lb-in ²
EI _o	Product of modulus of elasticity and moment of inertia at wing root	lb-in ²

NOMENCLATURE

<u>Symbol</u>	<u>Definition</u>	<u>Units</u>
$E_{NF_{1 \rightarrow 4}}$	Coefficients in the equation for the change in normal force coefficient with longitudinal cyclic angle	1/deg
$E_{PM_{1 \rightarrow 7}}$	Coefficients in the equation for the change in hub pitching moment coefficient with longitudinal cyclic angle	1/deg
$E_{SF_{1 \rightarrow 4}}$	Coefficients in the equation for the change in side force coefficient with longitudinal cyclic angle	1/deg
$E_{YM_{1 \rightarrow 7}}$	Coefficients in the equation for the change in hub yawing moment coefficient with longitudinal cyclic angle	1/deg
e	Oswald efficiency of wing or tail	ND
F	Generalized force or force on nacelle	lb
FPR	Lateral-directional SAS function	--
FRL	Lateral-directional SAS function	--
F_{ϕ}	Lateral-directional SAS function	--
$F_{\phi 1}$	Lateral-directional SAS function	--
$F_{\phi 2}$	Lateral-directional SAS function	--
$F_{\psi 1}$	Lateral-directional SAS function	--
$F_{\psi 2}$	Lateral-directional SAS function	--
F_a	Aerodynamic force on nacelle	lb
F_{qzn}	Landing gear oleo strut vertical force	lb
F_{sn}	Landing gear oleo strut lateral force	lb
F_x	Longitudinal generalized force	lb
F_y	Lateral generalized force	lb
F_z	Vertical generalized force	lb
$F_{\mu n}$	Landing gear oleo strut longitudinal force	lb

NOMENCLATURE

<u>Symbol</u>	<u>Definition</u>	<u>Units</u>
f_{e_u}	Leading edge umbrella drag	ft ²
f_{NF}	Multiplier on rotor normal force	ND
f_p	Multiplier on rotor power	ND
f_{PM}	Multiplier on rotor hub pitching moment	ND
f_Q	Multiplier on rotor torque	ND
f_{SF}	Multiplier on rotor side force	ND
f_T	Multiplier on rotor thrust	ND
f_{YM}	Multiplier on rotor hub yawing moment	ND
G	Generalized moment	ft-lb
GEF	Ground effect factor = $\left[1 - \frac{(\Delta \epsilon)_g}{\epsilon}\right]$	ND
$G_{A1\alpha}$	Load alleviation system gain - change in lateral cyclic with angle of attack	deg/deg
$G_{A1\beta}$	Load alleviation system gain - change in lateral cyclic with angle of sideslip	deg/deg
$G_{B1\alpha}$	Load alleviation system gain - change in longitudinal cyclic with angle of attack	deg/deg
G_{G1}	Governor gain	deg/sec/rad/sec
G_{G2}	Governor gain	deg/sec/rad/sec
G_{G3}	Governor gain	deg/sec/deg
G_p	Lateral directional SAS gain	inches/rad/sec
G_{pr1}	Lateral directional SAS gain	inches/rad/sec
$G_{p\delta_s}$	Lateral directional SAS gain	inches/inch
G_q	Longitudinal SAS gain	deg/rad/sec
G_r	Lateral directional SAS gain	inches/rad/sec

NOMENCLATURE

<u>Symbol</u>	<u>Definition</u>	<u>Units</u>
G_{r2}	Lateral directonal SAS gain	inches/rad/sec
$G_{r\delta r}$	Lateral directional SAS gain	inches/rad/sec
$G_{\beta p}$	Lateral directional SAS gain	inches/rad
$G_{\beta r}$	Lateral directional SAS gain	inches/rad
$G_{\beta\delta r}$	Lateral directional SAS gain	inches/inch
$G_{\delta B1}$	Longitudinal SAS gain	deg/inch
$G_{\delta B2}$	Longitudinal SAS gain	deg/inch
$G_{\delta TH}$	Governor throttle gain	deg/inch
G_{θ}	Longitudinal SAS gain	deg/rad/sec
G_{ϕ}	Lateral-directional SAS gain	inches/rad/sec
G_{ψ}	Lateral directional SAS gain	inch/inch
$G_{\psi\delta r}$	Lateral directional SAS gain	inch/inch
g	Gravitational constant	ft/sec ²
H	Height	ft
HP	Horsepower	--
$H_{PM(u+4v)}$	Coefficients in the equation for the change in hub pitching moment with pitch rate	--
$H'_{w'FUEL}$	Horizontal distance between wing mass element center of gravity and fuel center of gravity	ft
$H'_{w'NF}$	Horizontal distance between wing mass element center of gravity and fixed nacelle center of gravity	ft
$H'_{w'w}$	Horizontal distance between wing mass element center of gravity and fixed nacelle center of gravity	ft

NOMENCLATURE

<u>Symbol</u>	<u>Definition</u>	<u>Units</u>
h	Height or angular momentum	ft or lb-ft-sec
h_{CG}^N	Angular momentum of nacelle about aircraft center of gravity	lb-ft-sec
h_F	Distance from wing pivot plane to fuselage mass element center of gravity	ft
h_p	Height of pivot above wing chord line or angular momentum of nacelle about the pivot	
h_T	Landing gear oleo strut deflection during ground contact	ft
h_w	Distance from wing pivot plane to wing mass element center of gravity	ft
h_o	Angular momentum of an element of mass about its own center of gravity	lb-ft-sec
h_1	Wing vertical bending deflection	ft
h/D	Rotor hub height to rotor diameter ratio	ND
h_θ	Distance from aircraft center of gravity bottom of right main gear following a positive pitch rotation	ft
h_ϕ	Distance from aircraft center of gravity to bottom of right main gear following a positive roll	ft
I	Mass moment of inertia	slug-ft ²
I_{xx}	Vehicle mass roll moment of inertia about center of gravity	slug-ft ²
I_{xx_o}	Mass roll moment of inertia of aircraft components about their own center of gravity	slug-ft ²
$I_{xx}^{(F)}$	Mass roll moment of inertia of fuselage mass element about its center of gravity	slug-ft ²

NOMENCLATURE

<u>Symbol</u>	<u>Definition</u>	<u>Units</u>
$I_{xx}^{(W)}$	Mass roll moment of inertia of wing mass element about its center of gravity	slug-ft ²
I'_{xx}	Mass roll moment of inertia of the tilting portion of <u>each</u> nacelle about its center of gravity	slug-ft ²
I_{YY}	Vehicle mass pitch moment of inertia about center of gravity	slug-ft ²
I_{YY_0}	Mass pitch moment of inertia of aircraft components about their own center of gravity	slug-ft ²
$I_{YY}^{(F)}$	Mass pitch moment of inertia of fuselage mass element about its center of gravity	slug-ft ²
$I_{YY}^{(W)}$	Mass pitch moment of inertia of wing mass element about its center of gravity	slug-ft ²
I'_{YY}	Mass pitch moment of inertia of the tilting portion of <u>each</u> nacelle about its center of gravity	slug-ft ²
I_{xz}	Vehicle mass product of inertia about center of gravity	slug-ft ²
I_{xz_0}	Mass product of inertia of aircraft components about their own center of gravity	slug-ft ²
$I_{xz}^{(F)}$	Mass product of inertia of fuselage mass element about its center of gravity	slug-ft ²
$I_{xz}^{(W)}$	Mass product of inertia of wing mass element about its center of gravity	slug-ft ²
I'_{xz}	Mass product of inertia of the tilting portion of <u>each</u> nacelle about its center of gravity	slug-ft ²

NOMENCLATURE

<u>Symbol</u>	<u>Definition</u>	<u>Units</u>
I_{zz}	Vehicle mass yaw moment of inertia about center of gravity	slug-ft ²
I_{zz_0}	Mass yaw moment of inertia of aircraft components about their own center of gravity	slug-ft ²
$I(F)_{zz}$	Mass yaw moment of inertia of fuselage mass element about its center of gravity	slug-ft ²
$I(W)_{zz}$	Mass yaw moment of inertia of wing mass element about its center of gravity	slug-ft ²
I'_{zz}	Mass yaw moment of inertia of the tilting portion of <u>each</u> nacelle about its center of gravity	slug-ft ²
i	Incidence angle	deg or rad
\hat{i}	Unit vector in i direction	--
J_{xx}	Dummy inertia = $(I_{zz} - I_{yy})$	slug-ft ²
$J_{YM(u+4v)}$	Coefficients of curve fit equation for rotor hub moment with hub yaw rate	--
J_{yy}	Dummy inertia = $(I_{xx} - I_{zz})$	slug-ft ²
J_{zz}	Dummy inertia = $(I_{yy} - I_{xx})$	slug-ft ²
\hat{j}	Unit vector in j direction	--
K'_A	Wing slipstream correction factor	ND
$\frac{K_{D1}}{T} \rightarrow \frac{K_{D4}}{T}$	Coefficients of curve fit equation for wing download as a function of rotor height/diameter ratio	ND
$\frac{K_{M1}}{T} \rightarrow \frac{K_{M4}}{T}$	Coefficients of curve fit equation for wing pitching moment as a function of rotor height/diameter ratio	ND
$K_{\mathcal{L}}$	Multiplier on slipstream rolling moment coefficient	ND
K_{γ}	Multiplier on slipstream yawing moment coefficient	ND

NOMENCLATURE

<u>Symbol</u>	<u>Definition</u>	<u>Units</u>
$K_{ST\eta}$	Landing gear spring constants	lb/ft
$K_{WI} \rightarrow K_{W10}$	Coefficients for wing bending equations	--
$K_{\delta B}$	Multiplier on longitudinal cyclic pitch available from longitudinal stick	inch/inch
$K_{\delta e}$	Ratio between longitudinal stick motion and elevator deflection	deg/inch
$K_{\delta R}$	Multiplier on longitudinal cyclic pitch available from pedal displacement	inch/inch
$K_{\delta RUD}$	Ratio between pedal and rudder deflection	deg/inch
$K_{\delta s}$	Multiplier on longitudinal cyclic pitch and differential collective available from lateral stick	inch/inch
$K_{\delta's}$	Provision for lateral cyclic pitch on lateral stick	deg/deg
K_{θ}	Wing stiffness	ft-lb/rad
K_O	Coefficient of fuselage drag coefficient equation to account for drag due to sideslip	1/rad ³
K_1	Coefficient of fuselage drag coefficient equation	1/rad ²
K_2	Coefficient of fuselage drag coefficient equation	1/rad
K_3	Coefficient of fuselage lift coefficient equation	1/rad
K_4	Coefficient of fuselage lift coefficient equation	1/rad ²
K_5	Coefficient of fuselage pitching moment coefficient equation	1/rad

NOMENCLATURE

<u>Symbol</u>	<u>Definition</u>	<u>Units</u>
K ₆	Coefficient of fuselage pitching moment coefficient equation	1/rad ²
K ₇	Coefficient of fuselage side force coefficient equation	1/rad
K ₈	Coefficient of fuselage side force coefficient equation	1/rad
K ₉	Coefficient of fuselage yawing moment coefficient equation	1/rad
K ₁₀	Coefficient of fuselage yawing moment coefficient equation	1/rad ²
K ₂₀	Wing/body interference effects on C _{Lβ}	1/rad
K ₂₁	Wing planform effects on C _{Lβ}	1/rad
K ₂₂	Wing planform and lift effects on C _{ηβ}	1/rad
K ₃₀	Coefficient of nacelle drag coefficient equation	1/rad
K ₃₁	Coefficient of nacelle drag coefficient equation	1/rad ²
K ₃₂	Coefficient of nacelle lift coefficient equation	1/rad
K ₃₄	Coefficient of nacelle pitching moment coefficient equation	1/rad
K ₃₅	Coefficient of nacelle pitching moment coefficient equation	1/rad ²
K ₃₆	Coefficient of nacelle side force coefficient equation	1/rad
K ₃₇	Coefficient of nacelle side force coefficient equation	1/rad ²
K ₃₈	Coefficient of nacelle yawing moment coefficient equation	1/rad
K ₃₉	Coefficient of nacelle yawing moment coefficient equation	1/rad ²

NOMENCLATURE

<u>Symbol</u>	<u>Definition</u>	<u>Units</u>
K_{40}	Coefficient of nacelle yawing moment coefficient equation	1/rad
K_{41}	Coefficient of nacelle yawing moment coefficient equation	1/rad ²
K_{42}	Coefficient of fuselage lift coefficient equation	ND
\hat{k}	Unit vector in k direction	--
L	Rolling moment or nacelle shaft length	ft-lb ,ft
L	Rolling Moment	ft-lb
l	Distance from nacelle pivot to nacelle center of gravity	ft
l'	Horizontal distance from nacelle pivot to noted aircraft component center of gravity position - positive forward from pivot	ft
l _{AC}	Horizontal distance from horizontal tail quarter chord to wing aerodynamic center	ft
l _F	Horizontal distance from pivot to center of gravity of fuselage mass element	ft
l ₀	Wing root lift/foot	lb/ft :
l _{PA}	Horizontal distance from pivot to center of gravity of pilots station - positive forward from pivot	ft
l _w	Horizontal distance from pivot to wing mass element center of gravity	
M	Pitching moment	ft-lb
m	Pitching moment	ft-lb
M/T	Pitching moment/rotor thrust	ft-lb/lb
m	Aircraft total mass	slugs

NOMENCLATURE

<u>Symbol</u>	<u>Definition</u>	<u>Units</u>
m_f	Mass of fuselage mass element	slugs
m_N	Mass of one nacelle	slugs
m_w	Mass of wing mass element	slugs
N	Yawing moment	ft-lb
η	Yawing moment	ft-lb
NF	Rotor normal force	lb
N_I	Engine gas generator speed	rev/min
N_1 IND	Engine gas generator indicator	--
N_I^*	Engine gas generator speed at sea level standard, static conditions	rev/min
$N_{1\theta}$ IND	Referred engine gas generator speed indicator	--
N_{II}	Engine power turbine speed	
N_{II}^*	Engine power turbine speed at sea level standard static conditions	
P	Body axes roll rate	rad/sec
PC	Horizontal distance from wing leading edge to pivot location	ft.
P_N	Nacelle axes roll rate	rad/sec
P_R	Nacelle wind axes roll rate	rad/sec
p	Body axes roll rate	rad/sec
Q	Body axes pitch rate or rotor torque	rad/sec or lb-ft
Q_{IND}	Torque indicator	ND
Q_{MAX}	Maximum engine torque available	lb-ft
Q_N	Nacelle axes pitch rate	rad/sec
Q_R	Nacelle wind axes pitch rate	rad/sec

NOMENCLATURE

<u>Symbol</u>	<u>Definition</u>	<u>Units</u>
Q*	Engine torque at sea level standard static condition	lb-ft
q	Body axes pitch rate or freestream dynamic pressure	rad/sec or lb/ft ²
q _s	Dynamic pressure based on rotor slipstream = (q + T/A)	lb/ft ²
R	Body axes yaw rate or rotor resultant force or rotor radius	rad/sec or lb or ft
RHP	Rotor horsepower	--
R ^N	Nacelle axes yaw rate	rad/sec
R ^R	Nacelle wind axes yaw rate	rad/sec
r	Body axes yaw rate	rad/sec
<u>r</u>	Radius vector	--
r _n	Landing gear tire radius	ft.
S	Surface area	ft ²
SF	Rotor side force	lb
SHP	Shaft horsepower	--
SHP*	Engine shaft horsepower at sea level standard static conditions	
T	Rotor thrust	lb
TEA	Engine referred turbine inlet temperature	degrees
(T _{I GE} /T _{O GE})	Ratio of the rotor thrust in ground effect to the thrust out of ground effect	--
T ₁ →T ₃	Coefficients of curve fit equations for rotor/rotor interference	ND
t	Time	sec

NOMENCLATURE

<u>Symbol</u>	<u>Definition</u>	<u>Units</u>
u	Body axes longitudinal component of velocity at aircraft center of gravity or rotor hub, wing, horizontal and vertical tail velocities referred to rotor shaft and local surface chord axes respectively.	ft/sec
u'	Body axes longitudinal component of velocity at rotor hub and wing aerodynamic center	ft/sec
u _{PA}	Body axes longitudinal component of velocity at pilots station	ft/sec
V	Total velocity	ft/sec
V _t	Rotor tip speed	ft/sec
V'	Resultant flow through rotor disc	ft/sec
V*	Non-dimensional rotor forward velocity	N.D.
<u>V</u>	Total Velocity Vector	—
v	Body axes lateral component of velocity at aircraft center of gravity or rotor hub wing, horizontal and vertical tail velocities referred to rotor shaft and local surface chord axes respectively	ft/sec
v'	Body axes lateral component of velocity at rotor hub and wing aerodynamic center	ft/sec
v _i	Rotor induced velocity	ft/sec
v _{PA}	Body axes lateral component of velocity at pilots station.	ft/sec
v*	Non-dimensional rotor induced velocity	N.D.
W.L.	Fuselage water line position	inches
W'	Weight of aircraft components	lb.
WDTIND	Fuel flow indicator	—
w	Body axes vertical component of velocity at aircraft center of gravity or rotor	ft/sec

NOMENCLATURE

<u>Symbol</u>	<u>Definition</u>	<u>Units</u>
	hub, wing, horizontal and vertical tail velocities referred to rotor shaft and local surface chord axes respectively	
w'	Body axes vertical component of velocity at rotor hub and wing aerodynamic center	ft/sec
w_{PA}	Body axes vertical component of velocity at pilots station.	
$X_{\text{subscript}}$	Longitudinal distance, measured positive forward from nacelle pivot along body axes	ft.
$\Delta X_{\text{subscript}}$	Longitudinal force, measured positive forward along body axes	lb.
X_{aero}	Total longitudinal aerodynamic force at center of gravity measured positive forward along body axes.	lb.
$X_{\text{subscript}}^{\text{sprscript}}$	Longitudinal force, measured positive forward along body axes.	lb.
\dot{X}_{North}	Longitudinal ground track velocity	ft/sec
$Y_{\text{subscript}}$	Lateral distance, measured positive along right wing along body axes	ft.
$\Delta Y_{\text{subscript}}$	Lateral force, measured positive along right wing in body axes	lb.
Y_{aero}	Total lateral aerodynamic force at center of gravity measured positive along right wing in body axes	lb.
$Y_{\text{subscript}}^{\text{sprscript}}$	Lateral force, measured positive along right wing in body axes	lb.
\dot{Y}_{East}	Lateral ground track velocity	ft/sec
$Z_{\text{subscript}}$	Vertical distance, measured positive down nacelle pivot along body axes	ft.
$\Delta Z_{\text{subscript}}$	Vertical force, measured positive down along body axes	lb.
Z_{aero}	Total vertical aerodynamic force at center	lb.

NOMENCLATURE

<u>Symbol</u>	<u>Definition</u>	<u>Units</u>
	of gravity, measured positive down along body axes.	
$z_{\text{sprscript}}^{\text{subscript}}$	Vertical force, measured positive down along body axes	lb.
\dot{z}_{down}	Vertical ground track velocity	ft/sec
z	Vertical distance from nacelle pivot to center of gravity of aircraft component, positive down from nacelle pivot along body axes.	ft.
α	Angle of attack	rad
β	Angle of sideslip	rad
$\Delta'_{W'fuel}$	Vertical distance between wing fuel center of gravity and wing mass element center of gravity	ft.
$\Delta'_{W'NF}$	Vertical distance between fixed nacelle center of gravity and wing mass element center of gravity.	ft.
$\Delta'_{W'W}$	Vertical distance between wing center of gravity and wing mass element center of gravity.	ft.
δ	Control element (surface or stick) angular or linear displacement	deg. or in.
δ'_{C}	Vertical distance between cargo center of gravity and fuselage mass element center of gravity	ft.
δ'_{CR}	Vertical distance between crew center of gravity and fuselage mass element center of gravity	ft.
$\delta'_{F'}$	Vertical distance between fuselage center of gravity and fuselage mass element center of gravity.	ft.
δ'_{HT}	Vertical distance between horizontal tail center of gravity and fuselage mass element center of gravity	ft.

<u>Symbol</u>	<u>NOMENCLATURE</u>	<u>UNITS</u>
	<u>Definition</u>	
δ'_{VT}	Vertical distance between vertical tail center of gravity and fuselage mass element center of gravity	ft.
ϵ	Wing or rotor downwash angle	rad
ϵ_0	Wing downwash angle at zero wing angle of attach	rad
ϵ_{iLR}	Rotor/rotor interference angle, left rotor on right rotor	rad
ϵ_{iRL}	Rotor/rotor interference angle, right rotor on left rotor	rad
ϵ_w	Wing on rotor interference	rad
ζ	Rotor sideslip angle or damping ratio	rad or N.D.
$\zeta_{w1} \rightarrow \zeta_{w4}$	Wing damping ratio	N.D.
$H'_{w'fuel}$	Horizontal distance between wing fuel center of gravity and wing mass element center of gravity	ft.
$H'_{w'NF}$	Horizontal distance between fixed nacelle center of gravity and wing mass element center of gravity	ft.
$H'_{w'w}$	Horizontal distance between wing center of gravity and wing mass element center of gravity	ft.
η'_c	Horizontal distance between cargo center of gravity and fuselage mass element center of gravity	ft.
η'_{CR}	Horizontal distance between crew center of gravity and fuselage mass element center of gravity	ft.
η'_F	Horizontal distance between fuselage center of gravity and fuselage mass	ft

<u>Symbol</u>	<u>NOMENCLATURE</u> <u>Definition</u>	<u>Units</u>
	element center of gravity	
η_{HT}	Horizontal tail efficiency	N.D.
η'_{HT}	Horizontal distance between horizontal tail center of gravity and fuselage mass element center of gravity.	lb.
η_{VT}	Vertical tail efficiency factor	N.D.
η'_{VT}	Horizontal distance between vertical tail center of gravity and fuselage mass element center of gravity	ft.
η_{TR}	Transmission efficiency	N.D.
θ	Aircraft pitch or Euler angle or temperature ratio	rad or N.D.
θ_t	Wing twist angle	rad
$\theta_{0.75}$	Rotor collective pitch angle at three quarter radius	deg.
λ	Angle between the rotor shaft and a line drawn through the nacelle center of gravity from the pivot.	rad
μ	Rotor advance ratio = $V/\Omega R$	N.D.
μ_s	Tire sliding coefficient of friction when sliding sideways (for concrete)	N.D.
μ_0	Tire rolling coefficient of friction (for concrete)	N.D.
μ_1	Coefficient of rolling friction for brakes	N.D.
$\xi_{R1} \rightarrow \xi_{R4}$	Terms of wing immersed area calculation	—
π	3.14159	—
ρ	Ambient air density	slug/ft ³
σ	Fuselage sidewash angle	rad

<u>Symbol</u>	<u>NOMENCLATURE</u>	<u>Units</u>
	<u>Definition</u>	
σ_h	Ambient density ratio	N.D.
τ	Angle between freestream velocity and rotor resultant force	rad
τ_D	Engine response time constant	sec.
τ_E	Engine response time constant	sec.
τ_{HT}	Horizontal tail effectiveness	rad/rad
τ_{LAS}	Load alleviation system time constant	sec
τ_{VT}	Vertical tail effectiveness	rad/rad
τ_P	Lateral directional SAS time constant	sec
τ_r	Lateral directional SAS time constant	sec
τ_ϕ	Lateral directional SAS time constant	sec
$\tau_{\phi\delta_s}$	Lateral directional SAS time constant	sec
τ_ψ	Lateral directional SAS time constant	sec
$\tau_{\psi\delta_r}$	Lateral directional SAS time constant	sec
τ_1	Rotor thrust response time constant	sec
τ_2	Rotor thrust response time constant	sec
ϕ	Aircraft roll angle or Euler angle	rad
ϕ_P	Rotor swashplate phase angle	rad
$\phi_1 \rightarrow \phi_5$	Functions in wing vertical bending equations	—
χ	Rotor wake skew angle	rad
ψ	Aircraft yaw angle or Euler angle	rad
Ω	Rotor or engine rotational speed	rad/sec
$\underline{\Omega}$	Rotational speed vector	rad/sec
ω	Natural frequency	rad/sec
$\omega_{w1} \rightarrow \omega_{w3}$	Wing natural frequency	rad/sec

Subscripts

A	Available
AC	Aerodynamic center
ACT	Actuator
AERO	Aerodynamic force
a	Aileron
B	Longitudinal stick
c	Cargo
CG	Center of gravity
CR	Crew
C/4	Quarter chord
DUM	Dummy variable
E	Engine
EFF	Effective
e	Elevator or effective
F	Fuselage
FAC	Fuselage aerodynamic center
FUEL	Fuel in wing
FUEL _{CG}	Fuel center of gravity
FUS	Fuselage
F'	Fuselage less landing gear
f	Flap
GLAS	Load alleviation system
GYRO	Gyroscopic
g	Ground or gust
HL	Left rotor hub

Subscripts

HR	Right rotor hub
HT	Horizontal tail
HTCG	Horizontal tail center of gravity
IGE	In ground effect
i	Immersed
L	Left wing or rotor
LAS	Load alleviation system
LE	Left engine
LG	Landing gear
L-L	Rotor lead-lag
LN	Left nacelle
LR	Left rotor
LRH	Left rotor hub
LT	Left wing tip
LW	Left wing
LW _o	Left wing referred to freestream
MAX	Maximum
N	Nacelle or natural frequency
NF	Fixed portion of nacelle
NFCG	Fixed portion of nacelle center of gravity
NL	Left nacelle
NR	Right nacelle
NT	Tilting portion of nacelle
n	Landing gear index, n=1 left gear, n=2 right gear, n=3 nose gear

Subscripts

OGE	Out of ground effect
P	Power, nacelle pivot, or rotor polar moment of inertia
POWER	Power
PA	Pilot station
R	Right wing, rotor or rudder pedal
RE	Right engine
REQ	Required
RIGID	Rigid
RN	Right nacelle
RR	Right rotor
RRH	Right rotor hub
RT	Right wing tip
RUD	Rudder
RW	Right wing
RW _o	Right wing referred to freestream
S	Rotor shaft, side, or lateral stick
SP	Spoiler
STALL	Stall
T	Tail, total or wing tip
TH	Throttle
VT	Vertical tail
VTCG	Vertical tail center of gravity
W	Wing
WAC	Wing aerodynamic center
WCG	Wing center of gravity

Subscripts

- x Along the lonitudinal body axes, positive forward
- y Along the lateral body axes, positive out right wing
- z Along the vertical body axes, positive down
- Denotes a vector quantity

Superscripts

- (c) Referes to cargo or payload weight
- (CR) Refers to aircraft crew weight
- F Fuselage
- F' Fuselage less landing gear
- HT Horizontal tail
- (HT) Refers to horizontal tail weight component
- IGE In ground effect
- LW Left wing
- N Nacelle
- NL Left wing tip at pivot
- NR Right wing tip at pivot
- (p) Roll axes
- (q) Pitch axes
- RW Right wing
- (r) Yaw axes
- T Total of horizontal and vertical tail
- VT Vertical tail
- (VT) Referes to vertical tail weight component
- W Wing

Superscripts

(W' FUEL)	Refers to wing fuel weight
(W _F ')	Refers to fuselage weight component
(W' _{NF})	Refers to weight of fixed portion of nacelle
(W' _W)	Refers to wing weight component
•	First derivative with respect to time; represents velocity
••	Second derivative with respect to time; represents acceleration
"	Denotes an interim calculation or coefficient in local wind axes
'''	Denotes an interim calculation
-	Denotes average value
*	Denotes interim calculation or calculation in freestream wind axes
'	Denotes an interim calculation
+	Denotes an interim calculation
^	Denotes an interim calculation
	Absolute values

NOTES

1. Some symbols not defined in this section, but used in this report, are defined in the section of the report they are used.
2. Alternate definitions, where applicable, for each symbol are given. Select the appropriate definition for each particular section
3. All distances are measured with respect to the nacelle pivot. Distances are positive forward, down and to the right of the pivot. Forces are positive forward, down, and to the right.
4. Δ or δ preceding a symbol generally denotes an incremental change.

1.0 INTRODUCTION

Piloted simulation is a useful and important tool in the design, development and test of new flight vehicles. Figure 1.1 shows a summary of some of these uses as they could be applied to the Model 222 tilt rotor aircraft.

As part of Contract NAS2-6598 Boeing Vertol developed a complex mathematical model of the Model 222 tilt rotor, intended primarily for use with the NASA Flight Simulator for Advanced Aircraft (FSAA) at Ames Research Center. The purpose of this report is to document the development of that mathematical model and to substantiate the methods which were uniquely developed for this purpose.

- Evaluation of Tilt Rotor Handling Qualities
 - Stability and Control
 - Control System Optimization
 - Evaluation of Man-in-the-Loop System Compatibility
 - Evaluation of Malfunction Effects
- Evaluation of Tilt Rotor Performance
 - Maneuver Capability
 - VTOL and STOL Takeoff and Landing Capability
- As a Tool to Evaluate Configuration Changes
 - Changes in Cockpit Layout
 - Changes in Tail Size
 - Changes in Geometry
 - Changes in SAS Configuration
 - Changes in Elastic Characteristics
- As a Flight Test Support Tool
 - Development of Emergency Techniques
 - Familiarization of Flight Crews with Aircraft Characteristics Prior to Flight
 - Correlation Studies
 - Exploration of Flight-Discovered Phenomena

Figure No. 1.1. Summary of Uses for Piloted Simulation

2.0 GENERAL DESCRIPTION OF SIMULATION

The objective of this program was to develop a real time simulation program for a tilt rotor aircraft to be used at the NASA-Ames simulation facility in conjunction with the Flight Simulator for Advanced Aircraft (FSAA) for evaluation of tilt rotor aircraft performance and handling characteristics throughout the flight envelope and identifying problem areas within the envelope.

The mathematical model developed under this contract includes the basic 6 degree of rigid body freedom outer loop equations written about the instantaneous center of gravity with all inertial and aerodynamic coupling terms included. Euler angles are used to properly orient the aircraft in space.

Rotor forces and moments are input to the equations from curve-fit data. The rotor data bank applies to the Boeing Model 222 tilt rotor. Calculation of the rotor forces and moments on-line for real time simulation is not practical because of the complexity of the programs required to represent the lag-flap coupling effects of the soft-in-plane hingless rotor. Analytical studies show that the lag-flap coupling has a large effect upon the phasing of the hub forces and moments of the rotor thereby altering the direct rotor effects on aircraft stability significantly. The rotor rotational degree of freedom is included to represent the effects of rotor inertia which are included in the representation of the thrust management system.

The effects of rotor-on-wing, wing-on-rotor, and rotor-on-horizontal tail are included in this program. The effects of rotor-on-wing are represented by calculation of the slipstream angle of attack of the portions of the aircraft operating in the rotor slipstream by momentum methods and resolving the associated forces and moments to body axes. Correlation with test data are shown in Section 6.5.2 to verify these interference effects. The effects of the rotor slipstream on the horizontal tail downwash are also calculated by momentum methods. The angle through which the flow through the rotor is turned is assumed to represent the change in tail downwash. Provisions are made to incorporate the upwash effects of the wing on the rotor. Lifting line theory should be used to compute these effects.

The effects on lateral/directional parameters caused by rotor wake skew on the wing are included by computing the change in immersed wing area during sideways flight and sideslips.

Structural dynamics effects included consist of the first mode wing vertical bending and the first wing torsion mode. These wing structural modes have been included on a "quasistatic" basis; i.e. the natural frequencies of vibration of the structure are much higher than the frequencies of the rigid body motion, and the coupling is in the aerodynamic terms.

The aerodynamics of the fuselage, empennage, nacelles, wings and rotors are included in detail. The aerodynamics of the

wing and rotors are written separately for the left and right sides. The effects of the wing leading edge umbrellas are included, with provisions for the direct effects of wing down-load and pitching moment with the umbrellas open in slow flight. Ground effects are considered on the rotors, wing and horizontal tail. The effects of Mach number on the airplane are treated by application of the Prandtl-Glauert rule. The effects of Mach number on the rotor data have been included in the curve fit equations.

The control system elements represented include pilot command, three axis stability augmentation systems, a load alleviation system (LAS) and a thrust management system. Control system actuator dynamics are represented by appropriate first order and second order lags. The systems are assumed to be "tight" in that thresholds, biases and hysteresis loops are neglected.

Turbine engine performance with appropriate dynamic responses are included. Engine power is computed for the range of flight condition necessary to cover the flight envelope. A relatively simple engine dynamic response model modulates the power output in response to pilot control of throttle position.

Landing gear is represented by a spring-damper system without complex calculation of oleo strut response.

The effects of rotor tilt angle on the aircraft center of gravity and inertia are included. Forces and moments resulting from

acceleration of the nacelles during tilting maneuvers are calculated in the program.

An airframe representation/preprocessor calculation is included that enables the user to input the location of major structural elements of the aircraft in terms of water line, butt line and station line location. All lengths and inertias required by the equation are then calculated. This feature enables the user to quickly change the location of major elements to assess their impact on vehicle response. The rest of the input data required has been kept to a minimum to augment the programs' usefulness. Provisions have been included to provide a very flexible design tool which enables the astute user to perform a wide variety of studies. Figure 2.1 summarizes the salient features of the mathematical model described in this document. It should be emphasized that this model has full flight envelope capability.

- Full Flight Envelope Capability with Total Force Representation
- 6 Rigid Body Degrees of Freedom
- Independent Nacelle Pitch Degree of Freedom
- 2 Elastic Degrees of Freedom
- 1 Rotor Rotational Degree of Freedom
- Includes the Aerodynamics of:
 - Rotors
 - Wings
 - Rotor/Wing & Wing/Rotor Interference
 - Fuselage
 - Landing Gear
 - Tail Surfaces
 - Engines
- Control System Elements:
 - Pilot Command
 - SAS
 - Load Alleviation System (LAS)
 - Thrust and Power Management System
- Aeroelastic Representation
 - Wing Vertical Bending
 - Wing Torsion

Figure 2.1. Salient Features of Math Model

3.0 SIGN CONVENTIONS

Standard aircraft sign conventions have been used throughout this report. Sign conventions are as follows:

Positive X axis forward

Positive Y axis outward along the right wing.

Positive Z axis downward perpendicular to the XY plane.

Lift is positive along the negative Z axis.

Pitching moment is positive nose-up about the Y axis.

Sideforce is positive outward in the direction of the positive Y axis.

Yawing moment is positive nose-right.

Rolling moment is positive right wing down.

Positive elevator deflection is trailing edge down

Positive rudder deflection is rudder-trailing-edge-left.

Positive aileron deflection is right-flaperon-trailing-edge-down.

Positive spoiler deflection is left-hand-spoiler-deflected-upward.

Positive deflection of the pilot's stick and rudder pedals yields positive aircraft pitch, roll, and yaw moments from negative control deflections.

Rotor sign conventions are illustrated in Section 7.0

Special sign convention; used in the derivations are noted in the appropriate section.

4.0 MODEL 222 TILT ROTOR AIRCRAFT DESCRIPTION

The Boeing Model 222 Tilt Rotor Research Aircraft, shown in Figure 4.1 uses two 26-foot diameter soft in-plane hingeless rotors of the same design that has already been demonstrated in the NASA/Ames 40 by 80-foot tunnel. The soft in-plane rotor is mechanically simple and provides excellent flying qualities characteristics as well as freedom from aeroelastic problems. It is service proven on the FAA certified BO-105 helicopter. For transition, the rotors tilt from hover position (rotor disk horizontal) to cruise position (rotor disk vertical). Intermediate nacelle positions provide optimum performance capability for climb, descent and for STOL operations.

The Model 222 is powered by two modified Lycoming T53-L-13B turboshaft engines mounted in fixed (nontilting) nacelles at each wing tip. The rotors are interconnected by a cross shaft for single engine operation. The engine power available yields excellent single engine and temperature-altitude performance.

Fuselage and empennage are production (MU-2J) components, modified to accept the Model 222 wing and two production (OV-10) ejection seats. The retractable tricycle landing gear is also the existing MU-2J gear modified to provide increased energy absorption.

Collective and cyclic pitch of the rotors, together with nacelle tilt, provide high control power in hover. In the cruise mode, control is by conventional airplane elevators,

rudder, flaperons and spoilers. Leading-edge "umbrella" flaps and large deflection trailing-edge flaps reduce download and ground effect turbulences in hover. Operation of flaps, umbrellas and elevator as well as phasing out of the rotor controls is mechanically programmed with nacelle tilt to relieve pilot workload.

A limited-authority stability augmentation system includes feedback from angle-of-attack, yaw angle, and dynamic pressure. In cruise flight it feeds back two axes of cyclic pitch to the rotor control. This provides increased static stability and reduces blade loads to increase fatigue margins. The feedback system is not required for either stability or structural integrity. This system permits easy variation of the stability characteristics of the aircraft.

5.0 EQUATIONS OF MOTION

This section presents the derivation of the airframe equations of motion and the simplifications that were made in order to obtain the final equations as presented in Appendix E. The treatment accounts for all six rigid-body degrees-of-freedom including the effects of the tilting nacelles and rotors. The principal features of the derivation are:

- Assumption of X-Z plane of symmetry
- The basic equations are derived about the instantaneous center of gravity of the aircraft since the center of gravity is strongly dependent on nacelle incidence.
- Rotor and engine gyroscopic terms are included
- The wing elastic degrees of freedom do not couple inertially. The coupling occurs through the aerodynamic terms in the equations as discussed in Section 12.
- Wing aeroelastic effects are not included in the center of gravity calculations.

5.1 AXES SYSTEM

A set of right-handed orthogonal axes OXYZ is placed at the center of mass of the aircraft and is fixed in the aircraft such that OX lies in the lateral plane of symmetry and is positive forward parallel to the fuselage water line zero. The remaining axes are placed as shown in Figure 5.1.

The orientation of the aircraft is defined with respect to a

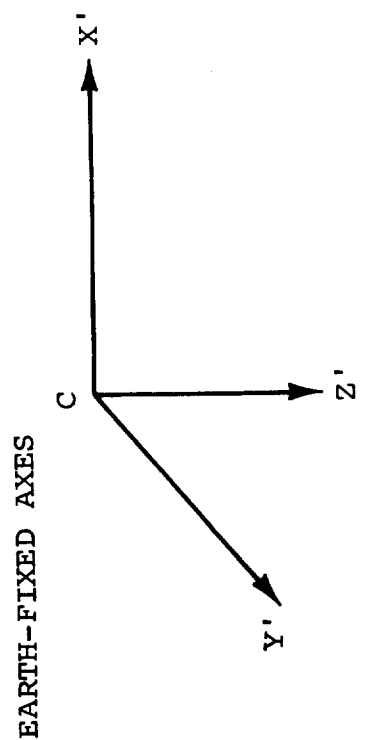
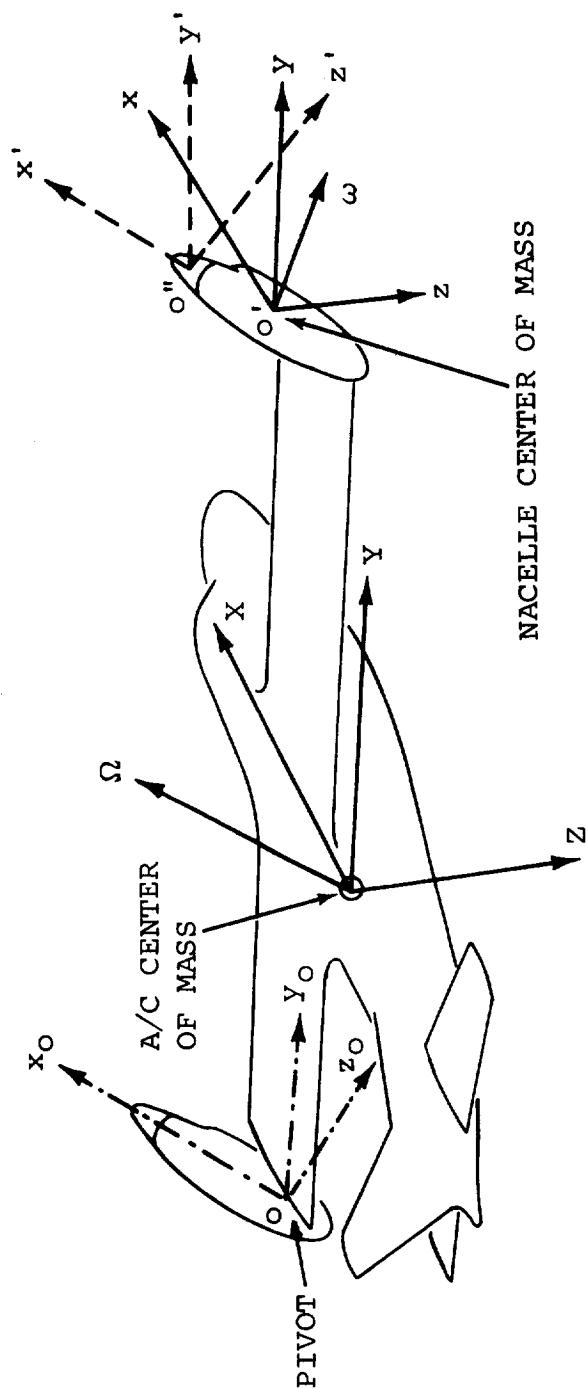


Figure 5.1. Axes Systems

set of earth-fixed axes C X'Y'Z'. With the axes OXYZ initially parallel to C X'Y'Z', the aircraft is yawed to the right about O through an angle ψ , then pitched up about OZ through the angle θ and finally rolled right about OX through the angle ϕ .

If \underline{V} and $\underline{\Omega}$ are the aircraft velocity and angular velocity vectors relative to the earth-fixed axes, the projections of these vectors on the moving axes are U, V, and W, for the components along OX, OY and OZ, and P, Q and R for the angular velocity components.

Thus

$$\underline{V} = U\hat{i} + V\hat{j} + W\hat{k} \quad (5.1)$$

$$\underline{\Omega} = P\hat{i} + Q\hat{j} + R\hat{k} \quad (5.2)$$

where the unit vectors \hat{i} , \hat{j} and \hat{k} lie along OX, OY and OZ.

5.2 AIRCRAFT GROUND TRACK

The components of \underline{V} relative to the earth-fixed axes are obtained in terms of U, V, W and ψ, θ, ϕ as, (See Reference 10),

$$\begin{aligned} \frac{dX'}{dt} = & U \cos \theta \cos \psi + V(\sin \phi \sin \theta \cos \psi - \cos \phi \sin \psi) \\ & + W (\cos \phi \sin \theta \cos \psi + \sin \theta \sin \psi) \end{aligned}$$

$$\begin{aligned} \frac{dY'}{dt} = & U \cos \theta \sin \psi + V(\sin \phi \sin \theta \sin \psi + \cos \phi \cos \psi) \\ & + W (\cos \phi \sin \theta \sin \psi - \sin \phi \cos \psi) \end{aligned} \quad (5.3)$$

$$\frac{dZ'}{dt} = -U \sin \theta + V \sin \phi \cos \theta + W \cos \phi \cos \theta$$

Integration of these equations gives the aircraft ground track.

A further relationship may be obtained between the rate of

change of the Euler angles (ψ, θ, ϕ) and the components of the angular velocity in the moving axes system, viz,

$$\begin{aligned}\dot{\psi} &= (R \cos \phi + Q \sin \phi) \sec \theta \\ \dot{\theta} &= Q \cos \phi - R \sin \phi \\ \dot{\phi} &= P + \dot{\psi} \sin \theta\end{aligned}\tag{5.4}$$

5.3 FORCE EQUATION

The total external force, \underline{F} , acting at the aircraft center of mass is given by

$$\underline{F} = \frac{d}{dt} (m\underline{V}) = m \left[\frac{\delta \underline{V}}{\delta t} + \underline{\Omega} \times \underline{V} \right]\tag{5.5}$$

where m is the mass of the aircraft and $\frac{\delta \underline{V}}{\delta t}$ is the rate of change of \underline{V} with respect to the moving reference frame OXYZ i.e.

$$\frac{\delta \underline{V}}{\delta t} = U \hat{i} + V \hat{j} + W \hat{k}\tag{5.6}$$

If \underline{F} has components F_x , F_y and F_z along the respective axes then

$$\underline{F} = F_x \hat{i} + F_y \hat{j} + F_z \hat{k} = m \left\{ U \hat{i} + V \hat{j} + W \hat{k} + \begin{vmatrix} \hat{i} & \hat{j} & \hat{k} \\ P & Q & R \\ U & V & W \end{vmatrix} \right\}$$

thus

$$\begin{aligned}F_x &= m (\dot{U} + QW - RV) \\ F_y &= m (\dot{V} + RU - PW) \\ F_z &= m (\dot{W} + PV - QU)\end{aligned}\tag{5.7}$$

The forces F_x , F_y and F_z are given by

$$\begin{aligned}
F_x &= X_{\text{AERO}} - mg \sin \theta \\
F_y &= Y_{\text{AERO}} + mg \sin \phi \cos \theta \\
F_z &= Z_{\text{AERO}} + mg \cos \phi \cos \theta
\end{aligned}
\tag{5.8}$$

where X_{AERO} , etc., are the components of the total aerodynamic force acting at the aircraft center of mass.

Substituting equations (5.8) in equations (5.7), the following equations are obtained for the aircraft accelerations,

$$\begin{aligned}
\dot{U} &= \frac{X_{\text{AERO}}}{m} - g \sin \theta - QW + RV \\
\dot{V} &= \frac{Y_{\text{AERO}}}{m} + g \cos \theta \sin \phi - RU + PW \\
\dot{W} &= \frac{Z_{\text{AERO}}}{m} + g \cos \theta \cos \phi + QU - PV
\end{aligned}
\tag{5.9}$$

5.4 MOMENT EQUATION

The derivation of the equations for the total moment acting about the aircraft center of mass is complicated by the fact that the center of mass changes position due to the tilting nacelles. Thus the centers of gravity of the principal aircraft component masses of the wings (m_w), fuselage (including tails) (m_f), and nacelles (m_N), move with respect to the reference axes OXYZ placed at the instantaneous overall center of gravity of the aircraft. The equation of motion for such a mass element will first be obtained and the total moment found by adding the contributions of all the elements.

5.5 EQUATION OF MOTION FOR A MASS ELEMENT

With reference to Figure (5.1) $O'xyz$ is a right-handed set of axes placed at the center of gravity of the representative mass. The axes are parallel to the set OXYZ. The mass, m ,

rotates about its own center of gravity with angular velocity $\underline{\omega}$ which, in general, differs from $\underline{\Omega}$ the angular velocity of the aircraft. If \underline{r} is the radius vector from O to O' then the velocity of the center of mass of the element is

$$\underline{V} = \frac{\delta \underline{r}}{\delta t} + \underline{\Omega} \times \underline{r} \quad (5.10)$$

The angular momentum of this mass about O is

$$\underline{h} = m (\underline{r} \times \underline{V}) + \underline{h}_o \quad (5.11)$$

where \underline{h}_o is the angular momentum of m about its own center of mass and is given by

$$\underline{h}_o = \bar{I} \underline{\omega} \quad (5.12)$$

where

$$\bar{I} = \begin{bmatrix} I_{xx} & -I_{xy} & -I_{xz} \\ -I_{yx} & I_{yy} & -I_{yz} \\ -I_{zx} & -I_{zy} & I_{zz} \end{bmatrix} \quad (5.13)$$

and I_{xx} , etc., are the moments and products of inertia of the mass about O'xyz.

The total moment, \underline{G} , about the aircraft center of mass is given by

$$\underline{G} = \frac{d\underline{h}}{dt} = \frac{\delta \underline{h}}{\delta t} + \underline{\Omega} \times \underline{h} \quad (5.14)$$

Using equations (5.10), (5.11) and (5.12) in (5.14) the moment becomes

$$\begin{aligned} \underline{G} = m \left[\frac{\delta \underline{r}}{\delta t} \times \left(\frac{\delta \underline{r}}{\delta t} + \underline{\Omega} \times \underline{r} \right) + \underline{r} \times \frac{\delta}{\delta t} \left(\frac{\delta \underline{r}}{\delta t} + \underline{\Omega} \times \underline{r} \right) \right] + \frac{\delta}{\delta t} (\bar{I} \underline{\omega}) \\ + m \underline{\Omega} \times \left[\underline{r} \times \left(\frac{\delta \underline{r}}{\delta t} + \underline{\Omega} \times \underline{r} \right) \right] + \underline{\Omega} \times (\bar{I} \underline{\omega}) \end{aligned} \quad (5.15)$$

which reduces to

$$\underline{G} = 2m\underline{\Omega} \left(\underline{r} \cdot \frac{\delta \underline{r}}{\delta t} \right) + m \underline{r} \times \frac{\delta^2 \underline{r}}{\delta t^2} + m \frac{\delta \Omega}{\delta t} (\underline{r} \cdot \underline{r}) - m \underline{r} \left(\underline{r} \cdot \frac{\delta \Omega}{\delta t} \right) \quad (5.16)$$

$$- 2m \frac{\delta \underline{r}}{\delta t} (\underline{\Omega} \cdot \underline{r}) - m (\underline{r} \cdot \underline{\Omega}) (\underline{\Omega} \times \underline{r}) + I \frac{\delta \underline{\omega}}{\delta t} + \underline{\Omega} \times (\underline{I} \underline{\omega})$$

The only masses that possess angular velocities different from that of the aircraft are the nacelles, which are free to pitch about O' with angular rate $\dot{\hat{i}} = \frac{d\hat{i}_N}{dt}$. Thus $\underline{\omega}$ may be written generally as

$$\underline{\omega} = P \hat{i} + (Q + \dot{\hat{i}}_N) \hat{j} + R \hat{k} \quad (5.17)$$

Now, with $\underline{r} = X \hat{i} + Y \hat{j} + Z \hat{k}$, where X, Y, and Z are the instantaneous coordinates of the individual mass center relative to the aircraft mass center, the various terms of equation (5.16) are, in component form,

$$\underline{r} \cdot \frac{\delta \underline{r}}{\delta t} = \dot{X}X + \dot{Y}Y + \dot{Z}Z$$

$$\underline{r} \times \frac{\delta^2 \underline{r}}{\delta t^2} = (YZ - ZY) \hat{i} - (XZ - ZX) \hat{j} + (XY - YX) \hat{k}$$

$$\frac{\delta \Omega}{\delta t} (\underline{r} \cdot \underline{r}) = (X^2 + Y^2 + Z^2) (\dot{P} \hat{i} + \dot{Q} \hat{j} + \dot{R} \hat{k})$$

$$\underline{r} \cdot \frac{\delta \Omega}{\delta t} = X \dot{P} + Y \dot{Q} + Z \dot{R}$$

$$\underline{\Omega} \cdot \underline{r} = XP + YQ + ZR$$

$$(\underline{r} \cdot \underline{\Omega}) (\underline{\Omega} \times \underline{r}) = (XP + YQ + ZR) \left[(QZ - RY) \hat{i} - (PZ - RX) \hat{j} + (PY - XQ) \hat{k} \right]$$

$$\underline{I} \frac{\delta \underline{\omega}}{\delta t} = (I_{xx} \dot{P} - I_{xz} R) \hat{i} + I_{yy} (\dot{Q} + \dot{\hat{i}}_N) \hat{j} + (I_{zz} \dot{R} - I_{xz} \dot{P}) \hat{k}$$

$$\underline{\Omega} \times (\underline{I} \underline{\omega}) = (QR I_{zz} - QP I_{xz} - RQ I_{yy} - R \dot{\hat{i}}_N I_{yy}) \hat{i}$$

$$- (PR I_{zz} - P^2 I_{xz} - PR I_{xx} + R^2 I_{xz}) \hat{j}$$

$$+ (QR I_{xz} + PQ I_{yy} + P \dot{\hat{i}}_N I_{yy} - PQ I_{xx}) \hat{k}$$

where, in the last two terms, the products of inertia I_{xy} and I_{yz} are zero from symmetry considerations.

Substituting the above relations into equation (5.16) and noting that \dot{Y} and \ddot{Y} are always zero (no lateral motion of the individual masses) the following expressions are obtained for the components of the moment $\underline{G} = \Delta L \hat{i} + \Delta M \hat{j} + \Delta N \hat{k}$:

$$\begin{aligned} \Delta L = & \dot{P} [I_{XX} + m(Y^2 + Z^2)] - (\dot{R} + PQ) [I_{XZ} + mXZ] \\ & + RQ [I_{ZZ} - I_{YY} + m(Y^2 - Z^2)] + mYZ(R^2 - Q^2) - I_{YY} R \dot{i}_N \\ & + m(Y\ddot{Z} - 2\dot{X}YR - 2\dot{X}ZR + 2Z\dot{Z}P - XY(\dot{Q} - PR)) \\ \Delta M = & \dot{Q} [I_{YY} + m(X^2 + Z^2)] - (R^2 - P^2) [I_{XZ} + mXZ] \\ & + PR [I_{XX} - I_{ZZ} + m(Z^2 - X^2)] + I_{YY} \dot{i}_N \end{aligned} \quad (5.19)$$

$$\begin{aligned} & + m[\ddot{X}Z - X\ddot{Z} + 2Q(Z\dot{Z} + X\dot{X}) - XY(\dot{P} + RQ) + YZ(PQ - \dot{R})] \\ \Delta N = & \dot{R} [I_{ZZ} + m(X^2 + Y^2)] - (\dot{P} - RQ) [I_{XZ} + mXZ] \end{aligned} \quad (5.20)$$

$$\begin{aligned} & + PQ [I_{YY} - I_{XX} + m(X^2 - Y^2)] + I_{YY} P \dot{i}_N \\ & + m[2X\dot{X}R - Y\ddot{X} - 2XZP - 2Y\dot{Z}Q - YZ(\dot{Q} + PR) + XY(Q^2 - P^2)] \end{aligned}$$

Summing the rolling moment equation:

$$\begin{aligned} L = & I_{XX} \dot{P} - I_{XZ} (\dot{R} + PQ) + (I_{ZZ} - I_{YY}) RQ \quad (5.21) \\ & + m_N (R^2 - Q^2) (Z_{NR} - Z_{NL}) Y_N + m_N \left\{ Y_N (\ddot{Z}_{NR} - \ddot{Z}_{NL}) \right. \\ & - 2Q (\dot{X}_{NR} - \dot{X}_{NL}) Y_N - 2R (\dot{X}_{NR} Z_{NR} + \dot{X}_{NL} Z_{NL}) + 2P (\dot{Z}_{NR} Z_{NR} + \\ & \left. \dot{Z}_{NL} Z_{NL}) - (\dot{Q} - PR) (X_{NR} - X_{NL}) Y_N \right\} + 2m_f Z_f (P\dot{Z}_f - \\ & R\dot{X}_f) + 2m_w Z_w (P\dot{Z}_w - R\dot{X}_w) - R I_{YY}^N (\dot{i}_{NL} + \dot{i}_{NR}) \end{aligned}$$

where I_{XX} , I_{XZ} , I_{ZZ} and I_{YY} are the inertias of the aircraft about its center of gravity, and the subscripts f, w, NL and NR stand for fuselage, wing, left nacelle and right nacelle. The remaining symbols are defined in the List of Symbols. Similar expressions are obtained for the pitching moment and yawing

moment. In the interests of brevity the remainder of the discussion will be limited to equation (5.21).

Evaluation of the terms of the rolling moment equation indicate that this equation may be simplified considerably without a significant change in accuracy. For example, terms containing $(\dot{X}_{NR} - \dot{X}_{NL})$ may be dropped because \dot{X}_{NR} is normally identical to \dot{X}_{NL} , i.e. the nacelles are raised or lowered together at the same rate. Equation (5.21) may thus be written

$$L = I_{XX} \dot{P} - I_{XZ} (\dot{R} + P\dot{Q}) + (I_{ZZ} - I_{YY}) R\dot{Q} + m_N Y_N (\ddot{X}_{NR} - \ddot{Z}_{NL}) \quad (5.22)$$

where the last term has been retained in consideration of the high differential nacelle accelerations encountered during hover maneuvers.

From the relationships presented in Appendix C the last term of equation (5.22) may be rewritten as

$$-2m_N Y_N [\ddot{i}_{NR} \cos (i_{NR} - \lambda) + i_{NL}^2 \sin (i_{NL} - \lambda) - i_{NR}^2 \sin (i_{NR} - \lambda) - \ddot{i}_{NL} \cos (i_{NL} - \lambda)] \quad (5.23)$$

which may be approximated to

$$-2m_N Y_N [\ddot{i}_{NR} \cos (i_{NR} - \lambda) - \ddot{i}_{NL} \cos (i_{NL} - \lambda)] \quad (5.24)$$

since the nacelle rates appear as squared terms.

Similar treatment of the pitching moment and yawing moment equations results in the following final form of the moment equations.

$$\begin{aligned}
L_{AERO} &= I_{XX} \dot{P} - I_{XZ} (\dot{R} + PQ) + (I_{ZZ} - I_{YY}) RQ \\
&\quad - \ell m_N Y_N [\ddot{i}_{NR} \cos(i_{NR} - \lambda) - \ddot{i}_{NL} \cos(i_{NL} - \lambda)] \\
M_{AERO} &= I_{YY} \dot{Q} - I_{XZ} (R^2 - P^2) + (I_{XX} - I_{ZZ}) PR \\
&\quad + \ddot{i}_{NR} \left\{ I_{YY_O}^N + \ell m_N [X_R \cos(i_{NR} - \lambda) - Z_R \sin(i_{NR} - \lambda)] \right\} \\
&\quad + \ddot{i}_{NL} \left\{ I_{YY_O}^N + \ell m_N [X_L \cos(i_{NL} - \lambda) - Z_L \sin(i_{NL} - \lambda)] \right\} \\
N_{AERO} &= I_{ZZ} \dot{R} - I_{XZ} (\dot{P} - RQ) + (I_{YY} - I_{XX}) PQ \\
&\quad + \ell m_N Y_N [\ddot{i}_{NR} \sin(i_{NR} - \lambda) - \ddot{i}_{NL} \sin(i_{NL} - \lambda)]
\end{aligned} \tag{5.25}$$

where the moments L_{AERO} , M_{AERO} and N_{AERO} represent the sum of the aerodynamic moments and rotor/engine gyroscopic moments about the aircraft center of mass. $I_{YY_O}^N$ is the nacelle pitch inertia referred to the nacelle-fixed axes system described in Appendix C. Equations for the aircraft inertias are also presented in that Appendix.

5.6 EQUATIONS OF MOTION FOR NACELLES

The equation of motion for a nacelle is required in order to obtain the moment exerted by the nacelle on the wing tip at the pivot. This moment is then used in the equations for wing twist.

The angular momentum of a nacelle about its pivot point is given by

$$\begin{aligned}
\underline{h}_p &= (\underline{r} - \underline{r}_p) \times m_N \underline{V} + \underline{h}_{O_N} \\
&= m_n (\underline{r} \times \underline{V}) + \underline{h}_O - m_n \underline{r}_p \times \underline{V}
\end{aligned} \tag{5.26}$$

where \underline{r} is the radius vector from aircraft c.g. to nacelle c.g.
 \underline{V} is the velocity of the nacelle c.g.

\underline{h}_{O_N} is the angular momentum of the nacelle about its own c.g.

m_N is the nacelle mass

and \underline{r}_p is the radius vector from aircraft c.g. to nacelle pivot

The term $m_n (\underline{r} \times \underline{V}) + \underline{h}_{O_N}$ is the angular momentum of the nacelle about the aircraft c.g. ($= \underline{h}_{CG}^N$)

$$\text{i.e. } \underline{h}_p = \underline{h}_{CG}^N - m_N (\underline{r}_p \times \underline{V})$$

The moment about the pivot is

$$G_p = \frac{d\underline{h}_p}{dt} = \frac{d\underline{h}_N}{dt} - m_n \frac{d}{dt} (\underline{r}_p \times \underline{V}) = \underline{G}_{CG}^N - \underline{\Delta G} \quad (5.27)$$

Since the quantity \underline{G}_{CG}^N has already been obtained (equations (5.18), (5.19) and (5.20)), only the remaining term needs to be evaluated.

$$\begin{aligned} \underline{\Delta G} &= m_N \frac{d}{dt} (\underline{r}_p \times \underline{V}) = m_N \left\{ \frac{\delta \underline{r}_p}{\delta t} \times \underline{V} + \underline{r}_p \times \frac{\delta \underline{V}}{\delta t} + \underline{\Omega} (\underline{r}_p \times \underline{V}) \right\} \\ &= m_N \left\{ \frac{\delta \underline{r}_p}{\delta t} \times \left(\frac{\delta \underline{r}}{\delta t} + \underline{\Omega} \times \underline{r} \right) + \underline{r}_p \times \frac{\delta}{\delta t} \left(\frac{\delta \underline{r}}{\delta t} + \underline{\Omega} \times \underline{r} \right) \right. \\ &\quad \left. + \underline{\Omega} \times \left[\underline{r}_p \times \left(\frac{\delta \underline{r}}{\delta t} + \underline{\Omega} \times \underline{r} \right) \right] \right\} \quad (5.28) \end{aligned}$$

Expansion of these terms results in the following expression

$$\begin{aligned} \underline{\Delta G} &= m_N \left\{ \frac{\delta \underline{r}_p}{\delta t} \times \frac{\delta \underline{r}}{\delta t} + \underline{\Omega} \left(\underline{r} \cdot \frac{\delta \underline{r}_p}{\delta t} \right) - \underline{r} \left(\frac{\delta \underline{r}_p}{\delta t} \cdot \underline{\Omega} \right) + \underline{r}_p \times \frac{\delta^2 \underline{r}}{\delta t^2} + \frac{\delta \underline{\Omega}}{\delta t} (\underline{r} \cdot \underline{r}_p) \right. \\ &\quad - \underline{r} \left(\underline{r}_p \cdot \frac{\delta \underline{\Omega}}{\delta t} \right) + \underline{\Omega} \left(\frac{\delta \underline{r}}{\delta t} \cdot \underline{r}_p \right) - 2 \frac{\delta \underline{r}}{\delta t} (\underline{r}_p \cdot \underline{\Omega}) \\ &\quad \left. + \underline{r}_p \left(\frac{\delta \underline{r}}{\delta t} \cdot \underline{\Omega} \right) - (\underline{r}_p \cdot \underline{\Omega}) (\underline{\Omega} \times \underline{r}) \right\} \end{aligned}$$

We require only the \hat{j} component of this vector in order to obtain the nacelle pivot pitching moment.

The components of the vectors \underline{r}_p , \underline{r} and $\underline{\Omega}$ are

$$\underline{r}_p = x_p \hat{i} + y_N \hat{j} + z_p \hat{k} = -x_{CG} \hat{i} + y_N \hat{j} - z_{CG} \hat{k}$$

$$\underline{r} = x_N \hat{i} + y_N \hat{j} + z_N \hat{k}$$

$$\underline{\Omega} = P \hat{i} + Q \hat{j} + R \hat{k}$$

Noting that the \hat{j} components of $\frac{\delta \underline{r}_p}{\delta t}$, $\frac{\delta \underline{r}}{\delta t}$ are zero (since y_N is a constant), the above expression yields

$$\Delta M = m_N \left\{ \ddot{x}_N z_{CG} - \ddot{z}_N x_{CG} + \dot{z}_{CG} \dot{x}_N + \dot{z}_N \dot{x}_{CG} + PQ y_N z_N - RQ x_N y_N \right\} \quad (5.30)$$

Combining this equation with Equation (5.19) and using the transformations given in Appendix C, the final equation for the right-hand nacelle pivot actuator pitching moment becomes, after some simplification,

$$\begin{aligned} M_{NR} = & -I_{NR} \left[I_{YY_0}^N + \ell^2 m_N \left(1 - \frac{m_N}{m} \right) - \ell^2 m_N \left(1 - \frac{m_N}{m} \right) \left[\dot{Q} - PR \cos 2(i_{NR} - \lambda) \right. \right. \\ & \left. \left. + (R^2 - P^2) \sin(i_{NR} - \lambda) \cos(i_{NR} - \lambda) \right] - (R^2 - P^2) I_{zz_0}^N \sin i_{NR} \cos i_{NR} \right. \\ & \left. - I_{YY_0} \dot{Q} + \ell \frac{m_N}{m} \left[X_{AERO} \sin(i_{NR} - \lambda) + Z_{AERO} \cos(i_{NR} - \lambda) \right] \right. \\ & \left. - \ell m_N y_N \left\{ (\dot{R} - PQ) \sin(i_{NR} - \lambda) - (\dot{P} + RQ) \cos(i_{NR} - \lambda) \right\} \right] \\ & + M_{NRAERO} \end{aligned} \quad (5.31)$$

where M_{NRAERO} includes the moment resulting from nacelle aerodynamic loads and the rotor gyroscopic moments. The terms X_{AERO} and Z_{AERO} are, respectively, the total aircraft aerodynamic X and Z forces.

The corresponding equation for the left nacelle actuator moment is obtained by substituting $-y_N = y_N$ and changing the R subscript to L.

5.7 DETERMINATION OF ROTOR GYROSCOPIC MOMENTS

The gyroscopic moments are most readily obtained as follows. A set of axes $O''x'y'z'$ is taken at the rotor hub (rotor c.g.) parallel to the nacelle-fixed set of axes $Ox_0y_0z_0$. Associated with each axis are the corresponding unit vectors \hat{i}' , \hat{j}' and \hat{k}' . The angular velocity of the rotor with respect to these axes is the vector

$$\underline{\omega} = \Omega_R \hat{i}' \quad (5.32)$$

where Ω_R is the rotor rotational speed.

The angular momentum of the rotor with respect to its c.g. is

$$\underline{h}_O = \bar{I}_R \underline{\omega} \quad (5.33)$$

where \bar{I}_R is the inertia matrix

$$\begin{bmatrix} I_{R_x'} & & \\ & I_{R_y'} & \\ & & I_{R_z'} \end{bmatrix}$$

the off-diagonal terms being zero since the axes $O''x'y'z'$ are principal axes of inertia of the rotor and hub.

In component form the angular momentum of the rotor is

$$\underline{h}_O = I_{R_y'} \Omega_R \hat{i}' = I_R \Omega_R \hat{i}' \quad (5.34)$$

With respect to the inertial axes OXYZ, the components of \underline{h}_O are

$$\underline{h}_O = I_R \Omega_R \cos i_{N\hat{i}} - I_R \Omega_R \sin i_{N\hat{k}} \quad (5.35)$$

The hub moment is therefore given by

$$\underline{G}_{HUB} = \frac{d\underline{h}_O}{dt} = \frac{\delta \underline{h}_O}{\delta t} + \underline{\Omega} \times \underline{h}_O \quad (5.36)$$

$$\text{where } \underline{\Omega} = P \hat{i} + Q \hat{j} + R \hat{k} \quad (5.37)$$

Substitution of equations (5.35) and (5.37) into equation (5.36) results in the following equations for the rotor gyroscopic moments.

$$L_{\text{gyro}} = I_R \dot{\Omega}_R \cos i_N - I_R \Omega_R (\dot{i}_N + Q) \sin i_N \quad (5.38)$$

$$M_{\text{gyro}} = I_R P \Omega_R \sin i_N + I_R R \Omega_R \cos i_N \quad (5.39)$$

$$N_{\text{gyro}} = -I_R \dot{\Omega}_R \sin i_N - I_R \Omega_R (\dot{i}_N + Q) \cos i_N \quad (5.40)$$

The above terms appear in the Computer Representation (Appendix E) as additions to the rotor aerodynamic forces and moments.

6.0 AIRFRAME AERODYNAMICS

This section presents the mathematical equations and representations of the aerodynamic data for the aircraft without rotors. The contribution of the rotors is described in Section 7. The overall airframe aerodynamics are obtained from the following components:

- (a) Fuselage
- (b) Wings
- (c) Horizontal Tail
- (d) Vertical Tail
- (e) Nacelles

The data and equations for each of the aerodynamic components are discussed below, together with the substantiating methods. The aerodynamic data are presented in local wind axes. Resolution to aircraft body axes is accomplished as described in the mathematical model (Appendix E). Where required, the equations have been written so as to be applicable over the entire range of angle of attack ± 180 degrees.

6.1 FUSELAGE

The aerodynamic lift, drag and pitching moment coefficients of the fuselage were estimated using the methods of Reference 1. The forces and moments are referred to the point on the fuselage corresponding to the wing quarter chord position. This reference point was selected in order to minimize the number of force and moment transfer equations in the mathematical

model. Wing-to-body carryover effects have been included in fuselage loads.

The equations for the fuselage forces and moments are:

$$\text{Lift:} \quad C_{LF} = K_{42} + K_3 \text{Sin}\alpha_F \text{Cos}\alpha_F + K_4 \text{Sin}\alpha_F \text{Cos}\alpha_F | \text{Sin}\alpha_F \text{Cos}\alpha_F |$$

$$\text{Drag:} \quad C_{DF} = C_{DOF} (1 + K_O |\beta_F|^3) + K_2 (\text{Sin}\alpha_F \text{Cos}\alpha_F)^2 + K_1 | \text{Sin}\alpha_F \text{Cos}\alpha_F | + \Delta C_{D_{LG}}$$

$$\text{Side Force:} \quad C_{YF} = K_7 \text{Sin}\beta_F \text{Cos}\beta_F + K_8 \text{Sin}\beta_F \text{Cos}\beta_F | \text{Sin}\beta_F \text{Cos}\beta_F |$$

$$\text{Pitching Moment:} \quad C_{MF} = C_{MOF} + K_5 \text{Sin}\alpha_F \text{Cos}\alpha_F + K_6 \text{Sin}\alpha_F \text{Cos}\alpha_F | \text{Sin}\alpha_F \text{Cos}\alpha_F | + \Delta C_{M_{LG}}$$

$$\text{Yawing Moment:} \quad C_{NF} = C_{NOF} + K_9 \text{Sin}\beta_F \text{Cos}\beta_F + K_{10} \text{Sin}\beta_F \text{Cos}\beta_F | \text{Sin}\beta_F \text{Cos}\beta_F |$$

$$\text{Rolling Moment:} \quad C_{RF} = 0$$

$$\text{where } \alpha_F = \text{Tan}^{-1} \left(\frac{W}{U} \right), \quad C_{LF} = \frac{L_F}{\frac{1}{2} \rho V_{FUS}^2 S_W} \quad \text{etc.}$$

$$\beta_F = \text{Tan}^{-1} \left[\frac{V}{\sqrt{U^2 + W^2}} \right], \quad C_{MF} = \frac{M_F}{\frac{1}{2} \rho V_{FUS}^2 S_W C_W} \quad \text{etc.}$$

and $\Delta C_{D_{LG}}$, $\Delta C_{M_{LG}}$, are the landing gear contributions to fuselage drag and pitching moment coefficients, when the landing gear is extended.

The fuselage forces and moments are then resolved into body axes at the aircraft C.G.

6.2 NACELLES

The forces and moments acting on the nacelles were estimated using the cross-flow methods of Reference 12. For convenience the resulting forces and moments are referred to the rotor hub, so that they may be added directly to the rotor forces and moments. The following equations are for the forces and moments on two nacelles:

$$C_{L_N} = K_{32} \sin \alpha_N \cos \alpha_N$$

$$C_{D_N} = C_{D_{O_N}} + K_{30} |\alpha_N| + K_{31} \alpha_N^2$$

$$C_{M_N} = C_{M_{O_N}} + K_{34} \sin \alpha_N \cos \alpha_N + K_{35} \sin \alpha_N \cos \alpha_N |\sin \alpha_N \cos \alpha_N|$$

$$C_{Y_N} = K_{36} \sin \beta_N \cos \beta_N + K_{37} \sin \beta_N \cos \beta_N |\sin \beta_N \cos \beta_N|$$

$$C_{N_N} = C_{N_{O_N}} + K_{38} \sin \beta_N \cos \beta_N + K_{39} \sin \beta_N \cos \beta_N |\sin \beta_N \cos \beta_N|$$

$$C_{X_N} = 0$$

The nacelle forces and moments in nacelle axes are:

$$\Delta X'_N = q_N S_W [-C_{D_N} \cos \alpha_N + C_{L_N} \sin \alpha_N - C_{Y_N} \sin \beta_N \cos \alpha_N]^{1/2}$$

$$\Delta Y'_N = q_N S_W [C_{Y_N} \cos \beta_N - C_{D_N} \sin \beta_N]^{1/2}$$

$$\Delta Z'_N = q_N S_W [-C_{L_N} \cos \alpha_N - C_{D_N} \cos \beta_N \sin \alpha_N - C_{Y_N} \sin \beta_N \sin \alpha_N]^{1/2}$$

$$\Delta X''_N = q_N S_W b_W \left[-\left(\frac{C_W}{b_W}\right) C_{M_N} \sin \beta_N \cos \alpha_N - C_{N_N} \sin \alpha_N \right]^{1/2}$$

$$\Delta M'_N = q_N S_W C_W [C_{M_N} \cos \beta_N]^{1/2}$$

$$\Delta N'_N = q_N S_W b_W [C_{N_N} \cos \alpha_N - \left(\frac{C_W}{b_W}\right) C_{M_N} \sin \beta_N \cos \alpha_N]^{1/2}$$

6.3 HORIZONTAL TAIL

Aerodynamics of the horizontal tail were obtained using the methods of Reference 1 in combination with test data. The horizontal tail includes a plain elevator.

The angle of attack of the horizontal tail, including interference effects, for zero elevator deflection, is

$$\alpha_{HT} = \tan^{-1} \left[\frac{w_{HT}}{u_{HT}} \right] - \epsilon + i_{HT}$$

where ϵ is the total downwash at the tail due to wing, rotor and ground effects and i_{HT} is the tail incidence angle.

The effect of elevator deflection on the effective tail angle of attack is introduced through the elevator effectiveness parameter, τ_{HT} , which is a function of the elevator and horizontal tail areas. Thus the effective horizontal tail angle of attack is

$$\alpha_{e_{HT}} = \alpha_{HT} + \tau_{HT} \delta_e$$

where δ_e is the elevator deflection.

The tail downwash angle, ϵ , depends on wing angle of attack and on rotor slipstream deflection. At a given rotor angle of attack, the slipstream deflection is a function of rotor thrust coefficient, C_{TS} , where the coefficient is based on the slipstream dynamic pressure. Figure 6.1 presents data on downwash angles measured during tests on a tilt rotor wind tunnel model (Reference 7). As can be seen, the downwash at low values of thrust coefficient is the same as the value of the power-off wing

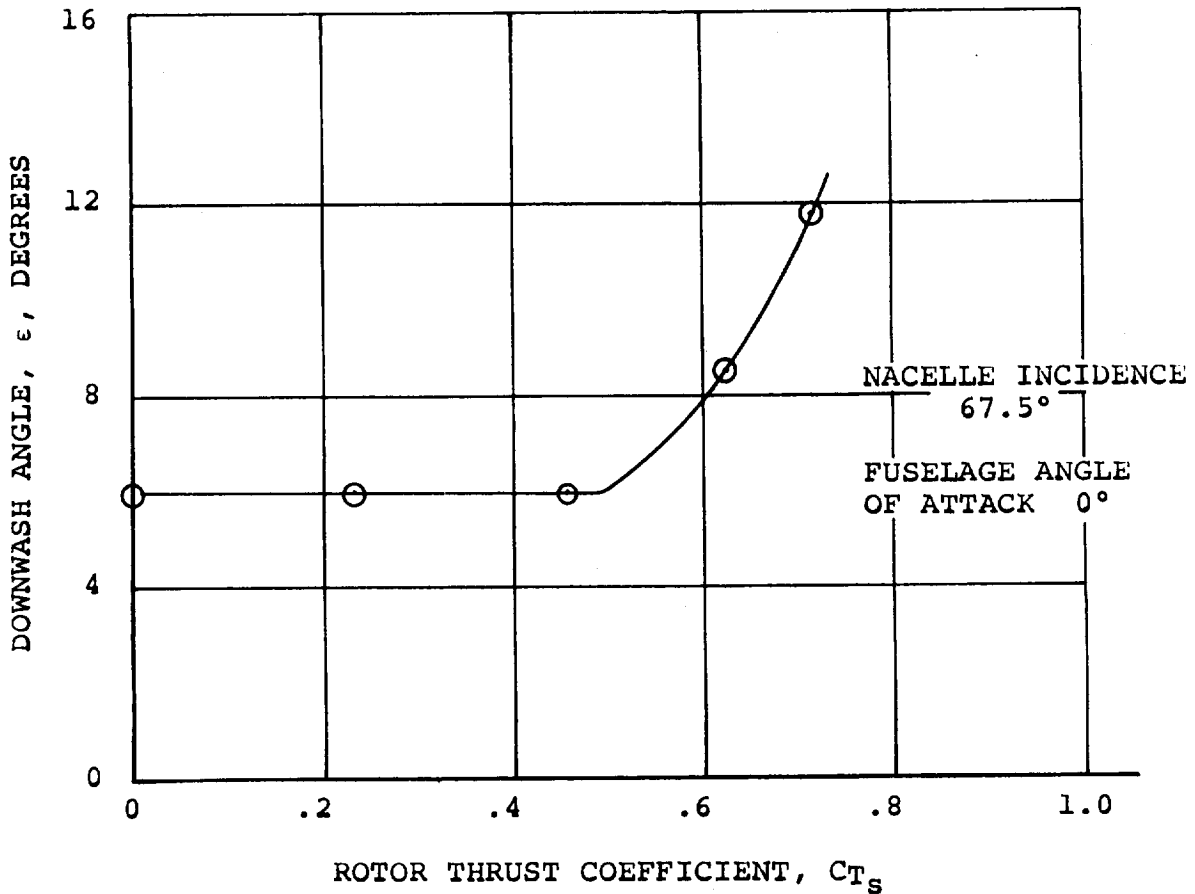


Figure 6.1. Variation of Horizontal Tail Downwash Angle with Thrust Coefficient

downwash ($C_{TS}=0$). Above values of C_{TS} in the neighborhood of $C_{TS}=0.5$ the downwash increases with increasing thrust coefficient. The values in the increasing portion of ϵ vs C_{TS} were found to correspond approximately to the slipstream deflection angle ϵ_p . Therefore, the approach adopted in the mathematical

model was to test if the rotor slipstream downwash ($\bar{\epsilon}_p$) exceeded the wing downwash and, if so, to use the computed slipstream downwash value as the tail downwash angle. Otherwise the wing downwash value was used.

Thus if

$$\bar{\epsilon}_p \geq \epsilon_0 + \frac{d\epsilon}{d\alpha} (\bar{\alpha}_w - l_{AC} \frac{\dot{W}}{U^2})$$

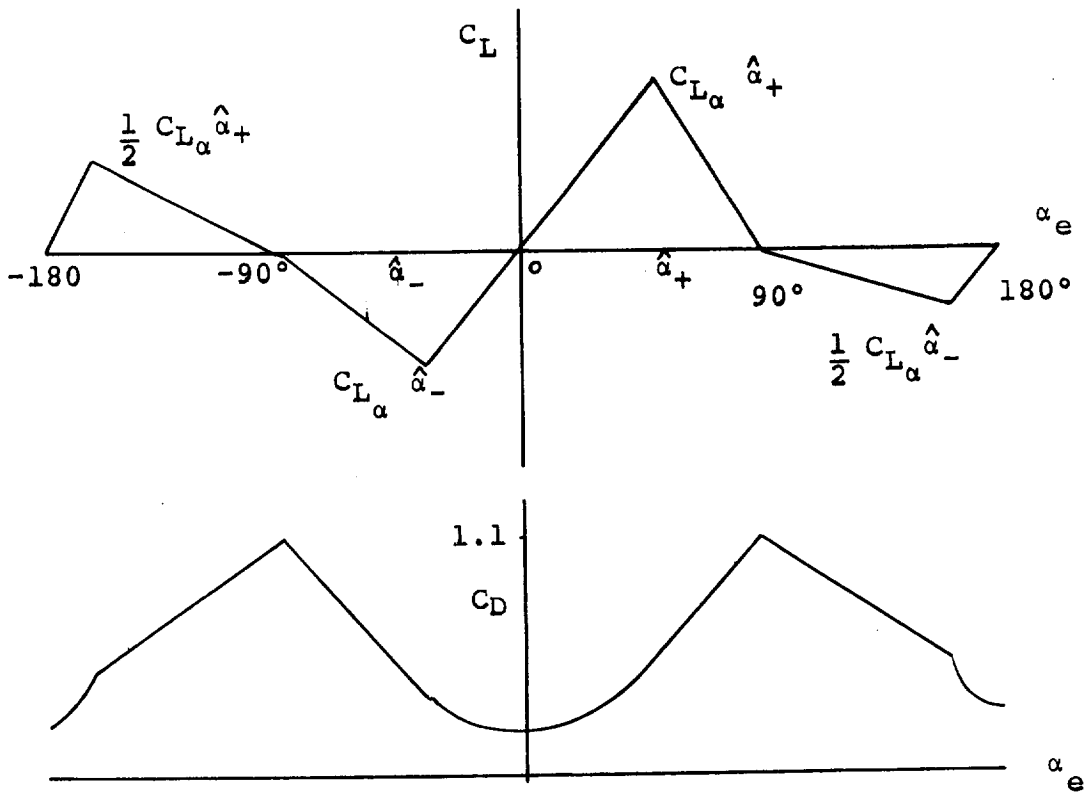
$$\text{then } \epsilon = \frac{\bar{\epsilon}_p (1-GEF)}{\sqrt{1-M^2}}$$

otherwise

$$\epsilon = \left[\epsilon_0 + \frac{d\epsilon}{d\alpha} (\bar{\alpha}_w - l_{AC} \frac{\dot{W}}{U^2}) \right] \frac{(1-GEF)}{\sqrt{1-M^2}}$$

In these expressions ϵ_0 is the wing downwash angle at zero wing angle-of-attack, $\frac{d\epsilon}{d\alpha}$ is the downwash derivative, l_{AC} is the distance from the wing to the tail aerodynamic centers, and $l_{AC} \frac{\dot{W}}{U^2}$ is the familiar downwash lag term. In general, the quantities ϵ_0 and $\frac{d\epsilon}{d\alpha}$ depend on the average of the left and right flaperon deflections. The effect of differential deflection of aileron/spoiler in producing an asymmetrical downwash field at the horizontal tail was not included because of the small contribution this makes to total aircraft rolling moment. The term (1-GEF) in the above equations is the ground effect factor. This quantity was obtained from Reference 10 and is a function of the wing span and height of the horizontal tail above the ground. This factor, when multiplied by the downwash which would be found out of ground effect, yields the downwash in ground effect. Ground effect is discussed in more detail in Section 10.

The lift and drag forces acting on the horizontal tail are required over the complete range of angle of attack -180° to $+180^\circ$, since the tilt rotor can fly backwards. The following sketch shows the schematic variation of lift and drag coefficients over this range plotted as a function of the effective horizontal tail angle of attack, α_{eHT} .



The angle of attack for C_{LHTMAX} is denoted by $\hat{\alpha}_{HT+}$ and is the value of the effective angle of attack at the stall less 2 degrees i.e.

$$\hat{\alpha}_{HT+} = (\alpha_{HTSTALL} - 2^\circ) + \tau_{HT} \delta_e$$

Similarly the angle of attack for stall at negative angles of attack is

$$\hat{\alpha}_{HT-} = -(\alpha_{HTSTALL} - 2^\circ) + \tau_{HT} \delta_e$$

The slope of the lift curve within this range of positive and negative angles of attack is given by

$$C_{L_\alpha} = \frac{C_{L_{\alpha HT}} \left(\frac{a_g}{a} \right)}{\sqrt{1-M^2}}$$

where a_g/a is the ratio of tail lift-curve slopes in and out of ground effect, and $\sqrt{1-M^2}$ is the Prandtl-Glauert correction factor for the effect of Mach number on lift-curve slope.

Within this region on the lift curve the value of lift coefficient is given by $C_{L_{HT}} = C_{L_\alpha} \alpha_{eHT}$ and the corresponding drag coefficient by

$$C_{D_{HT}} = C_{D_{OHT}} + \frac{2C_{L_{HT}}^2}{\pi AR_{HT}}$$

After stall angle of attack is passed the lift is assumed to fall linearly to zero at $\alpha_e = \pm 90^\circ$.

In these regions the lift is given by

$$C_{L_\alpha} = C_{L_\alpha} \frac{\hat{\alpha}_\pm \frac{(+90 - \alpha_{eHT})}{(+90 - \hat{\alpha}_{HT\pm})}}$$

where the appropriate signs are taken depending on the sign of α_{eHT} .

The corresponding drag is obtained by assuming a linear variation of drag from the value at $C_{L_{MAX}}$ to a value of $C_D = 1.1$ (flat plate normal to stream) at $\alpha_{eHT} = 90^\circ$. Thus

$$C_{L_{HT\text{STALL}}} = C_{L_{\alpha}} \hat{\alpha}_{HT+}$$

$$C_{D_{HT\text{STALL}}} = C_{D_{OHT}} + \frac{2C_{L_{HT\text{STALL}}}^2}{\pi AR_{HT}}$$

and

$$C_{D_{HT}} = C_{D_{HT\text{STALL}}} + \frac{(\alpha_{e_{HT}} - \hat{\alpha}_{HT+})(1.1 - C_{D_{HT\text{STALL}}})}{(+90 - \hat{\alpha}_{HT+})}$$

If the effective angle of attack of the horizontal tail exceeds $+90^\circ$ the tail will point trailing-edge first into the relative wind. Under this condition early stalling is precipitated because of the sharp "leading edge" and blunt "trailing edge". In order to represent this, it was assumed that the attainable $C_{L_{MAX}}$ of the tail under these conditions is half that occurring in normal flight.

$$\text{Thus if } 90^\circ < \alpha_{e_{HT}} \leq (180 - \frac{1}{2} \hat{\alpha}_{HT-})$$

$$\text{or } (-180 + \frac{1}{2} \hat{\alpha}_{HT+}) \leq \alpha_{e_{HT}} < -90^\circ$$

then

$$C_{L_{HT}} = .5C_{L_{\alpha}} \hat{\alpha}_{HT-} \frac{(\alpha_{e_{HT}} - 90^\circ)}{(90^\circ - \frac{1}{2} \hat{\alpha}_{HT-})}$$

$$\text{or } C_{L_{HT}} = .5C_{L_{\alpha}} \hat{\alpha}_{HT+} \frac{(\alpha_{e_{HT}} + 90^\circ)}{(-90 + \frac{1}{2} \hat{\alpha}_{HT+})}$$

The corresponding drag coefficients are:

$$\text{for } 90^\circ < \alpha_{e_{HT}} \leq (180 - \frac{1}{2} \hat{\alpha}_{HT-});$$

$$C_{L_{HT\text{STALL}}} = 0.5 C_{L_{\alpha}} \hat{\alpha}_{HT-}$$

$$C_{D_{HT\text{STALL}}} = \frac{2C_{L_{HT\text{STALL}}}^2}{\pi AR_{HT}} + C_{D_{OHT}}$$

which gives $C_{DHT} = C_{DHTSTALL} + \frac{(\alpha_{eHT} + 0.5 \hat{\alpha}_{HT-} - 180^\circ)(1.1 - C_{DHTSTALL})}{(0.5 \hat{\alpha}_{HT-} - 90^\circ)}$

and for $(-180 + \frac{1}{2} \hat{\alpha}_{HT+}) \leq \alpha_{eHT} < -90^\circ$;

$$C_{LHTSTALL} = 0.5 C_{L\alpha} \hat{\alpha}_{HT+}$$

$$C_{DHTSTALL} = \frac{2C_{LHTSTALL}^2}{\pi AR_{HT}} + C_{D_{OHT}}$$

which gives $C_{DHT} = C_{DHTSTALL} - \frac{(\alpha_{eHT} + 180^\circ - .5\hat{\alpha}_{HT+})(1.1 - C_{DHTSTALL})}{(.5\hat{\alpha}_{HT+} - 90^\circ)}$

In the range $(180 - .5\hat{\alpha}_{HT-}) \leq \alpha_{eHT} \leq 180^\circ$ when the tail has unstalled

$$C_{LHT} = C_{L\alpha} (\alpha_{eHT} - 180^\circ)$$

$$C_{DHT} = C_{D_{OHT}} + \frac{2C_{LHT}^2}{\pi AR_{HT}}$$

and similarly for the range $-180^\circ \leq \alpha_{eHT} < (-180 + .5 \hat{\alpha}_{HT+})$

$$C_{LHT} = C_{L\alpha} (\alpha_{eHT} + 180^\circ)$$

$$C_{DHT} = C_{D_{OHT}} + \frac{2C_{LHT}^2}{\pi AR_{HT}}$$

The above equations define the variation of tail lift and drag over the entire range of angle of attack. The tail pitching moment is not computed since it makes only a small contribution to the total aircraft pitching moment.

6.4 VERTICAL TAIL

The aerodynamic forces and moments acting on the vertical tail were estimated using the methods of Reference 1. The angle of attack of the vertical tail is given by

$$\alpha_{VT} = - \tan^{-1} \left[\frac{v_{VT}}{\sqrt{u_{VT}^2 + w_{VT}^2}} \right] + \beta_F \left(\frac{d\sigma}{d\beta} \right)$$

where u_{VT} , v_{VT} and w_{VT} are the components of velocity at the vertical tail aerodynamic center as given in Appendix C. The term $\beta_F \left(\frac{d\sigma}{d\beta} \right)$ is the sidewash correction for the presence of the fuselage.

As in the treatment of the horizontal tail, the effect of rudder deflection is obtained using a rudder effectiveness parameter τ_{VT} . Thus the effective angle of attack of the vertical tail when the rudder is deflected is

$$\alpha_{eVT} = \alpha_{VT} + \tau_{VT} \delta_{RUD}$$

The treatment of the vertical tail aerodynamics through the complete angle of attack range -180° to $+180^\circ$ then follows the same lines as that for the horizontal tail aerodynamics previously described.

The vertical tail forces and moments in body axes are then obtained from:

$$\begin{aligned} X_{AERO}^{VT} &= \bar{q} S_{VT} n_{VT} \left[-C_{D_{VT}} \cos(\beta_{VT} - \sigma) \cos(\alpha_{HT} - i_{HT}) \right. \\ &\quad \left. - C_{Y_{VT}} \sin(\beta_{VT} - \sigma) \cos(\alpha_{HT} - i_{HT}) \right] \\ Y_{AERO}^{VT} &= \bar{q} S_{VT} n_{VT} \left[C_{Y_{VT}} \cos(\beta_{VT} - \sigma) - C_{D_{VT}} \sin(\beta_{VT} - \sigma) \right] \\ Z_{AERO}^{VT} &= \bar{q} S_{VT} n_{VT} \left[-C_{D_{VT}} \cos(\beta_{VT} - \sigma) \sin(\alpha_{HT} - i_{HT}) - C_{Y_{VT}} \sin(\beta_{VT} - \sigma) \right. \\ &\quad \left. \sin(\alpha_{HT} - i_{HT}) \right] \end{aligned}$$

$$M_{AERO}^{VT} = Z_{AERO}^{VT} (X_{CG} - X_{VT}) + X_{AERO}^{VT} (Z_{VT} - Z_{CG})$$

$$N_{AERO}^{VT} = -Y_{AERO}^{VT} (X_{CG} - X_{VT})$$

$$L_{AERO}^{VT} = -Y_{AERO}^{VT} (Z_{VT} - Z_{CG})$$

6.5 WING AERODYNAMICS

The treatment of the wing aerodynamics is the most complex of all the components. Because wing flexibility must be represented, each wing panel required a separate treatment. The approach adopted for simulation purposes was first to obtain the aerodynamic forces and moments on the complete wing considered as rigid and uninfluenced by slipstream interference effects. With this data as a basis the effects of elastic deflection were introduced as an increment in the effective angle of attack of each wing panel and the rotor slipstream interference was then calculated. This approach is described in detail below.

6.5.1 BASIC WING AERODYNAMICS

The basic wing lift, drag and pitching moment coefficients for the wing in the presence of the fuselage rotors-off, were calculated using the methods of Reference 1. This data is applicable to low speed flight. Corrections for Mach number effects are introduced through the Prandtl-Glauert factor $\sqrt{1-M^2}$. Beyond stall angle of attack, the lift, drag and pitching moment curves are extended linearly to $\pm 90^\circ$

angle of attack in order to provide a representation of wing behavior at low transition speeds when wing angles of attack approach 90° . The data was calculated for the complete range of flaperon settings.

The complete wing basic lift, drag and pitching moment data also applies to each individual wing panel provided the data is obtained at the appropriate panel angle of attack. This approximation is acceptable if the angles of attack of each wing panel are not substantially different. This condition is normally fulfilled.

In addition to the above data, the effects of spoiler deflection on panel lift, drag and pitching moment are required. These were estimated using the data of Reference 1. As can be seen from the equations presented in Appendix E the spoiler effectiveness is strongly dependent upon flaperon deflection, a result of the spoilers being slot-lip spoilers.

6.5.2 ROTOR SLIPSTREAM INTERFERENCE

Before the basic wing aerodynamic data can be utilized in the calculation of the wing forces, the effects of the rotor slipstream must be calculated. The calculation procedure presented here has been developed and used at Boeing for some years, and gives acceptable agreement with wind tunnel test data on a wide variety of both tilt rotor and tilt wing configurations.

The method uses momentum theory to obtain the direction and

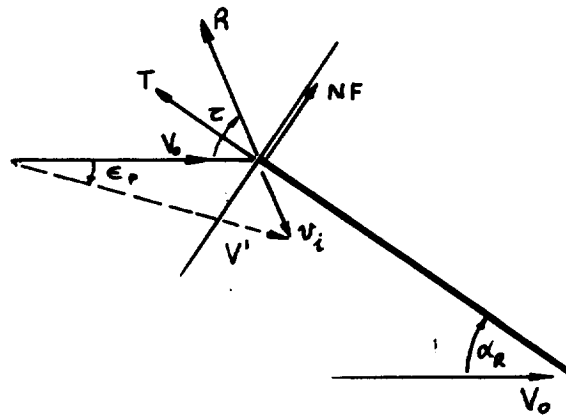
1

speed of the rotor slipstream in the neighborhood of the wing. From this the effective angle of attack of that part of the wing that is immersed in the slipstream is calculated. The lift, drag and pitching moment on the wing are then calculated for this angle of attack as if the entire wing were immersed. The area of the wing immersed in the slipstream is now computed and, using the ratio of the immersed to total wing area, the forces acting on the immersed portion are approximated.

At the angle of attack of the wing outside the slipstream, the wing forces and moments are obtained from the basic wing data as if no slipstream effects were present. These forces are then scaled by the ratio of unimmersed to total wing areas to obtain approximately the forces acting on the unimmersed wing. The sum of the approximations to immersed and unimmersed wing forces is now formed. This sum is then multiplied by a correction factor to obtain the final forces.

This correction factor is obtained from a consideration of the mass flows associated with the rotor-wing combination. In the following outline of the method only one rotor is considered.

From the following sketch, which shows the forces acting on the rotor, the inclination of



the resultant force on the rotor to the freestream direction is given by

$$\tau_R = \alpha_R + \text{Tan}^{-1} \left(\frac{NF}{T} \right)$$

The resultant force on the rotor is

$$R = \sqrt{T^2 + NF^2 + SF^2}$$

where T, NF and SF are the thrust, normal force and sideforce, respectively.

The mass flow through the disc is

$$m = \rho A V'$$

where A is the disc area and V' is obtained from the induced velocity triangle at the disc plane.

$$V' = \sqrt{(V_0 + v_i \cos \tau)^2 + (v_i \sin \tau)^2}$$

The resultant force on the rotor is related to the mass flow by (Glauert's assumption)

$$R = 2m v_i = 2\rho A V' v_i$$

From these equations the following quartic equation is obtained for the induced velocity at the disc.

$$v_*^4 + 2V_* v_*^3 \cos \tau + v_*^2 V_*^2 = 1$$

where the nondimensional notations

$$v_* = \frac{v_i}{\sqrt{\frac{R}{2\rho A}}} \quad V_* = \frac{V_o}{\sqrt{\frac{R}{2\rho A}}}$$

have been introduced.

This equation is then solved for v_* and the direction of the slipstream just behind the rotor disc is calculated from

$$\epsilon_p = \text{Tan}^{-1} \left[\frac{v_* \sin \tau}{v_* \cos \tau + V_*} \right]$$

The rotor thrust coefficient C_{T_s} is defined as

$$C_{T_s} = \frac{T}{(q + \frac{T}{A})A}$$

NOTE: Because the rotor diameter to wingchord is large the slipstream is considered to be uncontracted in the vicinity of the wing.

with $T = R \cos (\tau - \alpha_R)$

and $q = \frac{1}{2} \rho V^2 = \frac{1}{4} V_*^2 R$

then $C_{T_s} = \frac{\cos (\tau - \alpha_R)}{\cos (\tau - \alpha_R) + \frac{V_*^2}{4}}$

The aspect ratio of the slipstream-immersed wing area is given by

$$AR_i = \frac{S_i}{c^2}$$

where S_i is the immersed area calculated by the method described in Appendix D, and c is the wing chord.

The lift on the wing, if the slipstream were absent, is obtained by calculating the effective angle of attack of the wing outside the slipstream from

$$\alpha_o = \sin^{-1} \left[\frac{w_w}{\sqrt{u_w^2 + w_w^2}} \right] + \theta_t$$

where w_w , u_w are the velocities at the wing aerodynamic center and θ_t is the elastic twist at the point. The lift coefficient (C_L^*) for this angle of attack is obtained from the aerodynamic data for the appropriate flaperon/spoiler deflection.

Similarly the lift (C_L'') and drag (C_D'') coefficients of the wing in the slipstream (assuming wing is completely immersed) are obtained from the aerodynamic data at the angle of attack

$$\alpha_s = \alpha_o - \epsilon$$

The total lift coefficient of the wing with slipstream is therefore

$$C_{L_s} = K'_A \left[\frac{S_i}{S} (C_L'' \cos \epsilon - C_D'' \sin \epsilon) + C_L^* (1 - C_{T_s}) \left(1 - \frac{S_i}{S}\right) \right]$$

where

$$C_{L_s} = \frac{L}{q_s S_w}$$

in which q_s is the nominal slipstream dynamic pressure, defined

$$\text{by } q_s = q + \frac{T}{A}$$

The factor K'_A is a correction factor to account for the fact that the lift-sharing between the immersed and unimmersed portions

of the wing is not simply proportional to the respective areas.

From considerations of the mass flows associated with the wing-rotor combination the factor K'_A was obtained in the form

$$K'_A = \frac{V_* + \frac{C_{L\alpha i}}{C_{L\alpha}} v_*}{V_* + v_*}$$

where, from wing theory,

$$\frac{C_{L\alpha i}}{C_{L\alpha}} = \frac{1}{1 + \frac{C_{L\alpha}}{\pi} \left[\frac{1}{AR_i} - \frac{1}{AR} \right]}$$

The drag and pitching moments for the wing with slipstream are obtained similarly and are given by:

$$C_{D_S} = K'_A \left\{ \frac{S_i}{S} (C_L'' \sin \epsilon + C_D'' \cos \epsilon) + C_D^* (1 - C_{T_S}) \left(1 - \frac{S_i}{S}\right) \right\}$$

$$C_{M_S} = K'_A \left\{ \frac{S_i}{S} C_M'' + C_M^* (1 - C_{T_S}) \left(1 - \frac{S_i}{S}\right) \right\}$$

The rolling moment and yawing moment coefficients for the wing are given by

$$C_{\ell_S} = (K_{20} + K_{21} \bar{C}_L) (1 - \bar{C}_{T_S}) \beta_F + \bar{Y}_{AC} \left(\frac{1 - C_{T_S}}{2b_W} \right) (C_{L_{LW}}^* - C_{L_{RW}}^*) + \Delta C_{\ell_S}^{\text{POWER}}$$

$$C_{\eta_S} = K_{22} \bar{C}_L^2 (1 - C_{T_S}) \beta_F + \bar{Y}_{AC} \left(\frac{1 - C_{T_S}}{2b_W} \right) (C_{D_{RW}}^* - C_{D_{LW}}^*) + \Delta C_{\eta_S}^{\text{POWER}}$$

where the increment in rolling moment due to power is

$$\Delta C_{\ell_S}^{\text{POWER}} = \frac{1}{4} \left\{ \left[C_{L_{LW}} - (1 - \bar{C}_{T_S}) C_{L_{LW}}^* \right] \left[1 - \frac{1}{2} \left(\frac{S_i}{S} \right)_{LW} \right] - \left[C_{L_{RW}} - (1 - \bar{C}_{T_S}) C_{L_{RW}}^* \right] \left[1 - \frac{1}{2} \left(\frac{S_i}{S} \right)_{RW} \right] \right\}$$

and the increment in yawing moment is

$$\Delta C_{n_{S_{POWER}}} = \frac{1}{4} \left\{ \left[C_{D_{S_{RW}}} - (1 - \bar{C}_{TS}) C_{D_{RW}}^* \right] \left[1 - \frac{1}{2} \left(\frac{S_i}{S} \right)_{RW} \right] \right. \\ \left. - \left[C_{D_{S_{LW}}} - (1 - \bar{C}_{TS}) C_{D_{LW}}^* \right] \left[1 - \frac{1}{2} \left(\frac{S_i}{S} \right)_{LW} \right] \right\}$$

Figure 6.2 shows a correlation between the wing-in-slipstream method described above and experimental results for the Boeing Model 160 tilt rotor aircraft. As may be seen the simple treatment gives acceptable predictions of wing forces and moments.

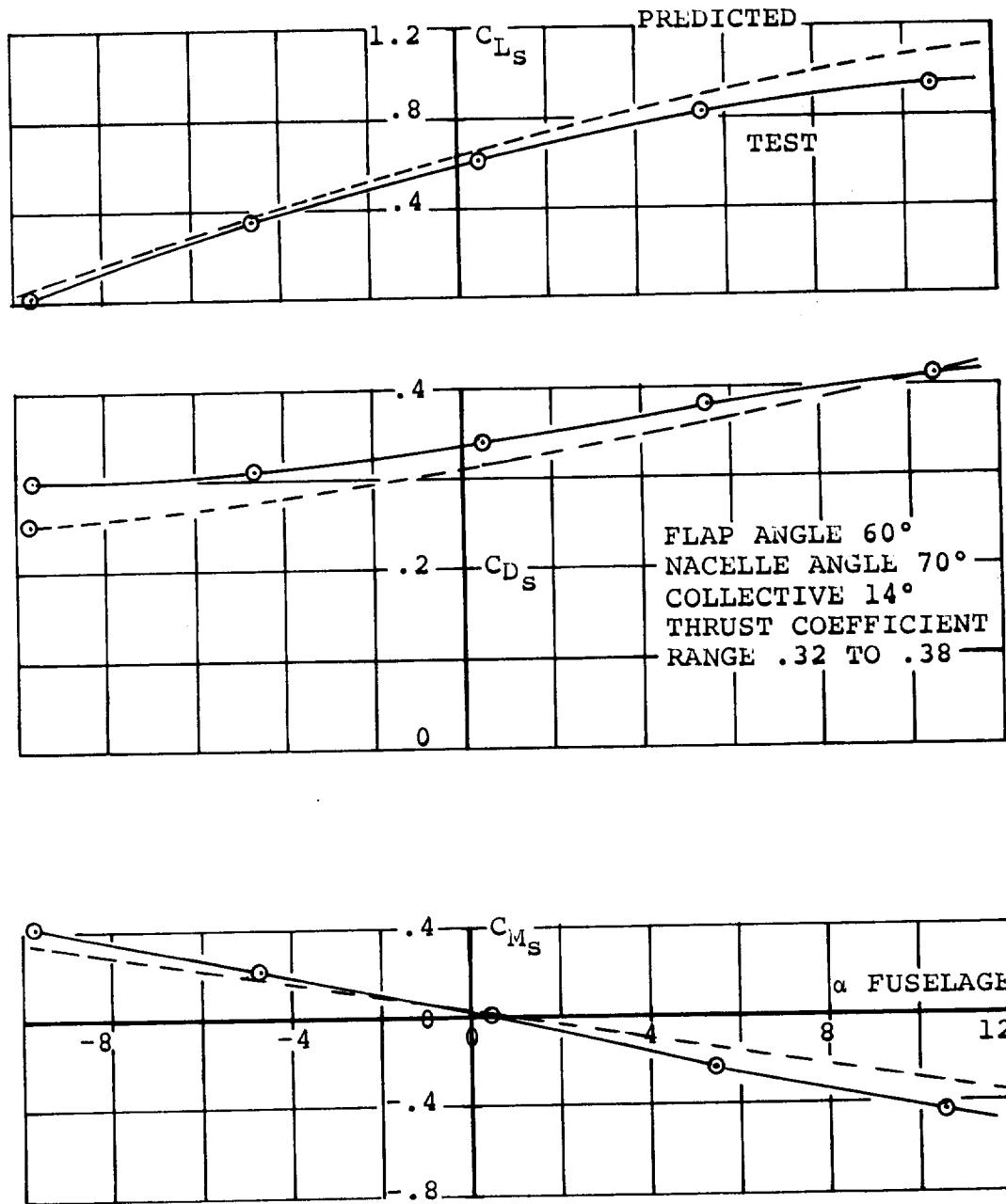


Figure 6.2. Correlation of Theory with Test for Predictions of Slipstream Forces and Moments

7.0 ROTOR AERODYNAMICS

The rotor aerodynamics as used in the mathematical model are described in this section. Also presented are the methods used to compute the rotor aerodynamics, a discussion on wing upwash as it effects the rotor, and a description of the technique used to account for rotor on rotor interference in skewed flight. In addition, correlation of the methods described in this section with test data for soft-in-plane hingeless rotors are presented. Calculation of the Model 222 rotor forces and moments was not practicable because of the complexity and size of the programs required to represent the lag-flap coupling effects of the rotor. In this mathematical model, the rotor forces and moments are input from a series of curve plot fit equations. These equations were generated by computing rotor data using the computer programs discussed in Section 7.2, and then a least squares curve fit program was used to obtain the curve fit equations. The rotor forces and moments used in the mathematical model include the six basic forces and moments (thrust, power, normal force, side force, pitching moment, yawing moment), hub pitching and yawing moments due to aircraft pitch and yaw rate, and changes to the six basic forces and moments due to cyclic pitch application.

7.1 FORMAT AND RANGE OF DATA

Rotor forces and moments are functions of thirteen variables. In order to reduce the size of the data bank, these variables were combined and non-dimensionalized. Each rotor force and

moment can be written as:

$$F = f(V, V_t, \theta_{0.75} \text{ or } T, \alpha, \beta, P, Q, R, A_1, B_1, P_N^R, Q_N^R, R_N^R) \quad (7-1)$$

where

- V = Forward speed
- V_t = Rotor tip speed
- $\theta_{0.75}$ = Collective pitch at the .75 radius
- T = Rotor thrust
- α = Rotor angle of attack
- β = Rotor sideslip angle
- P = Body axis roll rate
- Q = Body axis pitch rate
- R = Body axis yaw rate
- A_1 = Longitudinal cyclic pitch
- B_1 = Lateral cyclic pitch
- P_N^R = Rotor wind axis roll rate
- Q_N^R = Rotor wind axis pitch rate
- R_N^R = Rotor wind axis yaw rate

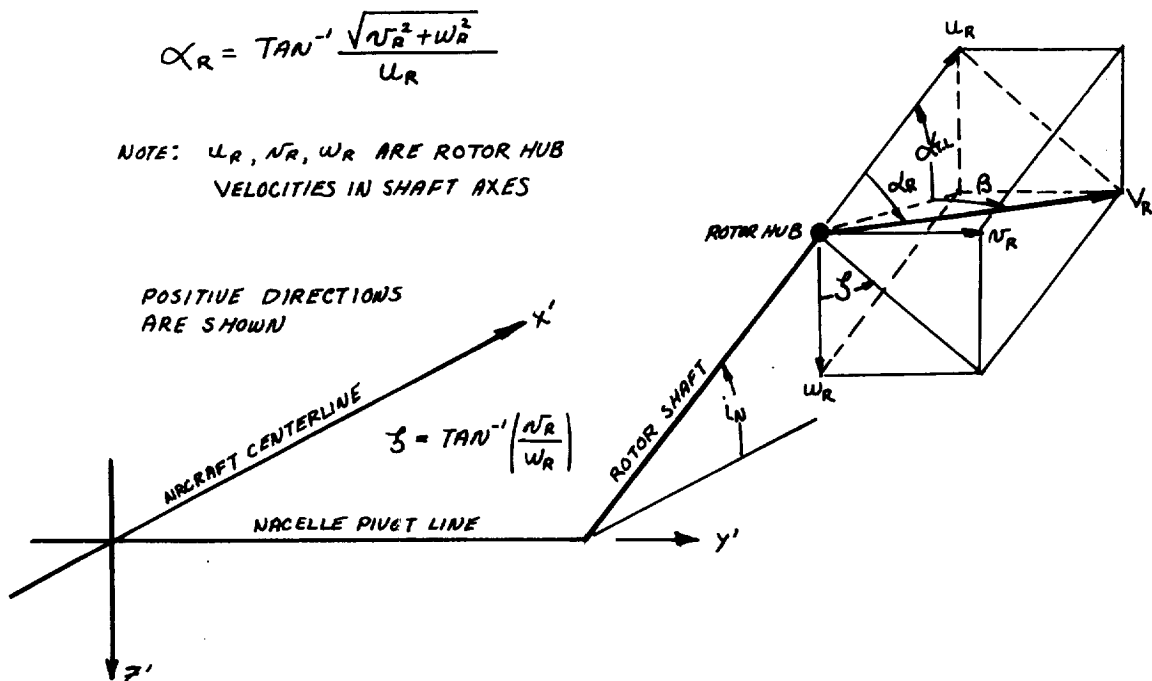
Forward speed and tip speed were combined to form rotor advance ratio and collective pitch or thrust were retained. Rotor angles of attack and sideslip and body axis roll, pitch and yaw rates were combined into a resultant angle of attack. Longitudinal and lateral cyclic pitch angles are retained. By combining the thirteen variables in this manner, Equation 7-1 can be expressed as:

$$F = f(\mu, \theta_{.75} \text{ or } C_T, \alpha_R) + [\Delta F = f(A_1, B_1)] + [\Delta F = f(P_N^R, Q_N^R, R_N^R)] \quad (7-2)$$

where

- μ = rotor advance ratio
- α_R = rotor resultant angle of attack

By using this functional relationship, basic rotor forces and moments can be written as functions of three variables plus increments due to cyclic pitch control application and wind axis pitch roll and yaw rates at the rotor hub. This is the format used in the mathematical model. In addition, the rotor forces and moments are non-dimensionalized by dividing forces by $(\rho \pi R^2 V_t^2)$, moments by $(\rho \pi R^2 V_t^2 R)$, and power by $(\rho \pi R^2 V_t^3)$.



The above sketch shows a rotor under condition of combined angle of attack ($\alpha_{T.L.}$) and sideslip (β). The resultant angle of attack (α_R) is the angle between the " u_R " component of velocity at the rotor hub and the total velocity (V_R) at the hub. The velocity components that define this resultant angle are the rotor hub velocities resolved to shaft axes and

derived in Appendix C. They include body axes pitch, roll and yaw rates. Other functional relationships that define the rotor resultant angle of attack are shown in Appendix D. Also shown on the sketch is the rotor sideslip angle (ζ). This angle represents the inclination of the plane containing the resultant velocity. Rotor wind axis forces and moments are defined relative to this plane. Since the resultant angle is defined from 0 through 180° the inclination of the rotor sideslip angle (ζ) determines the signs of the rotor forces and moments when they are resolved back to body axes.

After the functional format for the rotor data was established, the ranges of the variables were established. Discrete speeds and rotor rpm conditions were selected. A range of rotor resolved angles of attack and thrust levels were selected at each combination. These conditions were carefully selected to cover the total operating envelope of the Model 222. The ranges of the rotor data are shown in Table 7.1.

7.2 PROGRAMS USED TO COMPUTE ROTOR DATA

Rotor data used in the mathematical model were predicted from Boeing-developed computer programs. Hover and cruise performance (thrust-power) were obtained from a propeller performance analysis computer program (B-92). This analysis establishes a radial distribution of induced velocity based on a prescribed wake contraction schedule to calculate rotor induced and total power coefficients at specified thrust or

TABLE 7.1 RANGE OF ROTOR DATA

Total Velocity (V) ~ KTS	Rotor Speed (rpm)	Resultant Angle of Attack Range (α_R) ~ deg	Rotor Thrust (T) ~ Lb
0	551	0 → 180°	500 → 7000
45	551	0 → 180°	500 → 7000
60	551	0 → 180°	2000 → 6500
90	551	0 → 180°	2000 → 6500
120	400	0 → 45°	500 → 2600
142	386	0 → 20°	-700 → 3500
160	386	0 → 20°	-500 → 4750
200	386	0 → 20°	-500 → 6000
240	386	0 → 20°	0 → 3700
280	386	0 → 20°	0 → 3800
320	386	0 → 20°	0 → 4800
360	386	0 → 20°	0 → 3500

thrust coefficients. The radial airload distribution is also defined. A detailed description of this program is given in Reference 4.

Transition performance data, in-plane forces and moments and cyclic pitch effectiveness throughout the flight envelope were estimated using computer program D88 (Reference 5).

The D-88 computer program is an aeroelastic analysis for the study of aerodynamic, dynamic, and structural characteristics of current and advanced rotor and prop/rotor concepts. Airloads are calculated considering the effects of section geometry, compressibility and non-uniform inflow. An iterative process between the airloads and coupled flap-pitch dynamic response establishes blade accelerations which in turn are used to compute hub loads and rotor aerodynamic performance.

The rotor analysis is based on the idealization of a continuous, elastic, non-uniform beam into one composed of lumped discrete masses connected by weightless elastic sections. Associated with each mass is a flat rigid airfoil segment, with the mass center located at the midpoint. The aerodynamic loads generated by each segment are assumed to act at the mass center.

The effects of non-uniform inflow are included by considering a discontinuous constant circulation along part of the rotor blade, of sufficient strength to maintain the desired thrust. A vortex is assumed to trail from the inboard and outboard

circulation discontinuities, of equal and opposite strength. By summing the effects of all the vortices on a given blade around the azimuth the non-uniform induced flow for each blade at every dynamic bay is determined. Total velocity at each point in the blade is computed by vector addition of the velocity components.

The local angle of attack of each blade element is then computed at every blade station for specified azimuth angles and the aerodynamic coefficients (C_L , C_D , C_M) are looked up from tables of coefficients as a function of Mach number. From these coefficients the airloads are computed. The vertical, tangential and pitching aerodynamic loads are then harmonically analyzed into 10 harmonics and act as the forcing functions for each blade section.

To obtain a thrust match, an iteration process is performed on the airloads until a steady collective pitch angle is obtained which corresponds to the desired thrust. To perform the dynamic analysis, the lumped mass and elastic bay elements of the idealized rotor blade are transformed into a sequence of transfer matrix products, by means of the Associated Matrix Method. This method replaces each blade element by an equivalent "transfer matrix" that transfers the dynamic system variables, shear, moment, deflection and slope, inboard across the element. Therefore, multiplying the system variables outboard of the element by the transfer matrix gives the variables

inboard of the element. The whole mass, elastic blade idealization is then reduced to a sequence of transfer matrix products.

In-plane elastic rotor derivatives (both static and rate) in axial flow were calculated using computer program C-41 (Reference 2).

Dynamic derivatives for a rotor system are defined taking account of the modal behavior of the blades in two general flap-lag modes. These derivatives are given as matrix arrays of the partial derivatives of rotor forces with respect to unit amounts of elementary linear and angular motions of the hub and unit displacements in the blade modes. These effects are separated into inertial, damping and gyroscopic, and stiffness effects. Thus an element m_{ij} in the inertia derivative matrix is $\partial F_i / \partial g_j$, i.e., the force in the i direction due to unit acceleration in the j direction, all other quantities being held constant.

Similarly element d_{ij} of the damping derivative matrix will represent $\partial F_i / \partial g_j$ which might for appropriate (ij) be the aggregate gyroscopic and aerodynamic pitching moment due to unit velocity of yaw.

Similarly the elements of the stiffness derivative matrix represent such quantities as the normal force due to unit amount of shaft angle of attack, and generalized forces in the blade freedoms due to unit displacements in each of the other freedoms.

The matrices are of order 15 x 15 maximum. The first 6 rows and columns refer to forces in the vertical, lateral and axial directions and moments in the yaw pitch and roll directions due to unit acceleration, rates and displacements in each of the directions. These are the only numbers present if the rotor blades are assumed rigid. Three additional rows and columns are added for each blade mode considered. A limit of two blade modes is currently applied. The final three rows are for cyclic and collective pitch.

These derivative matrices provide a ready means for evaluating the contribution of the rotor to the coefficients of the aircraft dynamic equations. This program also provides the in-plane elastic rotor derivatives.

Elastic rotor rate derivatives in transition were estimated using computer program C-49 (Reference 3). This program evaluates hub force and moment derivatives for shaft angles varying from cruise to hover conditions. Dynamic derivatives suitable for transient analysis are computed. The dynamic derivatives are the partial differentials of hub forces and moments with respect to hub positions rates and accelerations and include inertial and gyroscopic effects as well as aerodynamic effects. For the static derivatives a constant shaft angle to the relative wind is assumed and the resulting blade motion computed. The effects of blade aerodynamic and inertia and gyroscopic forces are combined to give the hub derivatives

due to constant shaft angle and constant rate of change of shaft angle.

The output rotor forces and moments of these programs are in rotor wind axis.

7.3 ROTOR SIGN CONVENTION

The rotor sign conventions as used in this mathematical model are shown in Figure 7.1 . Positive directions of all rotor forces, moments and cyclic pitch angles are noted.

7.4 CURVE FIT FORMAT

The rotor data generated for the Model 222 mathematical model was curve fit at each advance ratio. A curve fit which is third order in angle of attack and second order in thrust coefficient or collective pitch was found to yield the most accurate results. The curve fits have the following general form.

$$C_F = \sum_{v=0}^2 \sum_{u=0}^3 \left[A(u+4v)\alpha^u C_T^v \right]$$

The double summation is expanded starting with the inner quantity i.e. set v and expand u from 0 to 3. Repeat until the summations are satisfied. The expansion of the generalized form is

$$\begin{aligned} C_F = & A_0 + A_1\alpha + A_2\alpha^2 + A_3\alpha^3 \\ & + (A_4 + A_5\alpha + A_6\alpha^2 + A_7\alpha^3)C_T \\ & + (A_8 + A_9\alpha + A_{10}\alpha^2 + A_{11}\alpha^3)C_T^2 \end{aligned}$$

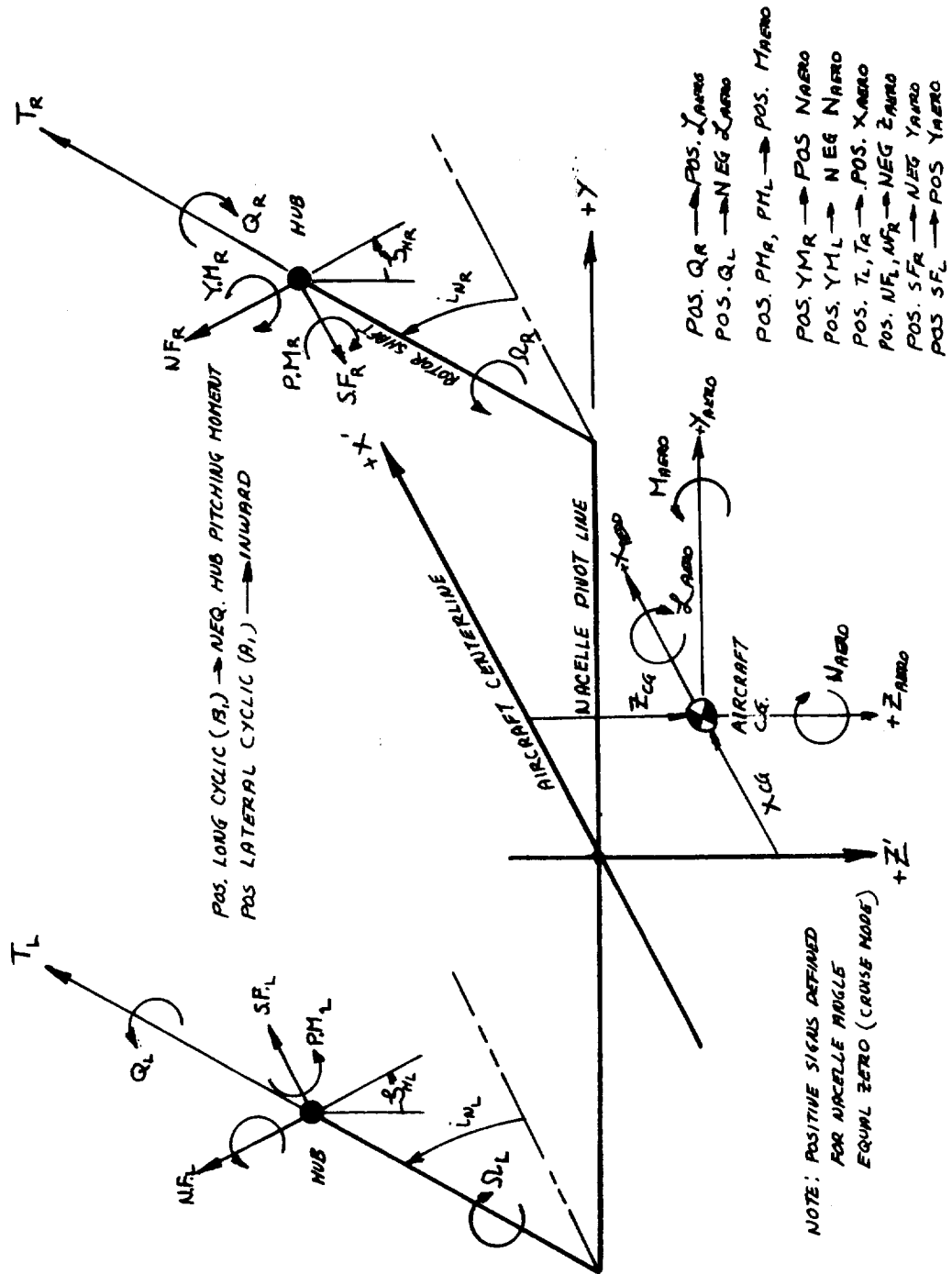


Figure 7.1. Rotor Sign Conventions

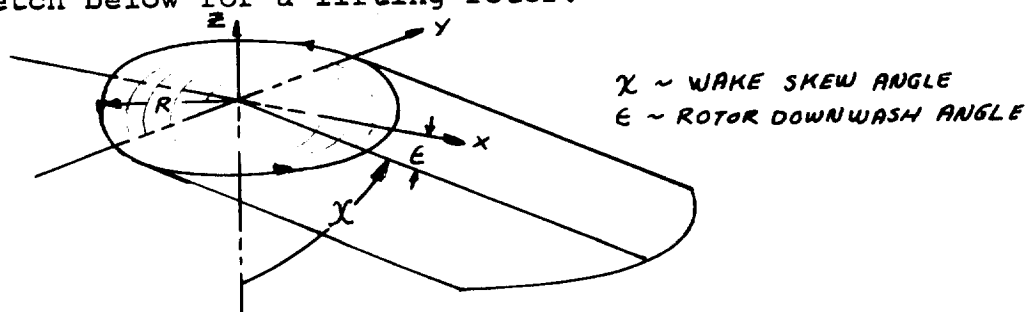
All of the rotor forces and moments are curve fit in this format. The coefficients of the equation were obtained from a least squares fit of the computed rotor data. The criteria used to determine the final coefficients was to have not more than a 5% difference between the curve fit equations and the computed rotor data at the nominal aircraft trim condition. In general this criteria was met.

7.5 EFFECT OF WING UPWASH ON ROTOR PERFORMANCE

The rotor operates in the upwash field associated with the lifting wing. Thus, the rotor behaves as if it were operating at an increased angle of attack. The effective upwash angles were calculated using lifting line theory. In the mathematical model the upwash angles are input in the form of a table of upwash angles as a function of wing lift coefficient, and nacelle incidence angle.

7.6 ROTOR/ROTOR INTERFERENCE

In order to obtain the correct lateral stick gradient when flying sideways or at large sideslip angles, a calculation for rotor-on-rotor interference is included in the mathematical model. In Reference 11, the wake skew angle is defined as in the sketch below for a lifting rotor.



Also presented in this reference are contour charts of the normal component of induced velocity near a rotor with a triangular disc loading for six different skew angles in the range from 0° to 90°. For the Model 222 geometry, a curve of normal induced velocity/average induced velocity as a function of skew angle was obtained. For the case of the Model 222 flying sideways, the downwind rotor is assumed to be operating at a lower angle of attack than the upwind rotor, and will therefore generate different forces and moments. The downwash angle is calculated from the normal component of induced velocity. The rotor/rotor interference is washed out as a function of nacelle angle and sideslip angle such that there is no interference in the high transition speed and cruise modes. The equations derived are shown in Appendix E, under the rotor/rotor interference section.

7.7 ISOLATED ROTOR AERODYNAMICS

The equations utilized to represent the isolated rotor aerodynamics are presented below. These equations are then resolved into body axis forces and moments to be used in the equation of motion.

7.7.1 Thrust (1)

$$C_{T_R}^i = [C_{T_{ORR}} \cos A_{1CR} \cos B_{1CR}]$$

$$\text{where } C_{T_{ORR}} = \sum_{v=0}^2 \sum_{u=0}^3 [A_T (u+4v) \alpha_{RR}^u \theta_{RR}^v] 0.75$$

(1) In the equations that follow, subscript RR denotes right rotor. The left rotor is identical provided due regard is paid to sign convention and azimuth reference.

$A_{T(u+4v)}$ = function of $\mu \left(\mu = \frac{V}{V_t} \right)$ and is obtained from Appendix F

A_{1C_R} = Lateral cyclic pitch

B_{1C_R} = Longitudinal cyclic pitch

$\theta_{0.75}$ = Blade pitch angle at 75% blade radius

$$\alpha_{RR} = \tan^{-1} \left\{ \frac{\sqrt{V_{RR}^2 + (W_{RR} + u_{RR} \epsilon_{wRR})^2}}{u_{RR}} \right\} + \epsilon_{iLR}$$

u_{RR}, V_{RR}, W_{RR} = rotor shaft axis velocity components

ϵ_{wRR} = Wing upwash angle

ϵ_{iLR} = Rotor/rotor interference angle

The effect of close proximity to the ground is accounted for by use of the following relationships

$$C_{T_{RR}} = C_{T_{RR}}' \left(\frac{T_{IGE}}{T_{OGE}} \right)_{RR}$$

where $\left(\frac{T_{IGE}}{T_{OGE}} \right)$ is defined in Section 10 under the discussion of ground effect.

7.7.2 Power

$$C_{P_{RR}} = C_{P_{ORR}} = \sum_{v=0}^2 \sum_{u=0}^3 \left[A_p(u+4v) \alpha_{RR}^u C_{T_{RR}}^{1v} \right]$$

where: $A_p(u+4v)$ may be obtained from Appendix F as a function of μ_{RR}

7.7.3 Normal Force

$$C_{NF_{RR}} = C_{NF_{ORR}} + \frac{dC_{NF_{RR}}}{dA_{1C_R}} A_{1C_R} + \frac{dC_{NF_{RR}}}{dB_{1C_R}} B_{1C_R}$$

$$\text{where: } C_{NF_{ORR}} = \sum_{v=0}^2 \sum_{u=0}^3 \left[A_{NF}(u+4v) \alpha_{RR}^u C_{T_{RR}}^{1v} \right]$$

$A_{NF}(u+4v)$ = Function of μ_{RR} and may be obtained from Appendix F.

$$\frac{dC_{NFRR}}{dA_{1CR}} = D_{NF1} C_{T_{RR}} + D_{NF2} \mu_{RR}^2 + D_{NF3} \mu_{RR} + D_{NF4}$$

$$\frac{dC_{NFRR}}{dB_{1CR}} = E_{NF1} C_{T_{RR}} + E_{NF2} \mu_{RR}^2 + E_{NF3} \mu_{RR} + E_{NF4}$$

The coefficients in the above 2 equations may be obtained from Appendix F.

7.7.4 Side Force

$$C_{SFRR} = C_{SF_{ORR}} + \frac{dC_{SFRR}}{dA_{1CR}} A_{1CR} + \frac{dC_{SFRR}}{dB_{1CR}} B_{1CR}$$

$$\text{where: } C_{SF_{ORR}} = \sum_{v=0}^2 \sum_{u=0}^3 \left[A_{SF}(u+4v) \alpha_{RR}^u C_{T_{RR}}^v \right]$$

$A_{SF}(u+4v)$ = function of μ_{RR} and may be obtained from Appendix F.

$$\frac{dC_{SFRR}}{dA_{1CR}} = D_{SF1} C_{T_{RR}} + D_{SF2} \mu_{RR}^2 + D_{SF3} \mu_{RR} + D_{SF4}$$

$$\frac{dC_{SFRR}}{dB_{1CR}} = E_{SF1} C_{T_{RR}} + E_{SF2} \mu_{RR}^2 + E_{SF3} \mu_{RR} + E_{SF4}$$

The coefficients in the above 2 equations may be obtained from Appendix F.

7.7.5 Hub Pitching Moment

$$C_{PMRR} = C_{PM_{ORR}} + \frac{dC_{PMRR}}{dA_{1CR}} A_{1CR} + \frac{dC_{PMRR}}{dB_{1CR}} B_{1CR} + \frac{dC_{PMRR}}{dQ} Q_{NR}^R$$

$$\text{where: } C_{PM_{ORR}} = \sum_{v=0}^2 \sum_{u=0}^3 \left[A_{PM}(u+4v) \alpha_{RR}^u C_{T_{RR}}^v \right]$$

$A_{PM}(u+4v)$ = function of μ_{RR} and may be obtained from Appendix F.

$$\frac{dC_{PM_{RR}}}{dQ} = \sum_{v=0}^2 \sum_{u=0}^3 \left[H_{PM}(u+4v) \alpha_{RR}^u C_{T_{RR}}^{i_v} \right]$$

$H_{PM}(u+4v)$ = function of μ_{RR} and may be obtained from Appendix F

$$Q_{NR}^R = Q_{NR}^N \cos \zeta_{HR} + R_{NR}^N \sin \zeta_{HR}$$

$$Q_{NR}^N = Q + \dot{i}_{NR}$$

$$R_{NR}^N = -R \cos i_{NR} - P \sin i_{NR}$$

ζ_{HR} = right rotor sideslip angle

i_{NR} = right nacelle velocity

i_{NR} = right nacelle angle

$$\begin{aligned} \frac{dC_{PM_{RR}}}{dA_{1C_R}} &= D_{PM_1} C_{T_{RR}} + D_{PM_2} \mu_{RR}^2 + D_{PM_3} \mu_{RR} + D_{PM_4} \quad (\mu_{RR} \leq .35) \\ &= D_{PM_1} C_{T_{RR}} + D_{PM_5} \mu_{RR}^2 + D_{PM_6} \mu_{RR} + D_{PM_7} \quad (\mu_{RR} > .35) \end{aligned}$$

$$\begin{aligned} \frac{dC_{PM_{RR}}}{dB_{1C_R}} &= E_{PM_1} C_{T_{RR}} + E_{PM_2} \mu_{RR}^2 + E_{PM_3} \mu_{RR} + E_{PM_4} \quad (\mu_{RR} \leq .35) \\ &= E_{PM_1} C_{T_{RR}} + E_{PM_5} \mu_{RR}^2 + E_{PM_6} \mu_{RR} + E_{PM_7} \quad (\mu_{RR} > .35) \end{aligned}$$

Values for the coefficients in the above 2 sets of equations may be found in Appendix F.

7.7.6 Hub Yawing Moment

$$C_{YM_{RR}} = C_{YM_{ORR}} + \frac{dC_{YM_{RR}}}{dA_{1C_R}} A_{1C_R} + \frac{dC_{YM_{RR}}}{dB_{1C_R}} B_{1C_R} + \frac{dC_{YM_{RR}}}{dR} R_{NR}^R$$

$$\text{where: } C_{YM_{ORR}} = \sum_{v=0}^2 \sum_{u=0}^3 \left[A_{YM}(u+4v) \alpha_{RR}^u C_{T_{RR}}^{i_v} \right]$$

$A_{YM}(u+4v)$ is a function of μ_{RR} and may be obtained from Appendix F.

$$\frac{dC_{YM_{RR}}}{dR} = \sum_{v=0}^2 \sum_{u=0}^3 \left[J_{YM}(u+4v) \alpha_{RR}^u C_{T_{RR}}^v \right]$$

$J_{YM}(u+4v)$ is a function of μ_{RR} and may be obtained from Appendix F.

$$R_{NR}^R = R_{NR}^N \cos \zeta_{HR} - Q_{NR}^N \sin \zeta_{HR}$$

$$R_{NR}^N = -R \cos i_{NR} - P \sin i_{NR}$$

$$Q_{NR}^N = Q + i_{NR}$$

ζ_{HR} = Right rotor sideslip angle

i_{NR} = Right nacelle velocity

i_{NR} = Right nacelle angle

$$\begin{aligned} \frac{dC_{YM_{RR}}}{dA_{1CR}} &= D_{YM1} C_{T_{RR}} + D_{YM2} \mu_{RR}^2 + D_{YM3} \mu_{RR} + D_{YM4} (\mu_{RR} \leq .35) \\ &= D_{YM1} C_T + D_{YM5} \mu_{RR}^2 + D_{YM6} \mu_{RR} + D_{YM7} (\mu_{RR} > .35) \end{aligned}$$

$$\begin{aligned} \frac{dC_{YM_{RR}}}{dB_{1CR}} &= E_{YM1} C_T + E_{YM2} \mu_{RR}^2 + E_{YM3} \mu_{RR} + E_{YM4} (\mu_{RR} \leq .35) \\ &= E_{YM1} C_{T_{RR}} + E_{YM5} \mu_{RR}^2 + E_{YM6} \mu_{RR} + E_{EM7} (\mu_{RR} > .35) \end{aligned}$$

Values for the coefficients in the above 2 sets of equations may be found in Appendix F.

Notes: (1) Application of rotor equations for left rotor follow similar format with subscript "RR" changed to "LR".

(2) When solving equations with double summations for values of μ not given in tables, solve equations for the two values of μ closest to the value desired and then interpolate linearly for exact value of μ .

7.8 CORRELATIONS OF ROTOR PREDICTION METHODS WITH TEST DATA

This section presents the results of correlation studies that were conducted to verify the adequacy of the rotor prediction methods used for the Model 222 tilt rotor. In general, prediction of trends is excellent with quite good agreement in absolute magnitudes.

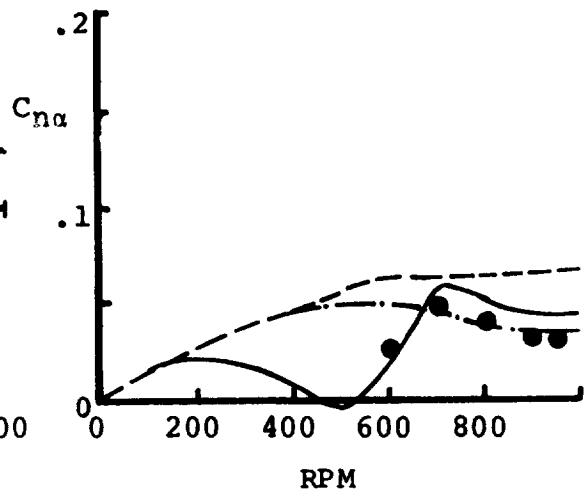
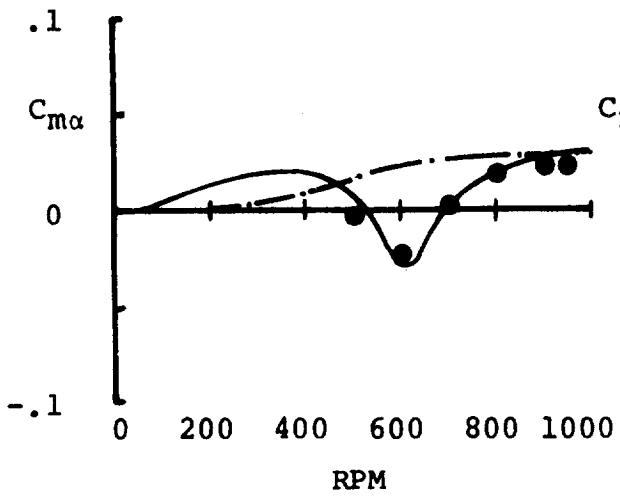
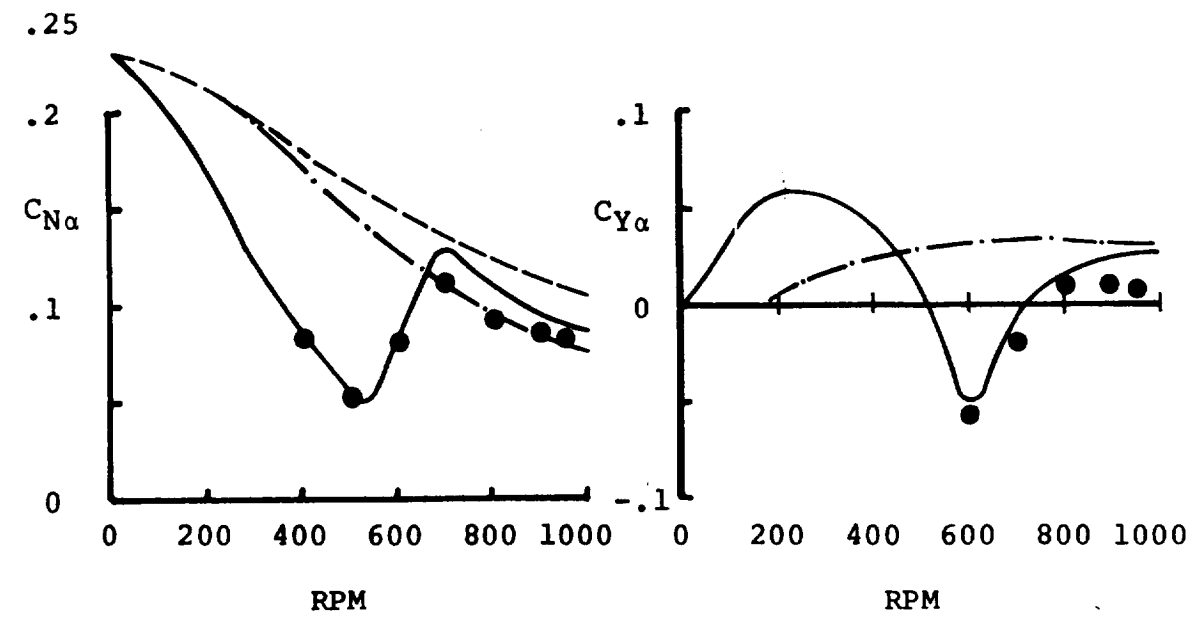
7.8.1 Model 213 Four Blade Hingeless Rotor Correlation

Figure 7.2 presents correlation with rotor derivatives measured on a 1/9 scale dynamically similar model of a tilt/stowed rotor conversion model. In this test the rotor hub forces and moments were carefully measured over a range of RPM in which the lead-lag modal frequency progressed from less than 1 per rev at 900 RPM to values significantly greater than 1 per rev as the rotor was feathered. The measured values confirm the predicted behavior trend and the quantitative correlation is also excellent.

7.8.2 Correlation with Model 222 26-Foot Diameter Rotor

Test in NASA-Ames 40 x 80-Foot Tunnel

Figure 7.3 shows the schematic of the windmilling test stand and its instrumentation. Test data were obtained from strain gages mounted on the outer portion of the wing as shown, and calibrated to measure normal force, pitching moment and yawing moment. Comparison with test data was made by calculating the moments about the wing strain gage locations using forces and moments predicted by the C-41 program. The results of this



Test Points ●
Theoretical Predictions
 - - - Rigid Blades
 - . - Flap Only
 - - - Flap & Lead Lag
 $\frac{dC_L}{d\alpha} = 5.7$

Definitions
 Normal Force = $1/2 \rho \pi R^2 V^2 C_{N\alpha} \cdot \alpha$
 Side Force = $1/2 \rho \pi R^2 V^2 C_{Y\alpha} \cdot \alpha$
 Pitching Moment = $\rho \pi R^3 V^2 C_{m\alpha} \cdot \alpha$
 Yawing Moment = $\rho \pi R^3 V^2 C_{n\alpha} \cdot \alpha$

Figure 7.2. Model 213 1/9 Scale Conversion Model – 85 Ft/Sec Derivative Variation with RPM

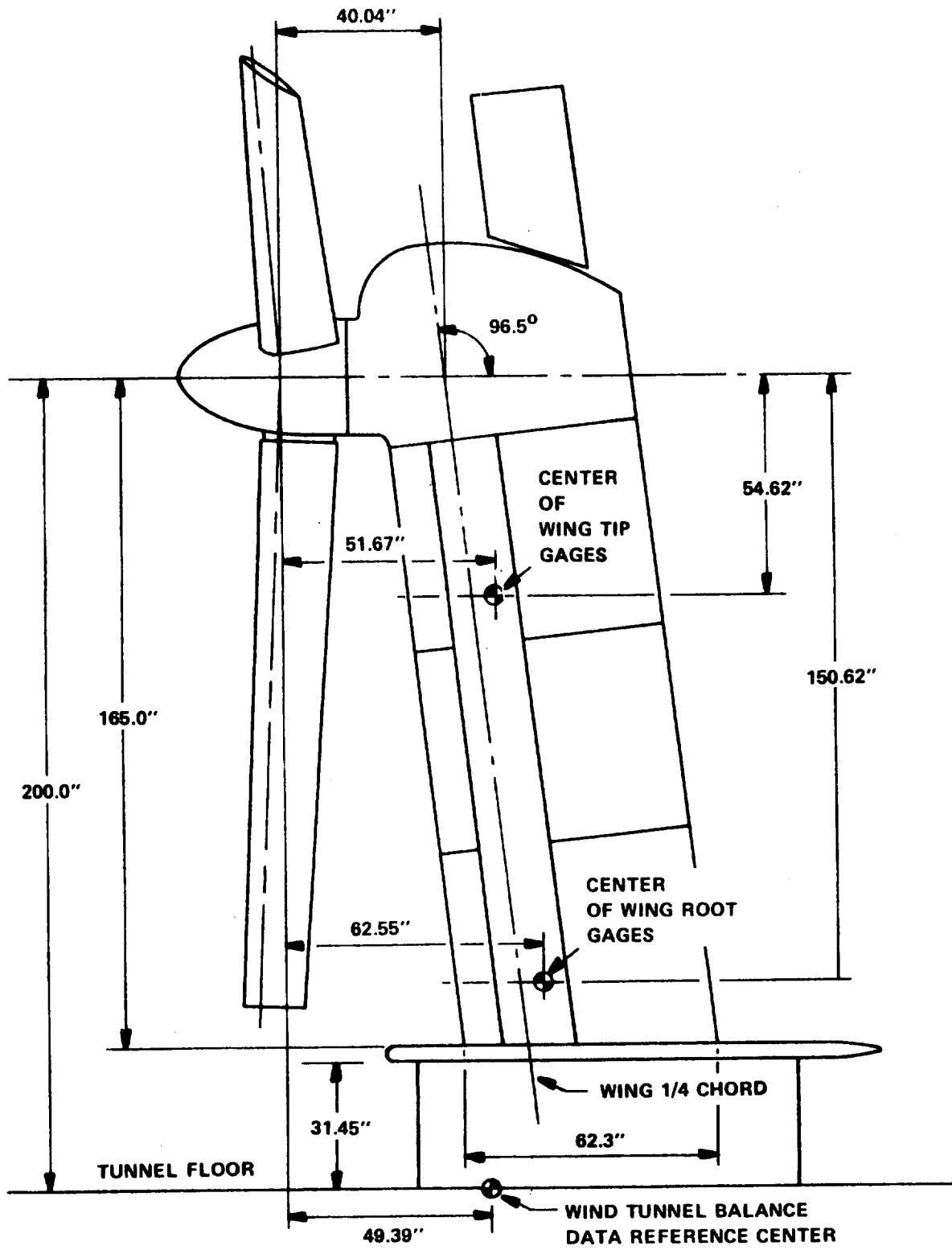


Figure 7.3. 26 Ft. Rotor Test Stand in NASA's 40' x 80' Tunnel

comparison for alpha derivatives are given in Figure 7.4 and for cyclic pitch derivatives in Figures 7.5 and 7.6 .

The analysis did not attempt to account for force and moment contributions from nacelle and wing aerodynamic interference. Nevertheless, quite good correlation is observed. These plots also show the values of derivatives predicted by several other programs. These include D-88 program which accounts for compressible non-linear downwash and L-22 which uses linear airfoil theory and uncoupled flap-lag freedoms. C-49 accounts for unsteady aerodynamics while C-41 uses a linear representation. C-41 and C-49 use a modal representation of blade freedoms (2 coupled flap-lag modes) while D-88 and L-22 make use of a finite element discrete mass representation.

The rotor derivative data was also compared with C-41 using a total unresolved moment approach. Total moments about the center of the wing tip gages and the reference azimuth position (orientation of the moment vector in the rotor disc plane) were calculated from the C-41 hub forces and moments and compared with test results (Figure 7.7). The interesting conclusion which is not apparent from the resolved forces and moments is that the total moment is predicted well but there are slight differences in the reference azimuth position.

7.8.3 Correlation with Model 222 1/4.622 Scale Model Data

The subject model is a dynamically similar version of the M222. The test data presented in Figures 7.8 and 7.9 were taken

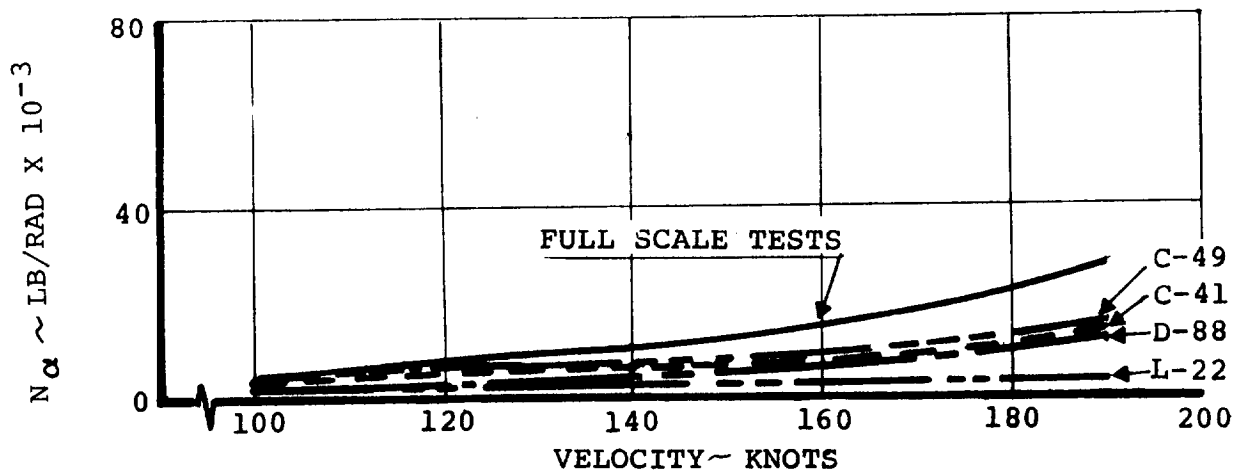
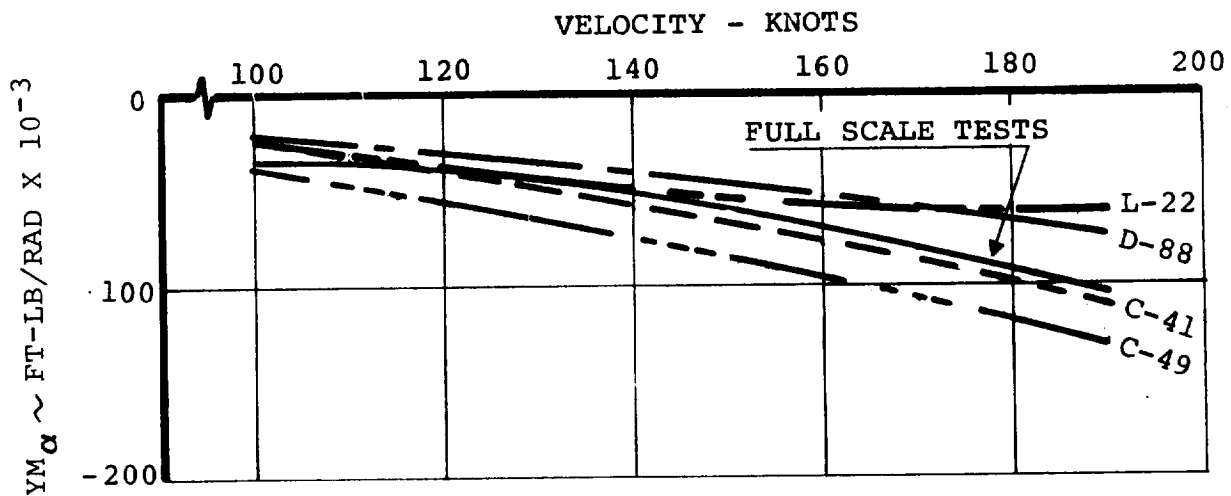
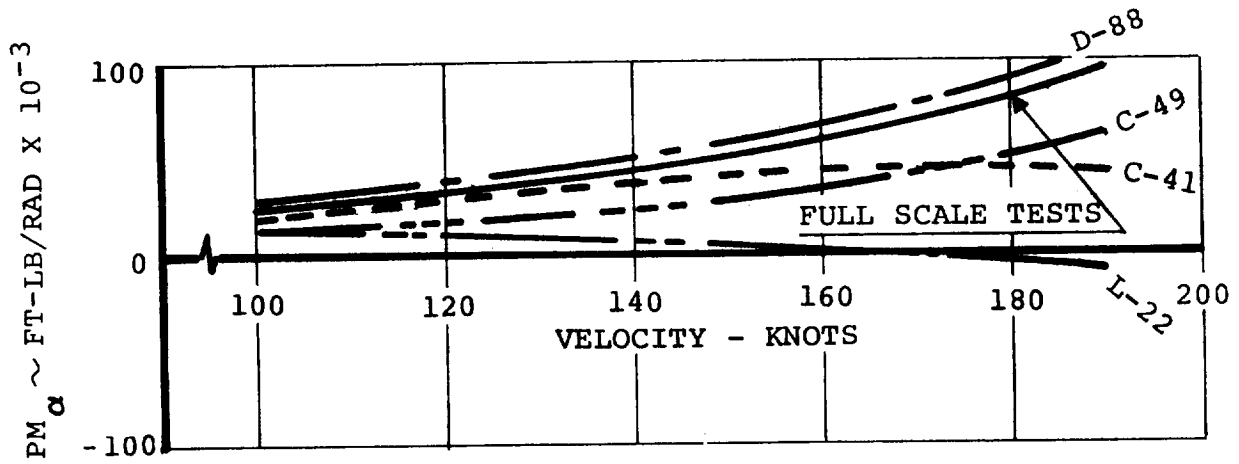


Figure 7.4. Correlation of 26 Ft Rotor Test Data with Various Rotor Derivative Programs

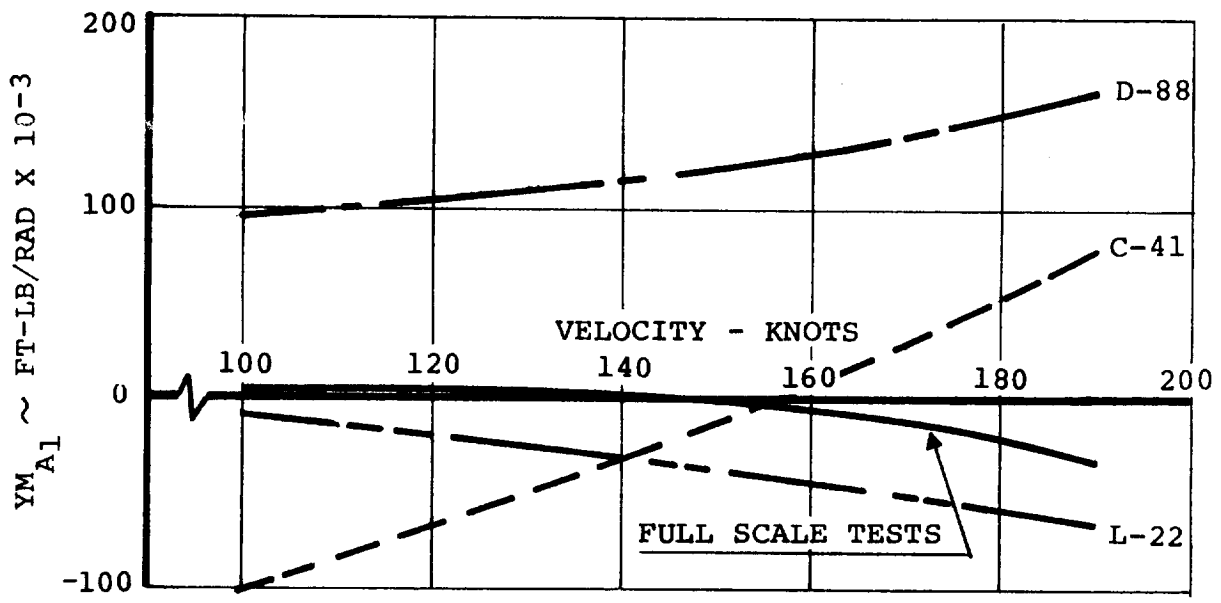
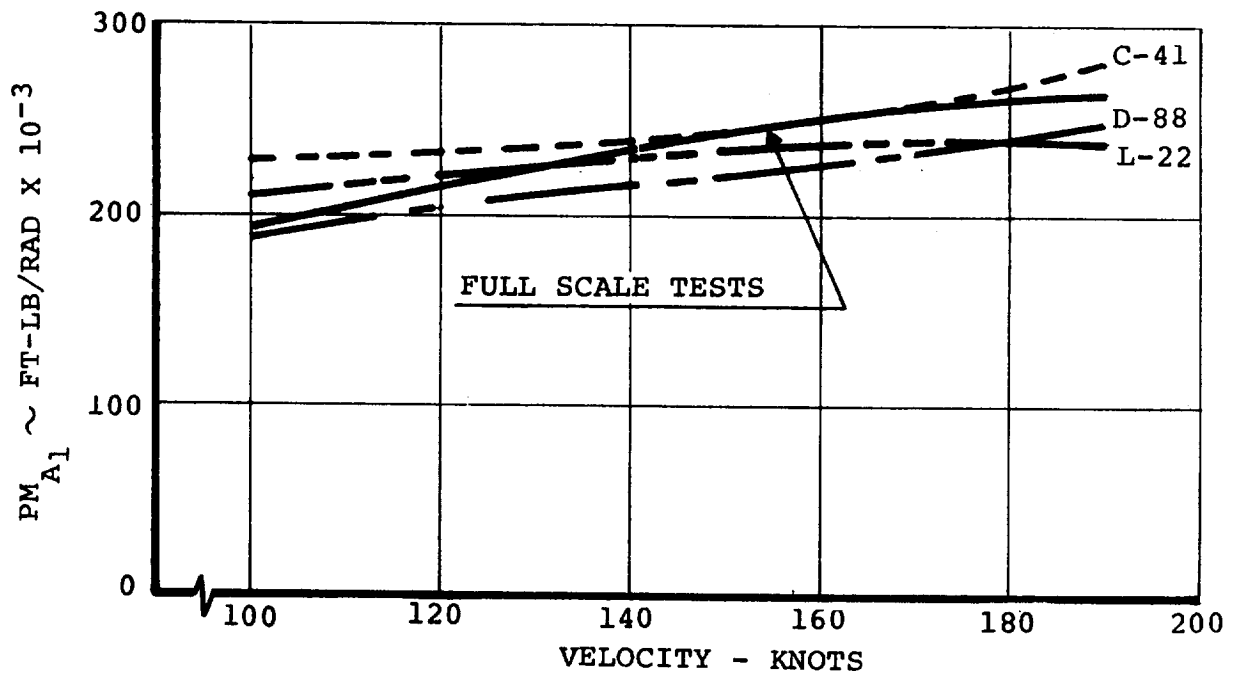


Figure 7.5. Correlation of 26 Ft Rotor Test Data with Various Rotor Derivative Programs – Cyclic Moment Derivatives

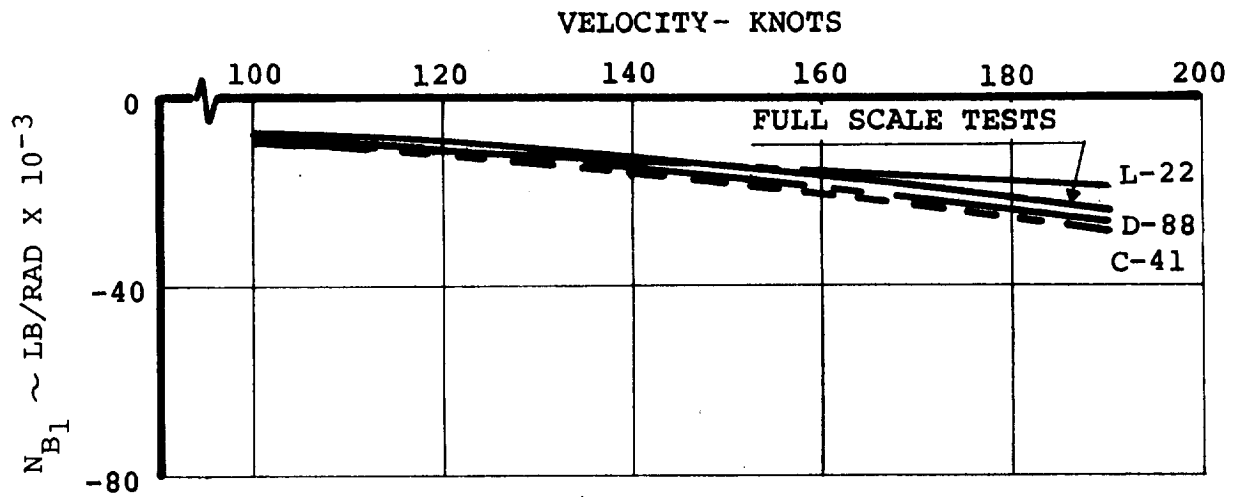
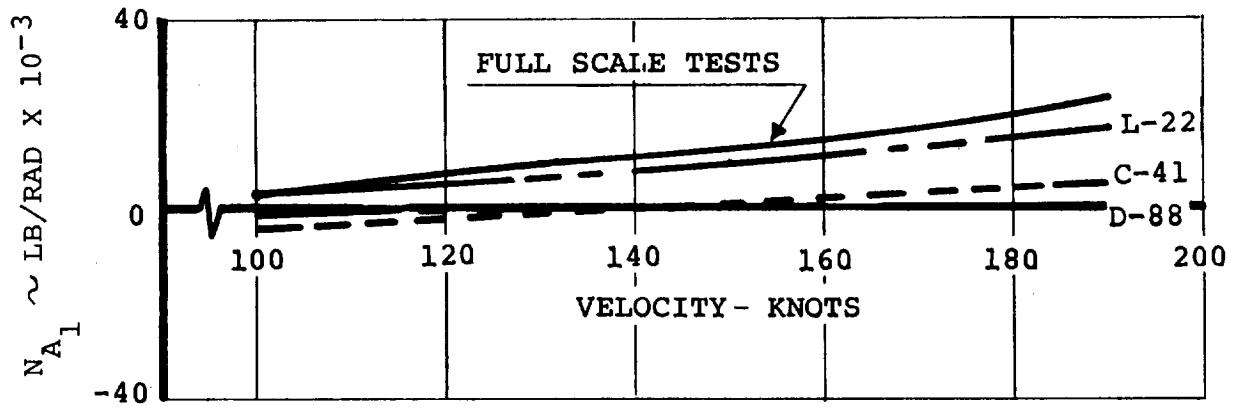


Figure 7.6. Correlation of 26 Ft Rotor Test Data with Various Rotor Derivative Programs – Cyclic Force Derivatives

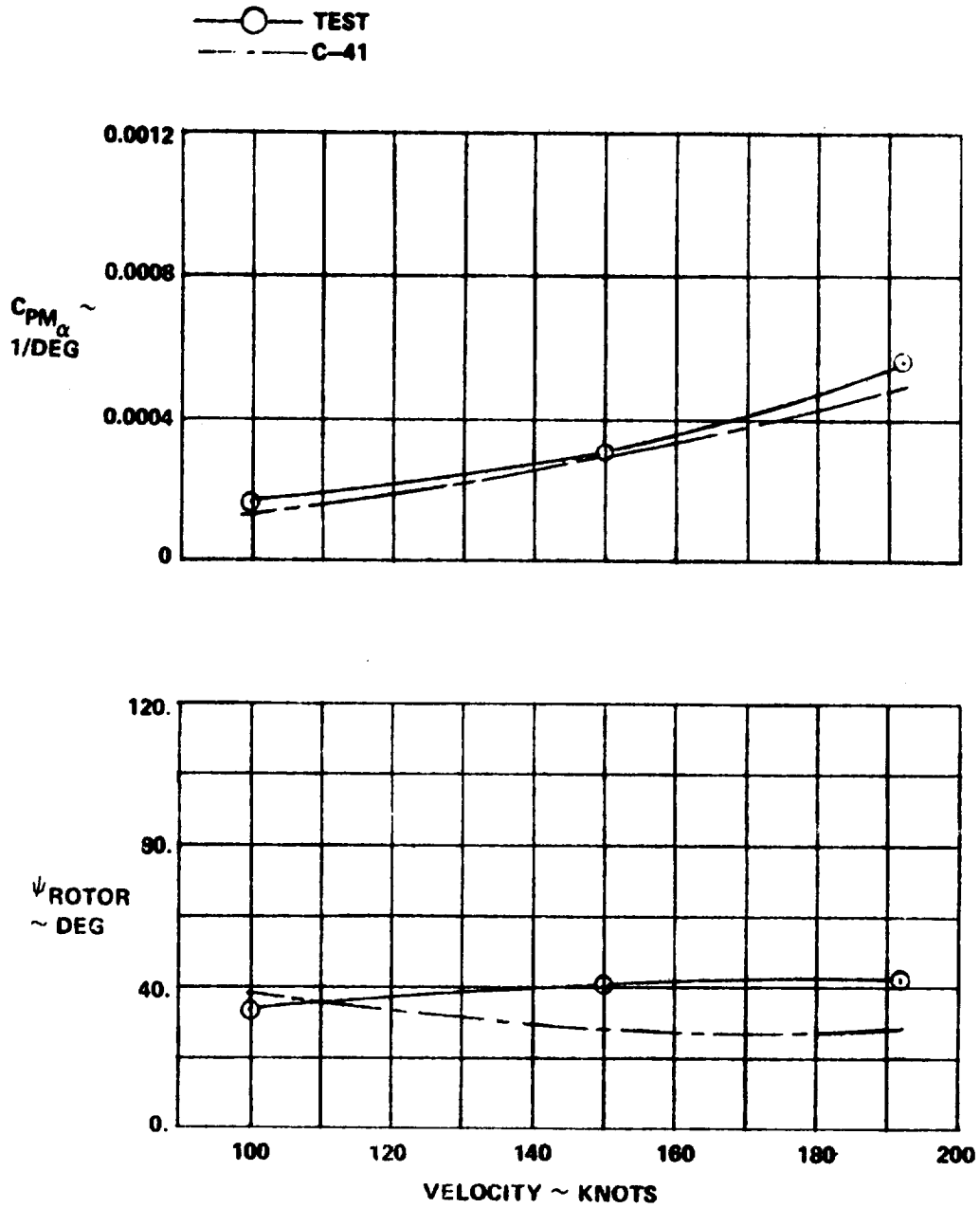


Figure 7.7. Rotor Moment and Azimuth Angle Due to Angle of Attack – Correlation with 26 Ft Rotor Data

with the model mounted on a pedestal in the tunnel. The rotors were given angles of attack to the free stream by pitching the complete model with zero sideslip angle and yawing the model at zero angle of attack. The yawing data contains minimal wing induced flow effects and comparison with the pitch data indicates the importance of induced flow on the rotor forces and moments. Forces and moments were computed for the isolated rotor and it is seen from Figure 7.8 that correlation with test data is excellent when wing induced effects are small; in Figure 7.9 wing effects introduce perceptible shifts which increase with dynamic pressure.

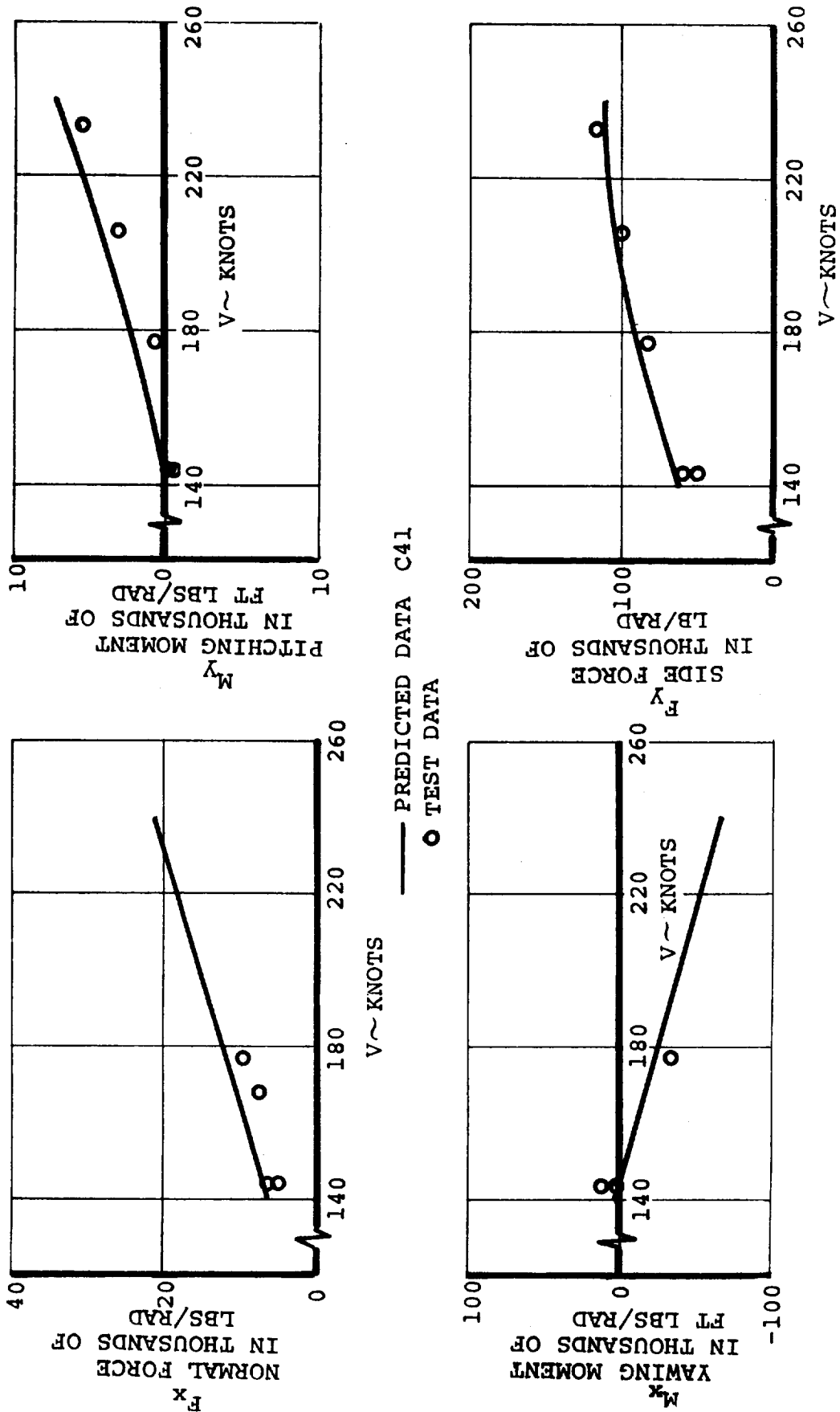


Figure 7.8. Comparison of Calculated and Test Rotor Hub Force and Moment Derivatives for M222
 1/4.622 Scale Model (Yaw Sweep) $\Omega = 386$ RPM

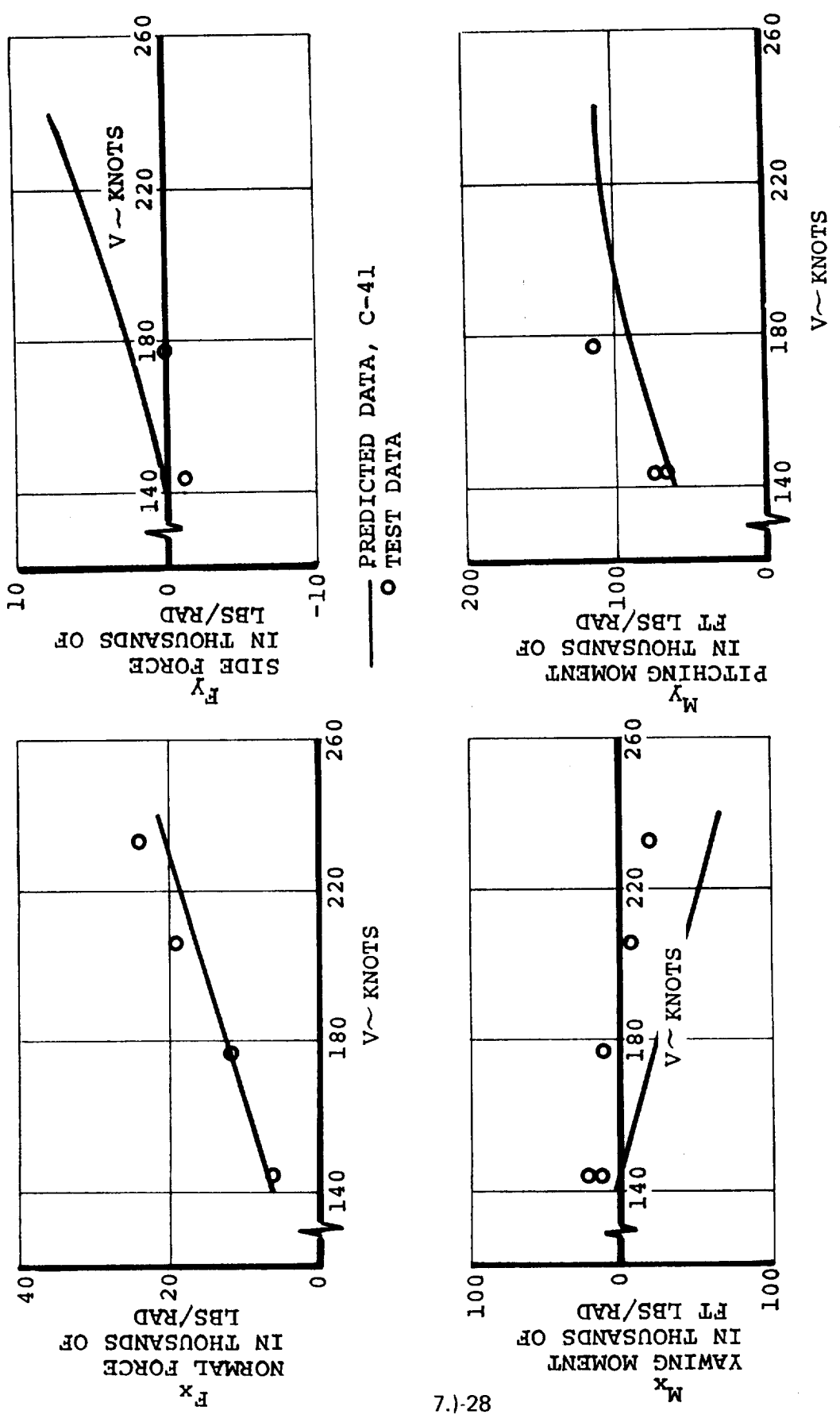


Figure 7.9. Comparison of Calculated and Test Rotor Hub Force and Moment Derivatives for M222 1/4.622 Scale Model (Pitch Sweep) $\Omega = 386$ RPM

8.0 CONTROL SYSTEM DESCRIPTION

This section describes the control system, stability augmentation systems, load alleviation system and thrust management system utilized in the mathematical model. A more complete description is given in Reference 8. .

8.1 CONTROL AERODYNAMIC CONFIGURATION

Control of the Model 222 aircraft is accomplished by utilization of longitudinal cyclic, differential longitudinal cyclic, collective and differential collective pitch, and differential nacelle tilt control in conjunction with the airplane control surfaces. The airplane control surfaces consist of conventional elevator and rudder and a flaperon and spoiler arrangement. The primary controls in each axis for each regime of flight are shown in Table 8.1.

The rotor controls provide a major portion of the control capability from hover through the low transition speed range, but airplane surface controls are operative in all regimes of flight, including hover. The rotor controls are phased out during transition as nacelle incidence decreases, speed increases, and the surface controls become more effective.

8.2 LONGITUDINAL CONTROL

Longitudinal control in hover is provided by longitudinal cyclic pitch. This is phased out through transition as the elevator becomes more effective. The elevator provides longitudinal control in the cruise mode.

TABLE 8.1 FLIGHT CONTROL MIXING

FLIGHT MODE	PRIMARY CONTROLS
<p><u>Helicopter (Hover)</u></p> <p>Pitch</p> <p>Roll</p> <p>Yaw</p> <p>Height Control</p>	<p>Longitudinal Cyclic</p> <p>Differential Collective</p> <p>Differential Longitudinal Cyclic and Differential Nacelle Tilt</p> <p>Collective/Engine Power</p>
<p><u>Transition</u></p> <p>Pitch</p> <p>Roll</p> <p>Yaw</p>	<p>Longitudinal Cyclic and Elevator</p> <p>Differential Collective, Differential Longitudinal Cyclic, Differential Nacelle Tilt, Aileron and Spoiler</p> <p>Differential Longitudinal Cyclic, Differential Nacelle Tilt, and Rudder</p>
<p><u>Airplane</u></p> <p>Pitch</p> <p>Roll</p> <p>Yaw</p>	<p>Elevator</p> <p>Aileron and Spoiler</p> <p>Rudder</p>

8.3 LATERAL CONTROL

Lateral control in hover is provided by differential collective pitch, together with differential engine fuel flow (power). The differential engine power is provided to ensure maintaining roll control in the event of a cross shaft failure. It also serves to minimize the cross shaft torque. In transition, differential collective and differential cyclic are scheduled as a function of nacelle tilt.

When differential cyclic pitch is commanded the nacelles are also actuated to tilt differentially, thereby increasing the thrust vectoring effect of the cyclic pitch. Differential deflection of the nacelles is ± 1.55 degrees per degree of cyclic plus approximately ± 0.20 degrees of differential nacelle tilt due to elasticity of wing and nacelles. This results in a large increase in control power as compared to the control power available from cyclic alone. The control power requirements may, therefore, be met with modest amounts of cyclic control resulting in low blade stresses and long rotor fatigue life. Collective pitch is also scheduled with nacelle tilt so that when the nacelles are tilted differentially, pitch is increased on the rotor whose disc is tilted down, and decreased on the rotor which is tilted up. This maintains the thrust approximately equal on the two rotors, ensuring that thrust vectoring rather than differential thrust is achieved by the differential cyclic pitch and differential nacelle tilt.

The wing has full span flaps and spoilers mounted on the trailing edge. The flaps are single slotted of 30 percent chord with a fixed hinge point 14.6 percent below the wing chord line. The flaps act as flaperons for roll control and deflect downward only by a maximum of 20 degrees from the nominal flap setting. Maximum incremental lift from the flaps is attained at approximately 35 degrees deflection and the maximum rolling moment occurs at the same time, so the flaperon deflection for roll control is limited to a maximum total flap deflection of 35 degrees. If, for example, the flaps are symmetrically deflected 30 degrees, only 5 degrees additional deflection is utilized for roll control. Full span spoilers of 12.7 percent chord are located forward of the flaps and hinged to the rear spar. The spoilers are "slot-lipped", i.e., they open up the slot forward of the flap with the flaps extended resulting in a large increase in roll control as compared to the control power with flaps closed. Maximum deflection of the spoilers for roll control is 45 degrees from the closed position.

Maximum spoiler rolling moment coefficient is also attained with flaps deflected approximately 35 degrees. Spoiler effectiveness with the flaps retracted is approximately one-third that attainable with the flaps extended. Spoiler rolling moment is further reduced at high speed by limiting the spoiler actuator force capability, thereby restricting the spoiler extension at speeds above 175 knots.

The spoilers and flaps are also used in conjunction with download alleviation devices referred to as umbrellas mounted on the leading edge of the wing for download relief in the hover and low-speed ranges. The umbrellas are 18.6 percent chord on the upper and lower wing surfaces. Maximum deflections of the surfaces for download alleviation are: flaps 70 degrees, spoilers 110 degrees from closed, and umbrellas aft-edge-of-the-upper surface up to 20 degrees from vertical and aft-edge-of-lower-surface down to 10 degrees from vertical. The umbrellas and spoilers retract at 50 knots automatically.

8.4 DIRECTIONAL CONTROL

Directional control in hover is provided by differential longitudinal cyclic pitch, which, as discussed above under lateral control, also actuates differential nacelle tilt to amplify the thrust vectoring effect of the cyclic pitch.

In transition, the differential cyclic and its associated nacelle tilt are phased out as the rudder becomes more effective. This results in near zero initial roll acceleration in response to a yaw input.

8.5 THRUST/COLLECTIVE CONTROL

In hover, forward motion of the thrust/collective lever mechanically commands both increased collective pitch and increased power. The governor provides a fine adjustment to the collective pitch to maintain rpm. Over travel of the pilot's lever, beyond the normal max power position, provides a collective

pitch landing flare capability. The over travel is entered by going through a "gate", which shuts down the rotor governor and leaves the pilot's lever directly connected to collective pitch, just like a helicopter collective pitch lever.

The collective pitch is also scheduled through transition as a function of nacelle incidence, minimizing the adjustment needed from the governor and also providing the pitch variation with differential nacelle tilt required for roll and yaw control.

In cruise the mechanical interconnection of the thrust/collective lever with collective pitch is phased out completely so that a pure power demand system with governed pitch, like a conventional fixed wing airplane, is provided. The control system block diagrams are shown in Appendix E.

8.6 CONTROL FEEL

Control force gradient variation with dynamic pressure prevents excessive sensitivity of control at high speed. In the model 222, the force gradients of the primary controls (longitudinal and lateral stick, and pedals) are varied linearly with dynamic pressure. The rudder and elevator deflections vary linearly with pilot's rudder pedal and longitudinal stick travel. Aileron deflection is programmed linearly and spoiler deflection nonlinearly with lateral stick deflection, to provide near-linear rolling moment effectiveness to near cruise speed. As mentioned earlier, spoiler deflection is limited at high speed by limiting the actuator capacity. The control force breakout forces and gradients are shown in Appendix F.

8.7 STABILITY AUGMENTATION SYSTEMS

Stability augmentation systems are provided to enhance aircraft flying qualities. The system consists of longitudinal, lateral and direction SAS. The longitudinal stability augmentation system incorporates a pitch rate feedback and a longitudinal stick pickoff. In addition, a lagged pitch rate signal is incorporated to provide some degree of attitude stabilization without the autopilot. (An autopilot is not represented in this simulation.) These signals are shaped and put through an authority limit. The longitudinal SAS commands longitudinal cyclic pitch to provide the required damping in hover and transition. It is not required in the cruise mode and is phased out at 175 knots. The block diagram of the longitudinal SAS is given in Appendix E.

The lateral stability augmentation system is operative in all flight modes. It consists of roll rate feedback for increased damping in roll, lagged roll rate feedback to provide roll attitude stability, and a lateral stick pickoff. In addition a sideslip feedback is incorporated to decrease the strong dihedral effect. These feedback loops are shaped and phased to yield good aircraft dynamic characteristics. A lateral SAS authority limit is incorporated in the circuit. The output of the lateral stability augmentation system is input to the control system in terms of equivalent lateral stick, since the drive actuator is in series with, and commands the same control as, the pilots lateral stick control linkage. The

lateral SAS never opposes the pilots' command. The block diagram of this system is shown in Appendix E.

A directional stability augmentation system is provided and operates in all flight regimes. The yaw channel consists of yaw rate feedback for increased directional damping in hover and low speed flight modes, lagged yaw rate feedback to provide yaw attitude stability, and a rudder pedal pickoff for quickening. Directional damping provided by the rotors is quite high in the higher transition and cruise speed ranges. No additional yaw rate damping is therefore needed in cruise. A feedback is provided to modify the effective yawing moment due to roll rate which exists in the basic unaugmented aircraft configuration in the cruise speed range. The feedback gains, and the relative phasing of these gains have been optimized to provide good directional dynamic response. A directional SAS authority limit is incorporated. The SAS command is input to the control system in terms of equivalent inches of rudder pedal. The block diagram for the directional stability augmentation system is shown in Appendix E.

The stability augmentation systems used for the simulation are not set up to investigate individual component failures. Modifications are required in order to do malfunction type studies with this simulation.

8.8 LOAD ALLEVIATION SYSTEM (LAS)

Propeller type aircraft experience significant blade loads during exposure to skewed flow due to steady state or transient conditions (climb, sideslip, gusts, etc). The tilt rotor configuration can have similar problems. However, since cyclic pitch is a basic part of the tilt rotor control system it provides the means to significantly reduce the sensitivities to these effects. It also can be used to reduce the destabilizing moments which come from the rotors and thus improve static stability.

An automatic load alleviation system is provided and operates via the swashplate to reduce both transient and steady state hub forces and moments and the destabilizing moments at the nacelle pivot. It is not a required system for the Model 222, but will significantly enhance the static stability and the fatigue margins of the aircraft.

The overall objectives to be achieved through the use of cyclic feedback control are:

- Reduce rotor hub forces and moments for both steady state operation and gust encounter
- Improve flying qualities of the aircraft by using the cyclic control system to reduce pilot workload and improve short period response by reducing destabilizing forces and moments of the rotors

- Reduce aircraft structural loads resulting from gust turbulence
- Improve ride qualities by damping the response to gust turbulence

The load alleviation system, as mechanized in this simulation consists of angle of attack, angle of sideslip, and dynamic pressure sensors which drive through appropriate gains and filters to reduce the longitudinal and lateral moments at the nacelle pivot. The lateral cyclic pitch used for load alleviation is authority limited and drives separate actuators in each hub. The longitudinal cyclic pitch is summed in with the longitudinal SAS. The block diagram for this system as mechanized is shown in Appendix . This system is operative from low transition speed (approx. 50 knots) through dive speed and reduces the pivot moments from 50% in the 150 to 200 knot range to 100% in all other modes of flight.

8.9 THRUST MANAGEMENT SYSTEM

The thrust and power management system for a tilt rotor aircraft must be compatible with both the helicopter and airplane configurations. Thrust control for the hover task, rpm control, gust response (especially in the cruise flight regime), and effect on aircraft flying qualities must all be considered. Classically, helicopters have used collective pitch demand to control thrust and fuel governing to control rpm while fixed-wing aircraft have used fuel flow demand to control thrust and

collective pitch governing to control rpm. Each system has its advantages. For a tilt rotor aircraft it is desirable from a practical viewpoint to have one type of governing for both the helicopter and fixed-wing flight regimes. Collective pitch governing was chosen for Model 222 for several reasons:

- It is more readily adapted to the hover flight regime than the fuel governor is to cruise
- It has better gust response characteristics
- It is fast acting and has high accuracy
- Thrust response to pilot control can be easily shaped with feed forward loops
- It has been demonstrated successfully in hover, transition and cruise in the CL-84 aircraft

With collective pitch governing there are two areas in the thrust management system to be considered: (1) style of the collective pitch governor; and (2) the feed forward loops for shaping pilot thrust control. The block diagram for this system as mechanized in this simulation is shown in Appendix E.

Several different governor configurations were considered for The M222 in order to determine the governor system best suited to meet the following objectives: (1) 0.3 percent steady state error in 2.5 to 3 seconds; (2) 2 percent rpm overshoot; and (3), satisfactory effect on aircraft flying qualities in the

all-operational mode (i.e., all aircraft components operational and performing as designed) and various failure modes. A single governor reference which used the rpm signal from each rotor and averaged them was chosen as the configuration that best satisfied the design criteria. To achieve the required accuracy and transient response goals, integral as well as proportional feedback of rpm was necessary in both the hover and cruise regimes. Governor gain is scheduled with nacelle incidence to maintain a near optimum level of governing throughout the flight envelope. Gains are varied linearly as the rotor rpm is changed from 551 in hover to 386 in cruise. The second requirement of the governor system is shaping the rotor thrust output for a pilot throttle input. Considerations in determining the proper shaping include:

- (1) throttle sensitivity;
- (2) time constant to reach 63% of steady-state thrust; and
- (3) allowable thrust overshoot

Variable pilot's control sensitivity is employed to give the optimum sensitivity in the hover power range yet maintain full power control within a reasonable throttle throw (8 inches). Shaping of the pilot command with collective quickening is done to improve the thrust time constant and thrust response transient shaping so that the pilot may perform the precision hover task with a minimum of difficulty. In the cruise regime, shaping of the thrust output is unnecessary and is phased out during transition.

The thrust/collective pitch control system is designed in such a manner that, during hover, when the pilot moves his control, he commands both a change in engine fuel setting and, mechanically, a change in collective setting. The governor then operates with a time lag to trim the collective to the value required to maintain rpm. The mechanical collective change feature is washed out as a function of nacelle incidence so that when nacelle incidence is decreased to zero, the pilot commands only engine fuel. In addition, the reference setting schedule for collective has been established to maintain equal thrust output from both rotors during application of differential nacelle tilt.

As was mentioned previously, additional details on the Model 222 control system may be obtained from Reference 8.

9.0 ENGINE REPRESENTATION

This section describes the engine performance and dynamic model representation that is used in the mathematical model. The basic engine cycle performance data consists of tabulated values of four variables: power, fuel flow, gas generator shaft rpm, and power turbine shaft rpm. These parameters are a function of Mach number and turbine inlet temperature. All data are in referred, normalized format as shown in Table 9.1. Because of the normalized, referred format, all data are valid for any ambient conditions. The effects on engine performance of operating at non-optimum power turbine speed are included in this model. The referred format also facilitates including engine thermodynamic and mechanical limits. Limitations on engine cycle operation may be input on any combination of the following: fuel flow, torque, gas generator speed, gas generator referred rpm or output shaft speed. A detailed description of this routine is in Reference 9. The flow charts which describe this routine mathematically are shown in Appendix E.

A simplified dynamic model of the Lycoming T53-L-13 engine was formulated for use in the tilt rotor mathematical model. This model was coupled to the output of the engine performance program described above. The model consists basically of 2 first order lags in series with variable time constants and gains. The output of the model is rate limited to reflect actual engine performance. This simplified model gives satisfactory

results for both large and small power transients. The block diagram for this system is shown as part of the thrust management system block diagram shown in Appendix E.

TABLE 9.1 ENGINE CYCLE DATA FORMAT

VARIABLE	SYMBOL	REFERRED, NORMALIZED FORM
Thrust	F_N	$F_N / \delta F_N^*$
Power	SHP	$SHP / \delta \sqrt{\theta} SHP^*$
Gas Generator rpm	N_I	$N_I / \sqrt{\theta} N_I^*$
Power Turbine rpm	N_{II}	$N_{II} / \sqrt{\theta} N_{II}^*$
Fuel Flow	W_F	$W_F / \delta \sqrt{\theta} F_N^*$
Turbine Inlet Temperature	T	$W_F / \delta \sqrt{\theta} SHP^*$ T / θ
Where:	<p>* = Max. Power Setting, Static, Sea Level, Standard Day</p> <p>θ = Ambient Temperature ($^{\circ}R$) Divided by 518.69$^{\circ}R$</p> <p>δ = Ambient Pressure (psia) Divided by 14.696 psia</p>	

10.0 GROUND EFFECTS

The effects of operating near the ground on the rotors and airframe are included in this model. The presence of the ground on the airframe imposes a boundary condition which inhibits the downward flow of air normally associated with the lifting action of the wing and tail. The reduced downwash has three main effects;

- A reduction in the downwash angle at the tail
- An increase in the wing lift curve slope
- An increase in the tail lift curve slope

These have been accounted for by the methods given in Reference 10 Appendix B-7. The data given in the reference for the change in wing and tail lift curve slope has been used directly. The equation specified for the change in downwash angle at the tail due to ground proximity was modified for convenience. The equation as stated is:

$$\frac{(\Delta\varepsilon)_g}{\varepsilon} = \frac{b_1^2 + 4(h-H)^2}{b_1^2 + 4(h+H)^2}$$

where $(\Delta\varepsilon)_g$ = the change in tail downwash angle due to ground proximity

ε = the downwash remote from ground

h = the height of the tail root quarter chord point above the ground

H = the height of the wing root quarter chord point above the ground

b_1 = a function of wing lift and wing flap geometry

For this mathematical model, the b_1 in the above equation was taken to be equal to the wing span, b_w . This results in a small error in the change in horizontal tail downwash. It is, however, sufficiently accurate for this simulation.

Ground effects on the rotor are difficult to predict analytically, especially in forward flight. Wind tunnel test data for the Model 160 powered model, Reference 6 was plotted as a thrust ratio versus effective rotor height/diameter ratio, for two rotor advance ratios. This data, shown in Figure 10.1 was curve fit and linearly interpolated for advance ratio. The resulting equation is as follows: - (for the right rotor. The left rotor is identical except for subscripts)

$$\left(\frac{T_{IGE}}{T_{OGE}} \right)_{RR} = \left[\left(\frac{h}{D} \right)_{EFF}^2 (.1741 - .6216 \mu_{RR}) + \left(\frac{h}{D} \right)_{EFF} (1.4779 \mu_{RR} - .4143) + 1.2479 - .8806 \mu_{RR} \right]$$

where $\left(\frac{h}{D} \right)_{EFF} = \frac{2R[|\sin(\theta + i_{NR})\cos\phi| + .0174]}{h_{RR}}$

$$h_{RR} = -Z_{DOWN} + (L_S \cos i_{NR} - X_{CG}) \sin \theta + [(L_S \sin i_{NR} + Z_{CG}) \cos \phi - Y_N \sin \phi] \cos \theta$$

= Rotor hub height above the ground

- L_S = Distance from the nacelle pivot to the rotor hub
- X_{CG} = Longitudinal distance from the pivot to the CG
- Z_{CG} = Vertical distance from the pivot to the CG
- θ = Aircraft pitch attitude
- ϕ = Aircraft roll attitude
- i_{NR} = Right rotor nacelle angle
- Y_N = Wing semispan

$$\left(\frac{T_{IGE}}{T_{OGE}}\right) = \left[\left(\frac{h}{D}\right)_{EFF}^2 (.1741 - .6216\mu) + \left(\frac{h}{D}\right)_{EFF} (1.4779\mu - .4143) + 1.2479 - .8806\mu\right]$$

NOTE: If $\mu > 0.283$; $\left(\frac{T_{IGE}}{T_{OGE}}\right) = 1.0$
 or
 If $\left(\frac{h}{D}\right)_{EFF} > 1.3$; $\left(\frac{T_{IGE}}{T_{OGE}}\right) = 1.0$

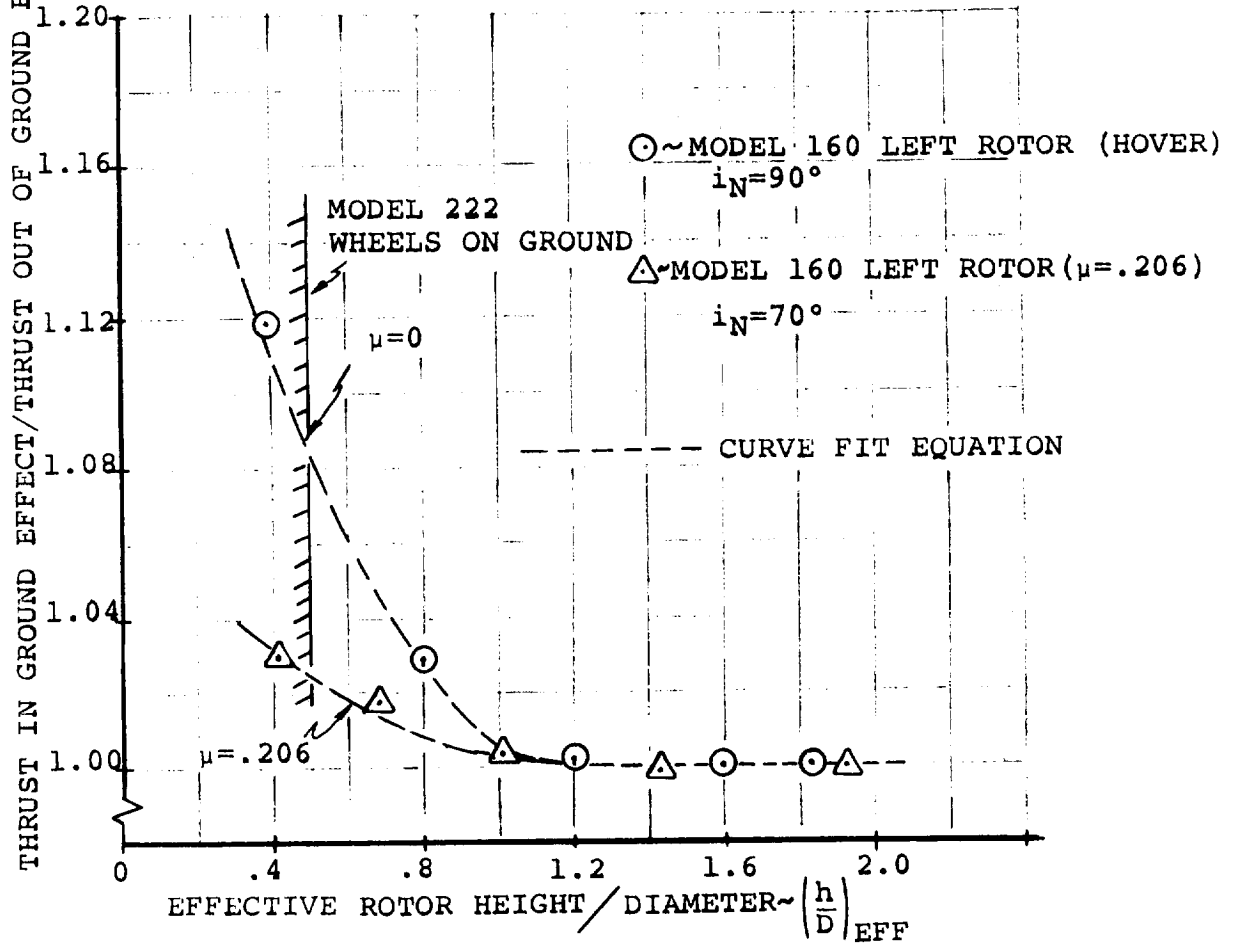


Figure 10.1. Effect of Rotor Height on Thrust Augmentation Ratio

The equation for the effective rotor height to diameter ratio $(h/D)_{EFF}$ was derived by dividing the rotor hub height by $[\sin(\theta+i_N)\cos \phi]$. This yields the rotor height along the shaft. For the cruise condition the hub height is infinite, $(h/D)_{EFF}$ is infinite and the augmentation ratio due to ground effect is unity. Some special conditions which must be observed when using these equations are noted in Figure 10.1.

11.0 AIRFRAME REPRESENTATION (PREPROCESSOR)

An airframe representation/preprocessor calculation is included in the mathematical model that enables the user to input the location of major structural elements of the aircraft in terms of water line, butt line and station line location. All lengths, center of gravity distances and inertias used in the equations are then calculated. This feature enables the user to quickly change the location of major structural elements to assess their impact on vehicle response.

In the derivation of the basic equations of motion, the aircraft was divided into three principal mass elements. The fuselage mass element (m_f), the wing mass element (m_W) and the tilting nacelle mass element (m_N). The components of the three mass elements are shown below and are available from a standard mass properties buildup of the Model 222.

- fuselage mass element (m_f) { Fuselage and contents
Horizontal tail and contents
Vertical tail and contents
Crew and trapped liquids
Cargo
- wing mass element (m_W) { Wing and contents
Fuel carried in wing
Fixed nacelles and/or engines
- tilting nacelle mass element (m_N) { Tilting nacelle (including rotors)

These three mass elements along with their respective distances from the nacelle pivot to the center of each mass element are used to compute the aircraft center of gravity distances with

The quantities required to compute m_f , l_f , m_w , l_w , m , l , m_N , λ , h_f , h_w are available from an aircraft three-view drawing and a standard mass properties buildup. The quantities l and λ (defined in the sketch) are easily obtainable from a drawing. The mass quantities (m , m_N , m_f , m_w) are computed from a mass properties buildup by adding up the components of each mass element as described in the previous paragraph. The lengths l_f , l_w , h_f and h_w are computed by summing the weight moments of the components of each mass element about the nacelle pivot. The equations for these operations have been derived and are presented in Appendix E under the preprocessor equations. The input data to these equations include the weight of each component, and its location in terms of water line, fuselage station line, and butt line.

When the center of gravity distance of each mass element has been determined, the component and total aircraft mass moments of inertia can be computed. The equations for the total aircraft mass moments of inertia are presented in Appendix C. The moments of inertia of each mass element are computed by application of the parallel axis theorem. The moments of inertia of each component about its own center of gravity must be known. The parallel axis theorem states:

$$I_{xx} = \sum_{i=1}^N [I_{xxO_i} + m_i (y_i^2 + z_i^2)]$$

$$I_{YY} = \sum_{i=1}^N \left[I_{YYO_i} + m_i (z_i^2 + x_i^2) \right]$$

$$I_{ZZ} = \sum_{i=1}^N \left[I_{ZZO_i} + m_i (x_i^2 + y_i^2) \right]$$

$$I_{XZ} = \sum_{i=1}^N \left[I_{XZO_i} + m_i (x_i z_i) \right]$$

where N represents the number of component masses.

These equations have been expanded to compute the moments of inertia of each mass element and are shown in Appendix E under the preprocessor section. The only additional input data required are the inertias of each component about their own centers of gravity. These are readily available from the mass properties buildup of the Model 222.

Other lengths required for the mathematical model are computed in this section. The input data for these computations are in terms of the water line, butt line and fuselage station line locations of the elements in question.

12.0 AERO-ELASTIC REPRESENTATION

Two aero-elastic degrees of freedom are included in the tilt rotor mathematical model. These are first mode wing vertical bending and first mode wing torsion. The stability and control characteristics of flexible airplanes may be significantly influenced by distortions of the structure under transient loading conditions. When the separation in frequency between the elastic degrees of freedom and the rigid body motions is not large, then significant aerodynamic and inertial coupling can occur between the two. Many of the important effects of elastic distortion, however, can be accounted for simply by modifying the aerodynamic equations. The assumption is made that the changes in aerodynamic loading take place so slowly that the structure is at all times in static equilibrium. This is equivalent to assuming that the natural frequencies of vibration of the structure are much higher than the frequencies of the rigid body motions. Thus a change in load produces a proportional change in the shape of the airplane, which in turn influences the load. This is known as the method of "quasistatic" deflections where all the coupling occurs in the aerodynamic equations.

The wing uncoupled natural frequencies were investigated to determine which method would be used. Table 12.1 shows the

TABLE 12.1 WING UNCOUPLED FREQUENCIES (BLADES OFF)
CRUISE CONFIGURATION

<u>Symmetric Mode</u>	<u>Frequency</u>
Vertical Bending	3.6 cps
Chordwise Bending	5.4 cps
Torsion	6.1 cps
<u>Antisymmetric Mode</u>	<u>Frequency</u>
Vertical Bending	11.2 cps
Chordwise Bending	9.1 cps
Torsion	5.7 cps

Model 222 wing uncoupled frequencies for the cruise condition for both the symmetric and anti-symmetric modes. As can be noted in the table, the lowest vertical bending frequency is 3.6 cps and the lowest wing torsional frequency is 5.7 cps. The rigid body short period mode varies from approximately 0.40 cps to 1.35 cps. Since the rigid body short period modes are separated from the elastic modes by a substantial margin, the method of "quasistatic" deflection is used to represent the wing bending and torsion modes, with the only coupling in the aerodynamic terms (through angle of attack). The wing twists and bends instantaneously when subjected to an applied load. The assumptions made in deriving the wing bending and torsion relationships are as follows:

- No coupling between bending and torsion modes
- Wings are cantilevered from the fuselage
- Elliptical loading assumed for the rigid untwisted wing
- Aerodynamic loads act at the wing quarter chord
- Wing elastic axis coincident with cross shaft
- Wing center of mass assumed to lie on the elastic axis
- First wing torsional mode assumed linear from tip to root

In the mathematical model, wing twist at the tip is calculated using the following equation:

$$K_{\theta_t} \theta_t = M_{ACT} - I_E \Omega_E R + q \frac{c_w^2 b_w}{C_w} C_{m_0} + q C_w^2 \left(\frac{dC_{m_c/4}}{dC_l} + \frac{x_{WAC}}{C_w} \right) \left(\frac{C_{L_\alpha}^2 b_w}{6\pi} \right) (4\theta_t + 3\pi \alpha_{RIGID})$$

where: K_{θ_t} = Wing torsional spring constant

θ_t = Wing twist angle in degrees

M_{ACT} = Nacelle actuator pitching moment

I_E = Engine inertia

Ω_E = Engine speed

R = Body yaw rate

q = Dynamic pressure

c_w = Wing reference chord

b_w = Wing reference span

C_{m_0} = Wing zero lift pitching moment coefficient

$\frac{dC_{m_c/4}}{dC_l}$ = Wing pitching moment slope with lift coefficient

C_{L_α} = Wing lift curve slope

α_{RIGID} = Wing angle of attack without twist

Assuming a linear mode shape from the wing tip to the root and a cantilevered wing (zero twist at root), the wing twist at the aerodynamic center location of the wing is obtained by linear interpolation. The wing twist represents the change in angle of attack of the wing tip and aerodynamic center and are used in the aerodynamic equations.

Wing vertical bending deflection is also treated on a "quasi-static" basis. The form of the equation used in the mathematical model for the wing tip deflection is as follows:

$$h_1 = K_{W_1} Z_{AERO}^N + K_{W_2} Z_{AERO}^W - K_{W_3} L_{AERO}^N - K_{W_4} \bar{a}_T - K_{W_5} \bar{a}_{WAC}$$

where: h_1 = Wing tip deflection
 Z_{AERO}^W = Wing lift
 Z_{AERO}^N = Total wing lift
 L_{AERO}^N = Nacelle rolling moment
 \bar{a}_T = Vertical acceleration of the nacelle
 \bar{a}_{WAC} = Vertical acceleration of the wing aerodynamic center
 $K_{W_1} \rightarrow K_{W_5}$ = Constants for Model 222 wing

The form of the equation for the wing deflection at the aerodynamic center is written similarly:

$$h_{1_{WAC}} = K_{W_6} Z_{AERO}^N + K_{W_7} Z_{AERO}^W - K_{W_8} L_{AERO}^N - K_{W_9} \bar{a}_T - K_{W_{10}} \bar{a}_{WAC}$$

The symbols represent the same quantities as the tip deflections except the quantities K_{W_6} to $K_{W_{10}}$ are different from K_1 to K_5 .

These equations are derived in Appendix A. Since the wings are assumed cantilevered, these equations may be written for

the left and right sides. The equations as used in the mathematical model are written in Appendix E.

The wing tip and aerodynamic center vertical bending velocities are computed by dividing the change in vertical bending deflection by the simulation time frame. The vertical bending deflections and velocities are then added to the velocity components at the wing tip and aerodynamic center. These velocity components are then used in the calculation of the aerodynamic angle of attack.

In addition to the aerodynamic coupling via angle of attack, as discussed above, the wing tip vertical forces and moments act as the driving functions to a set of second order equations that are forced at the wing vertical bending frequency. This results in giving the pilot a "seat of the pants" feel for the vibratory aspects of the wing vertical bending mode. The equations were written in this manner to see if the pilot could induce a P.I.O. (pilot induced oscillation) during the piloted simulations due to wing vertical bending.

13.0 CONCLUSIONS AND RECOMMENDATIONS

1. Formulation of an eleven degree of freedom tilt rotor mathematical model and setting up an in-house hybrid simulation program using this model have been successfully completed.
2. The simulation model has been successfully checked out and validated at the Ames Research Center.
3. The in-house simulation model is "real time" and executes in 40 milliseconds. The Ames simulation is also real time with a 50 millisecond time frame. This increased time is due to the all digital nature of the Ames simulation.
4. It is desirable to shorten the frame time of the simulation. This may be accomplished by streamlining the following elements of the mathematical model:
 - Slipstream aerodynamics
 - Input aerodynamic data in body axes rather than wind axes to eliminate axes transforms
5. The simulation could be improved by incorporating advances in methodology in such areas as:
 - Rotor Representation - Formulate a simplified analytical model to adequately represent the dynamics and aerodynamics of soft-in-plane hingeless

rotors for all flight regimes. This would avoid the necessity for complex time-consuming table look ups of rotor data.

- Slipstream Aerodynamics - Simplify the analytical representation based on wind tunnel test data.
- Interference Effects - Improve the prediction of the tail downwash environment at low transition speeds.

14.0 REFERENCES

1. USAF Stability and Control DATCOM, Air Force Flight Dynamics Laboratory, October 1960, (Revised September 1970).
2. Reed, T. J., "User Report" Prop/Rotor Dynamic Derivative Program C41 J.N.", Boeing Document D210-10116-1, Vertol Division, The Boeing Company, Philadelphia, Pa., June 1970.
3. Amos, A. K.; Miao, W., "Program C-49: Rotor Stability Derivatives", Boeing Interoffice Memorandum, 8-7453-1-2483, Vertol Division, The Boeing Company, Philadelphia, Pa., July 1971.
4. Davenport, F. J., "Analysis of Propeller and Rotor Performance in Static and Axial Flight by an Explicit Vortex Influence Technique", Boeing Document R-372, Boeing Company, Vertol Division, Philadelphia, Pa., February 1965.
5. Tarzanin, F. and Thomas, E., "Aeroelastic Rotor Analysis", Boeing Document D8-0614, Boeing Company, Vertol Division, Philadelphia, Pa., May 1967.
6. Magee, J. P., et al, "Test Program II, Wind Tunnel Test of a Powered Tilt Rotor Performance Model, Volume VI, Results and Analysis", Boeing Document D213-10000-6, Boeing Company, Vertol Division, Philadelphia, Pa., August 1970.
7. Smith, M. C., "University of Maryland Wind Tunnel Test 489, Force, Moment and Downwash Measurements on a Rigid Rotor

and Semispan Wing", (4 volumes), Boeing Document D8-1062-1, The Boeing Company, Vertol Division, Philadelphia, Pa., March 1968.

8. "Study of V/STOL Tilt Rotor Research Aircraft Program (Phase I)", Volumes II and III, Prepared under contract NAS2-7259 for NASA, Ames Research Center, Boeing Vertol Company, Philadelphia, Pa., January 1973.
9. Schoen, A. H., "User's Manual for VASCOMP II, The V/STOL Aircraft Sizing and Performance Computer Program", Boeing Document D8-0375, Volume VI, Boeing Company, Vertol Division, Philadelphia, Pa., March 1968.
10. Etkin, Bernard, "Dynamics of Flight", John Wiley and Sons, Inc., 1959.
11. Heyson, Harry H. and Katzoff, S.; "Induced Velocities Near a Lifting Rotor with Non-uniform Disk Loading", NACA Report 1319, December 7, 1956.
12. Allen, H.J. and Perkins, E.W., "A Study of Effects of Viscosity on Flow Over Slender Inclined Bodies of Revolution", NACA TR 1048, 1951.

APPENDIX A - TREATMENT OF WING FLEXIBILITY

As described in Section 12 the large separation which exists between the natural frequencies of vibration of the wing structure and the aircraft rigid body motions, enables the elastic deformations of the wing structure to be calculated on a quasi-static basis.

In the simple treatment presented below, the bending and torsion modes are considered to be uncoupled. The wing is treated as a cantilever with a built-in root end. The wing is free to twist about the elastic axis which is assumed to coincide with the nacelle pivot line. The center of mass of each chordwise strip is also taken to lie on the pivot line. The unloaded wing has neither geometric nor aerodynamic twist.

WING TWIST

Spanwise twisting of the wing takes place under the action of the nacelle aerodynamic and inertial moments, the wing lift distribution, and the spanwise distribution of aerodynamic pitching moment. The nacelle aerodynamic moments consist of rotor hub loads, transferred to the pivot, together with the aerodynamic loads on the nacelle itself. Nacelle inertial moments include the gyroscopic effects of the rotor drive system.

With reference to Figure A.1, M_N is the moment supplied or absorbed by the nacelle tilt actuator. If K_θ is the wing stiffness as seen by the wing tip, then

$$M_N = K_\theta \theta_T \quad (A-1)$$

The total moment about the elastic axis due to wing aerodynamics, nacelle loads and engine gyroscopic torque is

$$T = \int_0^{b/2} m \, dy + M_N + M_{gyro} \quad (A-2)$$

The aerodynamic moment about the elastic axis at any station y is given by

$$m = m_{c/4} + \ell x \quad (A-3)$$

where ℓ is the section lift and x is the distance from the quarter chord to the elastic axis. In terms of the section aerodynamic coefficients,

$$m(y) = \frac{1}{2} \rho V^2 c^2 C_{m_{c/4}} + \frac{1}{2} \rho V^2 c^2 C_\ell \frac{x}{c} \quad (A-4)$$

The section lift coefficient, C_ℓ , is given by

$$\begin{aligned} C_\ell &= k \frac{dC_\ell}{d\alpha} (\alpha - \alpha_o) \sqrt{1 - \left(\frac{2y}{b}\right)^2} \\ &= k a_o (\alpha_R - \epsilon_p - \alpha_o + \theta_t(y)) \sqrt{1 - \left(\frac{2y}{b}\right)^2} \end{aligned} \quad (A-5)$$

where α_R is the wing root section angle of attack
 ϵ_p is the rotor induced downwash, assumed constant spanwise
 α_o is the section zero-lift angle
 θ_t is the structural twist at station y

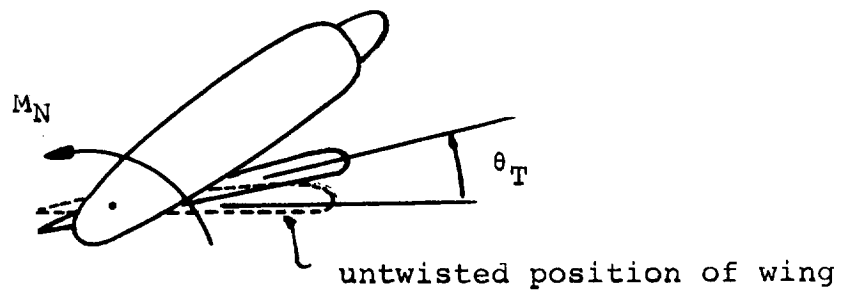
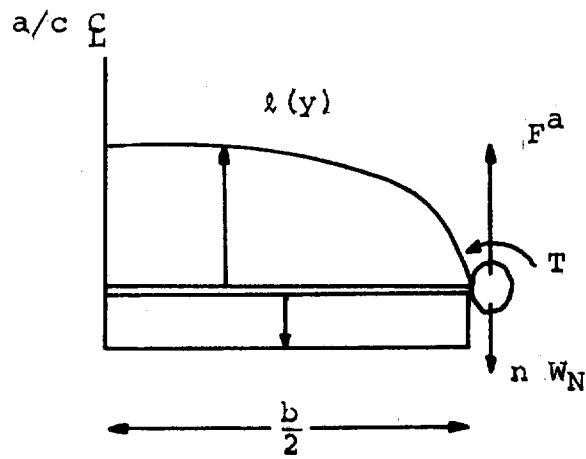


Figure A.1. Wing Geometry for Derivation of Flexibility

The factor $k\sqrt{1-\left(\frac{2y}{b}\right)^2}$ is introduced so that, for the untwisted wing, the lift distribution is elliptical. The value of k is obtained from the rigid wing elliptical loading as

$$k = \frac{4}{\pi} \frac{C_{L\alpha}}{a_0} \quad (A-6)$$

Thus the equation for C_ℓ becomes, with $\alpha_{RIGID} = \alpha_R - \epsilon \bar{p} \alpha_0$,

$$C_\ell = \frac{4}{\pi} C_{L\alpha} \left[\alpha_{RIGID} \sqrt{1-\left(\frac{2y}{b}\right)^2} + \theta_t \sqrt{1-\left(\frac{2y}{b}\right)^2} \right] \quad (A-7)$$

In equation (A-4) we can write, for low angles of attack,

$$C_{m_{c/4}} = C_{m_0} + \frac{dC_{m_{c/4}}}{dC_\ell} C_\ell \quad (A-8)$$

and therefore

$$m(y) = \frac{1}{2} \rho V^2 c^2 \left\{ C_{m_0} + \left(\frac{dC_{m_{c/4}}}{dC_\ell} + \frac{x}{c} \right) C_\ell \right\} \quad (A-9)$$

The equation for the total wing twisting moment, equation (A-2), can now be written as,

$$T = M_{actuator} + M_{GYRO} + \frac{1}{4} \rho V^2 c^2 C_{m_0} b + \frac{1}{2} \rho V^2 c^2 \left(\frac{dC_{m_{c/4}}}{dC_\ell} + \frac{x}{c} \right) \int_0^{b/2} C_\ell dy \quad (A-10)$$

Using equation (A-7), assuming a linear structural twist from root to tip and performing the indicated integrations, the equation for total wing twisting moment becomes

$$T = K_\theta \theta_T = M_{actuator} + M_{gyro} + \frac{1}{4} \rho V^2 b c^2 C_{m_0} + \frac{1}{2} \rho V^2 c^2 \left(\frac{dC_{m_{c/4}}}{dC_\ell} + \frac{x}{c} \right) \times \frac{C_{L\alpha} b}{6\pi} \left(3\pi \alpha_{RIGID} + 4\theta_T \right) \quad (A-11)$$

The equation for the actuator moment is given in the equations of motion, Section 5.0.

Rearranging, and writing $q = q_s (1-C_{T_s}) = \frac{1}{2} \rho V^2$

$$\theta_T = \frac{M_N + M_{gyro} + \frac{1}{2} q_s (1-C_{T_s}) c_w^2 \left[6\pi\alpha \text{ rigid} \left(\frac{dC_m}{dC_L} + \frac{x}{c} \right) + b_w C_{m_0} \right]}{K_\theta - \frac{2}{3\pi} q_s b_w c_w^2 C_{L_\alpha} (1-C_{T_s}) \left(\frac{dC_m}{dC_L} + \frac{x}{c} \right)} \quad (A-12)$$

where C_{m_0} , the zero-lift wing section pitching moment coefficient, is a function of flap deflection:

$$C_{m_0} = C_1 + C_2 \delta_f + C_3 \delta_f^2 \quad (A-13)$$

Knowing the tip value of twist, the twist at any other spanwise station is obtained by assuming a linear variation of twist from zero at the root to the tip value.

WING VERTICAL BENDING

The spanwise bending moment at any spanwise station y , on the wing is the sum of the bending moments due to wing aerodynamic lift, wing weight, nacelle lift, nacelle weight and net torque on the nacelle. The expressions for each contribution to the bending moments are derived below.

- Bending moment due to wing loading.

Assuming an elliptical distribution of lift the bending moment is given by

$$\begin{aligned} M^a(y_1) &= \int_{y_1}^{b/2} \ell(y) (y-y_1) dy \\ &= \frac{\ell_0 b^2}{4} \int_{y_1}^{b/2} \sqrt{1 - \left(\frac{2y}{b}\right)^2} \left(\frac{2y}{b} - \frac{2y_1}{b}\right) d\left(\frac{2y}{b}\right) \end{aligned} \quad (A-14)$$

where ℓ_0 is the lift per unit length at the wing root. Introducing the spanwise variable $\theta = \cos^{-1}\left(\frac{2y}{b}\right)$ making the required substitutions and integrating, the bending moment at any point y is:

$$M^a(y) = \frac{\ell_0 b^2}{4} \left[\frac{1}{2} (\sin \theta - \theta \cos \theta) - \frac{1}{6} \sin^3 \theta \right] \quad (A-15)$$

● Bending due to nacelle net vertical load.

The net vertical force on nacelle is

$$F = F^a - nW_N$$

where F^a is the aerodynamic force and nW_N is the inertial load on the nacelle. The bending moment due to nacelle force is

$$M^N(y) = \frac{Fb}{2} (1 - \cos \theta) \quad (A-16)$$

● Bending due to wing weight.

Assuming a uniform distribution of wing weight

$$M^W(y_1) = -n \int_{y_1}^{b/2} w(y) (y - y_1) dy$$

and $w(y) = 2W/b$ where W is the weight of one wing panel

$$\therefore M^W(y_1) = \frac{2nW}{b} \int_{y_1}^{b/2} (y - y_1) dy \quad (A-17)$$

i.e.
$$M^W(y) = -\frac{nWb}{2} (1 - \cos \theta - \frac{1}{2} \sin^2 \theta)$$

● Bending due to nacelle torque (rolling moment)

$$T(y) = \text{constant} = T \quad (A-18)$$

Total bending moment at station y is therefore

$$M(y) = M^a(y) + M^N(y) + M^W(y) + T \quad (A-19)$$

Assuming a linear variation of EI from root to tip given by

$$EI(y) = EI_0 \left[1 - a \left(\frac{2y}{b} \right) \right] = EI_0 (1 - a \cos \theta), \quad (A-20)$$

the curvature of the wing due to bending is

$$\begin{aligned} \frac{M(y)}{EI(y)} = \frac{d^2z}{dy^2} = & \frac{L_0 b^2}{8EI_0} \left[\frac{(\sin \theta - \theta \cos \theta) - \frac{1}{3} \sin^3 \theta}{1 - a \cos \theta} \right] + \frac{F_a b}{2EI_0} \left[\frac{1 - \cos \theta}{1 - a \cos \theta} \right] \\ & - \frac{nW_N b}{2EI_0} \left[\frac{1 - \cos \theta}{1 - a \cos \theta} \right] - \frac{nW_w b}{2EI_0} \left[\frac{1 - \cos \theta - \frac{1}{2} \sin^2 \theta}{1 - a \cos \theta} \right] \\ & + \frac{T}{EI_0} \left[\frac{1}{(1 - a \cos \theta)} \right] \end{aligned} \quad (A-21)$$

Double integration of this equation yields the following expression for the bending deflection of the wing at any point y on the span:-

$$\begin{aligned} z(y) = & \frac{Lb^3}{8\pi EI_0} \phi_1 + \frac{b^3 F_a}{8EI_0} \phi_2 - \frac{nW_N b^3}{8EI_0} \phi_3 \\ & - \frac{nW_w b^3}{8EI_0} \phi_4 + \frac{Tb^3}{4EI_0} \phi_5 \end{aligned} \quad (A-22)$$

$$\text{where } \phi_1 = \int_0^Y \left\{ \int_0^Y \frac{(\sin \theta - \theta \cos \theta) - \frac{1}{3} \sin^3 \theta}{1 - a \cos \theta} dy \right\} dy$$

$$\phi_2 = \phi_3 = \int_0^Y \left\{ \int_0^Y \frac{1 - \cos \theta}{1 - a \cos \theta} dy \right\} dy$$

$$\phi_4 = \int_0^Y \left\{ \int_0^Y \frac{1 - \cos \theta - \frac{1}{2} \sin^2 \theta}{1 - a \cos \theta} dy \right\} dy$$

$$\phi_5 = \int_0^y \left\{ \int_0^y \frac{dy}{1-a \cos \theta} \right\} dy$$

and where the wing lift (2 wing panels) $L = \frac{\pi}{4} \rho_0 b$. The function ϕ_1 through ϕ_5 were obtained numerically and are presented in Figure A.2 .

$$\text{Since } L = -2 z_{\text{AERO}}^W$$

$$F^a = - z_{\text{AERO}}^N$$

$$T = - L_{\text{AERO}}^N$$

$$nW_w = \frac{1}{2} m_w \frac{z_{\text{AERO}}}{m} = \frac{1}{2} m_w \bar{a}_{\text{WAC}}$$

$$nW_N = m_N \bar{a}_T$$

where m_w is the mass of two wing panels

m is the total aircraft mass

\bar{a}_{WAC} is the acceleration of the wing aerodynamic center

\bar{a}_T is the acceleration of the wing tip

and since the values of ϕ_1 through ϕ_5 are constant for any given station y on the wing we can write the final equation for wing bending in the form

$$h_1 = K_{W_1} z_{\text{AERO}}^N + K_{W_2} z_{\text{AERO}}^W - K_{W_3} L_{\text{AERO}}^N - K_{W_4} \bar{a}_T - K_{W_5} \bar{a}_{\text{WAC}}$$

where $h_1 = -z$

$$K_{W_1} = \frac{b^3 \phi_2}{8EI_0}$$

$$K_{W_2} = \frac{b^3 \phi_1}{4\pi EI_0}$$

$$K_{W_3} = \frac{b^3 \phi_5}{4EI_0}$$

$$K_{W_4} = \frac{m_N b^3 \phi_2}{8EI_0}$$

$$K_{W_5} = \frac{m_W b^3 \phi_4}{8EI_0}$$

This is the form given in the computer representation. The bending deflection at the aerodynamic center and at the wing tip are obtained using the values of $\phi_1 \rightarrow \phi_5$ appropriate to these stations.

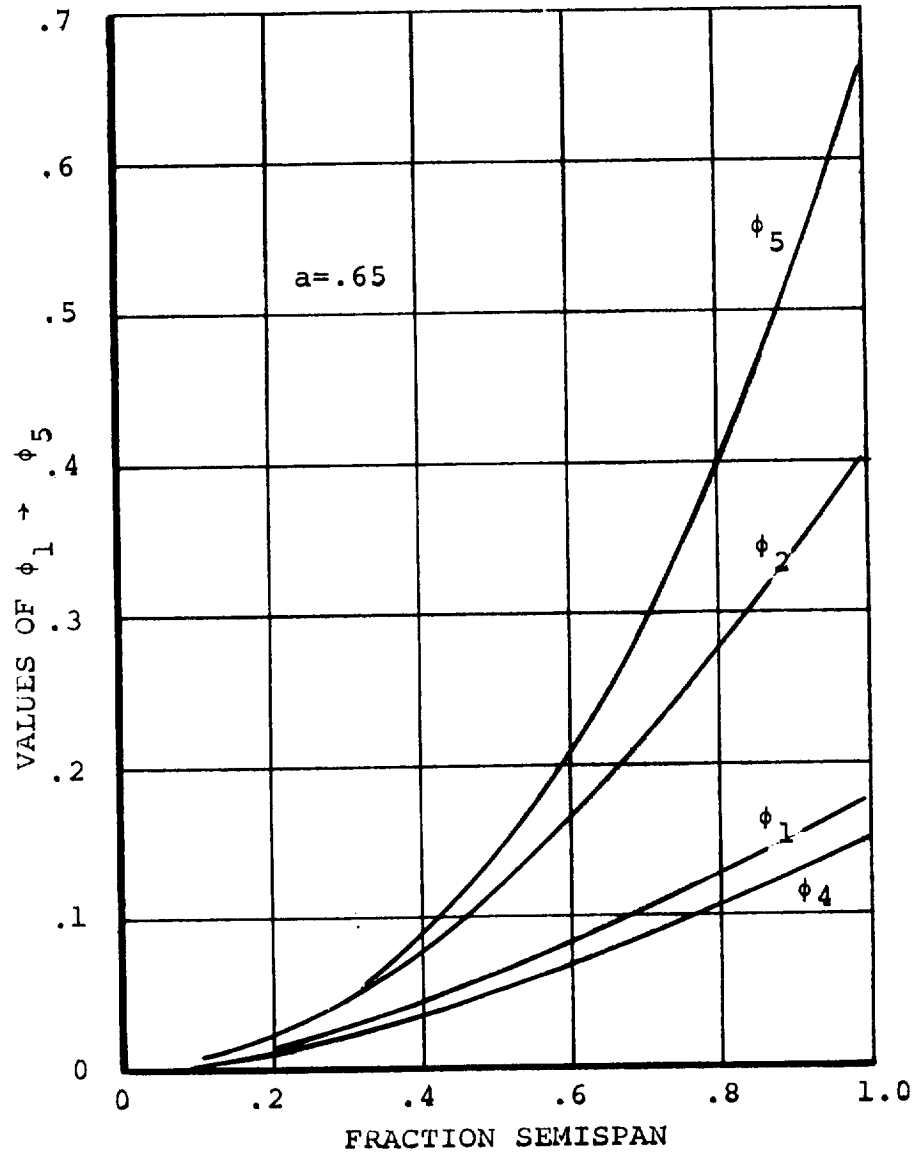


Figure A.2. Wing Bending Functions

APPENDIX B - DERIVATION OF LANDING GEAR EQUATIONS

Presented below are the equations for landing gear forces and moments arising from ground contact. The derivation accounts for brake and friction forces together with a simplified representation of the oleo dynamics. Nose wheel steering is not included.

With reference to Figure B-1 the distance from the center of gravity to the bottom of the right main wheel following a positive pitch rotation is

$$h_{\theta} = X \sin \theta - Z \cos \theta - r \quad (\text{B-1})$$

where X and Z are the coordinates of the hub of the wheel relative to the C.G. and r is the tire radius. If the aircraft is now rolled right, through the angle ϕ , the bottom of the right gear moves through a distance

$$h_{\phi} = \left[Y \sin \phi + (Z+r)(\cos \phi - 1) \right] \cos \theta \quad (\text{B-2})$$

The height of the bottom of the wheel above the ground is therefore

$$h = H_{CG} + h_{\theta} - h_{\phi} \quad (\text{B-3})$$

and the oleo deflection during ground contact is given by

$$h_T = \frac{H_{CG} + h_{\theta} - h_{\phi}}{\cos \phi \cos \theta} \quad (\text{B-4})$$

By differentiation of equation B-4 and making small angle assumptions regarding the aircraft pitch and roll angles during touchdown, the rate of change of oleo strut deflection is

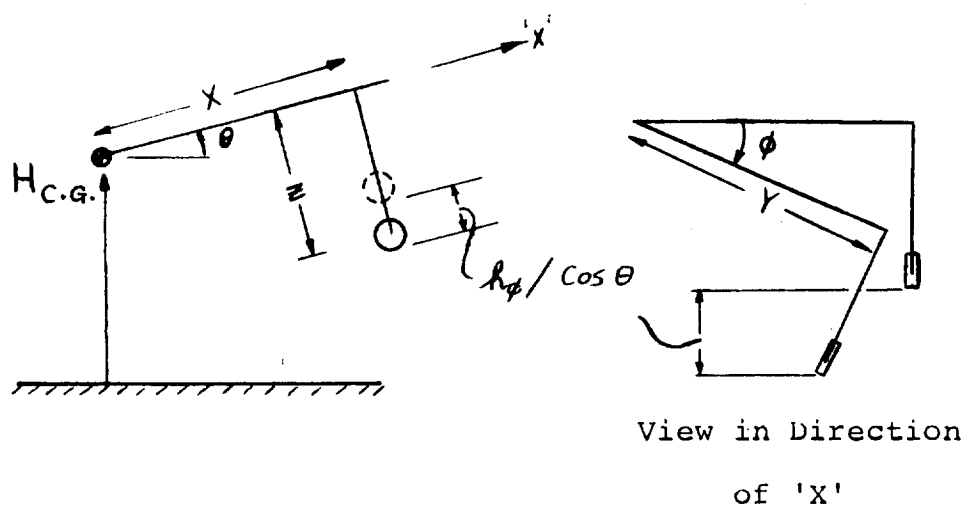


Figure B.1. Geometry of Landing Gear

obtained as

$$\dot{h}_T = \frac{\dot{h}_{CG}}{\cos \phi \cos \theta} + XQ - YP \quad (B-5)$$

Assuming that the oleo response is that of a second order system, the equation of motion for the landing gear is

$$F_G = K_{ST} h_T + D_{ST} \dot{h}_T \quad (B-6)$$

where K_{ST} and D_{ST} are the equivalent spring rates and damping for the oleo, and F_G is the force on the landing gear strut.

Tire Friction and Side Force

The friction force acting on each tire during ground contact is resolved into a force F_μ along the line of intersection of the plane of the wheel and the ground plane, positive forward, and a side force F_s at right angles to F_μ lying in the ground plane and positive to starboard. The friction force F_s is assumed to be proportional to oleo force and the amount of braking exerted by the pilot. The side force is proportional to the oleo force.

The components of tire friction are:

$$F_\mu = (\mu_0 + \mu_1 B_G) F_{GZ} \frac{u}{|u|} \quad (B-7)$$

$$F_s = \mu_s F_{GZ} \frac{v}{|v|} \quad (B-8)$$

where μ_0 , μ_1 and μ_s are the coefficients for rolling friction, brake friction and sliding friction. B_G is expressed as a percentage of full brake pedal deflection. The signs of the forward and sideways velocity are introduced to properly orient the tire forces.

The force and moment contributions of each landing gear to the aircraft total forces and moments are, assuming small angles;

$$\Delta X_n = F_{\mu_n} - F_{GZ_n} \theta \quad (B-9)$$

$$\Delta Y_n = F_{s_n} + F_{GZ_n} \phi \quad (B-10)$$

$$\Delta Z_n = F_{\mu_n} \theta - F_{s_n} \phi + F_{GZ_n} \quad (B-11)$$

$$\Delta M_n = -\Delta Z_n X_n + \Delta X_n (Z_n + r_n + h_{T_n}) \quad (B-12)$$

$$\Delta L_n = \Delta Z_n Y_n - \Delta Y_n (Z_n + r_n + h_T) \quad (B-13)$$

$$\Delta N_n = -\Delta X_n Y_n + X_n \Delta Y_n \quad (B-14)$$

where $n=1,2$ and 3 denote the left main gear, right main gear and nose gear, respectively.

The total contribution of the landing gear forces to the forces and moments at the center of gravity of the aircraft are:

$$\Delta X_{LG} = \sum_{n=1}^3 \Delta X_n$$

$$\Delta Y_{LG} = \sum_{n=1}^3 \Delta Y_n$$

$$\Delta Z_{LG} = \sum_{n=1}^3 \Delta Z_n$$

$$\Delta L_{LG} = \sum_{n=1}^3 \Delta L_n$$

$$\Delta M_{LG} = \sum_{n=1}^3 \Delta M_n$$

$$\Delta N_{LG} = \sum_{n=1}^3 \Delta N_n$$

APPENDIX C - VELOCITY AND ACCELERATION TRANSFORMATIONS AND
CENTER OF GRAVITY/INERTIA EQUATIONS

C.1 Velocity Transformations

The calculation of aerodynamic forces on wings, fuselage, nacelles and tail surfaces requires that the angle of attack and relative wind velocity at these surfaces be known. These velocities are obtained most conveniently in terms of the velocity of the pivot reference point.

With reference to Figure C.1, the velocity of a general point in the aircraft relative to the airplane center of gravity is

$$\underline{V} = \frac{\delta \underline{r}}{\delta t} + \underline{\Omega} \times \underline{r} \quad (C-1)$$

where \underline{r} is the radius vector from the c.g. to the point and $\underline{\Omega}$ is the angular velocity of the aircraft. Thus, expanding equation C-1, the velocity of the pivot relative to the c.g. is

$$\begin{aligned} u'_p &= \dot{X}_p + QZ_p - Y_p R \\ v'_p &= \dot{Y}_p - PZ_p + X_p R \\ w'_p &= \dot{Z}_p + PY_p - QX_p \end{aligned} \quad (C-2)$$

where X_p , Y_p and Z_p are the distances of the pivot from the c.g., measured positively forward, to the right and downwards, respectively. If we measure all distances from the pivot location then $X_p = -X_{CG}$, $Y_p = -Y_{CG} = 0$, $Z_p = -Z_{CG}$ and the velocity of the pivot relative to inertial space can be written,

$$\begin{aligned} u_p &= U + u'_p = U - \dot{X}_{CG} - QZ_{CG} \\ v_p &= V + v'_p = V + PZ_{CG} - X_{CG} R \\ w_p &= W + w'_p = W + QX_{CG} - \dot{Z}_{CG} \end{aligned} \quad (C-3)$$

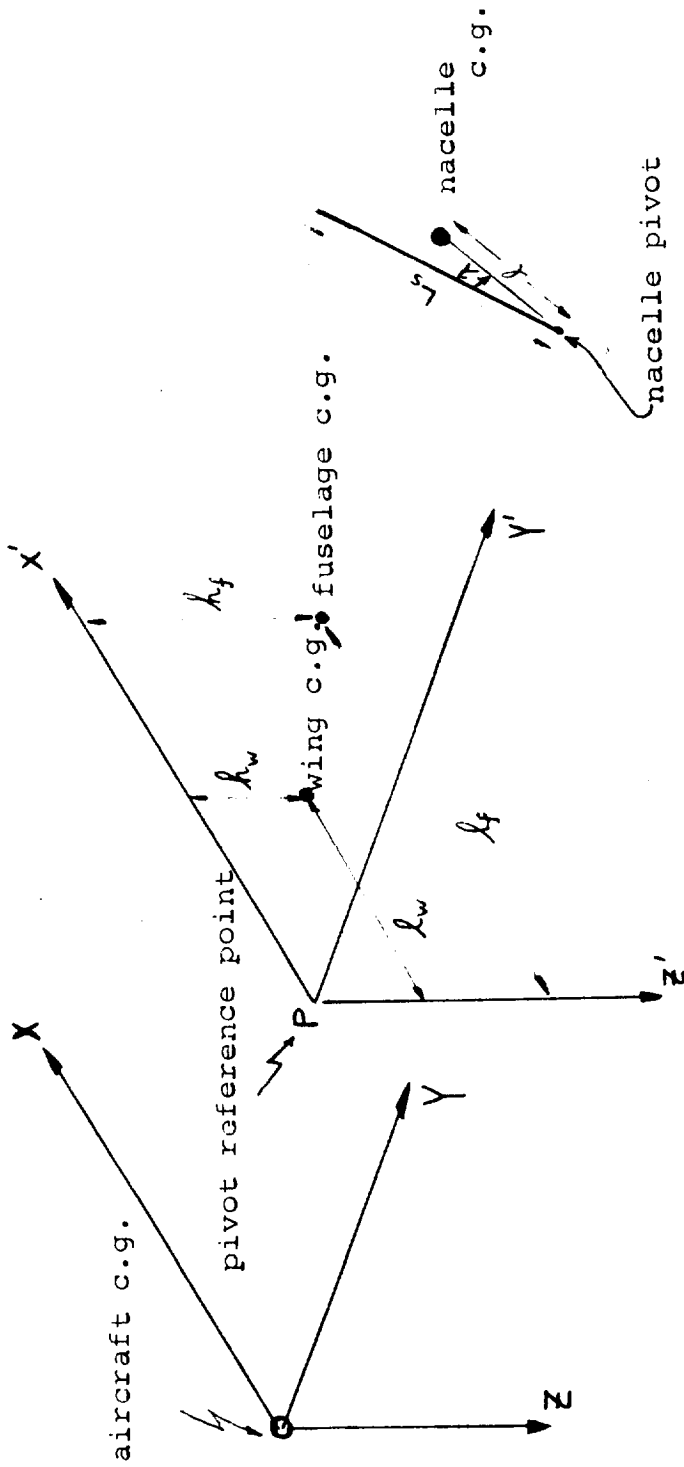


Figure C.1. Reference Axes Systems

where U, V and W are the components of the velocity of the airplane center of gravity.

The velocity of a point in the aircraft relative to the pivot is

$$\begin{aligned} u &= \dot{X} + QZ - YR \\ v &= \dot{Y} + RX - PZ \\ w &= \dot{Z} + PY - QX \end{aligned} \tag{C-4}$$

where X, Y, and Z are measured from the pivot to the point. By adding equations (C-3) and (C-4) the velocities of the following components are obtained relative to inertial space. The indicated distances are measured relative to the pivot.

Velocity of Horizontal Tail Aerodynamic Center

$$\begin{aligned} u_{HT} &= u_P + Z_{HT}Q \\ v_{HT} &= v_P + X_{HT}R - Z_{HT}P \\ w_{HT} &= w_P - X_{HT}Q \end{aligned} \tag{C-5}$$

Velocity of Vertical Tail Aerodynamic Center

$$\begin{aligned} u_{VT} &= u_P + Z_{VT}Q \\ v_{VT} &= u_P + X_{VT}R - Z_{VT}P \\ w_{VT} &= w_P + X_{VT}Q \end{aligned} \tag{C-6}$$

Velocity of Left Wing Aerodynamic Center - Body Axes

$$\begin{aligned} u'_{LW} &= u_P + Q (Z_{WAC} + h_{1LWAC}) + Y_{WAC}R \\ v'_{LW} &= u_P + X_{WAC}R - P (Z_{WAC} + h_{1LWAC}) \\ w'_{LW} &= w_P - Y_{WAC}P - X_{WAC}Q + \dot{h}_{1LWAC} \end{aligned} \tag{C-7}$$

where h_{1LWAC} is the elastic deflection of the left wing aerodynamic center. The equations for the right wing are obtained by substituting

$$Y_{RWAC} = -Y_{LWAC}$$

and $h_{1RWAC} = h_{1LWAC}$

Velocity of Left Wing Aerodynamic Center-Chord Axes

In order to compute wing angle-of-attack the velocity components are required relative to the wing chord line. If the wing chord makes an angle i_w with the body centerline then

$$\begin{aligned} u_{LW} &= u'_{LW} \cos i_w - w'_{LW} \sin i_w \\ v_{LW} &= v'_{LW} \\ w_{LW} &= w'_{LW} \cos i_w + u'_{LW} \sin i_w \end{aligned} \tag{C-8}$$

The equations for the right wing are obtained by changing the subscript.

Velocity of Left Rotor Hub - Body Axes

$$\begin{aligned} u'_{RL} &= u_P + RY_N - L_S (\dot{i}_{NL} + Q) \sin i_{NL} + Qh_{1L} \\ v'_{RL} &= v_P + L_S (R \cos i_{NL} + P \sin i_{NL}) - Ph_{1L} \\ w'_{RL} &= w_P - PY_N - L_S (\dot{i}_{NL} + Q) \cos i_{NL} + \dot{h}_{1L} \end{aligned} \tag{C-9}$$

where L_S is the distance from the rotor pivot point to the rotor hub and h_{1L} is the deflection of the wing tip. The equations for the right hub are obtained by changing subscripts and substituting $Y_N = -Y_N$.

Velocity of Left Rotor Hub - Shaft Axes

Since the rotor aerodynamic forces and moments are functions of the shaft angle of attack and sideslip, the velocity components are required relative to shaft axes.

$$\begin{aligned}u_{RL} &= u_{RL}' \cos i_{NL} - w_{RL}' \sin i_{NL} \\v_{RL} &= v_{RL}' \\w_{RL} &= w_{RL}' \sin i_{NL} + u_{RL}' \cos i_{NL}\end{aligned}\tag{C-10}$$

The corresponding equations for the right hub are obtained by changing the subscript.

C.2 Center of Gravity and Inertia Equations

Equations are required that express the overall aircraft center of gravity position and inertias in terms of the centers of gravity and inertias of the individual mass components. In order to do this a fixed reference point is chosen in the aircraft defined by the intersection of the line joining the nacelle pivots and the vertical plane of symmetry of the aircraft, see Figure C.1. A set of axes $PXPYPZP$ is taken at this pivot reference point, parallel to the axes $OXYZ$ at the aircraft center of gravity. If the location of the aircraft center of gravity with respect to the pivot reference axes is $(X'_{CG}, Y'_{CG}, Z'_{CG})$ and if (l_f, h_f) and (l_w, h_w) are the x and z coordinates of the fuselage and wing masses measured from the pivot, then the following relationships are obtained between the centers of mass of the components and the aircraft center of gravity.

Fuselage CG Relative to Aircraft CG

$$x_f = \ell_f - x'_{CG} \quad (C-11)$$

$$x_f = h_f - z_{CG}$$

Wing CG Relative to Aircraft CG

$$x_w = \ell_w - x'_{CG} \quad (C-12)$$

$$z_w = h_w - z'_{CG}$$

Nacelle CG Relative to Aircraft CG

$$x_{NR} = \ell \cos (i_{NR} - \lambda) - x'_{CG}$$

$$x_{NL} = \ell \cos (i_{NL} - \lambda) - x'_{CG} \quad (C-13)$$

$$z_{NR} = \ell \sin (i_{NR} - \lambda) - z'_{CG}$$

$$z_{NL} = \ell \sin (i_{NL} - \lambda) - z'_{CG}$$

where ℓ is the distance from the nacelle pivot point to the nacelle c.g., and λ is the angular depression of the nacelle center of mass below the nacelle pivot, when the nacelle is in the down position, see Figure C.1.

Aircraft Center of Gravity Position

By taking moments about the pivot, the aircraft center of gravity is given by

$$X'_{CG} = \frac{m_f l_f + m_w l_w}{m} + l \left(\frac{m_N}{m} \right) \left[\cos(i_{NL}-\lambda) + \cos(i_{NR}-\lambda) \right] \quad (C-14)$$

$$Z'_{CG} = \frac{m_f h_f + m_w h_w}{m} - l \left(\frac{m_N}{m} \right) \left[\sin(i_{NL}-\lambda) + \sin(i_{NR}-\lambda) \right]$$

The equations of motion (Section 5) require the first and second time derivatives of the center of gravity position. They are as follows:

Center of Gravity Velocity Relative to Pivot Point

$$\dot{X}'_{CG} = -l \left(\frac{m_N}{m} \right) \left[\dot{i}_{NR} \sin(i_{NR}-\lambda) + \dot{i}_{NL} \sin(i_{NL}-\lambda) \right] \quad (C-15)$$

$$\dot{Z}'_{CG} = -l \left(\frac{m_N}{m} \right) \left[\dot{i}_{NR} \cos(i_{NR}-\lambda) + \dot{i}_{NL} \cos(i_{NL}-\lambda) \right]$$

Center of Gravity Acceleration Relative to Pivot Point

$$\ddot{X}'_{CG} = -l \left(\frac{m_N}{m} \right) \left[\ddot{i}_{NR} \sin(i_{NR}-\lambda) + \ddot{i}_{NL} \sin(i_{NL}-\lambda) + \dot{i}_{NL}^2 \cos(i_{NL}-\lambda) + \dot{i}_{NR}^2 \cos(i_{NR}-\lambda) \right] \quad (C-16)$$

$$\ddot{Z}'_{CG} = -l \left(\frac{m_N}{m} \right) \left[\ddot{i}_{NR} \cos(i_{NR}-\lambda) + \ddot{i}_{NL} \cos(i_{NL}-\lambda) - \dot{i}_{NL}^2 \sin(i_{NL}-\lambda) - \dot{i}_{NR}^2 \sin(i_{NR}-\lambda) \right]$$

Pilot Station Velocities - Body Axes

The velocities at the pilot's station are required in order to drive the visual display. From equations (C-3) and (C-4) the components of velocity of the pilot's station in body axes are:

$$u_{PA} = u_P + QZ_{PA} - RY_{PA}$$

$$v_{PA} = v_P + Rl_{PA} - PZ_{PA}$$

$$w_{PA} = w_P + PY_{PA} - Ql_{PA}$$

C-3 Pilot Station Acceleration - Body Axes

The pilot station acceleration is also required to drive the visual display. These accelerations are derived here.

The velocity at the pilot's station is

$$\underline{v}_{PA} = \underline{v}_{CG} + \underline{\Omega} \times \underline{r}_{PA} + \frac{\delta \underline{r}_{PA}}{\delta t}$$

where \underline{r}_{PA} is the vector from the aircraft CG to the pilot's station and $\frac{\delta \underline{r}_{PA}}{\delta t}$ is the rate of change of the pilot's station with respect to the aircraft CG.

The pilot's station acceleration is

$$\begin{aligned} \underline{a}_{PA} &= \frac{d\underline{v}_{PA}}{dt} = \frac{d\underline{v}_{CG}}{dt} + \frac{d}{dt} (\underline{\Omega} \times \underline{r}_{PA}) + \frac{d}{dt} \left(\frac{\delta \underline{r}_{PA}}{\delta t} \right) \\ &= \underline{a}_{CG} + \frac{\delta}{\delta t} (\underline{\Omega} \times \underline{r}_{PA}) + \underline{\Omega} \times (\underline{\Omega} \times \underline{r}_{PA}) + \frac{\delta^2 \underline{r}_{PA}}{\delta t^2} + \underline{\Omega} \times \frac{\delta \underline{r}_{PA}}{\delta t} \\ &= \underline{a}_{CG} + \frac{\delta \underline{\Omega}}{\delta t} \times \underline{r}_{PA} + 2\underline{\Omega} \times \frac{\delta \underline{r}_{PA}}{\delta t} + \underline{\Omega} (\underline{r}_{PA} \cdot \underline{\Omega}) - \Omega^2 \underline{r}_{PA} + \frac{\delta^2 \underline{r}_{PA}}{\delta t^2} \end{aligned}$$

$$\text{with } \underline{\Omega} = P\hat{i} + Q\hat{j} + R\hat{k}$$

$$\frac{\delta \underline{\Omega}}{\delta t} = \dot{P}\hat{i} + \dot{Q}\hat{j} + \dot{R}\hat{k}$$

$$\underline{r}_{PA} = (x_{PA} - x_{CG})\hat{i} + (y_{PA} - y_{CG})\hat{j} + (z_{PA} - z_{CG})\hat{k}$$

$$\frac{\delta \underline{r}_{PA}}{\delta t} = (\dot{x}_{PA} - \dot{x}_{CG})\hat{i} + (\dot{y}_{PA} - \dot{y}_{CG})\hat{j} + (\dot{z}_{PA} - \dot{z}_{CG})\hat{k}$$

and noting that Y_{CG} and the time derivatives of X_{PA} , Y_{PA} , Z_{PA} are always zero, the above equation yields the pilot's station accelerations as: -

$$a_{x_{PA}} = \frac{X_{AERO}}{m} + (\dot{Q} + PR)(Z_{PA} - Z_{CG}) + (Q^2 + R^2)(X_{CG} - l_{PA}) \\ + Y_{PA}(PQ - \dot{R}) - 2Q\dot{Z}_{CG} - \ddot{X}_{CG}$$

$$a_{y_{PA}} = \frac{Y_{AERO}}{m} + (\dot{P} - QR)(Z_{CG} - Z_{PA}) + (\dot{R} + PQ)(l_{PA} - X_{CG}) \\ - Y_{PA}(R^2 + P^2) + 2(P\dot{Z}_{CG} - R\dot{X}_{CG})$$

$$a_{z_{PA}} = \frac{Z_{AERO}}{m} + (\dot{Q} - PR)(X_{CG} - l_{PA}) + (P^2 + Q^2)(Z_{CG} - Z_{PA}) \\ + Y_{PA}(\dot{P} + QR) + 2Q\dot{X}_{CG} - \ddot{Z}_{CG}$$

where $a_{x_{CG}} = \frac{Z_{AERO}}{m}$ etc.

$X_{PA} = l_{PA}$, the distance from the pivot to the pilot's station

C.4 Aircraft Inertias

The aircraft roll inertia about the aircraft center of gravity is, from the parallel axis theorem,

$$I_{XX} = I_{XX}^f + I_{XX}^w + I_{XX}^{NL} + I_{XX}^{NR} + m_f Z_f^2 + m_w Z_w^2 + 2m_N Y_N^2 + m_N Z_{NL}^2 + m_N Z_{NR}^2 \quad (C-17)$$

where I_{XX}^f , etc., are the inertias of the various components about their individual centers of gravity.

In the case of the nacelles the inertias I_{xx}^{NL} , I_{xx}^{NR} are dependent on the nacelle tilt angle, i_N . These inertias are related to the inertias of the nacelle with respect to a set of nacelle-fixed axes $O''xyz$ placed as shown in Figure 5.1. The relationships are

$$I_{xx}^N = I_{xx_0}^N + (I_{zz_0}^N - I_{xx_0}^N) \sin^2 i_N - I_{xz_0} \sin 2i_N$$

$$I_{yy}^N = I_{yy_0}^N \tag{C-18}$$

$$I_{zz}^N = I_{zz_0}^N + (I_{xx_0}^N - I_{zz_0}^N) \sin^2 i_N + I_{xz_0} \sin 2i_N$$

$$I_{xz}^N = I_{xz_0}^N \cos 2i_N + \frac{1}{2} (I_{xx_0}^N - I_{zz_0}^N) \sin 2i_N$$

Using equations (C-18) together with (C-13), (C-11) and (C-12), in equation (C-17), the roll inertia becomes

$$\begin{aligned} I_{xx} = & I_{xx}^f + I_{xx}^w + 2I_{xx_0}^N + (I_{zz_0}^N - I_{xx_0}^N) (\sin^2 i_{NL} + \sin^2 i_{NR}) \\ & - I_{xz_0}^N (\sin 2i_{NL} + \sin 2i_{NR}) + 2 m_N Y_N^2 + m_f h_f z_f \\ & + m_w h_w z_w - m_f z_f z'_{CG} - m_w z_w z'_{CG} \\ & - m_N z_{NL} z'_{CG} - m_N z_{NR} z'_{CG} \\ & - 2m_N \left[z_{NR} \sin(i_{NR} - \lambda) + z_{NL} \sin(i_{NL} - \lambda) \right] \end{aligned}$$

$$\begin{aligned}
&= I_{xx}^f + I_{xx}^w + 2I_{xx_0}^N + (I_{zz_0}^N - I_{xx_0}^N) (\sin^2 i_{NL} + \sin^2 i_{NR}) \\
&\quad - I_{xz_0}^N (\sin 2i_{NL} + \sin 2i_{NR}) + 2 m_N Y_N^2 + m_f h_f Z_f \\
&\quad + m_w h_w Z_w - \ell m_N \left[Z_{NR} \sin (i_{NR} - \lambda) + Z_{NL} \sin (i_{NL} - \lambda) \right]
\end{aligned}$$

since the terms containing Z_{CG} sum to zero.

Similarly

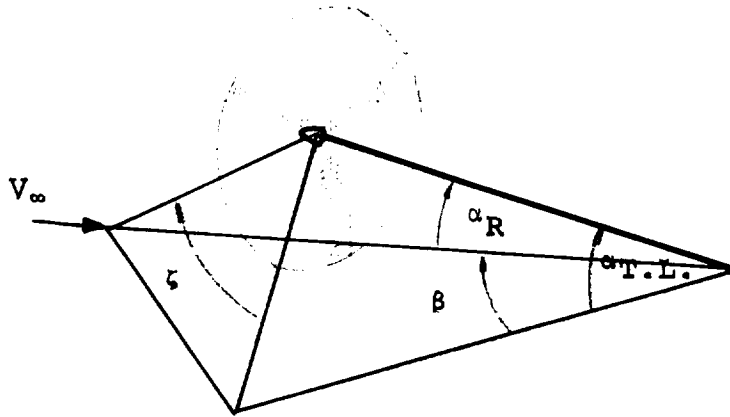
$$\begin{aligned}
I_{xz} &= I_{xz}^f + I_{xz}^w + I_{xz}^N (\cos 2i_{NL} + \cos 2i_{NR}) \\
&\quad + \frac{1}{2} (I_{xx_0}^N - I_{zz_0}^N) (\sin 2i_{NL} + \sin 2i_{NR}) + m_f \ell_f Z_f \\
&\quad + m_w Z_w \ell_w + \ell m_N \left[Z_{NR} \cos (i_{NR} - \lambda) + Z_{NL} \cos (i_{NL} - \lambda) \right]
\end{aligned}$$

$$\begin{aligned}
(I_{zz} - I_{yy}) &= I_{zz}^f - I_{yy}^f + I_{zz}^w - I_{yy}^w + 2(I_{zz_0}^N - I_{yy_0}^N) \\
&\quad + (I_{xx_0}^N - I_{zz_0}^N) (\sin^2 i_{NL} + \sin^2 i_{NR}) + I_{xz_0}^N (\sin 2i_{NL} + \sin 2i_{NR}) \\
&\quad - (m_f h_f Z_f + m_w h_w Z_w) + m_N \ell \left[Z_{NL} \sin (i_{NL} - \lambda) \right. \\
&\quad \left. + Z_{NR} \sin (i_{NR} - \lambda) \right] + 2m_N Y_N^2
\end{aligned}$$

Similar expressions are obtained for I_{yy} and I_{zz} and these are presented in Appendix E.

APPENDIX D - CALCULATION OF SLIPSTREAM-IMMERSED WING AREAS

The wing areas washed by the rotor slipstreams are required in the calculation of wing lift and drag. These immersed areas depend on rotor shaft inclination, wing angle of attack and sideslip, and rotor thrust. The equations presented in Appendix E for the immersed areas S_{iL} and S_{iR} were obtained as follows.



The above sketch shows a rotor under conditions of combined angle of attack ($\alpha_{T.L.}$) and sideslip (β). The resultant angle of attack of the shaft is given by

$$\alpha_R = \cos^{-1} (\cos \alpha_{T.L.} \cos \beta) \quad (D-1)$$

If the rotor shaft is inclined to the fuselage centerline at angle i_N and the fuselage is at angle of attack α_f then

$$\alpha_{T.L.} = \alpha_f + i_N \quad (D-2)$$

The rotor "sideslip" angle, ζ , is defined by

$$\zeta = \text{Tan}^{-1} \left[\frac{\text{Tan } \beta}{\text{Sin } \alpha_{\text{T.L.}}} \right] \quad (\text{D-3})$$

and is the angle shown in the sketch.

Figure D.1 presents four views of the geometry of rotor slipstream/wing planform interaction.

Figure D.1[a] is a view of the plane taken through the rotor shaft parallel to the aircraft vertical plane of symmetry. The line PT is the wing chord, the distances PC and h_p are the horizontal and vertical coordinates of the pivot measured from the wing leading edge, and l is the spinner-to-pivot shaft length.

Figure D.1[b] is a view taken normal to the rotor disc plane. In this view, the traces of the slipstream on planes taken through the wing leading and trailing edges parallel to the disc plane appear as circles. This assumes that the slipstream is a sheared circular cylinder.

Figure D.1[c] is a section taken in the plane containing the rotor shaft and the freestream velocity vector V_∞ . The angle ϵ is the deflection of the slipstream relative to the free-stream direction. Planes are taken through the wing leading and trailing edges parallel to the rotor disc. These intersect the rotor shaftline at the points O and T, and intersect the slipstream centerline at the points O' and O". These points enable the slipstream traces shown in (b) to be constructed.

Figure (D.1[d]) is a view taken perpendicular to the wing surface showing the areas washed by the slipstream. For convenience this view combines the immersed areas of both left and right wings. In general, the imprint of the slipstream on the wing will be bounded in the chordwise direction by curved lines; however, the approximation is made that these lines are straight.

The immersed area of the right wing panel is (assuming that the tip is immersed),

$$\begin{aligned} S_{i_R} &= \frac{1}{2}(PM + TN)c \\ &= \frac{1}{2}(PR + RM + TS + SN)c \end{aligned} \quad (D-4)$$

$$\text{From Figure D.1[b]} \quad PR = OO' \sin \zeta \quad (D-5)$$

$$\text{From Figure D.1[c]} \quad OO' = (\ell - OD) \tan (\alpha_R - \epsilon) \quad (D-6)$$

$$\text{From Figure D.1[a]} \quad OD = PC \cos (i_N - i_W) - h_p \sin (i_N - i_W) \quad (D-7)$$

$$\text{From Figure D.1[b]} \quad RM = R'M' = \sqrt{\frac{D_S^2}{4} - O'R'^2} \quad (D-8)$$

$$\text{From Figure D.1[b]} \quad O'R' = OO' \cos \zeta + OP \quad (D-9)$$

$$\text{From Figure D.1[a]} \quad OP = PC \sin (i_N - i_W) + h_p \cos (i_N - i_W) \quad (D-10)$$

These equations define the leading edge intersection PM. If RM is zero or negative, the slipstream does not intersect the leading edge and the wing is considered to be unaffected by the slipstream.

For the trailing edge intersection, TN:

$$TS = OO'' \sin \zeta \quad (D-11)$$

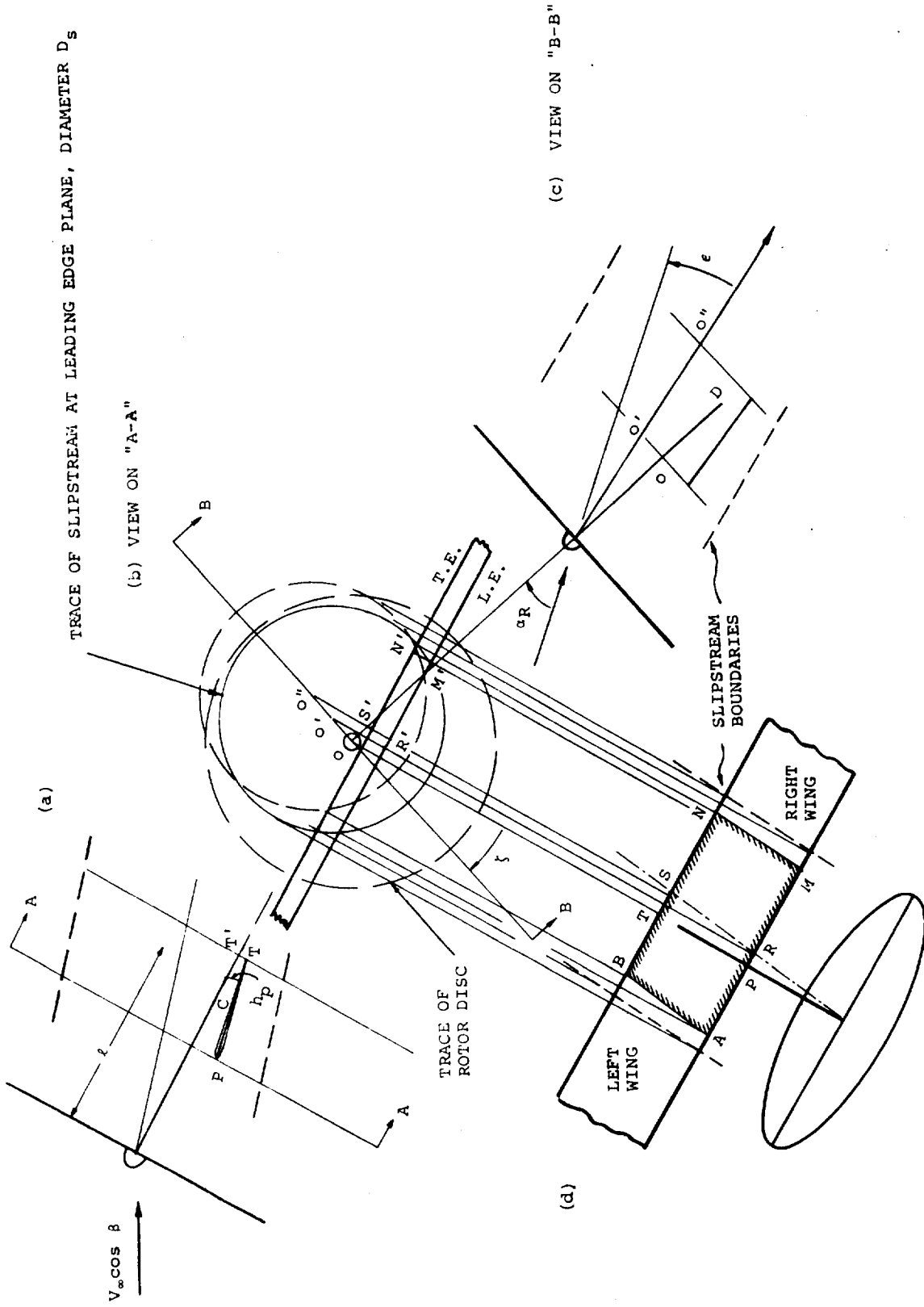


Figure D.1. Geometry of Rotor Slipstream/Wing Planform Interaction

$$OO'' = (\ell + c \cos (i_N - i_W) - OD) \tan (\alpha_R - \epsilon) \quad (D-12)$$

$$SN = S'N' = \frac{D_S^2}{4} - O''S'^2 \quad (D-13)$$

$$O''S' = OO'' \cos \zeta + TT' \quad (D-14)$$

$$TT' = OP - c \sin (i_N - i_W) \quad (D-15)$$

If we write

$$\xi_1 = PR, \xi_2 = RM, \xi_3 = TS, \text{ and } \xi_4 = SN$$

then, using the above equations,

$$\xi_1 = [\ell - PC \cos (i_N - i_W) + h_p \sin (i_N - i_W)] \tan (\alpha_R - \epsilon) \sin \zeta \quad (D-16)$$

and

$$\xi_2 = \sqrt{\frac{D_S^2}{4} - \{[\ell - PC \cos (i_N - i_W) + h_p \sin (i_N - i_W)] \tan (\alpha_R - \epsilon) \cos \zeta + PC \sin (i_N - i_W) + h_p \cos (i_N - i_W)\}^2} \quad (D-17)$$

The corresponding equations for ξ_3 and ξ_4 are obtained by replacing PC in (D-16) and (D-17) with (PC-c)

Thus the immersed area of the right wing panel is given

$$\text{by } S_{i_R} = \frac{1}{2} c (\xi_1 + \xi_2 + \xi_3 + \xi_4) \quad (D-18)$$

From the symmetry of Figure D.1(d), SN=BS and RM=AR. The total immersed area of both wing panels is

$$S_{i_T} = \frac{1}{2} c (AM + BN) = \frac{1}{2} c (2\xi_2 + 2\xi_4) = c (\xi_2 + \xi_4) \quad (D-19)$$

and therefore the immersed area of the left wing is obtained from

$$S_{i_L} = S_{i_T} - S_{i_R} \quad (D-20)$$

The above equations correspond to those presented in Appendix E for calculating immersed wing area.

APPENDIX E COMPUTER REPRESENTATION

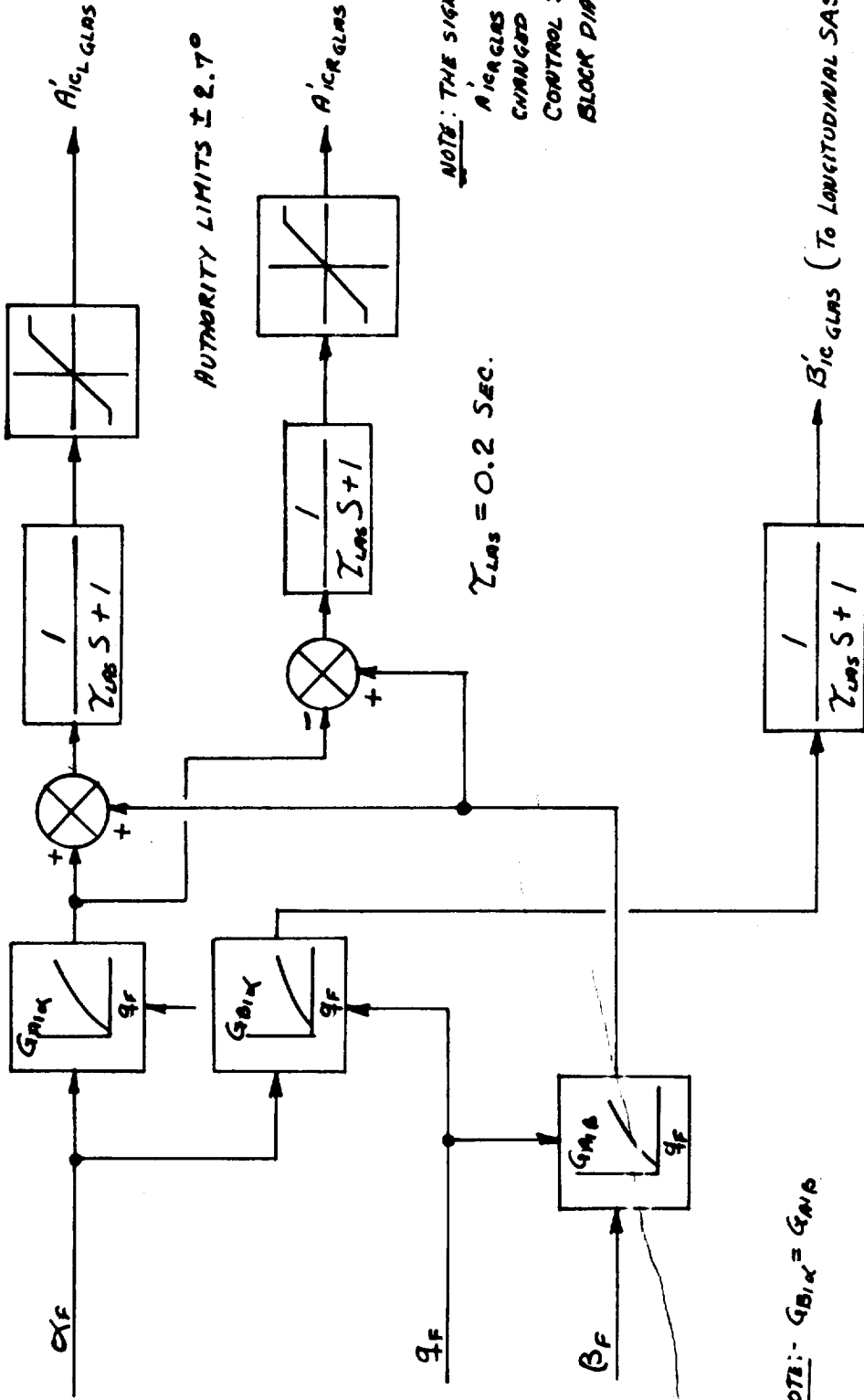
The equations derived in previous sections of this report have been collected and written in a format to facilitate computer programming. The complete set of equations which define the Model 222 simulation mathematical model are contained in this section. The computer block diagram for the simulation is also included. Each element of this block diagram contains an index number. Figure E.1 lists the index number, the name of the element, and its page number in this appendix. In addition the input and output, where appropriate, to each element are identified by their index numbers.

INDEX NUMBER	BLOCK DIAGRAM ELEMENT NAMES	PAGE NUMBER
1.	Control Mixing, Load Alleviation System and Actuator Dynamics	E-4
2.	Stability Augmentation System	E-7
3.	Density Calculation	E-9
4.	Engines and Thrust Management System	E-10
5.	Rotor Control Coordinate Axis Transforms	E-14
6.	Center of Gravity Calculation	E-15
7.	Aerodynamic Coordinate Transforms	E-16
8.	Wing Equations (Including Interference)	E-19
9.	Wing A.C. to Elastic Axis Transform	E-33
10.	Wing Force and Moment Resolution to Center of Gravity	E-34
11.	Horizontal and Vertical Tail Aerodynamics (Including Interference)	E-35
12.	Tail Force and Moment Resolution to Center of Gravity	E-43
13.	Nacelle Aerodynamics	E-44
14.	Landing Gear Equations	E-46
15.	Fuselage Aerodynamics	E-49
16.	Fuselage Force and Moment Resolution to Center of Gravity (Includes Landing Gear)	E-50
17.	Wing/Rotor Interference	E-51
18.	Rotor/Rotor Interference	E-52
19.	Rotor Aero Input Equations	E-53
20.	Rotor Equations	E-54
21.	Rotor Force and Moment Resolution	E-61
22.	Wing Vertical Bending	E-64
23.	Wing Torsion	E-66
24.	Total Force and Moment Summation About Center of Gravity	E-67
25.	Basic Equations of Motion	E-68
26.	Euler Angle Calculation	E-77
27.	Aircraft Condition Calculation and Ground Track	E-78
28.	Gust Model	E-80
29.	Preliminary Calculation (Preprocess)	E-81
30.	Trim Loops	E-87

Figure E.1. Block Diagram Element Index Numbers

MODEL 222 LOAD ALLEVIATION SYSTEM (LAS)

(FOR PIVOT MOMENTS - SINGLE COMMON LONG. ACTUATOR)



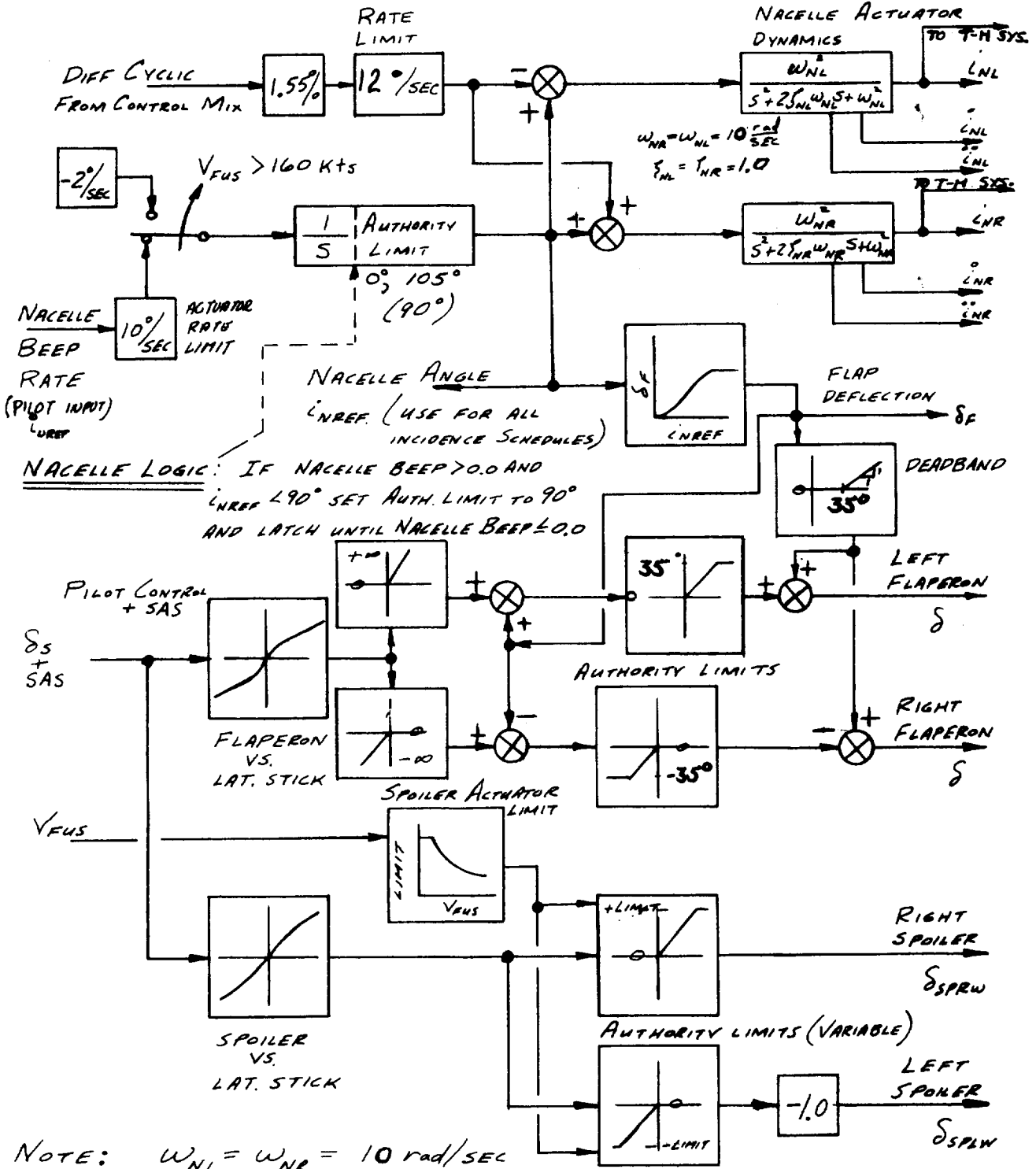
NOTE: $G_{B1\alpha} = G_{M1\beta}$

GOVERNING EQUATIONS

- $A_{ICLGLAS} = G_{M1\alpha} \alpha + G_{M1\beta} \beta$
- $A_{ICRGLAS} = G_{M1\alpha} \alpha - G_{M1\beta} \beta$
- $B_{ICGLAS} = G_{M1\alpha} \alpha$

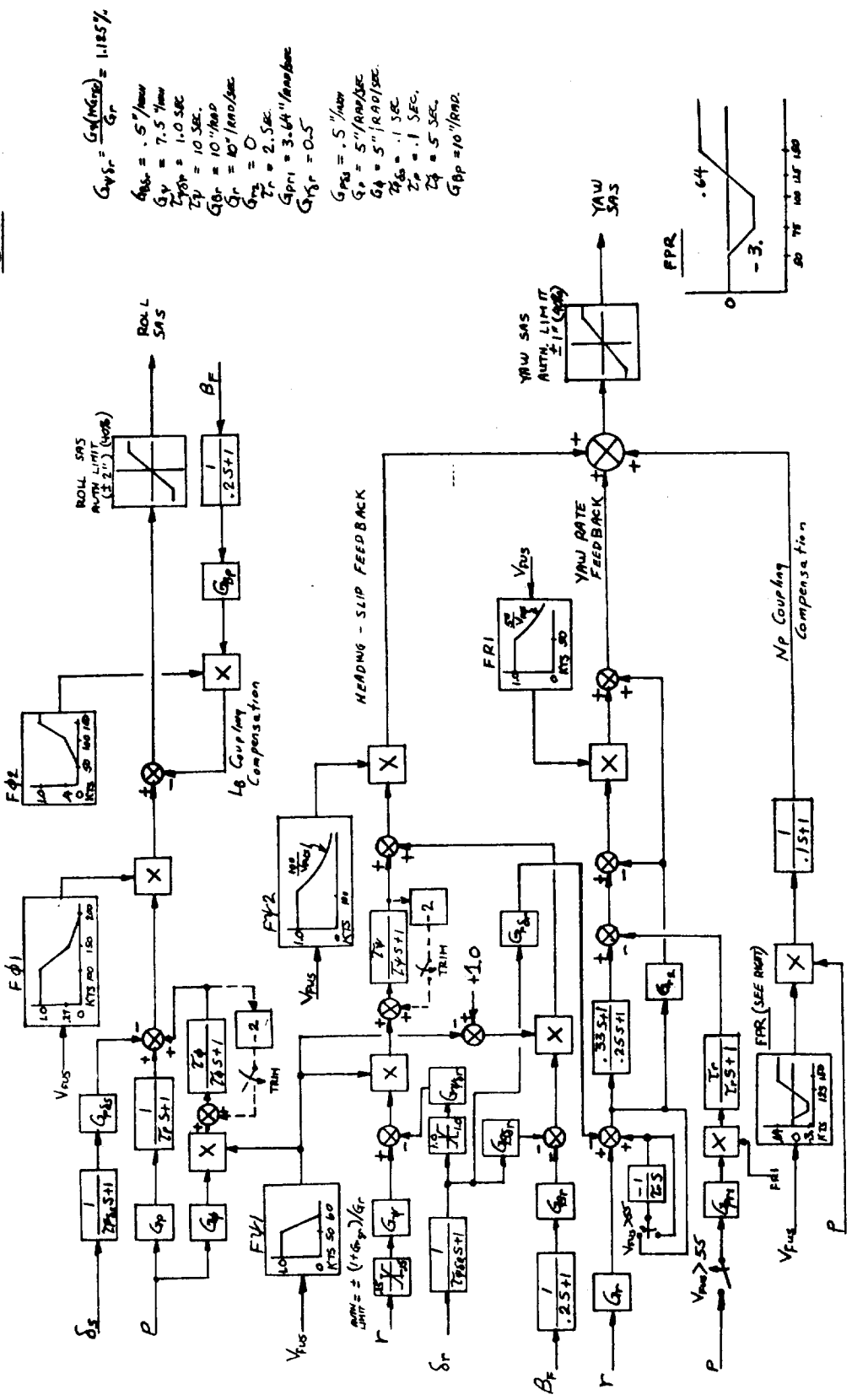
MODEL 222

NACELLE, FLAP, FLAPERON, & SPOILER CONTROLS

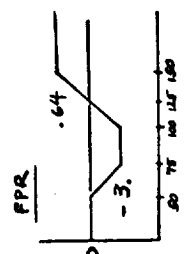


NOTE: $W_{NL} = W_{NR} = 10 \text{ rad/SEC}$
 $\zeta_{NL} = \zeta_{NR} = 1.0$ (critical.)

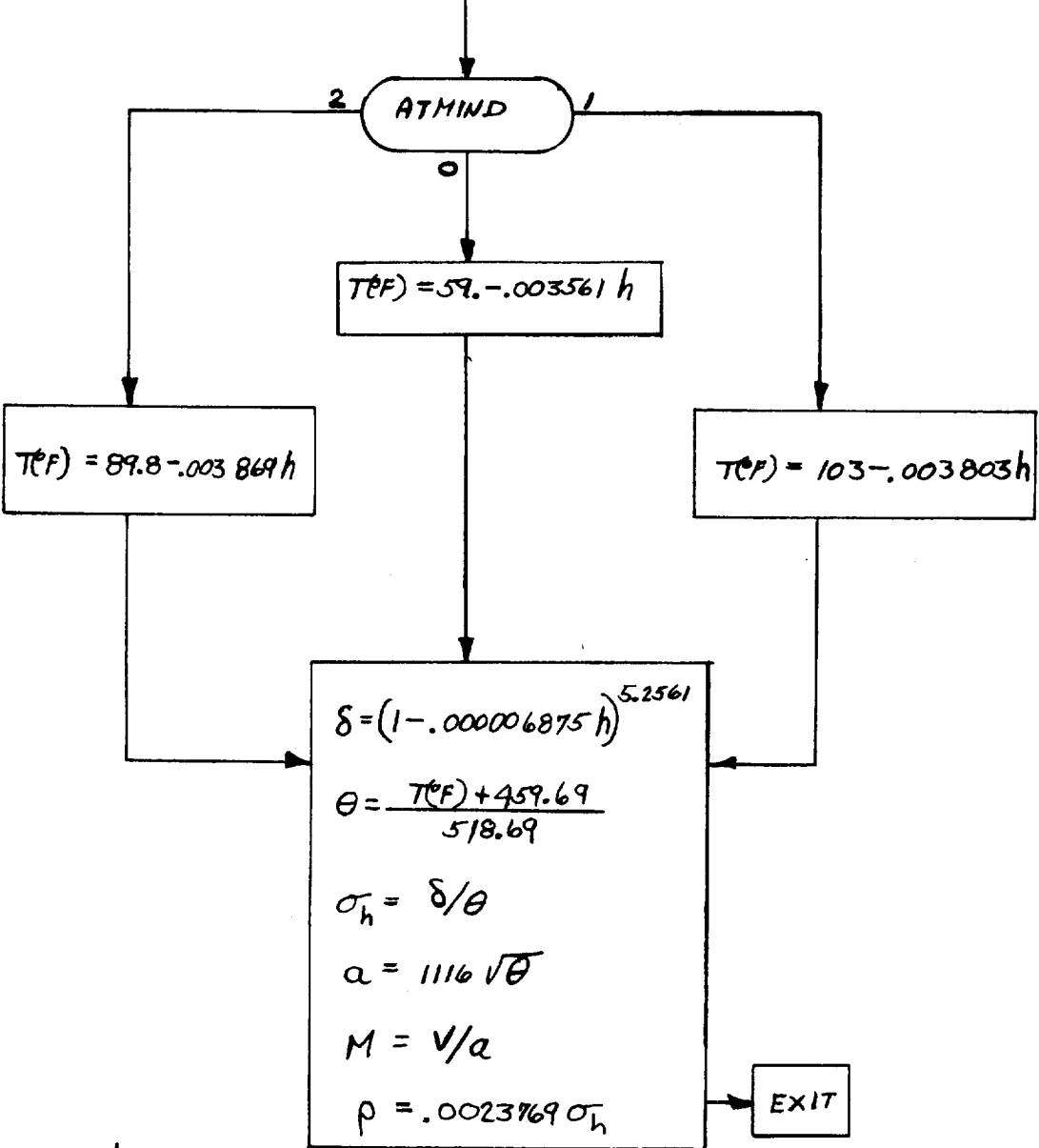
LATERAL - DIRECTIONAL
SAS



- $G_{\rho} = \frac{G_{\rho}(V_{us})}{G_r} = 1.185\%$
 $G_{\rho} = .5''/1000$
 $G_r = 7.5''/1000$
 $T_{\rho} = 1.0 \text{ SEC}$
 $T_r = 10''/1000$
 $G_r = 10''/1000$
 $G_{\rho} = 0$
 $T_r = 2.5 \text{ SEC}$
 $G_{\rho} = 3.64''/1000$
 $G_{\rho} = 0.5$
 $G_{\rho} = .5''/1000$
 $G_r = 5''/1000$
 $G_r = 5''/1000$
 $T_{\rho} = .1 \text{ SEC}$
 $T_r = .1 \text{ SEC}$
 $T_r = .5 \text{ SEC}$
 $G_{\rho} = 10''/1000$

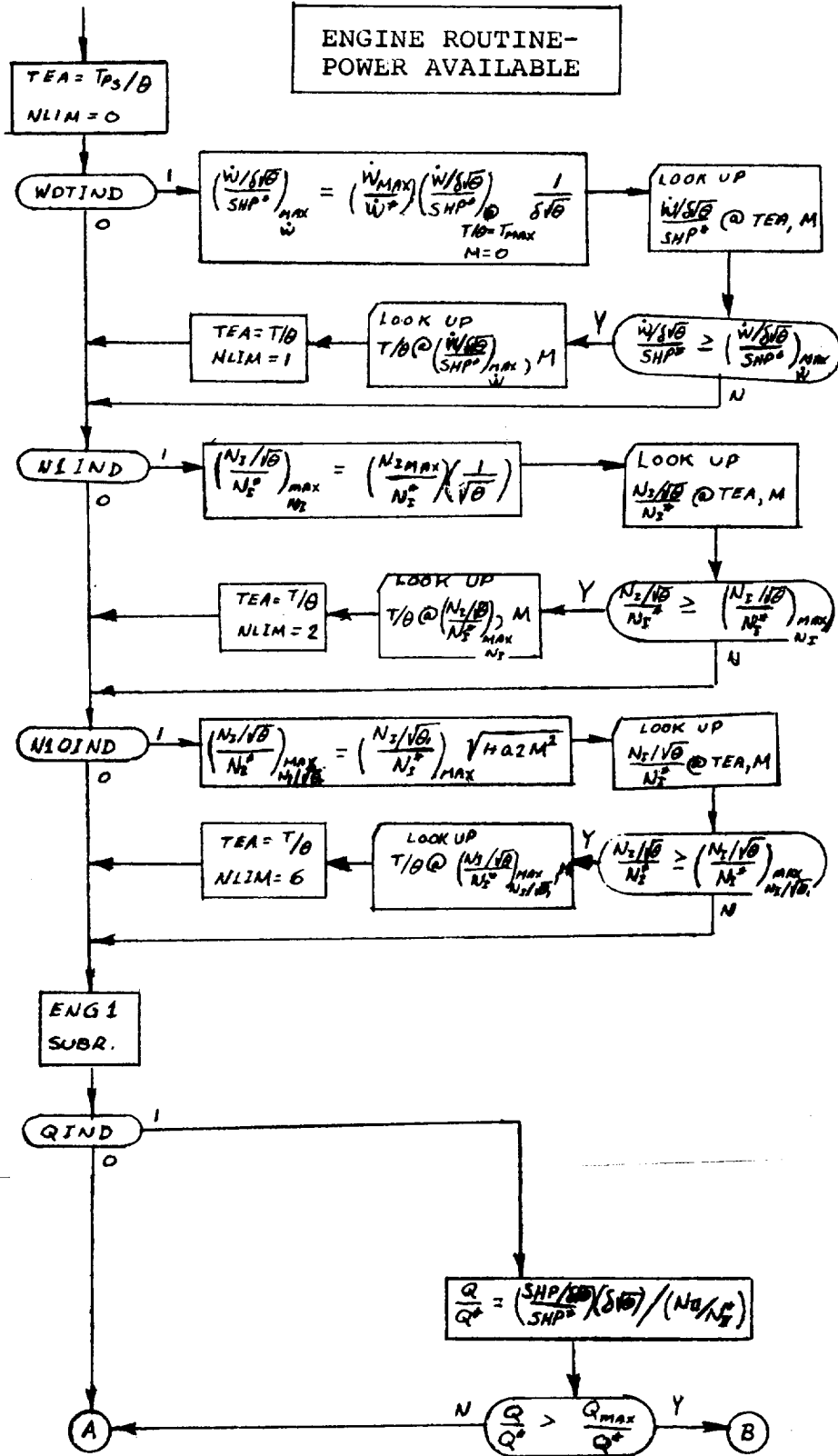


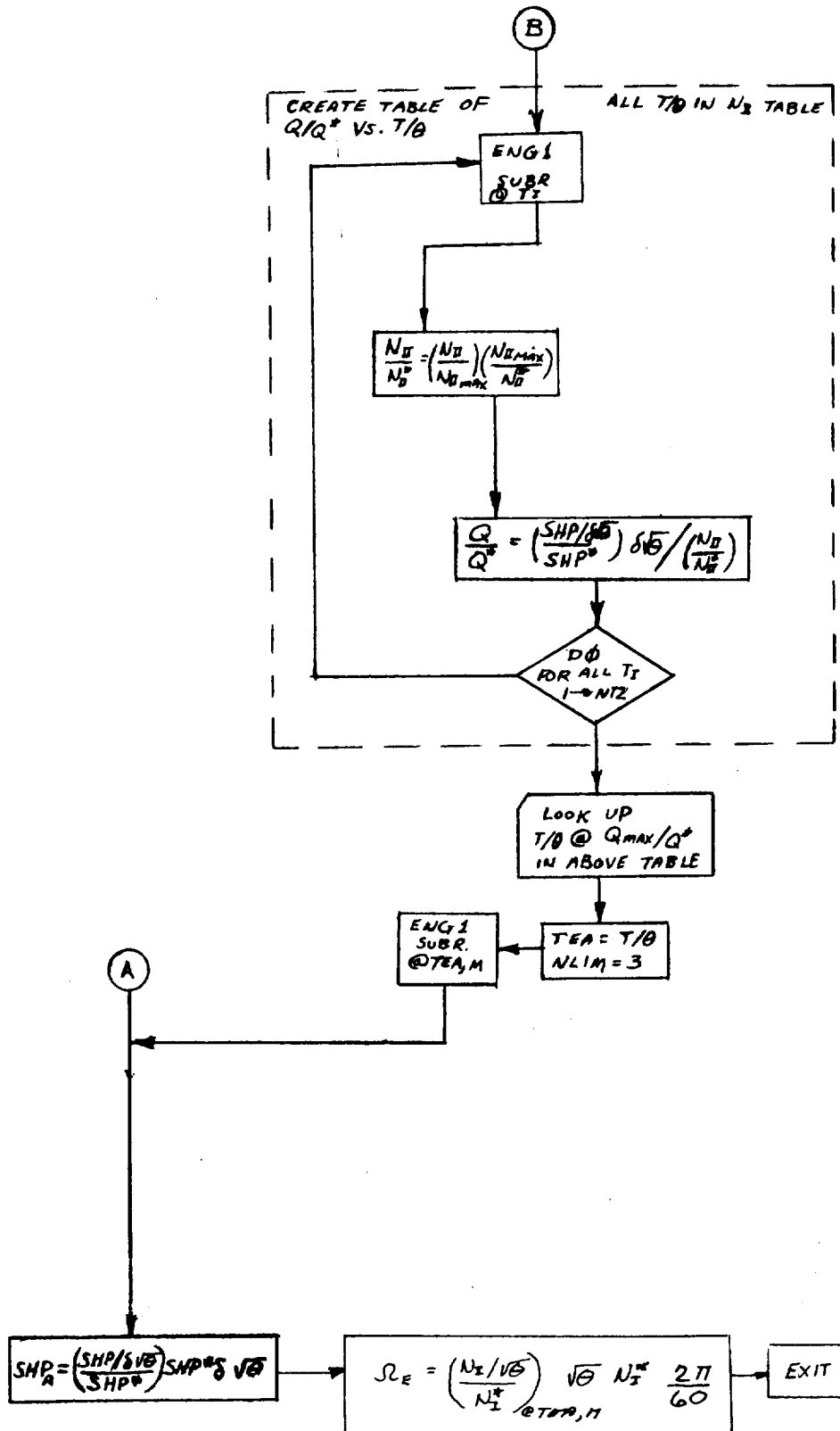
DENSITY CALCULATIONS

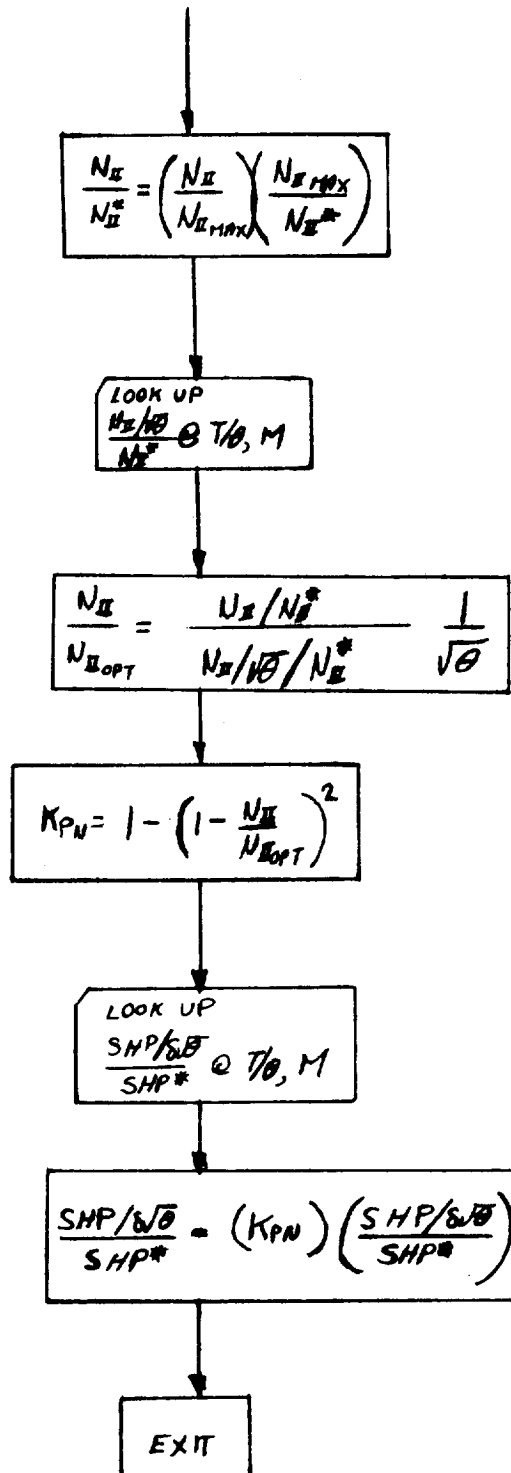


INPUT: h
 ATMIND: 0 ~ STD ATMOS
 1 ~ HOT ATMOS
 2 ~ TROPICAL ATMOS

OUTPUT: $\delta, \theta, \sigma_h, a, M, \rho$







ENG 1 SUBROUTINE, FLOW CHART

ROTOR CONTROL COORDINATE AXIS TRANSFORM

LEFT

$$A_{iCL}'' = A_{iCL}' \cos \phi_p + B_{iCL}' \sin \phi_p$$

$$B_{iCL}'' = -A_{iCL}' \sin \phi_p + B_{iCL}' \cos \phi_p$$

$$A_{iCL} = A_{iCL}'' \cos \zeta_{HL} - B_{iCL}'' \sin \zeta_{HL}$$

$$B_{iCL} = A_{iCL}'' \sin \zeta_{HL} + B_{iCL}'' \cos \zeta_{HL}$$

RIGHT

$$A_{iCR}'' = A_{iCR}' \cos \phi_p + B_{iCR}' \sin \phi_p$$

$$B_{iCR}'' = -A_{iCR}' \sin \phi_p + B_{iCR}' \cos \phi_p$$

$$A_{iCR} = +A_{iCR}'' \cos \zeta_{HR} + B_{iCR}'' \sin \zeta_{HR}$$

$$B_{iCR} = -A_{iCR}'' \sin \zeta_{HR} + B_{iCR}'' \cos \zeta_{HR}$$

ROTOR SIDE SLIP ANGLE

$$\zeta_{HR} = \tan^{-1} \frac{v_{RR}}{w_{RR} + \epsilon_{wRR} u_{RR}}$$

$$\zeta_{HL} = \tan^{-1} \frac{v_{RL}}{w_{RL} + \epsilon_{wRL} u_{RL}}$$

FORM THE SIN & COS OF ζ_{HR} & ζ_{HL}

NOTE: ϕ_p IS THE CONTROL PHASE ANGLE. ϕ_p IS POSITIVE

FOR THE CONTROL AXIS MOVED OPPOSITE TO ROTOR ROTATION.

CENTER OF GRAVITY CALCULATION

C.G. LOCATION w.r.t. PIVOT

$$X_{CG} = \frac{m_f l_f + m_w l_w}{m} + l \left(\frac{m_N}{m} \right) \left[\cos(i_{NL} - \lambda) + \cos(i_{NR} - \lambda) \right]$$

$$Z_{CG} = \frac{m_f h_f + m_w h_w}{m} - l \left(\frac{m_N}{m} \right) \left[\sin(i_{NL} - \lambda) + \sin(i_{NR} - \lambda) \right]$$

C.G. VELOCITY w.r.t. PIVOT

$$\dot{X}_{CG} = -l \frac{m_N}{m} \left[\dot{i}_{NL} \sin(i_{NL} - \lambda) + \dot{i}_{NR} \sin(i_{NR} - \lambda) \right]$$

$$\dot{Z}_{CG} = -l \frac{m_N}{m} \left[\dot{i}_{NL} \cos(i_{NL} - \lambda) + \dot{i}_{NR} \cos(i_{NR} - \lambda) \right]$$

C.G. ACCELERATION w.r.t. PIVOT

$$\ddot{X}_{CG} = -l \frac{m_N}{m} \left[\ddot{i}_{NL} \sin(i_{NL} - \lambda) + \dot{i}_{NL}^2 \cos(i_{NL} - \lambda) \right. \\ \left. + \ddot{i}_{NR} \sin(i_{NR} - \lambda) + \dot{i}_{NR}^2 \cos(i_{NR} - \lambda) \right]$$

$$\ddot{Z}_{CG} = -l \frac{m_N}{m} \left[\ddot{i}_{NL} \cos(i_{NL} - \lambda) - \dot{i}_{NL}^2 \sin(i_{NL} - \lambda) \right. \\ \left. + \ddot{i}_{NR} \cos(i_{NR} - \lambda) - \dot{i}_{NR}^2 \sin(i_{NR} - \lambda) \right]$$

FUSELAGE PIVOT VELOCITY

$$U_P = U - Z_{CG} \dot{q} - \dot{X}_{CG}$$

$$V_P = V + Z_{CG} p - X_{CG} r$$

$$W_P = W + X_{CG} \dot{q} - \dot{Z}_{CG}$$

AERO DYNAMIC COORDINATE TRANSFORM

LEFT WING A.C. VELOCITY - BODY AXES

$$U'_{LW} = U_p + Z_{WAC} q + Y_{WAC} r + g h_{LWAC}$$

$$V'_{LW} = V_p + X_{WAC} r - Z_{WAC} p - p h_{LWAC}$$

$$W'_{LW} = W_p - Y_{WAC} p - X_{WAC} q + \dot{h}_{LWAC}$$

RIGHT WING A.C. VELOCITY - BODY AXES

$$U'_{RW} = U_p + Z_{WAC} q - Y_{WAC} r + g h_{RWAC}$$

$$V'_{RW} = V_p + X_{WAC} r - Z_{WAC} p - p h_{RWAC}$$

$$W'_{RW} = W_p + Y_{WAC} p - X_{WAC} q + \dot{h}_{RWAC}$$

LEFT ROTOR HUB VELOCITY - BODY AXES

$$U'_{RL} = U_p + r Y_N - L_s \sin i_{NL} (\dot{i}_{NL} + q) + g h_{IL}$$

$$V'_{RL} = V_p + L_s (r \cos i_{NL} + p \sin i_{NL}) - p h_{IL}$$

$$W'_{RL} = W_p - p Y_N - L_s (\dot{i}_{NL} + q) \cos i_{NL} + \dot{h}_{IL}$$

RIGHT ROTOR HUB VELOCITY - BODY AXES

$$U'_{RR} = U_p - r Y_N - L_s \sin i_{NR} (\dot{i}_{NR} + q) + g h_{IR}$$

$$V'_{RR} = V_p + L_s (r \cos i_{NR} + p \sin i_{NR}) - p h_{IR}$$

$$W'_{RR} = W_p + p Y_N - L_s (\dot{i}_{NR} + q) \cos i_{NR} + \dot{h}_{IR}$$

AERODYNAMIC COORDINATE TRANSFORM (CONT'D.)

LEFT ROTOR HUB VELOCITY - SHAFT AXES

$$U_{RL} = U'_{RL} \cos i_{NL} - W'_{RL} \sin i_{NL}$$

$$V_{RL} = V'_{RL}$$

$$W_{RL} = U'_{RL} \sin i_{NL} + W'_{RL} \cos i_{NL}$$

RIGHT ROTOR HUB VELOCITY - SHAFT AXES

$$U_{RR} = U'_{RR} \cos i_{NR} - W'_{RR} \sin i_{NR}$$

$$V_{RR} = V'_{RR}$$

$$W_{RR} = U'_{RR} \sin i_{NR} + W'_{RR} \cos i_{NR}$$

LEFT WING A.C. VELOCITY - CHORD AXES

$$U_{LW} = U'_{LW} \cos i_w - W'_{LW} \sin i_w$$

$$V_{LW} = V'_{LW}$$

$$W_{LW} = U'_{LW} \sin i_w + W'_{LW} \cos i_w$$

RIGHT WING A.C. VELOCITY - CHORD AXES

$$U_{RW} = U'_{RW} \cos i_w - W'_{RW} \sin i_w$$

$$V_{RW} = V'_{RW}$$

$$W_{RW} = U'_{RW} \sin i_w + W'_{RW} \cos i_w$$

AERODYNAMIC COORDINATE TRANSFORM (Cont'd)

HORIZONTAL STABILIZER A.C. VELOCITY

$$U_{HT} = U_P + Z_{HT} \dot{\alpha}$$

$$V_{HT} = V_P + X_{HT} \dot{r} - Z_{HT} P$$

$$W_{HT} = W_P - X_{HT} \dot{q}$$

VERTICAL FIN A.C. VELOCITY

$$U_{VT} = U_P + Z_{VT} \dot{\alpha}$$

$$V_{VT} = V_P + X_{VT} \dot{r} - Z_{VT} P$$

$$W_{VT} = W_P - X_{VT} \dot{q}$$

WING EQUATIONS

$$\Gamma_{RR} = \alpha_{RR} + \tan^{-1} \left(\frac{N.F_R}{T_R} \right)$$

$$R_{RR} = \sqrt{T_R^2 + N.F_R^2 + S.F_R^2}$$

$$V_{*R} = \frac{V_{RR}}{\sqrt{\frac{|R_{RR}| + 10}{2\rho A}}}$$

$$V_{*R}^4 + 2 V_{*R}^3 \cos \Gamma_{RR} + V_{*R}^2 V_{RR}^2 = 1 \quad (\text{solve for } V_{*R})$$

$$E_{PRR} = \tan^{-1} \frac{V_{*R} \sin \Gamma_{RR}}{V_{RR} + V_{*R} \cos \Gamma_{RR}}$$

$$C_{TSRR} = \frac{\cos(\Gamma_{RR} - \alpha_{RR})}{\cos(\Gamma_{RR} - \alpha_{RR}) + \frac{V_{*R}^2}{4}}$$

$$\Gamma_{LR} = \alpha_{LR} + \tan^{-1} \left(\frac{N.F_L}{T_L} \right)$$

$$R_{LR} = \sqrt{T_L^2 + N.F_L^2 + S.F_L^2}$$

$$V_{*L} = \frac{V_{LR}}{\sqrt{\frac{|R_{LR}| + 10}{2\rho A}}}$$

$$V_{*L}^4 + 2 V_{*L}^3 \cos \Gamma_{LR} + V_{*L}^2 V_{LR}^2 = 1 \quad (\text{solve for } V_{*L})$$

$$E_{PLR} = \tan^{-1} \frac{V_{*L} \sin \Gamma_{LR}}{V_{LR} + V_{*L} \cos \Gamma_{LR}}$$

$$C_{TSLR} = \frac{\cos(\Gamma_{LR} - \alpha_{LR})}{\cos(\Gamma_{LR} - \alpha_{LR}) + \frac{V_{*L}^2}{4}}$$

WING EQUATIONS (Cont'd.)

$$\bar{\xi} = (\xi_{HR} + \xi_{HE}) \cdot 5$$

$$\bar{\alpha}_R = (\alpha_{RR} + \alpha_{LR}) \cdot 5$$

$$\bar{E}_P = (E_{PRR} + E_{PLR}) \cdot 5$$

$$\bar{C}_{TS} = (C_{TSRR} + C_{TSLR}) \cdot 5$$

} Used in Tail Aerodynamics

$$\bar{i}_N = (i_{NL} + i_{NR}) \cdot 5$$

$$C_{LW} = \frac{(C_{LSRW} + C_{LSLW})}{(1 - \bar{C}_{TS})} \cdot 5$$

} Used in Wing/Rotor Interfer.

$$\xi_{R1} = [L_s - PC \cos(\bar{i}_N - i_w) + h_p \sin(\bar{i}_N - i_w)] \tan(\bar{\alpha}_R - \bar{E}_p) \sin \bar{\xi}$$

$$\xi_{R2} = \sqrt{\frac{D^2}{4} - \left\{ [L_s - PC \cos(\bar{i}_N - i_w) + h_p \sin(\bar{i}_N - i_w)] \tan(\bar{\alpha}_R - \bar{E}_p) \cos \bar{\xi} + PC \sin(\bar{i}_N - i_w) + h_p \cos(\bar{i}_N - i_w) \right\}^2}$$

IF: $\xi_{R2} = 0$ OR Imaginary, $S_{iRW} = 0$ and $S_{iLW} = 0$,
also $\left(\frac{C_{Lwi}}{C_{Lw}}\right)_{RW} = 0$ and $\left(\frac{C_{Lwi}}{C_{Lw}}\right)_{LW} = 0.0$

FORM ξ_{R3} BY REPLACING PC IN ξ_{R1} EQUATION WITH (PC - C_w)

FORM ξ_{R4} BY REPLACING PC IN ξ_{R2} EQUATION WITH (PC - C_w)

IF: $\xi_{R4} = 0$ OR Imaginary; $S_{iRW} = 0$ and $S_{iLW} = 0$,
also $\left(\frac{C_{Lwi}}{C_{Lw}}\right)_{RW} = 0.0$ and $\left(\frac{C_{Lwi}}{C_{Lw}}\right)_{LW} = 0.0$

IF: UMBRELLAS OPEN; SET $C_{LW} = 0.0$

UMBRELLA LOGIC:

IF: $i_{NREF} < F_{iN}$ OR $q_F > 8.479 \frac{LB}{FT^2}$
SET UMBRELLAS CLOSED (Hysteresis $F_{iN} \pm 1^\circ$; $q_F \pm 0.1 \frac{LB}{FT^2}$)

WING EQUATIONS (CONT'D)

$$S_{iRW} = \frac{C_W}{2} [\bar{F}_{R1} + \bar{F}_{R2} + \bar{F}_{R3} + \bar{F}_{R4}]$$

$$\left(\frac{S_i}{S}\right)_{RW} = 2 \left(\frac{S_{iR}}{S_W}\right)$$

$$S_{iT} = C_W [\bar{F}_{R2} + \bar{F}_{R4}]$$

$$S_{iLW} = S_{iT} - S_{iR}$$

$$\left(\frac{S_i}{S}\right)_{LW} = 2 \left(\frac{S_{iL}}{S_W}\right)$$

$$(R_i)_{LW} = \left(\frac{S_{iL}}{C_W^2}\right)$$

$$(R_i)_{RW} = \left(\frac{S_{iR}}{C_W^2}\right)$$

$$R_W = \frac{S_W}{C_W^2} \text{ (PRELIMINARY)}$$

$$\left(\frac{C_{L\alpha i}}{C_{L\alpha}}\right)_{LW} = \frac{1}{1 + \frac{C_{L\alpha W}}{\pi} \left[\frac{1}{(R_i)_{LW}} - \frac{1}{R_W} \right]}$$

$$\left(\frac{C_{L\alpha i}}{C_{L\alpha}}\right)_{RW} = \frac{1}{1 + \frac{C_{L\alpha}}{\pi} \left[\frac{1}{(R_i)_{RW}} - \frac{1}{R_W} \right]}$$

$$K'_{AL} = \frac{V_{\infty L} + \left(\frac{C_{L\alpha i}}{C_{L\alpha}}\right)_{LW} N_{\infty L}}{V_{\infty L} + N_{\infty L}}$$

$$K'_{AR} = \frac{V_{\infty R} + \left(\frac{C_{L\alpha i}}{C_{L\alpha}}\right)_{RW} N_{\infty R}}{V_{\infty R} + N_{\infty R}}$$

WING EQUATIONS (CONTINUED)

$$\bar{q}_S = \left[\frac{1}{2} \rho (u^2 + v^2 + w^2) + \frac{(T_L + T_R) \cdot S}{A} \right]$$

$$q_{SRW} = \left[\frac{1}{2} \rho (u_{RW}^2 + v_{RW}^2 + w_{RW}^2) + \frac{T_R}{A} \right]$$

$$q_{SLW} = \left[\frac{1}{2} \rho (u_{LW}^2 + v_{LW}^2 + w_{LW}^2) + \frac{T_L}{A} \right]$$

WING EQUATIONS (Cont'd.)

WING ANGLE OF ATTACK AND SIDESLIP

$$\alpha_{LWO} = \sin^{-1} \left[\frac{W_{LW}}{\sqrt{U_{LW}^2 + W_{LW}^2}} \right] + \theta_{ELWAC}$$

$$\alpha_{RWO} = \sin^{-1} \left[\frac{W_{RW}}{\sqrt{U_{RW}^2 + W_{RW}^2}} \right] + \theta_{ERWAC}$$

$$\beta_{LWO} = \sin^{-1} \left[\frac{V_{LW}}{\sqrt{U_{LW}^2 + V_{LW}^2 + W_{LW}^2}} \right]$$

$$\beta_{RWO} = \sin^{-1} \left[\frac{V_{RW}}{\sqrt{U_{RW}^2 + V_{RW}^2 + W_{RW}^2}} \right]$$

$$\alpha_{LWSSO} = \alpha_{LWO} - \epsilon_{PLR}$$

$$\alpha_{RWSSO} = \alpha_{RWO} - \epsilon_{PRR}$$

$$\bar{\alpha}_W = (\alpha_{LWO} + \alpha_{RWO}) \cdot 0.5$$

$$\alpha_{LWrigid} = \sin^{-1} \left[\frac{W_{LW}}{\sqrt{U_{LW}^2 + W_{LW}^2}} \right] - \epsilon_{PLR}$$

$$\alpha_{RWrigid} = \sin^{-1} \left[\frac{W_{RW}}{\sqrt{U_{RW}^2 + W_{RW}^2}} \right] - \epsilon_{PRR}$$

$$\alpha'_{LWO} = \alpha_{LWO} - i_W - \theta_{ELWAC}$$

$$\alpha'_{RWO} = \alpha_{RWO} - i_W - \theta_{ERWAC}$$

NOTE: IF α_{LWSSO} OR $\alpha_{RWSSO} \geq \alpha_{MAX}$; PRINT OUT STALL WARNING

WING EQUATIONS (CONT'D)

CALCULATION OF INCREMENTAL LIFT, DRAG AND MOMENT COEFFICIENTS

CALCULATE:

$$C_{L_{LW0}} = C_L @ \alpha = \alpha_{LWSS0}, \quad \delta = \delta_{a_{LW}} + \delta_f, \quad \delta_{SP} = \delta_{SP_L}$$

$$C_{L_{RW0}} = C_L @ \alpha = \alpha_{RWSS0}, \quad \delta = \delta_{a_{RW}} + \delta_f, \quad \delta_{SP} = \delta_{SP_R}$$

$$C_{L_{LW0}}^* = C_L @ \alpha = \alpha_{LW0}, \quad \delta = \delta_{a_{LW}} + \delta_f, \quad \delta_{SP} = \delta_{SP_L}$$

$$C_{L_{RW0}}^* = C_L @ \alpha = \alpha_{RW0}, \quad \delta = \delta_{a_{RW}} + \delta_f, \quad \delta_{SP} = \delta_{SP_R}$$

$$C_{L_0} = C_L @ \alpha_F + i_w, \quad \delta = \delta_f$$

CALCULATE:

$$\alpha_{N.L.}^+ = 14.6^\circ - 0.12 \delta \quad (0^\circ \leq \delta \leq 40^\circ)$$

$$= 9.8^\circ \quad (\delta > 40^\circ)$$

$$\alpha_{N.L.}^- = -16.7^\circ - .1138\delta \quad (0^\circ \leq \delta \leq 40^\circ)$$

$$= -21.25^\circ \quad (\delta > 40^\circ)$$

IF: $\alpha_{N.L.}^- \leq \alpha \leq \alpha_{N.L.}^+$

$$C_L = 0.134 + C_{L_{RW}} \alpha + \Delta C_{L_\delta} + F \Delta C_{L_{SP}}$$

WHERE:

$$\Delta C_{L_\delta} = .0269 \delta \quad (0^\circ \leq \delta \leq 22.22906^\circ)$$

$$= -2.437137 + .20607 \delta - .003128 \delta^2 \quad (22.22906^\circ < \delta \leq 29.786^\circ)$$

$$= .442100 + .0263 \delta - .000338 \delta^2 \quad (\delta > 29.786^\circ)$$

$$\Delta C_{L_{SP}} = -0.01132 \delta_{SP} \quad (0^\circ \leq \delta_{SP} \leq 30^\circ)$$

$$= .076 - .018666 \delta_{SP} + .00016 \delta_{SP}^2 \quad (\delta_{SP} > 30^\circ)$$

$$F = 1.003412 + .011163 \delta + .002168 \delta^2 \quad (0^\circ \leq \delta \leq 20.1665^\circ)$$

$$F = -.756323 + .185684 \delta - .002159 \delta^2 \quad (\delta > 20.1665^\circ)$$

WING EQUATIONS (CONT'D)

IF: $\alpha_{N.L}^+ < \alpha \leq \alpha_{N.L}^+ + 8.534^\circ$

CALCULATE: $C'_{L,N.L} = 0.134 + C_{L\alpha_w} \alpha_{N.L}^+ + \Delta C_{L_S} + F \Delta C_{L_{SP}}$

$$\alpha_{DUM} = \alpha - \alpha_{N.L}^+ + 14.6^\circ$$

$$\Delta C_{L,N.L} = -0.00547619 \alpha_{DUM}^2 + 0.18254762 \alpha_{DUM} - 1.421571513$$

$$C_L = C'_{L,N.L} + \Delta C_{L,N.L} \quad \text{AND PRINT STALL WARNING}$$

IF: $(\alpha_{N.L}^+ + 8.534^\circ) < \alpha < 90^\circ$

CALCULATE: $C'_{L,N.L} = 0.134 + C_{L\alpha_w} \alpha_{N.L}^+ + \Delta C_{L_S} + F \Delta C_{L_{SP}}$

$$C_L = \frac{C'_{L,N.L} (90^\circ - \alpha)}{90^\circ - (\alpha_{N.L}^+ + 8.534^\circ)} \quad \text{AND PRINT STALL WARNING.}$$

IF: $(\alpha_{N.L}^- - 8.534^\circ) \leq \alpha < \alpha_{N.L}^-$

CALCULATE:

$$C'_{L,N.L} = 0.134 + C_{L\alpha_w} \alpha_{N.L}^- + \Delta C_{L_S} + F \Delta C_{L_{SP}}$$

$$\alpha_{DUM} = \alpha_{N.L}^- - \alpha + 14.6^\circ$$

$$\Delta C_{L,N.L} = -0.00547619 \alpha_{DUM}^2 + 0.18254762 \alpha_{DUM} - 1.421571513$$

$$C_L = C'_{L,N.L} - \Delta C_{L,N.L} \quad \text{AND PRINT STALL WARNING}$$

IF: $-90^\circ \leq \alpha < (\alpha_{N.L}^- - 8.534^\circ)$

CALCULATE:

$$C'_{L,N.L} = 0.134 + C_{L\alpha_w} \alpha_{N.L}^- + \Delta C_{L_S} + F \Delta C_{L_{SP}}$$

$$C_L = \frac{C'_{L,N.L} (90^\circ + \alpha)}{90^\circ + \alpha_{N.L}^- - 8.534^\circ} \quad \text{AND PRINT STALL WARNING}$$

NOTE: - α , α_{DUM} , δ , δ_{sw} , δ_{amb} , δ_f , $\alpha_{N.L}^-$, $\alpha_{N.L}^+$, $\delta_{SP,L}$, $\delta_{SP,R}$, IN DEGREES; $C_{L\alpha_w} \sim \text{1/DIGREES}$

WING EQUATIONS (CONT'D)

CALCULATE:-

$$C_{D_{LW}} = C_D @ \alpha = \alpha_{LWSSO}, \quad \delta = \delta_f + \delta_{aLW}, \quad \delta_{SP} = \delta_{SP_L}$$

$$C_{D_{RW}} = C_D @ \alpha = \alpha_{RWSSO}, \quad \delta = \delta_f + \delta_{aRW}, \quad \delta_{SP} = \delta_{SP_R}$$

$$C_{D_{LW}}^* = C_D @ \alpha = \alpha_{LW0}, \quad \delta = \delta_f + \delta_{aLW}, \quad \delta_{SP} = \delta_{SP_L}$$

$$C_{D_{RW}}^* = C_D @ \alpha = \alpha_{RW0}, \quad \delta = \delta_f + \delta_{aRW}, \quad \delta_{SP} = \delta_{SP_R}$$

AS FOLLOWS:

IF:- $-20^\circ \leq \alpha \leq 20^\circ$

CALCULATE: $C_D = 0.00059250 \alpha^2 + 0.002109993 \alpha + 0.01765$
 $+ \sum_{n=0}^4 \sum_{u=0}^4 [A_D(u+n) \delta^u \alpha^n] + \Delta C_{D_{SP}}$

WHERE: $\Delta C_{D_{SP}} = -0.000098784 \delta_{SP} + 0.000009622 \delta_{SP}^2$

IF: $20^\circ < \alpha \leq 90^\circ$, $\alpha_{DUM} = 20^\circ$

CALCULATE: $C_D^+ = 0.31105749 + \sum_{n=0}^4 \sum_{u=0}^4 [A_D(u+n) \delta^u \alpha_{DUM}^n] + \Delta C_{D_{SP}}$

$$C_D = C_D^+ + \frac{(1 - C_D^+)(\alpha - 20^\circ)}{70^\circ}$$

IF: $-90^\circ \leq \alpha < -20^\circ$, $\alpha_{DUM} = -20^\circ$

CALCULATE: $C_D^- = 0.19124389 + \sum_{n=0}^4 \sum_{u=0}^4 [A_D(u+n) \delta^u \alpha_{DUM}^n] + \Delta C_{D_{SP}}$

$$C_D = C_D^- - \frac{(1 - C_D^-)(\alpha + 20^\circ)}{70^\circ}$$

NOTE: α , α_{DUM} , δ , δ_{aRW} , δ_{aLW} , δ_{SP_R} , δ_{SP_L} IN DEGREES

WING EQUATIONS (CONT'D)

CALCULATE:

$$C_{MLW} = C_M @ \alpha = \alpha_{LWSSO} , \quad \delta = \delta_f + \delta_{aLW}$$

$$C_{MARW} = C_M @ \alpha = \alpha_{RWSO} , \quad \delta = \delta_f + \delta_{aRW}$$

$$C_{MLW_0}^* = C_M @ \alpha = \alpha_{LW_0} , \quad \delta = \delta_f + \delta_{aLW}$$

$$C_{MARW_0}^* = C_M @ \alpha = \alpha_{RW_0} , \quad \delta = \delta_f + \delta_{aRW}$$

AS FOLLOWS:

IF:- $-20^\circ \leq \alpha \leq 20^\circ$

CALCULATE:- $C_M' = -.030117 - .0003162 \alpha$

$$\Delta C_{M\delta} = .0000778 \delta^2 - .010033 \delta \quad (0^\circ \leq \delta \leq 45^\circ)$$

$$\Delta C_{M\delta} = .0000322 \delta^2 - .0049045 \delta - .1384272 \quad (\delta > 45^\circ)$$

$$C_M = C_M' + \Delta C_{M\delta}$$

IF: $\alpha > 20^\circ$

CALCULATE: $C_M' = -.036441 + \Delta C_{M\delta}$

$$C_M = C_M' \frac{(90^\circ - \alpha)}{70^\circ}$$

IF $\alpha < -20^\circ$

CALCULATE $C_M' = -.023793 + \Delta C_{M\delta}$

$$C_M = C_M' \frac{(90^\circ + \alpha)}{70^\circ}$$

NOTE: $\alpha, \alpha_{down}, \delta, \delta_{aRW}, \delta_{aLW}, \delta_{aP}, \delta_{aR}$ IN DEGREES

WING EQUATIONS (CONT'D)

CALCULATE :-

$$C_{LW}''' = C_{LW0} \quad ; \quad C_{DLW}''' = C_{D0} \quad ; \quad C_{MLW}'' = C_{M0}$$

$$C_{LRW}''' = C_{LRW0} \quad ; \quad C_{DRW}'' = C_{D0} \quad ; \quad C_{MRW}'' = C_{M0}$$

$$C_{LLWMAX}'' = C_{LMAX} + \Delta C_{L_S} + \Delta C_{L_{SP}}$$

$$C_{LRWMAX}'' = C_{LMAX} + \Delta C_{L_S} + \Delta C_{L_{SP}}$$

$$C_{LRW}^{*'} = C_{LRW0}^{*'} \quad ; \quad C_{DRW}^{*'} = C_{D0}^{*'} \quad ; \quad C_{MRW}^{*'} = C_{M0}^{*'}$$

$$C_{LLW}^{*'} = C_{LLW0}^{*'} \quad ; \quad C_{DLW}^{*'} = C_{D0}^{*'} \quad ; \quad C_{MLW}^{*'} = C_{M0}^{*'}$$

$$C_{LLWMAX}^{*'} = C_{LLWMAX}''$$

$$C_{LRWMAX}^{*'} = C_{LRWMAX}''$$

$$\bar{C}_L = \frac{C_{L0} \left(\frac{a_1}{a} \right)_W}{\sqrt{1-M^2}}$$

$$C_{LLW}''^{IGE} = C_{LLW}''' \frac{\left(\frac{a_1}{a} \right)_W}{\sqrt{1-M^2}} \quad ; \quad C_{LRW}''^{IGE} = C_{LRW}''' \frac{\left(\frac{a_1}{a} \right)_W}{\sqrt{1-M^2}} \quad ;$$

$$C_{LLW}^{*'}^{IGE} = C_{LLW}^{*'} \frac{\left(\frac{a_1}{a} \right)_W}{\sqrt{1-M^2}} \quad ; \quad C_{LRW}^{*'}^{IGE} = C_{LRW}^{*'} \frac{\left(\frac{a_1}{a} \right)_W}{\sqrt{1-M^2}}$$

WING EQUATIONS (CONT'D)

$$\Delta C_{DLW}^{IGE} = K_{99} \frac{(C_{LLW}^{IGE} - C_{LLW}''')^2}{\pi AR_w}; \quad \Delta C_{DRW}^{IGE} = K_{99} \frac{(C_{LRW}'' - C_{LRW}')^2}{\pi AR_w};$$

$$\Delta C_{DLW}^{IGE*} = K_{99} \frac{(C_{LLW}^{IGE*} - C_{LLW}^{*1})^2}{\pi AR_w}; \quad \Delta C_{DRW}^{IGE*} = K_{99} \frac{(C_{LRW}^{IGE*} - C_{LRW}^{*1})^2}{\pi AR_w}$$

$$\text{IF: } C_{LLW}^{IGE} \geq C_{LLW}''; \quad \text{SET } \Delta C_{DLW}^{IGE} = 0.0 \text{ \& } C_{LLW}^{IGE} = C_{LLW}''$$

$$\text{IF: } C_{LRW}^{IGE} \geq C_{LRW}''; \quad \text{SET } \Delta C_{DRW}^{IGE} = 0.0 \text{ \& } C_{LRW}^{IGE} = C_{LRW}''$$

$$\text{IF: } C_{LLW}^{IGE*} \geq C_{LLW}^{*1}; \quad \text{SET } \Delta C_{DLW}^{IGE*} = 0.0 \text{ \& } C_{LLW}^{IGE*} = C_{LLW}^{*1}$$

$$\text{IF: } C_{LRW}^{IGE*} \geq C_{LRW}^{*1}; \quad \text{SET } \Delta C_{DRW}^{IGE*} = 0.0 \text{ \& } C_{LRW}^{IGE*} = C_{LRW}^{*1}$$

$$\text{IF: } (a_2/a) > 1.0; \quad \text{SET } K_{99} = -1.0$$

$$(a_2/a) \leq 1.0; \quad \text{SET } K_{99} = +1.0$$

CALCULATE

$$C_{LLW}'' = C_{LLW}^{IGE}$$

$$C_{DLW}'' = C_{DLW}''' + \Delta C_{DLW}^{IGE}$$

$$C_{LRW}'' = C_{LRW}^{IGE}$$

$$C_{DRW}'' = C_{DRW}''' + \Delta C_{DRW}^{IGE}$$

$$C_{LLW}^{*1} = C_{LLW}^{IGE*}$$

$$C_{DLW}^{*1} = C_{DLW}^{*1} + \Delta C_{DLW}^{IGE*}$$

$$C_{LRW}^{*1} = C_{LRW}^{IGE*}$$

$$C_{DRW}^{*1} = C_{DRW}^{*1} + \Delta C_{DRW}^{IGE*}$$

WING EQUATIONS (cont'd.)

$$C_{LSLW} = K'_L \left\{ \left(\frac{S_i}{S} \right)_{LW} \left(C''_{LLW} \cos \epsilon_{PLR} - C''_{DLW} \sin \epsilon_{PLR} \right) + C^*_{LLW} (1 - C_{TSLR}) \left[1 - \left(\frac{S_i}{S} \right)_{LW} \right] \right\}$$

$$C_{LSRW} = K'_R \left\{ \left(\frac{S_i}{S} \right)_{RW} \left(C''_{LRW} \cos \epsilon_{PRR} - C''_{DRW} \sin \epsilon_{PRR} \right) + C^*_{LRW} (1 - C_{TSRR}) \left[1 - \left(\frac{S_i}{S} \right)_{RW} \right] \right\}$$

$$C_{DSLW} = K'_L \left\{ \left(\frac{S_i}{S} \right)_{LW} \left(C''_{LLW} \sin \epsilon_{PLR} + C''_{DLW} \cos \epsilon_{PLR} \right) + C^*_{DLW} (1 - C_{TSLR}) \left[1 - \left(\frac{S_i}{S} \right)_{LW} \right] \right\}$$

$$C_{DSRW} = K'_R \left\{ \left(\frac{S_i}{S} \right)_{RW} \left(C''_{LRW} \sin \epsilon_{PRR} + C''_{DRW} \cos \epsilon_{PRR} \right) + C^*_{DRW} (1 - C_{TSRR}) \left[1 - \left(\frac{S_i}{S} \right)_{RW} \right] \right\}$$

$$C_{MSLW} = K'_L \left\{ \left(\frac{S_i}{S} \right)_{LW} (C''_{MLW}) + C^*_{MLW} (1 - C_{TSLR}) \left[1 - \left(\frac{S_i}{S} \right)_{LW} \right] \right\}$$

$$C_{MSRW} = K'_R \left\{ \left(\frac{S_i}{S} \right)_{RW} (C''_{MRW}) + C^*_{MRW} (1 - C_{TSRR}) \left[1 - \left(\frac{S_i}{S} \right)_{RW} \right] \right\}$$

WING EQUATIONS (cont'd.)

$$\Delta C_{Y5 \text{ POWER}} = \frac{1}{4} \left\{ [C_{LSLW} - (1 - \bar{C}_{TS}) C_{LLW}^*] \left[1 - \frac{1}{2} \left(\frac{S_i}{S} \right)_{LW} \right] - [C_{LSRW} - (1 - \bar{C}_{TS}) C_{LRW}^*] \left[1 - \frac{1}{2} \left(\frac{S_i}{S} \right)_{RW} \right] \right\}$$

$$\Delta C_{N5 \text{ POWER}} = \frac{1}{4} \left\{ [C_{DSRW} - (1 - \bar{C}_{TS}) C_{DRW}^*] \left[1 - \frac{1}{2} \left(\frac{S_i}{S} \right)_{RW} \right] - [C_{DSLW} - (1 - \bar{C}_{TS}) C_{DLW}^*] \left[1 - \frac{1}{2} \left(\frac{S_i}{S} \right)_{LW} \right] \right\}$$

$$C_{Y5W} = (K_{20} + K_{21} \bar{C}_L) (1 - \bar{C}_{TS}) \beta_f + \left(\frac{1 - \bar{C}_{TS}}{2b_w} \right) (K_{22}) (C_{LLW}^* - C_{LRW}^*) \bar{Y}_{AC}$$

$$+ \Delta C_{Y5 \text{ POWER}}$$

$$C_{N5W} = (K_{22} \bar{C}_L^2) (1 - \bar{C}_{TS}) \beta_f + \left(\frac{1 - \bar{C}_{TS}}{2b_w} \right) (K_{22}) \left\{ (C_{DRW}^* - C_{DLW}^*) - [C_{LRW}^* \sin(\alpha_{RW0} - i_w) + C_{LLW}^* \sin(i_w - \alpha_{LW0})] \right\} \bar{Y}_{AC}$$

$$+ \Delta C_{N5 \text{ POWER}}$$

WING EQUATIONS

SPECIAL CONDITIONS (FOR UMBRELLAS OPEN)

IF : UMBRELLAS CLOSED; GO THROUGH WING EQUATIONS

IF : UMBRELLAS OPEN ; CALCULATE THE WING FORCES AND MOMENTS AS FOLLOWS:

$$X_{AERO}^{LW} = f_{e_h} q_{SLW} (1 - C_{TSLR}) \left[\frac{-U_{LW}}{|U_{LW}| + 1} \right]$$

$$X_{AERO}^{RW} = f_{e_h} q_{SRW} (1 - C_{TSRR}) \left[\frac{-U_{RW}}{|U_{RW}| + 1} \right]$$

$$Y_{AERO}^{LW} = 0.0$$

$$Y_{AERO}^{RW} = 0.0$$

$$\left. \begin{aligned} Z_{AERO}^{LW} &= T_L \left(\frac{D}{T} \right)_L \\ Z_{AERO}^{RW} &= T_R \left(\frac{D}{T} \right)_R \end{aligned} \right\} \text{GO TO WING BENDING}$$

$$M_{AERO}^{LW} = -X_{\frac{c}{z}} Z_{AERO}^{LW} + \left(\frac{M}{T} \right)_L T_L \left. \begin{aligned} & \\ & \end{aligned} \right\} Z_{AERO}^{LW} \text{ \& } Z_{AERO}^{RW} \text{ FROM}$$

$$M_{AERO}^{RW} = -X_{\frac{c}{z}} Z_{AERO}^{RW} + \left(\frac{M}{T} \right)_R T_R \left. \begin{aligned} & \\ & \end{aligned} \right\} \text{WING BENDING}$$

$$Z_{AERO}^W = \left(\frac{b_w}{z} \right) \left\{ Z_{AERO}^{RW} \left[1 - \left(\frac{S_i}{S} \right)_{RW} \right] - Z_{AERO}^{LW} \left[1 - \left(\frac{S_i}{S} \right)_{LW} \right] \right\}$$

$$M_{AERO}^W = 0.0$$

$$\underline{\text{IF}}: \left[\frac{h}{D} \right]_{EFF}^{LR} \leq 1.3 ; \left(\frac{D}{T} \right)_L = K_{\frac{D1}{T}} \left[\frac{h}{D} \right]_{EFF}^{LR} + K_{\frac{D2}{T}} \left[\frac{h}{D} \right]_{EFF}^{LR} + K_{\frac{D3}{T}} ;$$

$$\text{ \& } \left(\frac{M}{T} \right)_R = K_{\frac{M1}{T}} \left[\frac{h}{D} \right]_{EFF}^{LR} + K_{\frac{M2}{T}} \left[\frac{h}{D} \right]_{EFF}^{LR} + K_{\frac{M3}{T}}$$

$$\underline{\text{IF}}: \left[\frac{h}{D} \right]_{EFF}^{LR} > 1.3 ; \left(\frac{D}{T} \right)_L = K_{\frac{D4}{T}} ; \text{ \& } \left(\frac{M}{T} \right)_L = K_{\frac{M4}{T}}$$

$$\underline{\text{IF}}: \left[\frac{h}{D} \right]_{EFF}^{RR} \leq 1.3 ; \left(\frac{D}{T} \right)_R = K_{\frac{D1}{T}} \left[\frac{h}{D} \right]_{EFF}^{RR} + K_{\frac{D2}{T}} \left[\frac{h}{D} \right]_{EFF}^{RR} + K_{\frac{D3}{T}}$$

$$\text{ \& } \left(\frac{M}{T} \right)_R = K_{\frac{M1}{T}} \left[\frac{h}{D} \right]_{EFF}^{RR} + K_{\frac{M2}{T}} \left[\frac{h}{D} \right]_{EFF}^{RR} + K_{\frac{M3}{T}}$$

$$\underline{\text{IF}}: \left[\frac{h}{D} \right]_{EFF}^{RR} > 1.3 ; \left(\frac{D}{T} \right)_R = K_{\frac{D4}{T}} ; \text{ \& } \left(\frac{M}{T} \right)_R = K_{\frac{M4}{T}}$$

WING A.C. TO ELASTIC AXIS TRANSFORM

PITCHING MOMENT

$$M_{AERO}^{RW} = C_{MSRW} q_{SRW} \frac{S_W}{Z} C_W - X_{WAC} Z_{AERO}^{RW} + Z_{WAC} X_{AERO}^{RW}$$

$$M_{AERO}^{LW} = C_{MSLW} q_{SLW} \frac{S_W}{Z} C_W - X_{WAC} Z_{AERO}^{LW} + Z_{WAC} X_{AERO}^{LW}$$

VERTICAL FORCES

$$Z_{AERO}^{RW'} = [-C_{LSRW} - C_{DSRW} \alpha'_{RWO}] q_{SRW} \frac{S_W}{Z}$$

$$Z_{AERO}^{LW'} = [-C_{LSLW} - C_{DSLW} \alpha'_{LWO}] q_{SLW} \frac{S_W}{Z}$$

NOTE: $Z_{AERO}^{RW'}$ & $Z_{AERO}^{LW'}$ ARE USED IN VERTICAL BENDING EQ.'S

WING FORCE & MOMENT RESOLUTION - BODY AXES @ C.G.

$$X_{AERO}^{LW} = [-C_{DSLW} + C_{LSLW} \alpha'_{LW0}] \bar{q}_{SLW} \frac{S_w}{2}$$

$$X_{AERO}^{RW} = [-C_{DSRW} + C_{LSRW} \alpha'_{RW0}] \bar{q}_{SRW} \frac{S_w}{2}$$

$$Y_{AERO}^{LW} = [-C_{PSLW} \beta_{LW0}] \bar{q}_{SLW} \frac{S_w}{2}$$

$$Y_{AERO}^{RW} = [-C_{PSRW} \beta_{RW0}] \bar{q}_{SRW} \frac{S_w}{2}$$

$$\left. \begin{array}{l} Z_{AERO}^{LW} \\ Z_{AERO}^{RW} \end{array} \right\} \text{FROM VERTICAL BENDING}$$

$$L_{AERO}^{W} = C_{L_{SW}} \bar{q}_s S_w b_w$$

$$M_{AERO}^W = M_{AERO}^{LW} + M_{AERO}^{RW} + X_{CG} (Z_{AERO}^{LW} + Z_{AERO}^{RW}) - Z_{CG} (X_{AERO}^{LW} + X_{AERO}^{RW})$$

$$N_{AERO}^W = C_{N_{SW}} \bar{q}_s S_w b_w$$

NOTE: OBSERVE WING EQUATION SPECIAL CONDITIONS

HORIZONTAL AND VERTICAL TAIL AERODYNAMICS

WING AND TAIL ALTITUDE - GROUND EFFECT

$$h_{w c/4} = -Z_{down} + (X_{wac} - X_{cg}) \sin \theta + (Z_{cg} - Z_{wac}) \cos \theta$$

$$h_{t c/4} = -Z_{down} + (X_{ht} - X_{cg}) \sin \theta + (Z_{cg} - Z_{ht}) \cos \theta$$

HORIZONTAL TAIL ANGLE OF ATTACK

$$l_{ac} = X_{wac} - X_{ht} \quad (\text{PRELIMINARY})$$

$$GEF = \left[b_w^2 + 4(h_{t c/4} - h_{w c/4})^2 \right] / \left[b_w^2 + 4(h_{t c/4} + h_{w c/4})^2 \right]$$

$$\underline{\text{IF:}} \quad \bar{E}_p \frac{(1-GEF)}{\sqrt{1-M^2}} \geq \left[E_0 + \frac{dE}{d\alpha} \left(\alpha_w - l_{ac} \frac{\dot{w}}{U^2} \right) \right] \frac{(1-GEF)}{\sqrt{1-M^2}}$$

$$E = \frac{\bar{E}_p (1-GEF)}{\sqrt{1-M^2}}$$

$$\underline{\text{IF:}} \quad \frac{\bar{E}_p (1-GEF)}{\sqrt{1-M^2}} < \left[E_0 + \frac{dE}{d\alpha} \left(\alpha_w - l_{ac} \frac{\dot{w}}{U^2} \right) \right] \frac{(1-GEF)}{\sqrt{1-M^2}}$$

$$E = \left[E_0 + \frac{dE}{d\alpha} \left(\alpha_w - l_{ac} \frac{\dot{w}}{U^2} \right) \right] \frac{(1-GEF)}{\sqrt{1-M^2}}$$

USE FOR
RESOLUTION
OF
FORCES

$$\alpha_{HT} = \tan^{-1} \left[\frac{W_{HT}}{U_{HT}} \right] - E + i_{HT}; \quad \text{NOTE: - IF } U < 0 \quad \alpha_{HT} = \tan^{-1} \left[\frac{W_{HT}}{U_{HT}} \right] + i_{HT}$$

$$\text{WHERE } E_0 = f(\delta_L + \delta_a) \cdot 5 \quad \text{AND} \quad \frac{dE}{d\alpha} = f(\delta_L + \delta_a) \cdot 5$$

$$\underline{\text{IF:}} \quad |\alpha_{HT}| > 180^\circ ;$$

$$\alpha_{HT} = -(\text{SIGN } \alpha_{HT}) 360^\circ + \alpha_{HT}$$

USE ONLY IN EQ. FOR FORCE AND
MOMENT COEFF.

HORIZONTAL AND VERTICAL TAIL AERODYNAMICS (CONT'D)

HORIZONTAL TAIL LIFT AND DRAG

$$\alpha_{eHT} = \alpha_{HT} + I_{HT} \delta_e$$

$$\hat{\alpha}_{HT+} = (\alpha_{HTSTALL} - 2^\circ) + I_{HT} \delta_e$$

$$\hat{\alpha}_{HT-} = -(\alpha_{HTSTALL} - 2^\circ) + I_{HT} \delta_e$$

$$C_{L\alpha} = C_{L\alpha HT} \left(\frac{a_q}{a_{HT}} \right) / \sqrt{1-M^2}$$

$$\text{WHERE } \left(\frac{a_q}{a} \right)_{HT} = f(h_{TC/a}); \quad I_{HT} = f(s_e/s_T)$$

IF:- $\hat{\alpha}_{HT-} \leq \alpha_{eHT} \leq \hat{\alpha}_{HT+}$

$$C_{LHT} = C_{L\alpha} \alpha_{eHT}$$

$$C_{DHT} = C_{D0HT} + \frac{2C_{LHT}^2}{\pi R_{HT}}$$

IF:- $\hat{\alpha}_{HT+} < \alpha_{eHT} \leq 90^\circ$

$$C_{LHT} = C_{L\alpha} \hat{\alpha}_{HT+} \left[\frac{90^\circ - \alpha_{eHT}}{90^\circ - \hat{\alpha}_{HT+}} \right]$$

$$C_{LHTSTALL} = C_{L\alpha} \hat{\alpha}_{HT+}$$

$$C_{DHTSTALL} = C_{D0HT} + \frac{2C_{LHTSTALL}^2}{\pi R_{HT}}$$

$$C_{DHT} = C_{DHTSTALL} + \frac{(\alpha_{eHT} - \hat{\alpha}_{HT+})(1.1 - C_{DHTSTALL})}{90^\circ - \hat{\alpha}_{HT+}}$$

HORIZONTAL AND VERTICAL TAIL AERODYNAMICS (CONT'D)

HORIZONTAL TAIL LIFT AND DRAG (CONT'D)

IF:- $90^\circ < \alpha_{HT} < (180^\circ - .5 \hat{\alpha}_{HT-})$

$$C_{LHT} = .5 C_{L\alpha} \hat{\alpha}_{HT-} \frac{(\alpha_{HT} - 90^\circ)}{(90^\circ - .5 \hat{\alpha}_{HT-})}$$

$$C_{LHTSTALL} = .5 C_{L\alpha} \hat{\alpha}_{HT-}$$

$$C_{DHTSTALL} = \frac{2 C_{LHTSTALL}^2}{\pi R_{HT}} + C_{D_{0HT}}$$

$$C_{DHT} = C_{DHTSTALL} + \frac{(\alpha_{HT} + .5 \hat{\alpha}_{HT-} - 180^\circ)(1.1 - C_{DHTSTALL})}{(.5 \hat{\alpha}_{HT-} - 90^\circ)}$$

IF:- $(180^\circ - .5 \hat{\alpha}_{HT-}) \leq \alpha_{HT} \leq 180^\circ$

$$C_{LHT} = C_{L\alpha} (\alpha_{HT} - 180^\circ)$$

$$C_{DHT} = C_{D_{0HT}} + \frac{2 C_{LHT}^2}{\pi R_{HT}}$$

IF:- $-90^\circ \leq \alpha_{HT} < \hat{\alpha}_{HT-}$

$$C_{LHT} = C_{L\alpha} \hat{\alpha}_{HT-} \frac{(-90^\circ - \alpha_{HT})}{(-90^\circ - \hat{\alpha}_{HT-})}$$

$$C_{LHTSTALL} = C_{L\alpha} \hat{\alpha}_{HT-}$$

$$C_{DHTSTALL} = C_{D_{0HT}} + \frac{2 C_{LHTSTALL}^2}{\pi R_{HT}}$$

$$C_{DHT} = C_{DHTSTALL} + \frac{(\alpha_{HT} - \hat{\alpha}_{HT-})(1.1 - C_{DHTSTALL})}{(-90^\circ - \hat{\alpha}_{HT-})}$$

HORIZONTAL AND VERTICAL TAIL AERODYNAMICS (CONT'D)

HORIZONTAL TAIL LIFT AND DRAG (CONT'D)

IF: $(-180^\circ + .5\hat{\alpha}_{HT}) < \alpha_{HT} < -90^\circ$

$$C_{LHT} = .5 C_{L\alpha} \hat{\alpha}_{HT} \frac{(\alpha_{HT} + 90^\circ)}{(-90^\circ + .5\hat{\alpha}_{HT})}$$

$$C_{LHTSTALL} = .5 C_{L\alpha} \hat{\alpha}_{HT}$$

$$C_{DHTSTALL} = C_{DHT} + \frac{2 C_{LHTSTALL}^2}{\pi R_{HT}}$$

$$C_{DHT} = C_{DHTSTALL} - \frac{(\alpha_{HT} + 180^\circ - .5\hat{\alpha}_{HT})(1.1 - C_{DHTSTALL})}{(.5\hat{\alpha}_{HT} - 90^\circ)}$$

IF: $-180^\circ \leq \alpha_{HT} < (-180^\circ + .5\hat{\alpha}_{HT})$

$$C_{LHT} = C_{L\alpha} (\alpha_{HT} + 180^\circ)$$

$$C_{DHT} = C_{DHT} + \frac{2 C_{LHT}^2}{\pi R_{HT}}$$

HORIZONTAL AND VERTICAL TAIL AERODYNAMICS (CONT'D)

VERTICAL TAIL AERODYNAMICS

VERTICAL TAIL ANGLE OF ATTACK AND SIDESLIP

$$\beta_{VT} = \tan^{-1} \frac{V_{VT}}{\sqrt{U_{VT}^2 + W_{VT}^2}}$$

$$\alpha_{VT} = -\beta_{VT} + \beta_f \left(\frac{d\sigma}{dB} \right) \quad \left\{ \begin{array}{l} \text{NOTE: THIS VALUE OF } \alpha_{VT} \text{ IS USED IN RESOLUTION} \\ \text{OF FORCES AND MOMENTS} \end{array} \right\}$$

$$\text{IF: } |\alpha_{VT}| > 180^\circ; \quad \alpha_{VT} = \alpha_{VT} - (\text{SIGN } \alpha_{VT}) (360^\circ) \quad \left\{ \begin{array}{l} \text{NOTE: THIS VALUE OF } \alpha_{VT} \text{ ONLY USED} \\ \text{IN CALC. OF FORCE AND} \\ \text{MOMENT COEFFICIENTS} \end{array} \right\}$$

$$\alpha_{eVT} = (\alpha_{VT} + I_{VT} \delta_{RU})$$

$$\hat{\alpha}_{VT+} = (\alpha_{VT_{STALL}} - 2^\circ) + I_{VT} \delta_{RU}$$

$$\hat{\alpha}_{VT-} = -(\alpha_{VT_{STALL}} - 2^\circ) + I_{VT} \delta_{RU}$$

$$C_{Y\alpha} = C_{Y\alpha_{VT}} / \sqrt{1-M^2}$$

TAIL DYNAMIC PRESSURE AND SIDESWASH

$$\bar{q} = \frac{\rho}{2} (U^2 + V^2 + W^2)$$

$$\sigma = \frac{d\sigma}{dB} \beta_f$$

VERTICAL TAIL LIFT AND DRAG

$$\text{IF: } \hat{\alpha}_{VT-} \leq \alpha_{eVT} \leq \hat{\alpha}_{VT+}$$

$$C_{YVT} = C_{Y\alpha} \alpha_{eVT}$$

$$C_{DVT} = C_{DOUT} + \frac{2 C_{YVT}^2}{\pi A_{VT}}$$

HORIZONTAL AND VERTICAL TAIL AERODYNAMICS (CONT'D)

VERTICAL TAIL LIFT AND DRAG (CONT'D)

IF:- $\hat{\alpha}_{VT+} < \alpha_{eVT} < 90^\circ$

$$C_{YVT} = C_{Y\alpha} \hat{\alpha}_{VT+} \left[\frac{90^\circ - \alpha_{eVT}}{90^\circ - \hat{\alpha}_{VT+}} \right]$$

$$C_{YVTSTALL} = C_{Y\alpha} \hat{\alpha}_{VT+}$$

$$C_{DVTSTALL} = C_{D0VT} + \frac{2 C_{YVTSTALL}^2}{\pi R_{VT}^2}$$

$$C_{DVT} = C_{DVTSTALL} + \frac{(\alpha_{eVT} - \hat{\alpha}_{VT+}) \times 1.1 - C_{DVTSTALL}}{90^\circ - \hat{\alpha}_{VT+}}$$

IF:- $90^\circ < \alpha_{eVT} \leq (180^\circ - 0.5 \hat{\alpha}_{VT-})$

$$C_{YVT} = 0.5 C_{Y\alpha} \hat{\alpha}_{VT-} \left(\frac{\alpha_{eVT} - 90^\circ}{90^\circ - 0.5 \hat{\alpha}_{VT-}} \right)$$

$$C_{YVTSTALL} = 0.5 C_{Y\alpha} \hat{\alpha}_{VT-}$$

$$C_{DVTSTALL} = C_{D0VT} + \frac{2 C_{YVTSTALL}^2}{\pi R_{VT}^2}$$

$$C_{DVT} = C_{DVTSTALL} + \frac{(\alpha_{eVT} + 0.5 \hat{\alpha}_{VT-} - 180^\circ) \times 1.1 - C_{DVTSTALL}}{(0.5 \hat{\alpha}_{VT-} - 90^\circ)}$$

IF:- $(180^\circ - 0.5 \hat{\alpha}_{VT-}) \leq \alpha_{eVT} \leq 180^\circ$

$$C_{YVT} = C_{Y\alpha} (\alpha_{eVT} - 180^\circ)$$

$$C_{DVT} = C_{D0VT} + \frac{2 C_{YVT}^2}{\pi R_{VT}^2}$$

HORIZONTAL AND VERTICAL TAIL AERODYNAMICS (CONT'D)

VERTICAL TAIL LIFT AND DRAG (CONT'D)

IF:- $-90^\circ \leq \alpha_{eVT} < \hat{\alpha}_{VT-}$

$$C_{YVT} = C_{Y\alpha} \hat{\alpha}_{VT-} \frac{(-90^\circ - \alpha_{eVT})}{(-90^\circ - \hat{\alpha}_{VT-})}$$

$$C_{YVT\text{STALL}} = C_{Y\alpha} \hat{\alpha}_{VT-}$$

$$C_{DVT\text{STALL}} = C_{D0VT} + \frac{2 C_{YVT\text{STALL}}^2}{\pi R_{VT}}$$

$$C_{DVT} = C_{DVT\text{STALL}} + \frac{(\alpha_{eVT} - \hat{\alpha}_{VT-})(1.1 - C_{DVT\text{STALL}})}{(-90^\circ - \hat{\alpha}_{VT-})}$$

IF:- $(-180^\circ + .5 \hat{\alpha}_{VT+}) < \alpha_{eVT} < -90^\circ$

$$C_{YVT} = .5 C_{Y\alpha} \hat{\alpha}_{VT+} \frac{(\alpha_{eVT} + 90^\circ)}{(-90^\circ + .5 \hat{\alpha}_{VT+})}$$

$$C_{YVT\text{STALL}} = .5 C_{Y\alpha} \hat{\alpha}_{VT+}$$

$$C_{DVT\text{STALL}} = C_{D0VT} + \frac{2 C_{YVT\text{STALL}}^2}{\pi R_{VT}}$$

$$C_{DVT} = C_{DVT\text{STALL}} - \frac{(\alpha_{eVT} + 180^\circ - .5 \hat{\alpha}_{VT+})(1.1 - C_{DVT\text{STALL}})}{(.5 \hat{\alpha}_{VT+} - 90^\circ)}$$

IF:- $-180^\circ \leq \alpha_{eVT} < (-180^\circ + .5 \hat{\alpha}_{VT+})$

$$C_{YVT} = C_{Y\alpha} (\alpha_{eVT} + 180^\circ)$$

$$C_{DVT} = C_{D0VT} + \frac{2 C_{YVT}^2}{\pi R_{VT}}$$

HORIZONTAL AND VERTICAL TAIL AERODYNAMICS (CONT'D)

TAIL EQUATIONS LOGIC

HORIZONTAL TAIL

1. IF $hw_{CH} > 100 \text{ FT.}$, SET $G_{EF} = 0.0$
2. IF THE UMBRELLAS OPEN; SET $\epsilon = \frac{\bar{\epsilon}_p (1 - G_{EP})}{\sqrt{1 - M^2}}$
3. IF $\alpha_{ENT} > \hat{\alpha}_{HT+}$ PRINT STALL WARNING.
4. IF $\alpha_{ENT} < \hat{\alpha}_{HT-}$ PRINT STALL WARNING

VERTICAL TAIL

1. IF $\alpha_{VT} > \hat{\alpha}_{VT+}$ PRINT STALL WARNING
2. IF $\alpha_{VT} < \hat{\alpha}_{VT-}$ PRINT STALL WARNING

TAIL FORCE AND MOMENT RESOLUTION TO C.G.

HORIZONTAL TAIL

NOTES: - IF UMBRELLAS OPEN AND $M > 0$; SET $\eta_{HT} = .5 \eta_{NT}$

$$X_{AERO}^{HT} = [-C_{DHT} \cos(\alpha_{HT} - i_{HT}) \cos(\beta_{VT} - \sigma) + C_{LHT} \sin(\alpha_{HT} - i_{HT})] \bar{q} S_{HT} \eta_{HT}$$

$$Y_{AERO}^{HT} = [-C_{DHT} \sin(\beta_{VT} - \sigma)] \bar{q} S_{HT} \eta_{HT}$$

$$Z_{AERO}^{HT} = [-C_{LHT} \cos(\alpha_{HT} - i_{HT}) - C_{DHT} \cos(\beta_{VT} - \sigma) \sin(\alpha_{HT} - i_{HT})] \bar{q} S_{HT} \eta_{HT}$$

$$L_{AERO}^{HT} = -Y_{AERO}^{HT} (Z_{HT} - Z_{CG})$$

$$M_{AERO}^{HT} = Z_{AERO}^{HT} (X_{CG} - X_{HT}) + X_{AERO}^{HT} (Z_{HT} - Z_{CG})$$

$$N_{AERO}^{HT} = -Y_{AERO}^{HT} (X_{CG} - X_{HT})$$

VERTICAL TAIL

$$X_{AERO}^{VT} = [-C_{DVT} \cos(\beta_{VT} - \sigma) \cos(\alpha_{HT} - i_{HT}) - C_{YVT} \sin(\beta_{VT} - \sigma) \cos(\alpha_{HT} - i_{HT})] \bar{q} S_{VT} \eta_{VT}$$

$$Y_{AERO}^{VT} = [C_{YVT} \cos(\beta_{VT} - \sigma) - C_{DVT} \sin(\beta_{VT} - \sigma)] \bar{q} S_{VT} \eta_{VT}$$

$$Z_{AERO}^{VT} = [-C_{DVT} \cos(\beta_{VT} - \sigma) \sin(\alpha_{HT} - i_{HT}) - C_{YVT} \sin(\beta_{VT} - \sigma) \sin(\alpha_{HT} - i_{HT})] \bar{q} S_{VT} \eta_{VT}$$

$$L_{AERO}^{VT} = -Y_{AERO}^{VT} (Z_{VT} - Z_{CG})$$

$$M_{AERO}^{VT} = Z_{AERO}^{VT} (X_{CG} - X_{VT}) + X_{AERO}^{VT} (Z_{VT} - Z_{CG})$$

$$N_{AERO}^{VT} = -Y_{AERO}^{VT} (X_{CG} - X_{VT})$$

TOTAL TAIL CONTRIBUTION

$$X_{AERO}^T = X_{AERO}^{VT} + X_{AERO}^{HT} ; Z_{AERO}^T = Z_{AERO}^{VT} + Z_{AERO}^{HT} \quad M_{AERO}^T = M_{AERO}^{VT} + M_{AERO}^{HT}$$

$$Y_{AERO}^T = Y_{AERO}^{VT} + Y_{AERO}^{HT} ; L_{AERO}^T = L_{AERO}^{VT} + L_{AERO}^{HT} \quad N_{AERO}^T = N_{AERO}^{VT} + N_{AERO}^{HT}$$

NACELLE AERODYNAMICS

NACELLE ANGLE OF ATTACK AND SIDESLIP

$$\alpha_{RN} = \tan^{-1} \frac{W_{RR}}{U_{RR}} \quad ; \quad q_{RN} = \frac{1}{2} \rho V_{RR}^2$$

$$\alpha_{LN} = \tan^{-1} \frac{W_{RL}}{U_{RL}} \quad ; \quad q_{LN} = \frac{1}{2} \rho V_{LR}^2$$

$$\beta_{RN} = \tan^{-1} \frac{V_{RR}}{\sqrt{U_{RR}^2 + W_{RR}^2}}$$

$$\beta_{LN} = \tan^{-1} \frac{V_{RL}}{\sqrt{U_{RL}^2 + W_{RL}^2}}$$

NACELLE WIND AXIS FORCE & MOMENT COEF.'S

$$\left. \begin{aligned} C_{DRN} &= C_{DORN} + K_{30} |\alpha_{RN}| + K_{31} |\alpha_{RN}|^2 \\ C_{DLN} &= C_{DOLN} + K_{30} |\alpha_{LN}| + K_{31} |\alpha_{LN}|^2 \end{aligned} \right\} \begin{array}{l} \text{NOTE: CHECK RANGE} \\ \text{OF } \alpha_{RN} \text{ \& } \alpha_{LN} \text{ TO} \\ \text{DETERMINE VALUES FOR} \\ \text{CONSTANTS.} \end{array}$$

WHERE: $C_{DORN} = C_{DON}$

$$C_{DOLN} = C_{DON}$$

$$C_{LRN} = K_{32} \sin \alpha_{RN} \cos \alpha_{RN}$$

$$C_{LLN} = K_{32} \sin \alpha_{LN} \cos \alpha_{LN}$$

$$C_{MNRN} = C_{MON} + K_{34} \sin \alpha_{RN} \cos \alpha_{RN} + K_{35} (\sin \alpha_{RN} \cos \alpha_{RN}) |\sin \alpha_{RN} \cos \alpha_{RN}|$$

$$C_{MLN} = C_{MON} + K_{34} \sin \alpha_{LN} \cos \alpha_{LN} + K_{35} (\sin \alpha_{LN} \cos \alpha_{LN}) |\sin \alpha_{LN} \cos \alpha_{LN}|$$

SPECIAL CONDITIONS

1. IF: $V_{RR}^2 \leq 1 (\text{ft/sec})^2$; RIGHT NACELLE AERO $\equiv 0.0$ & HOLD VALUE OF α_{RN} & β_{RN}
2. IF: $V_{LR}^2 \leq 1 (\text{ft/sec})^2$; LEFT NACELLE AERO $\equiv 0.0$ & HOLD VALUE OF α_{LN} & β_{LN}

NACELLE AERODYNAMICS (Cont'd.)

$$C_{YRN} = K_{36} \sin \beta_{RN} \cos \beta_{RN} + K_{37} (\sin \beta_{RN} \cos \beta_{RN}) |\sin \beta_{RN} \cos \beta_{RN}|$$

$$C_{YLN} = K'_{36} \sin \beta_{LN} \cos \beta_{LN} + K'_{37} (\sin \beta_{LN} \cos \beta_{LN}) |\sin \beta_{LN} \cos \beta_{LN}|$$

$$C_{NRN} = C_{NORN} + K_{38} \sin \beta_{RN} \cos \beta_{RN} + K_{37} (\sin \beta_{RN} \cos \beta_{RN}) |\sin \beta_{RN} \cos \beta_{RN}|$$

$$C_{NLN} = C_{NOLN} + K'_{38} \sin \beta_{LN} \cos \beta_{LN} + K'_{37} (\sin \beta_{LN} \cos \beta_{LN}) |\sin \beta_{LN} \cos \beta_{LN}|$$

$$C_{XRN} = C_{ZLN} \equiv 0.0$$

NACELLE FORCES & MOMENTS - NACELLE AXES

RIGHT

$$\Delta X'_{RN} = q_{RN} S_w \left[-C_{DRN} \cos \alpha_{RN} + C_{LRN} \sin \alpha_{RN} - C_{YRN} \sin \beta_{RN} \cos \alpha_{RN} \right] \frac{1}{2}$$

$$\Delta Y'_{RN} = q_{RN} S_w \left[C_{YRN} \cos \beta_{RN} - C_{DRN} \sin \beta_{RN} \right] \frac{1}{2}$$

$$\Delta Z'_{RN} = q_{RN} S_w \left[-C_{LRN} \cos \alpha_{RN} - C_{DRN} \cos \beta_{RN} \sin \alpha_{RN} - C_{YRN} \sin \beta_{RN} \sin \alpha_{RN} \right] \frac{1}{2}$$

$$\Delta X'_{LN} = q_{RN} S_w b_w \left[-\left(\frac{C_w}{b_w}\right) C_{MRN} \sin \beta_{RN} \cos \alpha_{RN} - C_{NRN} \sin \alpha_{RN} \right] \frac{1}{2}$$

$$\Delta M'_{RN} = q_{RN} S_w C_w \left[C_{MRN} \cos \beta_{RN} \right] \frac{1}{2}$$

$$\Delta N'_{RN} = q_{RN} S_w b_w \left[C_{NRN} \cos \alpha_{RN} - \left(\frac{C_w}{b_w}\right) C_{MRN} \sin \beta_{RN} \cos \alpha_{RN} \right] \frac{1}{2}$$

$$\Delta X'_{LN} = q_{LN} S_w \left[-C_{DLN} \cos \alpha_{LN} + C_{LLN} \sin \alpha_{LN} - C_{YLN} \sin \beta_{LN} \cos \alpha_{LN} \right] \frac{1}{2}$$

$$\Delta Y'_{LN} = q_{LN} S_w \left[C_{YLN} \cos \beta_{LN} - C_{DLN} \sin \beta_{LN} \right] \frac{1}{2}$$

$$\Delta Z'_{LN} = q_{LN} S_w \left[-C_{LLN} \cos \alpha_{LN} - C_{DLN} \cos \beta_{LN} \sin \alpha_{LN} - C_{YLN} \sin \beta_{LN} \sin \alpha_{LN} \right] \frac{1}{2}$$

LEFT

$$\Delta X'_{RN} = q_{LN} S_w b_w \left[-\left(\frac{C_w}{b_w}\right) C_{MLN} \sin \beta_{LN} \cos \alpha_{LN} - C_{NLN} \sin \alpha_{LN} \right] \frac{1}{2}$$

$$\Delta M'_{LN} = q_{LN} S_w C_w \left[C_{MLN} \cos \beta_{LN} \right] \frac{1}{2}$$

$$\Delta N'_{LN} = q_{LN} S_w b_w \left[C_{NLN} \cos \alpha_{LN} - \left(\frac{C_w}{b_w}\right) C_{MLN} \sin \beta_{LN} \cos \alpha_{LN} \right] \frac{1}{2}$$

LANDING GEAR EQUATIONS

PERFORM THE FOLLOWING CALCULATIONS FOR EACH OF THREE LANDING GEAR i.e. $n = 1, 2, 3$.

LANDING GEAR-A/C LOCATION

$$X_n = -X_{CG} + X_{Gn}$$

$$Y_n = Y_{Gn}$$

$$Z_n = -Z_{CG} + Z_{Gn}$$

$n=1$ LEFT MAIN GEAR
 $n=2$ RIGHT MAIN GEAR
 $n=3$ NOSE GEAR

Strut Deflection

$$h_{G0n} = X_n \sin \theta - Z_n \cos \theta - r_n$$

$$h_{G\phi n} = [Y_n \sin \phi + (Z_n + r_n)(\cos \phi - 1)] \cos \theta$$

$$h_{TN} = (-Z_{down} + h_{G0n} - h_{G\phi n}) / (\cos \phi \cos \theta)$$

Rate of Strut Deflection

$$\dot{h}_{TN} = -\dot{Z}_{down} \left(\frac{1}{\cos \phi \cos \theta} \right) + X_n q - Y_n p$$

Vertical force

$$F_{G2n} = K_{STN} h_{TN} + D_{STN} \dot{h}_{TN}$$

NOTE: COMPUTE F_{G2n} ONLY IF $h_{TN} < 0$;

IF $h_{TN} > 0$; $F_{G2n} = 0.0$

REMAINING CALCULATIONS MAY BE SET TO ZERO.

LANDING GEAR EQUATIONS (cont'd.)

Longitudinal force:

$$F_{Ln} = + (\mu_0 + \mu_1 B_{Gn}) F_{Gzn} \frac{+u}{|u|}$$

i.e. IF $u > 0$ F_{Ln} is negative
IF $u < 0$ F_{Ln} is positive
IF $u = 0$ $F_{Ln} = 0.0$

NOTE: B_{Gn} is percent brake pedal deflection

Side force:

$$F_{Sn} = \mu_s F_{Gzn} \frac{+v}{|v|}$$

i.e. IF $v > 0$ F_{Sn} is negative
IF $v < 0$ F_{Sn} is positive
IF $v = 0$ $F_{Sn} = 0.0$

FORCE & MOMENT CONTRIBUTION OF EACH GEAR

$$\Delta X_n = F_{Ln} - F_{Gzn} \theta$$

$$\Delta Y_n = F_{Sn} + F_{Gzn} \phi$$

$$\Delta Z_n = F_{Ln} \theta - F_{Sn} \phi + F_{Gzn}$$

$$\Delta M_n = -\Delta Z_n X_n + \Delta X_n (Z_n + r_n + h_{Tn})$$

$$\Delta L_n = \Delta Z_n Y_n - \Delta Y_n (Z_n + r_n + h_{Tn})$$

$$\Delta N_n = -\Delta X_n Y_n + X_n \Delta Y_n$$

LANDING GEAR EQUATIONS (Cont'd.)

$$\Delta X_{LG} = \sum_1^3 \Delta X_n$$

$$\Delta Y_{LG} = \sum_1^3 \Delta Y_n$$

$$\Delta Z_{LG} = \sum_1^3 \Delta Z_n$$

$$\Delta \alpha_{LG} = \sum_1^3 \Delta \alpha_n$$

$$\Delta M_{LG} = \sum_1^3 \Delta M_n$$

$$\Delta N_{LG} = \sum_1^3 \Delta N_n$$

FUSELAGE AERODYNAMICS

FUSELAGE INPUT EQUATIONS

$$\alpha_F = \tan^{-1} \frac{W}{U}$$

$$\beta_F = \tan^{-1} \frac{V}{\sqrt{U^2 + W^2}}$$

$$\alpha'_F = \sin \alpha_F \cos \beta_F$$

$$\beta'_F = \sin \beta_F \cos \beta_F$$

$$V_F = \sqrt{U^2 + V^2 + W^2}$$

$$q_F = \frac{1}{2} \rho V_F^2$$

(q) SAME AS TAIL DYNAMIC PRESSURE

$$V_{FUS} = V_F \sqrt{\sigma_h}$$

FUSELAGE WIND AXIS COEF'S

$$C_{DF} = C_{DOF} (1 + K_0 |\beta_F|^3) + K_2 \alpha_F^2 + K_1 |\alpha_F| + \Delta C_{DLG}$$

$$C_{LF} = K_3 \alpha'_F + K_4 \alpha'_F |\alpha'_F| + K_{42}$$

$$C_{YF} = K_7 \beta'_F + K_8 \beta'_F |\beta'_F|$$

$$C_{MF} = C_{MOF} + K_5 \alpha'_F + K_6 \alpha'_F |\alpha'_F| + \Delta C_{MLG}$$

$$C_{NF} = C_{NOF} + K_9 \beta'_F + K_{10} \beta'_F |\beta'_F|$$

NOTE: IF GEAR IS UP; $\Delta C_{DLG} \neq \Delta C_{MLG} = 0.0$

SPECIAL CONDITIONS

1. IF $V_F^2 \leq 1$ (ft/sec)² FUSELAGE AERO = 0.0 \neq
HOLD VALUE OF $\alpha_F \neq \beta_F$

FUSELAGE FORCES & MOMENT ABOUT A/C C.G.

$$X_{AERO}^{F'} = [-C_{DF} \cos \alpha_F + C_{LF} \sin \alpha_F - C_{YF} \sin \beta_F \cos \alpha_F] q_F S_W$$

$$Y_{AERO}^{F'} = [C_{YF} \cos \beta_F - C_{DF} \sin \beta_F] q_F S_W$$

$$Z_{AERO}^{F'} = [-C_{LF} \cos \alpha_F - C_{DF} \cos \beta_F \sin \alpha_F - C_{YF} \sin \beta_F \sin \alpha_F] q_F S_W$$

$$\begin{aligned} \mathcal{L}_{AERO}^{F'} = & \left[-\left(\frac{C_W}{b_W}\right) C_{MF} \sin \beta_F \cos \alpha_F - C_{NF} \sin \alpha_F \right] q_F S_W b_W + \\ & + Y_{AERO}^{F'} [Z_{CG} - Z_{FAC}] \end{aligned}$$

$$\begin{aligned} \mathcal{M}_{AERO}^{F'} = & [C_{MF} \cos \beta_F] q_F S_W C_W + Z_{AERO}^{F'} [X_{CG} - X_{FAC}] \\ & - X_{AERO}^{F'} [Z_{CG} - Z_{FAC}] + \end{aligned}$$

$$\begin{aligned} \mathcal{N}_{AERO}^{F'} = & [C_{NF} \cos \alpha_F - \left(\frac{C_W}{b_W}\right) C_{MF} \sin \beta_F \sin \alpha_F] q_F S_W b_W \\ & - Y_{AERO}^{F'} [X_{CG} - X_{FAC}] + \end{aligned}$$

$$X_{AERO}^F = X_{AERO}^{F'} + \Delta X_{LG}$$

$$Y_{AERO}^F = Y_{AERO}^{F'} + \Delta Y_{LG}$$

$$Z_{AERO}^F = Z_{AERO}^{F'} + \Delta Z_{LG}$$

$$\mathcal{L}_{AERO}^F = \mathcal{L}_{AERO}^{F'} + \Delta \mathcal{L}_{LG}$$

$$\mathcal{M}_{AERO}^F = \mathcal{M}_{AERO}^{F'} + \Delta \mathcal{M}_{LG}$$

$$\mathcal{N}_{AERO}^F = \mathcal{N}_{AERO}^{F'} + \Delta \mathcal{N}_{LG}$$

WING ON ROTOR INTERFERENCE

AVERAGE NACELLE INCIDENCE

$$\bar{i}_N = 0.5 (i_{NL} + i_{NR})$$

AVERAGE LIFT COEF.

$$C_{LW} = 0.5 \frac{(C_{LSRW} + C_{LSLW})}{(1 - \bar{C}_{TS})}$$

LOOK-UP: E_{WRR} & E_{WRL} @ \bar{i}_N & C_{LW}

WING INTERFERENCE LOGIC

1. IF: UMBRELLAS OPEN, SET $C_{LW} = 0.0$ & $E = \frac{E_p(1 - GEP)}{\sqrt{1 - M^2}}$

ROTOR / ROTOR INTERFERENCE

POSITIVE SIDESLIP i.e., $v > 0.0$ (LOGIC REQUIRED)

$$\chi = 1.5708 - \epsilon_{PRR}$$

$$\left(\frac{\delta v_{RL}^*}{v_{RR}^*} \right) = T_1 + T_2(\chi) + T_3(\chi)^2$$

$$\delta v_{RL} = \left(\frac{\delta v_{RL}^*}{v_{RR}^*} \right) v_{RR} \sqrt{\frac{R_{RR}}{2\rho\pi R^2}}$$

$$\epsilon'_{iRL} = -\tan^{-1} \left[\frac{\delta v_{RL}}{v_{LR} + 1.0} \right]$$

$$\epsilon_{iRL} = (|\beta_F|)(.40528 i_{NL}) \epsilon'_{iRL}$$

$$\epsilon_{iLR} = 0.0$$

NEGATIVE SIDESLIP i.e. $v < 0.0$

$$\chi = 1.5708 - \epsilon_{PLR}$$

$$\left(\frac{\delta v_{LR}^*}{v_{LR}^*} \right) = T_1 + T_2(\chi) + T_3(\chi)^2$$

$$\delta v_{LR} = \left(\frac{\delta v_{LR}^*}{v_{RR}^*} \right) v_{NL} \sqrt{\frac{R_{LR}}{2\rho\pi R^2}}$$

$$\epsilon'_{iLR} = -\tan^{-1} \left[\frac{\delta v_{LR}}{v_{RR} + 1.0} \right]$$

$$\epsilon_{iLR} = (|\beta_F|)(.40528 i_{NR}) \epsilon'_{iLR}$$

$$\epsilon_{iRL} = 0.0$$

NOTE: $v_{RR} \neq v_{NL}$ FROM WING EQUATIONS.

ROTOR AERO INPUT EQUATIONS

RIGHT ROTOR

$$\alpha_{RR} = \tan^{-1} \left\{ \frac{\sqrt{V_{RR}^2 + (W_{RR} + U_{RR} \epsilon_{WRR})^2}}{U_{RR}} \right\} + \epsilon_{iLR}$$

$$V_{RR} = \sqrt{U_{RR}^2 + V_{RR}^2 + W_{RR}^2} \quad ; \quad \mu_{RR} = \frac{V_{RR}}{\Omega_{LR}}$$

LEFT ROTOR

$$\alpha_{LR} = \tan^{-1} \left\{ \frac{\sqrt{V_{RL}^2 + (W_{RL} + U_{RL} \epsilon_{WRL})^2}}{U_{RL}} \right\} + \epsilon_{iLR}$$

$$V_{LR} = \sqrt{U_{RL}^2 + V_{RL}^2 + W_{RL}^2} \quad ; \quad \mu_{LR} = \frac{V_{LR}}{\Omega_{LR}}$$

ROTOR ANGULAR RATE TRANSFORMS

RIGHT - NACELLE AXES

$$P_{NR}^N = -p \cos i_{NR} + r \sin i_{NR}$$

$$Q_{NR}^N = q + \dot{i}_{NR}$$

$$R_{NR}^N = -r \cos i_{NR} - p \sin i_{NR}$$

LEFT - NACELLE AXES

$$P_{NL}^N = p \cos i_{NL} - r \sin i_{NL}$$

$$Q_{NL}^N = q + \dot{i}_{NL}$$

$$R_{NL}^N = r \cos i_{NL} + p \sin i_{NL}$$

RIGHT WIND AXES

$$P_{NR}^R = P_{NR}^N$$

$$Q_{NR}^R = Q_{NR}^N \cos \beta_{HR} + R_{NR}^N \sin \beta_{HR}$$

$$R_{NR}^R = R_{NR}^N \cos \beta_{NR} - Q_{NR}^N \sin \beta_{NR}$$

LEFT WIND AXES

$$P_{NL}^R = P_{NL}^N$$

$$Q_{NL}^R = Q_{NL}^N \cos \beta_{HL} - R_{NL}^N \sin \beta_{HL}$$

$$R_{NL}^R = R_{NL}^N \cos \beta_{NL} + Q_{NL}^N \sin \beta_{NL}$$

NOTE: USE WIND AXIS RATES IN ROTOR ROUTINE

ROTOR EQUATIONS

RIGHT ROTOR

THRUST

$$C'_{TRR} = \left[\frac{Z_1 S + 1}{Z_2 S + 1} \right] \left[C_{TORR} \cos A_{IGR} \cos B_{IOR} \right]$$

WHERE:-

$$C_{TORR} = \sum_{N=0}^2 \sum_{U=0}^3 \left[A_T(U+4N) \alpha_{RR}^U \theta_{O75R}^N \right] \left. \begin{array}{l} \text{INTERPOLATE } C_{TORR} \\ \text{LINEARLY BETWEEN } \mu\text{'S} \end{array} \right\}$$

$$A_T(U+4N) = f(\mu_{RR})$$

GROUND EFFECT

$$h_{RR} = -Z_{DOWN} + (L_S \cos i_{NR} - X_{CG}) \sin \theta \\ + \left[(L_S \sin i_{NR} + Z_{CG}) \cos \phi - Y_N \sin \phi \right] \cos \theta$$

$$\left(\frac{h}{D} \right)_{EFF_{RR}} = \frac{h_{RR}}{2R \left[\left| \sin(\theta + i_{NR}) \cos \phi \right| + 0.0174 \right]}$$

$$\left(\frac{T_{IGE}}{T_{OGE}} \right)_{RR} = \left[\left(\frac{h}{D} \right)_{EFF_{RR}}^2 (0.1741 - 0.6216 \mu_{RR}) \right. \\ \left. + \left(\frac{h}{D} \right)_{EFF_{RR}} (1.4779 \mu_{RR} - 0.4143) \right. \\ \left. + 1.2474 - 0.8806 \mu_{RR} \right]$$

$$C_{TRR} = C'_{TRR} \left(\frac{T_{IGE}}{T_{OGE}} \right)_{RR}$$

SPECIAL CONDITIONS: IF $\mu_{RR} \geq 0.203$; $\left(\frac{T_{IGE}}{T_{OGE}} \right)_{RR} = 1.0$

OR IF $\left(\frac{h}{D} \right)_{EFF_{RR}} \geq 1.3$; $\left(\frac{T_{IGE}}{T_{OGE}} \right)_{RR} = 1.0$

ROTOR EQUATIONS (CONTINUOUS)

POWER

$$C_{PRR} = C_{PORR}$$

WHERE:-

$$C_{PORR} = \sum_{N=0}^2 \sum_{u=0}^3 \left[A_P(u+4N) \alpha_{RR}^u C_{TRR}^{iN} \right] \left. \begin{array}{l} \text{INTERPOLATE } C_{PORR} \\ \text{LINEARLY BETWEEN } \mu\text{'S} \end{array} \right\}$$

$$A_P(u+4N) = f(\mu_{RR})$$

NORMAL FORCE

$$C_{NFR} = C_{NFORR} + \frac{dC_{NFR}}{dA_{ICR}} A_{ICR} + \frac{dC_{NFR}}{dB_{ICR}} B_{ICR}$$

WHERE:-

$$C_{NFORR} = \sum_{N=0}^2 \sum_{u=0}^3 \left[A_{NP}(u+4N) \alpha_{RR}^u C_{TRR}^{iN} \right] \left. \begin{array}{l} \text{INTERPOLATE } C_{NFORR} \\ \text{LINEARLY BETWEEN} \\ \mu\text{'S} \end{array} \right\}$$

$$A_{NP}(u+4N) = f(\mu_{RR})$$

$$\frac{dC_{NFR}}{dA_{ICR}} = D_{NF1} C_{TRR} + D_{NF2} \mu_{RR}^2 + D_{NF3} \mu_{RR} + D_{NF4}$$

$$\frac{dC_{NFR}}{dB_{ICR}} = E_{NF1} C_{TRR} + E_{NF2} \mu_{RR}^2 + E_{NF3} \mu_{RR} + E_{NF4}$$

ROTOR EQUATIONS (CONTINUED)

SIDE FORCE

$$C_{SF_{RR}} = C_{SF_{ORR}} + \frac{dC_{SF_{RR}}}{dA_{ICR}} A_{ICR} + \frac{dC_{SF_{RR}}}{dB_{ICR}} B_{ICR}$$

WHERE:-

$$C_{SF_{ORR}} = \sum_{n=0}^2 \sum_{u=0}^3 \left[A_{SF}(u+4n) \alpha_{RR}^u C_{TRR}^{IN} \right] \left. \begin{array}{l} \text{INTERPOLATE } C_{SF_{ORR}} \\ \text{LINEARLY} \\ \text{BETWEEN } \mu\text{'S} \end{array} \right\}$$

$$A_{SF}(u+4n) = f(\mu_{RR})$$

$$\frac{dC_{SF_{RR}}}{dA_{ICR}} = D_{SF1} C_{TRR} + D_{SF2} \mu_{RR}^2 + D_{SF3} \mu_{RR} + D_{SF4}$$

$$\frac{dC_{SF_{RR}}}{dB_{ICR}} = E_{SF1} C_{TRR} + E_{SF2} \mu_{RR}^2 + E_{SF3} \mu_{RR} + E_{SF4}$$

ROTOR EQUATIONS (CONTINUED)

HUB PITCHING MOMENT

$$C_{PMRR} = C_{PMORR} + \frac{dC_{PMORR}}{dA_{ICR}} A_{ICR} + \frac{dC_{PMORR}}{dB_{ICR}} B_{ICR} + \frac{dC_{PMORR}}{dQ} Q_{NR}^R$$

WHERE:-

$$C_{PMORR} = \sum_{N=0}^2 \sum_{u=0}^3 \left[A_{PM}(u+4\pi) \alpha_{RR}^u C_{TRR}^{iN} \right]$$

$$A_{PM}(u+4\pi) = f(\mu_{RR})$$

$$\frac{dC_{PMORR}}{dQ} = \sum_{N=0}^2 \sum_{u=0}^3 \left[H_{PM}(u+4\pi) \alpha_{RR}^u C_{TRR}^{iN} \right]$$

$$H_{PM}(u+4\pi) = f(\mu_{RR})$$

INTERPOLATE
C_{PMORR} AND
 $\frac{dC_{PMORR}}{dQ}$
LINEARLY
BETWEEN μ 'S

NOTE:-

FOR $\mu_{RR} \leq 0.35$

$$\frac{dC_{PMORR}}{dA_{ICR}} = D_{PM1} C_{TRR} + D_{PM2} \mu_{RR}^2 + D_{PM3} \mu_{RR} + D_{PM4}$$

FOR $\mu_{RR} > 0.35$, THE COEFFS. ABOVE CHANGE AS FOLLOWS

$$D_{PM2} \equiv D_{PM5}$$

$$D_{PM3} \equiv D_{PM6}$$

$$D_{PM4} \equiv D_{PM7}$$

ROTOR EQUATIONS (CONTINUED)

HUB PITCHING MOMENT (CONTINUED)

$$\frac{d C_{PMR}}{d B_{ICR}} = E_{PM1} C_{TRR} + E_{PM2} \mu_{RR}^2 + E_{PM3} \mu + E_{PM4}$$

NOTE:- USE THE ABOVE EQUATION FOR $\mu_{RR} \leq 0.35$

FOR $\mu_{RR} > 0.35$: $E_{PM2} \equiv E_{PM5}$

$$E_{PM3} \equiv E_{PM6}$$

$$E_{PM4} \equiv E_{PM7}$$

HUB YAWING MOMENT

$$C_{YMRR} = C_{YMORR} + \frac{d C_{YMRR}}{d A_{ICR}} A_{ICR} + \frac{d C_{YMRR}}{d B_{ICR}} B_{ICR} + \frac{d C_{YMRR}}{d R} R_{UR}^R$$

WHERE:-

$$C_{YMORR} = \sum_{N=0}^2 \sum_{u=0}^3 \left[A_{YM}(u+4N) \alpha_{RR}^u C_{TRR}^{1u} \right]$$

$$A_{YM}(u+4N) = f(\mu_{RR})$$

$$\frac{d C_{YMRR}}{d R} = \sum_{N=0}^2 \sum_{u=0}^3 \left[J_{YM}(u+4N) \alpha_{RR}^u C_{TRR}^{1u} \right]$$

$$J_{YM}(u+4N) = f(\mu_{RR})$$

INTERPOLATE

C_{YMRR} AND $\frac{d C_{YMRR}}{d R}$

LINEARLY BETWEEN

μ 's.

ROTOR EQUATIONS (CONTINUUM)

HUB YAWING MOMENT (CONTINUUM)

FOR $\mu_{RR} \leq 0.35$

$$\frac{d C_{YMRR}}{d A_{ICR}} = D_{YM1} C_{TRR} + D_{YM2} \mu_{RR}^2 + D_{YM3} \mu_{RR} + D_{YM4}$$

FOR $\mu_{RR} > 0.35$

$$D_{YM2} \equiv D_{YM5}$$

$$D_{YM3} \equiv D_{YM6}$$

$$D_{YM4} \equiv D_{YM7}$$

FOR $\mu_{RR} \leq 0.35$

$$\frac{d C_{YMRR}}{d B_{ICR}} = E_{YM1} C_{TRR} + E_{YM2} \mu_{RR}^2 + E_{YM3} \mu_{RR} + E_{YM4}$$

FOR $\mu_{RR} > 0.35$

$$E_{YM2} \equiv E_{YM5}$$

$$E_{YM3} \equiv E_{YM6}$$

$$E_{YM4} \equiv E_{YM7}$$

ROTOR EQUATIONS (Cont'd)

ROTOR FORCE & MOMENT CALCULATION

$$T_R = f_{TR} C_{TRR} \rho \pi R^4 \Omega_R^2$$

$$N.F.R. = f_{NFR} C_{NFR} \rho \pi R^4 \Omega_R^2$$

$$S.F.R. = f_{SFR} C_{SFR} \rho \pi R^4 \Omega_R^2$$

$$M_R = f_{MR} C_{MR} \rho \pi R^5 \Omega_R^2$$

$$N_R = f_{NR} C_{NR} \rho \pi R^5 \Omega_R^2$$

$$Q_{REQ} = f_{QR} C_{QR} \rho \pi R^5 \Omega_R^2$$

$$RHP_{RR} = f_{PR} C_{PR} \rho \pi R^5 \Omega_R^3 / 550 \quad \text{OR} \quad RHP_{RR} = Q_{REQ} \left(\frac{\Omega_R}{550} \right)$$

LEFT ROTOR FOLLOWS SIMILAR FORMAT

WITH SUBSCRIPTS CHANGED.

THE LEFT ROTOR ALTITUDE EQUATION IS AS FOLLOWS:

$$h_{LR} = -Z_{DOWN} + (L_S \cos i_{NL} - X_{CG}) \sin \theta \\ + \left[(L_S \sin i_{NL} + Z_{CG}) \cos \phi + Y_N \sin \phi \right] \cos \theta$$

OR;

$$h_{LR} = h_{RR} + 2 Y_N \sin \phi \cos \theta$$

ROTOR FORCE & MOMENT RESOLUTION

HUB MOMENTS - NACELLE AXES

LEFT

$$I_{LRH} = -Q_{LREQ} - I_P \dot{\Omega}_L$$

$$M_{LRH} = M_L \cos \delta_{HL} - N_L \sin \delta_{HL} \\ - I_P \Omega_L (p \sin i_{NL} + r \cos i_{NL})$$

$$N_{LRH} = -N_L \cos \delta_{HL} - M_L \sin \delta_{HL} + I_P \Omega_L (i_{NL} + q)$$

RIGHT

$$I_{RRH} = Q_{RREQ} + I_P \dot{\Omega}_R$$

$$M_{RRH} = M_R \cos \delta_{HR} + N_R \sin \delta_{HR} \\ + I_P \Omega_R (p \sin i_{NR} + r \cos i_{NR})$$

$$N_{RRH} = N_R \cos \delta_{HR} - M_R \sin \delta_{HR} - I_P \Omega_R (i_{NR} + q)$$

NOTE: NACELLE AXES ARE RIGHT HANDED SYSTEMS

ROTOR FORCES & MOMENT RESOLUTION (Cont'd.)

LEFT TIP PIVOT - BODY AXES @ TIP (w/ NACELLE AERO)

$$X_{AERO}^{NL} = (T_L + \Delta X'_{LN}) \cos i_{NL} - \sin i_{NL} (N.F.L \cos \beta_{HL} + S.F.L \sin \beta_{HL} - \Delta Z'_{LN})$$

$$Y_{AERO}^{NL} = S.F.L \cos \beta_{HL} - N.F.L \sin \beta_{HL} + \Delta Y'_{LN}$$

$$Z_{AERO}^{NL} = -(T_L + \Delta X'_{LN}) \sin i_{NL} - \cos i_{NL} (N.F.L \cos \beta_{HL} + S.F.L \sin \beta_{HL} - \Delta Z'_{LN})$$

$$\mathcal{L}_{AERO}^{NL} = (\mathcal{L}_{LRH} + \Delta \mathcal{L}'_{LN}) \cos i_{NL} + \sin i_{NL} (\mathcal{M}_{LRH} + \Delta \mathcal{M}'_{LN} + L_S Y_{AERO}^{NL})$$

$$\mathcal{M}_{AERO}^{NL} = \mathcal{M}_{LRH} + \Delta \mathcal{M}'_{LN} + N.F.L L_S \cos \beta_{HL} + S.F.L L_S \sin \beta_{HL} - L_S \Delta Z'_{LN} - I_E \Omega_{EL} \nu$$

$$\mathcal{N}_{AERO}^{NL} = \cos i_{NL} (\mathcal{M}_{LRH} + \Delta \mathcal{M}'_{LN} + L_S Y_{AERO}^{NL}) - \sin i_{NL} (\mathcal{L}_{LRH} + \Delta \mathcal{L}'_{LN}) + I_E \Omega_{EL} \varphi$$

NACELLE EQUATION INPUT - LEFT

$$\mathcal{M}_{NLAERO} = \mathcal{M}_{LRH} + \Delta \mathcal{M}'_{LN} + (N.F.L \cos \beta_{HL} + S.F.L \sin \beta_{HL} - \Delta Z'_{LN}) L_S$$

GLAS INPUTS - LEFT

$$\mathcal{M}_{NLAERO}^{GLAS} = \mathcal{M}_{LRH} + L_S (N.F.L \cos \beta_{HL} + S.F.L \sin \beta_{HL})$$

$$\mathcal{N}_{NLAERO}^{GLAS} = \mathcal{M}_{LRH} + L_S (S.F.L \cos \beta_{HL} - N.F.L \sin \beta_{HL})$$

ROTOR FORCE & MOMENT RESOLUTION (Cont'd.)

RIGHT TIP PIVOT - BODY AXES @ TIP (w/ NACELLE AERO)

$$X_{AERO}^{NR} = (T_R + \Delta X'_{RN}) \cos i_{NR} + \sin i_{NR} (-N.F.R \cos \zeta_{HR} + S.F.R \sin \zeta_{HR} + \Delta Z'_{RN})$$

$$Y_{AERO}^{NR} = -S.F.R \cos \zeta_{HR} - N.F.R \sin \zeta_{HR} + \Delta Y'_{RN}$$

$$Z_{AERO}^{NR} = -(T_R + \Delta X'_{RN}) \sin i_{NR} + \cos i_{NR} (-N.F.R \cos \zeta_{HR} + S.F.R \sin \zeta_{HR} + \Delta Z'_{RN})$$

$$\mathcal{L}_{AERO}^{NR} = (\mathcal{L}_{RRH} + \Delta \mathcal{L}'_{RN}) \cos i_{NR} + \sin i_{NR} (M_{RRH} + L_S Y_{AERO}^{NR} + \Delta M'_{RN})$$

$$M_{AERO}^{NR} = M_{RRH} + \Delta M'_{RN} + N.F.R L_S \cos \zeta_{HR} - S.F.R L_S \sin \zeta_{HR} - L_S \Delta Z'_{RN} - I_E \Omega_{ER} \dot{\nu}$$

$$M_{AERO}^{NR} = \cos i_{NR} (M_{RRH} + \Delta M'_{RN} + L_S Y_{AERO}^{NR}) - \sin i_{NR} (\mathcal{L}_{RRH} + \Delta \mathcal{L}'_{RN}) + I_E \Omega_{ER} \dot{\eta}$$

NACELLE EQUATION INPUT - RIGHT

$$M_{NRAERO} = M_{RRH} + \Delta M'_{RN} + (N.F.R \cos \zeta_{HR} - S.F.R \sin \zeta_{HR} - \Delta Z'_{NR}) L_S$$

GLAS INPUTS - RIGHT

$$M_{GLAS}^{NRAERO} = M_{RRH} + L_S (N.F.R \cos \zeta_{HR} - S.F.R \sin \zeta_{HR})$$

$$M_{GLAS}^{NRAERO} = M_{RRH} - L_S (S.F.R \cos \zeta_{HR} + N.F.R \sin \zeta_{HR})$$

WING VERTICAL BENDING

RIGHT WING TIP DEFLECTION

$$\bar{a}_{RT} = \frac{Z_{AERO}}{m} + Y_N \dot{p}$$

$$\bar{a}_{RWAC} = \frac{Z_{AERO}}{m} + Y_{WAC} \dot{p}$$

$$h_{iR} = K_{W1} Z_{AERO}^{NR'} + K_{W2} Z_{AERO}^{RW'} + K_{W3} L_{AERO}^{NR'} - K_{W4} \bar{a}_{RT} - K_{W5} \bar{a}_{RWAC}$$

$$\dot{h}_{iR} = \Delta h_{iR} / \Delta t$$

WHERE: Δh_{iR} IS THE DIFFERENCE OF h_{iR} BETWEEN TIME FRAMES
AND Δt IS THE TIME FRAME

RIGHT WING A.C. DEFLECTION

$$h_{iRWAC} = K_{W6} Z_{AERO}^{NR'} + K_{W7} Z_{AERO}^{RW'} + K_{W8} L_{AERO}^{NR'} - K_{W9} \bar{a}_{RT} - K_{W10} \bar{a}_{RWAC}$$

$$\dot{h}_{iRWAC} = \Delta h_{iRWAC} / \Delta t$$

WHERE: Δh_{iRWAC} IS THE DIFFERENCE OF h_{iRWAC} BETWEEN TIME
FRAMES AND Δt IS THE TIME FRAME.

FORCE AND MOMENT EFFECTS

$$\ddot{Z}_{AERO}^{NR} = -Z \sum_{W1} W_{W1} \dot{Z}_{AERO}^{NR} - W_{W1}^2 Z_{AERO}^{NR} + W_{W1}^2 Z_{AERO}^{NR'}$$

$$\ddot{Z}_{AERO}^{RW} = -Z \sum_{W2} W_{W2} \dot{Z}_{AERO}^{RW} - W_{W2}^2 Z_{AERO}^{RW} + W_{W2}^2 Z_{AERO}^{RW'}$$

$$\ddot{L}_{AERO}^{NR} = -Z \sum_{W3} W_{W3} \dot{L}_{AERO}^{NR} - W_{W3}^2 L_{AERO}^{NR} + W_{W3}^2 L_{AERO}^{NR'}$$

FORM Z_{AERO}^{NR} , Z_{AERO}^{RW} , L_{AERO}^{NR}

WING VERTICAL BENDING (Cont'd.)

LEFT WING TIP DEFLECTION

$$\bar{a}_{LT} = \frac{Z_{AERO}}{M} - Y_N \dot{P}$$

$$\bar{a}_{LWAC} = \frac{Z_{AERO}}{M} - Y_{WAC} \dot{P}$$

$$h_{iL} = K_{W1} Z_{AERO}^{NL'} + K_{W2} Z_{AERO}^{LW'} - K_{W3} Z_{AERO}^{NL'} - K_{W4} \bar{a}_{LT} - K_{W5} \bar{a}_{LWAC}$$

$$\dot{h}_{iL} = \Delta h_{iL} / \Delta t$$

WHERE: Δh_{iL} IS THE DIFFERENCE OF h_{iL} BETWEEN TIME FRAMES
AND Δt IS THE TIME FRAME

LEFT WING A.C. DEFLECTION

$$h_{iLWAC} = K_{W6} Z_{AERO}^{NL'} + K_{W7} Z_{AERO}^{LW'} - K_{W8} Z_{AERO}^{NL'} - K_{W9} \bar{a}_{LT} - K_{W10} \bar{a}_{LWAC}$$

$$\dot{h}_{iLWAC} = \Delta h_{iLWAC} / \Delta t$$

WHERE: Δh_{iLWAC} IS THE DIFFERENCE OF h_{iLWAC} BETWEEN TIME
FRAMES AND Δt IS THE TIME FRAME

FORCE AND MOMENT EFFECTS

$$\ddot{Z}_{AERO}^{NL} = -Z \sum_{W1} W_{W1} \dot{Z}_{AERO}^{NL} - W_{W1}^2 Z_{AERO}^{NL} + W_{W1}^2 Z_{AERO}^{NL'}$$

$$\ddot{Z}_{AERO}^{LW} = -Z \sum_{W2} W_{W2} \dot{Z}_{AERO}^{LW} - W_{W2}^2 Z_{AERO}^{LW} + W_{W2}^2 Z_{AERO}^{LW'}$$

$$\ddot{L}_{AERO}^{NL} = -Z \sum_{W3} W_{W3} \dot{L}_{AERO}^{NL} - W_{W3}^2 L_{AERO}^{NL} + W_{W3}^2 L_{AERO}^{NL'}$$

FORM Z_{AERO}^{NL} , Z_{AERO}^{LW} , & L_{AERO}^{NL}

WING TORSION

LEFT WING TWIST @ TIP

$$\begin{aligned}K_{\theta} \theta_{ELW} &= M_{NRACT} - I_E \Omega_{ELW} \\ &+ q_{SLW} \frac{c_w^2 b_w}{2} C_{M0} (1 - C_{TSLR}) \\ &+ (1 - C_{TSLR}) q_{SLW} c_w^2 \left(\frac{dC_{MWCA}}{dC_L} + \frac{X_{WAC}}{C_w} \right) \left(\frac{C_{LW} b_w}{6\pi} \right) \left(4\theta_{ELW} + 3\pi \alpha_{RWIGID} \right)\end{aligned}$$

RIGHT WING TWIST @ TIP

$$\begin{aligned}K_{\theta} \theta_{ERW} &= M_{NRACT} - I_E \Omega_{ERW} \\ &+ q_{SRW} \frac{c_w^2 b_w}{2} C_{M0} (1 - C_{TSRR}) \\ &+ (1 - C_{TSRR}) q_{SRW} c_w^2 \left(\frac{dC_{MWCA}}{dC_L} + \frac{X_{WAC}}{C_w} \right) \left(\frac{C_{LR} b_w}{6\pi} \right) \left(4\theta_{ERW} + 3\pi \alpha_{RWIGID} \right)\end{aligned}$$

WHERE: $C_{M0} = C_1 + C_2 \delta_F + C_3 \delta_F^2$

$$\theta_{ELWAC} = \frac{Y_{WAC}}{Y_N} \theta_{ELW}$$

$$\theta_{ERWAC} = \frac{Y_{WAC}}{Y_N} \theta_{ERW}$$

NOTE: IF UMBRELLAS ARE OPEN; SET TERMS CONTAINING

$q_s (1 - C_{TS})$ EQUAL TO ZERO

TOTAL FORCE AND MOMENT SUMMATION ABOUT C.G.

$$X_{AERO} = X_{AERO}^{NL} + X_{AERO}^{NR} + X_{AERO}^F + X_{AERO}^{LW} + X_{AERO}^{RW} + X_{AERO}^T$$

$$Y_{AERO} = Y_{AERO}^{NL} + Y_{AERO}^{NR} + Y_{AERO}^F + Y_{AERO}^{LW} + Y_{AERO}^{RW} + Y_{AERO}^T$$

$$Z_{AERO} = Z_{AERO}^{NL} + Z_{AERO}^{NR} + Z_{AERO}^F + Z_{AERO}^{LW} + Z_{AERO}^{RW} + Z_{AERO}^T$$

$$\begin{aligned} L_{AERO} = & L_{AERO}^{NL} + L_{AERO}^{NR} + L_{AERO}^F + L_{AERO}^W + L_{AERO}^T \\ & + Y_N (Z_{AERO}^{NR} - Z_{AERO}^{NL}) + Z_{CG} (Y_{AERO}^{NL} + Y_{AERO}^{NR}) \end{aligned}$$

$$\begin{aligned} M_{AERO} = & M_{AERO}^{NL} + M_{AERO}^{NR} + M_{AERO}^F + M_{AERO}^W + M_{AERO}^T \\ & + X_{CG} (Z_{AERO}^{NL} + Z_{AERO}^{NR}) - Z_{CG} (X_{AERO}^{NL} + X_{AERO}^{NR}) \end{aligned}$$

$$\begin{aligned} N_{AERO} = & N_{AERO}^{NL} + N_{AERO}^{NR} + N_{AERO}^F + N_{AERO}^W + N_{AERO}^T \\ & + Y_N (X_{AERO}^{NL} - X_{AERO}^{NR}) - X_{CG} (Y_{AERO}^{NL} + Y_{AERO}^{NR}) \end{aligned}$$

NOMENCLATURE

- $l_f, h_f \sim$ FUSELAGE MASS CENTER W. R. T. PIVOT FUSE. CENTER, AXES.
- $l_w, h_w \sim$ WING " " " " " " " "
- $l \sim$ NACELLE PIVOT TO NACELLE C.G. DISTANCE
- $\lambda \sim$ ANGLE BETWEEN NACELLE SHAFT AXIS AND ITS C.G. TO PIVOT AXIS.
- $m_f \sim$ MASS OF FUSELAGE
- $m_w \sim$ MASS OF BOTH WINGS
- $m_N \sim$ MASS OF ONE NACELLE
- $i_N \sim$ NACELLE SHAFT TO FUSELAGE X-AXIS ANGLE
- $I_{xx}^{(f)}, I_{yy}^{(f)}, I_{zz}^{(f)}, I_{xz}^{(f)} \sim$ FUSELAGE INERTIAS ABOUT ITS C.G.
- $I_{xx}^{(w)}, I_{yy}^{(w)}, I_{zz}^{(w)}, I_{xz}^{(w)} \sim$ WING INERTIAS ABOUT THEIR C.G.
- $I'_{xx}, I'_{yy}, I'_{zz}, I'_{xz} \sim$ MOMENTS OF INERTIA OF ONE NACELLE ABOUT ITS C.G.
- $p, q, r \sim$ FUSELAGE BODY AXIS ANGULAR RATES
- $u, v, w \sim$ FUSELAGE BODY AXIS LINEAR RATES
- $I_p \sim$ ROTOR POLAR MOMENT OF INERTIA
- $\Omega \sim$ ROTOR SPEED, ANGULAR
- $X_{AIR0}; Y_{AIR0}; Z_{AIR0} \sim$ TOTAL AERODYNAMIC FORCES IN THE BODY AXIS.

SUBSCRIPTS

- R ~ RIGHT
L ~ LEFT
W ~ WING
F ~ FUSELAGE

BASIC EQUATIONS OF MOTION

PRELIMINARY CALCULATIONS

FUSELAGE C.G. w.r.t. A/C C.G.

$$X_f = l_f - X_{CG}$$

$$Z_f = h_f - Z_{CG}$$

WING C.G. w.r.t. A/C C.G.

$$X_w = l_w - X_{CG}$$

$$Z_w = h_w - Z_{CG}$$

NACELLE C.G.'s w.r.t. A/C C.G.

$$X_R = l \cos(i_{NR} - \lambda) - X_{CG}$$

$$Z_R = -l \sin(i_{NR} - \lambda) - Z_{CG}$$

$$X_L = l \cos(i_{NL} - \lambda) - X_{CG}$$

$$Z_L = -l \sin(i_{NL} - \lambda) - Z_{CG}$$

PRELIMINARY CALCULATIONS

INERTIA TERMS

$$\sum_k I_{ij}^{(k)} = I_{ij}^{(f)} + I_{ij}^{(w)} + 2I'_{ij}$$

$$\begin{aligned} I_{xx} = & \sum_k I_{xx}^{(k)} + (I'_{zz} - I'_{xx})(\sin^2 i_{NR} + \sin^2 i_{NL}) \\ & - I'_{xz} (\sin 2i_{NR} + \sin 2i_{NL}) + 2m_N Y_N^2 \\ & + m_f h_f Z_f + m_w h_w Z_w + \\ & - \rho m_N [Z_R \sin(i_{NR} - \lambda) + Z_L \sin(i_{NL} - \lambda)] \end{aligned}$$

$$\begin{aligned} J_{xx} = & \sum_k (I_{zz}^{(k)} - I_{yy}^{(k)}) + (I'_{xx} - I'_{zz})(\sin^2 i_{NR} + \sin^2 i_{NL}) \\ & + I'_{xz} (\sin 2i_{NR} + \sin 2i_{NL}) + 2m_N Y_N^2 \\ & - (m_f h_f Z_f + m_w h_w Z_w) \\ & + \rho m_N [Z_R \sin(i_{NR} - \lambda) + Z_L \sin(i_{NL} - \lambda)] \end{aligned}$$

$$\begin{aligned} I_{xz}^{(p)} = & I_{xz}^{(f)} + I_{xz}^{(w)} + \frac{1}{2} (I'_{xx} - I'_{zz})(\sin 2i_{NR} + \sin 2i_{NL}) \\ & + I'_{xz} (\cos 2i_{NR} + \cos 2i_{NL}) + (m_f l_f Z_f + m_w l_w Z_w) \\ & + m_N \rho [Z_R \cos(i_{NR} - \lambda) + Z_L \cos(i_{NL} - \lambda)] \end{aligned}$$

INERTIA TERMS

$$I_{yy} = \sum_k I_{yy}^{(k)} + m_f (l_f X_f + h_f Z_f) + m_w (l_w X_w + h_w Z_w) \\ + m_N l [X_R \cos(i_{NR} - \lambda) - Z_R \sin(i_{NR} - \lambda)] \\ + m_N l [X_L \cos(i_{NL} - \lambda) - Z_L \sin(i_{NL} - \lambda)]$$

$$J_{yy} = (I_{xx}^{(f)} - I_{zz}^{(f)}) + (I_{xx}^{(w)} - I_{zz}^{(w)}) + \dots \\ + (I'_{xx} - I'_{zz}) (\cos 2i_{NR} + \cos 2i_{NL}) \\ - 2I'_{xz} (\sin 2i_{NR} + \sin 2i_{NL}) + m_f (-l_f X_f + h_f Z_f) \\ + m_w (-l_w X_w + h_w Z_w) \\ - m_N l [X_R \cos(i_{NR} - \lambda) + Z_R \sin(i_{NR} - \lambda) + X_L \cos(i_{NL} - \lambda) \\ + Z_L \sin(i_{NL} - \lambda)]$$

$$I_{xz}^{(g)} = I_{xz}^{(f)} + I_{xz}^{(w)} + \frac{1}{2} (I'_{xx} - I'_{zz}) (\sin 2i_{NR} + \sin 2i_{NL}) \\ + I'_{xz} (\cos 2i_{NR} + \cos 2i_{NL}) \\ - m_N l [X_R \sin(i_{NR} - \lambda) + X_L \sin(i_{NL} - \lambda)] \\ + m_f h_f X_f + m_w h_w X_w$$

INERTIA TERMS

$$\begin{aligned} I_{zz} = & \sum_A I_{zz}^{(A)} + (I'_{xx} - I'_{zz})(\sin^2 i_{NR} + \sin^2 i_{NL}) \\ & + I'_{xz} (\sin 2i_{NR} + \sin 2i_{NL}) + 2m_N Y_N^2 \\ & + m_f h_f X_f + m_w h_w X_w \\ & + m_N l [X_R \cos(i_{NR} - \lambda) + X_L \cos(i_{NL} - \lambda)] \end{aligned}$$

$$\begin{aligned} J_{zz} = & \sum_A (I_{yy}^{(A)} - I_{xx}^{(A)}) + (I'_{xx} - I'_{zz})(\sin^2 i_{NR} + \sin^2 i_{NL}) \\ & + I'_{xz} (\sin 2i_{NR} + \sin 2i_{NL}) - 2m_N Y_N^2 \\ & + m_f h_f X_f + m_w h_w X_w \\ & + m_N l [X_R \cos(i_{NR} - \lambda) + X_L \cos(i_{NL} - \lambda)] \end{aligned}$$

$$\begin{aligned} I_{xz}^{(r)} = & I_{xz}^{(f)} + I_{xz}^{(w)} + \frac{1}{2}(I'_{xx} - I'_{zz})(\sin 2i_{NR} + \sin 2i_{NL}) \\ & + I'_{xz} (\cos 2i_{NR} + \cos 2i_{NL}) + m_f h_f X_f + m_w h_w X_w \\ & - l m_N [X_R \sin(i_{NR} - \lambda) + X_L \sin(i_{NL} - \lambda)] \end{aligned}$$

BASIC EQUATIONS - FINAL SIMPLIFICATION

ROLL EQUATION

$$\begin{aligned} I_{xx} \dot{p} &= -J_{xx} r q + I_{xz}^{(p)} (\dot{r} + p q) \\ &+ \mathcal{L}_{MN} Y_N \left\{ \ddot{i}_{NR} \cos(i_{NR} - \lambda) - \ddot{i}_{NL} \cos(i_{NL} - \lambda) \right\} \\ &+ \mathcal{L}_{AERO} \end{aligned}$$

PITCH EQUATION

$$\begin{aligned} I_{yy} \dot{q} &= -J_{yy} p r - I_{xz}^{(q)} (p^2 - r^2) \\ &- \ddot{i}_{NR} \left\{ I'_{yy} + \mathcal{L}_{MN} [-Z_R \sin(i_{NR} - \lambda) + X_R \cos(i_{NR} - \lambda)] \right\} \\ &- \ddot{i}_{NL} \left\{ I'_{yy} + \mathcal{L}_{MN} [-Z_L \sin(i_{NL} - \lambda) + X_L \cos(i_{NL} - \lambda)] \right\} \\ &+ \mathcal{M}_{AERO} \end{aligned}$$

YAW EQUATION

$$\begin{aligned} I_{zz} \dot{r} &= -J_{zz} p q - (r q - \dot{p}) I_{xz}^{(r)} \\ &- \mathcal{L}_{MN} Y_N \left\{ \ddot{i}_{NR} \sin(i_{NR} - \lambda) - \ddot{i}_{NL} \sin(i_{NL} - \lambda) \right\} \\ &+ \mathcal{N}_{AERO} \end{aligned}$$

BASIC EQUATIONS

RIGHT NACELLE ACTUATOR PITCHING MOMENT EQUATION

$$\begin{aligned} M_{NRACT} = & -\ddot{i}_{NR} \left[I'_{yy} + l^2 m_N \left(1 - \frac{m_N}{m} \right) \right] \\ & - l^2 m_N \left(1 - \frac{m_N}{m} \right) \left[-pr \cos 2(i_{NR} - \lambda) + \dot{q} \right. \\ & \quad \left. + (r^2 - p^2) \sin(i_{NR} - \lambda) \cos(i_{NR} - \lambda) \right] \\ & - (r^2 - p^2) \left[I'_{zz} \sin i_{NR} \cos i_{NR} \right] - I'_{yy} \dot{q} \\ & + l \frac{m_N}{m} \left[X_{AERO} \sin(i_{NR} - \lambda) + Z_{AERO} \cos(i_{NR} - \lambda) \right] \\ & - l m_N Y_N \left\{ (\dot{r} - pq) \left[\sin(i_{NR} - \lambda) \right] \right. \\ & \quad \left. - (\dot{p} + rq) \left[\cos(i_{NR} - \lambda) \right] \right\} \\ & + M_{NRAERO} \end{aligned}$$

Note: The above equation must be calculated for wing torsion calculation only

BASIC EQUATIONS

LEFT NACELLE ACTUATOR PITCHING MOMENT EQUATION

$$\begin{aligned} M_{NLACT} = & - \ddot{i}_{NL} \left[I'_{yy} + l^2 m_N \left(1 - \frac{m_N}{m} \right) \right] \\ & - l^2 m_N \left(1 - \frac{m_N}{m} \right) \left[-pr \cos 2(i_{NL} - \lambda) + \dot{q} \right. \\ & \quad \left. + (r^2 - p^2) \sin(i_{NL} - \lambda) \cos(i_{NL} - \lambda) \right] \\ & - (r^2 - p^2) \left[I'_{zz} \sin i_{NL} \cos i_{NL} \right] - I'_{yy} \dot{q} \\ & + l \frac{m_N}{m} \left[X_{AERO} \sin(i_{NL} - \lambda) + Z_{AERO} \cos(i_{NL} - \lambda) \right] \\ & + l m_N Y_N \left\{ (\dot{r} - pq) \left[\sin(i_{NL} - \lambda) \right] \right. \\ & \quad \left. - (\dot{p} + rq) \left[\cos(i_{NL} - \lambda) \right] \right\} \\ & + M_{NLAERO} \end{aligned}$$

NOTE: The above equation must be calculated for wing torsion calculation ONLY.

HIRSCHFELD CONDITION CALCULATIONS
LINEAR EQUATIONS OF MOTION (ψ, θ, ϕ -EULER SYSTEM)

$$\dot{u} = \frac{X_{AERO}}{m} - g \sin \theta - \dot{\phi} \omega + r v$$

$$\dot{v} = \frac{Y_{AERO}}{m} + g \cos \theta \sin \phi - r u + p \omega$$

$$\dot{w} = \frac{Z_{AERO}}{m} + g \cos \theta \cos \phi + \dot{\theta} u - p v$$

EULER ANGLE CALCULATION - ψ, θ, ϕ SYSTEM

$$\dot{\psi} = (r \cos \phi + z \sin \phi) / \cos \theta$$

$$\dot{\theta} = z \cos \phi - r \sin \phi$$

$$\dot{\phi} = \rho + \dot{\psi} \sin \theta$$

AIRCRAFT CONDITION CALCULATIONS

GROUND TRACK

NORTHWARD VELOCITY

$$\begin{aligned}\dot{X}_{\text{NORTH}} = & U \cos \theta \cos \psi + V (\sin \phi \sin \theta \cos \psi \\ & - \cos \phi \sin \psi) \\ & + W (\cos \phi \sin \theta \cos \psi + \sin \phi \sin \psi)\end{aligned}$$

EASTWARD VELOCITY

$$\begin{aligned}\dot{Y}_{\text{EAST}} = & U \cos \theta \sin \psi + V (\sin \phi \sin \theta \sin \psi + \cos \phi \cos \psi) \\ & + W (\cos \phi \sin \theta \sin \psi - \sin \phi \cos \psi)\end{aligned}$$

DOWNWARD VELOCITY

$$\dot{Z}_{\text{DOWN}} = -U \sin \theta + V \sin \phi \cos \theta + W \cos \phi \cos \theta$$

AIRCRAFT CONDITION CALCULATIONS (CONTINUED)

PILOT STATION ACCELERATIONS (BODY AXES)

$$a_{xPA} = \frac{X_{AERO}}{m} + (\dot{q} + pr)(Z_{PA} - Z_{CG}) \\ + (\dot{q}^2 + r^2)(X_{CG} - l_{PA}) + Y_{PA}(pq - \dot{r}) \\ - Zq\dot{Z}_{CG} - \ddot{X}_{CG}$$

$$a_{yPA} = \frac{Y_{AERO}}{m} + (\dot{p} - qr)(Z_{CG} - Z_{PA}) + (\dot{r} + pq)(l_{PA} - X_{CG}) \\ - Y_{PA}(r^2 + p^2) + Z(p\dot{Z}_{CG} - r\dot{X}_{CG})$$

$$a_{zPA} = \frac{Z_{AERO}}{m} + (\dot{q} - pr)(X_{CG} - l_{PA}) + (p^2 + \dot{q}^2)(Z_{CG} - Z_{PA}) \\ + Y_{PA}(\dot{p} + qr) + Zq\dot{X}_{CG} - \ddot{Z}_{CG}$$

PILOT STATION VELOCITIES (BODY AXES)

$$U_{PA} = U_P + qZ_{PA} - rY_{PA}$$

$$V_{PA} = V_P + r l_{PA} - pZ_{PA}$$

$$W_{PA} = W_P + pY_{PA} - q l_{PA}$$

GUST MODEL

The Gust Model to be used with the simulation will consist of:

NASA-AMES program number NAPS-80.

The output of this program is in the form of gust components that will be added to the inertial components of the basic equations of motion. In practice, the following equations will be used in formulating the input to the aerodynamic coordinate transforms etc.,.

$$\begin{aligned}U &= U' + U_g & P &= P' + P_g \\V &= V' + V_g & Q &= Q' + Q_g \\W &= W' + W_g & R &= R' + R_g\end{aligned}$$

The primed terms above are derived from the basic equations.

Alterations to nomenclature in the vertical equations has been resisted at this time for the sake of simplicity.

7

PRELIMINARY CALCULATIONS (PREPROCESS)

CENTER OF GRAVITY CALCULATIONS

$$m = \frac{1}{32.174} [W'_f + W'_{NT} + W'_{HT} + W'_{VT} + W'_w + W'_{NF} + W'_{CR} + W'_{FUEL} + W'_c]$$

$$m_N = \frac{1}{32.174} \left(\frac{W'_{NT}}{2} \right)$$

$$m_f = \frac{1}{32.174} [W'_f + W'_{HT} + W'_{VT} + W'_{CR} + W'_c]$$

$$m_w = \frac{1}{32.174} [W'_w + W'_{FUEL} + W'_{NF}]$$

$$l'_f = [(FS)_p - (FS)_{f'}] \frac{1}{12}$$

$$l'_{HT} = [(FS)_p - (FS)_{HTCG}] \frac{1}{12}$$

$$l'_{VT} = [(FS)_p - (FS)_{VTCG}] \frac{1}{12}$$

$$l'_{PA} = [(FS)_p - (FS)_{PA}] \frac{1}{12}$$

$$l'_c = [(FS)_p - (FS)_c] \frac{1}{12}$$

$$l'_f = \frac{1}{m_f(32.174)} [W'_f l'_f + W'_{HT} l'_{HT} + W'_{VT} l'_{VT} + W'_{CR} l'_{PA} + W'_c l'_c]$$

$$l'_w = [(FS)_p - (FS)_w] \frac{1}{12}$$

$$l'_{FUEL} = [(FS)_p - (FS)_{FUEL}] \frac{1}{12}$$

$$l'_{NF} = [(FS)_p - (FS)_{NF}] \frac{1}{12}$$

$$l'_w = \frac{1}{m_w(32.174)} [W'_w l'_w + W'_{FUEL} l'_{FUEL} + W'_{NF} l'_{NF}]$$

PRELIMINARY CALCULATIONS (CONT'D.)

$$z'_f = \left[(WL)_p - (WL)_{f'} \right] \frac{1}{12}$$

$$z'_{HT} = \left[(WL)_p - (WL)_{HTCG} \right] \frac{1}{12}$$

$$z'_{VT} = \left[(WL)_p - (WL)_{VTG} \right] \frac{1}{12}$$

$$z'_{PA} = \left[(WL)_p - (WL)_{PA} \right] \frac{1}{12}$$

$$z'_c = \left[(WL)_p - (WL)_c \right] \frac{1}{12}$$

$$h_f = \frac{1}{(32.174) m_f} \left[W'_f z'_f + W'_{HT} z'_{HT} + W'_{VT} z'_{VT} + W'_{CR} z'_{PA} + W'_c z'_c \right]$$

$$z'_w = \left[(WL)_p - (WL)_w \right] \frac{1}{12}$$

$$z'_{FUEL} = \left[(WL)_p - (WL)_{FUEL} \right] \frac{1}{12}$$

$$z'_{NF} = \left[(WL)_p - (WL)_{NF} \right] \frac{1}{12}$$

$$h_w = \frac{1}{(32.174) m_w} \left[W'_w z'_w + W'_{FUEL} z'_{FUEL} + W'_{NF} z'_{NF} \right]$$

$$X_{WAC} = \left[(FS)_p - (FS)_{WAC} \right] \frac{1}{12}$$

$$Y_{WAC} = \left[(BL)_{WAC} \right] \frac{1}{12}$$

$$Z_{WAC} = \left[(WL)_p - (WL)_{WAC} \right] \frac{1}{12}$$

$$Y_N = \left[(BL)_N \right] \frac{1}{12}$$

8.

PRELIMINARY CALCULATIONS (CONT'D)

$$X_{HT} = [(FS)_P - (FS)_{HT}] \frac{1}{12}$$

$$Z_{HT} = [(WL)_P - (WL)_{HT}] \frac{1}{12}$$

$$X_{VT} = [(FS)_P - (FS)_{VT}] \frac{1}{12}$$

$$Z_{VT} = [(WL)_P - (WL)_{VT}] \frac{1}{12}$$

$$A = 3.14159 R^2$$

$$\bar{Y}_{WAC} = [(\bar{BL})_{WAC}] \frac{1}{12}$$

$$X_{G2} = X_{G1} = [(FS)_P - (FS)_{G2}] \frac{1}{12}$$

$$Z_{G2} = Z_{G1} = [(WL)_P - (WL)_{G2}] \frac{1}{12}$$

$$Y_{G2} = [(BL)_{G2}] \frac{1}{12}$$

$$Y_{G1} = -Y_{G2}$$

$$Y_{G3} = 0.$$

$$Y_{PA} = [(BL)_{PA}] \frac{1}{12} ; \text{ POSITIVE FOR PILOT IN RIGHT SEAT}$$

$$X_{FAC} = [(FS)_P - (FS)_{FAC}] \frac{1}{12}$$

$$Z_{FAC} = [(WL)_P - (WL)_{FAC}] \frac{1}{12}$$

57

PRELIMINARY CALCULATIONS (CONT'D)

$$X_{CH_2} = [(FS)_P - (FS)_{CH_2}] \frac{1}{12}$$

$$Z_{G3} = [(WL)_P - (WL)_{G3}] \frac{1}{12}$$

$$X_{G3} = [(FS)_P - (FS)_{G3}] \frac{1}{12}$$

$$Y_{NF} = [(BL)_{NF CG}] \frac{1}{12}$$

$$Y_{HT} = [(BL)_{HT CG}] \frac{1}{12}$$

$$Y_w = [(BL)_{w CG}] \frac{1}{12}$$

$$Y_{FUEL} = [(BL)_{FUEL CG}] \frac{1}{12}$$

INERTIA CALCULATIONS

$$\eta'_{f'} = l_f - l'_{f'}$$

$$\delta'_{f'} = h_f - z'_{f'}$$

$$\eta'_{HT} = l_f - l'_{HT}$$

$$\delta'_{HT} = h_f - z'_{HT}$$

$$\eta'_{VT} = l_f - l'_{VT}$$

$$\delta'_{VT} = h_f - z'_{VT}$$

$$\eta'_{CA} = l_f - l_{PA}$$

$$\delta'_{CA} = h_f - z_{PA}$$

PRELIMINARY CALCULATIONS (CONT'D)

$$\eta'_c = l_f - l'_c$$

$$\delta'_c = h_f - z'_c$$

$$\begin{aligned} I_{yy}^{(p)} &= I_{yy_0}^{(w_p)} + I_{yy_0}^{(HT)} + I_{yy_0}^{(VT)} + I_{yy_0}^{(CR)} + I_{yy_0}^{(c)} + \frac{W'_f}{32.174} (\eta_{f'}'^2 + \delta_{f'}'^2) \\ &\quad + \frac{W'_{HT}}{32.174} (\eta_{HT}'^2 + \delta_{HT}'^2) + \frac{W'_{VT}}{32.174} (\eta_{VT}'^2 + \delta_{VT}'^2) \\ &\quad + \frac{W'_{CR}}{32.174} (\eta_{CR}'^2 + \delta_{CR}'^2) + \frac{W'_c}{32.174} (\eta_c'^2 + \delta_c'^2) \end{aligned}$$

$$\begin{aligned} I_{xx}^{(p)} &= I_{xx_0}^{(w_p)} + I_{xx_0}^{(HT)} + I_{xx_0}^{(VT)} + I_{xx_0}^{(CR)} + I_{xx_0}^{(c)} + \frac{W'_f}{32.174} \delta_{f'}'^2 + \frac{W'_{HT}}{32.174} (\delta_{HT}'^2 + Y_{HT}^2) \\ &\quad + \frac{W'_{VT}}{32.174} \delta_{VT}'^2 + \frac{W'_{CR}}{32.174} \delta_{CR}'^2 + \frac{W'_c}{32.174} \delta_c'^2 \end{aligned}$$

$$\begin{aligned} I_{zz}^{(p)} &= I_{zz_0}^{(w_p)} + I_{zz_0}^{(HT)} + I_{zz_0}^{(VT)} + I_{zz_0}^{(CR)} + I_{zz_0}^{(c)} + \frac{W'_f}{32.174} \eta_{f'}'^2 + \frac{W'_{HT}}{32.174} (\eta_{HT}'^2 + Y_{HT}^2) \\ &\quad + \frac{W'_{VT}}{32.174} \eta_{VT}'^2 + \frac{W'_{CR}}{32.174} \eta_{CR}'^2 + \frac{W'_c}{32.174} \eta_c'^2 \end{aligned}$$

$$\begin{aligned} I_{xz}^{(p)} &= I_{xz_0}^{(w_p)} + I_{xz_0}^{(HT)} + I_{xz_0}^{(VT)} + I_{xz_0}^{(CR)} + I_{xz_0}^{(c)} + \frac{W'_f}{32.174} \eta_{f'}' \delta_{f'}' \\ &\quad + \frac{W'_{HT}}{32.174} \eta_{HT}' \delta_{HT}' + \frac{W'_{VT}}{32.174} \eta_{VT}' \delta_{VT}' + \frac{W'_{CR}}{32.174} \eta_{CR}' \delta_{CR}' \\ &\quad + \frac{W'_c}{32.174} \eta_c' \delta_c' \end{aligned}$$

$$H'_{w'w} = l_w - l'_w$$

$$\Delta'_{w'w} = h_w - z'_w$$

$$H'_{w'_{FUEL}} = l_w - l'_{FUEL}$$

$$\Delta'_{w'_{FUEL}} = h_w - z'_{FUEL}$$

PRELIMINARY CALCULATIONS (CONT'D)

$$H'_{w'NF} = l_w - l'_{NF}$$

$$\Delta'_{w'NF} = h_w - z'_{NF}$$

$$I_{yy}^{(w)} = I_{yy_0}^{(w'_w)} + I_{yy_0}^{(w'_{FUEL})} + I_{yy_0}^{(w'_{NF})} + \frac{W'_w}{32.174} (H'^2_{w'_w} + \Delta'^2_{w'_w})$$
$$+ \frac{W'_{FUEL}}{32.174} (H'^2_{w'_{FUEL}} + \Delta'^2_{w'_{FUEL}}) + \frac{W'_{NF}}{32.174} (H'^2_{w'_{NF}} + \Delta'^2_{w'_{NF}})$$

$$I_{xx}^{(w)} = I_{xx_0}^{(w'_w)} + I_{xx_0}^{(w'_{FUEL})} + I_{xx_0}^{(w'_{NF})} + \frac{W'_w}{32.174} (\Delta'^2_{w'_w} + Y_w^2)$$
$$+ \frac{W'_{FUEL}}{32.174} (\Delta'^2_{w'_{FUEL}} + Y_{FUEL}^2) + \frac{W'_{NF}}{32.174} (\Delta'^2_{w'_{NF}} + Y_{NF}^2)$$

$$I_{zz}^{(w)} = I_{zz_0}^{(w'_w)} + I_{zz_0}^{(w'_{FUEL})} + I_{zz_0}^{(w'_{NF})} + \frac{W'_w}{32.174} (H'^2_{w'_w} + Y_w^2)$$
$$+ \frac{W'_{FUEL}}{32.174} (H'^2_{w'_{FUEL}} + Y_{FUEL}^2) + \frac{W'_{NF}}{32.174} (H'^2_{w'_{NF}} + Y_{NF}^2)$$

$$I_{xz}^{(w)} = I_{xz_0}^{(w'_w)} + I_{xz_0}^{(w'_{FUEL})} + I_{xz_0}^{(w'_{NF})} + \frac{W'_w}{32.174} H'_{w'_w} \Delta'_{w'_w}$$
$$+ \frac{W'_{FUEL}}{32.174} H'_{w'_{FUEL}} \Delta'_{w'_{FUEL}} + \frac{W'_{NF}}{32.174} H'_{w'_{NF}} \Delta'_{w'_{NF}}$$

MATH MODEL TRIM LOOPS - STEADY FLIGHT

INITIALIZE $u, v, \theta, h, \Omega, P, q, r$ AT DESIRED FLIGHT CONDITION.

CLOSE THE FOLLOWING TRIM FEEDBACK LOOPS TO TRIM MATH MODEL FOR FLIGHT.

$$i_{NREF} = K_{T1} \int \dot{u} dt + K_{T2} \dot{u}$$

$$\phi = -K_{T3} \int \dot{v}_i dt - K_{T4} \dot{v}_i$$

$$w = K_{T5} \int \dot{w} dt + K_{T6} \dot{w}$$

$$\delta_S = -K_{T7} \int \dot{p} dt - K_{T8} \dot{p}$$

$$\delta_R = -K_{T9} \int \dot{r} dt - K_{T10} \dot{r}$$

$$\delta_B = -K_{T11} \int \dot{q} dt - K_{T12} \dot{q}$$

$$i_{NR} = K_{T13} \iint \ddot{i}_{NR} dt dt + K_{T14} \int \ddot{i}_{NR} dt$$

$$i_{NL} = K_{T13} \iint \ddot{i}_{NL} dt dt + K_{T14} \int \ddot{i}_{NL} dt$$

$$\delta_{TH} = K_{T15} \int \dot{z}_{DOWN} dt + K_{T16} \dot{z}_{DOWN}$$

- NOTE:
- 1.) HOLD INTEGRATED VALUE WHEN GOING TO FLIGHT.
 - 2.) START SECOND TRIM FROM FIRST TRIM VALUES.
 - 3.) DETERMINE K'S EXPERIMENTALLY TO MINIMIZE TRIM TIME.
 - 4.) TRIM WITH ALL ACTUATOR DYNAMICS, SAS, AND GOVERNOR IN OPERATING CONDITION TO INSURE PROPER COCKPIT CONTROL AND COLLECTIVE POSITIONS.

5) $\dot{z}_{DOWN} = \dot{z}_{DOWN} - \dot{z}_{DOWN}^{TRIM}$; set \dot{z}_{DOWN}^{TRIM} at desired R/C

8

MATH MODEL TRIM LOOP OPTIONS

1.) When specifying i_{NREF} , form:

$$\theta = K_{TI1} \int \dot{u} dt + K_{TI2} \dot{u}$$

Note: This option will be commonly used in cruise flight when the nacelles are down and locked.

APPENDIX F MATHEMATICAL MODEL INPUT DATA

Presented in this section is the input data for the mathematical model. A general description of the Model 222 tilt rotor was given in Section 4.0. Model 222 dimensional data and control surface deflections and travels are given on the following pages. Weight, balance and moment of inertia data for five nominal design operating conditions are defined in Figure F.1 . Center of gravity envelopes for the condition of nacelle incidence zero (cruise configuration) and nacelle incidence 90 degrees (hover configuration) are illustrated in Figure F.2. The mathematical model input data are given in Section F.1 to F.5 and are referenced by page number to the equations presented in Appendix E.

MODEL 222 DIMENSIONAL DATA

WING

AREA (THEO.)	200 FT ²
ASPECT RATIO	5.61
SPAN (BETWEEN ROTOR ζ)	33.42 FT
TAPER RATIO	1.00
CHORDS:	
ROOT	71.8 IN
TIP	71.8 IN
MEAN AERODYNAMIC	71.8 IN
SWEEPBACK	0 DEGREES
DIHEDRAL	0 DEGREES
INCIDENCE	
ROOT	2.0 DEGREES
TIP	2.0 DEGREES
AIRFOIL SECTION	
ROOT	NACA 63 ₄ 221 (MODIFIED)
TIP	NACA 63 ₄ 221 (MODIFIED)

FUSELAGE

LENGTH	38.83 FT
DEPTH (NOT INCLUDING SPONSONS)	5.45 FT
WIDTH (NOT INCLUDING SPONSONS)	5.45 FT
WETTED AREA (INCLUDING SPONSONS)	582 FT ²

MODEL 222 DIMENSIONAL DATA (Continued)

NACELLES

ENGINE

LENGTH	5.58 FT
DEPTH	2.37 FT
WIDTH	2.37 FT
WETTED AREA (PER NACELLE)	21 FT ²

TILTING

LENGTH	3.70 FT
DEPTH	3.35 FT
WIDTH	2.37 FT
WETTED AREA (PER NACELLE)	22 FT ²

HORIZONTAL TAIL

AREA (EXPOSED)	46.3 FT ²
AREA (THEO)	58.3 FT ²
SPAN	15.75 FT
ASPECT RATIO	4.26
TAPER RATIO	.379
DISTANCE $(\bar{c}/4)_W$ to $(\bar{c}/4)_{HT}$	20.29 FT
CHORDS	
ROOT	66.0 IN
TIP	25.0 IN
MEAN AERODYNAMIC	48.0 IN
SWEEPBACK AT 0 PERCENT CHORD	14° 51'
DIHEDRAL	0 DEGREES

MODEL 222 DIMENSIONAL DATA (Continued)

INCIDENCE

ROOT 0 DEGREES
TIP 0 DEGREES

AIRFOIL SECTION

ROOT NACA 64A010 (MODIFIED)
TIP NACA 64A010 (MODIFIED)

VERTICAL TAIL

AREA (EXPOSED, EXCLUDES DORSAL) 35.5 FT²
AREA (REFERENCE) 43.3 FT²
SPAN (REFERENCE) 8.14 FT
ASPECT RATIO 1.53
TAPER RATIO .303
DISTANCE $(\bar{c}/4)_W$ to $(\bar{c}/4)_{VT}$ 18.88 FT
CHORDS (REFERENCE)
ROOT 8.17 FT
TIP 2.48 FT
MEAN AERODYNAMIC 5.83 FT
SWEEPBACK AT 0 PERCENT CHORD 46° 28'
AIRFOIL SECTION NACA 64A008

CONTROL SURFACES

FLAPERON

AREA (AFT OF HINGE) 52.5 FT
SPAN (LENGTH EACH SIDE) 151.56 IN
CHORD (% OF WING CHORD) 30
SWEEPBACK OF HINGE LINE 0°

SPOILERS

AREA 19.15 FT²

CONTROL SURFACE DEFLECTIONS AND CONTROL TRAVELS

Control Surface Deflections (Positive deflection is trailing edge down unless indicated otherwise)

Elevator	+20° (Pilot Stick Command-Deflection From Scheduled Elevator Position)
Flaperon (Flap Mode)	+70°, -0°
(Aileron Mode)	+20°, -0° (Flaperon Used for Roll Control to a Maximum of 35° Combined Flap + Aileron Mode Deflection)
Rudder	+20°
Spoiler (Roll Control)	45° (T.E. Up)
(Max. Download Alleviation in Hover)	110° (T.E. Up)
Umbrella Upper Surface	Aft Edge 20° From Vertical
Lower Surface	Aft Edge 10° From Vertical

Rotor Control Authorities

Longitudinal Cyclic	+2.5° for Pitch Trim Plus Maneuver
	+2.7° for Combined SAS + Load Alleviation
Differential Longitudinal Cyclic	+4.5° Maximum for Roll Command (Function of Nacelle Incidence)
Maximum Longitudinal Cyclic for Combined Inputs	±7°
Collective Pitch	0° to 56.5° (at .75R)
Differential Collective	+3.0° Maximum for Yaw Command & +4.8° for Maximum Roll Command (Function of Nacelle Incidence)
Lateral Cyclic	+2.7° for Rotor Load Alleviation

Nacelle Deflection Authorities

Nacelle Tilt	0° to 105°
Differential Nacelle Tilt	1.55° Per Degree Differential Longitudinal Cyclic

Pilot Control Movements

Stick - Longitudinal	+6 Inches
- Lateral	+5 Inches
Rudder Pedals	+2.5 Inches

MASS PROPERTIES

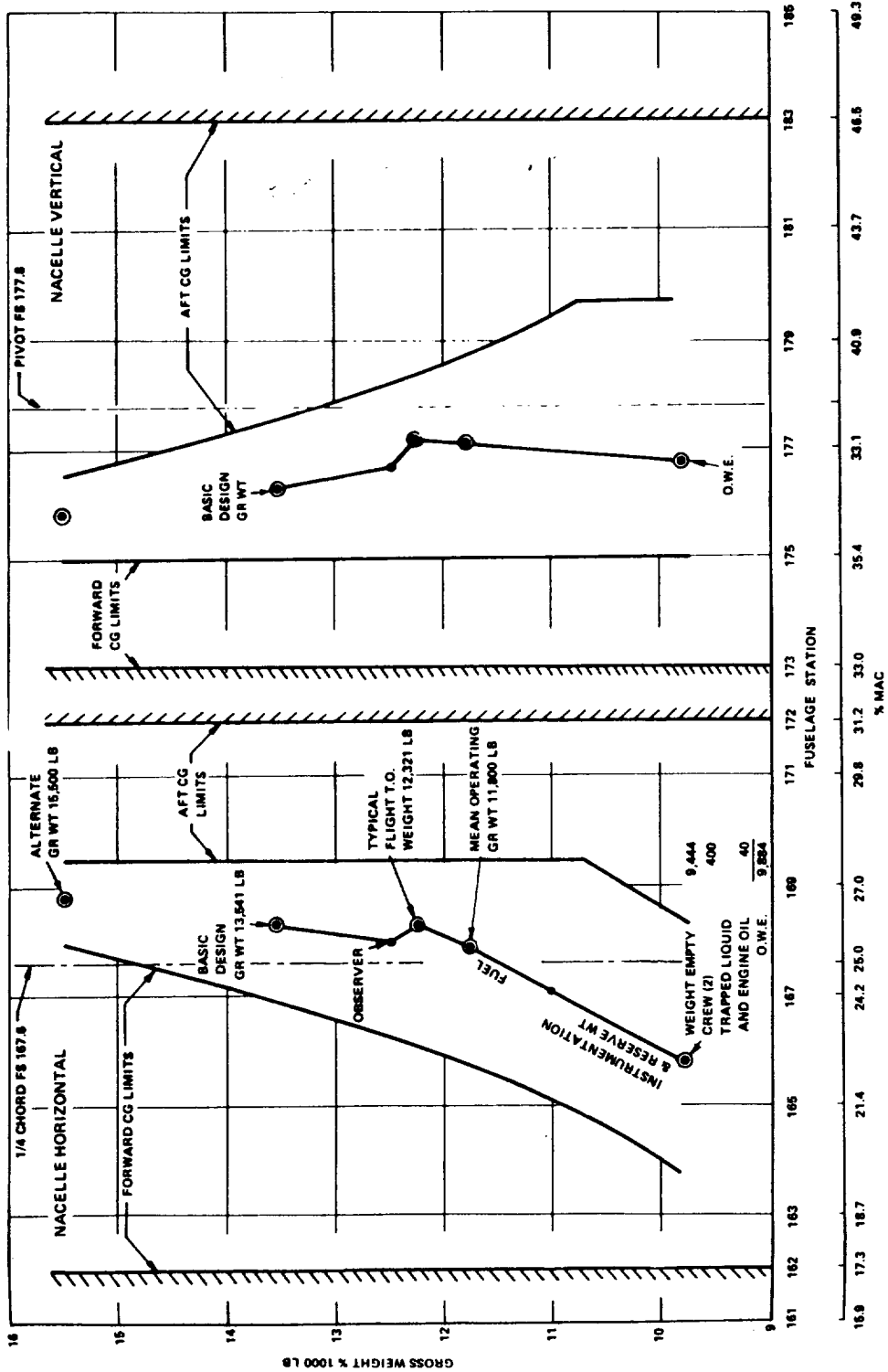
(WEIGHT BALANCE AND MOMENTS OF INERTIA)

SUB-GROUPS	N.A.C.E.L.L.F. BALANCE			HORIZONTAL INERTIA - SLUG FT ²			N.A.C.E.L.L.F. BALANCE			VERTICAL INERTIA - SLUG FT ²		
	WEIGHT	X (F.S.)	Z (W.L.)	IXX (ROLL)	IYY (PITCH)	IZZ (YAW)	IXX (ROLL)	IYY (PITCH)	IZZ (YAW)	IXX (ROLL)	IYY (PITCH)	IZZ (YAW)
* FUSELAGE & CONTENTS	3696	149.7	-9.0	903	6058	6152						
* HORIZONTAL TAIL	130	419.4	27.7	23	15	38						
* VERTICAL TAIL	96	406.7	63.8	15	22	7						
* WING & CONTENTS	1695	182.2	107.4	40.3	1266	200	1346					
* NACELLE & CONTENTS	(4267)	160.0	(210.1)	(42.4)	(224)	(1395)	(1507)					
FIXED TILTING	1475	202.7	227.8	43.1	43	115	61					
	2792	137.5	200.7	42.0	45	366	369	176.4	200.7	64.3	389	388
OPER. WEIGHT EMPTY	9884	165.8	22.6	48674	12256	57263	490	176.8		34.6	50751	13308
* OBSERVER	200	150.0	1.0	6	7	4						
* FUEL	1280	178.6	109.0	380	32	416						
* INSTRU. & RES	1157	178.6	.5	110	275	300	SAME					
* OTHER	1020	171.5	.5	110	250	225						
BASIC DESIGN GROSS WEIGHT	13541	168.3	20.1	52843	13191	61576	474	176.3		28.8	55176	14482
* OBSERVER	200	150.0	1.0	6	7	4						
* FUEL	1375	178.6	109.0	380	32	416						
* INSTRU. & RES	1157	178.6	.5	110	275	300	SAME					
* OTHER	1020	171.5	.5	110	250	225						
* BALMAST	1864	171.5	.5	120	350	375						
ALTERNATE GROSS WEIGHT	15500	168.8	17.9	53308	13697	62254	412	175.7		25.5	55781	15120
* FUEL	1280	178.6	109.0	380	32	416						
* INSTRU. & RES	1157	178.6	.5	110	275	300	SAME					
TYPICAL FLIGHT TAKE-OFF WEIGHT	12321	168.3	22.0	52573	12787	61359	453	177.1		31.6	54826	13971
* FUEL	759	178.6	109.0	187	12	195						
* INSTRU. & RES	1157	178.6	.5	110	275	300	SAME					
MEAN OPERATING GROSS WEIGHT	11800	167.9	21.1	51053	12717	59743	425	177.1		31.1	53291	13856

NOTE: * ROTOR BLADE INERTIAS (I₀) ARE NOT INCLUDED IN THE ABOVE VALUES. THE ROTOR BLADE WEIGHT IS ASSUMED TO BE ACTING AT THE HUB \bar{z} .

* ROTOR BLADE WEIGHT (COMPLETE AS REMOVED FROM HUB), BALANCE AND INERTIAS (I₀) ARE AS FOLLOWS:
 BLADE WEIGHT 124 LBS., SPAN BALANCE 54.9" FROM HUB \bar{z} , CHORD BALANCE FROM LEADING EDGE OF
 BLADE 4.7", INERTIAS (SLUG FT² AROUND BLADE C.G.) I_{XX} = 52, I_{YY} = 2, I_{ZZ} = 55.

Figure F.1. Mass Properties



- OPERATIONAL CG LIMITS
- ▨ STRUCTURAL DESIGN CG LIMITS
- MAC
- L.E. MAC
- ROTOR PLANE
- WING 1/4 CHORD
- PIVOT POINT
- LANDING GEAR IN DOWN POSITION
- MOMENT CHANGES: FOR ALL POINTS SHOWN
- NACELLE - CURISE TO HOVER + 108609 IN.-LB
- LANDING GEAR - DOWN TO UP - 6077 IN.-LB
- O.W.E. - OPERATING WEIGHT EMPTY
- BALLAST LOCATION AND AMOUNT DEFINED IN VOLUME IV

- 71.8 IN.
- F.S. 149.8
- F.S. 118.8
- F.S. 167.5
- F.S. 177.8

Figure F.2. C.G. Limit Diagram

F.1 CONTROL SYSTEM INPUT DATA

The input data for the control system, SAS, thrust management, and load alleviation system are in this section, and are referenced by page number to the equations presented in Appendix E. Figures F.3 to F.14 present the scheduled function.

F.1.1 Control System Input Data ⁽¹⁾

Control Mixing (Page E.4)

$$K_{\delta_{RUD}} = -8 \text{ deg/inch}$$

$$K_{\delta_R} = 1.0$$

$$K_{\delta_S} = 1.0$$

$$K_{\delta_B} = 1.0$$

$$K_{\delta_e} = -3.33 \text{ deg/inch}$$

$$K_{\delta's} = 0$$

Actuator Dynamics

$$\omega_N = 20 \text{ rad/sec}$$

$$\zeta = 1.0$$

Lead-lag Dynamics

$$\omega_{L-L} = 35.5 \text{ rad/sec}$$

$$\zeta = .18$$

Scheduled Functions - Refer to Graphs

- a) Scheduled Longitudinal Cyclic vs Nacelle Incidence

(1) Gains and time constants not shown on these pages are noted on the block diagrams.

- b) Cyclic Gain vs Nacelle Incidence (Pedals)
- c) Differential Collective Gain vs Nacelle Incidence (Pedals)
- d) Differential Collective Gain vs Nacelle Incidence (Lateral Stick)
- e) Longitudinal Cyclic Gain vs Nacelle Incidence (Long. Stick)
- f) Lateral Cyclic Gain vs Nacelle Incidence
- g) Elevator Deflection vs Nacelle Incidence
- h) Scheduled Lateral Cyclic vs Nacelle Incidence

Load Alleviation System (LAS) (Page E.5)

$$\tau_{LAS} = 0.2 \text{ sec.}$$

LAS Functions

$G_{B_{1\alpha}}$, $G_{A_{1\beta}}$, $G_{A_{1\alpha}}$ vs Dynamic Pressure

Nacelle and Airplane Controls (Page E.6)

Nacelle Actuator Dynamics

$$\omega_{NR} = \omega_{NL} = 10 \text{ rad/sec}$$

$$\zeta_{NL} = \zeta_{NR} = 1.0$$

Scheduled Functions

- a) Scheduled Flap Angle vs Nacelle Incidence
- b) Flaperon vs Lateral Stick
- c) Spoiler Deflection vs Lateral Stick
- d) Spoiler Actuator Limit

Stability Augmentation System (Page E.7 and E.8)

Gains, time constants and scheduled functions noted on block diagrams.

Roll SAS Authority Limit = +2 inches

Yaw SAS Authority Limit = + 1 inch

Pitch SAS Authority Limit = + 2.7°

Thrust Management System (Page E.13)

$$(N_{II}/N_{II_{MAX}})_{REF} = .8865$$

$$\Omega_{REF} = 57.6923 \text{ rad/sec}$$

$$\eta_{TR} = 1.0$$

$$I_P = 564 \text{ slug-ft}^2$$

$$G_{G1} = 2.5 \text{ deg/sec / rad/sec}$$

$$G_{G2} = 2.66 \text{ deg/rad/sec}$$

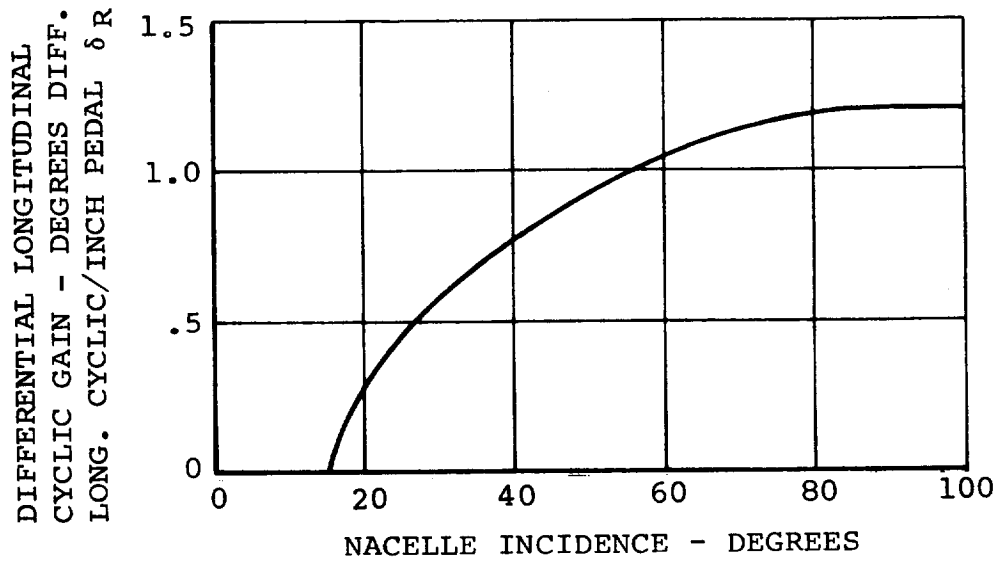
$$G_{G3} = .05 \text{ deg/sec/deg}$$

Scheduled Functions

- a) Turbine Inlet Temperature vs Throttle Position
- b) τ_D vs (ΔHP)
- c) $\tau_e \delta / \sqrt{\theta}$ vs SHP
- d) Output Gain Ratio vs Power Output
- e) Governor Gain Schedule
- f) RPM Select Schedule
- g) Throttle Collective Gain Schedule
- h) Incremental Collective Schedule
- i) Variable Authority Limit

Rotor Control Coordinate Axis Transforms (Page E.14)

$$\phi_P = -12 \text{ degrees}$$



NOTE: DIFFERENTIAL NACELLE TILT IS 1.55 DEGREES PER NACELLE PER DEGREE OF DIFF. CYCLIC

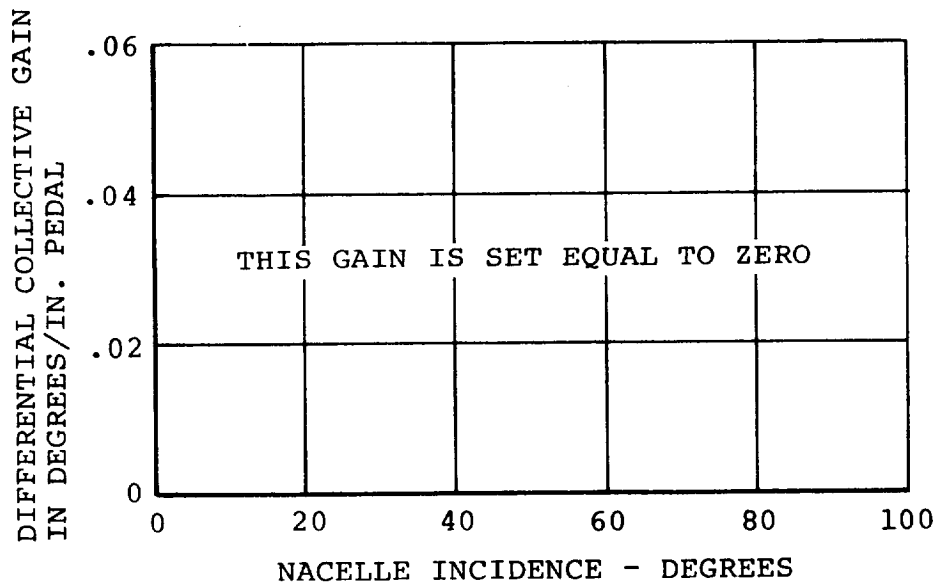
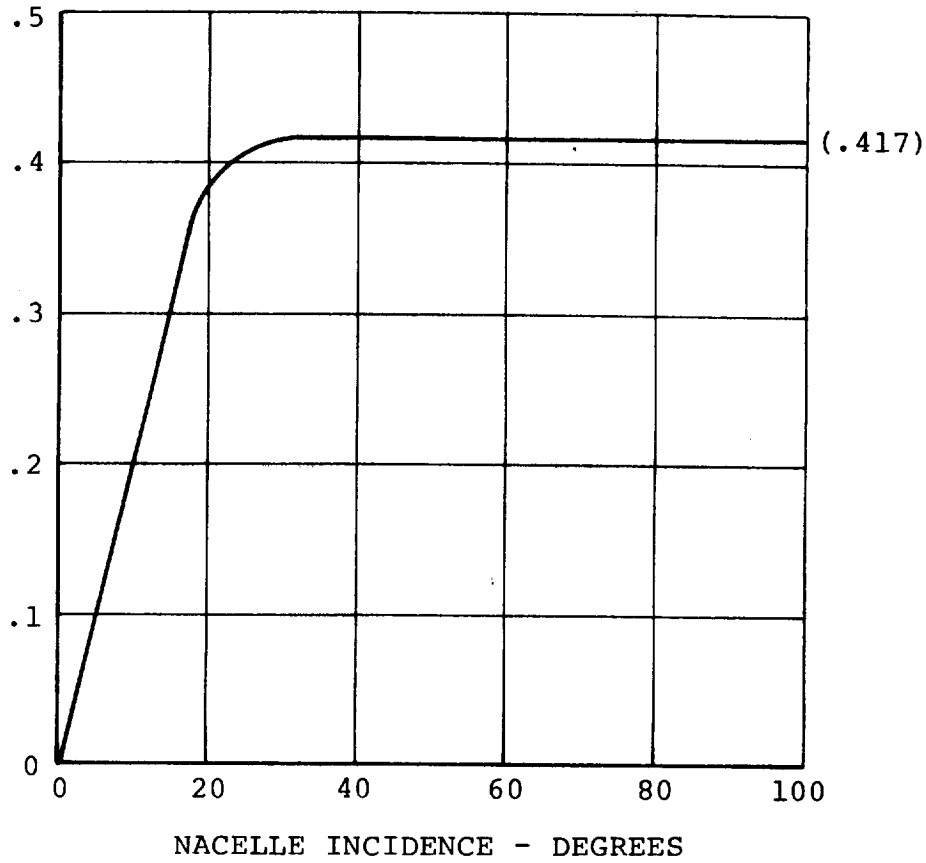


Figure F.3. Differential Long. Cyclic for Yaw Control vs Nacelle Incidence

LONGITUDINAL CYCLIC GAIN - $\frac{\text{DEGREES CUMMULATIVE CYCLIC}}{\text{INCH LONG. STICK } \delta B}$



NOTE: ELEVATOR DEFLECT 3.3333 DEGREES
PER INCH OF LONGITUDINAL STICK

MAXIMUM LONG. STICK TRAVEL IS ± 6 INCHES

Figure F.5. Longitudinal Cyclic for Pitch Control Gain vs Nacelle Incidence

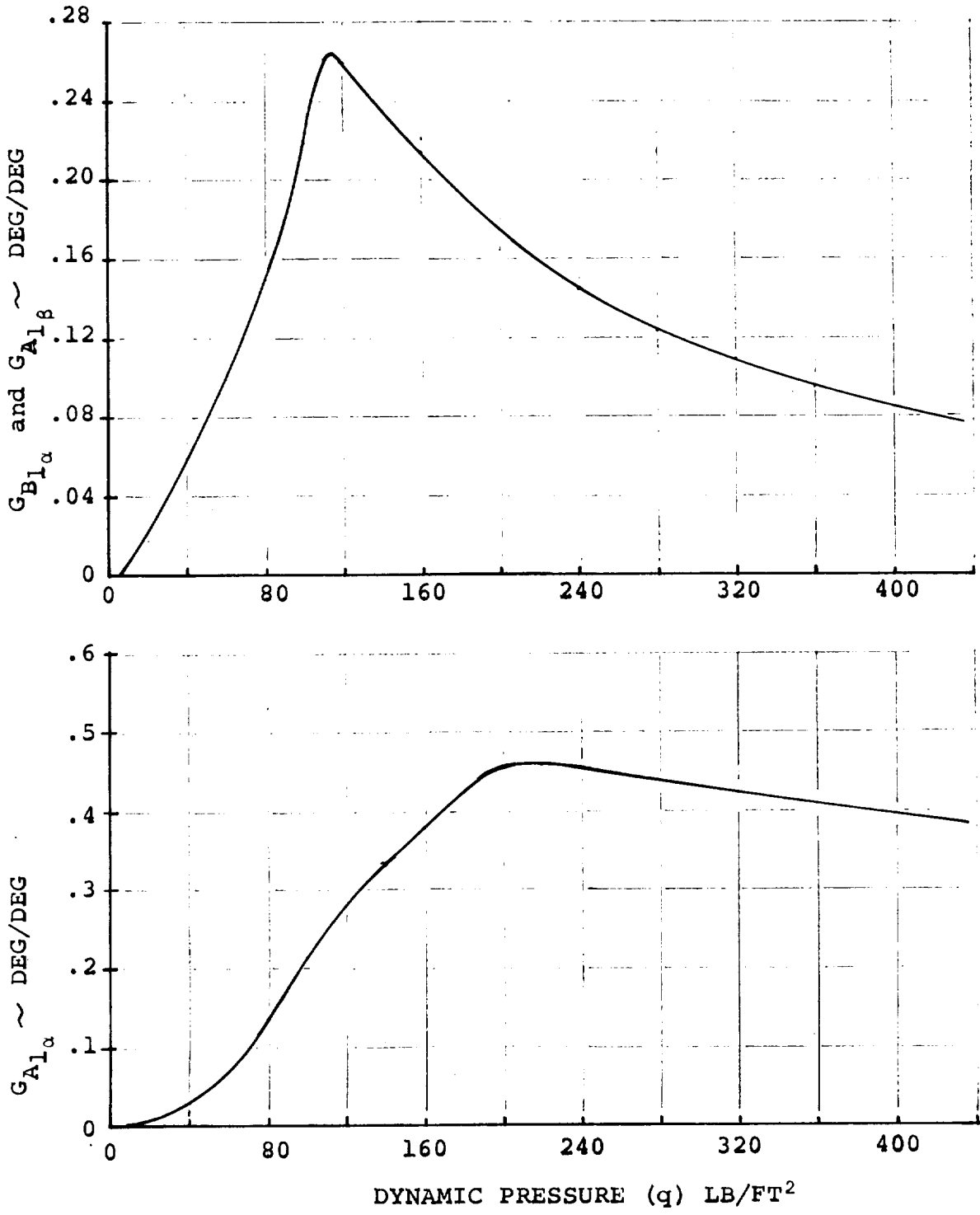


Figure F.6. Load Alleviation System Gain Schedule.

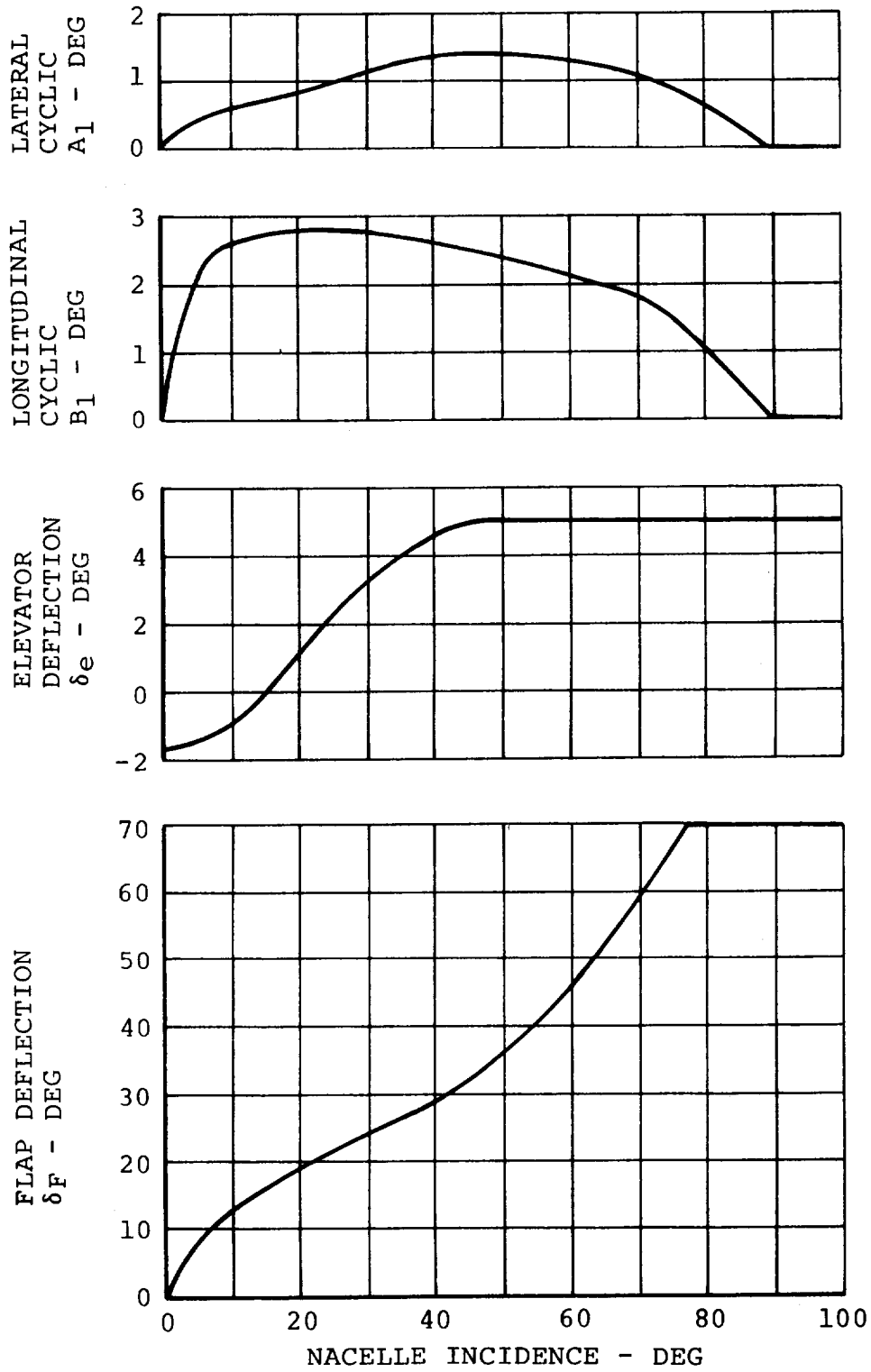
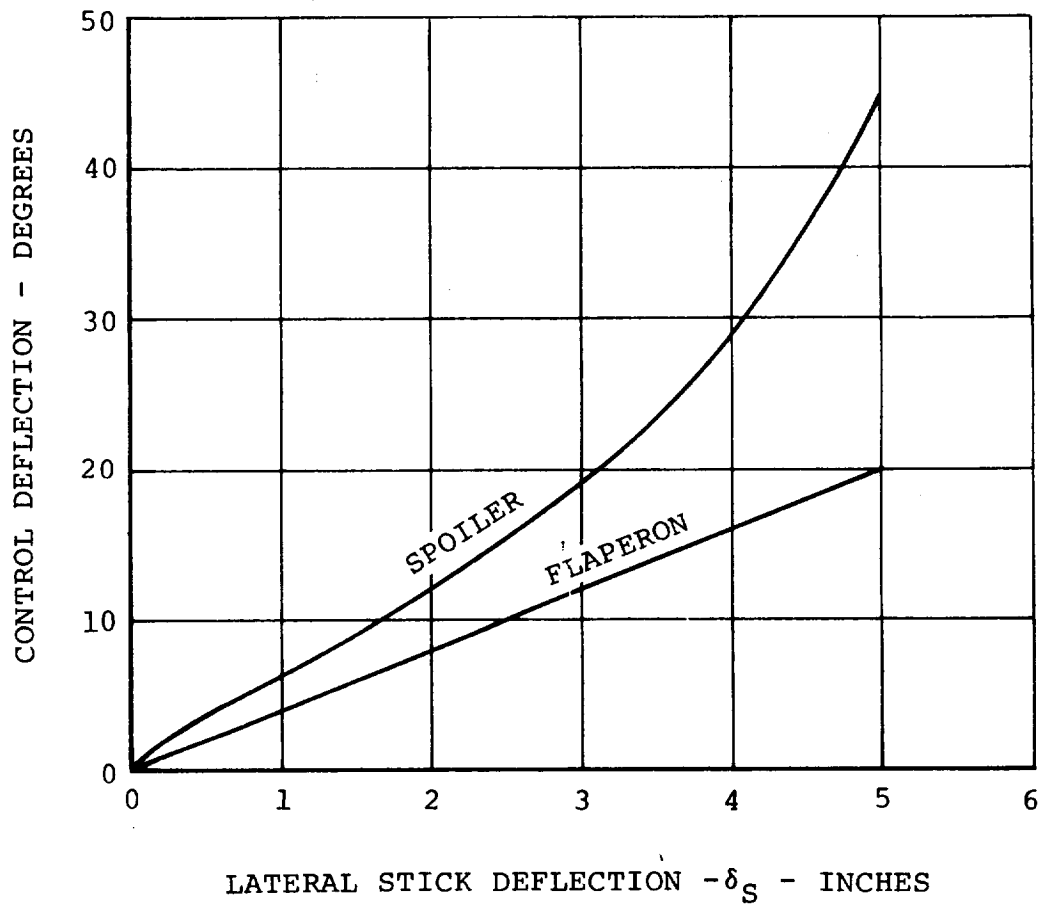


Figure F.7. Programmed Cyclic, Elevator, and Flap Deflection vs Nacelle Incidence



MAXIMUM LATERAL STICK TRAVEL IS ± 5 INCHES

Figure F.8. Roll Control Deflection vs Stick Deflection

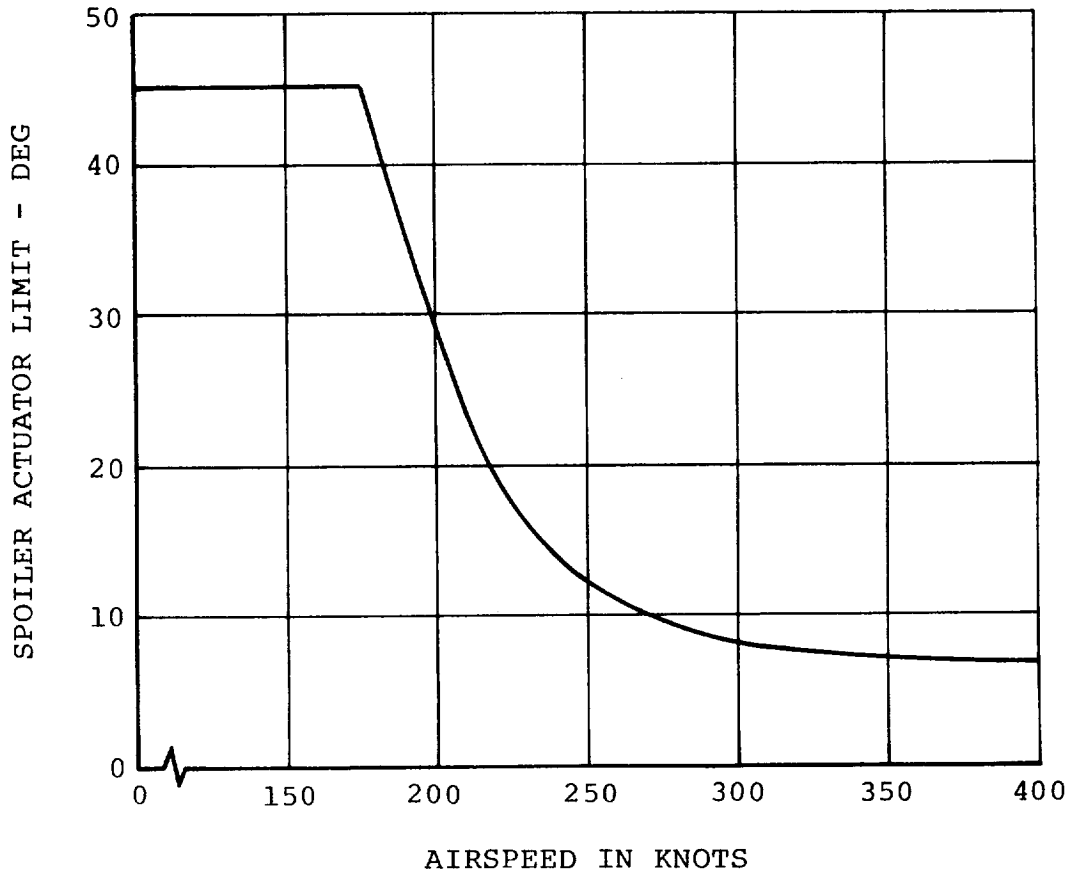


Figure F.9. Spoiler Actuator Limit vs Airspeed

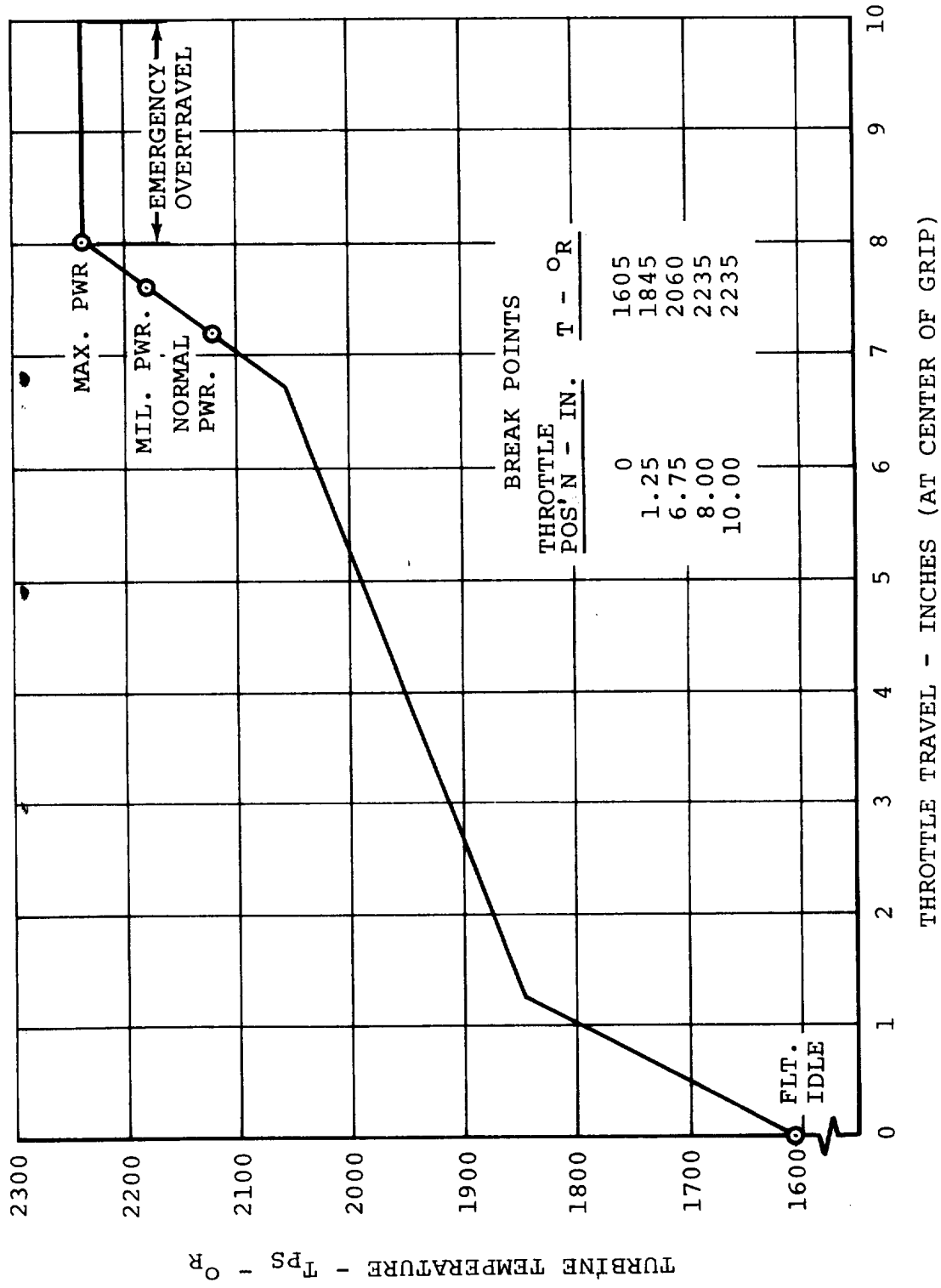


Figure F.10. Assumed Throttle Travel Model 222 Simulation Both Engines

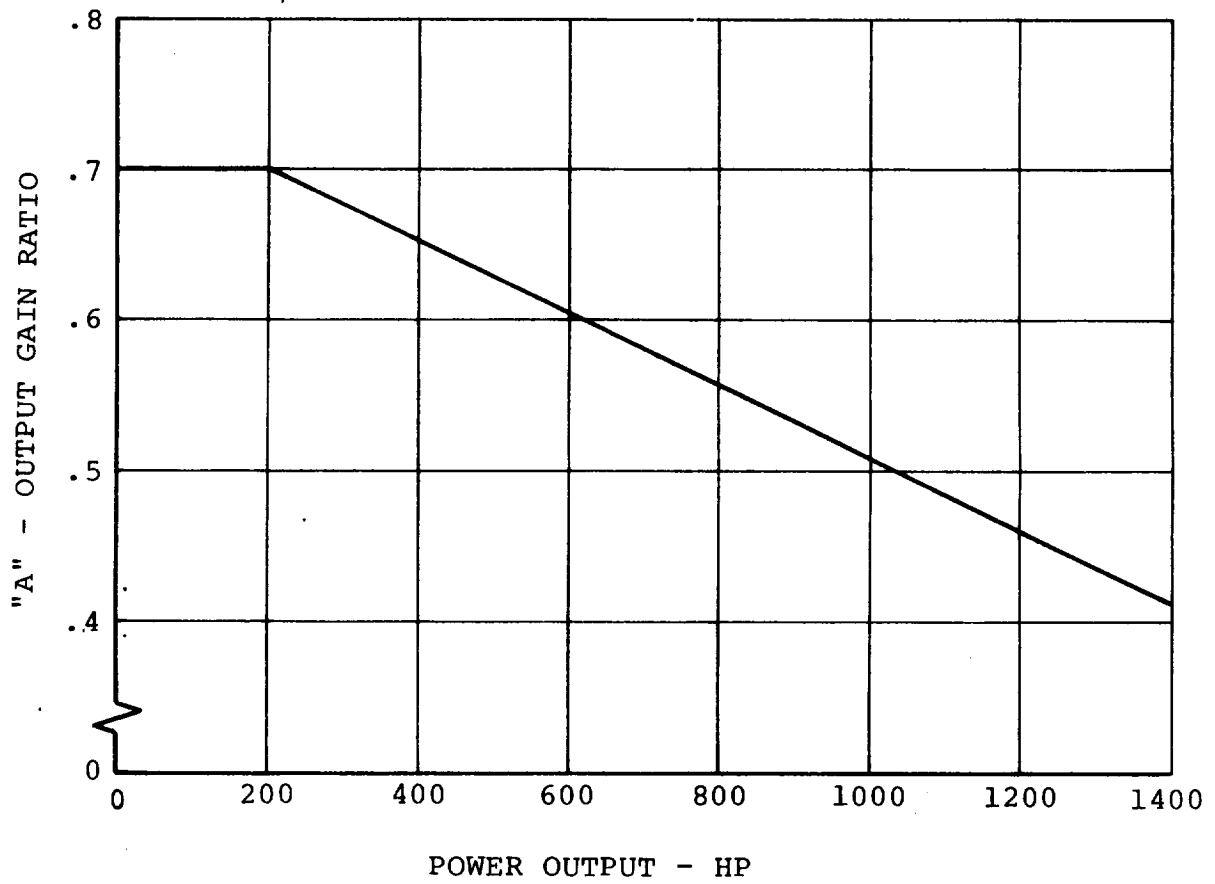


Figure F.12. Engine Characteristics Lycoming T53-L13 Engine

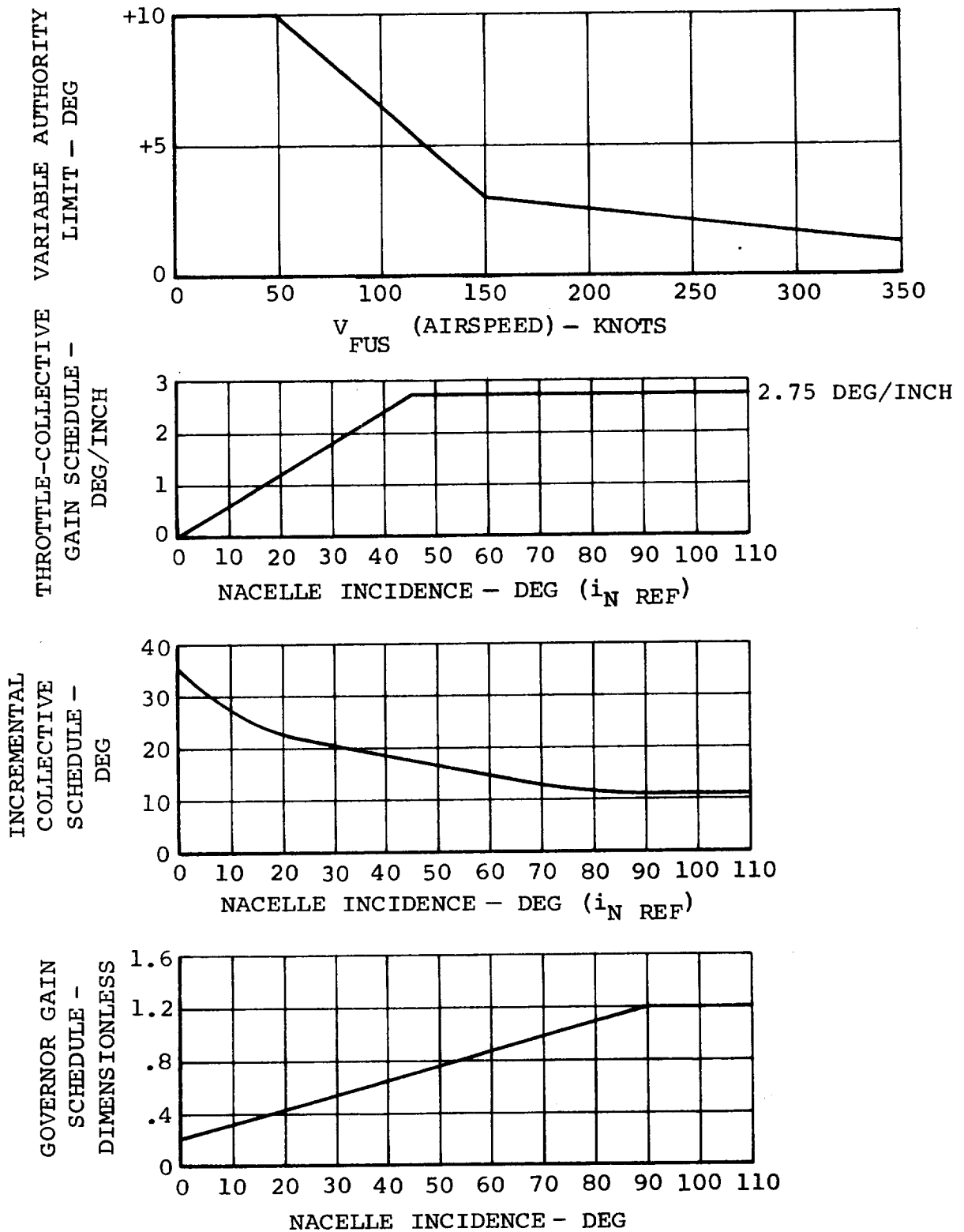


Figure F.13. Thrust Management System-Scheduled Parameters

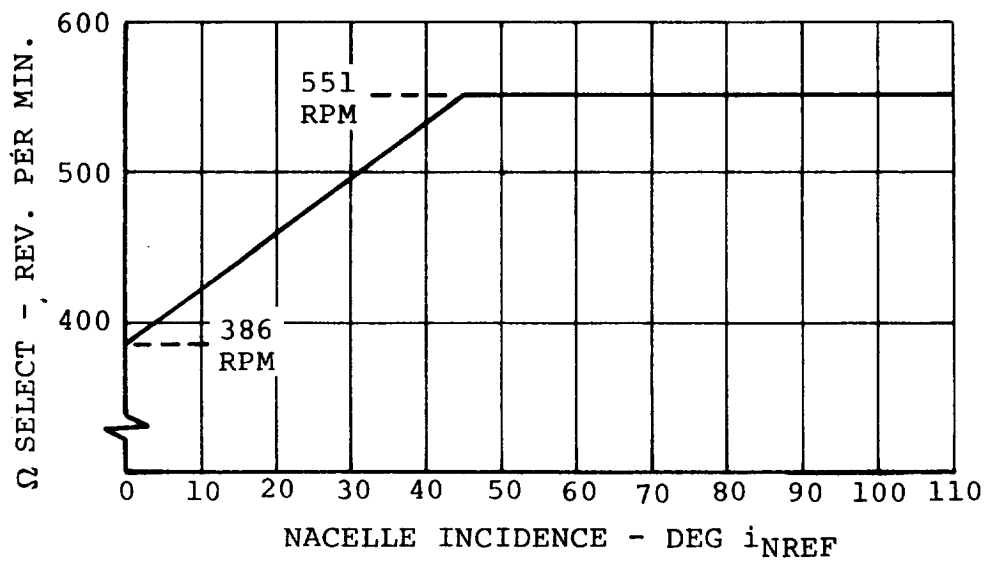


Figure F.14. Thrust Management System-Scheduled Parameters

F.2 ENGINE INPUT DATA

The input data for the engine performance subroutine is given in this section, and are referenced by page number to the equation presented in Appendix E. Plotted data are shown in Figures F.15 to F.18.

F.2.1 Turbine Engine Performance Input Data

Engine Performance Data (Pages E.10, E.11 and E.12)

$$\text{SHP}^* = 1550$$

$$\text{WDTIND} = 1.0$$

$$\text{N1IND} = 1.0$$

$$\text{N10IND} = 0$$

$$\text{QIND} = 1.0$$

$$\dot{w}_{\text{MAX}}^* / \dot{w}^* = 1.11$$

$$N_{\text{I MAX}}^* / N_{\text{I}}^* = 1.04$$

$$(N_{\text{I}} / \sqrt{\theta_1} / N_{\text{I}}^*)_{\text{MAX}} = 0$$

$$Q_{\text{MAX}} / Q^* = 1.446$$

$$N_{\text{II MAX}}^* / N_{\text{II}}^* = 1.128$$

$$N_{\text{I}}^* = 25425 \text{ RPM}$$

$$(N_{\text{II}} / N_{\text{II MAX}}^*)_{\text{REF}} = .8865$$

$$\Omega_{\text{REF}} = 57.6923$$

Tabular Engine Cycle Input Data

- a) Values of Referred Horsepower
- b) Values of Referred Fuel Flow
- c) Values of Referred Gas Generator Speed
- d) Values of Referred Power Turbine Speed

1. VALUES OF REFERRED HORSEPOWER $\frac{SHP}{\delta\sqrt{\theta}}/SHP^*$

MACH NO.	T/θ=1600	T/θ=1800	T/θ=2000	T/θ=2200	T/θ=2400	T/θ=2600	T/θ=2800
0	.035	.330	.630	.920	1.200	1.340	1.400
.2	.075	.375	.670	.960	1.245	1.390	1.450
.4	.125	.425	.720	1.010	1.295	1.440	1.500
.6	.180	.480	.775	1.065	1.350	1.495	1.550
.8	.240	.534	.835	1.125	1.410	1.550	1.600

2. VALUES OF REFERRED FUEL FLOW $\frac{W}{\delta\sqrt{\theta}}/SHP^*$

MACH NO.	T/θ=1600	T/θ=1800	T/θ=2000	T/θ=2200	T/θ=2400	T/θ=2600	T/θ=2800
0	.150	.278	.407	.535	.662	.750	.802
.2	.150	.278	.407	.535	.662	.750	.802
.4	.150	.278	.407	.535	.662	.750	.802
.6	.150	.278	.407	.535	.662	.750	.802
.8	.150	.278	.407	.535	.662	.750	.802

3. VALUES OF REFERRED GAS GENERATOR SPEED $N_{II}/\sqrt{\theta}/N_{II}^*$

MACH NO.	T/θ=1600	T/θ=1800	T/θ=2000	T/θ=2200	T/θ=2400	T/θ=2600	T/θ=2800
0	.722	.840	.925	.990	1.045	1.097	1.150
.2	.735	.846	.927	.992	1.048	1.100	1.154
.4	.748	.853	.933	.997	1.052	1.105	1.158
.6	.766	.860	.939	1.004	1.059	1.111	1.162
.8	.789	.871	.950	1.015	1.068	1.119	1.170

4. VALUES OF REFERRED POWER TURBINE SPEED $N_{II}/\sqrt{\theta}/N_{II}^*$

MACH NO.	T/θ=1600	T/θ=1800	T/θ=2000	T/θ=2200	T/θ=2400	T/θ=2600	T/θ=2800
0	.445	.685	.856	.983	1.084	1.178	1.264
.2	.461	.699	.880	.997	1.088	1.169	1.246
.4	.500	.734	.908	1.009	1.089	1.158	1.224
.6	.557	.789	.940	1.023	1.086	1.145	1.197
.8	.640	.858	.973	1.029	1.076	1.123	1.161

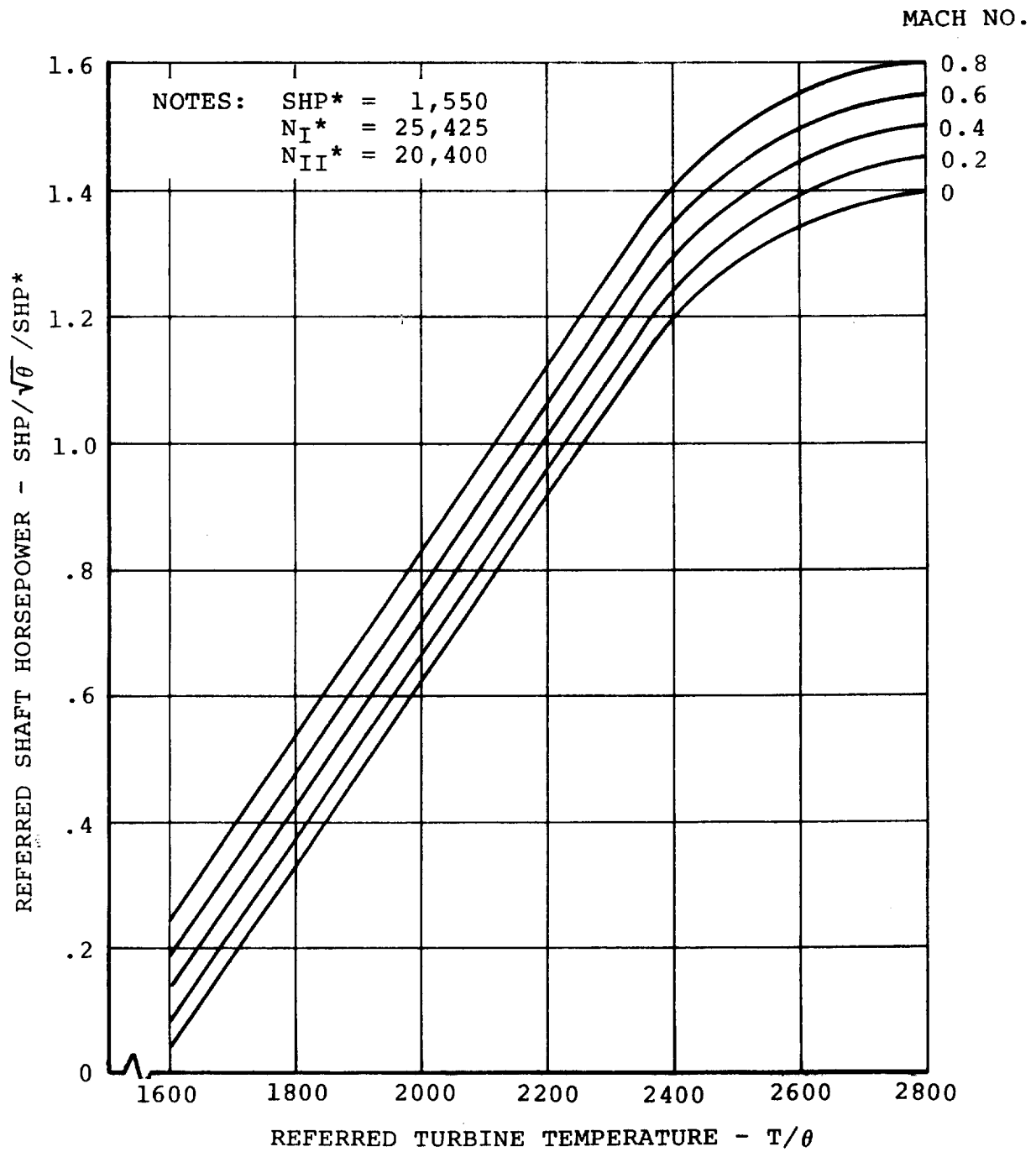


Figure F.15. Turbine Engine Performance - Engine Cycle 1.78

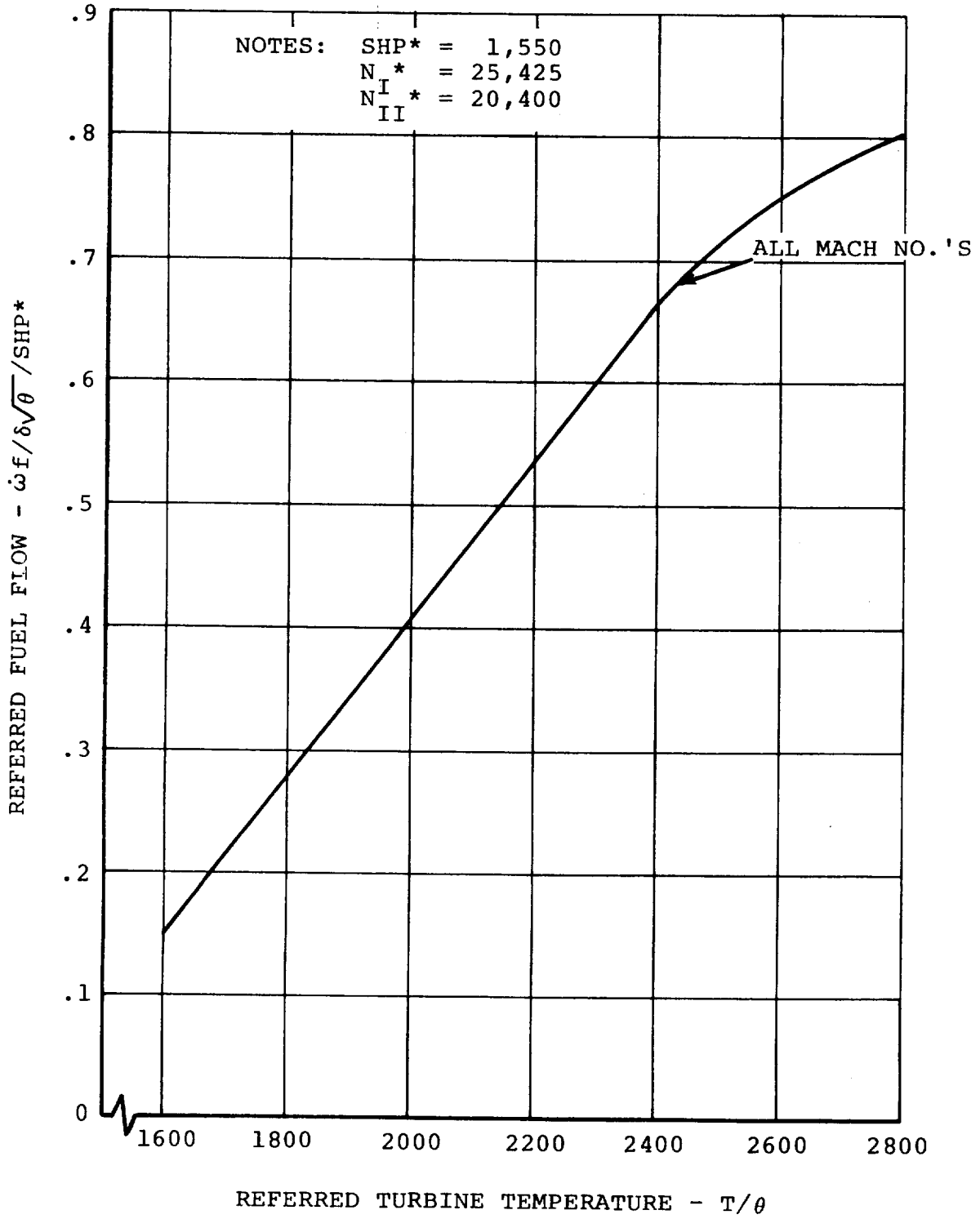


Figure F.16. Turbine Engine Performance - Engine Cycle 1.78

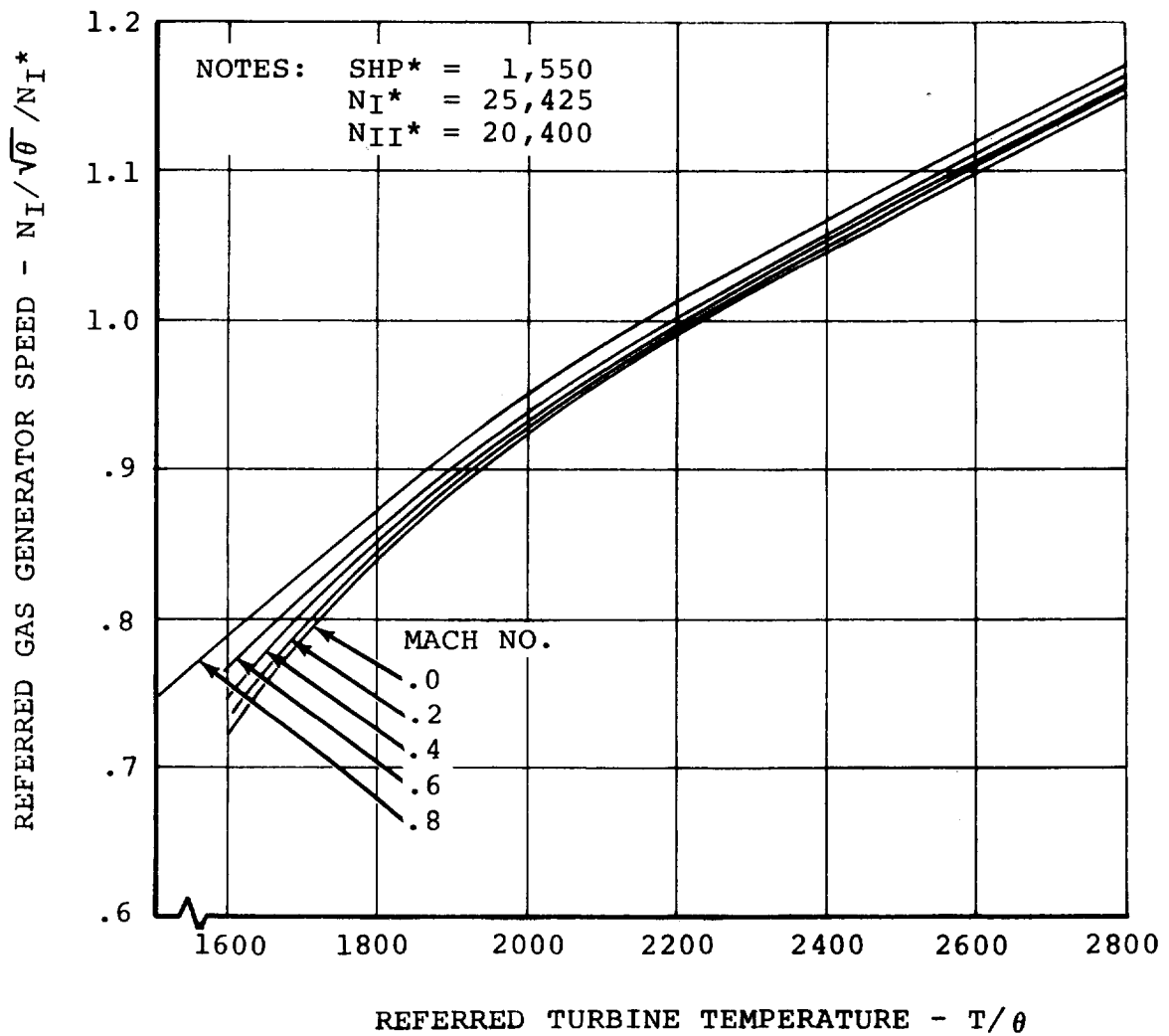


Figure F.17. Turbine Engine Performance - Engine Cycle 1.78

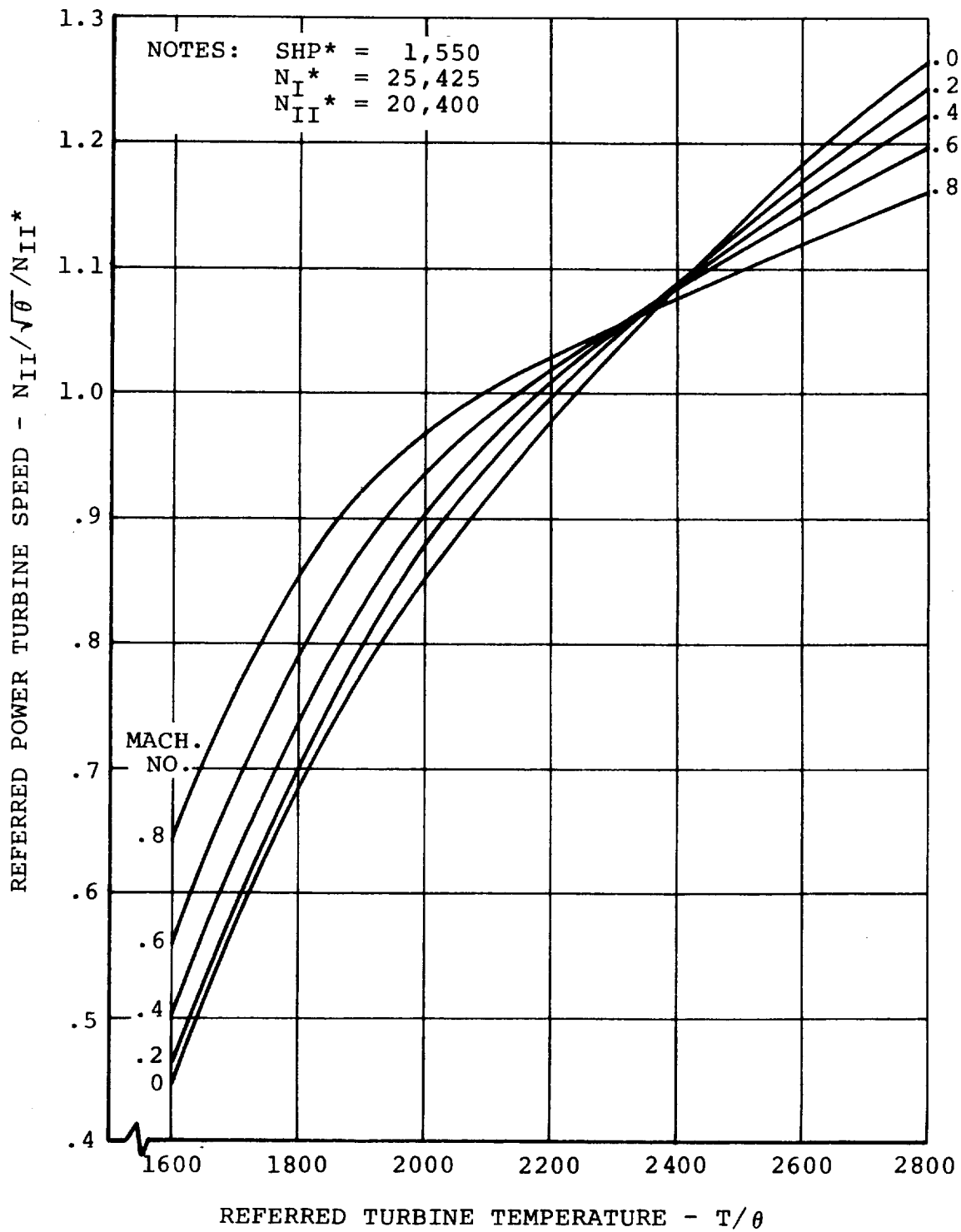


Figure F.18. Turbine Engine Performance - Engine Cycle 1.78

F.3 ROTOR AERODYNAMIC INPUT DATA

The input data for the rotor aerodynamics are given in this section, and are referenced by page number to the equations presented in Appendix E. Tabulated coefficients of the curve fit equations are shown in Figures F.19 to F.27.

F.3.1 Rotor Aerodynamic Input Data

Rotor Thrust (Page E.54)

$$\tau_1 = .10$$

$$\tau_2 = .10$$

$$R = 13 \text{ Ft.}$$

Rotor Force and Moment Calculations (Page E.60)

$$f_{TR} = f_{TL} = 1.0$$

$$f_{NFR} = f_{NF_L} = 1.0$$

$$f_{SFR} = f_{SF_L} = 1.0$$

$$f_{PMR} = f_{PM_L} = 1.0$$

$$f_{YMR} = f_{YM_L} = 1.0$$

$$f_{QR} = f_{Q_L} = 1.0$$

$$f_{PR} = f_{P_L} = 1.0$$

μ	0	.1014	.1351	.2027	.3723	.4565	.6432	.8038	1.125
A_{T0}	.131167x10 ⁻²	-.539532x10 ⁻²	-.203368x10 ⁻¹	-.427861x10 ⁻¹	-.470950x10 ⁻¹	-.439534x10 ⁻¹	-.522445x10 ⁻¹	-.708703x10 ⁻¹	-.878713x10 ⁻¹
A_{T1}	0	-.119838x10 ⁻³	.841758x10 ⁻⁴	.481855x10 ⁻³	.266417x10 ⁻³	0	0	0	0
A_{T2}	0	.26831x-10 ⁻⁵	.260200x10 ⁻⁵	.399507x10 ⁻⁶	-.596957x10 ⁻⁵	0	0	0	0
A_{T3}	0	-.904463x10 ⁻⁸	-.127543x10 ⁻⁷	-.681927x10 ⁻⁸	.36307x10 ⁻⁷	0	0	0	0
A_{T4}	.747733x10 ⁻³	.784148x10 ⁻³	.254258x10 ⁻²	.250025x10 ⁻²	.186317x10 ⁻²	.108914x10 ⁻²	.408704x10 ⁻³	.766317x10 ⁻³	.704819x10 ⁻³
A_{T5}	0	.8905x10	-.387201x10	-.220100x10	-.270408x10 ⁻⁴	0	0	0	0
A_{T6}	0	-.699401x10 ⁻⁷	.413387x10 ⁻⁶	.151901x10 ⁻⁶	-.510959x10 ⁻⁶	0	0	0	0
A_{T7}	0	.156844x10 ⁻⁹	-.151355x10 ⁻⁸	-.407612x10 ⁻⁹	.306610x10 ⁻⁷	0	0	0	0
A_{T8}	.120357x10 ⁻⁴	.996174x10 ⁻⁵	-.926255x10 ⁻⁴	-.825240x10 ⁻⁵	-.307987x10 ⁻⁵	.100012x10 ⁻⁴	.214303x10 ⁻⁴	.163128x10 ⁻⁴	.161866x10 ⁻⁴
A_{T9}	0	-.592706x10 ⁻⁸	.371573x10 ⁻⁵	.215847x10 ⁻⁶	-.111356x10 ⁻⁶	0	0	0	0
A_{T10}	0	-.10436x10 ⁻⁸	-.449157x10 ⁻⁷	-.725582x10 ⁻⁹	.769226x10 ⁻⁷	0	0	0	0
A_{T11}	0	.388825x10 ⁻¹¹	.168184x10 ⁻⁹	-.196520x10 ⁻¹¹	-.167159x10 ⁻⁸	0	0	0	0

NOTE: α and θ 0.75 must be in degrees when these coefficients are used in the thrust equation.

Figure F. 19. Coefficients of Curve Fit Equations for Thrust Coefficient

$\mu \rightarrow$.1014	.1351	.2027	.3723	.4565	.6432	.8038	1.125
AP0	.118188x10 ⁻³	.117752x10 ⁻³	.575597x10 ⁻³	.204675x10 ⁻³	.283014x10 ⁻³	.362823x10 ⁻³	.511711x10 ⁻³	.539983x10 ⁻³
AP1	0	.262107x10 ⁻⁵	-.835529x10 ⁻⁵	-.551959x10 ⁻⁵	-.952757x10 ⁻⁵	0	0	0
AP2	0	.379347x10 ⁻⁷	.973647x10 ⁻⁷	.145048x10 ⁻⁶	-.615163x10 ⁻⁷	0	0	0
AP3	0	-.147777x10 ⁻⁹	-.180303x10 ⁻⁹	-.391787x10 ⁻⁹	.131638x10 ⁻⁸	0	0	0
AP4	.223227x10 ⁻¹	.143376x10 ⁰	.143289x10 ⁰	.304517x10 ⁰	.383466x10 ⁰	.466013x10 ⁰	.662959x10 ⁰	.854989x10 ⁰
AP5	0	-.263395x10 ⁻²	-.391803x10 ⁻²	-.56844x10 ⁻²	-.278572x10 ⁻²	0	0	0
AP6	0	.115613x10 ⁻⁴	.421318x10 ⁻⁴	.336549x10 ⁻⁴	.129237x10 ⁻⁴	0	0	0
AP7	0	-.239424x10 ⁻⁷	-.174886x10 ⁻⁶	-.109523x10 ⁻⁶	-.595181x10 ⁻⁶	0	0	0
AP8	.601436x10 ¹	.153503x10 ¹	-.759331x10 ⁰	-.718612x10 ¹	-.297074x10 ⁻¹	.186185x10 ⁻¹	-.810072x10 ⁻¹	.960492x10 ⁻³
AP9	0	.212258x10 ⁰	.443411x10 ⁰	.50642x10 ⁰	-.477549x10 ⁻²	0	0	0
AP10	0	-.297147x10 ⁻²	-.703113x10 ⁻²	-.624918x10 ⁻²	.327815x10 ⁻³	0	0	0
AP11	0	.985059x10 ⁻⁵	.27991x10 ⁻⁴	.221158x10 ⁻⁴	-.543824x10 ⁻⁵	0	0	0

NOTE: α must be in degrees when these coefficients are used in the power equation.

Figure F.20. Coefficients of Curve Fit Equations for Power Coefficient

	$\mu=0$	$\mu=.1014$	$\mu=.1351$	$\mu=.2027$	$\mu=.3723$	$\mu=.4565$
ANF0	0	-.154857x10 ⁻⁵	.204691x10 ⁻⁵	.450018x10 ⁻⁴	-.982094x10 ⁻⁴	.179585x10 ⁻⁶
ANF1	0	.467546x10 ⁻⁵	.942028x10 ⁻⁵	.211604x10 ⁻⁴	.19641x10 ⁻³	.323623x10 ⁻³
ANF2	0	-.285003x10 ⁻⁷	-.100977x10 ⁻⁶	-.251209x10 ⁻⁶	-.639116x10 ⁻⁵	.684873x10 ⁻⁶
ANF3	0	.128888x10 ⁻¹⁰	.270048x10 ⁻⁹	.746916x10 ⁻⁹	.657985x10 ⁻⁷	-.249423x10 ⁻⁷
ANF4	0	-.102821x10 ⁻³	.224724x10 ⁻³	.929207x10 ⁻³	-.157595x10 ⁻²	-.809587x10 ⁻⁴
ANF5	0	.749984x10 ⁻³	.125801x10 ⁻²	.178593x10 ⁻²	.24356x10 ⁻²	.572817x10 ⁻²
ANF6	0	-.945697x10 ⁻⁵	-.132674x10 ⁻⁴	-.217638x10 ⁻⁴	.234598x10 ⁻³	.109167x10 ⁻²
ANF7	0	.293263x10 ⁻⁷	.348545x10 ⁻⁷	.65423x10 ⁻⁷	-.470641x10 ⁻⁵	-.963463x10 ⁻⁴
ANF8	0	.109342x10 ⁰	.275072x10 ⁻¹	-.543699x10 ⁻¹	.443939x10 ⁻¹	.53212x10 ⁻²
ANF9	0	.943903x10 ⁻¹	.696523x10 ⁻¹	.18035x10 ⁰	-.138981x10 ⁻¹	.159926x10 ⁰
ANF10	0	-.109604x10 ⁻²	-.923809x10 ⁻³	-.232838x10 ⁻²	.632501x10 ⁻³	-.115516x10 ⁰
ANF11	0	.317682x10 ⁻⁵	.29846x10 ⁻⁵	.738683x10 ⁻⁵	-.814596x10 ⁻⁵	.994553x10 ⁻²

	$\mu=.5147$	$\mu=.6432$	$\mu=.772$	$\mu=.9008$	$\mu=1.03$	$\mu=1.158$
ANF0	.137987x10 ⁻⁵	.161374x10 ⁻⁵	.245107x10 ⁻⁵	-.132502x10 ⁻⁶	-.173383x10 ⁻⁵	.585875x10 ⁻⁵
ANF1	.439095x10 ⁻³	.760961x10 ⁻³	.109347x10 ⁻²	.140037x10 ⁻²	.170687x10 ⁻²	.199778x10 ⁻²
ANF2	.228487x10 ⁻⁵	.440349x10 ⁻⁶	.823616x10 ⁻⁶	-.191532x10 ⁻⁶	-.139327x10 ⁻⁵	-.209278x10 ⁻⁵
ANF3	-.762918x10 ⁻⁷	-.152524x10 ⁻⁷	-.545001x10 ⁻⁷	.257742x10 ⁻⁷	.512513x10 ⁻⁷	.76607x10 ⁻⁷
ANF4	-.7923358x10 ⁻³	-.58501x10 ⁻³	-.578165x10 ⁻⁴	-.185878x10 ⁻³	.212865x10 ⁻²	-.228619x10 ⁻²
ANF5	.665352x10 ⁻²	.282596x10 ⁻²	-.625689x10 ⁻²	-.258884x10 ⁻²	-.513321x10 ⁻²	.123733x10 ⁻¹
ANF6	-.208908x10 ⁻³	.266667x10 ⁻³	.122656x10 ⁻²	.658596x10 ⁻³	.878786x10 ⁻³	-.583625x10 ⁻³
ANF7	.776787x10 ⁻⁵	-.517496x10 ⁻⁵	-.361453x10 ⁻⁴	-.249126x10 ⁻⁴	-.316126x10 ⁻⁴	.101001x10 ⁻⁴
ANF8	.324054x10 ⁻¹	.487661x10 ⁻¹	-.60177x10 ⁻¹	.804597x10 ⁻²	-.162981x10 ⁰	.466581x10 ⁻¹
ANF9	-.688518x10 ⁻¹	.113439x10 ⁰	.642961x10 ⁰	.208291x10 ⁻¹	.515108x10 ⁰	-.898786x10 ⁰
ANF10	.875982x10 ⁻²	-.243064x10 ⁻¹	-.967895x10 ⁻¹	-.520537x10 ⁻²	-.665886x10 ⁻¹	.324115x10 ⁻¹
ANF11	-.327294x10 ⁻³	.563958x10 ⁻³	.300992x10 ⁻²	.261473x10 ⁻³	.221409x10 ⁻²	-.439838x10 ⁻³

NOTE: α must be in degrees when these coefficients are used in the normal force equation.

Figure F.21. Coefficients of Curve Fit Equations for Normal Force Coefficient

	$\mu = .1014$	$\mu = .1351$	$\mu = .2027$	$\mu = .3723$	$\mu = .4565$
A SF0	0	.291745x10 ⁻⁶	.115843x10 ⁻⁵	.564885x10 ⁻⁴	.610186x10 ⁻⁸
A SF1	0	-.12407x10 ⁻⁵	-.106448x10 ⁻⁵	.633856x10 ⁻⁶	.557813x10 ⁻⁴
A SF2	0	.113747x10 ⁻⁷	.671759x10 ⁻⁸	-.252897x10 ⁻⁷	-.598734x10 ⁻⁶
A SF3	0	-.245443x10 ⁻¹⁰	-.440653x10 ⁻¹¹	.119483x10 ⁻⁹	-.659238x10 ⁻⁸
A SF4	0	.143202x10 ⁻³	.317272x10 ⁻³	.147537x10 ⁻²	-.842079x10 ⁻⁴
A SF5	0	-.830999x10 ⁻⁴	-.118232x10 ⁻³	-.544752x10 ⁻⁴	-.550991x10 ⁻⁴
A SF6	0	.958551x10 ⁻⁷	.242609x10 ⁻⁶	-.267651x10 ⁻⁵	-.171925x10 ⁻⁴
A SF7	0	.200043x10 ⁻⁸	.227584x10 ⁻⁸	.163762x10 ⁻⁷	.296356x10 ⁻⁶
A SF8	0	-.193731x10 ⁻²	-.509539x10 ⁻²	-.833551x10 ⁻¹	.686884x10 ⁻²
A SF9	0	.407909x10 ⁻²	.722497x10 ⁻²	.315085x10 ⁻²	-.101352x10 ⁻¹
A SF10	0	-.450147x10 ⁻⁴	-.916859x10 ⁻⁴	.612312x10 ⁻⁴	.130744x10 ⁻²
A SF11	0	.124524x10 ⁻⁶	.285967x10 ⁻⁶	-.428818x10 ⁻⁶	-.239885x10 ⁻⁴

	$\mu = .5147$	$\mu = .6432$	$\mu = .772$	$\mu = .9003$	$\mu = 1.158$
A SF0	.136092x10 ⁻⁵	.976607x10 ⁻⁶	-.97825x10 ⁻⁶	.786968x10 ⁻⁶	-.216019x10 ⁻⁵
A SF1	-.23559x10 ⁻⁴	-.130694x10 ⁻³	-.316773x10 ⁻³	-.557452x10 ⁻³	-.809093x10 ⁻³
A SF2	.127659x10 ⁻⁵	-.366955x10 ⁻⁶	-.859884x10 ⁻⁶	-.124574x10 ⁻⁶	-.856051x10 ⁻⁷
A SF3	-.572509x10 ⁻⁷	.121016x10 ⁻⁷	.301607x10 ⁻⁷	.115477x10 ⁻⁷	.178906x10 ⁻⁷
A SF4	.119258x10 ⁻²	-.100898x10 ⁻³	.725157x10 ⁻³	.258719x10 ⁻⁴	.167271x10 ⁻³
A SF5	-.740273x10 ⁻²	-.367008x10 ⁻²	-.55614x10 ⁻²	-.320731x10 ⁻²	-.721592x10 ⁻²
A SF6	.104627x10 ⁻²	.662111x10 ⁻⁴	.25791x10 ⁻³	-.165071x10 ⁻³	.327913x10 ⁻³
A SF7	-.487885x10 ⁻⁴	-.2585357x10 ⁻⁵	-.751767x10 ⁻⁵	.278601x10 ⁻⁶	-.134919x10 ⁻⁴
A SF8	-.177106x10 ⁰	.363417x10 ⁻²	-.600228x10 ⁻¹	-.274394x10 ⁻¹	.157176x10 ⁻¹
A SF9	.683888x10 ⁰	-.104633x10 ⁰	-.660259x10 ⁻¹	-.178098x10 ⁰	.175384x10 ⁰
A SF10	-.161739x10 ⁰	-.180444x10 ⁻²	-.812251x10 ⁻²	.208395x10 ⁻¹	-.938934x10 ⁻²
A SF11	.75356x10 ⁻²	.896371x10 ⁻⁴	.125335x10 ⁻³	-.295016x10 ⁻³	.401628x10 ⁻³

NOTE: α must be in degrees when these coefficients are used in the side force equation.

Figure F.22. Coefficients of Curve Fit Equations for Side Force Coefficient

	$\mu = 0$	$\mu = .1014$	$\mu = .1351$	$\mu = .2027$	$\mu = .3723$	$\mu = .4565$
A PM0	0	.377218x10 ⁻⁵	.688095x10 ⁻⁵	-.79344x10 ⁻⁵	-.310285x10 ⁻⁶	-.884622x10 ⁻⁸
A PM1	0	.539482x10 ⁻⁵	.125905x10 ⁻⁴	.316671x10 ⁻⁴	.820375x10 ⁻⁴	.141415x10 ⁻⁴
A PM2	0	-.12652x10 ⁻⁶	-.252414x10 ⁻⁶	-.581828x10 ⁻⁶	-.271116x10 ⁻⁶	.345339x10 ⁻⁷
A PM3	0	.537895x10 ⁻⁹	.101607x10 ⁻⁸	.226169x10 ⁻⁸	-.151223x10 ⁻⁷	-.105759x10 ⁻⁸
A PM4	0	.172117x10 ⁻³	.562525x10 ⁻³	.201324x10 ⁻²	.193688x10 ⁻³	-.738879x10 ⁻⁵
A PM5	0	.146772x10 ⁻²	.1652x10 ⁻²	.206142x10 ⁻²	.464123x10 ⁻²	-.159412x10 ⁻²
A PM6	0	-.11507x10 ⁻⁴	-.121292x10 ⁻⁴	-.131115x10 ⁻⁴	-.229179x10 ⁻⁴	.508798x10 ⁻⁵
A PM7	0	.185794x10 ⁻⁷	.164608x10 ⁻⁷	.913233x10 ⁻⁸	-.119169x10 ⁻⁶	-.10134x10 ⁻⁶
A PM8	0	-.165488x10 ⁻¹	-.189205x10 ⁻¹	.766096x10 ⁻¹	-.133686x10 ⁻¹	.955878x10 ⁻³
A PM9	0	.181983x10 ⁻²	.224173x10 ⁻³	-.692308x10 ⁻²	-.487350x10 ⁻²	.216812x10 ⁻¹
A PM10	0	-.236138x10 ⁻⁴	.16657x10 ⁻⁶	.684175x10 ⁻⁴	.362062x10 ⁻³	-.13177x10 ⁻²
A PM11	0	.796661x10 ⁻⁷	-.470343x10 ⁻⁸	-.176422x10 ⁻⁶	-.598035x10 ⁻⁵	.362472x10 ⁻⁴
$\mu = .5147$ $\mu = .6432$ $\mu = .772$ $\mu = .9008$ $\mu = 1.03$ $\mu = 1.158$						
A PM0	-.163818x10 ⁻⁶	-.771885x10 ⁻⁶	-.248968x10 ⁻⁵	.145349x10 ⁻⁶	.168996x10 ⁻⁵	.274231x10 ⁻⁶
A PM1	-.177418x10 ⁻⁵	-.922672x10 ⁻⁴	-.202383x10 ⁻³	-.308712x10 ⁻³	-.383796x10 ⁻³	-.470485x10 ⁻³
A PM2	.356703x10 ⁻⁷	.111958x10 ⁻⁶	.704986x10 ⁻⁶	.536055x10 ⁻⁷	-.912361x10 ⁻⁷	.25489x10 ⁻⁶
A PM3	-.137756x10 ⁻⁸	-.216285x10 ⁻⁹	-.328566x10 ⁻⁷	.532226x10 ⁻⁹	-.27077x10 ⁻⁹	-.640161x10 ⁻⁸
A PM4	.401368x10 ⁻⁴	.225413x10 ⁻⁴	.778302x10 ⁻³	-.483831x10 ⁻³	-.497667x10 ⁻³	-.321648x10 ⁻³
A PM5	-.240092x10 ⁻²	-.399324x10 ⁻²	-.641948x10 ⁻²	-.70195x10 ⁻²	-.100188x10 ⁻¹	-.687551x10 ⁻²
A PM6	-.120839x10 ⁻⁴	-.665199x10 ⁻⁴	-.128724x10 ⁻³	-.119008x10 ⁻³	-.416504x10 ⁻⁴	-.344122x10 ⁻³
A PM7	.387065x10 ⁻⁶	.204615x10 ⁻⁵	.638786x10 ⁻⁵	.396756x10 ⁻⁵	.168316x10 ⁻⁵	.12192x10 ⁻⁴
A PM8	-.227747x10 ⁻²	.261322x10 ⁻¹	-.424198x10 ⁻¹	.428319x10 ⁻¹	.392666x10 ⁻¹	.256492x10 ⁻¹
A PM9	-.751961x10 ⁻¹	-.183726x10 ⁰	.359543x10 ⁻¹	.143102x10 ⁻¹	.949637x10 ⁻¹	-.135728x10 ⁰
A PM10	.10527x10 ⁻²	.210223x10 ⁻¹	-.33401x10 ⁻³	.856042x10 ⁻²	.12569x10 ⁻¹	.336543x10 ⁻¹
A PM11	-.393332x10 ⁻⁴	-.726143x10 ⁻³	-.78287x10 ⁻⁴	-.33099x10 ⁻³	-.435573x10 ⁻³	-.115452x10 ⁻²

NOTE: α must be in degrees when these coefficients are used in the pitching moment equation.

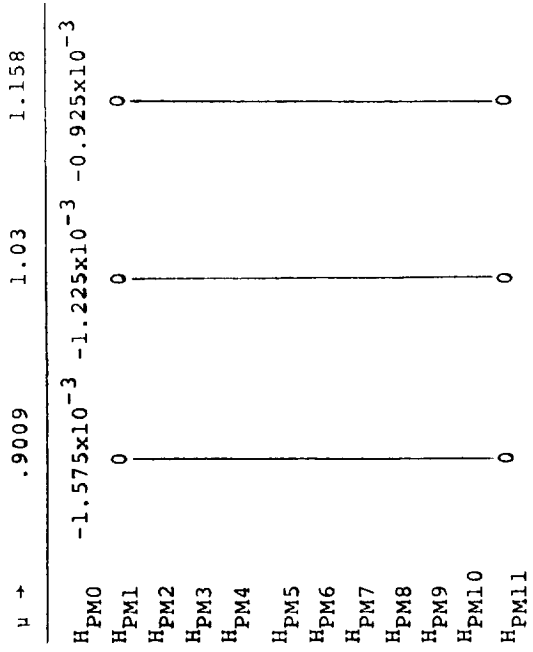
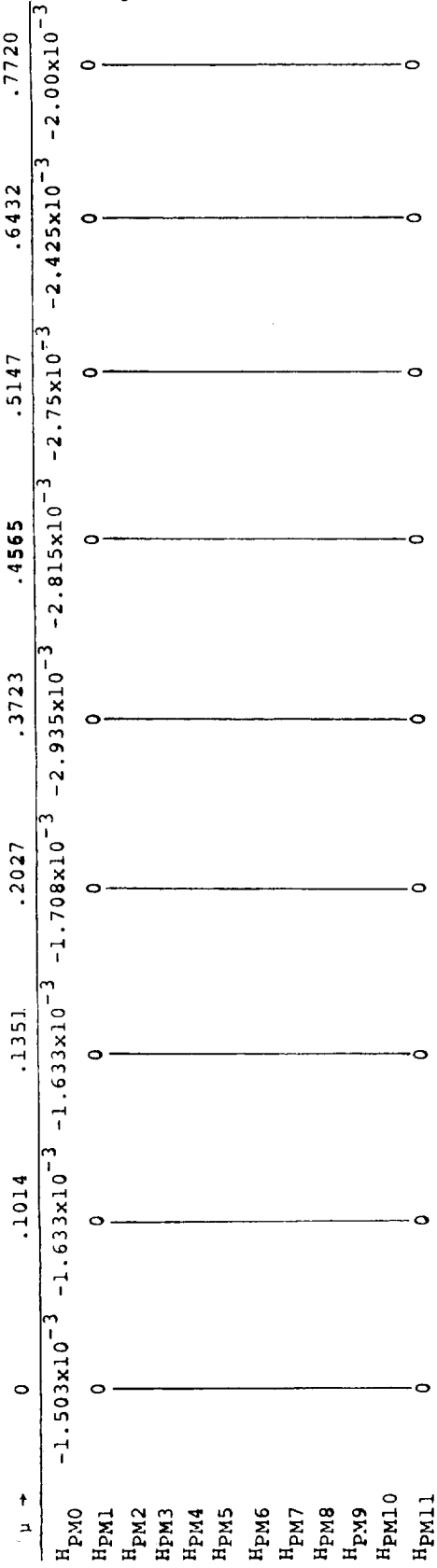
Figure F.23. Coefficients of Curve Fit Equations for Pitching Moment Coefficient

	$\mu = 1.014$	$\mu = 1.351$	$\mu = .2027$	$\mu = .3723$	$\mu = .4565$
A _{YM0}	.109092x10 ⁻⁵	.286933x10 ⁻⁷	-.110543x10 ⁻⁴	-.115949x10 ⁻⁴	.75428x10 ⁻⁶
A _{YM1}	.126647x10 ⁻⁴	.191392x10 ⁻⁴	.250948x10 ⁻⁴	.442163x10 ⁻⁴	.199993x10 ⁻³
A _{YM2}	-.148631x10 ⁻⁶	-.229016x10 ⁻⁶	-.220845x10 ⁻⁶	.979871x10 ⁻⁶	.672974x10 ⁻⁶
A _{YM3}	.435436x10 ⁻⁹	.68199x10 ⁻⁹	.154233x10 ⁻⁹	-.231738x10 ⁻⁷	-.198906x10 ⁻⁷
A _{YM4}	.216295x10 ⁻³	.61904x10 ⁻³	.303865x10 ⁻⁴	.76278x10 ⁻³	-.989016x10 ⁻⁴
A _{YM5}	.636091x10 ⁻⁴	.533431x10 ⁻⁴	.880677x10 ⁻³	.600766x10 ⁻²	.890334x10 ⁻²
A _{YM6}	.290233x10 ⁻⁵	.265736x10 ⁻⁵	-.16908x10 ⁻⁴	-.24055x10 ⁻³	.101251x10 ⁻⁴
A _{YM7}	-.182158x10 ⁻⁷	-.164399x10 ⁻⁷	.10332x10 ⁻⁶	.289645x10 ⁻⁵	-.239883x10 ⁻⁶
A _{YM8}	-.158447x10 ⁻¹	-.2112x10 ⁻¹	-.171322x10 ⁻¹	-.27995x10 ⁻¹	.646468x10 ⁻²
A _{YM9}	.147256x10 ⁻²	.323912x10 ⁻³	-.426356x10 ⁻²	.116529x10 ⁻¹	.486429x10 ⁻¹
A _{YM10}	-.178633x10 ⁻⁴	-.158877x10 ⁻⁵	.873694x10 ⁻⁴	-.78607x10 ⁻³	-.277348x10 ⁻²
A _{YM11}	.579483x10 ⁻⁷	.374405x10 ⁻⁸	-.533888x10 ⁻⁶	.133698x10 ⁻⁴	.407947x10 ⁻⁴

	$\mu = .5147$	$\mu = .6432$	$\mu = .772$	$\mu = .9008$	$\mu = 1.03$	$\mu = 1.158$
A _{YM0}	.811278x10 ⁻⁶	-.689819x10 ⁻⁶	-.140611x10 ⁻⁵	-.959155x10 ⁻⁶	.232776x10 ⁻⁵	.776742x10 ⁻⁶
A _{YM1}	.2549x10	.358353x10 ⁻³	.40651x10 ⁻³	.423457x10 ⁻³	.404494x10 ⁻³	.400109x10 ⁻³
A _{YM2}	.298133x10 ⁻⁶	-.483638x10 ⁻⁶	.711836x10 ⁻⁶	.366298x10 ⁻⁶	-.978679x10 ⁻⁶	.483519x10 ⁻⁶
A _{YM3}	-.7069x10 ⁻⁸	.165027x10 ⁻⁷	-.242848x10 ⁻⁷	-.201739x10 ⁻⁷	.384779x10 ⁻⁷	-.178582x10 ⁻⁷
A _{YM4}	-.138358x10 ⁻³	-.376316x10 ⁻³	-.111605x10 ⁻³	-.498142x10 ⁻³	-.859507x10 ⁻³	-.170495x10 ⁻³
A _{YM5}	.84517x10 ⁻²	.731418x10 ⁻²	.111654x10 ⁻¹	.700776x10 ⁻²	.495335x10 ⁻²	.937562x10 ⁻³
A _{YM6}	.511468x10 ⁻⁴	.25651x10 ⁻³	-.397326x10 ⁻³	-.179799x10 ⁻³	.475445x10 ⁻³	.428652x10 ⁻³
A _{YM7}	-.113402x10 ⁻⁵	-.882347x10 ⁻⁵	.127859x10 ⁻⁴	.100219x10 ⁻⁴	-.172489x10 ⁻⁴	-.224772x10 ⁻⁴
A _{YM8}	.135303x10 ⁻³	.322547x10 ⁻¹	.931734x10 ⁻²	.392748x10 ⁻¹	.62677x10 ⁻¹	.242592x10 ⁰
A _{YM9}	.664771x10 ⁻¹	.729796x10 ⁻¹	-.283071x10 ⁰	-.697861x10 ⁻¹	.101986x10 ⁰	.629868x10 ⁰
A _{YM10}	-.647118x10 ⁻²	-.170565x10 ⁻¹	.292923x10 ⁻¹	.166632x10 ⁻¹	-.284635x10 ⁻¹	-.600989x10 ⁻¹
A _{YM11}	.140141x10 ⁻³	.575827x10 ⁻³	-.960904x10 ⁻³	-.821801x10 ⁻³	.101423x10 ⁻²	.245749x10 ⁻²

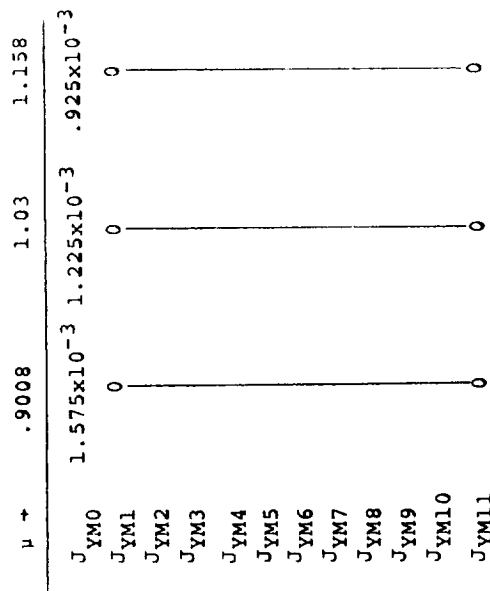
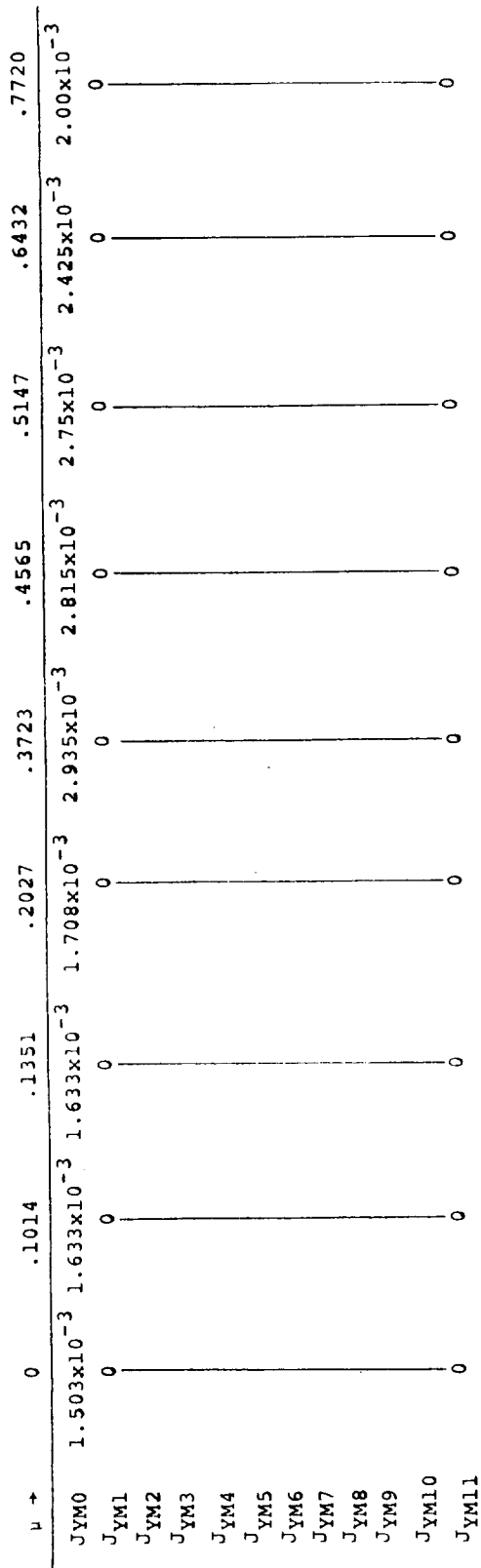
NOTE: β must be in degrees when these coefficients are used in the yawing moment equation.

Figure F.24. Coefficients of Curve Fit Equations for Yawing Moment Coefficient



NOTE: α must be in degrees when these coefficients are used in the pitching moment rate equation.

Figure F.25. Curve Fit Coefficients for αC_{PM}



NOTE: α must be in degrees when these equations are used in the hub yawing moment rate equation.

Figure F.26. Curve Fit Coefficients for αC_{YM}
 αR

$$\left. \begin{array}{l} \text{ENF}_1 = -.024 \\ \text{ENF}_2 = -.002703 \\ \text{ENF}_3 = -.000346 \\ \text{ENF}_4 = .00039 \end{array} \right\} \text{Coeff. of } \frac{dC_{NF}}{dB_{1C}} \sim \frac{1}{DEG}$$

$$\left. \begin{array}{l} D_{NF} = .006 \\ D_{NF1} = -.0012318 \\ D_{NF2} = .000033 \\ D_{NF3} = -.0000268 \end{array} \right\} \text{Coeff. of } \frac{dC_{NF}}{dA_{1C}} \sim \frac{1}{DEG}$$

$$\left. \begin{array}{l} \text{ESF}_1 = .0025 \\ \text{ESF}_2 = .0011896 \\ \text{ESF}_3 = -.00001246 \\ \text{ESF}_4 = .00001669 \end{array} \right\} \text{Coeff. of } \frac{dC_{SF}}{dB_{1C}} \sim \frac{1}{DEG}$$

$$\left. \begin{array}{l} D_{SF} = .025 \\ D_{SF1} = .0025356 \\ D_{SF2} = -.0002264 \\ D_{SF3} = -.000044 \end{array} \right\} \text{Coeff. of } \frac{dC_{SF}}{dA_{1C}} \sim \frac{1}{DEG}$$

$$\left. \begin{array}{l} \text{EPM}_1 = -.0025 \\ \text{EPM}_2 = -.0014304 \\ \text{EPM}_3 = .0003029 \\ \text{EPM}_4 = -.0002938 \\ \text{EPM}_5 = -.0001367 \\ \text{EPM}_6 = -.0004888 \\ \text{EPM}_7 = -.0001767 \end{array} \right\} \text{Coeff. of } \frac{dC_{PM}}{dB_{1C}} \sim \frac{1}{DEG}$$

$$\left. \begin{array}{l} D_{PM}_1 = -.0015 \\ D_{PM}_2 = .0010726 \\ D_{PM}_3 = -.0001564 \\ D_{PM}_4 = .0001762 \\ D_{PM}_5 = +.0000966 \\ D_{PM}_6 = .000571 \\ D_{PM}_7 = .0000422 \end{array} \right\} \text{Coeff. of } \frac{dC_{PM}}{dA_{1C}} \sim \frac{1}{DEG}$$

$$\left. \begin{array}{l} \text{EYM}_1 = .0025 \\ \text{EYM}_2 = -.0013888 \\ \text{EYM}_3 = .000336 \\ \text{EYM}_4 = -.000187 \\ \text{EYM}_5 = -.0000723 \\ \text{EYM}_6 = -.0006354 \\ \text{EYM}_7 = -.0000098 \end{array} \right\} \text{Coeff of } \frac{dC_{YM}}{dB_{1C}} \sim \frac{1}{DEG}$$

$$\left. \begin{array}{l} D_{YM}_1 = -.0025 \\ D_{YM}_2 = -.0009883 \\ D_{YM}_3 = .000089 \\ D_{YM}_4 = -.0002866 \\ D_{YM}_5 = -.0001503 \\ D_{YM}_6 = -.0004564 \\ D_{YM}_7 = -.0001993 \end{array} \right\} \text{Coeff of } \frac{dC_{YM}}{dA_{1C}} \sim \frac{1}{DEG}$$

Figure F.27. Constants for Cyclic Pitch Effectiveness in Rotor Equations

F.4 AIRFRAME AERODYNAMIC INPUT DATA

The input data for the airframe aerodynamic data are given in this section and are referenced by page number to the equations presented in Appendix E. Plotted aerodynamic data are presented in Figures F.28 to F.30 .

F.4.1 Input Data

<u>PAGE</u>		<u>PAGE</u>	
E.21	$C_{L_{\alpha w}} = 3.94 \text{ 1/rad}$	E.43	$\eta_{HT} = 1.0$
E.28	$C_{L_{MAX}} = 1.232$		$\eta_{VT} = 1.0$
E.31	$K_{20} = -.0975/\text{RAD}$ $K_{21} = -.0916/\text{RAD}$ $K_{22} = .015$ $K_{\alpha} = 1.0$ $K_{\eta} = 1.0$	E.44	$\alpha_N \leq .5236\text{RAD}/>.5236\text{RAD}$ $C_{DON} = .001821/- .016179$ $K_{30} = .04773/- .2034$ $K_{31} = .16086/- .071138$ $K_{32} = .1087$
E.32	$f_{eu} = 60 \text{ ft}^2$ $D/T = .05$ $K_{D1}/T = 0.0$ $K_{D2}/T = 0.0$ $K_{D3}/T = .05$ $K_{D4}/T = .05$ $K_{M1}/T = 0.0$ $K_{M2}/T = 0.0$ $K_{M3}/T = 0.0$ $K_{M4}/T = 0.0$		$C_{MON} = 0$ $K_{34} = 0$ $K_{35} = 0$ $K_{36} = -.1087$ $K_{37} = 0$ $K_{36} = -.1087$ $K_{37} = 0$ $C_{NON} = 0$ $K_{38} = 0$ $K_{39} = 0$ $K_{40} = 0$ $K_{41} = 0$
E.36	$\tau_{HT} = .52$ $\alpha_{HT\text{STALL}} = 16 \text{ DEG}$ $C_{L_{\alpha HT}} = .061 \text{ 1/DEG}$ $C_{D_{OHT}} = .0084202$	E.49	$C_{DOF} = .0075705$ $K_0 = 18$ $K_1 = -.03581$ $K_2 = .2561$ $\Delta C_{DLG} = .05$ $K_3 = .922/\text{RAD}$ $K_4 = 0$ $K_5 = .67709$ $K_6 = 0$ $K_7 = -.478$
E.39	$\frac{d\sigma}{d\beta} = -.025$ $\tau_{VT} = .55$ $\alpha_{VT\text{STALL}} = 20.0 \text{ DEG}$ $C_{x_{\alpha VT}} = .0546 \text{ 1/DEG}$ $C_{D_{OVT}} = .0078915$		

E.49

$$\begin{aligned}
 K_8 &= 0 \\
 K_9 &= -.131/\text{RAD} \\
 K_{10} &= 0 \\
 C_{\text{MOF}} &= .0001883 \\
 C_{\text{NOF}} &= 0 \\
 \Delta C_{\text{MLG}} &= 0 \\
 K_{42} &= .0537
 \end{aligned}$$

E.52

$$\begin{aligned}
 T_1 &= 0 \\
 T_2 &= -.04808 \\
 T_3 &= .3795
 \end{aligned}$$

E.54

$$\begin{aligned}
 \tau_1 &= .1 \\
 \tau_2 &= .1
 \end{aligned}$$

E.60

$$f_{\text{TR}} = f_{\text{NFR}} = f_{\text{SFR}} = f_{\text{PMR}} = f_{\text{YMR}} = f_{\text{QR}} = f_{\text{PR}} = 1.0$$

E.66

$$\begin{aligned}
 \frac{dC_{\text{Mwc}}/4}{dC_L} &= -.03215 \\
 C_1 &= -.065 \\
 C_2 &= -.0025 \text{ 1/DEG} \\
 C_3 &= 0.0 \text{ 1/DEG}^2 \\
 C_{L\alpha} &= 3.94/\text{RAD}
 \end{aligned}$$

Wing Aerodynamic Input Data

Coefficients of $\sum_{v=0}^4 \sum_{u=0}^4 [A_{D(u+5v)} \delta^u \alpha^v]$ (Page E.26)

A_{D0}	=	.582990	x	10^{-3}
A_{D1}	=	.126170	x	10^{-2}
A_{D2}	=	.391649	x	10^{-4}
A_{D3}	=	.110058	x	10^{-5}
A_{D4}	=	-.159415	x	10^{-7}
A_{D5}	=	.245484	x	10^{-3}
A_{D6}	=	.265950	x	10^{-3}
A_{D7}	=	.404673	x	10^{-5}
A_{D8}	=	-.152693	x	10^{-6}
A_{D9}	=	.102320	x	10^{-8}
A_{D10}	=	-.313543	x	10^{-5}
A_{D11}	=	.624554	x	10^{-6}
A_{D12}	=	.141804	x	10^{-6}
A_{D13}	=	-.821732	x	10^{-8}
A_{D14}	=	.119984	x	10^{-9}
A_{D15}	=	-.474069	x	10^{-5}
A_{D16}	=	.771740	x	10^{-6}
A_{D17}	=	-.800800	x	10^{-7}
A_{D18}	=	.208761	x	10^{-8}
A_{D19}	=	-.114899	x	10^{-10}
A_{D20}	=	.238184	x	10^{-6}
A_{D21}	=	.196213	x	10^{-7}
A_{D22}	=	-.204613	x	10^{-8}
A_{D23}	=	.133330	x	10^{-10}
A_{D24}	=	.492127	x	10^{-13}

NOTES: δ , α in degrees.

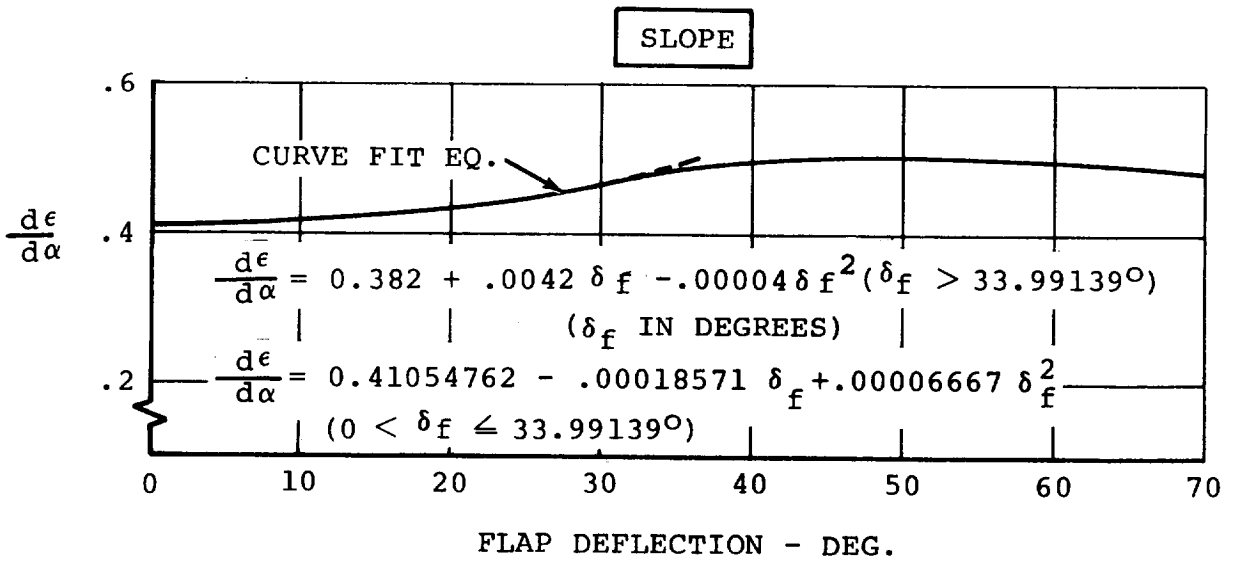
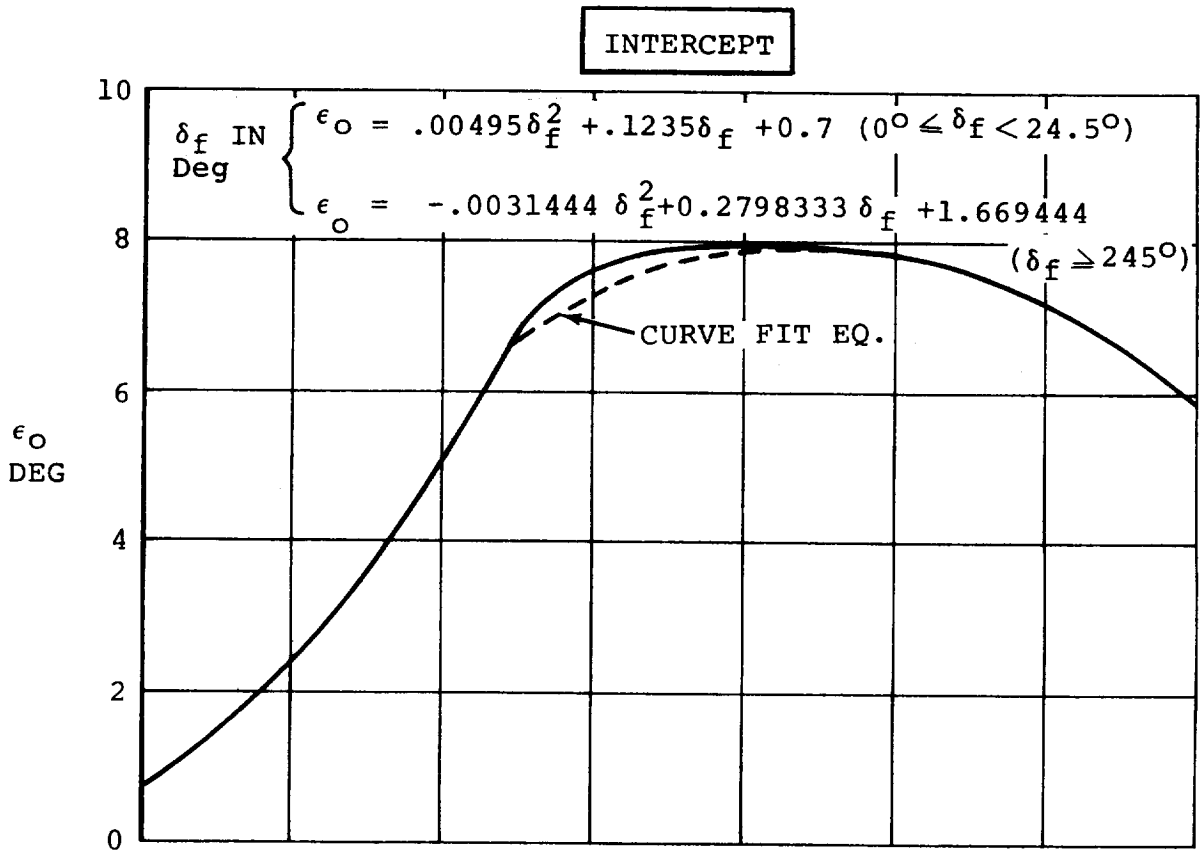


Figure F.28. Model 222 Downwash Functions @ $C_T = 0, i_w = +2.0^\circ$

REF: APPENDIX B-7 ETKIN

$$\left. \begin{array}{l} \text{FOR TAIL;} \\ \frac{ag}{a} = 1.2103 - .038 h_T + .00184h_T^2; h_T \leq 6.3219 \\ \frac{ag}{a} = 1.1096 - .01284 h_T + .00038h_T^2; h_T > 6.3219 \\ \frac{ag}{a} = 1.00; h_{TC/4} \geq 17.' \end{array} \right\}$$

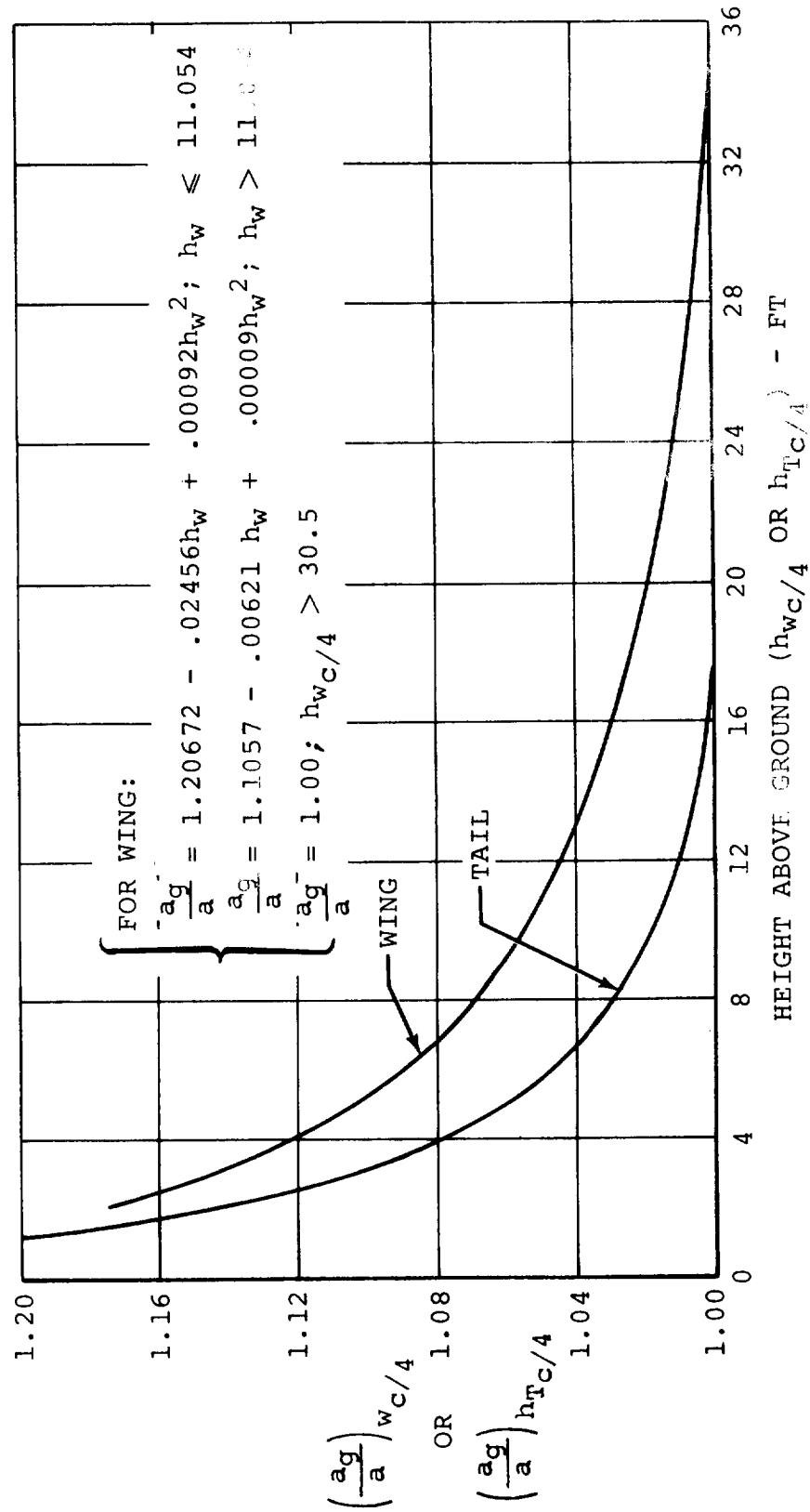
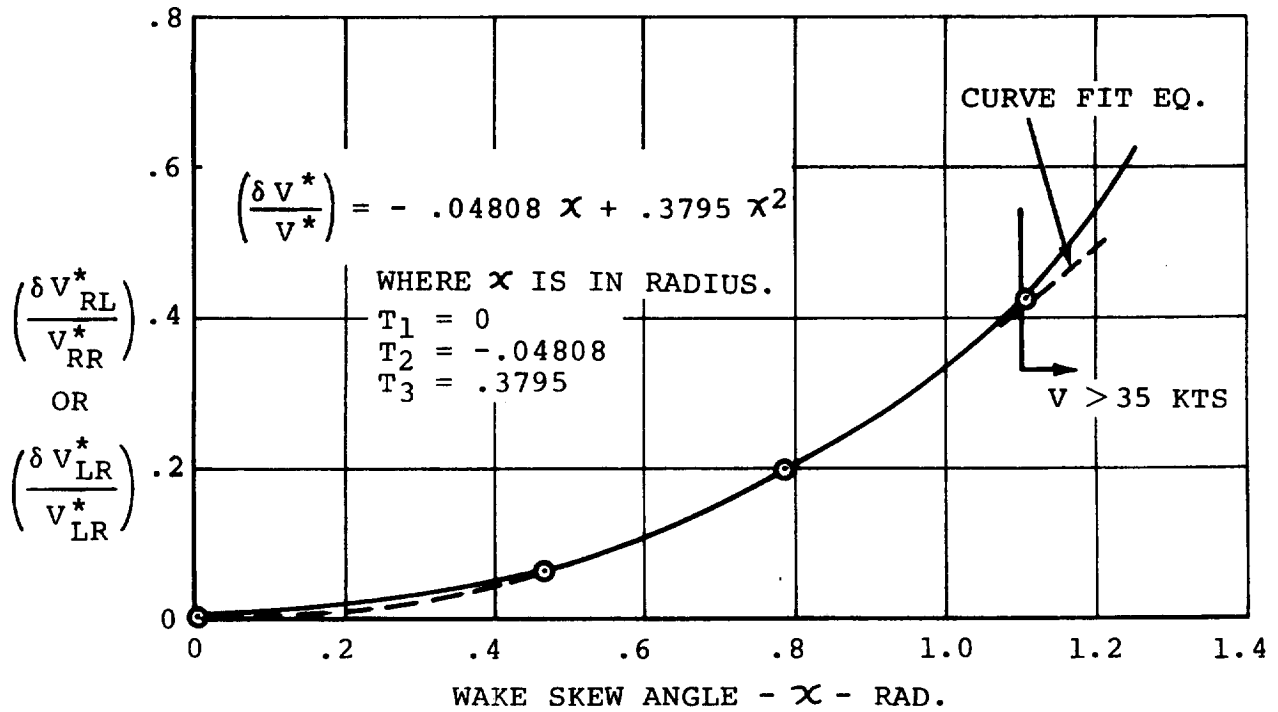
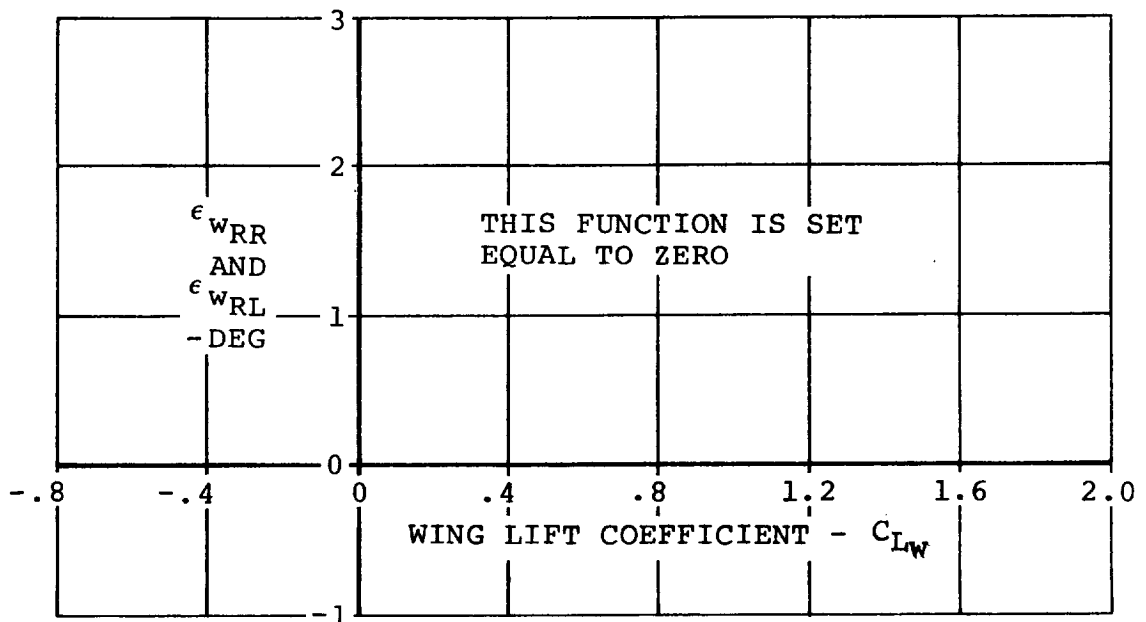


Figure F.29. Variation of Lift Curve Slope with Ground Height



ESTIMATED ROTOR/ROTOR INTERFERENCE PARAMETER



WING ON ROTOR INTERFERENCE

Figure F.30. Rotor/Rotor and Wing/Rotor Interference

F.5 GEOMETRIC, WEIGHTS AND BALANCE DATA

The input data for the Model 222 geometry, weights and balance are presented in this section, and are referenced in Appendix E. Input data for the preprocessor calculations are not presented, but are easily obtainable from an aircraft three-view drawing and the weights and balance data presented in this section. It should be emphasized that the lengths and inertias presented here were calculated using the preprocessor.

F.5.1 Input Data

<u>Page</u>		<u>Page</u>	
E.16	$X_{WAC} = .84 \text{ ft}$	E.23,E.17	$i_w = 2 \text{ DEG}$
	$Y_{WAC} = 8.333 \text{ ft}$	E.31	$b_w = 33.417 \text{ ft}$
	$Z_{WAC} = .4 \text{ ft}$		$\bar{Y} = 6.92 \text{ ft}$
	$L_S = 4.94 \text{ ft}$	E.32	$X_{C/2} = -.25 \text{ ft}$
	$Y_N = 16.666 \text{ ft}$	E.35	$i_{HT} = 0.0$
E.18	$X_{HT} = -19.45 \text{ ft}$	E.36	$AR_{HT} = 4.255$
	$Z_{HT} = 2.51 \text{ ft}$	E.39	$AR_{VT} = 1.768$
	$X_{VT} = -18.04 \text{ ft}$		$S_{HT} = 58.3 \text{ ft}^2$
	$Z_{VT} = -1.0226 \text{ ft}$		$S_{VT} = 43.3 \text{ ft}^2$
E.19	$A = 530929 \text{ ft}^2$	E.46	$Z_{G_1} = 7.08 \text{ ft}$
	$R = \text{ft}$		$Z_{G_2} = 7.08 \text{ ft}$
E.20	$PC = 2.36 \text{ ft}, F_{IN}=0^\circ$		$Z_{G_3} = 7.53 \text{ ft}$
	$h_p = .33 \text{ ft}$		$Y_{G_1} = -3.86 \text{ ft}$
	$c_w = 5.983 \text{ ft}$		$Y_{G_2} = 3.86 \text{ ft}$
	$S_w = 200 \text{ ft}^2$		$Y_{G_3} = 0$

Page

E.46 $X_{G_1} = -3.7 \text{ ft}$
 $X_{G_2} = -3.7 \text{ ft}$
 $X_{G_3} = 10.67$
 $r_1 = 1.065 \text{ ft}$
 $r_2 = 1.065 \text{ ft}$
 $r_3 = .60 \text{ ft}$
 $K_{ST_1} = 3840 \text{ lb/ft}$
 $K_{ST_2} = 3840 \text{ lb/ft}$
 $K_{ST_3} = 3840 \text{ lb/ft}$
 $D_{ST_1} = 600 \text{ lb/ft/sec}$
 $D_{ST_2} = 600 \text{ lb/ft/sec}$
 $D_{ST_3} = 600 \text{ lb/ft/sec}$
 $\mu_0 = .03$
 $\mu_1 = .005$
 $\mu_s = .5$
E.50 $X_{FAC} = .84 \text{ ft}$
 $Z_{FAC} = 3.66 \text{ ft}$
E.61 $I_P = 564 \text{ slu-ft}^2$
E.62 $I_E = 1.47 \text{ slug-ft}^2$
E.64 $K_{W_1} = .59678 \times 10^{-4}$
 $K_{W_2} = .1637 \times 10^{-4}$
 $K_{W_3} = .58356 \times 10^{-5}$
 $K_{W_4} = .2959 \times 10^{-2}$
 $K_{W_5} = .1656 \times 10^{-2}$

Page

E.64 $\zeta_{W_1} = .5$
 $\zeta_{W_2} = .5$
 $\zeta_{W_3} = .5$
 $\zeta_{W_4} = .5$
 $\zeta_{W_5} = .5$
 $K_{W_6} = .1709 \times 10^{-4}$
 $K_{W_7} = .05768 \times 10^{-4}$
 $K_{W_8} = .1221 \times 10^{-5}$
 $K_{W_9} = .0847 \times 10^{-2}$
 $K_{W_{10}} = .0559 \times 10^{-2}$
 $\omega_{W1} = 19.92 \text{ rad/sec}$
 $\omega_{W2} = 19.92 \text{ rad/sec}$
 $\omega_{W3} = 19.92 \text{ rad/sec}$
 $\omega_{W4} = 19.92 \text{ rad/sec}$
E.66 $K_{\theta t} = 0.98 \times 10^6 \text{ FT-LB/RAD}$
 $\frac{X_{WAC}}{C_w} = .275$
E.79 $Y_{PA} = 0$
 $l_{PA} = 6.75 \text{ ft}$
 $Z_{PA} = 4.75 \text{ ft}$

E.68 to
E.78

Equations of motion input constant (Weight = 12321 lb,
nominal CG)

$$m_W = 138.32 \text{ slugs}$$

$$m_N = 43.39 \text{ slugs}$$

$$m_f = 157.88$$

$$m = 382.98 \text{ (12321 LBS)}$$

$$I_{xx}^{(f)} = 789.3 \text{ slug-ft}^2$$

$$I_{yy}^{(f)} = 10845.6 \text{ slug-ft}^2$$

$$I_{zz}^{(f)} = 10707.4 \text{ slug-ft}^2$$

$$I_{xz}^{(f)} = 399.9 \text{ slug-ft}^2$$

$$I_{xx}^{(w)} = 23978.4 \text{ slug-ft}^2$$

$$I_{yy}^{(w)} = 664.8 \text{ slug-ft}^2$$

$$I_{zz}^{(w)} = 24513.6 \text{ slug-ft}^2$$

$$I_{xz}^{(w)} = 384.5 \text{ slug-ft}^2$$

$$I_{xx}' = 22.5 \text{ slug-ft}^2$$

$$I_{yy}' = 194.0 \text{ slug-ft}^2$$

$$I_{zz}' = 195.4 \text{ slug-ft}^2$$

$$I_{xz}' = -20.0 \text{ slug-ft}^2$$

$$l_f = .6917 \text{ ft}$$

$$h_f = 4.075 \text{ ft}$$

$$l_w = -.775 \text{ ft}$$

$$h_w = .30417$$

$$Y_N = 16.666 \text{ ft}$$

$$l = 3.3624 \text{ ft}$$

$$\lambda = 2.841 \text{ DEG}$$

$$L_s = 4.94 \text{ ft}$$

F.6 SIMULATION INPUT DATA

This section presents the input data required to drive the Flight Simulator for Advanced Aircraft (FSAA). Figure F.31 shows the instrumentation requirements and Figure F.32 shows the Model 222 control force gradients and breakout forces.

CAB INSTRUMENTATION:

<u>Instrument</u>	<u>Range</u>
Vertical Situation Indicator	+90° Pitch and Roll
Horizontal Situation Indicator	+120° Heading
Airspeed	0 → 520 KIAS
Pressure Altimeter	0 → 10,000 Ft
Radar Altimeter	0 → 1000 Ft
Rate of Climb	+ 6000 FT/MIN
Turn and Bank	+ 3 Needle Widths
"g" Meter	+ 1 1/2 Ball Widths
Nacelle Angle	-1, +3 "g"
Clock	0 → 120°
Sideward Velocity	+ 40 Knots
Angle of Attack	+ 20°
Wing Flap Position	0 → 100°
Rotor Speed	0 → 125%
Engine Torque Meters (2)	0 → 125%

PRIMARY FLIGHT CONTROLS

Stick (+6° Long.; +5" Lateral)
Pedals (+2.5")
Power Lever (0→8" Normal; 0→10" Emergency)
Nacelle Position thumb Switch

MISCELLANEOUS EQUIPMENT AND FEATURES

Back Drives to Trim Stick and Pedals while in Initial Condition (I.C.)
Landing Gear Up - Down Switch with Indicator Light
SAS ON-OFF Switch
Detent Switches on Spring Cartridges (Pedals & Lateral Stick)
Magnetic Brake on Pedals, Long. and Lateral Controls
Long. and Lateral Beep Force Trim on Stick
Power Lever Null Meter
Toe Brakes
Specified Force Feel System

Figure F.31. Model 222 Pilot Station Requirements

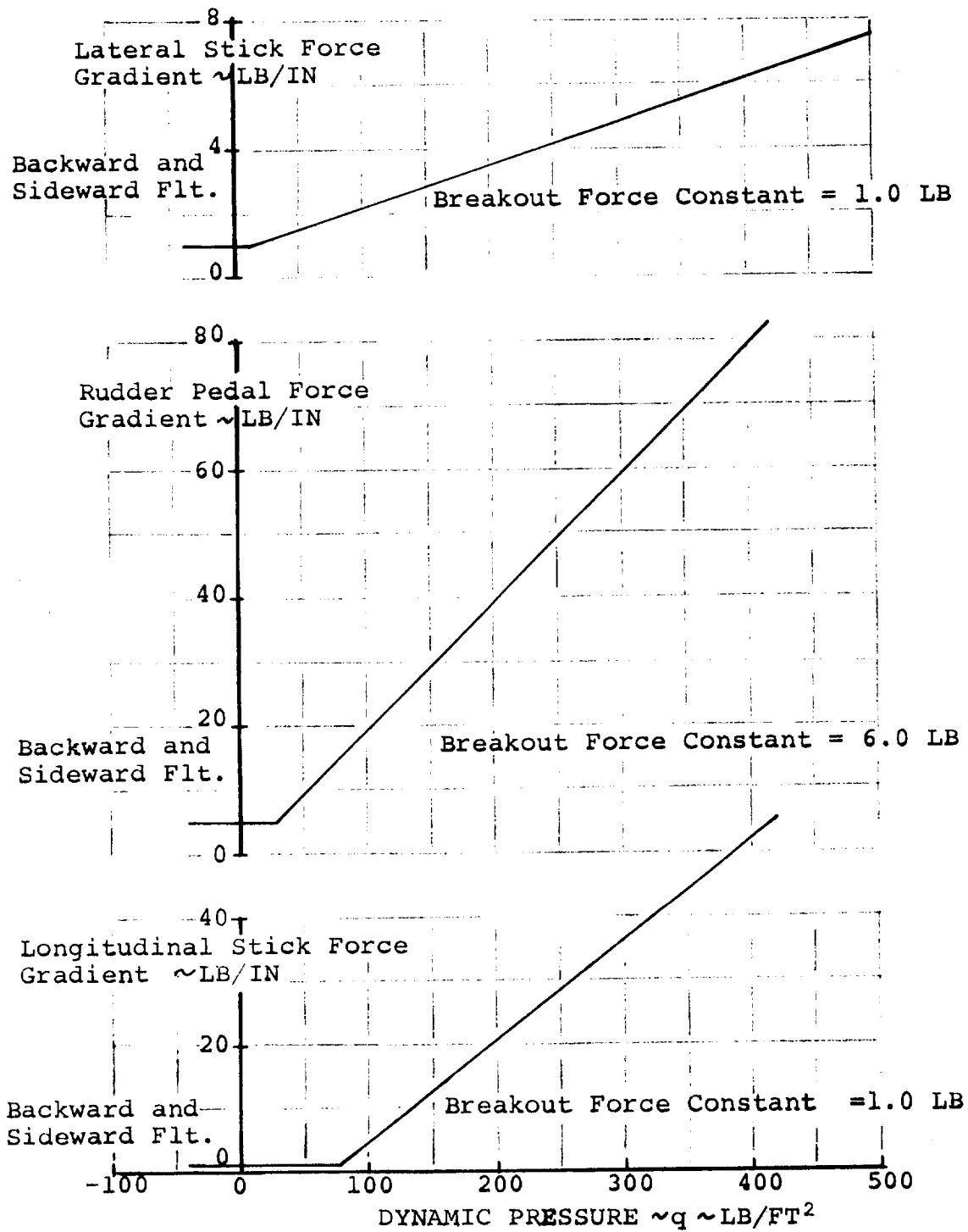


Figure F.32. Model 222 Control Force Gradients and Breakout Forces

APPENDIX G - IN-HOUSE HYBRID SIMULATION

The math model described in this report was mechanized in the Boeing Hybrid Simulation Laboratory for the purpose of developing and evaluating math model simplifications. This was accomplished in a parallel time frame to the NASA simulation, which also used the described math model.

The Hybrid Simulation Laboratory is a large scale hybrid computation complex. It is capable of providing simultaneous operation of several hybrid and analog simulations, depending on problem size. The complex is totally state of the art, with recent acquisition of two mini-computers for the purpose of multivariable function generation.

The Hybrid Simulation Laboratory complex is comprised of the following elements:

- Digital

- IBM 360/44 system

- 25600 byte core

- 32 priority interrupts

- 16 hi-speed floating point register

- 2 hi-speed, 1 low speed channels

- 2 - 800 B.P.I. tape transport

- 1 - 2311 disk system

- 2 - 2315 disk system

- 1 - hi-speed card read/punch

- 1 - hi-speed line printer

2 - alpha-meric scope/keyboard

1 - console typewriter

1 - ball printer

Basic Computer Arts Function Generation System (BOA)

1 - Interdata processor with 24000 byte core

1 - Interdata processor with 16000 byte core

2 - 16 channels analog to digital

2 - 16 channels digital to analog

2 - read only memory software systems

● Analog

4 - 3/4 expanded Applied Dynamics (AD-4)

771 amplifiers (all solid state)

4 resolver expansions

2 display consoles

10 ufd integrator system in 6 decades

1 - 1/8 expanded AD4 maintenance console

128 channels 100 KC analog to digital converters

128 channels digital to analog converters

1 applied dynamics 256

● Analog Output

4 - 8 channel Brush strip chart recorders

4 - 8 channel Varian Statos III strip chart recorders

4 - XY plotters

- Software System

Integrated disk resident state of the art system embracing

"real time" languages:

Assembly Language

Modified Fortran IV, Level G
and non-real time languages

Non-procedural block modeling, DSL/44

Fortran IV, Level G

Full utility system

Other special hybrid oriented programs

G.1 SIMULATION ARCHITECTURE

The tilt rotor simulation model utilized the entire hybrid facility. When tied to Boeing's Nudge Base Simulator, four consoles of Applied Dynamics from (AD-4's) analog, the Applied Dynamics 256 (AD-256) and two Simulator Laboratory analog computers were in use. In addition the IBM 360/44 digital computer and two Basic Computing Acts (BCA) function generators were utilized. Figure G.1 shows the utilization of the hybrid facility and also shows the location of the major elements of the tilt rotor mathematical model.

In programming the digital portion of the tilt rotor simulation, core size and execution time were of immediate concern. Along with the complex wing and rotor representations, there was a large number of functions which had to be handled in the digital computer with trade-offs considered on core used if functions were programmed as tables and execution time for digital table

look-up versus curve-fit equations. In most cases, curve-fit equations were used to program functions. A program was written to curve fit the various functions needed, and the equation programmed for the real time task.

The single largest difficulty was the rotor representation. To program the curve-fit equations for each of the eight functions, for both rotors, would take 30 milliseconds (timing estimates without rotor indicated only 10 milliseconds were available). To program as tables and look-up answers, would not only take too long, but use too much core. So the rotor data was put in the function generation mini-computers (BCA). To get the rotor data into format for the BCA, several steps had to be executed; 1) data points were input to the curve-fit program which punched out the coefficients of the curve-fit expansion, 2) these coefficients were input to a program that punched data in the correct format at the correct breakpoints to be input to 3) the BCA program which punched a deck of cards that are input to the function generator mini-computer.

Although the BCA enabled the programming of the rotor without using digital time or core, it did not have enough room to hold 8 functions x 2 rotors for the rotor 'maps' of the size required. To obviate this, the BCA was multiplexed, such that only one rotor's results would be calculated each BCA cycle, with the left and right rotor being alternated. In this case it took 8 milliseconds per BCA cycle, resulting in a total rotor update every 16 milliseconds.

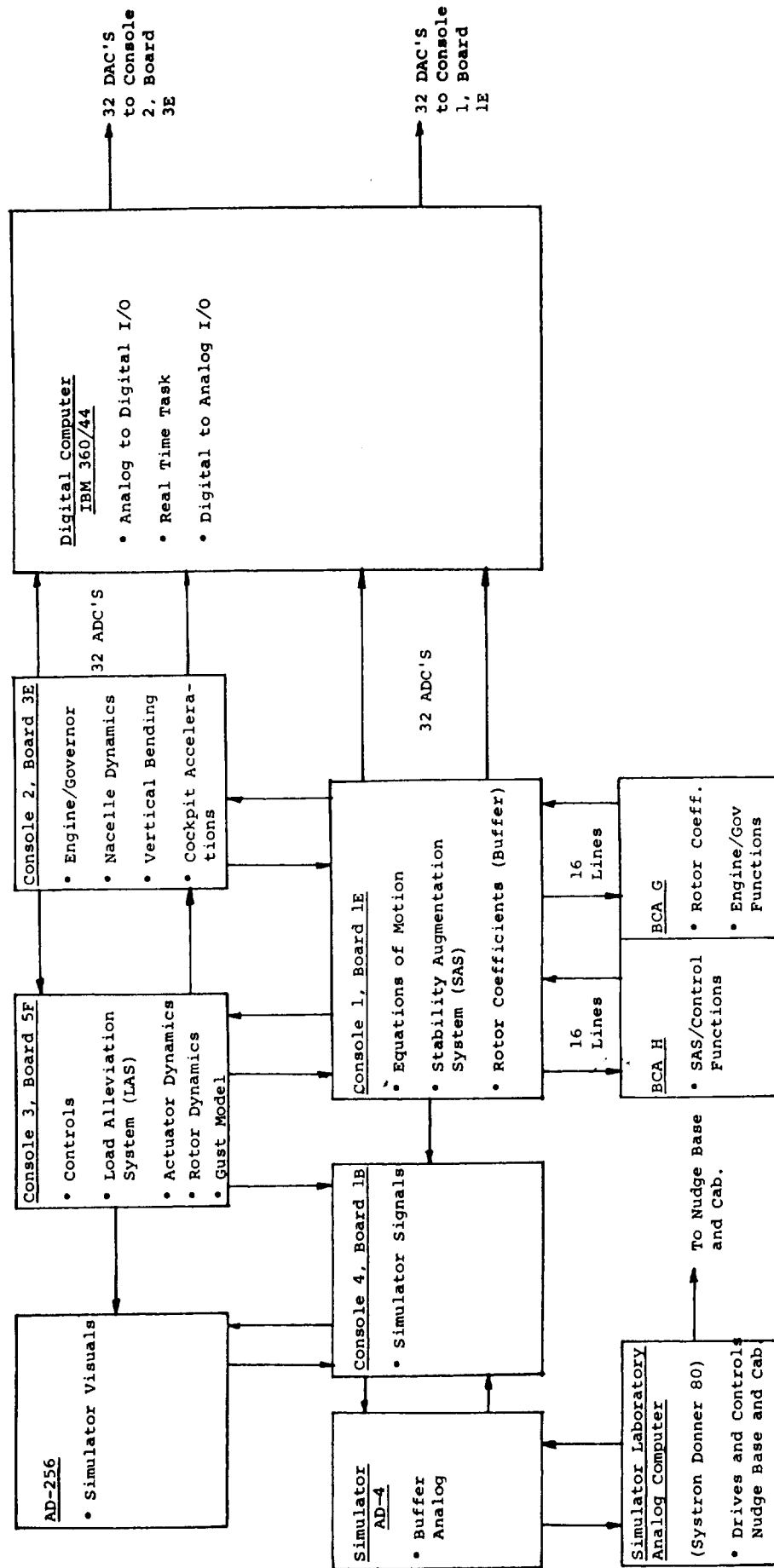


Figure G.1. Utilization of the Hybrid Laboratory for the Model 222 Math Model

As programming progressed, timing estimates showed the time frame would be a problem. The objective was a 40. millisecond (ms) time frame which results in 7 updates/cycle for the 3.5 cycle per second first mode vertical bending calculations. Due to the large number of angles and trigonometric functions, the complexity of the model and the real time requirement, every effort was made to reduce the time frame.

A parallel real time task method, where a 40 ms. time frame could be achieved, was selected. This method had two real time tasks, a 'Fast' real time task that was calculated every frame and a 'Slow' real time task that was executed every 3 frames. Thus, it was important to separate the equations to ensure only low frequency equations were placed in the slow loop. In order to minimize execution time, the system routines for taking the sine, cosine and square root, having unnecessary accuracy at the expense of time, were discarded and replaced by streamlined routines. Since there are a total of 21 sine-cosine pairs and 20 square-roots, the saving was substantial. The need for the time savings is emphasized by the fact that at present, using the parallel real time task, the total execution time is 38 ms. leaving 2 ms. for the foreground options, shown in Figure G.2 to be executed. The 40 ms. time frame objective has been achieved.

The digital portions of the simulation were programmed using the General Hybrid Program (GHP) structure, which utilizes a

- Direct control of the analog computer state and the interval timer (initial condition, hold, operate)
- Change aircraft trim conditions (airspeed, lateral speed, altitude, rate of climb, trim pitch attitude, trim nacelle angle)
- Control of line printer real-time printout
- Control of line printer trim printout
- Ability to change values of simulation flags (landing gear on/off ground effect on/off, vertical bending on/off, wing twist on/off)
- Ability to change real time phases (dual phase, total phase, plot phase; used to plot any digital function)

Figure G.2. Foreground Options

phase overlay scheme. The basic phase overlay structure is shown in Figure G.3. This figure also summarizes what is contained in each phase. Of most interest to this discussion are three phases; 1) the Preprocess phase, 2) the Run phase and 3) the Dual phase. The Preprocess phase loads the simulation data and sets up the analog computer by setting the potentiometers to the correct values and by reading out a test condition to ensure that no components are statically bad. Once the analogs are set up and checked, control is transferred by GHP to the run phase. This phase is in control while actually 'running' hybrid and executing the real time task. It is in the run phase that various options are provided, while the simulation is being used. These foreground options have been described in Figure G.2. The two line printer options, the line printer trim sheet and the line printer real time printout, are powerful tools allowing visibility into the simulation equations.

The Dual phase contains the two real time tasks, the fast (RTFAST) and the slow (RTSLOW). Figures G.4 and G.5 show what each real time task contains. The execution time of RTFAST is 32 ms. while that of RTSLOW is 18 ms. Since RTFAST is executed every 'frame' but RTSLOW only every 3 frames, the execution time is $32 + 18/3$ or 38 ms.

The digital listing for the simulation program is shown in Figure G.6. This listing contains the fast and slow real

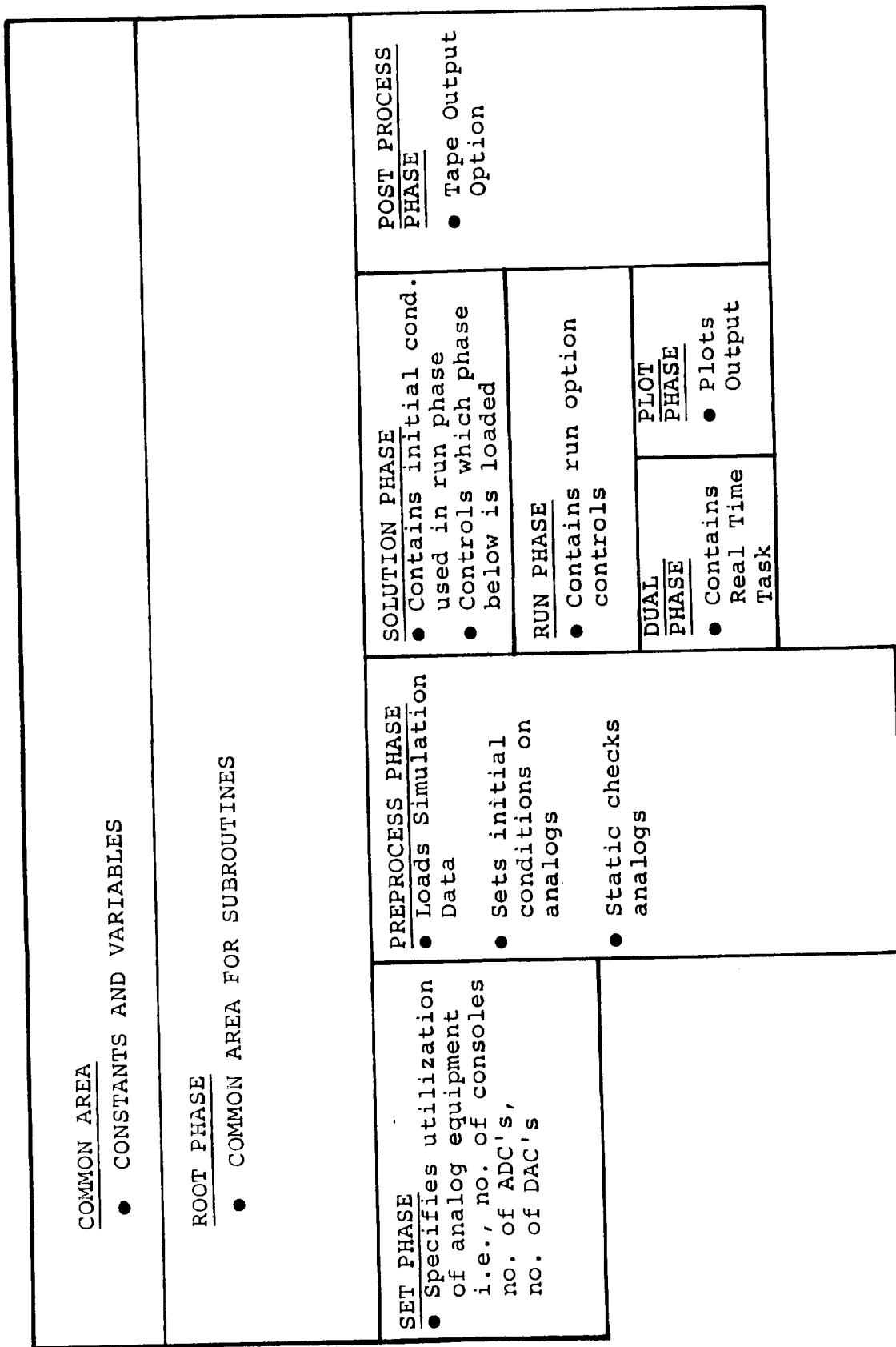


Figure G.3. GHP Phase Overlay Structure (Digital Core Allocations)

- | | |
|--|---|
| <p>1. <u>ANALOG TO DIGITAL I/O</u></p> <ul style="list-style-type: none"> ● Reads analog ADC lines ● Converts to floating point <p>2. <u>ENTRY FOR STATIC CHECK OF FAST REAL TIME TASK</u></p> <ul style="list-style-type: none"> ● Used for test cases W/O I/O <p>3. <u>ANGLE INITIALIZATION SECTION</u></p> <ul style="list-style-type: none"> ● Sin, cos i_{NL} & i_{NR} ● $i_{NACELLE}$ ● Sin, cos $i_{NL-\lambda}$, $i_{NR-\lambda}$ using trig ● δ_{FLAP}^2 <p>4. <u>VELOCITY SECTION (VELOCITIES, VELOCITIES², FREESTREAM, DYN. PRESSURE, TRANSFORM.)</u></p> <ul style="list-style-type: none"> ● Fuselage (also α_{fus}, β_{fus}, sin, cos) ● Doors open/close logic-f(i_{NAC}, α_{FUSE}) ● Rotor Hub - body axes, shaft axes, free-stream ● Wing A/C - body axes, chord axes, free-stream ● Tail <p>5. <u>ROTOR SECTION - LEFT AND RIGHT</u></p> <ul style="list-style-type: none"> ● α, ζ, sin, cos of α and ζ ● Rotor angular rate transform. p,q,R ● Ω, V_{TIP}, μ, Ω^2, μ^2 ● Rotor control axes transform A_{lc}, B_{lc} WRT ϕ_p, ζ ● Rotor EQS for CNF, CSF, CP, CYM ● Forces and moments from coefficients T, N.F., S.F., M,N,Q ● Hub moments - Nacelle axes ● Resolution of forces & moments - body axes at tip ● Summation with nacelle aero ● Gust load alleviation system <p>6. <u>WING SECTION - LEFT AND RIGHT</u></p> <ul style="list-style-type: none"> ● q_{LW}, q_{RW}, q_{WING} ● Doors open/close check ● If doors open <ul style="list-style-type: none"> ● Calc. X,Y,Z, L,M,NAERO ● Leave wing section & Set q's=0 ● If doors closed <ul style="list-style-type: none"> ● α, β, α_{SSO}, α_{RIG}, $\bar{\alpha}$ ● Aileron, Spoiler, Flap contribution to lift, drag, moment; Call AILSP ● Contribution due to totally washed wing; call CLDCM ● Contribution due to totally unwashed wing; call CLDCM ● C_L; Call CCF2 ● α, sin & $\cos \alpha$, sin & $\cos \beta$, sin & $\cos \epsilon_p$ ● α, β check for stall ● Aero Calc & resolution ● Wing/rotor interference <p>7. <u>TAIL SECTION</u></p> <ul style="list-style-type: none"> ● ϵ_{TAIL}, ϵ_0 if necessary; logic for doors open/closed ● α_{HT}, sin, cos ($\alpha_{HT} - i_{HT}$) ● 7 region C_{LHT}, C_{DHT} curve ● β_{VT}, α_{VT}, σ, sin, cos ($\beta_{VT} - \sigma$) ● 7 Region C_{LVT}, C_{DVT} curve ● If doors open; 1/2 efficiency of horizontal tail ● Vertical tail Aero ● Total tail Aero | <p>8. <u>EQUATION OF MOTION SECTION</u></p> <ul style="list-style-type: none"> ● Call gear subroutine ● Total Fuse Aero ● Calculate total aircraft Aero X_{AERO}, Y_{AERO}, Z_{AERO}, L_{AERO}, M_{AERO}, N_{AERO} ● Break Z_{AERO}, L_{AERO}, M_{AERO} into vertical bending/non-vertical bending parts ● BOM coefficients ● Vertical bending equations with flag ● Torsion equation with flag ● Fill DAC array (64) <p>9. <u>DIGITAL TO ANALOG I/O</u></p> <ul style="list-style-type: none"> ● Convert DACS to integer ● Write values |
|--|---|

1. ANALOG TO DIGITAL I/O
 - Reads discretos
 - Assigns flags to discretos
 - Check for trim sheet flag
 - Read 3rd console ADCS if required
2. ENTRY FOR STATIC CHECK OF SLOW REAL TIME TASK
 - Used for test cases w/o I/O
3. PRELIMINARY CALCULATIONS
 - $\sin^2 i_{NL}$, i_{NR} ; \sin , $\cos 2i_{NR}$, $2i_{NL}$; h^2 , q_{FUSE}
 - XCG, ZCG
 - V_{NORTH} , V_{EAST} , ground track
4. AIR & ENGINE MODEL
 - δ , $T^{\circ}F$, ρ , a , M , $\sqrt{1-M^2}$
 - TEA, preliminary engine routine calculations
 - SHP, ΩE , $\%Q$; call engine
5. FUSELAGE SECTION
 - C_{DF} , C_{LF} , C_{YF} , C_{MF} , C_{NF}
 - Aero calculation
6. GROUND EFFECT SECTION (WING & ROTOR)
 - $(a_q/a)_w$, K_{g9} , (T_{TGE}/T_{OGE}) , D/T , (M/T)
7. NACELLE SECTION LEFT & RIGHT
 - α_{NAC} , β_{NAC} ; \sin & $\cos \alpha_{NAC}$, β_{NAC}
 - C_D , C_L , C_Y , C_M , C_N nacelle
 - Aero calculation
8. WING IMMersed AREA SECTION - LEFT & RIGHT
 - τ , V^* , Look-up v^* ,
 - $\bar{\epsilon}_p$, C_{TSR}
 - $\bar{\zeta}$, $\bar{\alpha}_R$, $\bar{\epsilon}_p$, \bar{C}_{T_B} , $\sin \bar{\zeta} \cos \bar{\zeta}$, $\sin \bar{\zeta} \cos(\bar{I}_{NAC} - \bar{I}_w)$, $\tan(\bar{\alpha}_R - \bar{\epsilon}_p)$
 - ζ_{R1} , ζ_{R2} , ζ_{R3} , ζ_{R4}
 - S_{iR} , S_{iL} , S_{iL}/S , S_{iR}/S , S_{iT} , AR_L , CL_i , K_a
9. ROTOR/ROTOR INTERFERENCE
10. GROUND EFFECT - TAIL
 - $H_{wC/4}$, $H_{TC/4}$, $(a_q/a)_t$


```

300DLG ,DCMIG ,FTNPP ,GOVT ,JSD4ET,FFEH,EEFV, FIE ,FINDEG,
*EIP ,FIXPR,FIYX ,FIXZF ,FIXZR,FIKZM ,FIYF ,FIYPR,
*TIYM ,FIZF ,FIZPR,FIZM ,*P ,OMREF ,PC ,PI ,POTPAD,
*SEPR ,SRAP ,SC ,SHE ,SIm ,SKL ,SK2 ,SK3 ,
*SK4 ,SK5 ,SK6 ,SK7 ,SK8 ,SK9 ,SK10 ,SK20 ,SK21 ,
*SK22 ,CDNLG,SK310,SK311,SK32 ,CDNHI,SK34 ,SK35 ,SK36 ,
*SK37 ,SK38 ,SK39 ,SK40 ,SK41 ,SK42 ,SK43 ,SK44 ,SK45 ,
*SK46 ,SK47 ,SK48 ,SK49 ,SK50 ,SL ,SLPA ,SLW ,
*SM ,SMN ,SMW ,SPAN ,TAUHF ,TAUVT ,XFAC ,XHT ,
**MAC ,XVT ,YN ,YPA ,YMAC ,ZFAC ,ZHT ,ZPA ,ZMAC ,
*7VT ,CLOAL ,PHIPH ,SK3PHI ,ENZRF, XWC2 ,RTI ,RTZ ,RT3 ,
**KDT ,AKDZT ,AKDZT ,AKMT ,AKM2T ,AKM3T ,AKM4T ,SK31HI,
*EEI ,CLMAX ,ALR3K ,AKLSW ,BKNSH ,SQFRM, DEG20 ,DGTORD, HTVKT,
*IQV2 ,PDTQC, ROTPS, SKPS ,ALNFBK, TAURTI, TAURTZ
COMMON/DAC10/ DAC1(32) ,DAC2(32)
COMMON/XLITP/ AKEY(15) ,AME(2) ,BKEY(15) ,BME(2) ,CKEY(10) ,GME
COMMON/XFUP / VSTAR(33) ,TAIAG(9) ,SVSTA(33,9) ,SOFAR(35) ,
1 GAATAR(35) ,GPATAR(35) ,ALFTAB(35)
COMMON/XCNTR/ SKOLR ,SKOLS ,SKULR ,SKOLE ,SKOLRD, TH75LP ,TH75LN ,
TAUGLS ,GLSLM ,TAUGIC ,GICLM ,CNTRBL(4) ,DMA ,FTAA ,
2 SKDA ,GTH ,TAUTH ,OMG ,OMSLP ,OML4 ,OMG ,SKDCOL ,THRILM ,THMLP ,
3 THMLN ,SAPLM ,BTMGOV ,MRD ,FIARD ,TTNSLP ,TTMSLN ,GBRI ,G032 ,
4 TAUR3 ,GOATIG ,TAUR3 ,TAJ02 ,TAJ02 ,TAJ02 ,GLP ,GLP ,GLP ,GLP ,GLP ,
5 GP ,TAUP ,BEFP ,TAUHF ,GP41 ,TAJPHI ,GPSIDR ,GRETRD ,GRDR ,TAJDR ,
6 GPST ,TAURSI ,CBETR ,TAUPR ,*PRI ,TAUPRI ,GR ,TAJRI ,TAJZ ,TAUP3 ,
7 PLM ,DPLM ,DLBL4 ,DLSEM ,DL9L4 ,
8 TOMDM ,GULTM ,SKM1 ,SHM2 ,SHM3 ,SKM4 ,SKM5 ,
9 SKM6 ,SKM7 ,SKM8 ,SKM9 ,SKM10 ,GGUST ,TAUGST ,OMMR ,ETAM3 ,GINRF ,
0 OMRE ,ETATRF ,SKTHM ,SCI ,SC2 ,DCMCLL ,AINPLM ,TAUR01 ,TAUR02 ,
4 TAUFF ,TAUCYR ,DCYFLM ,ALASLP ,ALIM ,TAUSHP ,DELALM ,
DLFLP :
COMMON/INTVR/
1 AVEIN ,CILAML ,CILAMR ,COSINL ,COSINR ,COSPSI ,CZINL ,CZINR ,DLRPSO ,
2 HSD ,SILAML ,SILAMP ,SININL ,SININR ,SINPSI ,SSQINL ,SSQINR ,S2INL ,
3 SZINP
COMMON/EGSTV9/
1 VEAST ,VNPRT4 ,XCS ,YDTCC ,ZCS ,ZDTCC
COMMON/FSVAR/
1 AMAC ,AMACSO ,DEL ,EMAXN1 ,EMAXN2 ,EMXWOT ,ENZSTR ,FSMACH ,OMEGEL ,
2 OMCEP ,ONGVC ,ORVFSM ,QVSDTH ,QVTHDL ,XDE ,ROEQW2 ,SHPRRL ,SHPRR ,
3 SMA ,SD1MX ,S3HATC ,SQMDTX ,TDFE ,TEAL ,TEAR ,THODEL ,THEIC
4 ,PCTCL ,PCTOP
COMMON/VELVAR/
1 AMUL ,AMLSO ,AMIP ,AMKSO ,APOTL ,CMTL ,DMTR ,OMEGAL ,OMEGAR ,
2 MSOL ,MISR ,UHT ,UL4 ,JLMPR ,JLW50 ,JJP ,JRL ,JURLR ,
3 JURL ,JUR ,JURPR ,JRA ,JURPR ,JURMSO ,USO ,UVT ,
4 VALFL4 ,VALFR4 ,VALF5 ,VALVCL ,VALNC ,V3ETVT ,VLM ,VLMDE ,VLM50 ,
5 VP ,VRL ,VRLPR ,VRLVPL ,V2 ,VBRD ,VRRVR ,VRW ,VR402 ,
6 VMSO ,VSO ,VTI01 ,VTIPE ,VTOTAL ,VTOTLR ,VTOTRR ,VVT ,V7ETL ,
7 VZFR ,VMT ,VLM ,VLMDE ,VLSO ,VPL ,VRL ,VRLPR ,VRLWRL ,
8 WRW ,WRMPR ,WRMSO ,WR3 ,WR3PR ,WRWRR ,W50 ,WVT
COMMON/FUSVAR/
1 ALARF ,ALARFD ,ALFSD ,ALP4F ,AMAPF ,ANARF ,ANAREF ,TFTAF ,
2 BETFSO ,CRAME ,CDF ,CLE ,CMF ,CNF ,COSALF ,COSRTE ,CYE ,
3 CLLG ,DMLG ,DMLG ,DZL3 ,DZL3 ,DZL3 ,DZL3 ,DZL3 ,DZL3 ,DZL3 ,DZL3 ,

```

Figure G.6. (Continued)

SUPPLEMENTARY

LINE NO.

23	1	ATFL	ATGDDP	AICR	ALANNS	ALLSH	ALARM	ALARN	ALRRH	1	9
	2	ALPH9	ALPHR	AMARNC	AMAPNL	AMARNR	AMLRH	AMNLP	AMNRP	10	18
	3	AMRFP	AMRR4	AMVNC	ANARNL	ANARNR	ANR3H	ANROTL	ANRTR	19	27
	4	AMEL	ATLDP	ATCR	ATCRUP	CFEAL	CFEALR	CFEALR	CFEALR	28	36
	5	CMER	CP	CPAL	CPAL	CPAL	CPAL	CPAL	CPAL	47	45
	6	CPALL	CPALP	CPALP	CPALP	CPALP	CPALP	CPALP	CPALP	46	54
	7	CPYAL	CPYAL	CPYAL	CPYAL	CPYAL	CPYAL	CPYAL	CPYAL	55	53
	8	CPYAL	CPYAL	CPYAL	CPYAL	CPYAL	CPYAL	CPYAL	CPYAL	64	72
	9	CPYAL	CPYAL	CPYAL	CPYAL	CPYAL	CPYAL	CPYAL	CPYAL	73	81
	10	CPYAL	CPYAL	CPYAL	CPYAL	CPYAL	CPYAL	CPYAL	CPYAL	82	90
	11	CPYAL	CPYAL	CPYAL	CPYAL	CPYAL	CPYAL	CPYAL	CPYAL	91	99
	12	CPYAL	CPYAL	CPYAL	CPYAL	CPYAL	CPYAL	CPYAL	CPYAL	100	108
24	1	ALP4G	ALLWRP	ALDHL4	ALDHPM	ALDGL4	ALDGRM	ALDPR	ALDSS0	1	9
	2	ALP4G	ALLWRP	ALDHL4	ALDHPM	ALDGL4	ALDGRM	ALDPR	ALDSS0	10	18
	3	AVCL	AVCL	AVCL	AVCL	AVCL	AVCL	AVCL	AVCL	19	27
	4	CALL	CALL	CALL	CALL	CALL	CALL	CALL	CALL	28	36
	5	CCP4	CCP4	CCP4	CCP4	CCP4	CCP4	CCP4	CCP4	37	45
	6	CCSP4	CLAVE	CLCNTL	CLCNTL	CLCNTL	CLCNTL	CLCNTL	CLCNTL	46	54
	7	CLMSS	CLMAD	CLMSS	CLMSS	CLMSS	CLMSS	CLMSS	CLMSS	55	63
	8	CLMTR	CLMAD	CLMSS	CLMSS	CLMSS	CLMSS	CLMSS	CLMSS	64	72
	9	CLMTR	CLMAD	CLMSS	CLMSS	CLMSS	CLMSS	CLMSS	CLMSS	73	81
	10	CLMTR	CLMAD	CLMSS	CLMSS	CLMSS	CLMSS	CLMSS	CLMSS	82	90
	11	CLMTR	CLMAD	CLMSS	CLMSS	CLMSS	CLMSS	CLMSS	CLMSS	91	99
	12	CLMTR	CLMAD	CLMSS	CLMSS	CLMSS	CLMSS	CLMSS	CLMSS	100	108
25	1	CPYAL	CPYAL	CPYAL	CPYAL	CPYAL	CPYAL	CPYAL	CPYAL	1	9
	2	CPYAL	CPYAL	CPYAL	CPYAL	CPYAL	CPYAL	CPYAL	CPYAL	10	18
	3	CPYAL	CPYAL	CPYAL	CPYAL	CPYAL	CPYAL	CPYAL	CPYAL	19	27
	4	CPYAL	CPYAL	CPYAL	CPYAL	CPYAL	CPYAL	CPYAL	CPYAL	28	36
	5	CPYAL	CPYAL	CPYAL	CPYAL	CPYAL	CPYAL	CPYAL	CPYAL	37	45
	6	CPYAL	CPYAL	CPYAL	CPYAL	CPYAL	CPYAL	CPYAL	CPYAL	46	54
	7	CPYAL	CPYAL	CPYAL	CPYAL	CPYAL	CPYAL	CPYAL	CPYAL	55	63
	8	CPYAL	CPYAL	CPYAL	CPYAL	CPYAL	CPYAL	CPYAL	CPYAL	64	72
	9	CPYAL	CPYAL	CPYAL	CPYAL	CPYAL	CPYAL	CPYAL	CPYAL	73	81
	10	CPYAL	CPYAL	CPYAL	CPYAL	CPYAL	CPYAL	CPYAL	CPYAL	82	90
	11	CPYAL	CPYAL	CPYAL	CPYAL	CPYAL	CPYAL	CPYAL	CPYAL	91	99
	12	CPYAL	CPYAL	CPYAL	CPYAL	CPYAL	CPYAL	CPYAL	CPYAL	100	108
26	1	CPYAL	CPYAL	CPYAL	CPYAL	CPYAL	CPYAL	CPYAL	CPYAL	1	9
	2	CPYAL	CPYAL	CPYAL	CPYAL	CPYAL	CPYAL	CPYAL	CPYAL	10	18
	3	CPYAL	CPYAL	CPYAL	CPYAL	CPYAL	CPYAL	CPYAL	CPYAL	19	27
	4	CPYAL	CPYAL	CPYAL	CPYAL	CPYAL	CPYAL	CPYAL	CPYAL	28	36
	5	CPYAL	CPYAL	CPYAL	CPYAL	CPYAL	CPYAL	CPYAL	CPYAL	37	45
	6	CPYAL	CPYAL	CPYAL	CPYAL	CPYAL	CPYAL	CPYAL	CPYAL	46	54
	7	CPYAL	CPYAL	CPYAL	CPYAL	CPYAL	CPYAL	CPYAL	CPYAL	55	63
	8	CPYAL	CPYAL	CPYAL	CPYAL	CPYAL	CPYAL	CPYAL	CPYAL	64	72
	9	CPYAL	CPYAL	CPYAL	CPYAL	CPYAL	CPYAL	CPYAL	CPYAL	73	81
	10	CPYAL	CPYAL	CPYAL	CPYAL	CPYAL	CPYAL	CPYAL	CPYAL	82	90
	11	CPYAL	CPYAL	CPYAL	CPYAL	CPYAL	CPYAL	CPYAL	CPYAL	91	99
	12	CPYAL	CPYAL	CPYAL	CPYAL	CPYAL	CPYAL	CPYAL	CPYAL	100	108
27	1	CPYAL	CPYAL	CPYAL	CPYAL	CPYAL	CPYAL	CPYAL	CPYAL	1	9
	2	CPYAL	CPYAL	CPYAL	CPYAL	CPYAL	CPYAL	CPYAL	CPYAL	10	18
	3	CPYAL	CPYAL	CPYAL	CPYAL	CPYAL	CPYAL	CPYAL	CPYAL	19	27
	4	CPYAL	CPYAL	CPYAL	CPYAL	CPYAL	CPYAL	CPYAL	CPYAL	28	36
	5	CPYAL	CPYAL	CPYAL	CPYAL	CPYAL	CPYAL	CPYAL	CPYAL	37	45
	6	CPYAL	CPYAL	CPYAL	CPYAL	CPYAL	CPYAL	CPYAL	CPYAL	46	54
	7	CPYAL	CPYAL	CPYAL	CPYAL	CPYAL	CPYAL	CPYAL	CPYAL	55	63
	8	CPYAL	CPYAL	CPYAL	CPYAL	CPYAL	CPYAL	CPYAL	CPYAL	64	72
	9	CPYAL	CPYAL	CPYAL	CPYAL	CPYAL	CPYAL	CPYAL	CPYAL	73	81
	10	CPYAL	CPYAL	CPYAL	CPYAL	CPYAL	CPYAL	CPYAL	CPYAL	82	90
	11	CPYAL	CPYAL	CPYAL	CPYAL	CPYAL	CPYAL	CPYAL	CPYAL	91	99
	12	CPYAL	CPYAL	CPYAL	CPYAL	CPYAL	CPYAL	CPYAL	CPYAL	100	108

Figure G.6. (Continued)

SUBROUTINE DTFAST

I N D E X

```

C     COEFF1 = RKMS*AVFYAC/2./SPAN
C     COEFF14 = (F1VYDPR*SL*SM*(1.-SMN/SM))
C     COEFF16 = APE*SPAN (S * R)
C     COEFF17 = CH / SCAN (C / R) * WING CHARACTERISTICS
C     COEFF19 = S / 2
C     COEFF19 = F1ROTRAD*OTPA*ROTRAD*ROTRAD
C     COEFF20 = COEFF19 * 2.0
C     COEFF21 = 1./70.5*PI * ARHT
C     COEFF22 = 1./70.5*PI * ADVT
C     COEFF23 = ADEGHT * FEFT
C     COEFF24 = ADEGHT * FEFT
C     COEFF25 = 1./72.4*PI*ROTRAD*ROTRAD
C     COEFF26 = CHPD / 2.
C     COEFF27 = 1./CHD*CHD*CHD
C     COEFF28 = 1./70.5*PI*ARHT
C     COEFF29 = PI * ADVT*G
C     COEFF30 = 1./70.5*PI*ARHT
C     COEFF31 = S * C / 2
C     COEFF32 = S * C / 2 * CLALPHA*(CMOCL*WAC/C)
C     COEFF33 = S * C / 2 * CLALPHA*(CMOCL*WAC/C) * 4/3*PI * VNY/WAC
C     COEFF34 = WAC / VNY * X TH TRUST
C     COEFF35 = B
C     TABLE OF INTEGRATE CALCULATIONS
C     COS1 = 70.5 * SIN(TH-LAMDA)
C     XCOS = 70.5 * COS(TH-LAMDA)
C     XRSIN = XPR * SIN(TH-LAMDA)
C     XRCOS = XPR * COS(TH-LAMDA)
C     Z1SIN = 70.5 * SIN(TH-LAMDA)
C     Z1COS = 70.5 * COS(TH-LAMDA)
C     XLSIN = XLR * SIN(TH-LAMDA)
C     XLCOS = XLR * COS(TH-LAMDA)
C     Z2SIN = SWR * CH * 70.5
C     Z2COS = SWR * SM * 70.5
C     XMSIN = SWR * SL * X
C     XMCOS = SWR * SLW * X
C     TERM1 = (1/XCOS-1/70.5)*(SSDINR * SSJ1ML)
C     TERM2 = (1/XCOS)*(S21MR * S21ML)
C     TERM3 = (SL * SM)/(70.5 * SIN * Z1SIN)
C     TERM4 = (1/XCOS-1/70.5)*(S21MR * S21ML) * 0.5
C     TERM5 = (1/XPR * (C21MR * C21ML))
C     TERM6 = (SL * SM) * (C21MR * C21ML) * (LCOS)
C     DOWTIVE = 1./GTAX
C     DOWTIVE = 1./GTAY
C     DOWTIVE = 1./GTZZ
C     DQ = 0.0
C     DQ = 0.0
C     DQ = 0.0
C     DQ = 0.0
C     FOR ALL CALC USE FOLLOWING TRIG IDENTITIES WHERE
C     A = FACTOR * ANGLE IN RADIAN  A = LAMDA
C     COS(A-B) = COS(A)*COS(B) - SIN(A)*SIN(B)
C     SIN(A-B) = SIN(A)*COS(B) - COS(A)*SIN(B)
C     COS(A+B) = COS(A)*COS(B) + SIN(A)*SIN(B)
C     SIN(A+B) = SIN(A)*COS(B) + COS(A)*SIN(B)

```

Figure G.6. (Continued)

SUBROUTINE RTFAST

I N D E X

```

52 V = VPRIME + VGUST
53 A = APRIME + AGUST
54 P = PPRIME + PGUST
55 Q = QPRIME + QGUST
56 R = RPRIME + RGUST
57 USQ= U*U
58 VSQ= V*V
59 WSQ= W*W
60 VALF= F SORT(U SQ+MSQ,WORK)
61 ALPH= ATAN2(W,U)
62 RETAF= ATAN2(V,VALF)
63 VTOTAL= F SORT(U SQ+V SQ+W SQ,WORK)
64 SQF= RDETV2 *(USQ+VSQ+WSQ)
65 IF(SQF.GT.SQFPRM) GO TO 13C
66 NCLOSE = C
67 SQFPRM= DRPKIR*DRPKI9
68 GO TO 14C
69 NCLOSE= 1
70 SQFPRM= DRPKI4+DRPKI9
71 CONTINUE
72 GLAS SYSTEM
73 CALL LINT(CKEY,GMEM,GMEM,I STG,SOF,GATAR,GALF,GRATAB,GRIALF,
74 TAJRET = GRIALF
75 ALFGLS = ALPH*ROTDDG
76 RETGLS = RETAF*ROTDDG
77 AICPGS = ALFGLS*GALF+RETGLS*GALBET
78 BICGLS = RETGLS*GALBET-ALFGLS*GALALE
79 CUSELAG= PIVOT VELOCITY
80 JP = U - Q*ZCG - XDTCC
81 VP = V + W*ZCG - YDTCC
82 HP = W + Q*XCG - ZDTCC
83
84 LEFT ROTOR HUB VELOCITY - BODY AXES
85 UKRL = UP + P*YN - BL*SININL*(Q+AI*NDTL)*Q*HLL
86 VLPL = VP + BL*(P*COSINL + P*SININL) - P*HLL
87 WPLP = WP + P*YN - BL*(Q+AI*NDTL)*COSINL + HIDL
88
89 RIGHT ROTOR HUB VELOCITY - BODY AXES
90 URPR = UP - P*YN - BL*SININR*(Q+AI*NDTR)*Q*HIR
91 VRPR = VP + BL*(P*COSINR + P*SININR) - P*HIR
92 WRPR = WP + P*YN - BL*(Q+AI*NDTR)*COSINR + HIRDT
93
94 LEFT ROTOR HUB VELOCITY - SHAFT AXES
95 JPL = UKRL*COSINL - WPLP*SININL
96 VPL = VLPL
97 WPL = UKLPP*SININL + WPLP*COSINL
98
99 RIGHT ROTOR HUB VELOCITY - SHAFT AXES
100 JRR = URPR*COSINR - WRPR*SININR
101 VRR = VRPR
102 WRR = URPR*SININR + WRPR*COSINR

```

Figure G.6. (Continued)

SUBROUTINE RTFAST

INDEX

132

```

133 (BLANK CARD)
134 (BLANK CARD)
135 (BLANK CARD)
136 (BLANK CARD)
137 (BLANK CARD)
138 (BLANK CARD)
139 (BLANK CARD)
140 (BLANK CARD)
141 (BLANK CARD)
142 (BLANK CARD)
143 (BLANK CARD)
144 (BLANK CARD)
145 (BLANK CARD)
146 (BLANK CARD)
147 (BLANK CARD)
148 (BLANK CARD)
149 (BLANK CARD)
150 (BLANK CARD)
151 (BLANK CARD)
152 (BLANK CARD)
153 (BLANK CARD)

```

```

*****SYNTAX ERROR*****
C ROTOR INPUT EQUATIONS (AE?)
C NOTE ALPHA AND ALPHA R ARE DEFINED BETWEEN 0 AND 180 DEGREES
C I.E. 90 +DR- 90 DEGREES
133 ALPHA= ATAN2(VZFTL,URL) + FPIRL
134 ZETHL= ATAN2(VPL,PROTL)
135 CALL SINCS(FETHL,SINZHL,CCSZHL)
136 ALPHA= ATAN2(VZFTL,URL) + EPILR
137 ZETHR= ATAN2(VPR,PROPR)
138 CALL SINCS(FETHR,SINZHR,CCSZHR)
C VELOCITIES
C ROTOT ANGULAR RATE TRANSFORMS
C LEFT ROTOR - VACELLE AXES
139 PNLV= P*CSINL - R*SINLML
140 PNLN= Q+ATNDTL
141 PNLN= P*SINL +P*CSINL
C LEFT ROTOR - WIND AXES
142 PNLV= PNLV
143 PNLN= QNLN*CCSZHL -PMLN*SINZHL
144 PNLN= PNLN*CCSZHL +PMLN*SINZHL
C RIGHT ROTOR - VACELLE AXES
145 PNRN= -P*CSINR +R*SINRML
146 PNRN= Q+ATNDTR
147 PNRN= P*SINR +P*CSINR
C RIGHT ROTOR - WIND AXES
148 PNRV= PNRV
149 PNRN= QPNR*CCSZHR +RPNR*SINZHR
150 PNRN= PPNR*CCSZHR -QPNR*SINZHR
C WEGALE OMEGA + PNLV
C WEGALR OMEGA + PNRV
C WEGALS OMEGAL + CMEGAL

```

Figure G.6. (Continued)

SUBROUTINE RTFAST

I N D E X

```

CYMRIL = FYM1*CTL + FYM2*AMULSO + FYM3*AMUL + FYM4
CYMAIL = DYMI*CTL + DYM2*AMULSO + DYM3*AMUL + DYM4
30 TO 180
CONTINUE
CPMRIL = EPM1*CTL + EPM5*AMULSO + EPM6*AMUL + EPM7
CPMAIL = DPM1*CTL + DPM5*AMULSO + DPM6*AMUL + DPM7
CYMRIL = FYM1*CTL + FYM5*AMULSO + FYM6*AMUL + FYM7
CYMAIL = DYMI*CTL + DYM5*AMULSO + DYM6*AMUL + DYM7
CONTINUE
CNFL = CNFPL + CNFALL*AICL + CNFRIL * BICL
CSFL = CSFPL + CSFALL*AICL + CSFRIL * BICL
CPML = CPMP + CPMALL*AICL + CPMRIL * BICL
CYML = CYMPL + CYMALL*AICL + CYMRIL * BICL
    
```

C CALCULATIONS OF FORCES AND MOMENTS FROM COEFFICIENTS

```

ROPIR4 = COEF19 * ROE
ROPIR5 = COEF20 * ROE
CTL = CTLDPM*TIGEL
TL = CTL * FOPTR4 * OMSQL
FNORML = CNFL * ROPIR4 * OMSQL
FSTOEL = CSFL * ROPIR4 * OMSQL
ANROT1 = CPML * ROPIR5 * OMSQL
ANROT1 = CYML * ROPIR5 * OMSQL
TORQL = CPI * ROPIR5 * OMSQL
    
```

```

CTP = CTPORR*TIGER
TR = CTR * ROPIR4 * OMSQR
FNORMR = CNFR * ROPIR4 * OMSQR
ESIDER = CSFR * ROPIR4 * OMSQR
AMPOTR = CPMO * ROPIR5 * OMSQR
ANROT2 = CYMP * ROPIR5 * OMSQR
TORQR = CPP * ROPIR5 * OMSQR
OMD1L = OMDOT
OMDTR = OMDOT
    
```

```

C HUR MOMENTS - NACELLE AXES
FIPOML = FIP*OMEGAL
FIPOMR = FIP*OMEGAP
TRMR1 = FIP*OMEGEL * R
TRMR2 = FIP*OMEGER * R
TRMR3 = ANROT1*COSZHL - ANROT1*SINZHL
TRMR4 = -ANROT1*COSZHL - ANROT1*SINZHL
TRMR5 = ANROT2*COSZHR - ANROT2*SINZHR
TRMR6 = ANROT2*COSZHR - ANROT2*SINZHR
LEFT
ALLRH = -TORQL - FIP*OMD1L
ALPHR = TRMR3 - FIP*OMD1L*PNL
ANLRM = TRMR6 + FIP*OML*CNLN
RIGHT
ALPRM = TORQR + FIP*OMDTR
AMPRM = TRMR5 - FIP*OMR*PNRN
ANPRM = TRMR6 - FIP*OMR*PNRN
    
```

```

C RTCP FORCE AND MOMENT RESOLUTION
C PRELIMINARY CALCULATIONS
    
```

Figure G.6. (Continued)

SUBROUTINE BTCAST

BTCAST

```

241 TMAP2E = FMAP2E*COSS(PI) + FSTIPLES2E*SI
242 TMAP2E = FMAP2E*COSS(PI) + FSTIPLES2E*SI
243 TMAP2E = FMAP2E*COSS(PI) + FSTIPLES2E*SI
244 TMAP2E = FMAP2E*COSS(PI) + FSTIPLES2E*SI
245 TMAP2E = FMAP2E*COSS(PI) + FSTIPLES2E*SI
246 TMAP2E = FMAP2E*COSS(PI) + FSTIPLES2E*SI
247 TMAP2E = FMAP2E*COSS(PI) + FSTIPLES2E*SI
248 TMAP2E = FMAP2E*COSS(PI) + FSTIPLES2E*SI
249 TMAP2E = FMAP2E*COSS(PI) + FSTIPLES2E*SI
250 TMAP2E = FMAP2E*COSS(PI) + FSTIPLES2E*SI
251 TMAP2E = FMAP2E*COSS(PI) + FSTIPLES2E*SI
252 TMAP2E = FMAP2E*COSS(PI) + FSTIPLES2E*SI
253 TMAP2E = FMAP2E*COSS(PI) + FSTIPLES2E*SI
254 TMAP2E = FMAP2E*COSS(PI) + FSTIPLES2E*SI
255 TMAP2E = FMAP2E*COSS(PI) + FSTIPLES2E*SI
256 TMAP2E = FMAP2E*COSS(PI) + FSTIPLES2E*SI
257 TMAP2E = FMAP2E*COSS(PI) + FSTIPLES2E*SI
258 TMAP2E = FMAP2E*COSS(PI) + FSTIPLES2E*SI
259 TMAP2E = FMAP2E*COSS(PI) + FSTIPLES2E*SI
260 TMAP2E = FMAP2E*COSS(PI) + FSTIPLES2E*SI
261 TMAP2E = FMAP2E*COSS(PI) + FSTIPLES2E*SI
262 TMAP2E = FMAP2E*COSS(PI) + FSTIPLES2E*SI
263 TMAP2E = FMAP2E*COSS(PI) + FSTIPLES2E*SI
264 TMAP2E = FMAP2E*COSS(PI) + FSTIPLES2E*SI
265 TMAP2E = FMAP2E*COSS(PI) + FSTIPLES2E*SI
266 TMAP2E = FMAP2E*COSS(PI) + FSTIPLES2E*SI
267 TMAP2E = FMAP2E*COSS(PI) + FSTIPLES2E*SI
268 TMAP2E = FMAP2E*COSS(PI) + FSTIPLES2E*SI
269 TMAP2E = FMAP2E*COSS(PI) + FSTIPLES2E*SI

```

Figure G.6. (Continued)

SUBROUTINE RTFAST

I N D E X

```

270 ***** S Y N T A X E R R O R *****
271 SQWING = SQF + 0.5*DOVDSK*(T2 + TL)
272 SQLM = RDEOV2*(ULWSQ+VLNSQ+HLMSQ)+ TL * DOVDSK
273 SQRM = RDEOV2*(URWSQ+VRMSQ+HRMSQ) + TR * DOVDSK
274 IF(INCLOSE,FQ,1) GO TO 420
275 FTNPR = FINDEG-DBRK17
276 EQUATIONS FOR DOORS OPEN
277 SGNULM = 1.0
278 IF(UL.LT.0.) SGNULM = -1.0
279 SGNURM = 1.0
280 IF(UR.LT.0.) SGNURM = -1.0
281 XAERLM = -SGNULM*FEU*SQLM*(1.-CTSLR)
282 XAFORM = -SGNURM*FEU*SQRM*(1.-CTSPR)
283 YAERLM = 0.
284 YAERM = 0.
285 ZAERLM = DOVTL*TL
286 ZAFERM = DOVTR*TR
287 AMARLM = -XWC2*ZAERLM + AMOVL * TL
288 ALARM = -XWC2*ZAFERM + RMOVTR*TR
289 ANARMS = 0.
290 SET WING DYNAMIC PRESSURE = TO HARD 0.0 FOR THETA TWIST EQ
291 SOWING = 0.0
292 SOLM = 0.0
293 SQRM = 0.0
294 AVECLM = 0.0
295 TO TO 430
296 CONTINUE
297 EQUATIONS FOR DOORS CLOSED
298 FTNPR = FINDEG + DRPK17
299
300 ANGLE OF ATTACK AND SIDESLIP
301 ALPHA = ATAN2(MLN,ULW) + THTLAC
302 BETALW = ATAN2(VLM,VALFL4)
303 ALPHRW = ATAN2(PRW,UPW) + THTPAC
304 BETARW = ATAN2(VRW,VALFRW)
305
306 ALMSSO = ALPHA - EPLR
307 ALPHPW = ALPHRW - EPPR
308 ALRGLW = ALMSSO - THTLAC
309 ALRGPW = ALMSSO - THTPAC

```

Figure G.6. (Continued)

SUBROUTINE RTFAST

I N D E X

```

304 C
305 C
306 C
307 C
308 C
309 C
310 C
311 C
312 C
313 C
314 C
315 C
316 C
317 C
318 C
319 C
320 C
321 C
322 C
323 C
324 C
325 C
326 C
327 C
328 C
329 C
330 C

AVEALW = 0.5*(ALPHM + ALP+P)

CALCULATE LIFT AND DRAG INCREMENTS
FLAP , AILERON , SPOILER CONTRIBUTION

REVISED 11/29/72

CALL AILSP( DFLAIL ,DELSPI,DCLLDA,DCDLDA,DCMLDA,DCLLSP,DCDLSPI,
* DCMLSP)
CALL AILSP( DFLAIP ,DELSPI,DCLLDA,DCDLDA,DCMLDA,DCLLSP,DCDLSPI,
* DCMLSP)

CDCNTL= DCDLDA+DCDLSPI
CMCNTL= DCMLDA+DCMLSP

CDCNTR= DCDRDA+DCDRSP
CMCNTR= DCMRDA+DCMRSP

CONTRIBUTION DUE TO TOTALLY DOWNWASHED WING ( ALPHA - EPSILON)

CALL CLCDMIALWSSO, DFLAIL ,DCLLDA,DCLLSP,CDCNTL,CMCNTL,
* CLWSS,CDLWSS,CMLWSS,CLDUM,CDDUM)
CALL CLCDMIALPHM, DFLAIR ,DCLLDA,DCLLSP,CDCNTR,CMCNTR,
* CLWSS,CDRWSS,CMLWSS,CLDUM,CDDUM)

CONTRIBUTION DUE TO TOTALLY UN-WASHED WING ( ALPHA )

CALL CLCDMIALPHM, DFLAIL ,DCLLDA,DCLLSP,CDCNTL,CMCNTL,
* CLWAD,CDLWAD,CMLWAD,CLWPR,CDLWPR)
CALL CLCDMIALPHM, DFLAIR ,DCLLDA,DCLLSP,CDCNTR,CMCNTR,
* CLWAD,CDRWAD,CMLWAD,CLWPR,CDRWPR)

CALL CLP1(DELF1,CLZERO)
CALL CLP2(ALPH+ATW,CLZERO,0.5,CLAVE)

ALLWPR= ALPHM - ATW - THYLAC
ALRWPR= ALPHM - ATW - THTRAC
SALLW= ALLWPR
SALRW= 1.0
CALRW= 1.0
SRETLW= RETALW
SBFTLM= 1.0
SBFTRM= RETARW
CBFTPM= 1.0
IMARN1( 7)= .FALSE.
IMARN1( 8)= .FALSE.
IMARN1( 9)= .FALSE.
IMARN1(10)= .FALSE.

```

Figure G.6. (Continued)

SUBROUTINE RTFAST

T N D F X

```

331 IF(IALWSSO.GT.DEG20) IWARN1( 7) = .TRUE.
332 IF(IARWSSO.GT.DEG20) IWARN1( 9) = .TRUE.
333 IF(ALPHLW.GT.DEG20) IWARN1( 9) = .TRUE.
334 IF(ALPHRW.GT.DEG20) IWARN1(10) = .TRUE.
335 CALL SINCOSIEPLR,SEPLW,CEPLW
336 CALL SINCOSIEPRR,SEPRW,CEPRW
C
337 TRMW5 = (1.-CTSIR)* (1.-SILW)
338 TRMW6 = (1.-CTSRR)* (1.-SIRW)
339 CLSLW = (SILW*(CLLWSS*CEPLW-CDLWSS*SEPLW) + CLLWAD* TRMW5)*
* RKALPR
340 CDSLW = (SILW*(CLLWSS*SEPLW+CDLWSS*CEPLW) + CDLWAD* TRMW5)*
* RKALPP
341 CMSLW = (SILW*CDLWSS + CMLWAD* TRMW5)*BKALPR
C
342 CLSPW = (SIRW*(CLRWSS*CEPRW -CDRWSS*SEPRW)+ CLRWAD* TRMW6)*
* RKARPP
343 CDSPW = (SIRW*(CLRWSS*SEPRW +CDRWSS*CEPRW)+ CDRWAD* TRMW6)*
* RKARPP
344 CMSRW = (SIRW*CDRWSS + CRRWAD* TRMW6 )*RKARPR
C
345 DCLSPW = .25*(1.-.5*SIIW)*(CLSLW-CLLWAD*(1.-AVECTS))-(1.-.5*
* SIRW)*(CLSRW-CLRWAD*(1.-AVECTS))
346 DCNSPW = .25*(1.-.5*SIPW)*(CDSPW-CDRWAD*(1.-AVECTS))-(1.-.5*
* SILW)*(CDSLW-CDLWAD*(1.-AVECTS))
C
347 CLSM = (1.-AVECTS)*(9ETAF*(SK2+SK21*CLAVE)+COEF11*(CLLWAD
* -CLRWAD)) + DCLSPW
348 CNSM = (1.-AVECTS)*(9ETAF*(SK2+CLAVE*CLAVE+COEF12*(CDRWAD
* -CDLWAD- CLRWAD*(ALPHRW-ALPH )-LLWAD*(AINW-ALPHLW ))) +DCNSPW
C
349 TRMW7 = SOLW * COEF11
350 TRMW9 = SORW * COEF11
C
351 ZAEPLW = -TRMW7 *(CLSLW*CALL4 +CDSLW*CRETLW*SALLW )
352 XAEPLW = TRMW7 *(CLSLW*SALL4 -CDSLW*CBETLW*CALLW )
353 YAEPLW = -TRMW7 *CDSLW * SBETLW
354 AMAPLW = TRMW7 *CHORD *CMSLW * CRETLW
* -XMAC*ZAEPLW + ZMAC*XAEPLW
C
355 ZAEPRW = -TRMW9 *(CLSRW*CALRW +CDSRW*CBETRW*SALRW )
356 XAEPRW = TRMW9 *(CLSRW*SALRW -CDSRW*CBETRW*CALRW )
357 YAEPRW = -TRMW9 *CDSRW * SBETRW
358 AMAPRW = TRMW9 *CHORD *CMSRW * CBETRW
* -XMAC*ZAEPRW + ZMAC*XAEPRW
C
359 AVECLW = .5*(CLSPW+CLSLW)/(1.-AVECTS)
360 CONTINUE
361 XAEPMG = XAEPLW + XAEPRW
362 YAEPMG = YAEPLW + YAEPRW
363 ZAEPMG = ZAEPLW + ZAEPRW
364 ALAPMG = CLSW * SCMING + COEF11

```

Figure G.6. (Continued)

SUBROUTINE RTFAST

I N D E X

```

385 CONTINUE
386 EPTL1 = EPZER+DEPDAL*(AVEALN-SLAC*WDDT/(U*U+C.C11))
387 IF(AVEFP*LT.EPTL1) GO TO 265
388 EPTAIL = AVEFP*(1.-GEF)*DOVFSM
389 GO TO 265
390 CONTINUE
391 EPTAIL = EPTL1*(1.-GEF)*DOVFSM
392 CONTINUE
393 EPTAIL = EPTL1*(1.-GEF)*DOVFSM
394 CONTINUE
395 EPTAIL = EPTL1*(1.-GEF)*DOVFSM
396 EPTAIL = EPTL1*(1.-GEF)*DOVFSM
397 EPTAIL = EPTL1*(1.-GEF)*DOVFSM
398 EPTAIL = EPTL1*(1.-GEF)*DOVFSM
399 EPTAIL = EPTL1*(1.-GEF)*DOVFSM
400 EPTAIL = EPTL1*(1.-GEF)*DOVFSM
401 EPTAIL = EPTL1*(1.-GEF)*DOVFSM
402 EPTAIL = EPTL1*(1.-GEF)*DOVFSM
403 EPTAIL = EPTL1*(1.-GEF)*DOVFSM
404 EPTAIL = EPTL1*(1.-GEF)*DOVFSM
405 EPTAIL = EPTL1*(1.-GEF)*DOVFSM
406 EPTAIL = EPTL1*(1.-GEF)*DOVFSM
407 EPTAIL = EPTL1*(1.-GEF)*DOVFSM
408 EPTAIL = EPTL1*(1.-GEF)*DOVFSM
409 EPTAIL = EPTL1*(1.-GEF)*DOVFSM
410 EPTAIL = EPTL1*(1.-GEF)*DOVFSM
411 EPTAIL = EPTL1*(1.-GEF)*DOVFSM
412 EPTAIL = EPTL1*(1.-GEF)*DOVFSM
413 EPTAIL = EPTL1*(1.-GEF)*DOVFSM
414 EPTAIL = EPTL1*(1.-GEF)*DOVFSM
415 EPTAIL = EPTL1*(1.-GEF)*DOVFSM
416 EPTAIL = EPTL1*(1.-GEF)*DOVFSM
417 EPTAIL = EPTL1*(1.-GEF)*DOVFSM
418 EPTAIL = EPTL1*(1.-GEF)*DOVFSM
419 EPTAIL = EPTL1*(1.-GEF)*DOVFSM
420 EPTAIL = EPTL1*(1.-GEF)*DOVFSM
421 EPTAIL = EPTL1*(1.-GEF)*DOVFSM
422 EPTAIL = EPTL1*(1.-GEF)*DOVFSM
423 EPTAIL = EPTL1*(1.-GEF)*DOVFSM
424 EPTAIL = EPTL1*(1.-GEF)*DOVFSM
425 EPTAIL = EPTL1*(1.-GEF)*DOVFSM
426 EPTAIL = EPTL1*(1.-GEF)*DOVFSM
427 EPTAIL = EPTL1*(1.-GEF)*DOVFSM
428 EPTAIL = EPTL1*(1.-GEF)*DOVFSM
429 EPTAIL = EPTL1*(1.-GEF)*DOVFSM
430 EPTAIL = EPTL1*(1.-GEF)*DOVFSM
431 EPTAIL = EPTL1*(1.-GEF)*DOVFSM

```

Figure G.6. (Continued)

VERTICAL TAIL AERO COEFFICIENT TRANSFORM

CONTINUED

```

439 CONTST = CDMVT * CDMTAC(LMVT, CDEF2)
440 CDMVT = CDMVT * ((1.0 - CDMTAC(LMVT, CDEF2)) / (PI * DV2 - ALMVT))
441 DO TO 238
442 IF (ALMVT * CDMVT - T * TRMHT3) .GT. 0.02
443   SECTION 3
444   CONTST = CLAT * TRMHT3
445   CLMVT = CLMVT * (ALMVT - PI * DV2) / (PI * DV2 - TRMHT3)
446   CDMVT = CDMVT * CLMVT * CLMVT * CDEF2
447   CONT = CDMVT * ((1.0 - CDMTAC(LMVT, CDEF2)) / (TRMHT3 - PI * DV2))
448   DO TO 244
449   SECTION 4
450   CLMVT = CLMVT * (ALMVT - PI)
451   CDMVT = CDMVT * CLMVT * CDEF2
452   CONTINUED
453   VERTICAL TAIL AERO COEFFICIENT TRANSFORM
454   CDMVT = ATAN(PI * CDMVT)
455   ALMVT = -ACTVT * PI * CDEF2
456   IF (ALMVT * CDMVT - PI) .ALPHVT = ALMVT * CDEF2
457   IF (ALMVT * CDMVT - PI) .ALPHVT = ALMVT * CDEF2
458   SIGMA = DSDBET * PI * CDEF2
459   CALL SIGMA(BETVT - SIGMA, SHETS3, CDEF2)
460
461 SECTION 5
462 ALMVT = TRMVT * DELTA
463 ALMVT = ALMVT * ALMVT
464 ALMVT = V * STALL * ALMVT
465 ALMVT = -V * STALL * ALMVT
466 CDMVT = CDMVT * DELTA
467 TRMVT = CDMVT * DELTA
468 TRMVT = CDMVT * DELTA
469
470 IF (ALMVT * CDMVT - PI) .ALPHVT = ALMVT * CDEF2
471 IF (ALMVT * CDMVT - PI) .ALPHVT = ALMVT * CDEF2
472 IF (ALMVT * CDMVT - PI) .ALPHVT = ALMVT * CDEF2
473 IF (ALMVT * CDMVT - PI) .ALPHVT = ALMVT * CDEF2
474 IF (ALMVT * CDMVT - PI) .ALPHVT = ALMVT * CDEF2
475 IF (ALMVT * CDMVT - PI) .ALPHVT = ALMVT * CDEF2
476 IF (ALMVT * CDMVT - PI) .ALPHVT = ALMVT * CDEF2
477 IF (ALMVT * CDMVT - PI) .ALPHVT = ALMVT * CDEF2
478 IF (ALMVT * CDMVT - PI) .ALPHVT = ALMVT * CDEF2
479 IF (ALMVT * CDMVT - PI) .ALPHVT = ALMVT * CDEF2

```

Figure G.6. (Continued)

SUBROUTINE RTFAST

I N D E X

```

478 IWARN(6) = .FALSE.
479 GO TO 308
480 IF(ALVTE .GT. P1OV2) GO TO 300
279 C
481 REGION ?
482 CVTST = CVAT * ALVTP
483 CVVT = CVTST * (P1OV2 - ALVTE) / (P1OV2 - ALVTP)
484 CDVST = CDVST * CVTST * COEF22
485 CDVT = CDVST * (1.1 - CVTST) * (ALVTE - ALVTP) / (P1OV2 - ALVTP)
486 GO TO 309
300 IF(ALVTE .GT. (PI - TRMVT3)) GO TO 302
C
487 REGION 3
488 CVTST = CVAT * TRMVT3
489 CVVT = CVTST * (ALVTE - P1OV2) / (P1OV2 - TRMVT3)
490 CDVST = CDVST + CVTST * CVTST * COEF22
491 CDVT = CDVST * (1.1 - CVTST) * (ALVTE - PI + TRMVT3) / (TRMVT3 - P1OV2)
492 GO TO 308
C
493 REGION 4
494 CVT = CVAT * (ALVTE - PI)
495 CDVT = CDVST + CVT * CVT * COEF22
496 CONTINUE
C
C TOTAL TAIL FORCE AND MOMENT RESOLUTION
497 TRMHT = SQF * COEF23
C
C CHANGE MADE TO HALVE EFFHT FOR I NAC GT FINDEG
498 IF(INCLOSE .EQ. C.AND. UPRIME .GT. 0.1) TRMHT = TRMHT * 0.5
C
499 XARHT = TRMHT * (CLHT * SALIHT - CDHT * CALIHT * CBETS)
500 YARHT = -TRMHT * SBETS * CDHT
501 ALARHT = -YARHT * (LZHT - ZCG)
502 ANARHT = YARHT * (XCG - XHT) + XARHT * (ZHT - ZCG)
503 ANARHT = -YARHT * (XCG - XHT)
C
504 TRMVT = SQF * COEF24
C
505 XARVT = -TRMVT * CALIHT * (CDVT * CBETS + CVVT * SBETS)
506 YARVT = TRMVT * (CVVT * CBETS - CDVT * SBETS)
507 ALARVT = -YARVT * (ZVT - ZCG)
508 ANARVT = ZARVT * (XCG - XVT) + XARVT * (ZVT - ZCG)
509 ANARVT = -YARVT * (XCG - XVT)
C
510 XARPT = XARHT + XARVT
511 YARPT = YARHT + YARVT
512 ZARPT = ZARHT + ZARVT
513 ALARPT = ALARHT + ALARVT
514 ANARPT = ANARHT + ANARVT

```

Figure G.6. (Continued)

SUBROUTINE RTFAST

***** SYNTAX ERROR *****

***** SYNTAX ERROR *****

515
516

CALL DEAF
CONTINUE
KAEF=KAEF+DKLG
VAEF=VAEF+DKLG
ZAEF=ZAEF+DKLG
ALAE=ALAE+DKLG
MAEF=MAEF+DKLG
AAEF=AAEF+DKLG
LANK CARD
LANK CARD
LANK CARD
LANK CARD
LANK CARD
LANK CARD
LANK CARD
LANK CARD
LANK CARD
LANK CARD
LANK CARD

***** SYNTAX ERROR *****

517
518
519
520
521
522
523
524
525

IF (C.L.NE.1.) GO TO 80
CALL DEAF
CONTINUE
KAEF=KAEF+DKLG
VAEF=VAEF+DKLG
ZAEF=ZAEF+DKLG
ALAE=ALAE+DKLG
MAEF=MAEF+DKLG
AAEF=AAEF+DKLG

ELASTIC AXES TO C.G. TRANSFORM
DYNAMIC FORCES AND MOMENTS RESOLVED TO THE
TOTAL CENTER OF GRAVITY

KAEF=KAEF+MAEF+KAEF+KAEF
VAEF=VAEF+VAEF+VAEF+VAEF
ZAEF=ZAEF+ZAEF+ZAEF+ZAEF
ALAE=ALAE+ALAE+ALAE+ALAE
MAEF=MAEF+MAEF+MAEF+MAEF
AAEF=AAEF+AAEF+AAEF+AAEF

526
527
528
529
530
531
532
533

LAEP=LAEP+LAEP+LAEP+LAEP
VAEP=VAEP+VAEP+VAEP+VAEP
ZAEF=ZAEF+ZAEF+ZAEF+ZAEF
ALAE=ALAE+ALAE+ALAE+ALAE
MAEF=MAEF+MAEF+MAEF+MAEF
AAEF=AAEF+AAEF+AAEF+AAEF

534
535
536
537

LAEP=LAEP+LAEP+LAEP+LAEP
VAEP=VAEP+VAEP+VAEP+VAEP
ZAEF=ZAEF+ZAEF+ZAEF+ZAEF
ALAE=ALAE+ALAE+ALAE+ALAE
MAEF=MAEF+MAEF+MAEF+MAEF
AAEF=AAEF+AAEF+AAEF+AAEF

Figure G.6. (Continued)

SUBROUTINE RTFAST

I N D E X

```

538 * +YN*(XAERNL-XAERNR)-XCC*YAERNC
539 RQ = R*Q
540 PQ = P*Q
541 QR = R*R
542 PR = P*R
543 PP = P*P
544 RQ = R*Q
545 C POST EQUATION CROSS TERMS
546 TERMPI = -FJXX * RQ +FIXZP* PQ
547 C QDOT EQUATION CROSS TERMS
548 TERMQI = -FJYY * PR -FIXZO*(PP -RR)
549 C ROOT EQUATION CROSS TERMS
550 TERMRI = -FJZ * PQ -FIXZR* RQ
551 C AIMDDR EQUATION CROSS TERMS
552 TERMIR = COFFA*COEF2*( PR*(1.-2.*SILAMR*SILAMR) - (RR-PP)*SILAMR*
553 * CILAMR )
554 C TERM2K = -(RK -PP)* F177PR*SINI*NR *COSINR +COEF1*(XAER0*SILAMR
555 * + ZAFRO*CILAMP )
556 C TERM3Z = COFFO*(PQ*SILAMR +RQ*CILAMR)
557 C
558 C AIMDDL EQUATION CROSS TERMS
559 TERM1L = COFFA*COEF2*( PR*(1.-2.*SILAML*SILAML)-(RR-PP)*SILAML *
560 * CILAML )
561 C TERM2L = -(RQ-PP)* F177PR *SINI*ML *COSINL +COEF1*(XAER0*SILAML
562 * + ZAFRO*CILAPL )
563 C TERM3L = -COFFO*(PQ* SILAML + RQ*CILAML )
564 C IF(INV.EQ.1) GO TO 6C
565 HIR = .
566 HIOTR = 3.
567 HIL = .
568 HIOTL = 3.
569 HWACR = 3.
570 HDTACR = 0.
571 HWACL = 0.
572 HDTACL = 0.
573 GO TO 7C
574 C CONTINUE
575 TRMHIS = COFFLO*ZAERO
576 HIR = SKW1*ZAERNP+SKW2*ZAEHP+SKW3*ALARNR-TRMHIS*(SK#4+SK#5)
577 HIOTR = OVDTIM*(HIR-HIOTL)
578 HIROLD = HIR
579 HIL = SKW1*ZAERNL+SKW2*ZAFRLW+SKW3*ALARNL-TRMHIS*(SK#4+SK#5)
580 HIOTL = OVDTIM*(HIL-HIOTL)
581 HWACR = SKW6*ZAERNR+SKW7*ZAFRRM+SKW8*ALARNP-TRMHIS*(SKW9+SKW10)
582 HDTACR = OVDTIM*(HWACR-HACRDD)
583 HWACR = HWACR
584 HWACL = SKW4*ZAERNL+SKW5*ZAEPLM+SKW6*ALARNL-TRMHIS*(SKW9+SKW10)
585 HDTACL = OVDTIM*(HWACL-HACLOD)
586 HWACLD = HWACL
587 C CONTINUE
588 C TERMS FOR THETA TWIST EQUATION
589 C GMDW = SC1 + SC2*DELFLP
590 TRMTL = SOLW*(1.-CTSLR)

```

Figure G.6. (Continued)

SUBROUTINE RTFAST

I N D E X

```

622 C DAC1(11) = VTRIM
        WDOT EQUATION NON-WING BENDING TERMS
623 C DAC1(12) = ZARRG
        HTRIM DAC
624 C DAC1(13) = -HTRIM
        SORT(POE/ROEC)*VTOTAL FOR 9CA FUNCTIONS
625 C DAC1(14) = F*SORT(ROE/ROEK) * U
        COEFFICIENT OF AIMDDR IN THE QDOT EQUATION
626 C DAC1(15) = (FYPR+COEF4*(XKCOS-ZRSEMI)) * DDVIY
        VDOTLR FOR MU CALC ON ANALOG
627 C DAC1(16) = VTOTLR
        COEFFICIENT OF AIMDDL IN THE QDOT EQUATION
628 C DAC1(17) = (FYPR+COEF4*(XKCOS-ZLSINI)) * DDVIY
        LEFT ROTOR ALPHA FOR 9CA
629 C DAC1(18) = -ALPHR
        THETA TRIM DAC
630 C DAC1(19) = IHTRIM
        VDOTRR FOR MU CALC ON ANALOG
631 C DAC1(20) = VTOTRR
        AVERAGE ALPHA WING FOR SIMULATOR
632 C DAC1(21) = -AVEALW
        RIGHT ROTOR ALPHA TO USE IN 9CA
633 C DAC1(22) = -ALPHRR
        COEFFICIENT OF PDOT IN THE RDOT EQUATION
634 C DAC1(23) = FIXZR * DDVIYZ
        PNLR FOR MU CALC ON ANALOG
635 C DAC1(24) = PNLR
        COEFFICIENT OF AIMDDR IN THE RDOT EQUATION
636 C DAC1(25) = SILAMR * DDVIYZ
        PNR for MU CALC ON ANALOG
637 C DAC1(26) = PNR
        COEFFICIENT OF AIMDDL IN THE RDOT EQUATION
638 C DAC1(27) = SILAML * DDVIYZ
        VNRTH FOR SIMULATOR
639 C DAC1(28) = -VNRTH
        FUSELAGE DYNAMIC PRESSURE FOR SIMULATOR
640 C SGN5OF = 1.0
        (FUEL-T-0) SGN5OF = -1.0
641 C DAC1(29) = -SOF * SGN5OF
        VEAST FOR SIMULATOR
642 C DAC1(30) = -VEAST
        BETA FUSE FOR CONTROL SYSTEM FEEDBACK
643 C DAC1(31) = -BETAF
        DAC2( 1) = -CILAMR
644 C DAC2( 2) = HICGLS
        DAC2( 3) = COEFF3
645 C DAC2( 4) = -AICLGS
        DAC2( 5) = SILAMP
        MOMENT ARM FOR CG ACCELERATION EQS FOR SIMULATOR
646 C DAC2( 6) = KCG-SLPA
        HDOT TRIM DAC
647 C DAC2( 7) = HDOTRIM
        AVAILABLE HORSEPOWER RIGHT ENGINE
648 C DAC2( 8) = SHPPRR
        DAC2( 9) = CILAML
649 C

```

Figure G.6. (Continued)

SUBROUTINE RTFAST

I N D E X

```
461 CALL TRACK(RTFAST ,*2)
462 RETURN
463 DO 510 J=1,32
464 51) CALL DISABLI(J-1)
465 52) IPAN= KPAN
466 RETURN
467 END
```

Figure G.6. (Continued)

SUBROUTINE RTFAST

I N D E X

AIICLS	-	76=	528						
AIICLPR	-	9CJ	161						
AICR	-	23CJ	167=	186	187	188			
AICRDP	-	23CJ	165=	168					
AICRGS	-	77=	645						
AICRPR	-	9CJ	165						
AICRSP	-	3C5*	376*						
AINDTL	-	9CJ	49	82	84	140			
AINDTR	-	9CJ	49	85	87	146			
AINHTR	-	11CJ	395	398AG					
AINL	-	9CJ	41AG	42					
AINR	-	9CJ	40AG	42					
AINREF	-	9CJ							
AINRLM	-	15CJ							
AINRM	-	11CJ	317	318	348				
AITRIM	-	28CJ	639						
AKEY	-	13CJ							
ALAERC	-	27CJ	533=						
ALA4DA	-	11CJ	523=						
ALARF	-	20CJ	523						
ALARFP	-	20CJ	523						
ALARHT	-	26CJ	500=						
ALARHT	-	23CJ	266=						
ALARNC	-	23CJ	251=	568	574				
ALARNL	-	23CJ	259=	555	571				
ALARNF	-	532=	533						
ALARRG	-	26CJ	513=						
ALART	-	531=	533						
ALARVB	-	26CJ	507=						
ALARVT	-	26CJ	287=	537					
ALARWG	-	11CJ	76	77	78				
ALBRK	-	74=							
ALEGLS	-	72AG							
ALFREF	-	20CJ							
ALFSQ	-	14CJ							
ALFTAB	-	26CJ	72AG						
ALMTE	-	429	407	408	414	416	418	420	422
ALMTP	-	26CJ	431	437	441				424
ALMTPR	-	26CJ	402=	418	419				422
ALMTPR	-	26CJ	401=	424	431				433
ALMST	-	11CJ	390=	401	402				
ALM	-	15CJ							
ALLNSO	-	22CJ							
ALLPH	-	23CJ	235=	254					
ALLMPP	-	24CJ	317=						
ALNCBK	-	11CJ							
ALPH	-	20CJ	61=	316AG	592				
ALPH	-	26CJ	395=	397	398AS				
ALPHN	-	22CJ							
ALPHLP	-	23CJ	133=	304	313AS	317	333	348	
ALPHLP	-	24CJ	296=						
ALPHRN	-	22CJ							
ALPHR	-	23CJ	136=	613					
ALPHAS	-	24CJ	298=	304	314AS	319	334	348	
ALPHV	-	24CJ	455=	447	451				

Figure G.6. (Continued)

I N D E X

CONS10	-	29C0
CONS11	-	29C0
CONS12	-	29C0
CONS13	-	29C0
CONS14	-	29C0
CONS15	-	29C0
CONS16	-	29C0
CONS17	-	29C0
CONS18	-	29C0
CONS19	-	29C0
CONS20	-	29C0
CONS21	-	29C0
CONS22	-	29C0
CONS23	-	29C0
CONS24	-	29C0
CONS25	-	29C0
CONS26	-	29C0
CONS27	-	29C0
CONS28	-	29C0
CONS29	-	29C0
CONS30	-	29C0
CONS31	-	29C0
CONS32	-	29C0
CONS33	-	29C0
CONS34	-	29C0
CONS35	-	29C0
CONS36	-	29C0
CONS37	-	29C0
CONS38	-	29C0
CONS39	-	29C0
CONS40	-	29C0
CONS41	-	29C0
CONS42	-	29C0
CONS43	-	29C0
CONS44	-	29C0
CONS45	-	29C0
CONS46	-	29C0
CONS47	-	29C0
CONS48	-	29C0
CONS49	-	29C0
CONS50	-	29C0
CONS51	-	29C0
CONS52	-	29C0
CONS53	-	29C0
CONS54	-	29C0
CONS55	-	29C0
CONS56	-	29C0
CONS57	-	29C0
CONS58	-	29C0
CONS59	-	29C0
CONS60	-	29C0

376
376
376

Figure G.6. (Continued)

SUPPLEMENTARY RECAST

I N D E X

DRK6	-	29C0			
DRK7	-	29C0			
DRK8	-	29C0			
DRK9	-	29C0	173	193	
DC00F	-	24C0	375AG	377	
DCDL0A	-	11C0	305AG	307	
DCDLG	-	24C0	305AG	307	
DCDLSP	-	24C0	306AG	309	
DCRRDA	-	24C0	306AG	309	
DCRRSP	-	24C0	306AG	309	
DC00F	-	24C0	305AG	311AG	313AG
DCLL0A	-	24C0	305AG	311AG	313AG
DCLLSP	-	24C0	306AG	312AG	314AG
DCLRDA	-	24C0	306AG	312AG	314AG
DCLRSP	-	24C0	306AG	312AG	314AG
DCLS0W	-	24C0	345E	347	
DC0DCL	-	15C0			
DCMDF	-	24C0			
DCMLDA	-	24C0	305AG	309	
DCMLG	-	11C0	305AG	309	
DCMLSP	-	24C0	305AG	309	
DCMRDA	-	24C0	305AG	310	
DCMSP	-	24C0	345E	347	
DCMSPW	-	24C0	345E	347	
DCYPLM	-	15C0			
DEG2E	-	11C0	331	332	334
DEL	-	14C0	534		
DELALM	-	15C0			
DEL9S	-	9C0			
DEL9T	-	9C0			
DELELV	-	9C0	379	379	380
DELEP7	-	374E	375	378	381
DELELP	-	9C0	47	315AG	378
DELS	-	9C0			
DELS	-	9C0			
DELS	-	9C0	45		
DELRUD	-	9C0	375AG		
DELSPL	-	9C0	36AG		
DELSPP	-	9C0			
DELS	-	9C0			
DELS	-	9C0			
DELTH	-	9C0			
DEPOL	-	341E	494E	369	
DEFLAI	-	9C0	374E	311AG	374
DEFLATP	-	9C0	374E	312AG	374
DG00P	-	11C0	374	375	
DIGAV	-	6C0	562AG		
DIGAN2	-	6C0			
DIGARI	-	564E			
DRLM	-	15C0			
DLELPC	-	15C0			
DLEPST	-	16C0	47E		
DLLG	-	23C0	523		
DLLNC	-	22C0	251	254	
DPLM	-	15C0			
DLSAG	-	27C0	259	252	

Figure G.6. (Continued)

SUBROUTINE RTEAST

I N D E X

DLSL4	-	1500				
DNLG	-	2000	524			
DNLNC	-	2200	252			
DNPNC	-	2200	250			
DNF1	-	1000	170	190		
DNF2	-	1000	170	190		
DNF3	-	1000	170	190		
DNF4	-	1000	170	190		
DNLG	-	2000	525			
DNLNC	-	2200	250			
DNRNC	-	2200	258			
DDVT	-	1100				
DDVTL	-	2100	283			
DDVTR	-	2100	284			
DPA1	-	1000	175	181	195	201
DPA2	-	1000	175	195		
DPA3	-	1000	175	195		
DPA4	-	1000	175	195		
DPA5	-	1000	191	201		
DPA6	-	1000	191	201		
CP47	-	1000	181	201		
DRL4	-	1500				
DSDBET	-	1100	445			
DSF1	-	1000	172	192		
DSF2	-	1000	172	192		
DSF3	-	1000	172	192		
DSF4	-	1000	172	192		
DTIM	-	600				
DUM12	-	900				
DUM13	-	900				
DUM14	-	900				
DUM15	-	900				
DUM43	-	900				
DUM44	-	900				
CUM45	-	900				
DUM46	-	900				
DUM47	-	900				
DUM48	-	900				
DUM49	-	900				
DXLG	-	2000	520			
DXLNC	-	2200	247	249		
DXRNC	-	2200	254	257		
DYLG	-	2000	521			
CYLNC	-	2200	248			
DYMI	-	1000	177	183	197	203
DYM2	-	1000	177	197		
DYM3	-	1000	177	197		
DYM4	-	1000	177	197		
DYM5	-	1000	183	203		
CYM6	-	1000	183	203		
DYMT	-	1000	183	203		
DYRNC	-	2200	256			
DZLG	-	2000	522			
DZLNC	-	2200	243			
CZRNC	-	2200	244			
EFFHT	-	1100				

Figure G.6. (Continued)

SUBROUTINE RTFAST

I N D E X

FIC	-	1100	279	230	254	252
FINDEG	-	1100	274	295		
FINPR	-	1100	274=	295=		
FIP	-	1100	227	228	235	238
FIP04L	-	2300	277=	236	237	
FIP04R	-	2300	228=	239	240	
FIXX	-	2700				
FIXXF	-	1100				
FIXXPR	-	1100				
FIXXM	-	1100				
FIXZF	-	1100				
FIXZP	-	2700	544	594		
FIXZPR	-	1100				
FIXZQ	-	2700	545			
FIXZR	-	2700	546	614		
FIXZH	-	1100				
FIYY	-	2700				
FIYVF	-	1100	606	608		
FIYVPR	-	1100				
FIYYM	-	1100				
FIZZ	-	2700				
FIZZPR	-	1100	548	551		
FIZZW	-	1100	544			
FJXX	-	2700	545			
FJYY	-	2700	546			
FJZZ	-	4*				
FLAGS	-	4*				
FNOR4L	-	2300	213=	241	245	
FNOR4R	-	2300	220=	242	246	
FSIOEL	-	2300	214=	241	245	
FSIDER	-	2300	221=	242	246	
FSMACH	-	1800				
THE VARIABLE- FSORT - IS USED BEFORE IT IS DEFINED						
FSORT	-	60	63	100	101	105
FUSVAR	-	20*				121
GAATAB	-	1400	72AG			125
GAIALF	-	72AG	76	77		131
GAIBET	-	73=	76	77		
GBATAB	-	1400	72AG			
GBETDR	-	1500				
GBETP	-	1500				
GBETP	-	1500				
GRUTON	-	400				
GRIALF	-	72AG	73	78		
GDR1	-	1500				
GDR2	-	1500				
GDLTH	-	1500				
GEAR	-	518*				
GEF	-	2100	371	380	391	
GEFVAP	-	210*				
GGUST	-	1500				
GICLY	-	1500				
GINRF	-	1500				
GKFY	-	1300	72AG			

Figure G.6. (Continued)

SUBROUTINE RTFAST

I N D E X

GLPSLP	-	1500	
GLPP	-	1500	
GLSLM	-	1500	
GMEW	-	1300	72AG
GOMG	-	1500	
GP	-	1500	
GPOS	-	1500	
GPHI	-	1500	
GPRI	-	1500	
GPSI	-	1500	
GPSIDP	-	1500	
GO	-	1500	
GR	-	1500	
GDR	-	1500	
GTH	-	1500	
GTHF	-	1500	
GTHGV	-	1500	
H	-	900	
THE VARIABLE= MACRO - IS USED BEFORE IT IS DEFINED			
MACROD	-	575	57A=
THE VARIABLE= MACROD - IS USED BEFORE IT IS DEFINED			
MACROD	-	577	57A=
MCOT	-	700	
MTACL	-	2500	174 561= 575=
MTACR	-	2500	174 559= 572=
MTTRM	-	2800	631
MGEFLR	-	2100	
MGERR	-	2100	
MLHJR	-	2100	
MOLD	-	600	
MOLD2	-	600	
MP	-	1100	
MRHJR	-	2100	
MSO	-	1600	
MTCA	-	2100	
MTRM	-	2800	674
MTSTLL	-	800	472
MVTKT	-	1100	
MWACL	-	2500	176 561= 574= 575 576
MWACR	-	2500	176 559= 571= 572 573
MWC4	-	2100	
MVBCON	-	5*	
MYRIN	-	7*	
MIRTL	-	2500	94 557= 569=
MIOYR	-	2500	97 555= 566=
MIL	-	2500	92 83 555= 568= 560 570
THE VARIABLE= MILD - IS USED BEFORE IT IS DEFINED			
MILD	-	569	570=
MIR	-	2500	95 86 559= 555= 566 567
THE VARIABLE= MIRLD - IS USED BEFORE IT IS DEFINED			
MIRLD	-	566	557=
IAP	-	500	
IC	-	600	
ICDSP	-	200	
ICP	-	500	

* *

Figure G.6. (Continued)

* LINT	-	72*			
MICNT	-	201			
MIFCR	-	200			
MONDIG	-	603			
* MACVAC	-	22*			
NADCS	-	601			
NCHATA	-	601			
NCLOSE	-	66#	273	371	406
NCON	-	600			
NCONSL	-	600			
NDAACS	-	603			
NEP:FE	-	201			
NGFF	-	401			
NICS	-	600			
NOSIM	-	200			
NPCS	-	603			
NPLNT	-	401			
NPLNT2	-	600			
NPLN	-	300			
NPLN2	-	300			
NPLN3	-	300			
NPLN4	-	300			
NPLN5	-	300			
NPLN6	-	300			
NPLN7	-	300			
NPLN8	-	300			
NPLN9	-	300			
NPLN10	-	300			
NPLN11	-	300			
NPLN12	-	300			
NPLN13	-	300			
NPLN14	-	300			
NPLN15	-	300			
NPLN16	-	300			
NPLN17	-	300			
NPLN18	-	300			
NPLN19	-	300			
NPLN20	-	300			
NPLN21	-	300			
NPLN22	-	300			
NPLN23	-	300			
NPLN24	-	300			
NPLN25	-	300			
NPLN26	-	300			
NPLN27	-	300			
NPLN28	-	300			
NPLN29	-	300			
NPLN30	-	300			
NPLN31	-	300			
NPLN32	-	300			
NPLN33	-	300			
NPLN34	-	300			
NPLN35	-	300			
NPLN36	-	300			
NPLN37	-	300			
NPLN38	-	300			
NPLN39	-	300			
NPLN40	-	300			
NPLN41	-	300			
NPLN42	-	300			
NPLN43	-	300			
NPLN44	-	300			
NPLN45	-	300			
NPLN46	-	300			
NPLN47	-	300			
NPLN48	-	300			
NPLN49	-	300			
NPLN50	-	300			
NPLN51	-	300			
NPLN52	-	300			
NPLN53	-	300			
NPLN54	-	300			
NPLN55	-	300			
NPLN56	-	300			
NPLN57	-	300			
NPLN58	-	300			
NPLN59	-	300			
NPLN60	-	300			
NPLN61	-	300			
NPLN62	-	300			
NPLN63	-	300			
NPLN64	-	300			
NPLN65	-	300			
NPLN66	-	300			
NPLN67	-	300			
NPLN68	-	300			
NPLN69	-	300			
NPLN70	-	300			
NPLN71	-	300			
NPLN72	-	300			
NPLN73	-	300			
NPLN74	-	300			
NPLN75	-	300			
NPLN76	-	300			
NPLN77	-	300			
NPLN78	-	300			
NPLN79	-	300			
NPLN80	-	300			
NPLN81	-	300			
NPLN82	-	300			
NPLN83	-	300			
NPLN84	-	300			
NPLN85	-	300			
NPLN86	-	300			
NPLN87	-	300			
NPLN88	-	300			
NPLN89	-	300			
NPLN90	-	300			
NPLN91	-	300			
NPLN92	-	300			
NPLN93	-	300			
NPLN94	-	300			
NPLN95	-	300			
NPLN96	-	300			
NPLN97	-	300			
NPLN98	-	300			
NPLN99	-	300			
NPLN100	-	300			
NPLN101	-	300			
NPLN102	-	300			
NPLN103	-	300			
NPLN104	-	300			
NPLN105	-	300			
NPLN106	-	300			
NPLN107	-	300			
NPLN108	-	300			
NPLN109	-	300			
NPLN110	-	300			
NPLN111	-	300			
NPLN112	-	300			
NPLN113	-	300			
NPLN114	-	300			
NPLN115	-	300			
NPLN116	-	300			
NPLN117	-	300			
NPLN118	-	300			
NPLN119	-	300			
NPLN120	-	300			
NPLN121	-	300			
NPLN122	-	300			
NPLN123	-	300			
NPLN124	-	300			
NPLN125	-	300			
NPLN126	-	300			
NPLN127	-	300			
NPLN128	-	300			
NPLN129	-	300			
NPLN130	-	300			
NPLN131	-	300			
NPLN132	-	300			
NPLN133	-	300			
NPLN134	-	300			
NPLN135	-	300			
NPLN136	-	300			
NPLN137	-	300			
NPLN138	-	300			
NPLN139	-	300			
NPLN140	-	300			
NPLN141	-	300			
NPLN142	-	300			
NPLN143	-	300			
NPLN144	-	300			
NPLN145	-	300			
NPLN146	-	300			
NPLN147	-	300			
NPLN148	-	300			
NPLN149	-	300			
NPLN150	-	300			
NPLN151	-	300			
NPLN152	-	300			
NPLN153	-	300			
NPLN154	-	300			
NPLN155	-	300			
NPLN156	-	300			
NPLN157	-	300			
NPLN158	-	300			
NPLN159	-	300			
NPLN160	-	300			
NPLN161	-	300			
NPLN162	-	300			
NPLN163	-	300			
NPLN164	-	300			
NPLN165	-	300			
NPLN166	-	300			
NPLN167	-	300			
NPLN168	-	300			
NPLN169	-	300			
NPLN170	-	300			
NPLN171	-	300			
NPLN172	-	300			
NPLN173	-	300			
NPLN174	-	300			
NPLN175	-	300			
NPLN176	-	300			
NPLN177	-	300			
NPLN178	-	300			
NPLN179	-	300			
NPLN180	-	300			
NPLN181	-	300			
NPLN182	-	300			
NPLN183	-	300			
NPLN184	-	300			
NPLN185	-	300			
NPLN186	-	300			
NPLN187	-	300			
NPLN188	-	300			
NPLN189	-	300			
NPLN190	-	300			
NPLN191	-	300			
NPLN192	-	300			
NPLN193	-	300			
NPLN194	-	300			
NPLN195	-	300			
NPLN196	-	300			
NPLN197	-	300			
NPLN198	-	300			
NPLN199	-	300			
NPLN200	-	300			
NPLN201	-	300			
NPLN202	-	300			
NPLN203	-	300			
NPLN204	-	300			
NPLN205	-	300			
NPLN206	-	300			
NPLN207	-	300			
NPLN208	-	300			
NPLN209	-	300			
NPLN210	-	300			
NPLN211	-	300			
NPLN212	-	300			
NPLN213	-	300			
NPLN214	-	300			
NPLN215	-	300			
NPLN216	-	300			
NPLN217	-	300			
NPLN218	-	300			
NPLN219	-	300			
NPLN220	-	300			
NPLN221	-	300			
NPLN222	-	300			
NPLN223	-	300			
NPLN224	-	300			
NPLN225	-	300			
NPLN226	-	300			
NPLN227	-	300			
NPLN228	-	300			
NPLN229	-	300			
NPLN230	-	300			
NPLN231	-	300			
NPLN232	-	300			
NPLN233	-	300			
NPLN234	-	300			
NPLN235	-	300			
NPLN236	-	300			
NPLN237	-	300			
NPLN238	-	300			
NPLN239	-	300			
NPLN240	-	300			
NPLN241	-	300			
NPLN242	-	300			
NPLN243	-	300			
NPLN244	-	300			
NPLN245	-	300			
NPLN246	-	300			
NPLN247	-	300			
NPLN248	-	300			
NPLN249	-	300			
NPLN250	-	300			
NPLN251	-	300			
NPLN252	-	300			
NPLN253	-	300			
NPLN254	-	300			
NPLN255	-	300			
NPLN256	-	300			
NPLN257	-	300			
NPLN258	-	300			
NPLN259	-	300			
NPLN260	-	300			
NPLN261	-	300			
NPLN262	-	300			
NPLN263	-	300			
NPLN264	-	300			
NPLN265	-	300			
NPLN266	-	300			
NPLN267	-	300			
NPLN268	-	300			
NPLN269	-	300			
NPLN270	-	300			
NPLN271	-	300			
NPLN272	-	300			
NPLN273	-	300			
NPLN274	-	300			
NPLN275	-	300			
NPLN276	-	300			
NPLN277	-	300			
NPLN278	-	300			
NPLN279	-	300			
NPLN280	-	300			
NPLN281	-	300			
NPLN282	-	300			
NPLN283	-	300			
NPLN284	-	300			
NPLN285	-	300			
NPLN286	-	300			
NPLN287	-	300			
NPLN288	-	300			
NPLN289	-	300			
NPLN290	-	300			
NPLN291	-	300			
NPLN29					

SURROJTING RTFAST

I N D E X

RR11	-	2100			
RR12	-	2100			
RTFAST	-	1*			
RTPASS	-	9*			
SALHT	-	2500	398AC	497	499
SALLN	-	2200			514
SALLW	-	2400	313=	351	352
SALRN	-	2200			
SALRW	-	2400	321=	355	356
SAVINW	-	2400			
SAVZET	-	2400			
SRETLN	-	2200			
SRETLW	-	2400	323=	353	
SRETRN	-	2200			
SRETRW	-	2400	325=	357	
SRETSO	-	2600	465AC	409	414
SRECAF	-	2300			
SREPR	-	1100			
SRE5AF	-	2400			
SRWPR	-	1100			
SO1	-	2100			
SCADAC1	-	200	373		
SCADAC2	-	900			
SCADAC3	-	900			
SCADAC4	-	900			
SCDAC1	-	900	458AC		
SCDAC2	-	900			
SCDAC3	-	900			
SCDAC4	-	900			
SC1	-	1500	578		
SC2	-	1500	578		
SEPLM	-	2400	335AC	339	340
SEPRM	-	2400	336AC	342	343
SEHFL	-	2400			
SEHFR	-	2400			
SEPL	-	2400			
SEPLM	-	2400			
SEPMF	-	2400			
SEPR	-	2400			
SEPL	-	2400			
SEPR	-	2400			
SESEL	-	2400			
SESER	-	2400			
SETI	-	2400			
SETR	-	2400			
SEVML	-	2400			
SEVMR	-	2400			
SE	-	1100			
SEKSEF	-	620=	521=	472	
SEMLW	-	2400	275=	276=	279
SESHW	-	2400	277=	278=	280
SEH	-	1100			
SEHLY	-	1400			
SEHPP	-	1400			
SEHPP	-	1400			

* *

Figure G.6. (Continued)

SK21	1100						
SK22	1100						
SK23	1100						
SK24	1100						
SK25	1100						
SK26	1100						
SK27	1100						
SK28	1100						
SK29	1100						
SK30	1100						
SK31	1100						
SK32	1100						
SK33	1100						
SK34	1100						
SK35	1100						
SK36	1100						
SK37	1100						
SK38	1100						
SK39	1100						
SK40	1100						
SK41	1100						
SK42	1100						
SK43	1100						
SK44	1100						
SK45	1100						
SK46	1100						
SK47	1100						
SK48	1100						
SK49	1100						
SK50	1100						
SK51	1100						
SK52	1100						
SK53	1100						
SK54	1100						
SK55	1100						
SK56	1100						
SK57	1100						
SK58	1100						
SK59	1100						
SK60	1100						
SK61	1100						
SK62	1100						
SK63	1100						
SK64	1100						
SK65	1100						
SK66	1100						
SK67	1100						
SK68	1100						
SK69	1100						
SK70	1100						
SK71	1100						
SK72	1100						
SK73	1100						
SK74	1100						
SK75	1100						
SK76	1100						
SK77	1100						
SK78	1100						
SK79	1100						
SK80	1100						
SK81	1100						
SK82	1100						
SK83	1100						
SK84	1100						
SK85	1100						
SK86	1100						
SK87	1100						
SK88	1100						
SK89	1100						
SK90	1100						
SK91	1100						
SK92	1100						
SK93	1100						
SK94	1100						
SK95	1100						
SK96	1100						
SK97	1100						
SK98	1100						
SK99	1100						
SK100	1100						
SK101	1100						
SK102	1100						
SK103	1100						
SK104	1100						
SK105	1100						
SK106	1100						
SK107	1100						
SK108	1100						
SK109	1100						
SK110	1100						
SK111	1100						
SK112	1100						
SK113	1100						
SK114	1100						
SK115	1100						
SK116	1100						
SK117	1100						
SK118	1100						
SK119	1100						
SK120	1100						
SK121	1100						
SK122	1100						
SK123	1100						
SK124	1100						
SK125	1100						
SK126	1100						
SK127	1100						
SK128	1100						
SK129	1100						
SK130	1100						
SK131	1100						
SK132	1100						
SK133	1100						
SK134	1100						
SK135	1100						
SK136	1100						
SK137	1100						
SK138	1100						
SK139	1100						
SK140	1100						
SK141	1100						
SK142	1100						
SK143	1100						
SK144	1100						
SK145	1100						
SK146	1100						
SK147	1100						
SK148	1100						
SK149	1100						
SK150	1100						
SK151	1100						
SK152	1100						
SK153	1100						
SK154	1100						
SK155	1100						
SK156	1100						
SK157	1100						
SK158	1100						
SK159	1100						
SK160	1100						
SK161	1100						
SK162	1100						
SK163	1100						
SK164	1100						
SK165	1100						
SK166	1100						
SK167	1100						
SK168	1100						
SK169	1100						
SK170	1100						
SK171	1100						
SK172	1100						
SK173	1100						
SK174	1100						
SK175	1100						
SK176	1100						
SK177	1100						
SK178	1100						
SK179	1100						
SK180	1100						
SK181	1100						
SK182	1100						
SK183	1100						
SK184	1100						
SK185	1100						
SK186	1100						
SK187	1100						
SK188	1100						
SK189	1100						
SK190	1100						
SK191	1100						
SK192	1100						
SK193	1100						
SK194	1100						
SK195	1100						
SK196	1100						
SK197	1100						
SK198	1100						
SK199	1100						
SK200	1100						
SK201	1100						
SK202	1100						
SK203	1100						
SK204	1100						
SK205	1100						
SK206	1100						
SK207	1100						
SK208	1100						
SK209	1100						
SK210	1100						
SK211	1100						
SK212	1100						
SK213	1100						
SK214	1100						
SK215	1100						
SK216	1100						
SK217	1100						
SK218	1100						
SK219	1100						
SK220	1100						
SK221	1100						
SK222	1100						
SK223	1100						
SK224	1100						
SK225	1100						
SK226	1100						
SK227	1100						
SK228	1100						
SK229	1100						
SK230	1100						
SK231	1100						
SK232	1100						
SK233	1100						
SK234	1100						
SK235	1100						
SK236	1100						
SK237	1100		</				

SUBROUTINE REFERENCE

I N D E X

SCALING	240	777=	280=	364	356
SS-INTL	1600				
SS-INTP	1500				
STANLP	2400				
STANPR	2400				
SUMIXX	800				
SUMIXZ	800				
SUMIVV	800				
SUMIZZ	800				
SVSTAR	1400				
SVSTAR	2400				
SVSTARL	2400				
SMLG	400	517			
SMLG2	900				
SZINTL	1600				
SZINTP	1600				
TAILVP	26*				
TAIAC	1400				
TAUPBT	1500				
TAU-TP	1500				
TAU-DB	1500				
TAUDR	1500				
TAUFF	1500				
TAUSIC	1500				
TAUGLS	1500				
TAUGST	1500				
TAUMT	1100	313			
TAUL	600				
TAULR	2400				
TAUP	1500				
TAUPDS	1500				
TAUPHI	1500				
TAUPR	1500				
TAUPR1	1500				
TAUPR1	1500				
TAUQ1	1500				
TAUQ2	1500				
TAUR01	1500				
TAUR02	1500				
TAUR	2400				
TAUR1	1100				
TAUR2	1100				
TAUR1	1500				
TAUR2	1500				
TAUR3	1500				
TAUSHP	1500				
TAUTH	1500				
TAUTHE	1500				
TAUVT	1100	450			
TAUVEP	2400				
TCCOF	300				
TDEGF	1800				
TEAL	1800				
TEAR	1800				
TERMPI	2700	544=	503		

Figure G.6. (Continued)

SUBROUTINE ROSTER

I N D E X

Variable	1900	128#	131	62	90	107	113	120	121	125	130	131	605
UVT	1900	128#	131										
V	2700	52#	58										
VALFLW	1900	121#	207										
VALFRW	1900	125#	299										
VALFS	1900	60#	62										
VALNCL	1900												
VALNCP	1900												
VBETVT	1900	131#	444										
VEAST	1700	623											
VELVAP	19*												
VGNST	900	52											
VLM	1900	110#	118	207									
VLPR	1900	107#	110										
VLMSQ	1900	118#	271										
VNORTH	1700	610											
VP	1900	80#	93	86	107	113	120						
VPRIME	900	52											
VKL	1900	49#	95	134									
VLPR	1900	43#	89										
VPLVRL	1900	45#	101	104									
VRR	1900	92#	98	137									
VRRP	1900	86#	92										
VRRPR	1900	98#	100	105									
VRM	1900	116#	123	209									
VRPBR	1900	113#	114										
VRMSQ	1900	123#	272										
VSC	1900	58#	63	64									
VSTAR	2400												
VSTAR2	1400												
VSTARL	2400												
VTIPL	1900	155#	157										
VTIPL	1900	156#	158										
VTIPL	1900	63#											
VTOTAL	1900	101#	157	607									
VTOTAL	1900	102#	158	611									
VTRIM	2400	502											
VTRIM	300	452	453										
VSTILL	1900	129#	444										
VVT	1900	104#	133										
VZFTL	1900	105#	136										
VZFR	2700	53#	50	61	81								
W	900	386											
WDOT	900	53											
WGUST	1900	127#	195	254									
WHT	1900	111#	119	111									
WLW	1900	108#	109	111									
WLWDR	1900	119#	121	271									
WLWSQ	1900	24*											
WNGVAP	24*												
WNGVAP2	25*												
WORK	60	63	100	101	104	108	114	121	125	131	130	131	605
WP	1900	91#	84	87									
WPRIME	900	53											
WPL	1900	90#	96	102									
WRLPR	1900	94#	88	90									

Figure G.6. (Continued)

SUBROUTINE RTFAST

T N D F X

WRLWRL	-	1900	34=	101					
WROTL	-	1900	132=	104					
WROTR	-	103=	115	137					134
WRR	-	1900	93=	99					103
WRRPR	-	1900	47=	91					93
WRRWR	-	1900	99=	100					
WRW	-	1900	117=	124					298
WRWPR	-	1900	114=	115					117
WWSO	-	1900	124=	125					272
WSQ	-	1900	59=	60					64
WVT	-	1900	130=	131					63
XAERF	-	2000	523=	526					
XAERLW	-	2400	270=	352=					354
XAERNL	-	2300	263=	526					535
XAERNL	-	2300	247=	263					537
XAERNR	-	2300	255=	263					537
XAERQ	-	2700	526=	548					590
XAERRW	-	2400	290=	356=					351
XAERT	-	2600	517=	526					
XAERWG	-	2400	361=	365					526
XAIO	-	9*							
XAREP	-	2000	520						
XARHT	-	2600	497=	501					510
XARVT	-	2600	54=	508					510
XCG	-	1700	30	81					365
XCNTRL	-	15*							
XDTCC	-	1700	49=	70					
XF	-	2700							
XFAC	-	1100							
XFCON	-	800							
XFMLF	-	2700							
XFUNC	-	14*							
XHT	-	1100	127	501					502
XL	-	2700	619						508
XLGOS	-	2700							
XLJNTP	-	13*							
XLSTN	-	2700							
XMAP	-	10*							
XPAR1	-	11*							
XPAR3	-	20*							
XR	-	2700							
XRCOS	-	2700	606						
XRLCON	-	800							
XRSTN	-	2700							
XVT	-	1100	129	130					509
XW	-	2700							
XWAC	-	1100	107	109					354
XWCON	-	800							358
XWCZ	-	1100	295	286					
XWMLW	-	2700							
XXICON	-	800							
XXJCON	-	800							
XZICON	-	800							
YAERF	-	2000	521=	527					527
YAERLW	-	2400	291=	353=					362

*

*

*

*

*

*

Figure G.6. (Continued)

508 VOJTJIE RTEAST

I N D E X

YAERNC	-	2300	254#	527	533	537		
YAERNL	-	2300	255	264	264			
YAERNP	-	2300	256#	258	264			
YAERO	-	2700	277#	671				
YAERRW	-	2400	282#	357#	267			
YAERT	-	2600	511#	527				
YAEFAG	-	2400	362#	527				
YAEFEP	-	2900	521					
YARHT	-	2600	498#	500	532	511		
YARVT	-	2600	575#	509	509	511		
YN	-	1100	82	84	85	87	531	537
YPA	-	1100						
YMAC	-	1100	106	108	112	114		
YYJCON	-	RCO						
YYJCON	-	RCO						
ZAERE	-	2300	522#	529	287	351#	354	565
ZAERLW	-	2400	283#	285	287			574
ZAERNC	-	2300	255#	528	534			
ZAERNE	-	2300	249#	245	531	528	574	
ZAEPNR	-	2300	257#	255	531	555	571	
ZAEPN	-	2700	533#	546	551	564		
ZAERRW	-	2400	254#	236	287	350#	350	555
ZAERT	-	2400	512#	505				571
ZAEPJG	-	2400	463#	355	423			
ZAEFP	-	2300	527					
ZARHT	-	2600	499#	531	532			
ZAPRC	-	528#	535	533				
ZAPVJ	-	528#	536	433				
ZARVT	-	2400	574#	518	519			
ZCG	-	1700	79	81	80	800	601	537
ZDTCG	-	1700	57#	91	90			532
ZETHL	-	2300	134#	135AC				535
ZETHD	-	2300	137#	137B				
ZETRI	-	2400						
ZETRD	-	2400						
ZETP3	-	2400						
ZETP4	-	2400						
ZF	-	2700						
ZFAC	-	1100						
ZFCOJN	-	RCO						
ZFMPHF	-	2700						
ZMT	-	1100	126	500	401			
ZL	-	2700						
ZLCOJN	-	2700						
ZLSTH	-	2700						
ZPA	-	1100						
ZR	-	2700						
ZRCOS	-	2700						
ZRLCOJN	-	RCO						
ZRSIN	-	2700	576	129	537	508		
ZVT	-	1100	128					
ZW	-	2700						
ZWAC	-	1100	106	107	112	113	354	355
ZWCOJN	-	RCO						
ZWMMHW	-	2700						

Figure G.6. (Continued)

I N D E X

ZZJCON - ACO
ZZJCON - BCO



Figure G.6. (Continued)

SUBROUTINE RTSLOW

I N D E X

```

*SK44 ,SK47 ,SK48 ,SK49 ,SK50 ,SL ,SLF ,SLPA ,SLW , 99 TO 97
*SM ,SMW ,SPAN ,TAUHT ,TAUVT ,XFAC ,XHT , 98 TO 106
*XMAC ,XVT ,YPA ,YMAC ,ZFAC ,ZHT ,ZPA ,ZMAC ,
*ZVT ,CLOAD ,PHIPH ,SK37HI ,EM2REF ,XMC2 ,BT1 ,BT2 ,BT3 ,
*SKDI1 ,RKDZ1 ,RKMT ,BKMT ,BKMT ,BKMT ,SK31HI ,
*FEU ,CLMAX ,ALBRK ,BKLSW ,BKNSW ,SQPRM ,DEG20 ,DGTORD ,HTVTKT , 133 TO 141
*PIQV2 ,PDTODG ,ROTEPS ,SKFES ,ALNCBK ,TAURTI ,TAURT2
COMMON/SPIN/ RCBI(19),ISTRBI,IADCC(32)
COMMON/XLINTP/ AKY(16),AMEY(2),BKEY(16),BMEY(2),CKEY(10),GHEM
COMMON/XFUNC / VSTAR(33),TAUAG(9),SVSTAB(33,9),SOFARG(35),
1 GAATAR(35),GBATAR(35),ALFTAB(35)
COMMON/ZINIVR/
1 AVFIN ,CILAML,CILAMR,COSINL,COSINR,COSPSI,CZINL ,CZINR ,DLFSSQ, 1 - 9
2 HSO ,SILAML,SILAMR,SININL,SININR,SINPSI,SSQINL,SSQINR,SZINL , 10 - 18
3 SZINR
COMMON/CGGTVR/
1 VEAST ,VNRTH,XCG ,XDTCG ,ZCG ,ZDTCG 1 - 6
COMMON/ZENGVAR/
1 AMACH ,AMACSQ,DEL ,EMAXY1,EMAXY2,EMXADT,ENZSTR,FSMACH,OMEGEL, 1 - 9
2 DMFGR,DMOVTC,DOVFSM,DOVSOH,DVTHDL,ROE ,ROE0V2,SHPPRL,SHPPRR, 10 - 18
3 S4A ,SQNHMX,SQTHIC,SQWDTX,TJEGF ,TEAL ,TEAR ,TMCDL,THETC 19 - 27
4,PCQL,PCQTR
COMMON/VELVAR/
1 AMUL ,AMULSQ,AMUR ,AMJRSQ,AROTL ,OMDIL ,OMDTR ,OMEGAL,OMEGAR, 1 - 9
2 OMSQL ,OMSOR ,LHT ,UL4 ,ULMPR ,ULMSQ ,UP ,JRL ,URLPR , 10 - 18
3 URLURL,URP ,URRPR ,URRURR,URW ,URWPR ,JMSQ ,USQ ,UVT , 19 - 27
4 VALFLM,VALFRM,VALFS ,VALNCL,VALNCR,VBFTVT,VLW ,VLMWR ,VMSQ , 28 - 36
5 VP ,VRL ,VRLPR ,VRLVRL,VRR ,VRRPR ,VRRVRR,VRRM ,VRRPR , 37 - 45
6 VPSQ ,VSO ,VTIPL ,VTIPR ,VTOTAL,VTOTLR,VTOTR,VTVT ,VZETL , 46 - 54
7 VZETR ,VHT ,VWL ,VWLPR ,VMSQ ,VW ,VRL ,VRLPR ,VRLVRL, 55 - 53
9 WRW ,WRWPR ,WRMSQ ,WR3 ,WRRPR ,WRRRRR,WSQ ,WVT 64 - 71
COMMON/FUSVAR/
1 ALARF ,ALAPEP,ALFSD ,ALPHF ,AMARF ,AMARFP ,ANARF ,AVARFP,REAF , 1 - 9
2 RTTFSQ,CRCMF ,CDF ,CLF ,CMF ,CNF ,COSALF,COSBF,CYF , 10 - 18
3 DLG ,DLG ,DNLG ,DXLG ,DYLG ,QFSW ,QFSW ,SBSFCAF,SBESAF, 19 - 27
4 SINALF,SINRTF,SOF ,XAEPE ,XARFP ,YAERF ,YARFP ,ZARFP , 28 - 36
* ,SINTHE,COSTHF,SINPHI,COSPHI
COMMON/GFEVAR/
1 AGVAT,AGVAM,RIGX ,RK99 ,RMOVTL,BMOVTR,CORCOR,CLTCOR,CLMCR, 1 - 9
2 DOVTL ,DOVTR ,EPPPM ,GEF ,HGEFLR,HGEFRR,HLHUB ,HRMUR ,HTC4 , 10 - 18
3 HWC4 ,PRI1 ,PRI2 ,SRI ,TISEL ,TIGER 19 - 24
COMMON/NACVAR/
1 ALLNSQ,ALPHLN,ALPHRN,ALPNSQ,BETALN,BETARN,BTLNSQ,BTRNSQ,CALLY , 1 - 9
2 CALPN ,CBFTLN,CBETRN,CDLN ,CCLN ,CDDN ,CDSN ,CLLN ,CLRN , 10 - 18
3 CLN ,CMPN ,CNLN ,CMRN ,CYLN ,CYRN ,DLNLC ,DLNLC ,DMLNC , 19 - 27
4 DMNLC ,DNLNC ,DNPNC ,DXLNC ,DXRNC ,DYRNC ,DZLNC ,DZLNC , 27 - 36
5 SALLN ,SALRN ,SBFTLN,SBETRN,SQLNC ,SQRNC ,TNAI ,TNACZ 36 - 44
COMMON/ROTVAR/
1 ATCL ,ATCLDP,AIIC ,AICROP,ALARNC,ALLRH ,ALARNL,ALARNR,ALRRH , 1 - 9
2 ALPLR ,ALPHRR,AMARNC ,AMARNL,AMARNR,ANLRH ,AMRNL ,AMNRP,ANROTL , 10 - 18
3 AMROT ,AMRPH ,ANARNC ,ANARNL,ANARNR,ANLRH ,ANROTL,ANROTR,ANRRH , 19 - 27
4 RCL ,RCLDP,BIC ,BICRDP,CNFALL,CNFAIR,CNFBIL,CNFBIR,CNFL , 28 - 36
5 CNFR ,COSZHL,COSZHR,CPMAIL,CPMAIR,CPMBIL,CPMBIR,CPML ,CPMR , 37 - 45
6 CSFALL,CSFAIR,CSFBIL,CSFAIR,CSFL ,CSFR ,CYL ,CYR ,CYMAIL , 46 - 54
7 CYNMIP,CYNMIL,CYNMIR,CYNL ,CYNR ,FIPOML,FIPOMR,FNDRML,FNDRMR, 55 - 63

```

Figure G.6. (Continued)

SUBROUTINE RTSLOW

1 N T F X

9 FSIDL,FSIDER,PVNL,PHLR,PNRN,PNRR,QNLN,QNLR,QVYN, 64 - 72
 9 QVER,QVNL,QVNL,PNRP,RVRQ,RDP1R4,ROPIP5,SRP2CL,SHPROR, 73 - 81
 4 STRZHL,STRZHP,STL,STPOL,STOPQR,STR,STRMA1,TERMA2,TRMA3, 82 - 90
 4 TRMA4,TMHA1,TRMH12,TRM4NG,CATRML,XAERNK,YAERNC,YAEPNL,YAERNP, 91 - 99
 6 ZAE13C,ZAE1NL,ZAERNP,ZETHL,ZET14 100 - 108

22

COMMON/MSGVAR/
 1 ALAPHC,ALLMPR,ALPHLM,ALPHRM,ALRGLM,ALRGRM,ALRMRP,ALMSSD,AMARL4, 1 - 9
 2 AMARRM,AMR4WG,AMRWC,AMILM,AP1RM,ARUSSD,ATAULR,ATAURR,AVEALR, 10 - 19
 3 AVFALL,AVFCLM,AVECTS,AVEEPP,AVEZET,BETALA,BETAR4,AKALPR,AKARPR, 19 - 27
 4 CALL4,CALM4,CAVINM,CAVZET,CRETL4,CRETRM,CEPLM,CEPRM,CDCNL, 28 - 36
 5 CDNTR,CDM4,CDLWAD,CDLWPR,CDLWSS,CDR4AD,CDR4PR,CDR4SS,CDSLM, 37 - 45
 6 COSRM,CLAVE,CLCNL,CLCNTR,CLCNM,CLILM,CLIPM,CLLWAD,CLLMPR, 46 - 54
 7 CLLWSS,CLWAD,CLWRPR,CLWRSS,CLWSLM,CLSLM,CLZRO,CMCNL, 55 - 63
 8 CMNTE,CMWAD,CMWSS,CMWAD,CMRWS,CMSLM,CMSR4,CMSM,CTAULR, 64 - 72
 9 CTAURP,CTSLR,CTSRP,DCDOF,DCDLA,DCOLSP,DCDRDA,DCDRSP,DCDF, 73 - 81
 4 DELLVA,DELLSP,DELRPA,DELRSP,DELSM,DCNDF,DCMLD,DCMLSP,DCMRDA, 92 - 90
 4 DCMRSP,DCNDF,DEPLR,DEPLR,EPDRP,EPMEL,EPHAR,PELSL, 91 - 99
 6 DESSD,SAILM,SALM,SAZINH,SAVZE,SBEL4,SBETP4,SEPRM,SEPRM, 100 - 108
 7 SPMH,SPM4,SPM4,SPM4,SPM4,SPM4,SPM4,SPM4,SPM4,SPM4, 109 - 117
 8 SVST4,SVST4,SVST4,SVST4,SVST4,SVST4,SVST4,SVST4,SVST4, 118 - 126
 9 TAVAR,TRMGL1,TRMWS,TRMWS,TRMWS,TRMWS,TRMWS,TRMWS,TRMWS, 127 - 135
 4 TZETA,TZETA,TZETA,TVSTAR,VSTAR,VSTAR,XAE1,XAEP4,XAEP4, 136 - 144
 4 YAEPR,YAERMG,ZAERML,ZAERML,ZETA1,ZET2,ZET3,ZET4,ZET4, 145 - 153

23

1 YK24,TRMWS,XMGL1,XMGL1,XMGL1,XMGL1,XMGL1,XMGL1,XMGL1,XMGL1, 1 - 9
 2 XIDTP,XIDTP,XIDTP,XIDTP,XIDTP,XIDTP,XIDTP,XIDTP,XIDTP,XIDTP, 10 - 18
 3 XMPV/TAI14/ 19 - 27

24

1 ALAHT,ALAPT,ALAVT,ALPHHT,ALPHVT,AMARIT,AMART,AMAVT,ANAKHI, 1 - 9
 2 ANART,ANAVT,AREVT,CAHHT,CRETS,CNHI,COVT,CLHT,CYVT, 10 - 18
 3 EPAIL,EPFRO,SALHT,SHETS,SIGMA,TRMHT,TRMVT,XAERT,XARHT, 19 - 27
 4 XAPVT,XAHT,XARHT,XAVT,XAERT,XARHT,XARHT,XAVT,EPIL,ALMTP, 28 TO 36
 5 ALHTE,ALHTP,ALHTM,CLAT,TRMHT2,TRMHT3,CLHTST,CDHTST,ALVTPR, 37 TO 45
 6 ALVTE,ALVTP,ALVTP,ALVTP,ALVTP,TRMVT2,TRMVT3,CVVTST,COVST, 46 TO 53

25

COMMON/COMVAR/
 1 ALAERO,AMAFRO,AMAFRO,CM14,FLIX,FIKZP,FIKZP,FIKZP,FIKZP, 1 - 9
 2 FIZZ,FIJX,FIJY,FIJZ,FIKX,COVIVY,COVIZP,PO,PG, 10 - 18
 3 FRO,FR,FR,FR,FR,FR,FR,FR,FR,FR,FR,FR,FR,FR,FR,FR,FR,FR,FR, 19 - 27
 4 FRO,FR,FR,FR,FR,FR,FR,FR,FR,FR,FR,FR,FR,FR,FR,FR,FR,FR,FR, 28 TO 36
 5 FRO,FR,FR,FR,FR,FR,FR,FR,FR,FR,FR,FR,FR,FR,FR,FR,FR,FR,FR, 37 TO 45
 6 FRO,FR,FR,FR,FR,FR,FR,FR,FR,FR,FR,FR,FR,FR,FR,FR,FR,FR,FR, 46 TO 53
 7 FRO,FR,FR,FR,FR,FR,FR,FR,FR,FR,FR,FR,FR,FR,FR,FR,FR,FR,FR, 54 TO 62
 8 FRO,FR,FR,FR,FR,FR,FR,FR,FR,FR,FR,FR,FR,FR,FR,FR,FR,FR,FR, 63 TO 71
 9 FRO,FR,FR,FR,FR,FR,FR,FR,FR,FR,FR,FR,FR,FR,FR,FR,FR,FR,FR, 72 TO 80
 0 FRO,FR,FR,FR,FR,FR,FR,FR,FR,FR,FR,FR,FR,FR,FR,FR,FR,FR,FR, 81 TO 89
 1 FRO,FR,FR,FR,FR,FR,FR,FR,FR,FR,FR,FR,FR,FR,FR,FR,FR,FR,FR, 90 TO 98
 2 FRO,FR,FR,FR,FR,FR,FR,FR,FR,FR,FR,FR,FR,FR,FR,FR,FR,FR,FR, 99 TO 107
 3 FRO,FR,FR,FR,FR,FR,FR,FR,FR,FR,FR,FR,FR,FR,FR,FR,FR,FR,FR, 108 TO 116
 4 FRO,FR,FR,FR,FR,FR,FR,FR,FR,FR,FR,FR,FR,FR,FR,FR,FR,FR,FR, 117 TO 125
 5 FRO,FR,FR,FR,FR,FR,FR,FR,FR,FR,FR,FR,FR,FR,FR,FR,FR,FR,FR, 126 TO 134
 6 FRO,FR,FR,FR,FR,FR,FR,FR,FR,FR,FR,FR,FR,FR,FR,FR,FR,FR,FR, 135 TO 143
 7 FRO,FR,FR,FR,FR,FR,FR,FR,FR,FR,FR,FR,FR,FR,FR,FR,FR,FR,FR, 144 TO 152
 8 FRO,FR,FR,FR,FR,FR,FR,FR,FR,FR,FR,FR,FR,FR,FR,FR,FR,FR,FR, 153 TO 161
 9 FRO,FR,FR,FR,FR,FR,FR,FR,FR,FR,FR,FR,FR,FR,FR,FR,FR,FR,FR, 162 TO 170
 0 FRO,FR,FR,FR,FR,FR,FR,FR,FR,FR,FR,FR,FR,FR,FR,FR,FR,FR,FR, 171 TO 179

26

COMMON/EPAB3/
 1 CON51,CON52,CON53,CON54,CON55,CON56,CON57, 1 TO 7
 2 CON58,CON59,CON60,CON61,CON62,CON63,CON64,CON65,CON66,CON67, 8 TO 14
 3 CON68,CON69,CON70,CON71,CON72,CON73,CON74,CON75,CON76,CON77, 15 TO 21
 4 CON78,CON79,CON80,CON81,CON82,CON83,CON84,CON85,CON86,CON87, 22 TO 28
 5 CON88,CON89,CON90,CON91,CON92,CON93,CON94,CON95,CON96,CON97, 29 TO 35
 6 CON98,CON99,CON100,CON101,CON102,CON103,CON104,CON105,CON106, 36 TO 42
 7 CON107,CON108,CON109,CON110,CON111,CON112,CON113,CON114,CON115, 43 TO 49
 8 CON116,CON117,CON118,CON119,CON120,CON121,CON122,CON123,CON124, 50 TO 56
 9 CON125,CON126,CON127,CON128,CON129,CON130,CON131,CON132,CON133, 57 TO 63
 0 CON134,CON135,CON136,CON137,CON138,CON139,CON140,CON141,CON142, 64 TO 70
 1 CON143,CON144,CON145,CON146,CON147,CON148,CON149,CON150,CON151, 71 TO 77
 2 CON152,CON153,CON154,CON155,CON156,CON157,CON158,CON159,CON160, 78 TO 84
 3 CON161,CON162,CON163,CON164,CON165,CON166,CON167,CON168,CON169, 85 TO 91

Figure G.6. (Continued)

10670112
11370116

SUBROUTINE RTSLOW

I N D E X

```

D      *SFLL *SFNL *SFSL *SFMH *SFMH *SFQL *SFPL *
E      *SFNR *SFNR *SFNR *SFMH *SFMH *SFQR *SFQR *
F      *CONS71 *CONS72 *CONS73 *CONS74 *CONS75 *CONS76 *CONS77
G      *CONS78 *CONS79 *CONS80 *CONS81
      *PRE-COOKED COEFFICIENTS DEFINITION 0
      TABLE OF PRE-COOKED COEFFICIENTS DEFINITION 0
XFCO1 = SL*(1.-SMF/SM) -SLW*SMW/SM
ZFCO1 = SHF*(1.-SMF/SM) -SHW*SMW/SM
XWCO1 = SLW*(1.-SMH/SM) -SLF*SMF/SM
ZWCO1 = SHW*(1.-SMH/SM) -SHF*SMF/SM
XRLCO1 = -(SMF*SLF +SMW*SLW)/SM
ZRLCO1 = -(SMF*SHF +SMW*SHW)/SM
XXICO1 = SUMIXX + 2.*SMN*YN*YN
YYICO1 = SUMIYY
ZZICO1 = SUMIZZ + 2.*SMH* YN*YN
XZICO1 = FIXZF + FIXZM
XXJCO1 = SUMIZZ -SUMIYY +2.*SMN*YN*YN
YYJCO1 = (FIXXF -FIXZF)*(FIXXK-FIXZM)
ZZJCO1 = (SUMIYY-SLMTXX) -2.*SMH* YN*YN
COEF1 = SL*SMH/SM
COEF2 = SL*(1.-SMN/SM)
COEF3 = FIXXPR -FIXZPR
COEF4 = SL*SMN
COEF5 = SMF * SHF
COEF6 = SMW * SHW
COEF7 = SMF * SLF
COEF8 = SMW * SLW
COEF9 = SL*SMN*YN
CCEF10 = 1. / SM
COEF11 = BKLSM*AVEYAC/2./SPAN
COEF12 = BKNSM*AVEYAC/2./SPAN
COEF13 = (FIYPR+SL*SL*SMN*(1.-SMN/SM))
COEF16 = ARFAM*SPAN
COEF17 = CHORD/SPAN (C / B) * WING CHARACTERISTICS
COEF18 = S / 2
COEF19 = PI*ROTRAD*ROTRAD*ROTRAD*ROTRAD
COEF20 = COEF19 * ROTRAJ
COEF21 = 1./10.5*PI * ARHT)
COEF22 = 1./10.5*PI * ARVT)
COEF23 = AREAHT * EFFHT
COEF24 = AREAVT * EFFVT
COEF25 = 1./12.*PI* ROTRAD*ROTRAD)
COEF26 = CHORD / 2.
COEF27 = 1./CHORD/CHORD
COEF28 = 1./ARFAM/2.)
COEF29 = PI * ARWING
COEF30 = 1./PI*ARWING)
COEF31 = S * C / 2
COEF32 = S * C / 2 *CLALPH*(DCMDCL*YMAC/C )
COEF33 = S * C / 2 *CLALPH*(DCMDCL*YMAC/C ) *4/3/PI *YN/YMAC
COEF34 = YMAC / YN / K T4 TWIST
COEF35 = B * B
      TABLE OF INTERMEDIATE CALCULATIONS
ZRSIN = ZP* SIN(INR-LAMDA)
ZRCOS = ZR* COS(INR-LAMDA)
XPSIN = XR* SIN(INR-LAMDA)

```

Figure G.6. (Continued)

SUBROUTINE RTSLOW

I N D E X

```

C      XPRES = XP* COS(INR-LAMDA)
C      ZLSIN = ZI* SIN(INL-LAMDA)
C      ZLCS = ZI* COS(INL-LAMDA)
C      XLSIN = XI* SIN(INL-LAMDA)
C      X LCS = XI* COS(INL-LAMDA)
C      ZPWHF = SMF* SHF * ZF
C      ZPWHF = SMW* SHW * ZW
C      XF4LF = SMF* SLF * XF
C      XW4LW = SMW* SLW * XW
C      TERMI = (IXPR-17PI)*SSQINR + SSQINL)
C      TERM2 = (IXPR)*S2INR +S2INL)
C      TERM3 = (SL*SMI)*(ZRSIN +ZLSIN)
C      TERM4 = (IXPR-17PI)*(S2INR +S2INL) * 0.5
C      TERM5 = IXPR *(C2INR+C2INL)
C      TERM6 = (SL*SMN) *(IXRCS + XLCOS)
C      DOWIXX = 1./E1XX
C      DOWIYY = 1./E1YY
C      DOWIZZ = 1./E1ZZ
C      PQ = P*Q
C      RR = R*R
C      PR = P*R
C      RP = R*P
C      FOR BIT CALC USE FOLLOWING TRIG IDENTITIES WHERE
C      A = INCIDENCE ANGLE INR,INL R = LAMDA
C      COS(A-R) = COS(A)*COS(-R) -SIN(A)*SIN(-R)
C      COS(A+B) = COS(A)*COS(B) +SIN(A)*SIN(B)
C      SIN(A-R) = SIN(A)*COS(-B) +COS(A)*SIN(-R)
C      SIN(A+B) = SIN(A)*COS(B) -COS(A)*SIN(B)
C      SIN(2A) = 2.*SIN(A)*COS(A)
C      COS(2A) = 1. - 2.*SIN(A)*SIN(A)
C
C      DISCRETE LINE ALLOCATION:
C      CONSOLF = 1
C
C      PIT NUMBER    DEG NUMBER    FUNCTION
C      31            17            PANIC
C      30            16            TRIM
C      29            15            CONSOLE OPERATE
C
C      HORIZONTAL TAIL
C      1. IF HWC/4 GT 50 FT.   GFF = 0.
C      2. IF V LE 30 FT.   TAIL AERO = 0.
C      3. IF DEL FLAP GT 75 DEG   EPSILON TAIL = 0.
C      4. IF CTS LT 0.5   EPSILON P = 0.
C      5. LIMIT RANGE OF ABS(ALPHHT) TO (ALHTSTALL - 2. DEG) AND
C      PRINT WARNING
C
C      VERTICAL TAIL
C      1. LIMIT THE RANGE OF ABS(ALPHVT) TO (ALVTSTALL -2 DEG) AND
C      PRINT WARNING
C      READ DISCRETES FROM ANALOGS
    
```

Figure G.6. (Continued)

SUBROUTINE RTSLOW

I N D E X

```

130 IF(HGEFRR,GE,DBRK13) GO TO 412
131 TIGER = (HGEFRR*HGEFRR*(CONS51+CONS52*AMUL)+HGEFRR*(CONS53*AMUL
* +CONS54) +CONS55 +CONS56*AMUL)
132 DOVT = BKDIT*HGEFRR*HGEFRR+HKD2T*HGEFRR+BKD3T
133 3MOVTR = BKMIT*HGEFRR*HGEFRR+9KM2T*HGEFRR+BKM3T
134 GO TO 413
135 TIGER = 1.0
412 DOVT = DOVT
136 3MOVTR = 3KM4T
137 9MOVTR = 9KM4T
413 CONTINUE
138 IF(AMJL,GE,DBRK12) GO TO 414
139 HLHUR = HRHUR +2.0*YN*SINPHI*COSTHE
140 HGEFLR = HLHUR/12.*ROTTRAD*(CONS50+ARCS(COSPHI*(SINTHE*COSINL +
* COSTHE*SININL)))
141
142 IF(NGFF,NE,1) GO TO 414
143 IF(HGEFLR,GE,DBRK13) GO TO 414
144 TIGEL = (HGEFLR*HGEFLR*(CONS51+CONS52*AMUL)+HGEFLR*(CONS53*AMUL
* + CONS54) +CONS55 +CONS56*AMUL)
145 3OVTL = BKDIT*HGEFLR*HGEFLR+9KD2T*HGEFLR+BKD3T
146 9MOVTL = 9KMIT*HGEFLR*HGEFLR+3KM2T*HGEFLR+BKM3T
147 GO TO 415
148 TIGEL = 1.0
149 DOVT = DOVT
150 3MOVTL = 3KM4T
415 CONTINUE

```

NACEILF AFFDYNAMICS

```

152 ALPHA = ATAN2(WRL,URL)
153 ALPHR = ATAN2(WRR,URR)
154 4FTALN = ATAN2(VRL,VALNCL)
155 3FTAPN = ATAN2(VRR,VALNCR)
156 CALL SINCOS(ALPHN,SALLN,CALLN)
157 CALL SINCOS(ALPHR,SALRN,CALRN)
158 CALL SINCOS(BETLN,SBETLN,CBETLN)
159 CALL SINCOS(BETARN,SBETARN,CBETARN)
160 TRMNC1 = SALLN*CALLN

```

(B L A N K C A R D)
(B L A N K C A R D)
(B L A N K C A R D)
(B L A N K C A R D)
(B L A N K C A R D)
(B L A N K C A R D)
(B L A N K C A R D)
(B L A N K C A R D)
(B L A N K C A R D)
(B L A N K C A R D)
(B L A N K C A R D)

Figure G.6. (Continued)

SURROUNTING RTSLDM

LINE

```

161 TRMNC3= SAL*CALPN
162 TRMNC3= SBFTL*CRETLN
163 TRMNC4= SBETPN*CRETPN

C
164 WIND AXES
165 IF(CRS(ALPHEN).GT.ALNCRK) GO TO 72)
166 CDONE= CDONLO
167 SK3LE= SK3ELO
168 SK3LE= SK3ILO
169 GO TO 74)
170 CDONL= CDONHI
171 SK3LE= SK3CHI
172 SK3LE= SK3IHI
173 CONTINUE
174 COLN= COLN+SK3L*AP5(ALPHEN)+SK3LL*ALPHEN*ALPHN
175 CLLE= SK32*TRMNC1
176 CLME= CLM1+TRMNC1*(SK34+SK35*ATS(TRMNC1))
177 CLNE= TRMNC3*(SK43+SK44*ABS(TRMNC3))
178 CLN= COLN+TRMNC3*(SK42+SK41*ABS(TRMNC3))

C
179 IF(ABS(ALPHEN).GT.ALNCRK) GO TO 74)
180 CDONE= CDONLO
181 SK3LE= SK3ELO
182 SK3LE= SK3ILO
183 GO TO 77)
184 CDONL= CDONHI
185 SK3LE= SK3CHI
186 SK3LE= SK3IHI
187 CONTINUE
188 CDONE= CDONL+SK3R*ABS(ALPHEN)+SK3LR*ALPHEN*ALPHN
189 CLPN= SK32*TRMNC2
190 CLME= CLM1+TRMNC2*(SK34+SK35*ABS(TRMNC2))
191 CLNE= TRMNC4*(SK36+SK37*ABS(TRMNC4))
192 CLN= COLN+TRMNC4*(SK38+SK39*ABS(TRMNC4))

C
193 LEFT MACLE AERO FORCES - BODY AXES
194
195
196
197
198
199
200
201
202
203
204
205
206
207
208
209
210
211
212
213
214
215
216
217
218
219
220
221
222
223
224
225
226
227
228
229
230
231
232
233
234
235
236
237
238
239
240
241
242
243
244
245
246
247
248
249
250
251
252
253
254
255
256
257
258
259
260
261
262
263
264
265
266
267
268
269
270
271
272
273
274
275
276
277
278
279
280
281
282
283
284
285
286
287
288
289
290
291
292
293
294
295
296
297
298
299
300
301
302
303
304
305
306
307
308
309
310
311
312
313
314
315
316
317
318
319
320
321
322
323
324
325
326
327
328
329
330
331
332
333
334
335
336
337
338
339
340
341
342
343
344
345
346
347
348
349
350
351
352
353
354
355
356
357
358
359
360
361
362
363
364
365
366
367
368
369
370
371
372
373
374
375
376
377
378
379
380
381
382
383
384
385
386
387
388
389
390
391
392
393
394
395
396
397
398
399
400
401
402
403
404
405
406
407
408
409
410
411
412
413
414
415
416
417
418
419
420
421
422
423
424
425
426
427
428
429
430
431
432
433
434
435
436
437
438
439
440
441
442
443
444
445
446
447
448
449
450
451
452
453
454
455
456
457
458
459
460
461
462
463
464
465
466
467
468
469
470
471
472
473
474
475
476
477
478
479
480
481
482
483
484
485
486
487
488
489
490
491
492
493
494
495
496
497
498
499
500
501
502
503
504
505
506
507
508
509
510
511
512
513
514
515
516
517
518
519
520
521
522
523
524
525
526
527
528
529
530
531
532
533
534
535
536
537
538
539
540
541
542
543
544
545
546
547
548
549
550
551
552
553
554
555
556
557
558
559
560
561
562
563
564
565
566
567
568
569
570
571
572
573
574
575
576
577
578
579
580
581
582
583
584
585
586
587
588
589
590
591
592
593
594
595
596
597
598
599
600
601
602
603
604
605
606
607
608
609
610
611
612
613
614
615
616
617
618
619
620
621
622
623
624
625
626
627
628
629
630
631
632
633
634
635
636
637
638
639
640
641
642
643
644
645
646
647
648
649
650
651
652
653
654
655
656
657
658
659
660
661
662
663
664
665
666
667
668
669
670
671
672
673
674
675
676
677
678
679
680
681
682
683
684
685
686
687
688
689
690
691
692
693
694
695
696
697
698
699
700
701
702
703
704
705
706
707
708
709
710
711
712
713
714
715
716
717
718
719
720
721
722
723
724
725
726
727
728
729
730
731
732
733
734
735
736
737
738
739
740
741
742
743
744
745
746
747
748
749
750
751
752
753
754
755
756
757
758
759
760
761
762
763
764
765
766
767
768
769
770
771
772
773
774
775
776
777
778
779
780
781
782
783
784
785
786
787
788
789
790
791
792
793
794
795
796
797
798
799
800
801
802
803
804
805
806
807
808
809
810
811
812
813
814
815
816
817
818
819
820
821
822
823
824
825
826
827
828
829
830
831
832
833
834
835
836
837
838
839
840
841
842
843
844
845
846
847
848
849
850
851
852
853
854
855
856
857
858
859
860
861
862
863
864
865
866
867
868
869
870
871
872
873
874
875
876
877
878
879
880
881
882
883
884
885
886
887
888
889
890
891
892
893
894
895
896
897
898
899
900
901
902
903
904
905
906
907
908
909
910
911
912
913
914
915
916
917
918
919
920
921
922
923
924
925
926
927
928
929
930
931
932
933
934
935
936
937
938
939
940
941
942
943
944
945
946
947
948
949
950
951
952
953
954
955
956
957
958
959
960
961
962
963
964
965
966
967
968
969
970
971
972
973
974
975
976
977
978
979
980
981
982
983
984
985
986
987
988
989
990
991
992
993
994
995
996
997
998
999

```

Figure G.6. (Continued)

SUBROUTINE RTSLOW

I N D E X

```

220 ATAU1 = A*STAU1P)
221 CALL LINT (HKEY, HMEM, HMEM, IST1, VSTARL, ATAU1, SVSTAB, SVSTPL )
222 IWARN(12) = .FALSE.
223 KPAN = 321
224 IF (IST1.EQ.2) IWARN(12) = .TRUE.
C
225 TRMG4 = SVSTPL*STAU1
226 TRMG9 = VSTARL*SVSTPL*CTAU1
227 FDRP = ATAN2(TRMG4, TRMG9)
228 CTSLR = 4.7/(4.+ VSTARL*SVSTARL)
C
C      CALCULATE THE AMOUNT OF WING AREA IN DOWNWASH - USES AVERAGES
C
229 AVEZET = .5 *(ZETR4 + ZETHL )
230 AVELD = .5 *(ALPHRD + ALPHLR)
231 AVEPP = .5 *(EPDR + EPLR )
232 AVECTS = .5 *(CTSD + CTSL )
C
233 CALL SINGOSIAVEZET, SAVZET, CAVZET)
234 CALL SINGOSIAVEIN= AINW + SAVINW, CAVINW )
C
235 TAVAFP = TAN(AVEALR - AVEPPP )
C
236 ZFET1 = (RLS - PC*CAVINW + HPC SAVINW ) * TAVAFP
237 ZFET2 = ZET1*CAVZET + PC*SAVINW + HPC*CAVINW
238 ZFET3 = HPC*SAVINW*OTRAC - ZFET2*ZFET2
C
239 FC(ZFET3) 35,34,350
240 CONTINUE
241 ZFET2 = FC(ZFET3, MORR)
242 ZFET1 = ZFET1 + SAVZET
C
243 ZFET4 = (RLS - (PC-CHORD)*CAVINW + HPC*SAVINW ) * TAVAFP
244 ZFET5 = ZFET4 + CAVZET + (PC-CHORD)*SAVINW + HPC*CAVINW
245 ZFET6 = RCP*SAVINW*OTRAC - ZFET5*ZFET5
C
246 ZETR2 = ZFET5 + SAVZET
247 ZETR3 = FC(ZFET6) 36,36,355
248 CONTINUE
249 ZETR4 = FC(ZFET6, MORR)
C
250 ZETR1 = ZETR1 + ZETR2 + ZETR3 + ZETR4 )
251 STPW = COFF23 * SIR
252 SIT = CHORD *(ZETR2 + ZETR4 )
253 SIL = SIT - SIR
254 SILW = COFF24 * SIL
255 BOTLW = COFF27*SIL

```

Figure G.6. (Continued)

(B L A N K C A R D)
 (B L A N K C A R D)
 (B L A N K C A R D)
 (B L A N K C A R D)
 (B L A N K C A R D)
 (B L A N K C A R D)
 (B L A N K C A R D)
 (B L A N K C A R D)
 (B L A N K C A R D)
 (B L A N K C A R D)
 (B L A N K C A R D)
 (B L A N K C A R D)

C FUSFLAG
 XF = SLF - XCG
 ZF = SHE - ZCG
 C MEVC
 XN = SLW - XCG
 ZN = SHW - ZCG
 C MACELLES
 XF = SL* CILAW2 - XCG
 ZF = -SL* SILAW2 - ZCG
 C
 YL = SL* CILAW1 - XCG
 ZL = -SL* SILAW1 - ZCG
 C

INTERMEDIATE CALCULATIONS

C
 POSIN = ZR* SILAW2
 ZPOS = ZR* CILAW2
 XPOS = XR* SILAW1
 ZPOS = XR* CILAW1
 XLSIN = ZL* SILAW1
 ZLPOS = ZL* CILAW1
 XLSIN = XL* SILAW1
 ZLPOS = XL* CILAW1
 ZFMW2 = ZF* COEF6
 ZMMW2 = ZM* COEF6
 YEMFL = XG* COEF7
 XMMWL = XW* COEF8
 YERM1 = COEF2 * (SSQIN2 + SSQINI)
 YERM2 = FIXZP * (LS2IN2 + S2INI)
 YERM3 = COEF4 * (LS2IN1 + S2INI)
 YERM4 = COEF5 * (LS2IN2 + S2INI) * 0.5
 YERM5 = FIXZP * (C2IN2 + C2INI)
 YERM7 = COEF4 * (XPOS + ZLPOS)

RESULTS

C
 FIXX = XPOS - YERM1 - YERM2 - YERM3 - YERM4 + ZMMW2 + ZMMW1 - YERM5
 FIXZ = XZPOS + YERM6 + YERM7 + YERM8 + YERM9 + ZMMW4 + ZMMW3 - YERM6
 FIYV = YVICON * XEMFL + YEMFL * XMMWL + ZMMW4 + YERM6 - YERM3
 FIXZP = FIXZP
 FIZZ = ZVICON + YERM1 + YERM2 + YERM3 + YERM4 + YERM5 + YERM6
 FJXX = FIZZ - FIYV
 FJYY = FIXX - FIZZ
 FJZZ = FIYV - FIXX
 FIXZ4 = FIXZP

Figure G.6. (Continued)

SUBROUTINE RTSLOW

I N D E X

```

331      DDVIXX= 1./FIXX
332      DDVIYY= 1./FIYY
333      DDVIZZ= 1./FIZZ
334      ISLOW= 0
335      CALL TRACK(*RTSLOW ,*2)
336      RETURN
337      DO 510 J=1,32
338      510 CALL DISABLIJ(-1)
339      IPAN = KPAN
340      RETURN
341      END

```

Figure G.6. (Continued)

SUBROUTINE RTSLOW

I N D E X

ALAFNR	-	2100			
ALART	-	2400			
ALARVT	-	2400			
ALARWG	-	2200			
ALPRK	-	1000			
ALFSQ	-	1800			
ALFTAB	-	1300			
ALWTE	-	2400			
ALWTE	-	2400			
ALHTP	-	2400			
ALHTPR	-	2400			
ALHTST	-	1000			
ALLNSQ	-	2000			
ALLRH	-	2100			
ALLAPP	-	2200			
ALNCBK	-	1000			
ALPHF	-	1800			
ALPHFP	-	96=	178	91	
ALPHHT	-	2400			
ALPHLN	-	2000	152=	164	173
ALPHLR	-	2100	224	239	
ALPHLW	-	2000			
ALPHPN	-	2000	153=	170	137
ALPHRR	-	2100	209	230	
ALPHRW	-	2000			
ALPHVT	-	2400			
ALRGLW	-	2200			
ALRGRW	-	2200			
ALRNSQ	-	2000			
ALRRH	-	2100			
ALRWPP	-	2200			
ALVTE	-	2400			
ALVTM	-	2400			
ALVTP	-	2400			
ALVTPR	-	2400			
ALVTST	-	1000			
ALWSSQ	-	2200			
AMACH	-	1600	55=	56	
AMACLP	-	900			
AMACRP	-	900			
AMACSQ	-	1600	45=	47	
AMACTL	-	2300			
AMACTR	-	2300			
AMAFRO	-	2500			
AMARF	-	1800			
AMARFP	-	1800	39=		
AMARHT	-	2400			
AMARLW	-	2200			
AMARNC	-	2100			
AMARNL	-	2100			
AMARNR	-	2100			
AMARRW	-	2200			
AMART	-	2400			
AMARVT	-	2400			
AMARWG	-	2200			

Figure G.6. (Continued)

SUBROUTINE RTSLOW

I N D E X

AMEH	1200	215AG				
AMLRH	2100					
AMNLP	2100					
AMNAP	2100					
AMOTL	2100					
AMOTR	2100					
AMRRH	2100					
AMUL	1700	139	144			
AMULSO	1700					
AMUR	1700	127	131			
AMURSQ	1700					
ANAERO	2500					
ANARF	1800					
ANAREP	1900	107*				
ANARHT	2400					
ANARHC	2100					
ANAPNL	2100					
ANAPNR	2100					
ANART	2400					
ANARVT	2400					
ANARWC	2200					
ANDIC	300					
ANDIG2	300					
AMLRH	2100					
AMOTL	2100					
AMOTE	2100					
AMRSH	2100					
AREAM	1000					
AREAVT	1000					
AREAW	1000	69				
ARHT	1000					
ARILW	2200	270*	272			
ARIRM	2200	271*	273			
ADVT	1000					
ADWNG	800	272	273			
APWSSC	2200					
ATAN2	1500	153	154	155	200	200
ATAJLP	2200	220*	217AG			
ATAURP	2200	214*	215AG			
AVEALR	2200	239*	244			
AVEALW	2200					
AVECLW	2200					
AVFCTS	2200	241*	744			
AVEFPP	2200	242*				
AVEIN	1600	243AG				
AVEVAC	1900					
AVFYCS	1900					
AVEZET	2200	238*	242AG			
BDMOS	300					
BFTAF	1800	MSAG	282	288		
BETAFP	80	89	90			
BFTALN	2200	154*	158AG			
BETALW	2200					
BETARN	2200	155*	159AG			

Figure G.6. (Continued)

SUBROUTINE RTSIOW

INDEX

CDMHT	1700				
CDCLN	2700	169=	173		
CDONHI	1000	169	183		
CDONLO	1000	165	170		
CDORN	2000	179=	183=		
CDPVT	1000			197	198
CDRN	2000	187=	196		
CDRWAD	2200				
CDR4PR	2200				
CDR4SS	2200				
CDSLW	2200				
CDSRM	2200				
CDVT	2400				
CDWTST	2400				
CDWOP	1900				
CEPLY	2200	125=			
CEP2H	2200				
CGGTPV	1500				
CHORD	1000	199	205	252	267
CILAML	1400	52	302	309	311
CILAMR	1400	52	305	305	307
CLALHY	1700				
CLALPH	1000	172	273		
CLAT	2400				
CLAVE	2200				
CLCNTE	2200				
CLCNTR	2200				
CLDUN	2200				
CLF	1800	18=	96	97	
CLHT	2400				
CLHTST	2400				
CLILW	2200	272=	274		
CLLRW	2200	273=	275		
CLLN	2000	174=	272	293	
CLLWAD	2200				
CLLWPP	2200				
CLLWSS	2200				
CLWAX	1900				
CLDAL	1900	180=	196	197	
CLRN	2200				
CLRWAD	2200				
CLR4PR	2200				
CLR4SS	2200				
CLSLW	2200				
CLSRM	2200				
CLSA	2200				
CLTCOR	1900	112=			
CLWOP	1900	124=			
CLZERC	2200				
CNCNTL	2200				
CNCNTR	2200				
CWF	1800	21=	95	99	
CMLN	2200	175=	205	206	207
CMLWAD	2200				
CMLWSS	2200				

Figure G.6. (Continued)

I N D E X

CMDF	-	100	91		
CMON	-	100	175	189	
CMOW	-	250			
CMRN	-	200	190=	200	201
CMRMA0	-	220			
CMRMS	-	220			
CMSLW	-	220			
CMSRW	-	220			
CNF	-	180	92=	100	101
CNFAIL	-	210			
CNFAIR	-	210			
CNFBI1	-	210			
CNFAIR	-	210			
CNFL	-	210			
CNFPL	-	90			
CNPR	-	90			
CNFR	-	210			
CNLN	-	200	177=	206	207
CNDF	-	100	92		
CNOLN	-	100	177		
CNORN	-	100	191		
CMRN	-	200	191=	200	201
CNSW	-	220			
COEF1	-	80	52	53	
COEFIC	-	80			
COEF11	-	80			
COEF12	-	80			
COEF13	-	80			
COEF14	-	80			
COEF15	-	80			
COEF16	-	80			
COEF17	-	80	95	200	201
COEF18	-	80	194	195	
COEF19	-	80			
COEF2	-	80			
COEF20	-	90			
COEF21	-	80			
COEF22	-	80			
COEF23	-	80			
COEF24	-	80			
COEF25	-	80	211		
COEF26	-	80	265		
COEF27	-	80	270	271	
COEF28	-	80	266	269	
COEF29	-	80	272	273	
COEF3	-	80	316	319	
COEF30	-	80	125		
COEF31	-	90			
COEF32	-	80			
COEF33	-	80			
COEF34	-	80			
COEF35	-	80	294		
COEF36	-	80			
COEF37	-	80			
COEF38	-	90			

Figure G.6. (Continued)

SUPROJETINE RTSLW

I N D E X

COEF39	-	800		
COEF4	-	800		
COEF40	-	800		
COEF41	-	900		
COEF42	-	900		
COEF5	-	800		
COEF6	-	800		
COEF7	-	900	323	
COEF8	-	800	323	
COEF9	-	800		
CONS1	-	2600		
CONS10	-	2600		
CONS11	-	2600		
CONS12	-	2600		
CONS13	-	2600		
CONS14	-	2600		
CONS15	-	2600		
CONS16	-	2600		
CONS17	-	2600		
CONS18	-	2600		
CONS19	-	2600		
CONS2	-	2600		
CONS20	-	2600		
CONS21	-	2600		
CONS22	-	2600		
CONS23	-	2600		
CONS24	-	2600		
CONS25	-	2600		
CONS26	-	2600		
CONS27	-	2600		
CONS28	-	2600		
CONS29	-	2600		
CONS3	-	2600		
CONS30	-	2600		
CONS31	-	2600		
CONS32	-	2600		
CONS33	-	2600		
CONS34	-	2600		
CONS35	-	2600		
CONS36	-	2600		
CONS37	-	2600		
CONS38	-	2600		
CONS39	-	2600		
CONS4	-	2600		
CONS40	-	2600		
CONS41	-	2600		
CONS42	-	2600		
CONS43	-	2600		
CONS44	-	2600		
CONS45	-	2600		
CONS46	-	2600		
CONS47	-	2600		
CONS48	-	2600		
CONS49	-	2600		
CONS5	-	2600		

Figure G.6. (Continued)

I N D E X

CPMPL	-	900	
COMPR	-	900	
CPMP	-	2100	
CPR	-	900	
CSF11L	-	2100	
CSFALP	-	2100	
CSFRIL	-	2100	
CSF914	-	2100	
CSFL	-	2100	
CSEPL	-	900	
CSEPP	-	900	
CSFR	-	2100	
CTAULR	-	2200	235
CTAURR	-	2200	221
CTL	-	2100	
CTLPRM	-	900	
CTP	-	2100	
CTPRM	-	900	
CTSLP	-	2200	241
CTSR	-	2200	241
CYALVT	-	1000	
CYAT	-	2400	
CVF	-	1800	96
CYLN	-	2000	97
CYVAL	-	2100	202
CYVAL9	-	2100	202
CYVAL1	-	2100	
CYVAL19	-	2100	
CYVAL11	-	2100	
CYVAL1P	-	2100	
CYVAL	-	2100	
CYMP	-	900	
CYMP3	-	900	
CYMR	-	2100	
CYRN	-	2000	197
CVT	-	2400	197
CVTST	-	2400	197
CZINL	-	1400	320
CZINR	-	1400	322
DARK1	-	2400	
DARK10	-	2400	114
DARK11	-	2400	127
DARK12	-	2400	139
DARK13	-	2400	143
DARK14	-	2400	136
DARK15	-	2400	139
DARK16	-	2400	293
DARK17	-	2400	
DARK18	-	2400	
DARK19	-	2400	
DARK2	-	2400	
DARK21	-	2400	
DARK3	-	2400	
DARK4	-	2400	
DARK5	-	2400	
DARK6	-	2400	

Figure G.6. (Continued)

SUBROUTINE RTSLOH

I N D E X

DBRK7	-	26C0	
DBRK8	-	26C0	
DBRK9	-	26C0	
DCDDF	-	22C0	
DCDLDA	-	22C0	99
DCDLG	-	10C0	
DCMLSP	-	22C0	
DCORDA	-	22C0	
DCDRSP	-	22C0	
DCLDF	-	22C0	
ECLLDA	-	22C0	
DCLLSP	-	22C0	
ECLRDA	-	22C0	
DCLRSP	-	22C0	
DCLSPH	-	22C0	
DCMDF	-	22C0	
DCMLDA	-	22C0	91
DCMLG	-	10C0	
DCMLSP	-	22C0	
DCMRDA	-	22C0	
DCMRSP	-	22C0	
DCNSPM	-	22C0	
DEG20	-	10C0	
DEL	-	16C0	57=
DELRS	-	9C0	62
DELRT	-	9C0	69
DELELY	-	9C0	
DELFIP	-	9C0	
DELRS	-	9C0	
DELRT	-	9C0	
DELRTD	-	9C0	
DELSPL	-	9C0	
DELSPR	-	9C0	
DELS	-	9C0	
DELST	-	9C0	
DELTH	-	9C0	
DFLAIL	-	9C0	
DFLAIR	-	9C0	
DGTORD	-	10C0	
DIGAN	-	3C0	
DIGAN2	-	3C0	
DISABL	-	338*	
DLFPSQ	-	14C0	
DLG	-	18C0	
LLNC	-	20C0	207=
DLRNC	-	20C0	201=
DMLG	-	18C0	
DLNC	-	20C0	205=
DLRNC	-	20C0	199=
DMLG	-	18C0	
DLNC	-	20C0	206=
DLRNC	-	20C0	200=
DOVT	-	13C0	149
DOVTL	-	19C0	149
DOVTR	-	19C0	136

Figure G.6. (Continued)

SUBROUTINE RTSLW

INDEX

CSOART	-	1000		
DTM	-	300		
DUM12	-	900		
DUM13	-	900		
DUM14	-	900		
DUM15	-	900		
DUM43	-	900		
DUM44	-	900		
DUM45	-	900		
DUM46	-	900		
DUM47	-	900		
DUM48	-	900		
DXLG	-	1800		
DXLNC	-	2000	203=	
EXRNC	-	2000	197=	
DYLG	-	1800		
DYLNC	-	2000	204=	
LYRNC	-	2000	198=	
DZLG	-	1800		
DZLNC	-	2000	202=	
CZRNC	-	2000	196=	
EFFHT	-	1000		
EFFVT	-	1000		
EMAXN1	-	1500	74=	78
EMAXN2	-	1500	75=	74
EMAXD1	-	1600	73=	77
ENFL	-	900	31	
ENFR	-	900	32	
ENG	-	50		
ENGINE	-	700		
ENGVAR	-	160		
ENLX	-	500	74	
ENLSTP	-	500		
ENLTX	-	500		
ENZMX	-	500	75	
ENZREF	-	1000	75	
ENZSTR	-	1600	76=	
ENGVAP	-	250		
EPIL0	-	2200	291=	259=
EPIL1	-	2200	292=	299=
EPILR	-	2200	295=	260
EPP0M	-	1000	297=	299
EPPR0	-	2200	297=	277
EPTAIL	-	2400		
EPIL1	-	2400		
EP0RL	-	2200		
EPMPR	-	2200		
EPZERO	-	2400		
EQMX	-	500		
EMNTMX	-	500	77	
EMDTP	-	500	77	
FEU	-	1000		
FILE	-	1000		
FIN0EG	-	1000		
FINPR	-	1000		

Figure G.6. (Continued)

SUBROUTINE RTSLOW

I N D E X

HTVTKT	-	1300					
HWACL	-	2300					
HWACR	-	2300					
HWAC4	-	1900	1.2=	114	117	121	293 294
* HYBCCN	-	3*					
* HYBIC	-	4*					
HIOTL	-	2300					
HIOTR	-	2300					
HIL	-	2300					
HIR	-	2300					
IAD	-	300					
IADC3	-	1100					
IC	-	300					
ICDSCP	-	200					
ICLR	-	300					
ICOMP	-	600					
ICZ	-	300					
IDUC	-	300					
IFC	-	300					
IFCHAN	-	300					
IFLAG	-	200					
IFRAME	-	300					
IGN	-	300					
INHJ9	-	300					
ILEX	-	300					
INITVR	-	14*					
IOC	-	300					
IOC21	-	300					
IPAN	-	200					
IPHASE	-	600					
IPSNOS	-	300					
IRCTS	-	300					
IRCK	-	300					
IREVNT	-	29AG					
IRUNIT	-	300					
ISCOPE	-	200					
ISENCF	-	500					
ISETC	-	300					
ISMPC	-	300					
ISLOW	-	600					
ISTA	-	600					
ISTAD	-	300					
ISYAD2	-	300					
ISYA	-	600					
ISYB	-	300					
ISTDA	-	300					
ISTD42	-	300					
ISTGN	-	300					
ISTG22	-	300					
ISTHD	-	300					
ISTH02	-	300					
ISTIC	-	300					
ISTIC2	-	300					
ISTP1T	-	300					
ISTR81	-	1100					
ISTRN	-	300					

Figure G.6. (Continued)

SUBROUTINE RTSLOW

I N D E X

ISTRM2	-	300					
ISYNC	-	300					
ITRIM	-	600					
ITSC	-	300	32	35=			
IWARN1	-	600	7LG	217=	211=	233=	
IWARN2	-	600	7LG				
IWREV1	-	600					
J	-	33700	338AG				
JTRIM	-	600	32				
KAR	-	400					
KONFR	-	200					
KPAN	-	29=	34=	216=	232=	339	
KTRIM	-	600	31AG	32			
LETR	-	300					
LINT	-	215*	230*				
MICNT	-	200					
MIECR	-	200					
MONDIG	-	300					
NACVAR	-	20*					
NADCS	-	300					
NCHAIN	-	300					
NCON	-	300	28AG				
NCONSL	-	300					
NDACS	-	300					
NFRAME	-	200					
NREF	-	600	105	115	129	142	292
NRF	-	300					
NROS	-	300					
NOSIM	-	200					
NPCS	-	300					
NPLOT	-	600					
NPLOT2	-	600					
NQIND	-	500					
NRNDID	-	500					
NTMST	-	600					
NVB	-	600					
NWDTID	-	500					
N1IND	-	500					
N17HID	-	500					
N2IND	-	500					
OMDOT	-	900					
OMDTL	-	1700					
OMDYR	-	1700	75				
OMEGA	-	900					
OMEGAL	-	1700					
OMEGAR	-	1700					
OMEGEL	-	1600	91=	81	82=		
OMEGE	-	1600	79AG				
OMREF	-	1000	75				
CMSQL	-	1700					
OMSOR	-	1700					
OMDVTC	-	1600	61=	62	72		
OOVDSK	-	800					
OOVFSM	-	1600	6R=	112	124		
OOVIXX	-	2500	331=				
OOVIVY	-	2500	312=				

*

*

Figure G.6. (Continued)

SUBROUTINE LISTING

INDEX

ROUTINE	PC	PL	PR	PS	PT	PU	PV	PW	PX	PY	PZ
OV177	2500										
OPERA	300										
OPERA2	300										
OVDTM	900										
CVSOYH	1600	74									
CVHOL	1500	73									
P	2500										
PC	1000	245	246	252	253						
PCTOL	1600										
PCTQR	1600	79AG									
PGUST	900										
PHI	900	41AG									
PHIPH	1000										
PI	1000										
PILMSK	200										
PIDVZ	1000										
PNLN	2100										
PNLR	2100										
PNRN	2100										
PNRR	2100										
PP	2500										
PPRIME	900										
PQ	2500										
PQ	2500										
PRQJ	300										
PST	900	39AG									
C	2500										
CF54	1500	60E	96	97	98	99	100	101			
CGUST	900										
ONLN	2100										
ONLR	2100										
ONRN	2100										
ONRR	2100										
CPPIME	900										
R	2500										
RCPL	1100	33AG									
RDTDGG	1500										
RESLR	2200	27E	229								
RESRR	2200	21E	212								
RETURN	33E	34E									
REVENT	28E										
RGUST	900										
PNLN	2100										
PNLR	2100										
PNRN	2100										
PNRR	2100										
R7E	1600	62E	63	211							
RNEOV2	1600	63E	192	193							
ROFQ	500	62									
ROP1R4	2100										
ROP1R5	2100										
ROTFFS	1000										
ROTTRAD	1000	12E	141	247	254						
ROTVAR	21E										
APRIME	900										

* *

*

Figure G.6. (Continued)

I N D E X

SK48	1000								
SK49	1000								
SK5	1000	91							
SK50	1000								
SK6	1000	91							
SK7	1000	90							
SK8	1000	90							
SK9	1000	92							
SL	1000	300	301	302	303				
SLAC	800								
SLF	1000	296							
SLPA	1000								
SLW	1000	298							
SM	1000								
SMA	1600	64=							
SMB	1000								
SMM	1000								
SMV	1000								
SPAN	1000	100	101	200	201	206	207		
SPHIP	1000								
SPTD	800								
SQF	11*	49							
SOFARG	1800								
SOFPRM	1300								
SOLNC	1000								
SOLW	2000	192=	195						
SOM1MX	2200	78=							
SORES	2200	226=	227	286					
SOPRES	2200	212=	213	279					
SORNC	2000	193=	194						
SORW	2200								
SQTHC	1600	60=	64	69	71				
SQDIX	1600	77=							
SQWING	2200								
SSO1ML	1400	43=	44	315					
SSO1NR	1400	42=	45	316					
STAU	2200	228AG	234						
STAU	2200	219AG	220						
SUM1X	800								
SUM1X2	800								
SUM1Y	800								
SUM1Z	800								
SVSTAB	1300	215AG	230AG						
SVSTAR	2200	220	221	279					
SVSTR	2200	234	235	274	286				
SWLG	600								
SWLG2	900	89	91						
S21NL	1400	46=	317	319					
S21NR	1400	47=	317	319					
TAILVR	24*								
TAN	244								
TANAG	1300								
TAUHT	1000								
TAUL	300								
TAULR	2200	224=	228AG	229					

Figure G.6. (Continued)

SUBROUTINE RTSLOW

I N D E X

Label	Address	Address	Address	Address
TAURR	2200	214	219AG	
TAURT1	1000			
TAURT2	1000			
TAUVT	1000			
TAVSEP	2200	245	252	
TDEF	500			
TDEF	1600	59		
TEAL	1600			
TEAR	1600	72	79AG	
TERMP1	2500			
TERMQ1	2500			
TERMR1	2500			
TERM1	2500	316	326	
TERMIL	2500			
TERMR	2500			
TERM2	2500	317	326	
TERM2L	2500			
TERM2P	2500			
TERM3	2500	319	324	
TERM3L	2500			
TERM3R	2500			
TERM4	2500	319	323	
TERM5	2500	323		
TERM6	2500	321	324	
THODEL	1600	50	70	
THE	900	60AG		
THEFC	1600	50	61	
THLAC	2300			
THTRAC	2300			
TH75L	900			
TH75R	900			
TIDFL	1900	144	148	
TIGER	1900	131	135	
TL	2100	224	225	
TMG1C	2300	220	222	
TMG1L	2300	221	222	
TNAC1	2000	194	196	
TNAC2	2000	195	202	
TOROL	2100	197	197	
TOROR	2100	198	200	
TPSP	900	72	206	
TR	2100	205	206	
TRACK	27*	210		
TRIM	300			
TRIM2	300			
TRMARI	2100			
TRMAR2	2100			
TRMAP1	2100			
TRMAP4	2100			
TRMHR1	2100			
TRMHR2	2100			
TRMHT	2400			
TRMHT2	2400			
TRMHT3	2400			
TRMNC1	160*	174	175	

Figure G.6. (Continued)

SUBROUTINE RTSLOW

I N D E X

TRMNC2	-	161=	138	189	
TRMNC3	-	162=	176	177	
TRMNC4	-	163=	190	191	
TRMITL	-	2500			
TRMITR	-	2500			
TRMVT	-	2400			
TRMVT2	-	2400			
TRMVT3	-	2400			
TRMNC1	-	2200	211=	212	226
TRMNC4	-	2300	234=	236	
TRMNC5	-	2200			
TRMNC6	-	2200			
TRMNC7	-	2200			
TRMNC8	-	2200			
TRMNC9	-	2300	235=	236	
TSBASE	-	300			
TSREOD	-	300			
TSTRYS	-	38*			
TZERO	-	500	58		
TZET1	-	2200	245=	246	251
TZET2	-	2200	246=	247	
TZET3	-	2200	247=	248	250
TZET4	-	2200	252=	253	255
TZET5	-	2200	253=	254	
TZET6	-	2200	254=	255	258
U	-	2500			
UGUST	-	900			
UMT	-	1700			
ULW	-	1700			
ULWPR	-	1700			
ULWSQ	-	1700			
UP	-	1700			
UPRIME	-	900	54	55	
URL	-	1700	152		
URLPR	-	1700			
URLURL	-	1700	51	192	
URR	-	1700	153		
URRPR	-	1700			
URRURR	-	1700	50	193	
URN	-	1700			
URMPR	-	1700			
URMSQ	-	1700			
USEAID	-	33*			
USO	-	1700			
UVT	-	1700			
V	-	2900	276		
VALFLM	-	1700			
VALFRM	-	1700			
VALFS	-	1700			
VALNCL	-	1700	51=	154	
VALMCR	-	1700	50=	155	
VBETVT	-	1700			
VEAST	-	1500	55=		
VELVAR	-	17*			
VGUST	-	900			

Figure G.6. (Continued)

SUBROUTINE RTSLDW

I N D E X

Variable	Line	Line	Line	Line	Line	Line	Line	Line
VLW	1700							
VLMPR	1700							
VLMSQ	1700							
VNORTH	1500							
VP	1700	54=						
VPRI4F	900	54	55					
VRL	1700	154						
VRLPR	1700							
VRLVRL	1700	192						
VRR	1700	155						
VRRPR	1700							
VRRVRR	1700	193						
VRW	1700							
VRMPR	1700							
VRMSQ	1700							
VSO	1700							
VSTAR	2200	213=	215AG	221	223	275		
VSTARC	1300							
VSTARL	2200	227=	230AG	235	237	274		
VTIPL	1700							
VTIPR	1700							
VTOTAL	1700							
VTOTLR	1700	65						
VTOIIR	1700	227	2AG					
VTOIIR	1700	213	297					
VTSTLL	900							
VVT	1700							
VZETL	1700							
VZETR	1700							
W	2500							
WDOT	900							
WGUST	900							
WHT	1700							
WLW	1700							
WLWPR	1700							
WLMSQ	1700							
WNGVAR	220							
WNGVR2	230							
WORK	50							
WP	1700	51	60	67	212	225	226	250
WPRIME	900	54	55					
WRL	1700	152						
WRLPR	1700							
WRLWAL	1700	51	192					
WROTL	1700							
WRR	1700	153						
WRRPR	1700							
WRBWRR	1700	50	193					
WRW	1700							
WRMPR	1700							
WRMSQ	1700							
WSQ	1700							
WVT	1700							
XAERF	1800							
XAERLW	2200							

THE VARIABLE- WORK - IS USED BEFORE IT IS DEFINED

Figure G.6. (Continued)

SUBROUTINE ATLSP(DEL, SPOIL, DELA, DCJA, D'HA, DELS, DCDS, DCMS)

DCDS = CONSG9+SPOIL*(CCNSTC+CONST1*SPOIL)

DCMS = C.

RETURN
END

I N D E X

32

C

33

C

34

35

Figure G.6. (Continued)

SYMBOL	REFERENCES
5	8*
30	12*
40	15*
45	14
48	17
50	20*
55	25*
60	26*
65	30*
65	31*
AILSP	1*
AIRPK	20
ALNCRK	20
BRKLSW	20
BRKSW	20
CLFI	6*
CLMAX	20
CLZ	45
CLZ	18*
COMS1	30
COMS10	30
COMS11	30
COMS12	30
COMS13	30
COMS14	30
COMS15	30
COMS16	30
COMS17	30
COMS18	30
COMS19	30
COMS2	30
COMS20	30
COMS21	30
COMS22	30
COMS23	30
COMS24	30
COMS25	30
COMS26	30
COMS27	30
COMS28	30
COMS29	30
COMS3	30
COMS30	30
COMS31	30
COMS32	30
COMS33	30
COMS34	30
COMS35	30
COMS36	30
COMS37	30
COMS38	30
COMS39	30
COMS4	30
COMS40	30
COMS41	30
COMS42	30
COMS43	30
COMS44	30
COMS45	30
COMS46	30
COMS47	30
COMS48	30
COMS49	30
COMS50	30
COMS51	30
COMS52	30
COMS53	30
COMS54	30
COMS55	30
COMS56	30
COMS57	30
COMS58	30
COMS59	30
COMS60	30
COMS61	30
COMS62	30
COMS63	30
COMS64	30
COMS65	30
COMS66	30
COMS67	30
COMS68	30
COMS69	30
COMS70	30
COMS71	30
COMS72	30
COMS73	30
COMS74	30
COMS75	30
COMS76	30
COMS77	30
COMS78	30
COMS79	30
COMS80	30
COMS81	30
COMS82	30
COMS83	30
COMS84	30
COMS85	30
COMS86	30
COMS87	30
COMS88	30
COMS89	30
COMS90	30
COMS91	30
COMS92	30
COMS93	30
COMS94	30
COMS95	30
COMS96	30
COMS97	30
COMS98	30
COMS99	30
COMS100	30

Figure G.6. (Continued)

SUBROUTINE ATLSPIDEL, SPOIL, DCLA, DCDA, DCMA, DCLS, DCDS, DCMS)

I N D E X

CONS42	-	3C0
CONS43	-	3C0
CONS44	-	3C0
CONS45	-	3C0
CONS46	-	3C0
CONS47	-	3C0
CONS48	-	3C0
CONS49	-	3C0
CONS5	-	3C0
CONS50	-	3C0
CONS51	-	3C0
CONS52	-	3C0
CONS53	-	3C0
CONS54	-	3C0
CONS55	-	3C0
CONS56	-	3C0
CONS57	-	3C0
CONS58	-	3C0
CONS59	-	3C0
CONS6	-	3C0
CONS60	-	3C0
CONS61	-	3C0
CONS62	-	3C0
CONS63	-	3C0
CONS64	-	3C0
CONS65	-	3C0
CONS66	-	3C0
CONS67	-	3C0
CONS68	-	3C0
CONS69	-	3C0
CONS7	-	3C0
CONS70	-	3C0
CONS71	-	3C0
CONS72	-	3C0
CONS73	-	3C0
CONS74	-	3C0
CONS75	-	3C0
CONS76	-	3C0
CONS77	-	3C0
CONS78	-	3C0
CONS79	-	3C0
CONS8	-	3C0
CONS80	-	3C0
CONS81	-	3C0
CONS9	-	3C0
DBRK1	-	3C0
DBRK10	-	3C0
DBRK11	-	3C0
DBRK12	-	3C0
DBRK13	-	3C0
DBRK14	-	3C0
DBRK15	-	3C0
DBRK16	-	3C0
DBRK17	-	3C0
DBRK18	-	3C0

30
30
37
32
32

Figure G.6. (Continued)

SUBROUTINE CLCOCM(ALPHA,DEL,CLDEL,CLSP,CDFASP,CMFASP,CL,CD,CM,

INDEX

```

1 SUBROUTINE CLCOCM(ALPHA,DEL,CLDEL,CLSP,CDFASP,CMFASP,CL,CD,CM,
2 CLP,CDPI)
3 COMMON/XACDEF/ ACDW0,ACDW1,ACDW2,ACDW3,ACDW4,
4 ACDW5,ACDW6,ACDW7,ACDW8,ACDW9,
5 ACDW10,ACDW11,ACDW12,ACDW13,ACDW14,
6 ACDW15,ACDW16,ACDW17,ACDW18,ACDW19,
7 ACDW20,ACDW21,ACDW22,ACDW23,ACDW24
8 COMMON/XPAR1/ AINH1,AINH2,ALM0A,ALH1ST,ALVTST,AREAH1,AREAM,
9 AREAV1,ARHT,ARVT,AVEYAC,AVEYCS,BLS,COOF,COOHT,COOVT,
10 CHRD,CLALHT,CLALPH,CMOF,CMON,CMOF,CNDLN,CNORN,CYALVT,
11 DCOLG,DCMLG,FINPR,DOVT,DSDBET,EFFHT,EFFVT,FFIE,FINDEG,
12 *CIP, *FIXF, *FIXPR, *FIXW, *FIXZF, *FIXZR, *FIXZM, *FIYF, *FIYPR,
13 *FIYM, *FIZF, *FIZPR, *FIZM, *P, *OMREF, *PC, *PI, *ROTRAD,
14 *SBFPR, *SBWPP, *SG, *SHF, *SHW, *SK1, *SK2, *SK3,
15 *SK4, *SK5, *SK6, *SK7, *SK8, *SK9, *SK10, *SK20, *SK21,
16 *SK22, *CDNLD, *SK30L, *SK31L, *SK32, *CDNHI, *SK34, *SK35, *SK36,
17 *SK37, *SK38, *SK39, *SK40, *SK41, *SK42, *SK43, *SK44, *SK45,
18 *SK46, *SK47, *SK48, *SK49, *SK50, *SL, *SLF, *SLPA, *SLM,
19 *SM, *SME, *SMN, *SMW, *SPAN, *TAUHT, *TAUVT, *XFAC, *XHT,
20 *XMAC, *XVT, *YN, *YPA, *YMAC, *ZPAC, *ZHT, *ZPA, *ZMAC,
21 *ZVT, *CLOAL, *PHIPH, *SK30H1, *ENZREF, *KWC2, *BT1, *BT2, *BT3,
22 *RKDT, *RKDT1, *RKDT2, *RKDT3, *RKDT4, *BK41, *BK42, *SK31H1,
23 *FFI, *CLMAX, *AIRK, *PKLSM, *RKNSM, *SOFPNM, *DEG25, *DGTORD, *HTVTKT,
24 *PIQV2, *ROTORG, *ROTEPS, *SKEPS, *ALNCRK, *TAUR11, *TAUR12,
25 *CMNCR/GEFVAR/
26 1 ACVAT,AGVAM,RIGX, *RK99, *BMDVTL, *BMDVTS, *CMCOR, *CLTCOR, *CLWCR,
27 2 DOVT,DOVTR, *EPRM, *GFF, *HGFER, *HGFERR, *HLHUB, *HRHUB, *HTC4,
28 3 HNC4, *RR1, *RR12, *SBI, *TIGEL, *TIGER
29 COMMON/FLAGS/ IWARN1(16),IWARN2(16),ISENCE(2),IMREVT(2),ICOND,
30 1 ITPTM, *JTRIM, *KTRIM, *NPLDT, *NPLDT2, *IPHASE, *ISLDM, *SWLG, *GBUTON,
31 2 ISTA, *ISTB, *NCEF, *NWB, *NTWST
32 LOGICAL *I, *IWARN1, *IWARN2
33 COMMON/XPAR3/ CONS1, *CONS2, *CONS3, *CONS4, *CONS5, *CONS6, *CONS7,
34 1 CONS8, *CONS9, *CONS10, *CONS11, *CONS12, *CONS13, *CONS14,
35 2 CONS15, *CONS16, *CONS17, *CONS18, *CONS19, *CONS20, *CONS21,
36 3 CONS22, *CONS23, *CONS24, *CONS25, *CONS26, *CONS27, *CONS28,
37 4 CONS29, *CONS30, *CONS31, *CONS32, *CONS33, *CONS34, *CONS35,
38 5 CONS36, *CONS37, *CONS38, *CONS39, *CONS40, *CONS41, *CONS42,
39 6 CONS43, *CONS44, *CONS45, *CONS46, *CONS47, *CONS48, *CONS49,
40 7 CONS50, *CONS51, *CONS52, *CONS53, *CONS54, *CONS55, *CONS56,
41 8 CONS57, *CONS58, *CONS59, *CONS60, *CONS61, *CONS62, *CONS63,
42 9 CONS64, *CONS65, *CONS66, *CONS67, *CONS68, *CONS69, *CONS70,
43 0 DRAK1, *DRAK2, *DRAK3, *DRAK4, *DRAK5, *DRAK6, *DRAK7,
44 1 DRAK8, *DRAK9, *DRAK10, *DRAK11, *DRAK12, *DRAK13, *DRAK14,
45 2 DRAK15, *DRAK16, *DRAK17, *DRAK18, *DRAK19, *DRAK20, *DRAK21,
46 3 *SFL, *SFNL, *SFSL, *SFPL, *SFYML, *SFYQL, *SFPL,
47 4 *SFR, *SFRP, *SFRS, *SFRM, *SFRM, *SFRM, *SFRM, *SFRM,
48 5 *CONS71, *CONS72, *CONS73, *CONS74, *CONS75, *CONS76, *CONS77,
49 6 *CONS78, *CONS79, *CONS80, *CONS81
50 NOPT= 0
51 GO TO 5
52 ENTRY CLF2(1ALPHA,CLDEL,CLSP,CLZ)
53 NOPT= 1
54 CONTINUE
55 C

```

Figure G.6. (Continued)

```

13 ALDEG= ALPHA * ROTDQ
14 CLALDG= CLALDG+DGTQD
15
16 IF(DEL.GT.DARK2) GO TO 1
17 ALNLP= CONST1 +CONS2*DEL
18 ALNLM= CONS3+CONS4*DEL
19 GO TO 20
20 ALNLP= CONS5
21 ALNLM= CONS6
22 CONTINUE
23 ALRPK1= ALNLP+DARK3
24 ALRPK2= ALNLM+DARK3
25
26 IF(DEL.GT.DP+K6) GO TO 112
27 F= CONS21*DEL*(CONS22+(CONS23*DEL))
28 GO TO 114
29 F= (CONS24*DEL*(CONS25+(CONS26*DEL))
30 CONTINUE
31 CL1= CLDAL+CLDEL+CLSP*F
32 IMAPI(4)= .FALSE.
33 IF(ALDQ.GE.ALARK2) GO TO 100
34 CLNLP= CL1+CLALDG+ALNLM
35 CLP= CLNLP*(CONS7+ALDEG)/(CONS7+ALRPK2)
36 IMAPI(4)= .TRUE.
37 GO TO 140
38
39 IF(ALDEG.GE.ALNLM) GO TO 110
40 CLMP= CL1+CLALDG+ALNLM
41 ALDUM= ALNLM-ALDEG+CONS1
42 DCLNL= ALDUM*(CONS8*ALDUM+CONS9) +CONS10
43 CLP= CLNLP+DCLNL
44 IMAPI(4)= .TRUE.
45 GO TO 140
46
47 IF(ALDEG.GT.ALNLP) GO TO 120
48 CLP= CLALDG+ALDEG+CL1
49 GO TO 142
50
51 IF(ALDEG.GT.ALARK1) GO TO 130
52 CLNLP= CL1+CLALDG+ALNLP
53 ALDUM= ALDEG-ALNLP+CONS1
54 DCLNI= ALDUM*(CONS*ALDUM+CONS9)+CONS10
55 CLP= CLNLP+DCLNI
56 IMAPI(4)= .TRUE.
57 GO TO 140
58
59 CONTINUE
60 CLMP= CL1+CLALDG+ALNLP
61 CLP= CLMP*(CONS7-ALDEG)/(CONS7-ALRPK1)
62 CONTINUE
63 IF(INOPT.NE.1) GO TO 150
64 CL7= CLP*CLWCR
65 RETURN
66 CONTINUE
67
68 CLPMX= CLMAX+CLDEL+CLSP
69 CLICF= CLP*CLWCR
70 IF(CLICF.LT.CLPMX) GO TO 160
71 DDICE= CL

```

Figure G.6. (Continued)

SUBROUTINE CLDCM(ALPHA,DEL,CLDEL,CLSP,CDFASP,CMFASP,CL,CD,CM,

I N D E X

```

65 CLICE= CLPMX
66 GO TO 179
67 CLICE= CD*CP*(CLICE-CLP)*(CLICE-CLP)
68 CONTINUE
69
70 ALDUM= DRK5
71 IF(ALDEG.LT.DBRK4) ALDUM=DRK4
72 IF(ALDEG.GE.DBRK4.AND.ALDEG.LE.DBRK5) ALDUM= ALDEG
73
74 COT= ACDM0*DEL*(ACDM1+DEL*(ACDM2+DEL*(ACDM3+DEL*(ACDM4+DEL*(ACDM5+DEL*(ACDM6+DEL*(ACDM7+DEL*(ACDM8+DEL*(ACDM9+DEL*(ACDM10+DEL*(ACDM11+DEL*(ACDM12+DEL*(ACDM13+DEL*(ACDM14+DEL*(ACDM15+DEL*(ACDM16+DEL*(ACDM17+DEL*(ACDM18+DEL*(ACDM19+DEL*(ACDM20+DEL*(ACDM21+DEL*(ACDM22+DEL*(ACDM23+DEL*(ACDM24))))))))))))))))))
75
76 IF(ALDEG.GE.DBRK4) GO TO 183
77 CM= CONS11+CD1+CMFASP
78 CD= CM*(1.-CDM)*(ALDEG-DBRK4)*CONS12
79 CDP= (CONS17+CMFASP)*(CONS7+ALDEG)*CONS12
80 GO TO 200
81
82 IF(ALDEG.GT.DBRK5) GO TO 190
83 CDP= ALDEG*(CONS13+ALDEG+CONS14) +CONS15+CD1+CDFASP
84 CPM= CONS18+CONS19*ALDEG+CMFASP
85 GO TO 200
86
87 CDPPLUS= CONS10+CD1+CDFASP
88 CDP= CDPPLUS*(1.-CDPLUS)*(ALDEG-DBRK4)*CONS12
89 CPM= (CONS20+CMFASP)*(CONS7-ALDEG)*CONS12
90 CONTINUE
91
92 CL= CLICE
93 CD= CP+DCDIGE
94 CM= CPM
95
96 RETURN
97 END

```

Figure G.6. (Continued)

I N D E X

ALMCRK	-	300							
ALNLM	-	17=						37	38
ALNLD	-	16=						48	54
ALPHA	-	LAG							
ALVTSI	-	300							
AREAMT	-	300							
AREAVT	-	300							
AREA4	-	300							
ARHT	-	300							
ARVT	-	300							
AVEYAC	-	300							
AVEYCS	-	300							
BIGX	-	400							
BKDI1	-	300							
BKDI2	-	300							
BKDI3	-	300							
BKLSW	-	300							
BKMI1	-	300							
BKMI2	-	300							
BKMI3	-	300							
BKMI4	-	300							
BKNSW	-	300							
BKQ9	-	400							
BLS	-	300							
BMDVTL	-	400							
BMDVTR	-	400							
BT1	-	300							
BT2	-	300							
BT3	-	300							
CD	-	LAG							
CDFASP	-	LAG							
CDM	-	74=							
CDMF	-	300							
CDOHT	-	300							
CDPHI	-	300							
CDPMLD	-	300							
CDPVT	-	300							
CDP	-	LAG							
CDPLUS	-	92=							
CDWCOH	-	400							
CDI	-	72=							
CMTRD	-	300							
CL	-	LAG							
CLALDG	-	14=							
CLALHT	-	300							
CLALPH	-	300							
CLCOCM	-	1#							
CLDEL	-	LAG							
CLF2	-	10=							
CLIGE	-	62=							
CLMAX	-	300							
CLMLP	-	32=							
CLOAL	-	300							
CLP	-	LAG							
CLPMX	-	61=							

Figure G.6. (Continued)

SUBROUTINE CLC3CMIALP4A, DEL, CLDEL, CLSP, CDFASP, CMFASP, CL, CD, CM,

I N D E X

CONS48	-	TCO			
CONS49	-	TCO			
CONS5	-	TCO	19		
CONS5C	-	TCO			
CONS51	-	TCO			
CONS52	-	TCO			
CONS53	-	TCO			
CONS54	-	TCO			
CONS55	-	TCO			
CONS56	-	TCO			
CONS57	-	TCO			
CONS58	-	TCO			
CONS59	-	TCO			
CONS6	-	TCO			
CONS60	-	TCO			
CONS61	-	TCO			
CONS62	-	TCO			
CONS63	-	TCO			
CONS64	-	TCO			
CONS65	-	TCO			
CONS66	-	TCO			
CONS67	-	TCO			
CONS68	-	TCO			
CONS69	-	TCO	33	55	74
CONS7	-	TCO			
CONS70	-	TCO			
CONS71	-	TCO			
CONS72	-	TCO			
CONS73	-	TCO			
CONS74	-	TCO			
CONS75	-	TCO			
CONS76	-	TCO			
CONS77	-	TCO			
CONS78	-	TCO			
CONS79	-	TCO			
CONS8	-	TCO	19	49	
CONS80	-	TCO			
CONS81	-	TCO			
CONS8	-	TCO	39	47	
CONS9	-	TCO			
CYALVT	-	TCO			
DBRK1	-	TCO			
DBRK10	-	TCO			
DBRK11	-	TCO			
DBRK12	-	TCO			
DBRK13	-	TCO			
DBRK14	-	TCO			
DBRK15	-	TCO			
DBRK16	-	TCO			
DBRK17	-	TCO			
DBRK18	-	TCO			
DBRK19	-	TCO			
DBRK2	-	TCO	15		
DBRK2C	-	TCO			
DBRK21	-	TCO	22		
DBRK3	-	TCO		23	

Figure G.6. (Continued)

SURROUPTINE C1C0CM ALPHA, DEL, CLDEL, CLSP, CDFASP, CMFASP, CL, CD, CM,

I N D E X

CBRK 4	70	71	73	75
CBRK 5	69	71	78	83
CBRK 6	24			
CBRK 7				
CBRK 8				
CBRK 9				
CCDIGE	67=	87		
CCDLG	40	49=	50	
CCMLG				
DEG20	15	16	17	24
DEL	14		25	27
DGTORD				72
DOWT				
DOWTL				
DOWTR				
OSDBET				
EFFMT				
EFFVT				
EM2REF				
EMPRN				
F	27=	29		
FEU				
FTE				
FINDEG				
FIMPR				
FIP				
FIXF				
FIXPR				
FIXX				
FIXZF				
FIXZPR				
FIXZW				
FIVF				
FIVPR				
FIVW				
FIZF				
FIZPR				
FIZW				
FLAGS				
GUTOM				
GEF				
GEFVAR				
MGEFLR				
MGEFRR				
MLMJB				
MP				
MRMJB				
HTC4				
HTVTKT				
HMC4				
ICONOP				
IPHA5E				
ISENCE				
ISLOW				

Figure 6. (Continued)

I N D E X

ISTA	-	500
ISTR	-	500
ITRIM	-	500
IMARN1	-	500
IMARN2	-	500
IMREVT	-	500
JTPIM	-	500
KTRIM	-	500
NGFF	-	500
NOPT	-	8=
NPLT	-	57
NPLT2	-	500
NTWST	-	500
NVB	-	500
OMREF	-	300
PC	-	300
PIPH	-	300
PI	-	300
PIOV2	-	300
ROTODG	-	300
RETURN	-	13
ROTPS	-	59*
ROTRAD	-	300
RR11	-	300
RR12	-	400
SBFPR	-	300
SMPR	-	300
SBI	-	400
SFNL	-	700
SFNR	-	700
SFPL	-	700
SFPL	-	700
SFMR	-	700
SFPR	-	700
SFQL	-	700
SFOR	-	700
SFSL	-	700
SFSR	-	700
SFTL	-	700
SFTR	-	700
SFVHL	-	700
SFYMR	-	700
SG	-	300
SHF	-	300
SHW	-	300
SKFPS	-	300
SKO	-	300
SK1	-	300
SK10	-	300
SK2	-	300
SK20	-	300
SK21	-	300
SK22	-	300
SK3	-	300
SK30HI	-	300

*

Figure G.6. (Continued)

I N D E X

SK3CLD	-	300
SK3IMI	-	300
SK3ILD	-	300
SK32	-	300
SK34	-	300
SK35	-	300
SK36	-	300
SK37	-	300
SK38	-	300
SK39	-	300
SK4	-	300
SK40	-	300
SK41	-	300
SK42	-	300
SK43	-	300
SK44	-	300
SK45	-	300
SK46	-	300
SK47	-	300
SK48	-	300
SK49	-	300
SK5	-	300
SK50	-	300
SK6	-	300
SK7	-	300
SK8	-	300
SK9	-	300
SL	-	300
SLF	-	300
SLPA	-	300
SLW	-	300
SM	-	300
SME	-	300
SMM	-	300
SNN	-	300
SPAN	-	300
SOPRM	-	300
SMLG	-	500
TAUNT	-	300
TAURT1	-	300
TAURT2	-	300
TAURT	-	300
TIGEL	-	400
TIGER	-	400
XALDEF	-	2*
XFAC	-	300
XMT	-	300
XPAR1	-	3*
XPAR3	-	7*
XVT	-	300
XWAC	-	300
XMC2	-	300
YN	-	300
YPA	-	300
YWAC	-	300

* *

Figure G.6. (Continued)

SUBROUTINE CUCOCM(ALPHA, DEL, CLOFL, CLSP, CDFASP, CMFASP, CL, CD, CM,

I N D E X

ZFAC - 300
ZHT - 300
ZPA - 300
ZVT - 300
ZWAC - 300

Figure G.6. (Continued)

SUBROUTINE ENGINE1TEA, SHPOUT, OMENG, PCTORQ

I N D F X

```

1 SURROUTINE ENGINE (TFA, SHPOUT, OMENG, PCTORQ)
2 COMMON/ENG/ NWDOTD, NIIND, N1THID, N2IND, NOIND, NRNDID,
* FWDOTX, ENIMX, ENLTMX, EN2MX, EQMX, SHPSTR
* , ENDIPT, ENLSTR, ROE2, TZERO, TCDIF
3 COMMON/ENGVAR/
1 AMACH, AMACSO, DEL, FMAXNI, EMAXN2, EMXDT, EN2STR, FSMACH, OMEGEL,
2 OMEGER, ONOVC, OVFSM, OVSO, OVTHOL, ROE, ROE2, SHPRL, SHPRR,
3 SHA, SQNI, SQNYC, SQWDTX, TDEGF, TEAL, TEAR, THDEL, THETC
4, PCTOR, PCTOR
COMMON/FLAGS/ IWARN1(16), IWARN2(16), ISENCE(2), IREV(12), ICONDP,
1 ITRIM, JTRIM, KTRIM, NPLT, NPLT2, IPHASE, ISLOW, SMLG, GNOTON,
2 ISTR, NGEF, NVB, NTWST
5 LOGICAL*1 IWARN1, IWARN2
C
C ENGINE CHARACTERISTICS USED
C NWDOTD = 1 FUEL FLOW CUTOFF
C NIIND = 1 NI CUTOFF
C N1THID = 0 NO REFERRED NI CUTOFF
C N2IND = 2 N2 CUTOFF - NON-OPTIMUM N2 VARIATION
C NOIND = 1 TORQUE CUTOFF
C NRNDID = 0 NO REYNOLDS NUMBER CORRECTIONS
C
C TEASQ = TEA * TEA
C TFACUR = TFASQ * TEA
C TEAT4 = TEACUR * TEA
C NOTF TEA = TPS / THETC
C IF(NWDOTD.EQ.0) GO TO 1000
C FIND (WDOT/SHI) AT TEA,M
C
C W DOT = F(TFA) EQUATION FROM CURVE FIT PROGRAM
C 4TH ORDER IN TEA
C EMDOT = -2.050260368E-3531349133E-02*TEA - 2594440658E-05*TEASQ
* + 1.012475181E-08*TEACUR - 1.444138415E-12*TEAT4M
C
C IWARN1(1) = .FALSE.
C IF(EMDOT.LT.EMXDT) GO TO 1000
C IWARN1(1) = .TRUE.
C FIND TEA AT MAX WDOT,M
C
C TEA = F(W DOTMX) FROM CURVE FIT PROGRAM
C 4TH ORDER IN W DOTMX
C TFA = 1587.5624254398-1375.3423740761*EMXDT+12872.89968281*
* SQWDTX-22742.78987105*SQWDTX*EMXDT+13929.828136431*SQWDTX *
* SQWDTX
C
C TEASQ = TEA * TEA
C TFACUR = TEASQ * TEA
C TEAT4 = TEACUR * TEA
C
C IF(NIND.EQ.0) GO TO 2000
C FIND NI/N1STAR AT TEA,M
C
C NI = F(TEA,M) EQUATION FROM CURVE FIT PROGRAM
C 3RD ORDER IN TEA, 2ND ORDER IN M
C EN1 = -2.262254353 + 1.2512886559*AMACH + .9621240231*AMACSO

```

Figure G.6. (Continued)


```

30  * TEA = 7.9633431215-.2571992619*AMACH+.13604785869*AMACSQ
    *+(-.6857620249E-02+.7364751077E-03*AMACH-.1979318276E-02*AMACSQ)*
    * TEA +
    * (-.4348718891E-05-.3926992714E-06*AMACH+.1001305662E-05*AMACSQ)*
    * TEASO +
    * (-.7484074668E-09+.696958120E-10*AMACH+.1674167095E-09*AMACSQ)*
    * TEACUR
C
40  * ENGSHP = SHPMX*PROESH
    * END OF ENG 1 SUBR BLOCK
41  * IF(INZIND.EQ.1) GO TO 6000
42  * IF(INZIND.NE.1) GO TO 8000
    * THIS OPTION WILL BE LEFT BLANK UNTIL NEEDED
C
43  * GO TO 8000
44  * IF(INZIND.EQ.2) GO TO 7000
    * THIS OPTION WILL BE LEFT BLANK UNTIL NEEDED
C
45  * SHPMX = FOMX*EN2STR*OVTHDI
46  * IARMN1(1) = .FALSE.
47  * IF(ENGSHP.LT.SHPMAX) GO TO 9000
48  * IARMN1(3) = .TRUE.
49  * ENGSHP = SHPMX
    * FIND TEA AT MAX SHP * M
C
    * TEA = F(SHP,M) EQUATION FROM CURVE FIT PROGRAM
    * 3RD ORDER IN SHPMX * 2ND ORDER IN M
C
50  * TEA = 155C.0865704333-170.1433076663*AMACH-242.7678229176*AMACSQ
    *+(-1145.2371955474+149.9327819876*AMACH+706.56693216443*AMACSQ)*
    * SHPMX +
    * (-1125.4640744348+74.2324453353*AMACH-792.572236279916*AMACSQ)*
    * SHPMX + SHPMX +
    * (456.38766443477-226.4415181282*AMACH+311.0686620534*AMACSQ)*
    * SHPMX*SHPMX*SHPMX
    * TFASO = TEA * TEA
    * TEACUR = TEASO * TEA
    * TEA4TH = TEACUR * TEA
C
    * SINCE TORQUE LIMIT MET CAUSING A LOWER TEA TO BE REQ. THE
    * NI CALCULATION MUST BE RE-CALCULATED
    * EN1 = -2.242254353 +1.2312486559*AMACH+.9621240231*AMACSQ
    *+(-.3519585479E-07-.1539742133E-02*AMACH-.1308445977E-02*AMACSQ)*
    * TEA +
    * (-.13116093310E-05+.6259888594E-06*AMACH+.6764941537E-06*AMACSQ)*
    * TEASO +
    * (-.1745905983E-09-.8357285710E-10*AMACH-.9302102725E-10*AMACSQ)*
    * TEACUR
C
55  * IF(INZIND.NE.1) GO TO 9000
    * THIS OPTION WILL BE LEFT BLANK UNTIL NEEDED
C
56  * SHPOUT = ENGSHP*SHPMX*THCDEL
57  * OWENG = EN1*SQTHTC * EN1STR*0.10471356
58  * CTORQ = 10*. *THCDEL *ENGSHP /EN2STR
59  * RETURN
60  * END

```

Figure G.6. (Continued)

SURFUTINE GEAR

I N D E X

```

30 HCPHIN= COS(THETA*(YIN*SIGNPHI+(ZNR*ADIN))*COS(PHI-1.))
31 DDVCTP= 1./Z(COSTHETA*COSPHI)
32 HTN= (H+H*HTN-HCPHIN) * DDVCTP
C
33 IF(HTN.LT.0.) GO TO 100
34 DX(N)= 0.
35 DY(N)= 0.
36 DZ(N)= 0.
37 DL(N)= 0.
38 DM(N)= 0.
39 DN(N)= 0.
40 GO TO 200
C
41 RATE OF STRUT DEFLECTION
HTDTN= HDOT*DDVCTP+OPRIME*DXN-PPRIME*YIN
C
42 VERTICAL FORCE
FGZN= SKST(N)*HTN +SDST(N)*HTDTN
C
43 LONGITUDINAL FORCE
FMUN= (FRICTO+FRICTL*RG(N))*C57N*SIGNU
C
44 SINCE FGZN IS ALWAYS NEGATIVE
IF U GT 0. FMUN IS NEGATIVE
IF U LT 0. FMUN IS POSITIVE
IF U EQ 0. FMUN IS ZERO
C
45 SIDE FORCE
FSN= FRICTS*FGZN*SIGNV
C
46 SINCE FSN IS ALWAYS NEGATIVE
IF V GT 0. FSN IS NEGATIVE
IF V LT 0. FSN IS POSITIVE
IF V EQ 0. FSN IS ZERO
C
47 FORCE AND MOMENT CONTRIBUTION
DX(N)= FMUN - FGZN * THE
DY(N)= FSN+FGZN*PHI
DZ(N)= FMIN*THE-FSN*PHI+FGZN
DM(N)= -DZ(N)*XN+DX(1)*ZNR*ADIN+HTN
DL(N)= DZ(N)*YN -DY(N)*ZNR*ADIN+HTN
DN(N)= -DX(N)*YN +XN*DY(N)
N= N+1
IF(N.LF.3) GO TO 50
48 DXLG= DX(1)+DX(2)+DX(3)
49 DYLG= DY(1)+DY(2)+DY(3)
50 DZLG= DZ(1)+DZ(2)+DZ(3)
51 DMLG= DL(1)+DL(2)+DL(3)
52 DNLG= DN(1)+DN(2)+DN(3)
53 RETURN
54 END
55
56
57
58
59
60

```

Figure G.6. (Continued)

SYMBOL	REFERENCES	REFERENCES	REFERENCES
SC	74*	52	
75	12	13*	
I	31	51*	
11	12	15*	
12	12	17*	
12*	14	14	18*
13	19	20*	
14	19	22*	
15	19	24*	
15*	21	23	25*
20	6	51*	
ADC	203		
ADC3	203		
ALAF	500		
ALAREP	500		
ALES0	500		
ALPHE	500		
AMADE	500		
AMAREP	500		
ANARE	500		
ANAREP	500		
ASTAF	500		
BETEST	500		
BG	43	17*	43
BRKQUM	307	17*	
BRK1	307	17*	
BRK2	307		
BRK3	307		
CRCAR	500		
CDI	500		
CGTVP	4*		
CIF	500		
CMF	500		
CAF	500		
CNEPL	200		
CNEPD	207		
COSALF	500		
COSBTF	500		
COSPHI	31	31	
COSTHE	31	31	
CPL	200		
CPMPL	207		
CPMPR	207		
CPP	200		
CSFPL	207		
CSFPR	207		
CTLPRM	207		
CTPRM	200		
CVF	500		
CVMPL	200		
CVMPR	200		
DELSPL	207		
DELSPR	200		

Figure G.6. (Continued)

SUBROUTINE SEAP

I N D E X

SCPAC3	-	200			
SCDACC4	-	200			
SDET	-	701	9E0	42	
SOSTDM	-	300	9F0		
SOCT1	-	300			
SOCT2	-	300			
SOCT3	-	300			
SIGNU	-	13=	17=	43	
SIGNV	-	22=	24=	44	
SIGNALF	-	500			
SINRYF	-	500			
SINDHI	-	500			
SINTHE	-	500			
SKST	-	701	9F0	42	
SKSTDW	-	300	9F0		
SKST1	-	300			
SKST2	-	300			
SKST3	-	300			
SQF	-	500			
THE	-	200	45	47	
UPOLMF	-	200	12		
VEAST	-	400			
VNORTH	-	400			
VPOLMF	-	200	10		
WDET	-	200			
WPOLMF	-	200			
XAEFR	-	500			
XALD	-	200			
XARFP	-	500			
XCG	-	400	26		
XDTGG	-	400			
XG	-	701	9F0	26	
XGDM	-	300			
XGEAR	-	300			
XG1	-	300			
XG2	-	300			
XG3	-	300			
XN	-	200	20	41	49
XN	-	200			50
YAERF	-	500			
YARFP	-	500			
YG	-	701	9F0	27	
YGDUM	-	300			
YG1	-	300	9F0		
YG2	-	300			
YG3	-	300			
YN	-	27=	30	41	49
YN	-	27=			50
ZARFR	-	500			
ZARFP	-	500			
ZCG	-	400	20		
ZOTCG	-	400			
ZG	-	701	9F0	20	
ZGDUM	-	300			
ZG1	-	300	9F0		
ZG2	-	300			
ZG3	-	300			

Figure G.6. (Continued)

***** SUPER INDEX *****

T	A	D	F	X
ASS	-			RTSLOW
ACDMC	-			CLCOCM
ACDM1	-			CLCOCM
ACDM1C	-			CLCOCM
ACDM11	-			CLCOCM
ACDM12	-			CLCOCM
ACDM13	-			CLCOCM
ACDM14	-			CLCOCM
ACDM15	-			CLCOCM
ACDM16	-			CLCOCM
ACDM17	-			CLCOCM
ACDM18	-			CLCOCM
ACDM19	-			CLCOCM
ACDM2	-			CLCOCM
ACDM2C	-			CLCOCM
ACDM21	-			CLCOCM
ACDM22	-			CLCOCM
ACDM23	-			CLCOCM
ACDM24	-			CLCOCM
ACDM3	-			CLCOCM
ACDM4	-			CLCOCM
ACDM5	-			CLCOCM
ACDM6	-			CLCOCM
ACD47	-			CLCOCM
ACDMF	-			CLCOCM
ACDM9	-			CLCOCM
ADC	-			PTEFAST
ADCFLT	-			RTEFAST
AGDVAT	-			RTSLOW
AGDVAM	-			RTSLOW
ATCL	-			RTEFAST
ATCLDP	-			RTEFAST
ATCLOS	-			RTEFAST
ATCLPP	-			RTEFAST
ATC?	-			RTEFAST
ATCPN	-			RTEFAST
ATPCS	-			PTEFAST
ATCPPP	-			RTEFAST
AILSP	-			RTEFAST
ATNDYL	-			RTEFAST
ATNOTA	-			RTEFAST
AINHT	-			RTEFAST
AINL	-			RTEFAST
AINR	-			RTEFAST
AINW	-			RTEFAST
AITRIP	-			RTEFAST
AKEY	-			RTSLOW
ALAEFC	-			RTEFAST
ALARF	-			RTEFAST
ALARFP	-			RTEFAST
ALARHT	-			RTEFAST
ALARNC	-			PTEFAST
ALAFNL	-			PTEFAST
ALARAP	-			PTEFAST
ALARPC	-			PTEFAST

RTSLOW
 PTEFAST
 RTSLOW

RTSLOW

Figure G.6. (Continued)

***** SUPER INDEX *****

INDEX		
CLSP	-	CLC0CM
CLSRW	-	RTFAST
CLSW	-	RTFAST
CLTCOR	-	RTSLOW
CLWOPR	-	CLC0CM
CLZ	-	RTSLOW
CLZERO	-	RTFAST
CL1	-	CLC0CM
CM	-	CLC0CM
CMNTL	-	RTFAST
CMNTR	-	RTFAST
CMF	-	RTSLOW
CMFASP	-	CLC0CM
CMLN	-	RTSLOW
CMLMAD	-	RTFAST
CMLWSS	-	RTFAST
CMDF	-	RTSLOW
CMON	-	RTSLOW
CMOW	-	RTFAST
CMF	-	CLC0CM
CMRN	-	RTSLOW
CMRWAD	-	RTFAST
CMRWSS	-	RTFAST
CMSLW	-	RTFAST
CMSRW	-	RTFAST
CMF	-	RTSLOW
CMFAIL	-	RTFAST
CMFAIR	-	RTFAST
CMFBI	-	RTFAST
CMFBIR	-	RTFAST
CMFL	-	RTFAST
CMFPL	-	RTFAST
CMFPR	-	RTFAST
CMFR	-	RTFAST
CMNL	-	RTSLOW
CMOF	-	RTSLOW
CMOLN	-	RTSLOW
CMORN	-	RTSLOW
CMRN	-	RTSLOW
CNSW	-	RTFAST
COEF1	-	RTSLOW
COEFIC	-	RTFAST
COEF11	-	RTFAST
COEF12	-	RTFAST
COEF13	-	RTFAST
COEF16	-	RTFAST
COEF17	-	RTSLOW
COEF18	-	RTFAST
COEF19	-	RTFAST
COEF2	-	RTFAST
COEF20	-	RTFAST
COEF21	-	RTFAST
COEF27	-	RTFAST
COEF23	-	RTFAST
COEF24	-	RTFAST

Figure G.6. (Continued)

***** SUPER INDEX *****

I N D E X	
COEF25	- RTSLOW
COEF26	- RTSLOW
COEF27	- RTSLOW
COEF28	- RTSLOW
COEF29	- RTSLOW
COEF3	- RTSLOW
COEF30	- RTSLOW
COEF31	- RTEFAST
COEF32	- RTEFAST
COEF33	- RTEFAST
COEF34	- RTEFAST
COEF35	- RTSLOW
COEF4	- RTEFAST
COEF5	- RTSLOW
COEF6	- RTSLOW
COEF7	- RTSLOW
COEF8	- RTSLOW
COEF9	- RTEFAST
CONS10	- CLCOCM
CONS11	- CLCOCM
CONS12	- CLCOCM
CONS13	- CLCOCM
CONS14	- CLCOCM
CONS15	- CLCOCM
CONS16	- CLCOCM
CONS17	- CLCOCM
CONS18	- CLCOCM
CONS19	- CLCOCM
CONS2	- CLCOCM
CONS20	- CLCOCM
CONS21	- CLCOCM
CONS22	- CLCOCM
CONS23	- CLCOCM
CONS24	- CLCOCM
CONS25	- CLCOCM
CONS26	- CLCOCM
CONS27	- AILSP
CONS28	- AILSP
CONS29	- AILSP
CONS3	- CLCOCM
CONS30	- AILSP
CONS31	- AILSP
CONS32	- AILSP
CONS33	- AILSP
CONS34	- AILSP
CONS35	- AILSP
CONS36	- AILSP
CONS37	- AILSP
CONS38	- AILSP
CONS39	- AILSP
CONS4	- CLCOCM
CONS40	- AILSP
CONS41	- RTEFAST
CONS42	- RTEFAST

RTSLOW

Figure G.6. (Continued)

***** SUPER INDEX *****

I	N	D	E	X	
CONS43	-	RTFAST			
CONS44	-	RTSLOW			
CONS45	-	RTSLOW			
CONS46	-	RTSLOW			
CONS47	-	RTSLOW			
CONS48	-	RTSLOW			
CONS49	-	RTSLOW			
CONS50	-	CLCDCM			
CONS51	-	RTSLOW			
CONS52	-	RTSLOW			
CONS53	-	RTSLOW			
CONS54	-	RTSLOW			
CONS55	-	RTSLOW			
CONS56	-	RTSLOW			
CONS57	-	RTSLOW			
CONS58	-	RTSLOW			
CONS59	-	RTSLOW			
CONS60	-	CLCDCM			
CONS61	-	RTSLOW			
CONS62	-	RTSLOW			
CONS63	-	RTSLOW			
CONS64	-	RTSLOW			
CONS65	-	RTFAST			
CONS66	-	RTFAST			
CONS67	-	AILSP			
CONS68	-	AILSP			
CONS69	-	AILSP			
CONS70	-	CLCDCM			
CONS71	-	AILSP			
CONS72	-	RTFAST			
CONS73	-	RTFAST			
CONS74	-	RTFAST			
CONS75	-	RTFAST			
CONS76	-	RTFAST			
CONS77	-	RTFAST			
CONS78	-	RTFAST			
CONS79	-	RTFAST			
CONS80	-	CLCDCM			
CONS81	-	RTFAST			
CONS82	-	CLCDCM			
CONS83	-	RTFAST			
CONS84	-	RTFAST			
CONS85	-	RTFAST			
CONS86	-	RTFAST			
CONS87	-	RTFAST			
CONS88	-	RTFAST			
CONS89	-	RTFAST			
CONS90	-	RTFAST			
CONS91	-	RTFAST			
CONS92	-	RTFAST			
CONS93	-	RTFAST			
CONS94	-	RTFAST			
CONS95	-	RTFAST			
CONS96	-	RTFAST			
CONS97	-	RTFAST			
CONS98	-	RTFAST			
CONS99	-	RTFAST			
CONS100	-	RTFAST			

RTSLOW
RTSLOW
RTSLOW
RTSLOW
RTSLOW
RTSLOW

Figure G.6. (Continued)

***** SUPER INDEX *****

T N D F X	-	RTFAST
COSZHR	-	RTFAST
CPHIP	-	RTFAST
CPL	-	RTFAST
CPMAIL	-	RTFAST
CPMAILR	-	RTFAST
CPMAIL	-	RTFAST
CPMAILR	-	RTFAST
CPML	-	RTFAST
CPMPL	-	RTFAST
CPMPR	-	RTFAST
CPMR	-	RTFAST
CPR	-	RTFAST
CSFAIL	-	RTFAST
CSFAIR	-	RTFAST
CSFBIL	-	RTFAST
CSFBIR	-	RTFAST
CSEFL	-	RTFAST
CSEPL	-	RTFAST
CSEPR	-	RTFAST
CSFR	-	RTFAST
CTAULF	-	RTSLOW
CTAURR	-	RTSLOW
CTL	-	RTFAST
CTLPPM	-	RTFAST
CTR	-	RTFAST
CTRPPM	-	RTFAST
CTSLLP	-	RTFAST
CTSRP	-	RTFAST
CYALVT	-	RTFAST
CYAT	-	RTFAST
CYF	-	RTSLOW
CYLY	-	RTSLOW
CYMAIL	-	RTFAST
CYMAIP	-	RTFAST
CYMBIL	-	RTFAST
CYMBIR	-	RTFAST
CYML	-	RTFAST
CYMP	-	RTFAST
CYMPR	-	RTFAST
CYMR	-	RTFAST
CYRN	-	RTSLOW
CYVT	-	RTFAST
CYVTST	-	RTFAST
CZINL	-	RTSLOW
CZINP	-	RTSLOW
CACFLT	-	RTFAST
LACIO	-	RTFAST
LAC1	-	RTFAST
LAC2	-	RTFAST
DBRK1	-	RTFAST
DBRK1C	-	RTSLOW
DBRK11	-	RTSLOW
DBRK12	-	RTSLOW
DBRK13	-	RTSLOW
DBRK14	-	RTSLOW

RTSLOW
RTSLOW

Figure G.6. (Continued)

***** SUPER INDEX *****

I N D E X

DBRK 15	-	RTSLOW
DBRK 16	-	RTSLOW
DBRK 17	-	RTFAST
DBRK 18	-	RTFAST
DBRK 19	-	RTFAST
DBRK 2	-	CLCOCM
DBRK 20	-	AILSP
DBRK 21	-	AILSP
DBRK 22	-	CLCOCM
DBRK 23	-	CLCOCM
DBRK 3	-	CLCOCM
DBRK 4	-	CLCOCM
DBRK 5	-	CLCOCM
DBRK 6	-	CLCOCM
DBRK 7	-	AILSP
DBRK 8	-	AILSP
DBRK 9	-	RTFAST
DCCA	-	AILSP
DCDTGE	-	CLCOCM
DCDLDA	-	RTFAST
DCDLG	-	RTSLOW
DCDLSP	-	RTFAST
DCDRDA	-	RTFAST
DCDRSP	-	RTFAST
DCDS	-	AILSP
DCLA	-	AILSP
DCLLCA	-	RTFAST
DCLLSP	-	RTFAST
DCLML	-	CLCOCM
DCLRDA	-	RTFAST
DCLRSP	-	RTFAST
DCLS	-	AILSP
DCLSPH	-	RTFAST
DCMA	-	AILSP
DCMLDA	-	RTFAST
DCMLG	-	RTSLOW
DCMLSP	-	RTFAST
DCMRDA	-	RTFAST
DCMRSP	-	RTFAST
DCMS	-	AILSP
DCNSPM	-	RTFAST
DEGZO	-	RTFAST
DEL	-	AILSP
DELELV	-	RTFAST
DELEPZ	-	RTFAST
DELFLP	-	RTFAST
DELKUN	-	RTFAST
DELSPL	-	RTFAST
DELSPR	-	RTFAST
DEPDAL	-	RTFAST
DPLATL	-	RTFAST
DFLATR	-	RTFAST
DGTORD	-	CLCOCM
DIGAN	-	RTFAST
DISARI	-	RTFAST
DL	-	GEAR
DLFPSQ	-	RTFAST

CLCOCM RTFAST RTSLOW

RTFAST

RTSLOW

***** SUPER INDEX *****

T N P F X

ENF2	-	RTFAST		
ENF3	-	RTFAST		
ENF4	-	RTFAST		
ENG	-	ENGINE	RTSLOW	
ENGINE	-	RTSLOW		
ENG5MP	-	ENGINE		
ENGVAR	-	ENGINE	RTFAST	
EN1	-	ENGINE		
EN1X	-	RTSLOW		
EN1STR	-	ENGINE		
EN2	-	ENGINE		
EN2X	-	RTSLOW		
EN2DPT	-	ENGINE		
EN2REF	-	RTSLOW		
EN2STR	-	ENGINE		
EN2VAR	-	RTFAST	RTSLOW	
EP1LR	-	RTFAST	RTSLOW	
EP1R	-	RTFAST	RTSLOW	
EP1	-	RTFAST		
EP2	-	RTFAST		
EP3	-	RTFAST		
EP4	-	RTFAST		
EP5	-	RTFAST		
EP6	-	RTFAST		
EP7	-	RTFAST		
EPPLR	-	RTFAST	RTSLOW	
EPPRM	-	RTSLOW		
EPPT	-	RTFAST		
EPTAIL	-	RTFAST		
EPTL1	-	RTFAST		
EPURL	-	RTFAST		
EPURR	-	RTFAST		
EP7ER	-	RTFAST		
EQX	-	ENGINE		
ESF1	-	RTFAST		
ESF2	-	RTFAST		
ESF3	-	RTFAST		
ESF4	-	RTFAST		
ESMP	-	ENGINE		
EMDOT	-	ENGINE		
EMDT4X	-	RTSLOW		
EMDTPR	-	RTSLOW		
EY1	-	RTFAST		
EY2	-	RTFAST		
EY3	-	RTFAST		
EY4	-	RTFAST		
EY5	-	RTFAST		
EY6	-	RTFAST		
EY7	-	RTFAST		
F	-	CLDCM		
FU	-	RTFAST		
FGZN	-	GEAR		
FIE	-	RTFAST		
FINDEF	-	RTFAST		
FINPR	-	RTFAST		

Figure G.6. (Continued)

***** SUPER INDEX *****

I N D E X			
HTDTN	-	GEAR	
HTN	-	GEAR	
HTTRM	-	RTFAST	
HTSLL	-	RTFAST	
HWACL	-	RTFAST	
HWACR	-	RTFAST	
HWC4	-	RTSLOW	
HWBCOM	-	RTFAST	RTSLOW
HWBIO	-	RTFAST	RTSLOW
HIDTL	-	RTFAST	
HIDTR	-	RTFAST	
HIL	-	RTFAST	
HILOLD	-	RTFAST	
HIR	-	RTFAST	
HIROLD	-	RTFAST	
HICMOP	-	RTSLOW	
IFC	-	RTSLOW	
IMITVR	-	RTFAST	RTSLOW
IPAN	-	RTFAST	RTSLOW
IPSMS	-	RTFAST	
IREVNT	-	RTSLOW	
ISENCE	-	RTSLOW	
ISLOW	-	RTSLOW	
ISTA	-	RTFAST	
ISTAD	-	RTFAST	
ISTB	-	RTSLOW	
ISTDA	-	RTFAST	
ISTFLT	-	RTFAST	
ISTG	-	RTFAST	
ISTRBI	-	RTSLOW	
ITRIM	-	RTSLOW	
IWARN1	-	CLDCM	ENGINE
J	-	RTFAST	RTSLOW
JTRM	-	RTSLOW	
KAR	-	RTFAST	
KONFR	-	RTFAST	
KPAN	-	RTFAST	RTSLOW
KTRIM	-	RTSLOW	
LINT	-	RTFAST	RTSLOW
N	-	GEAR	
NACVAR	-	RTFAST	RTSLOW
NCLOSE	-	RTFAST	
NCON	-	RTSLOW	
NEEF	-	RTSLOW	
NEFT	-	RTSLOW	
NOPT	-	ATLSP	
NOIND	-	ENGINE	CLDCM
NRNDID	-	ENGINE	
NTWST	-	RTFAST	
NVB	-	RTFAST	
NMDTD	-	ENGINE	
N1IND	-	ENGINE	
N1THD	-	ENGINE	
N2IND	-	ENGINE	
OMDOT	-	RTFAST	
OMDTL	-	RTFAST	

Figure G.6. (Continued)

***** SUPER INDEX *****

INDEX			
CMDTR	-	RTFAST	
OMEGA	-	RTFAST	RTSLOW
OMEGAL	-	RTFAST	
OMEGAR	-	RTFAST	
OMEGEL	-	RTFAST	RTSLOW
OMEGEP	-	RTFAST	RTSLOW
CMENG	-	ENGINE	
OMREF	-	RTSLOW	
OMSQL	-	RTFAST	
OMSOR	-	RTFAST	
OMOVTC	-	RTSLOW	
OMOVCTP	-	GEAR	
OOVDSK	-	RTFAST	
OOVFSM	-	RTFAST	RTSLOW
OOVIXX	-	RTFAST	RTSLOW
OOVIVY	-	RTFAST	RTSLOW
OOVIZZ	-	RTFAST	RTSLOW
OVDTIM	-	RTFAST	
OVSOIH	-	ENGINE	RTSLOW
OVTHDL	-	ENGINE	RTSLOW
P	-	RTFAST	
PC	-	RTSLOW	
PCTORO	-	ENGINE	
PCTQR	-	RTFAST	RTSLOW
PGUST	-	RTFAST	
PHI	-	GEAR	RTSLOW
PI	-	RTFAST	
PIOV2	-	RTFAST	
PNLN	-	RTFAST	
PNLR	-	RTFAST	
PNRN	-	RTFAST	
PNRR	-	RTFAST	
PP	-	RTFAST	
PPRIME	-	GEAR	RTFAST
PQ	-	RTFAST	
PR	-	RTFAST	
PSI	-	RTSLOW	
O	-	RTFAST	
QFSW	-	RTSLOW	
OGUST	-	RTFAST	
QNLN	-	RTFAST	
QNLR	-	RTFAST	
QNRN	-	RTFAST	
QNR	-	RTFAST	
QPRIME	-	GEAR	RTFAST
R	-	RTFAST	
RAD	-	GEAR	
RADI	-	GEAR	
RCBI	-	RTSLOW	
ROTODG	-	CLCDCM	RTFAST
RESLR	-	RTSLOW	
RESKR	-	RTSLOW	
RETURN	-	RTSLOW	
REVENT	-	RTSLOW	
RGUST	-	RTFAST	
		ENGINE	RTFAST
		GEAR	RTFAST
		CLCDCM	RTSLOW

Figure G.6. (Continued)

***** SUPER INDEX *****

I N D E X		
SK40	-	RTSLOW
SK41	-	RTSLOW
SK42	-	RTSLOW
SK43	-	RTSLOW
SK44	-	RTSLOW
SK45	-	RTSLOW
SK6	-	RTSLOW
SK7	-	RTSLOW
SK8	-	RTSLOW
SK9	-	RTSLOW
SL	-	RTSLOW
SLAC	-	RTFAST
SLF	-	RTSLOW
SLPA	-	RTFAST
SLW	-	RTSLOW
SMA	-	RTSLOW
SPAN	-	RTFAST
SPHIP	-	RTFAST
SPID	-	RTSLOW
SPOIL	-	AILSP
SQF	-	RTFAST
SQFPM	-	RTFAST
SOLNC	-	RTSLOW
SOLM	-	RTFAST
SOLMPI	-	ENGINE
SORES	-	RTSLOW
SORES	-	RTSLOW
SOMNC	-	RTSLOW
SORW	-	RTFAST
SQHTC	-	ENGINE
SQMDTX	-	ENGINE
SQWING	-	RTFAST
SSQIML	-	RTSLOW
SSQIMR	-	RTSLOW
STAIR	-	RTSLOW
STAIR	-	RTSLOW
SVSTAR	-	RTSLOW
SVSTAR	-	RTSLOW
SVSTRL	-	RTSLOW
SWLG	-	RTFAST
SWLG2	-	RTSLOW
S2INL	-	RTSLOW
S2IMP	-	RTSLOW
TAILWR	-	RTFAST
TAN	-	RTSLOW
TAUNT	-	RTFAST
TAULR	-	RTSLOW
TAULR	-	RTSLOW
TAUVT	-	RTFAST
TAVAEP	-	RTSLOW
TODEF	-	RTSLOW
TDEGF	-	RTSLOW
TEA	-	ENGINE
TEACUR	-	ENGINE
TEAR	-	RTSLOW

RTSLOW

RTSLOW

RTSLOW

RTFAST
RTSLOW

RTSLOW

Figure G.6. (Continued)

***** SUPER INDEX *****

I N D E X		
TFASQ	-	ENGINE
TFATH	-	ENGINE
TERMP1	-	PTFAST
TERMQ1	-	PTFAST
TERMP1	-	PTFAST
TERM1	-	RTSLOW
TERMIL	-	RTFAST
TERM1R	-	PTFAST
TERM2	-	RTSLOW
TERM2L	-	RTFAST
TERM2R	-	RTFAST
TERM3	-	RTSLOW
TERM3L	-	RTFAST
TERM3R	-	RTFAST
TERM4	-	RTSLOW
TERM5	-	RTSLOW
TERM6	-	RTSLOW
THCODEL	-	ENGINE
THE	-	GEAR
THEYC	-	RTSLOW
THTLAC	-	RTFAST
THTRAC	-	RTFAST
THTRIP	-	RTFAST
TIGEL	-	RTFAST
TIGER	-	RTFAST
TL	-	RTFAST
TMHRIC	-	RTFAST
TMHR11	-	RTFAST
TMHR12	-	RTFAST
TMGIC	-	RTSLOW
TMG11	-	RTSLOW
TNAC1	-	RTSLOW
TNAC2	-	RTSLOW
TOROL	-	RTFAST
TOROP	-	RTFAST
TPSR	-	RTSLOW
TP	-	RTFAST
TRACK	-	RTFAST
TRMARI	-	PTFAST
TRMAR2	-	PTFAST
TRMAR3	-	PTFAST
TRMAP4	-	PTFAST
TPMCKK	-	RTFAST
TPMHBI	-	RTFAST
TPMHR2	-	RTFAST
TPMHR3	-	RTFAST
TPMHR4	-	RTFAST
TPMHPK	-	PTFAST
TRMHR6	-	RTFAST
TRMHR7	-	RTFAST
TRMHR8	-	RTFAST
TRMHR9	-	RTFAST
TRMHT	-	RTFAST
TPMHT2	-	RTFAST
TPMHT3	-	RTFAST

RTSLOW
RTSLOW

RTSLOW
RTSLOW
RTSLOW

RTSLOW
RTSLOW

Figure G.6. (Continued)

I N D E X

TRM15	-	RFEAST
TRM1C1	-	RTSLOW
TRM1C2	-	RTSLOW
TRM1C3	-	RTSLOW
TRM1C4	-	RTSLOW
TRM1L1	-	RFEAST
TRM1R1	-	RFEAST
TRM1T1	-	RFEAST
TRM1V1	-	RFEAST
TRM1W1	-	RFEAST
TRM1X1	-	RFEAST
TRM1Y1	-	RFEAST
TRM1Z1	-	RFEAST
TRM2	-	RTSLOW
TRM3	-	RTSLOW
TRM4	-	RTSLOW
TRM5	-	RFEAST
TRM6	-	RFEAST
TRM7	-	RFEAST
TRM8	-	RFEAST
TRM9	-	RTSLOW
TSTR1E	-	RFEAST
TSTR1S	-	RTSLOW
TZERO	-	RTSLOW
TZET1	-	RTSLOW
TZET2	-	RTSLOW
TZET3	-	RTSLOW
TZET4	-	RTSLOW
TZET5	-	RTSLOW
TZET6	-	RTSLOW
U	-	RFEAST
UGUST	-	RFEAST
UNT	-	RFEAST
ULM	-	RFEAST
ULMPR	-	RFEAST
ULMSQ	-	RFEAST
UP	-	RFEAST
UPR1NE	-	GEAR
URL	-	RFEAST
URLPR	-	RFEAST
URLURL	-	RFEAST
URR	-	RFEAST
URPP	-	RFEAST
URRUPP	-	RFEAST
URW	-	RFEAST
URMPR	-	RFEAST
URMSO	-	RFEAST
USEATO	-	RFEAST
USQ	-	RFEAST
UTR1P	-	RFEAST
UVT	-	RFEAST
V	-	PTFEAST
VALFLM	-	PTFEAST
VALFRM	-	RFEAST
VALFS	-	RFEAST
VALNCL	-	RTSLOW
VALNCR	-	RTSLOW
VRETVT	-	RFEAST

RTFAST RTSLOW

RTFAST
RTSLOW

RTSLOW
RTSLOW

RTFAST
RTSLOW

RTSLOW

RTSLOW

Figure G.6. (Continued)

***** SUPER INDEX *****

I N D E X

YARHT	-	RTFAST
YARVT	-	RTFAST
YG	-	GEAR
YGI	-	GEAR
YN	-	GEAR
YNAC	-	RTFAST
YYICON	-	RTSLOW
ZAERF	-	RTFAST
ZARLW	-	RTFAST
ZAERNL	-	RTFAST
ZAERNR	-	RTFAST
ZAERO	-	RTFAST
ZAERNM	-	RTFAST
ZAERT	-	RTFAST
ZAERMG	-	RTFAST
ZARFP	-	RTFAST
ZARHT	-	RTFAST
ZARRG	-	RTFAST
ZARVB	-	RTFAST
ZARVT	-	RTFAST
ZCG	-	GEAR
ZDTGG	-	RTFAST
ZFYHL	-	RTFAST
ZETHR	-	RTFAST
ZETRI	-	RTSLOW
ZETR2	-	RTSLOW
ZETR3	-	RTSLOW
ZETR4	-	RTSLOW
ZF	-	RTSLOW
ZFAC	-	RTSLOW
ZFMFH	-	RTSLOW
ZG	-	GEAR
ZGI	-	GEAR
ZHT	-	RTFAST
ZL	-	RTSLOW
ZLCS	-	RTSLOW
ZLSIN	-	RTFAST
ZN	-	GEAR
ZR	-	RTSLOW
ZRCOS	-	RTSLOW
ZPLCON	-	RTSLOW
ZRSIN	-	RTFAST
ZVT	-	RTFAST
ZW	-	RTSLOW
ZWAC	-	RTFAST
ZMMHM	-	RTSLOW
ZZICCN	-	RTSLOW

Figure G.6. (Continued)

***** TABLE OF CONTENTS *****

I N D E X

AILSP	94
CLCOCM	99
CLF1	-94
CLF2	-99
ENGINE	110
GEAR	115
RTFAST	1
RTSLOW	55
TSTRF	-1
TSTRS	-55
SUPER INDEX	120

Figure G.6. (Continued)

time tasks (RTFAST and RTSLOW), the aileron-spoiler subroutine (AILSP), the total lift, drag and moment subroutine (CLCDCM), the engine power subroutine (ENGINE), and the landing gear subroutine (GEAR) . The aileron spoiler subroutine calculates the lift, drag and pitching moment increments. The total wing lift, drag, and moment characteristics are computed in subroutine CLCDCM. Engine performance is computed in the engine subroutine and landing gear forces and moments in the gear subroutine. This listing contains an index of all the variables immediately following each subroutine. The index specifies by location number where the particular variable is defined and used in the subroutine. A master index is provided at the end which specifies the subroutine in which a particular variable is located.

In programming the analog portion of the simulation, size also was of prime concern, where in this case size implies an equipment limitation. From the beginning, equipment was allocated with maximum efficiency, but due to the complexity of the engine/governor, the phasing of the controls, the number of second order representations of actuators, and the number of functions needed to program these sections, the result was 1) three analogs used with a minimum of spare equipment and 2) 31 out of 32 BCA channels needed to program functions (includes

rotor). When the capability of using the nudge-base simulator is added, the simulation uses every piece of hardware available in the hybrid laboratory. Figure G.7 shows the definition of the symbols used on the analog diagrams for the Model 222 simulation presented in Figure G.8.

The scale factors for any of the elements shown in the analog diagrams may be determined by referring to Figure G.9, which is the subroutine used to static check the analog boards. The subroutine shows all the equations on the analogs and all of the scale factors. This program is used for static check only, in the operate mode the real time task continuously updates the analog. As an example, if the scale factor (and value) for potentiometer 240, which is used in the pitch equation of motion on board 1E console 1 is required the following steps are taken. Refer to the potentiometer calculation section of Figure G.9. This lies between statement numbers 0416 and 0518. Look up the definition of pot 240 [P1(240)]. This appears in statement number 0444 and is $P1(240) = P1C/PMX$. P1C is contained in common |X1C|, statement number 0008 and PMX is contained in common |XMAX|, statement number 0013. Substituting numerical values and dividing would yield the scale factor for pot 240.

G.2 TRIM LOOPS

The Model 222 trim loops are on the analog. The aircraft accelerations are used in feedback loops to drive the aircraft into

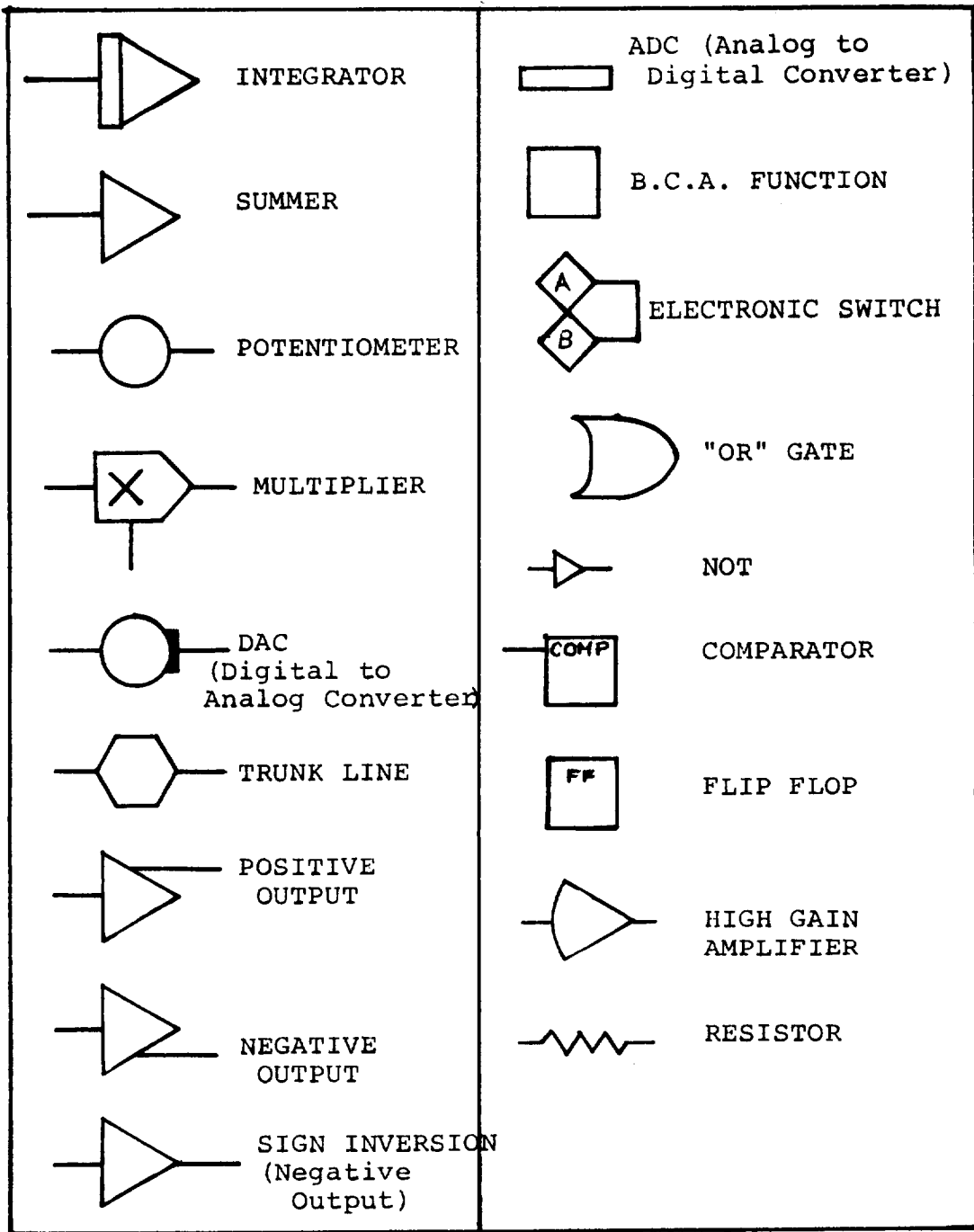


Figure G.7. Analog Symbols

TRIM LOOPS

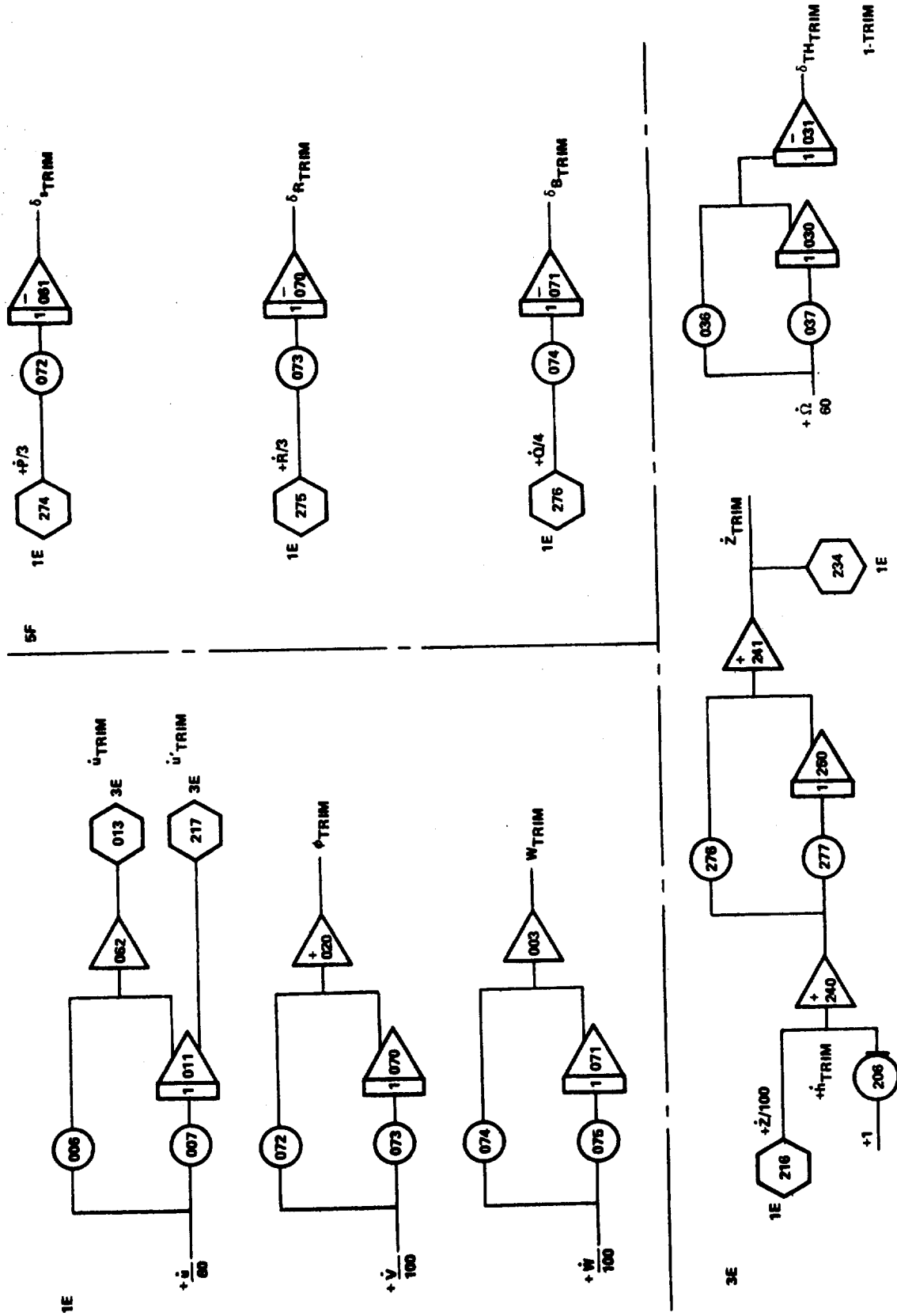
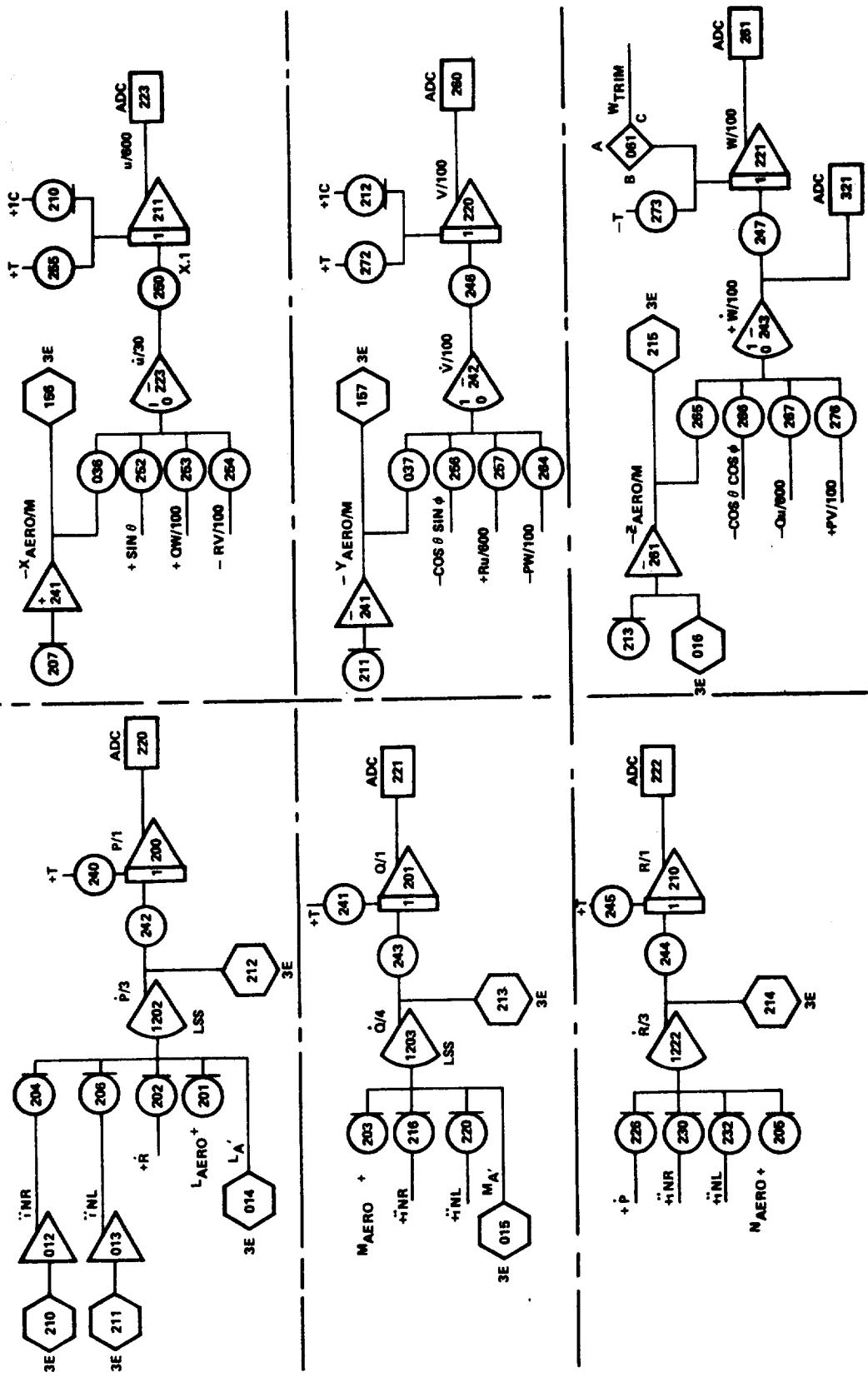


Figure G.8. Analog Diagrams for Model 222 Simulation

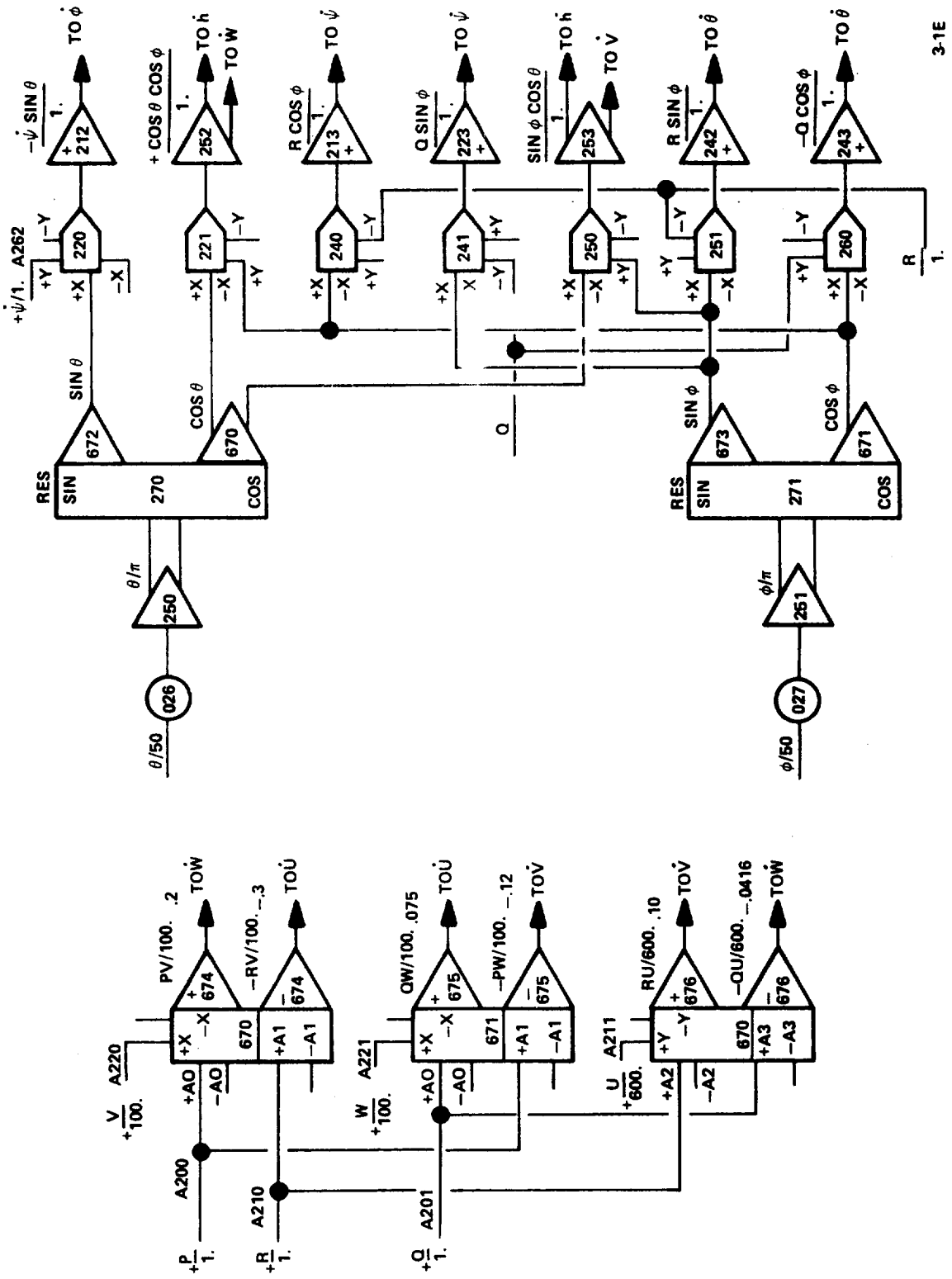
EQUATIONS OF MOTION: P,Q,R,U,V,W.



1-1E

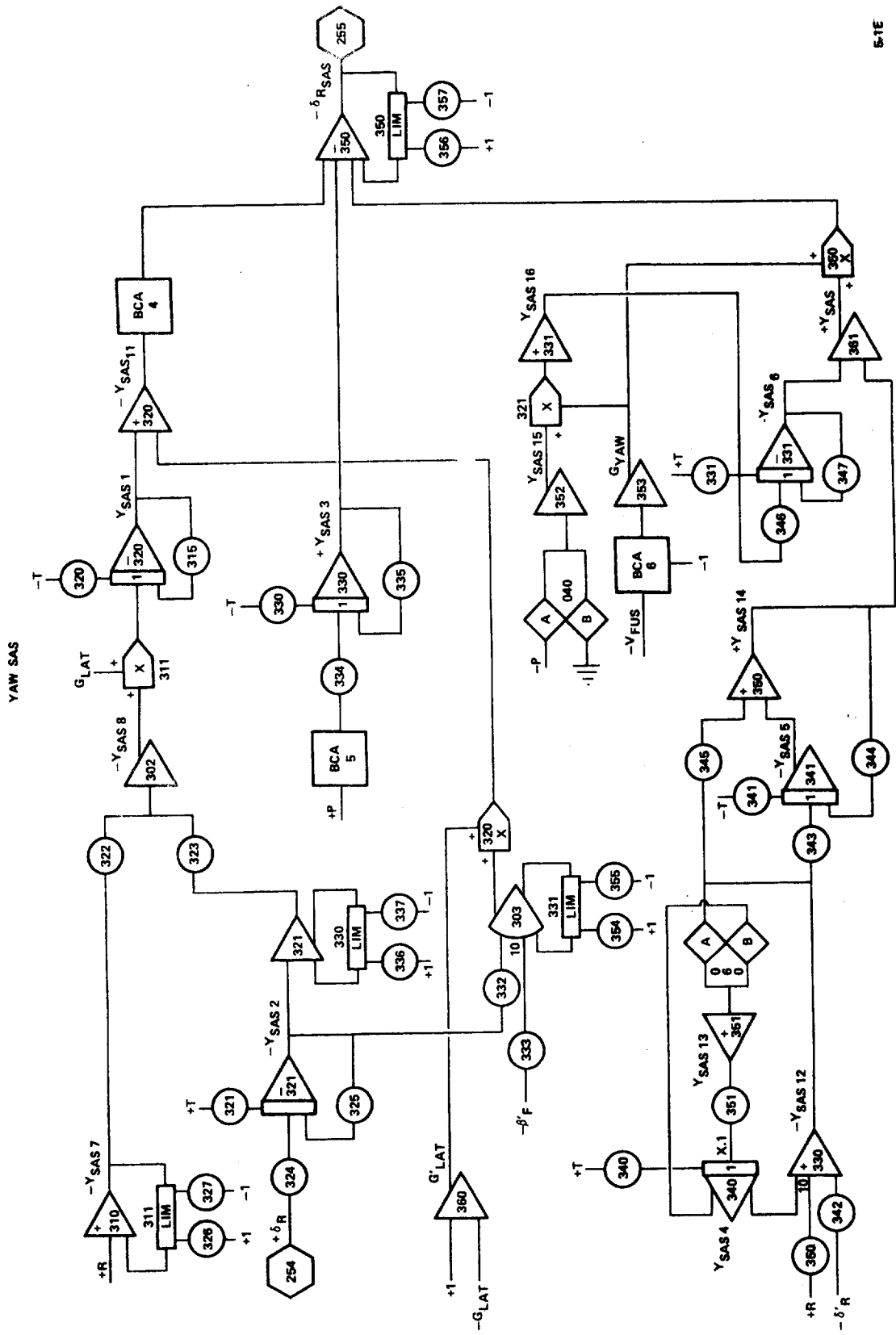
Figure G.8. (Continued)

EQUATIONS OF MOTION MULTIPLICATIONS



3-1E

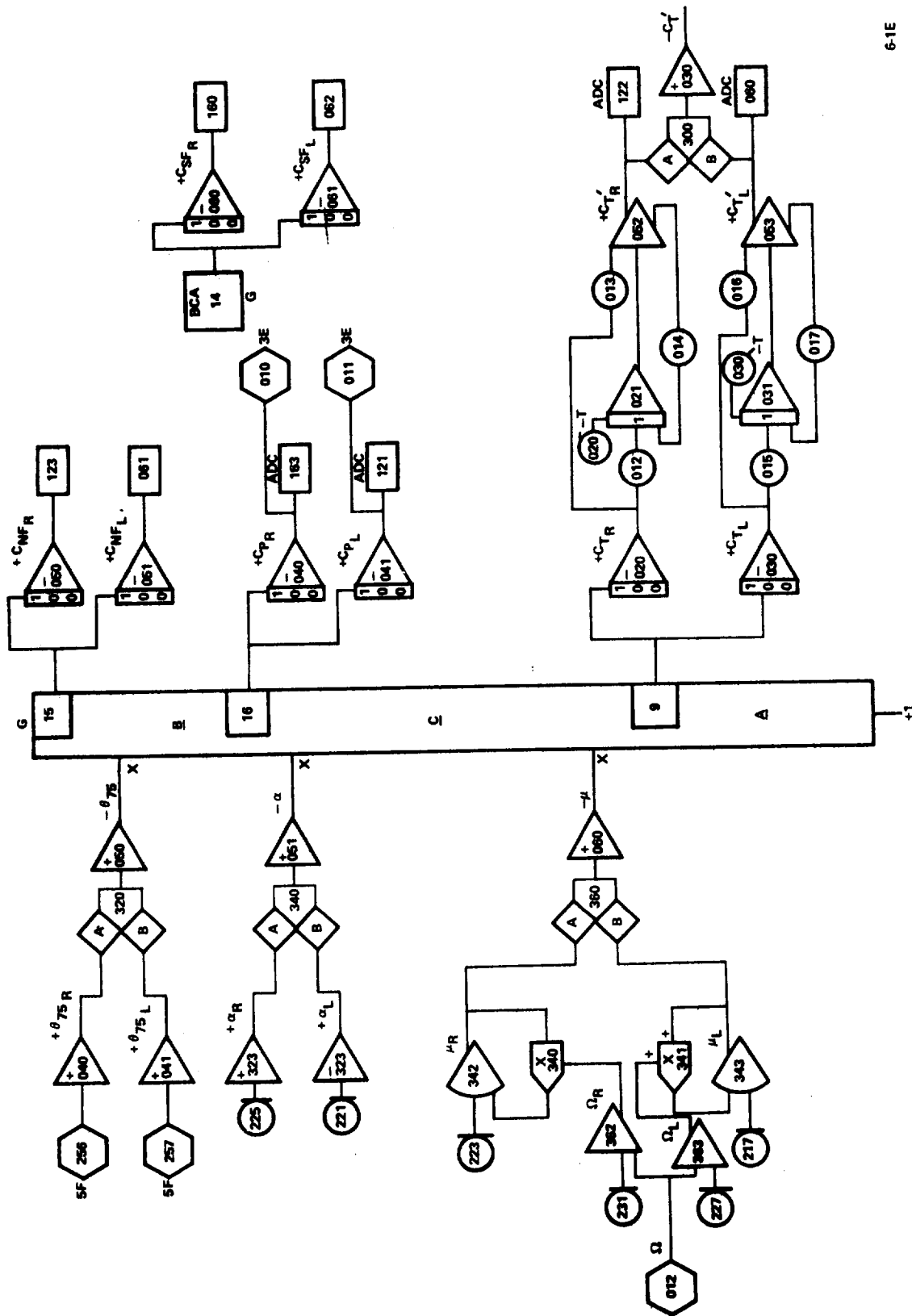
Figure G.8. (Continued)



5:1E

Figure G.8. (Continued)

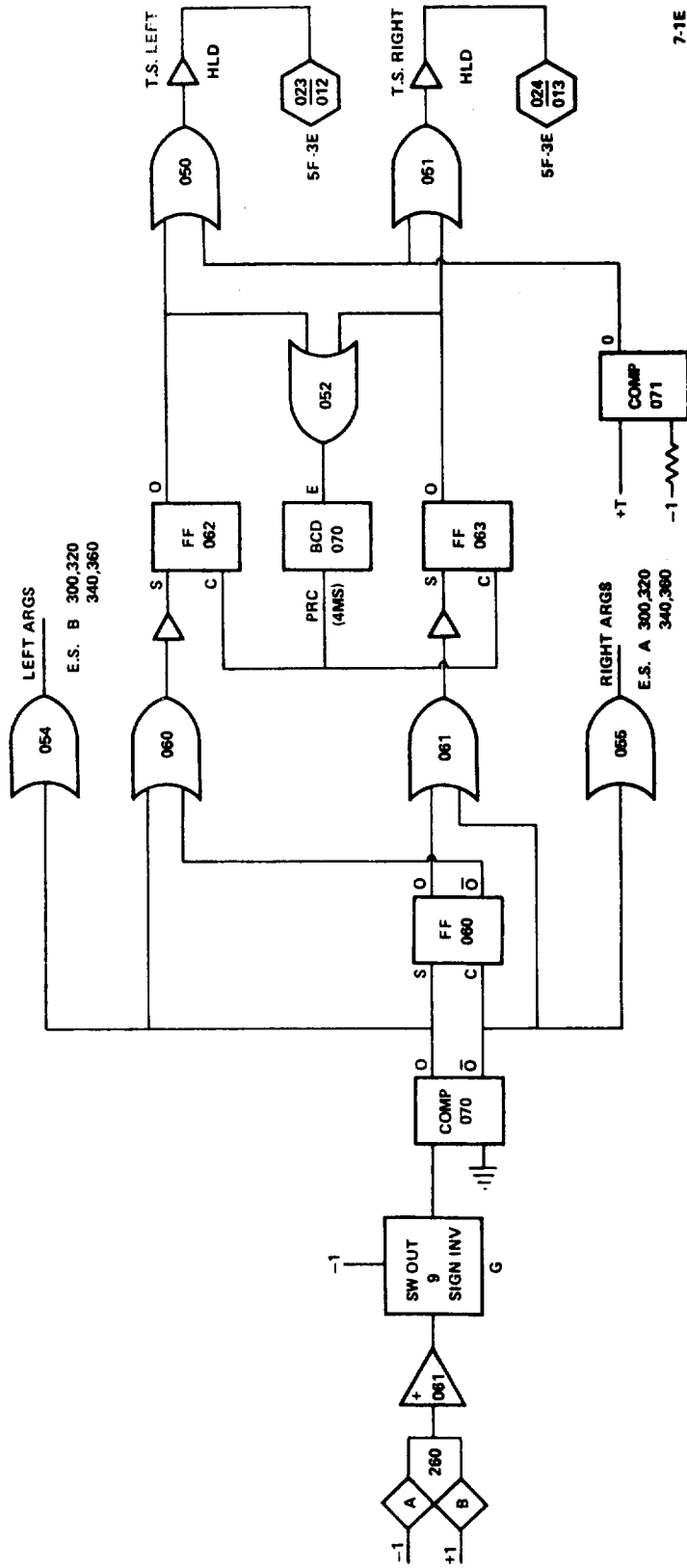
ROTOR FUNCTIONS



6-1E

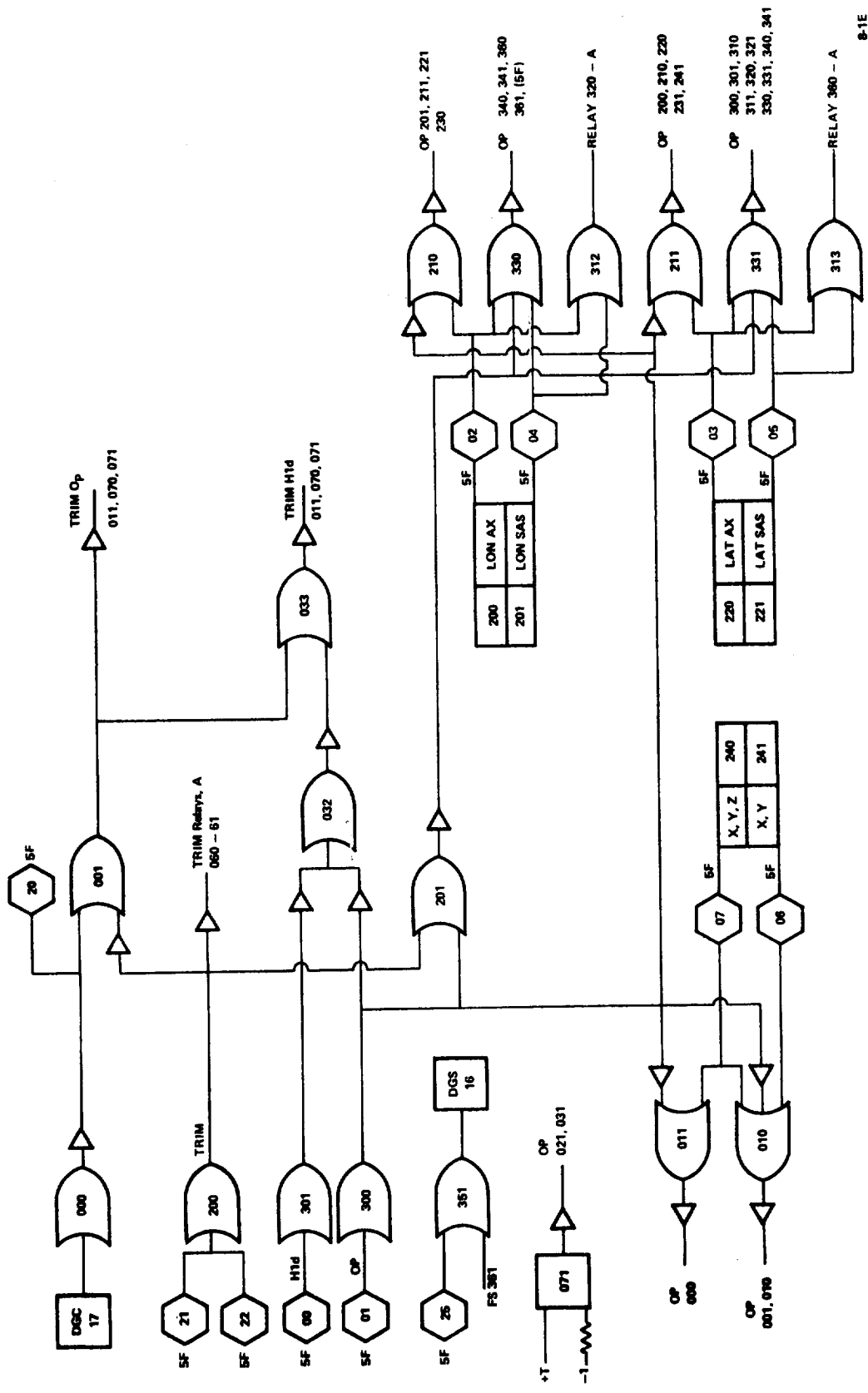
Figure G.8. (Continued)

ROTOR FUNCTION LOGIC



7-1E

Figure G.8. (Continued)



G-170

Figure G.8. (Continued)

TRIM LOGIC

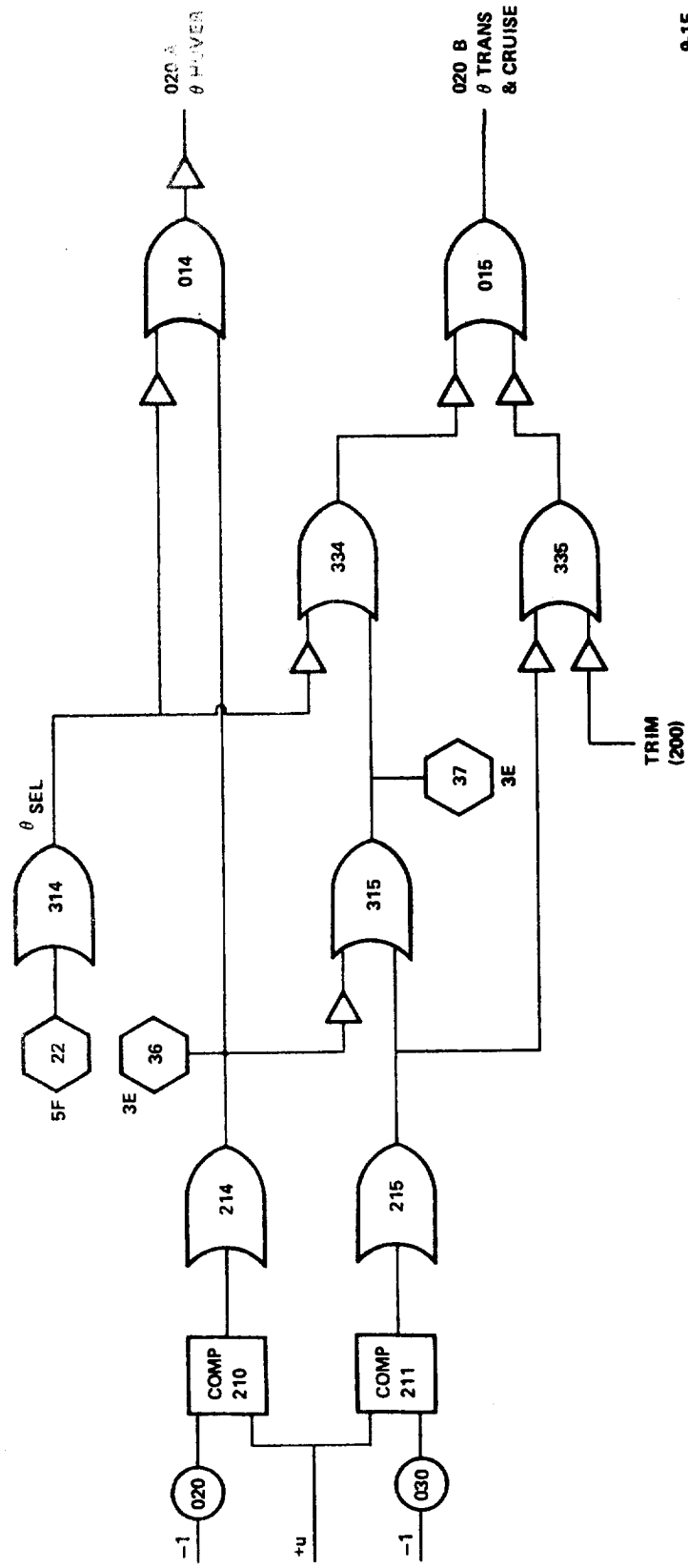


Figure G.8. (Continued)

NACELLES

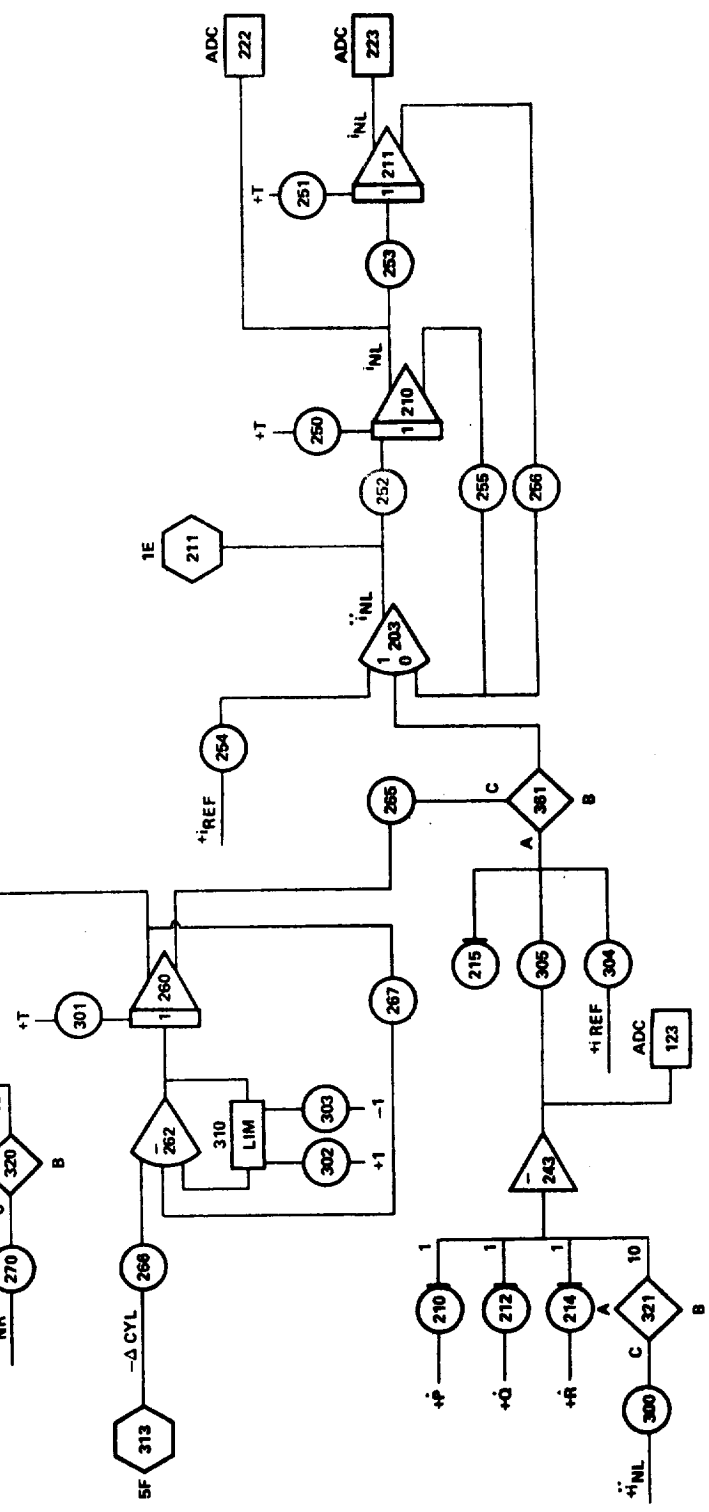
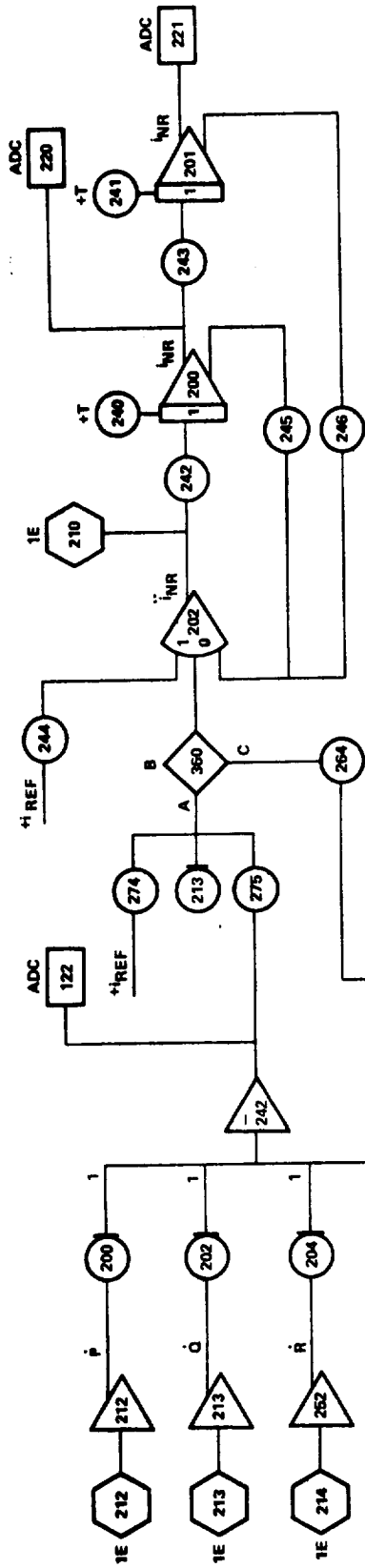
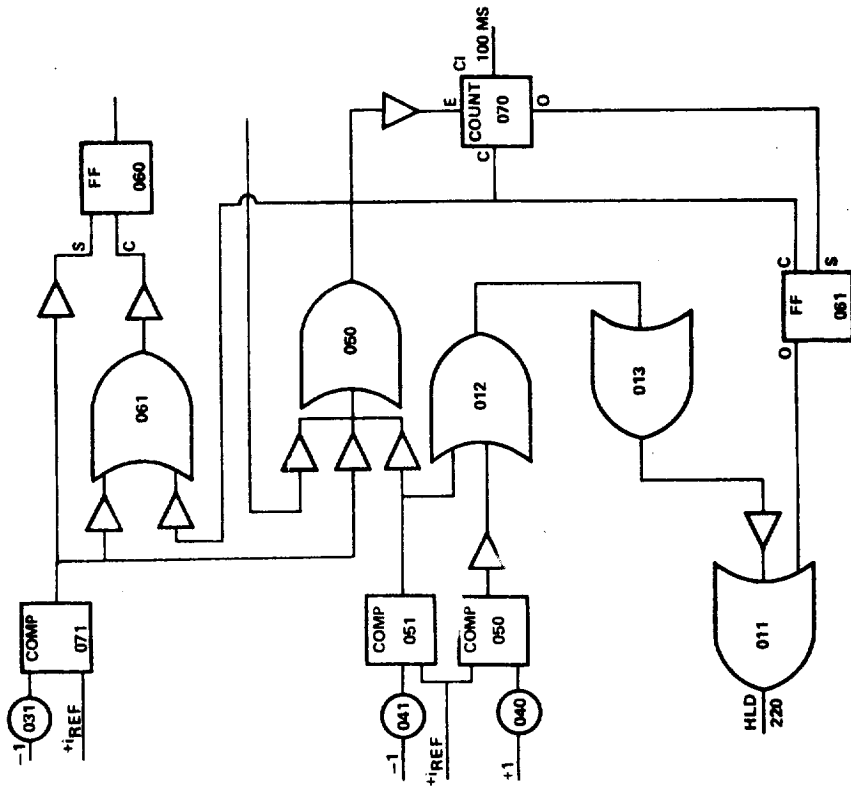
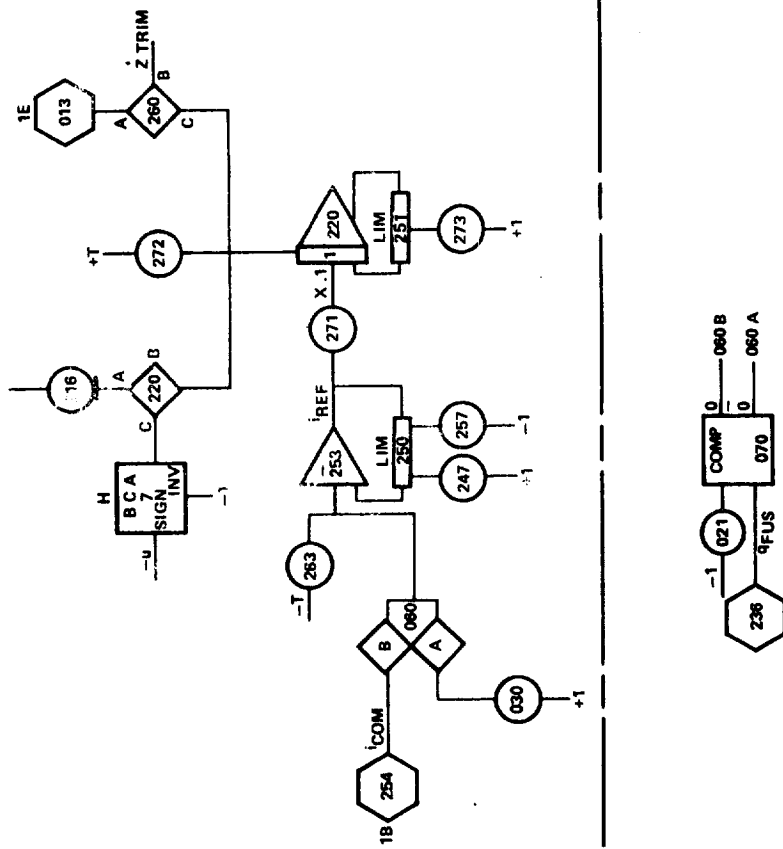


Figure G.8. (Continued)

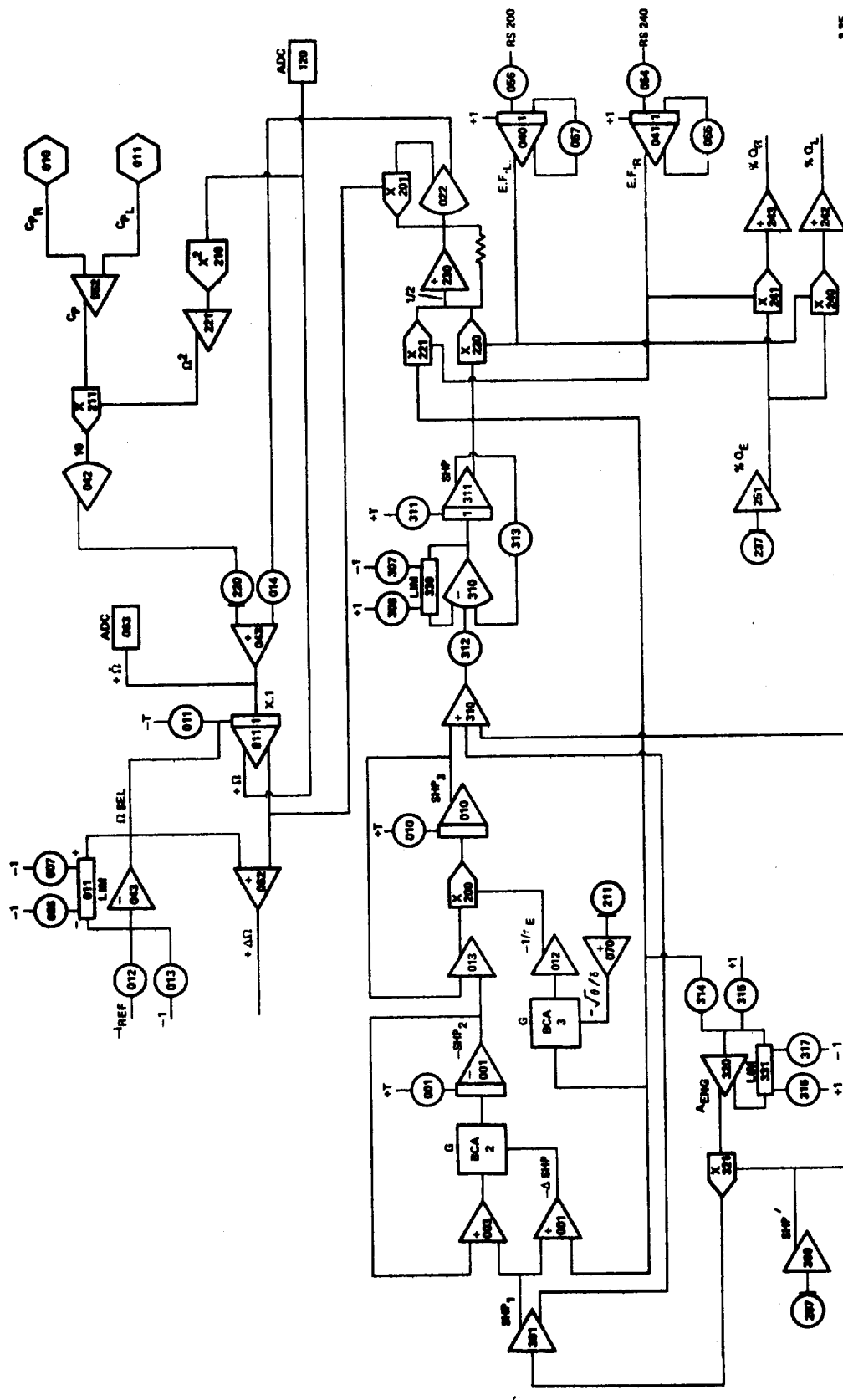
NACELLE CONTROL



23E

Figure G.8. (Continued)

ENGINE DYNAMICS



3-3E

Figure G.8. (Continued)

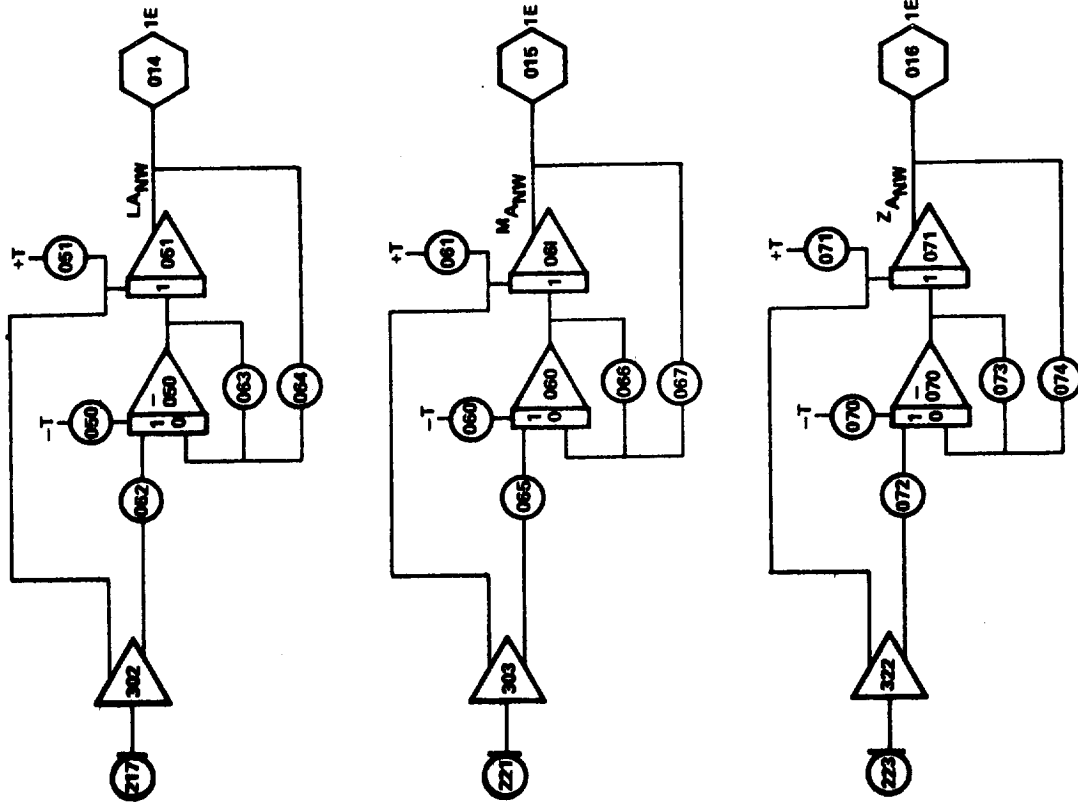
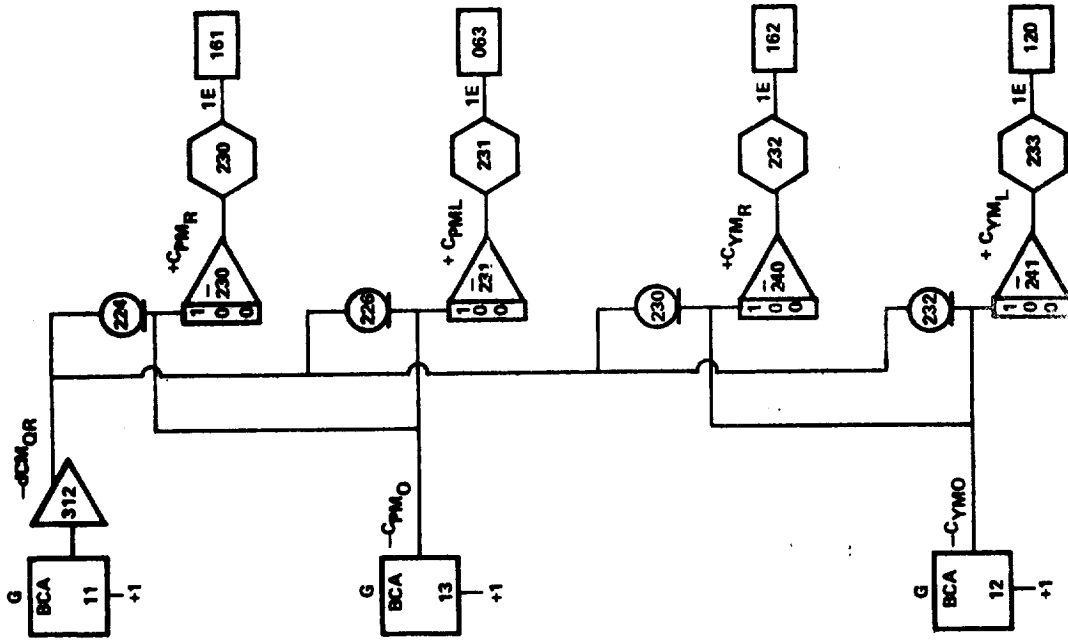


Figure G.8. (Continued)

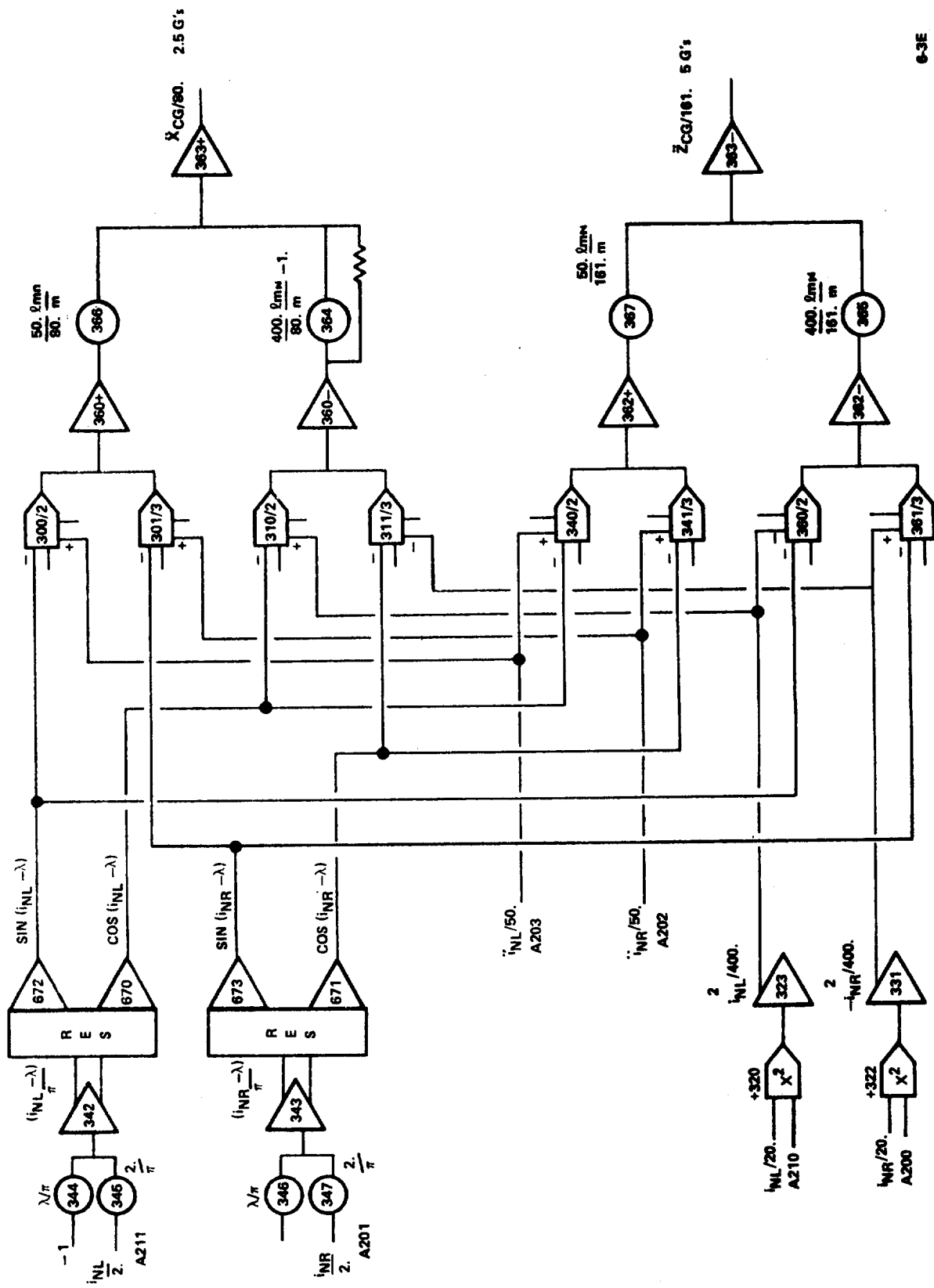
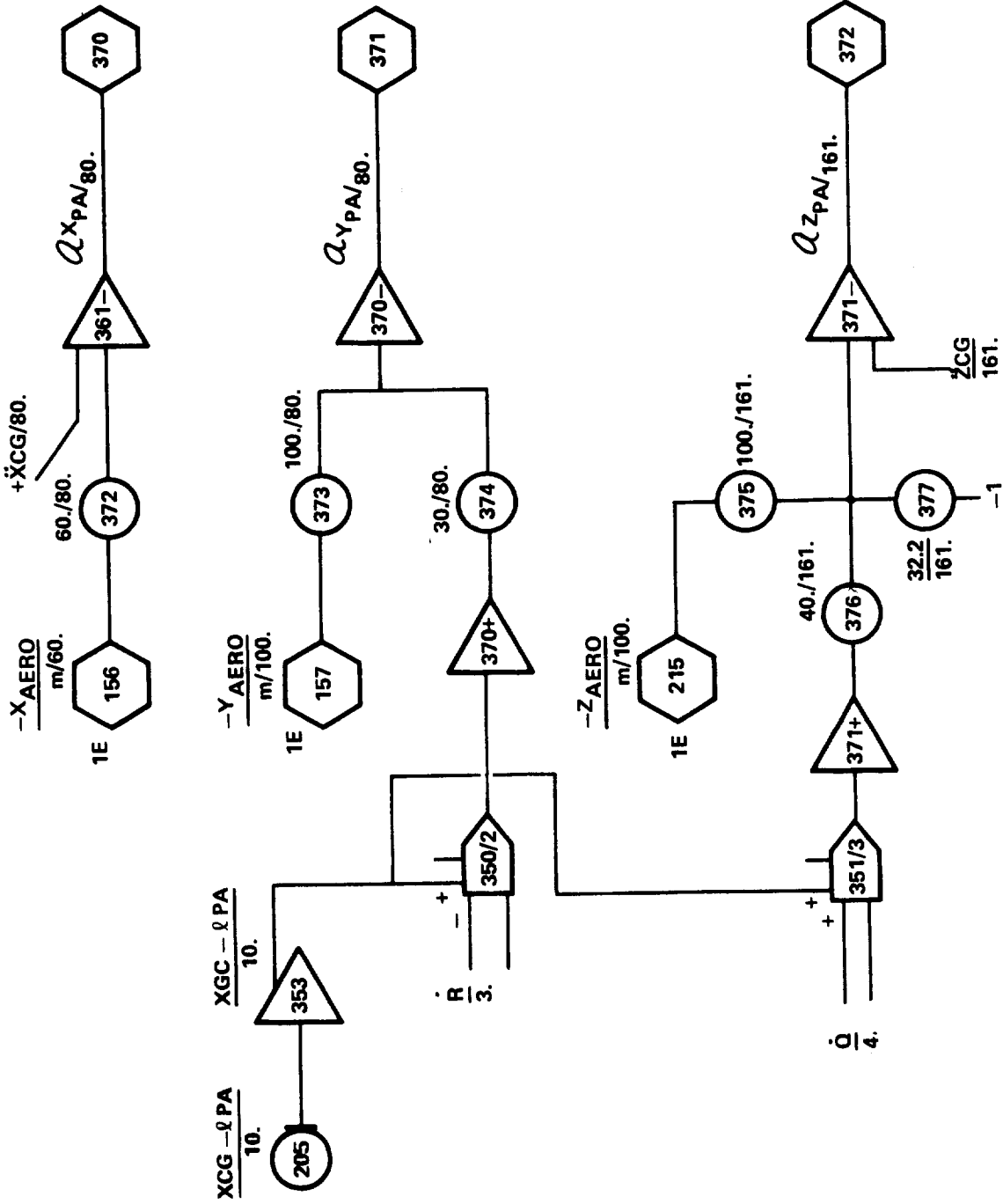


Figure G.8. (Continued)



7-3E

Figure G.8. (Continued)

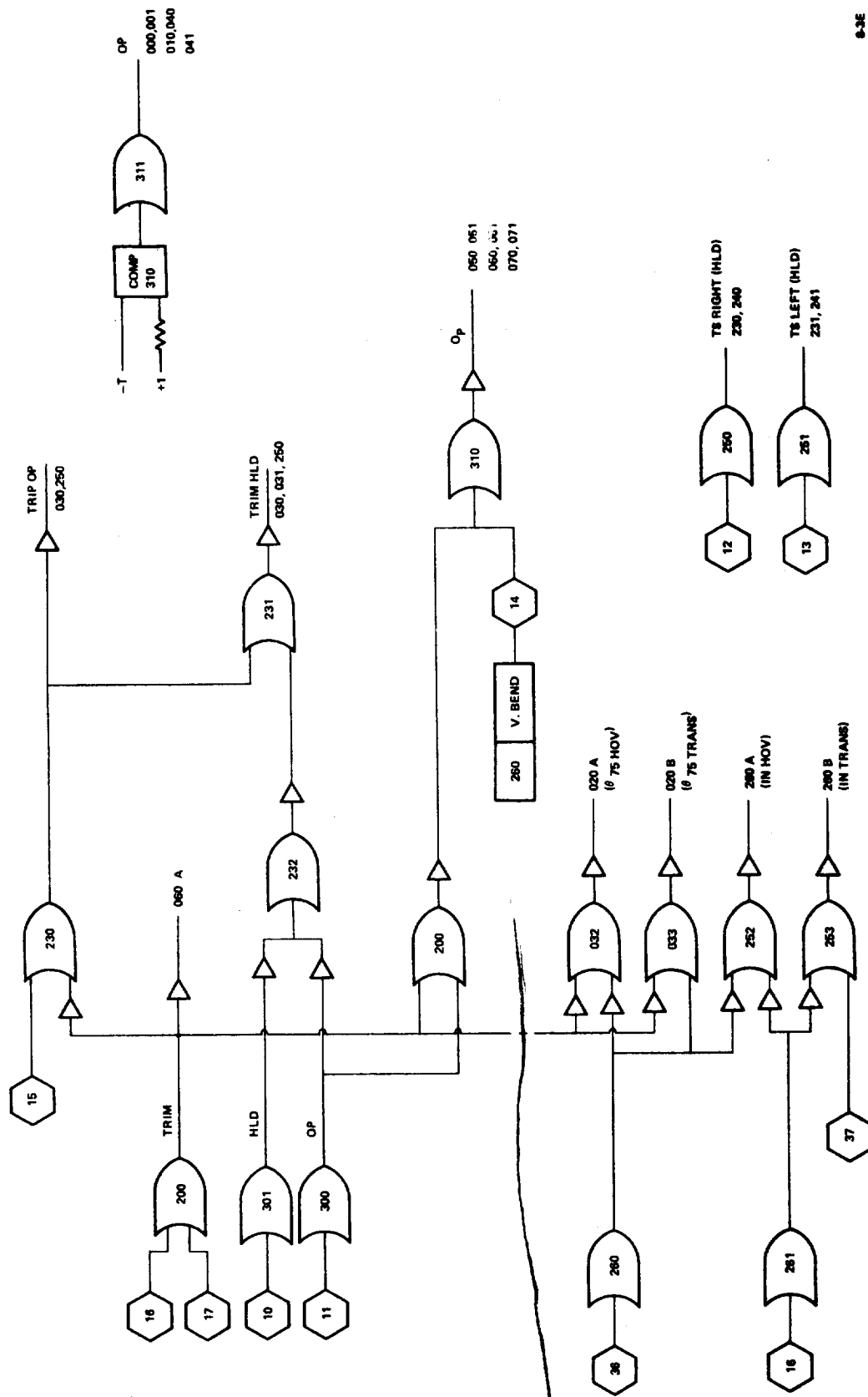


Figure G.8. (Continued)

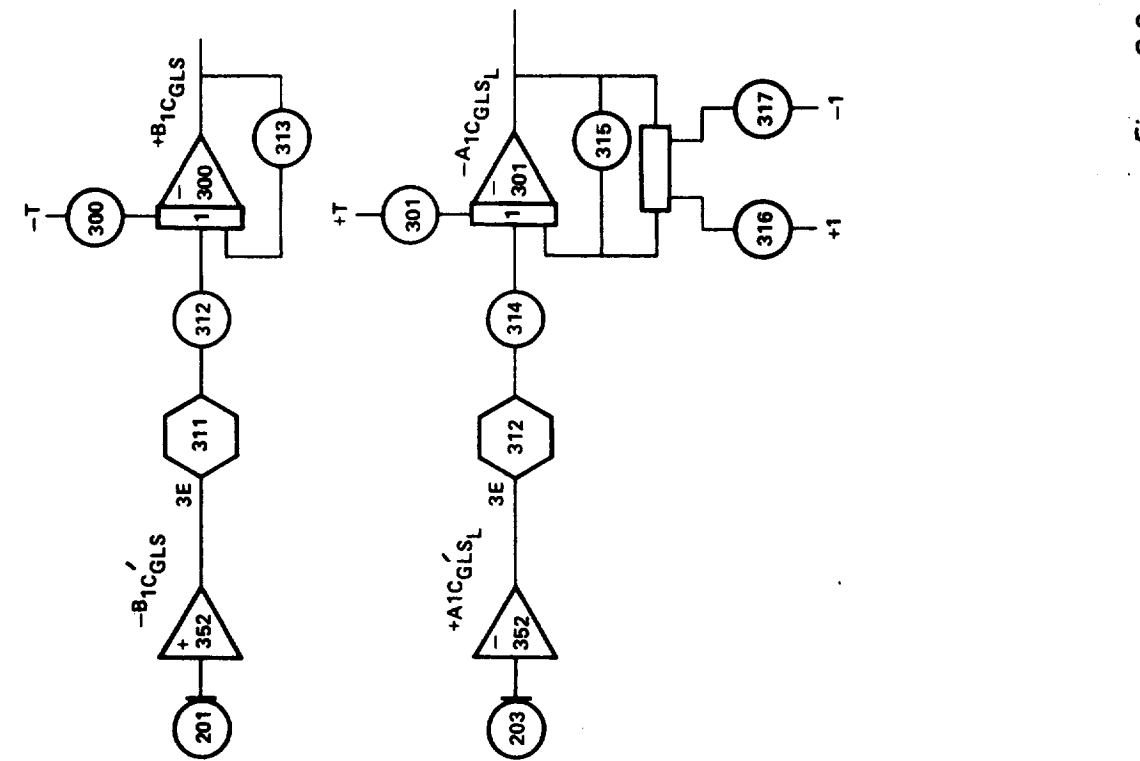
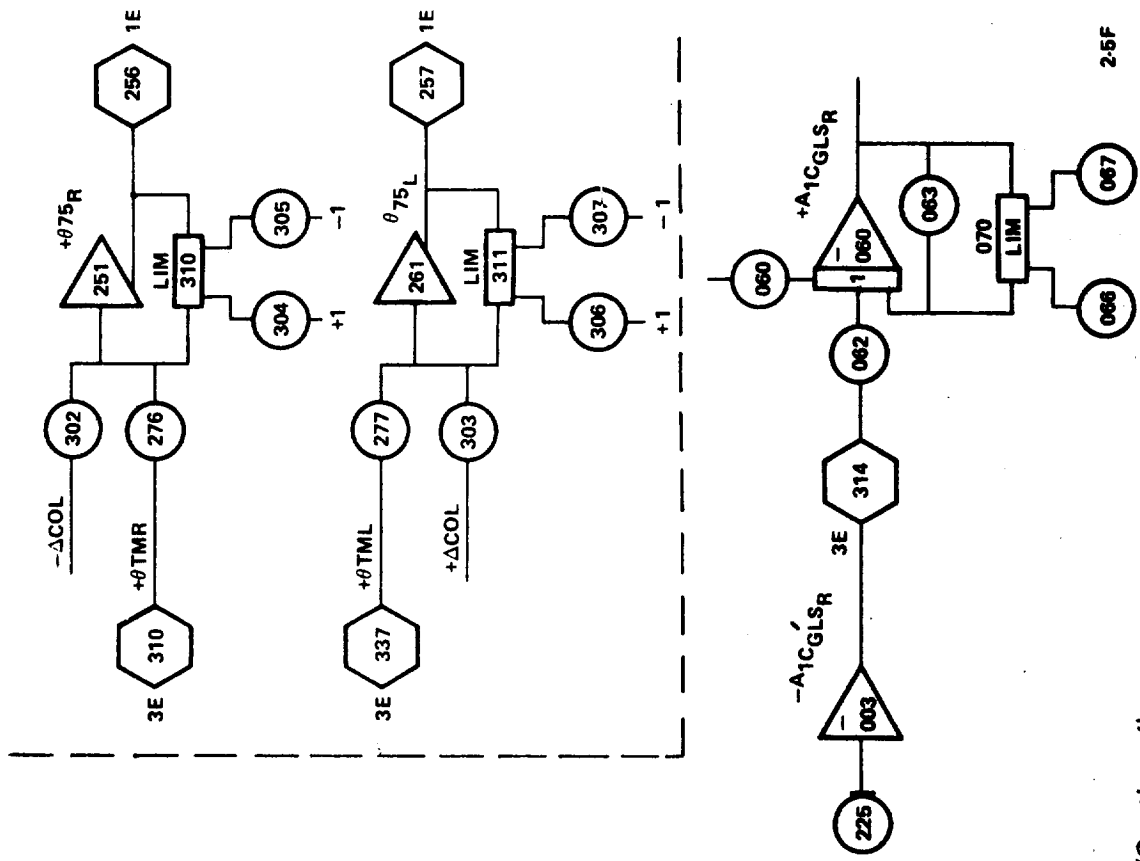
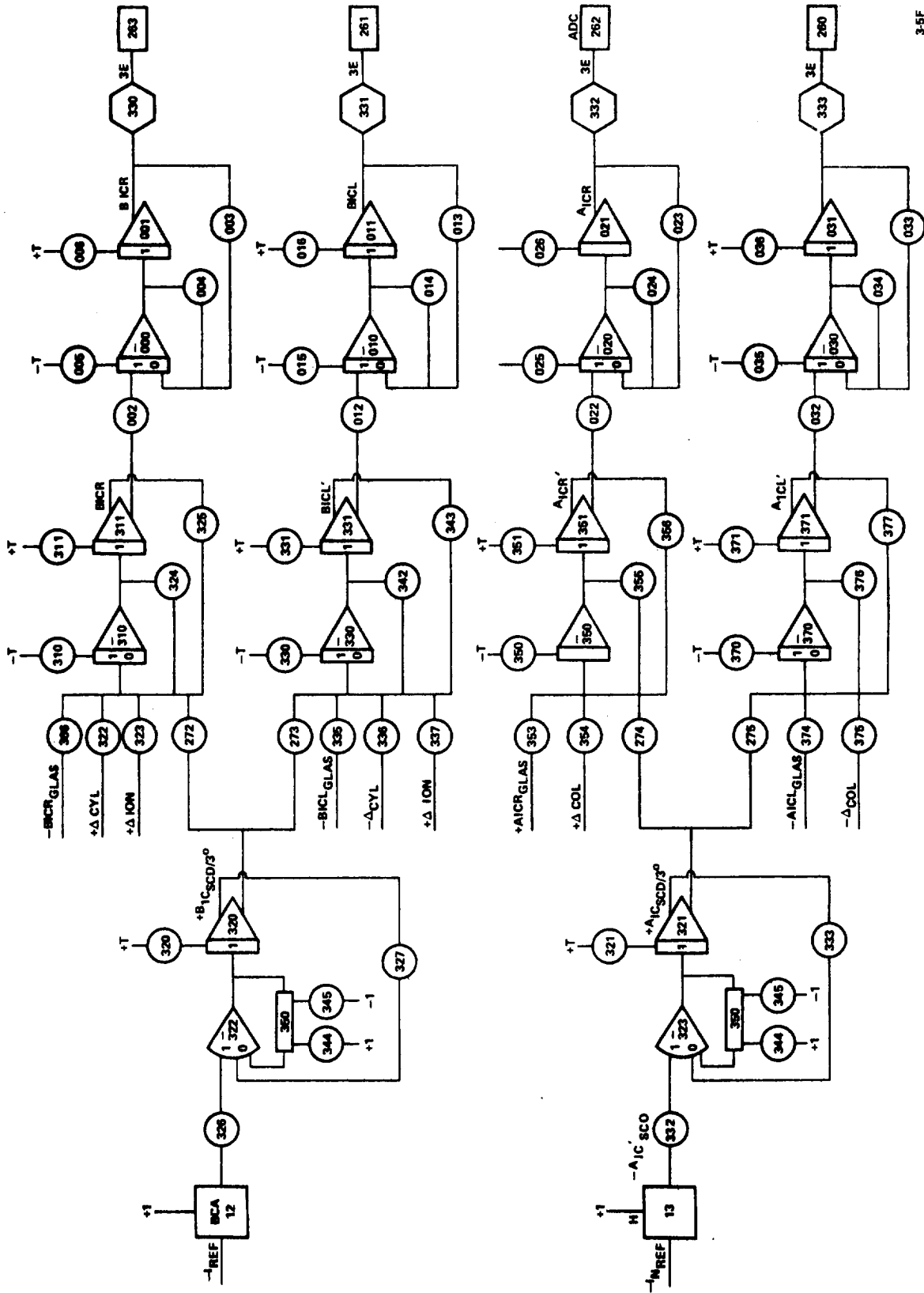
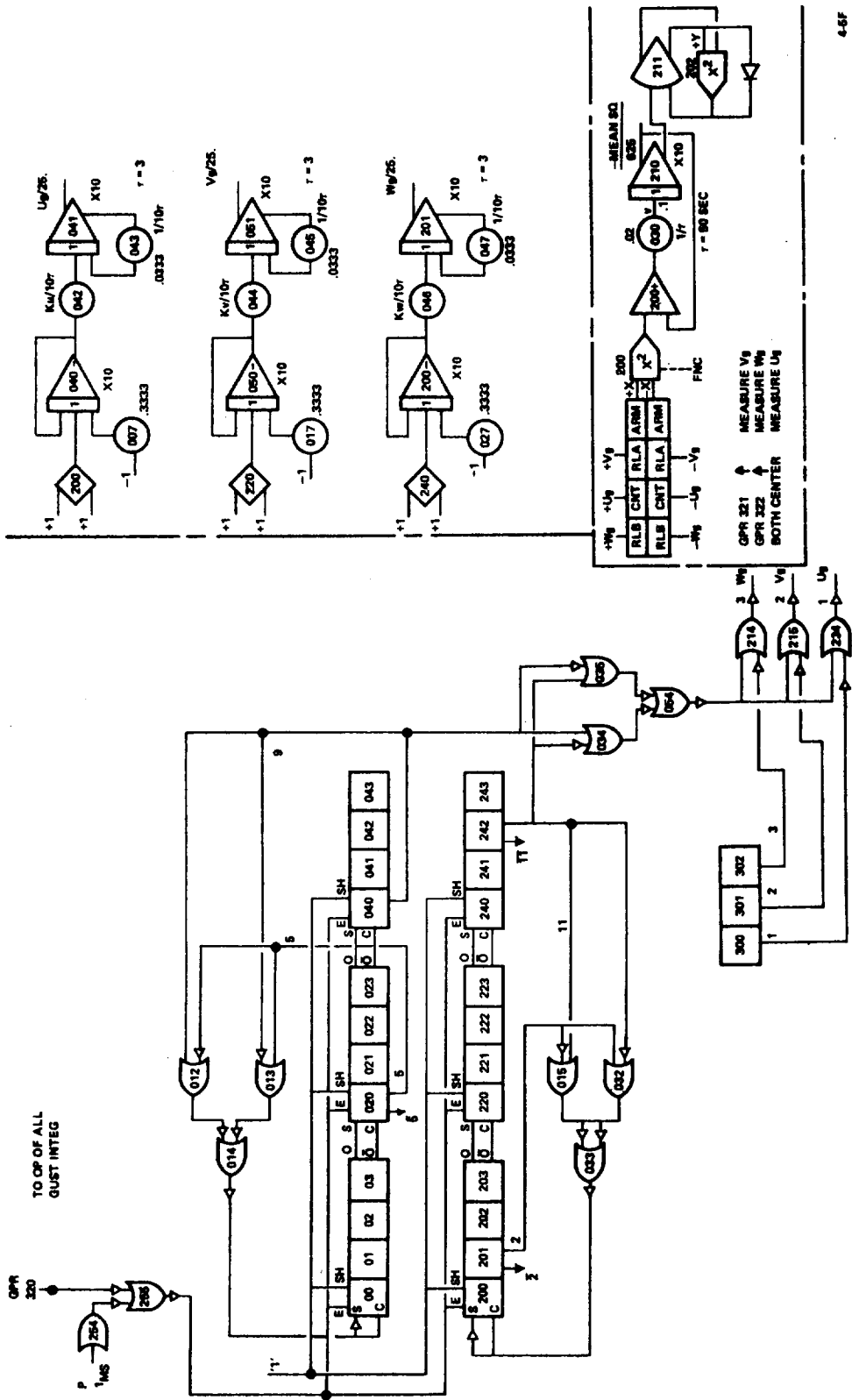


Figure G.8. (Continued)

25F





4-5F

Figure G.8. (Continued)

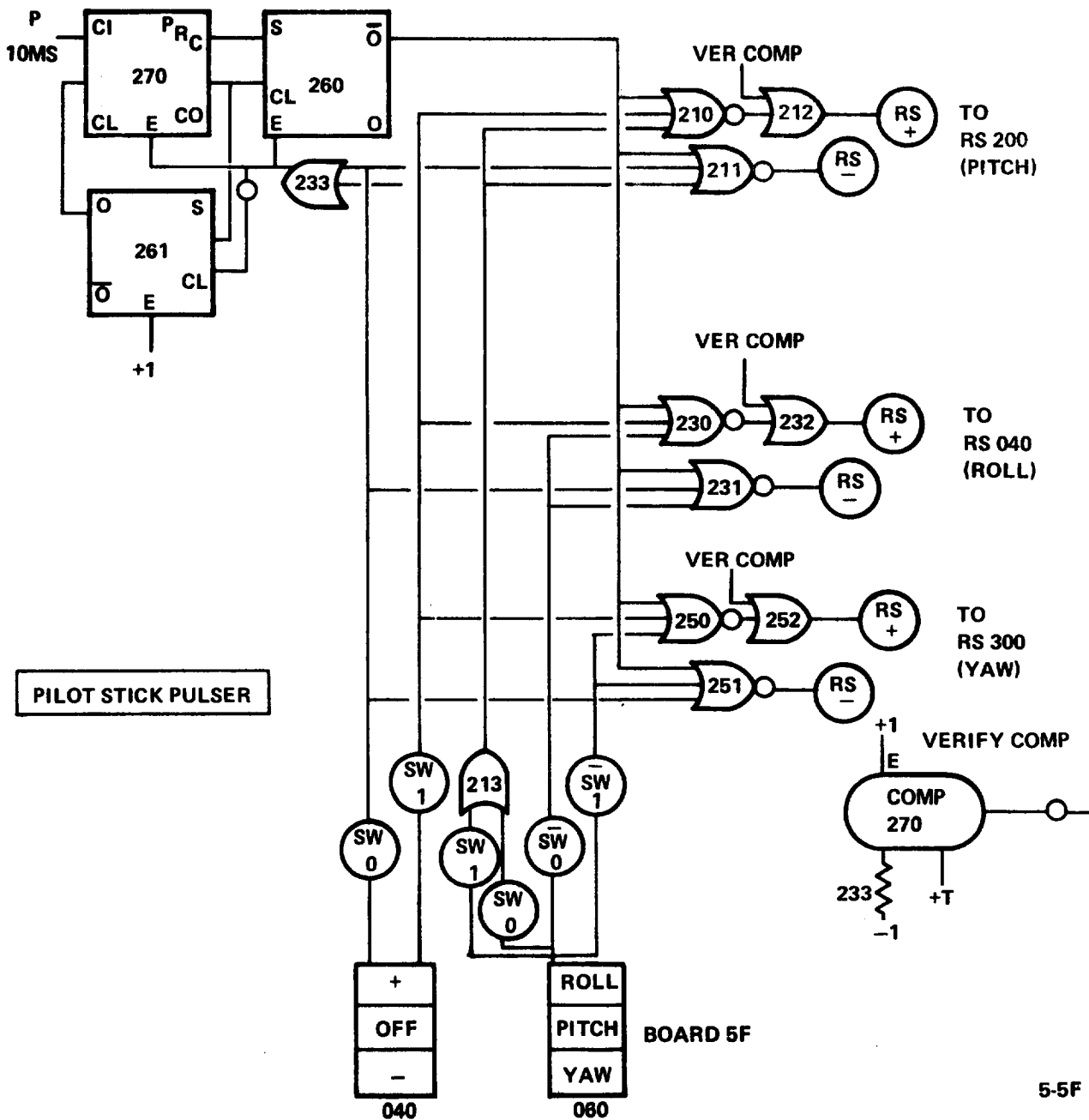


Figure G.8. (Continued)

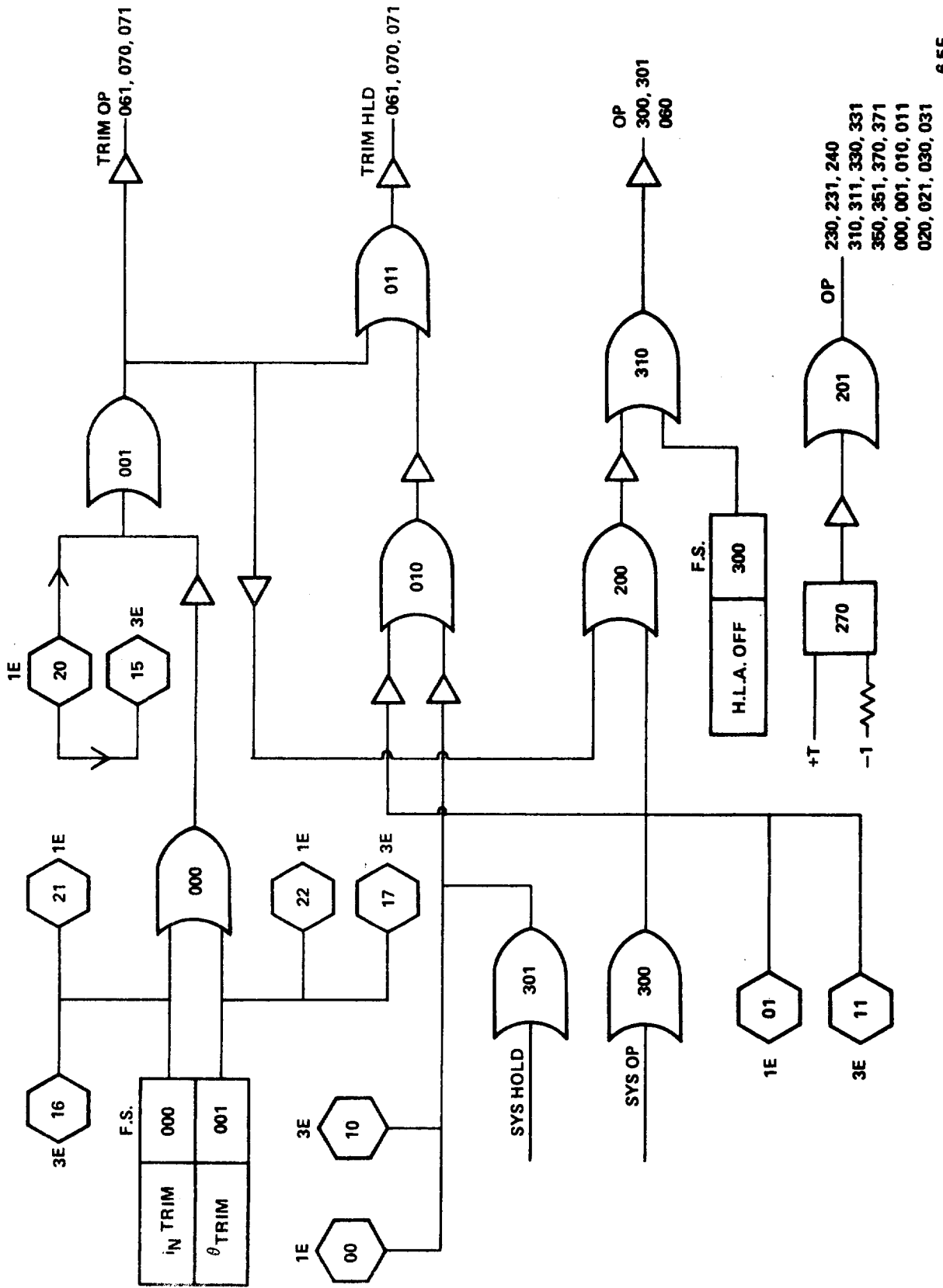
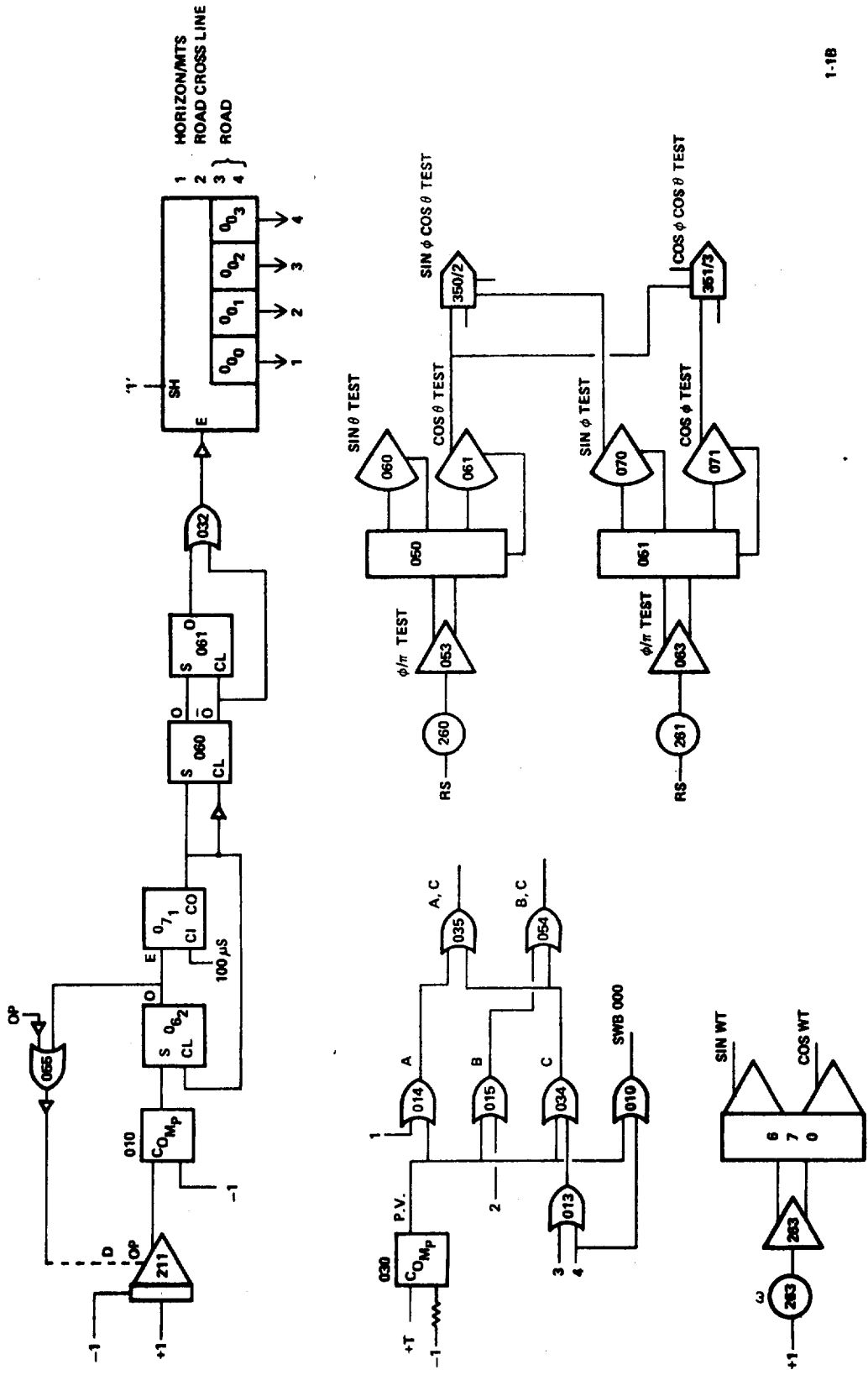
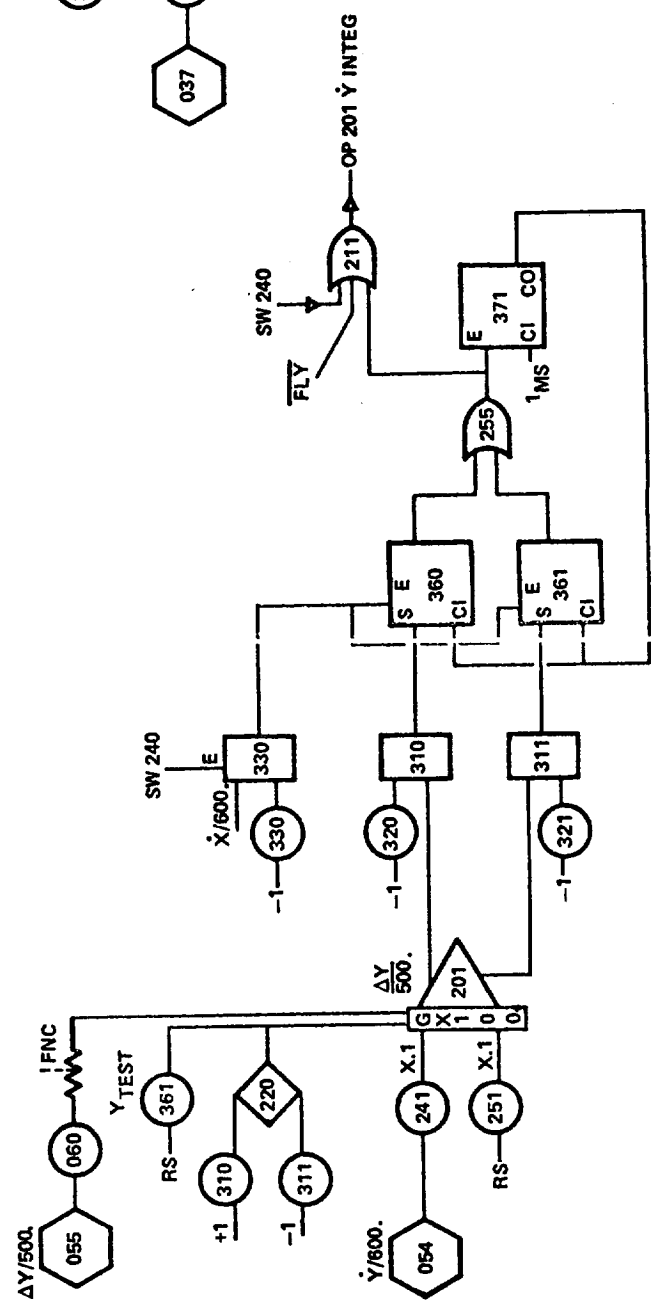
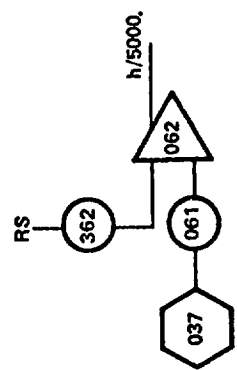
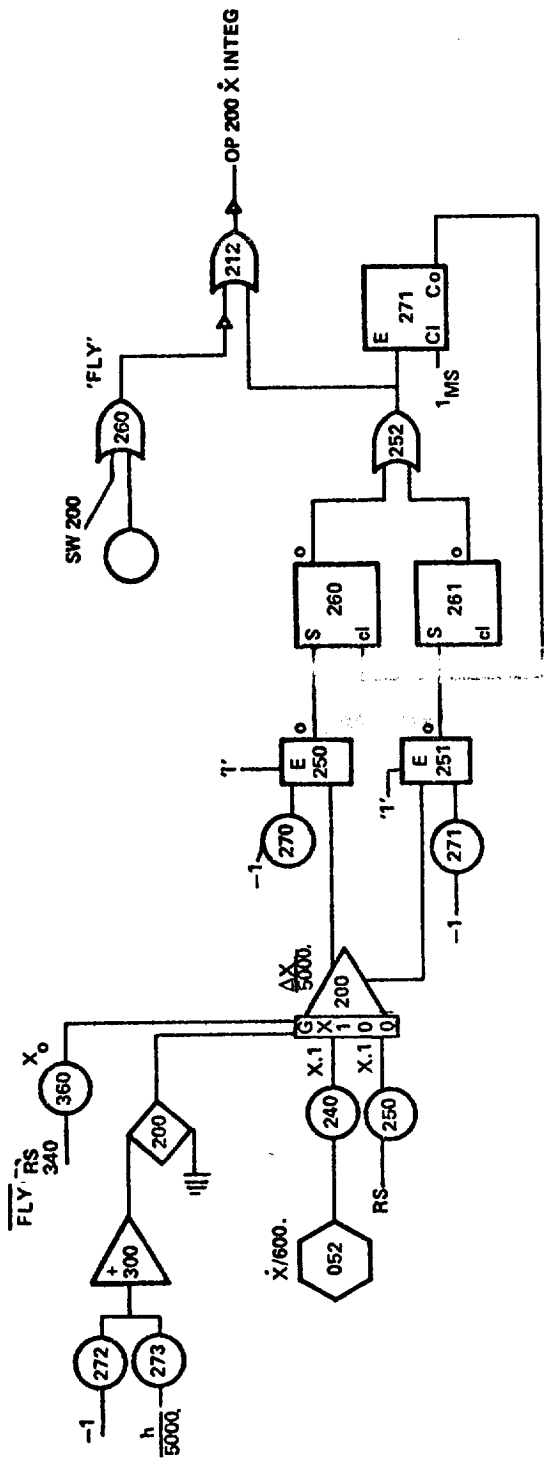


Figure G.8. (Continued)



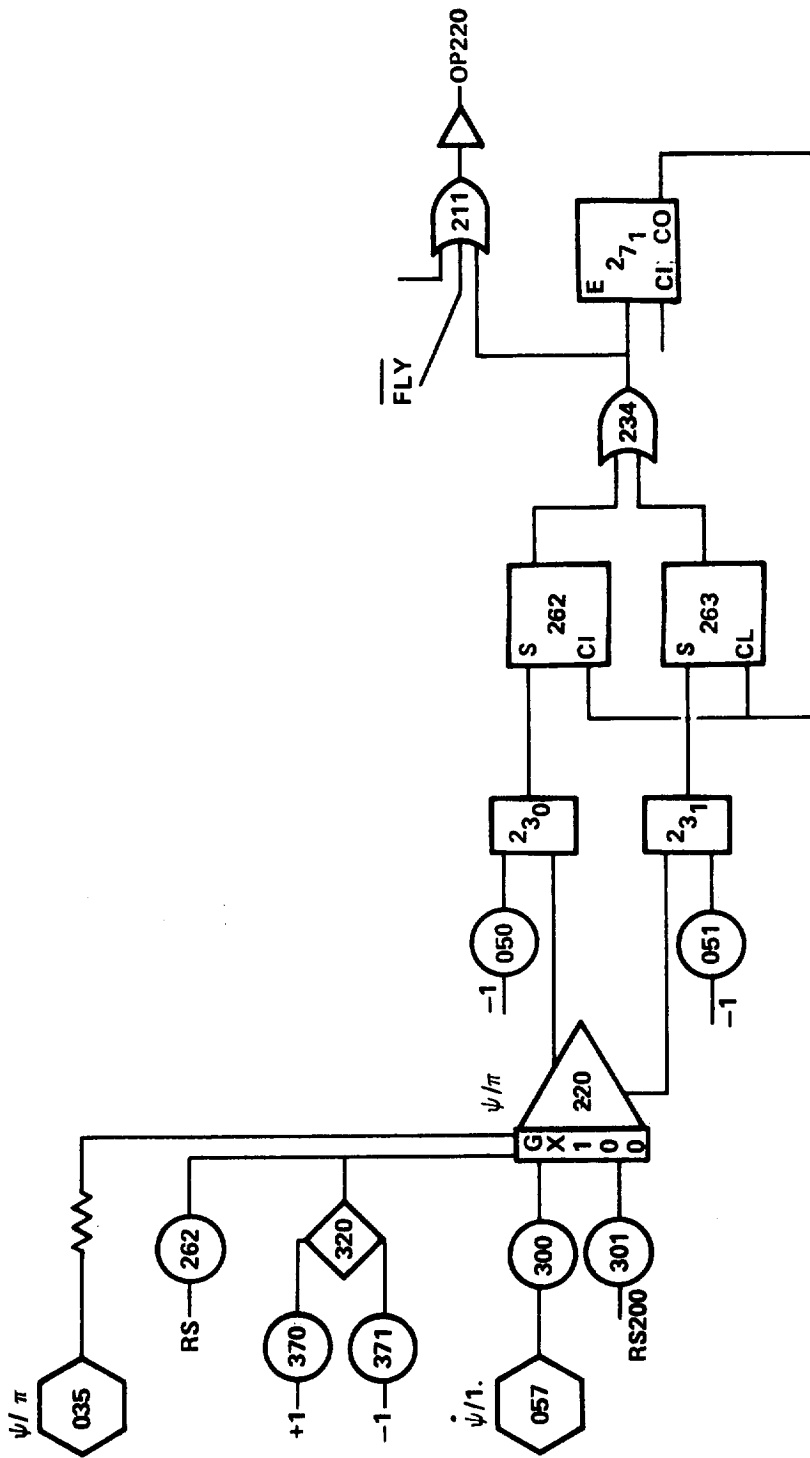
1-1B

Figure G.8. (Continued)



2-1B

Figure 3.8. (Continued)



3-1B

Figure G.8. (Continued)

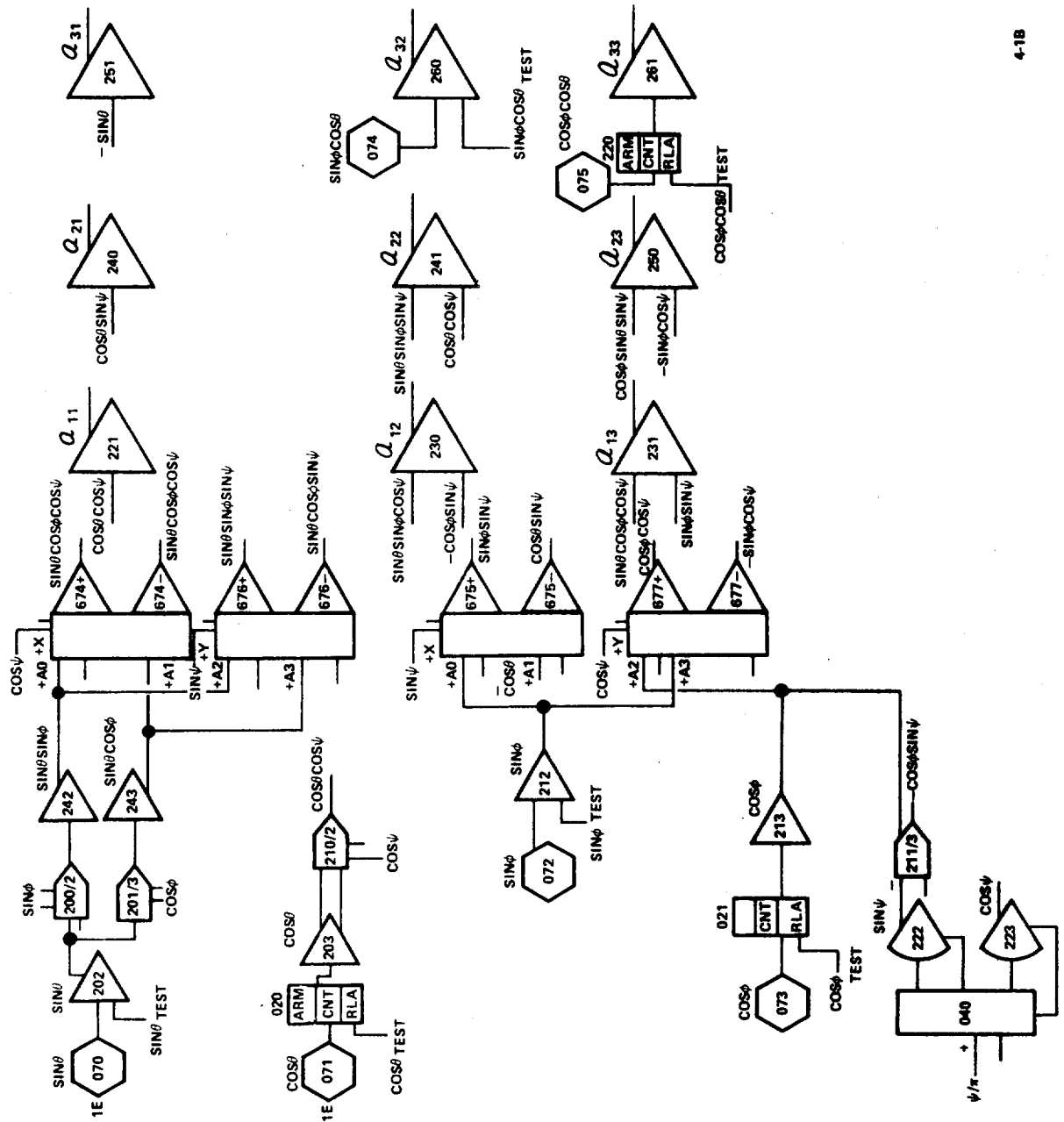


Figure G.8. (Continued)

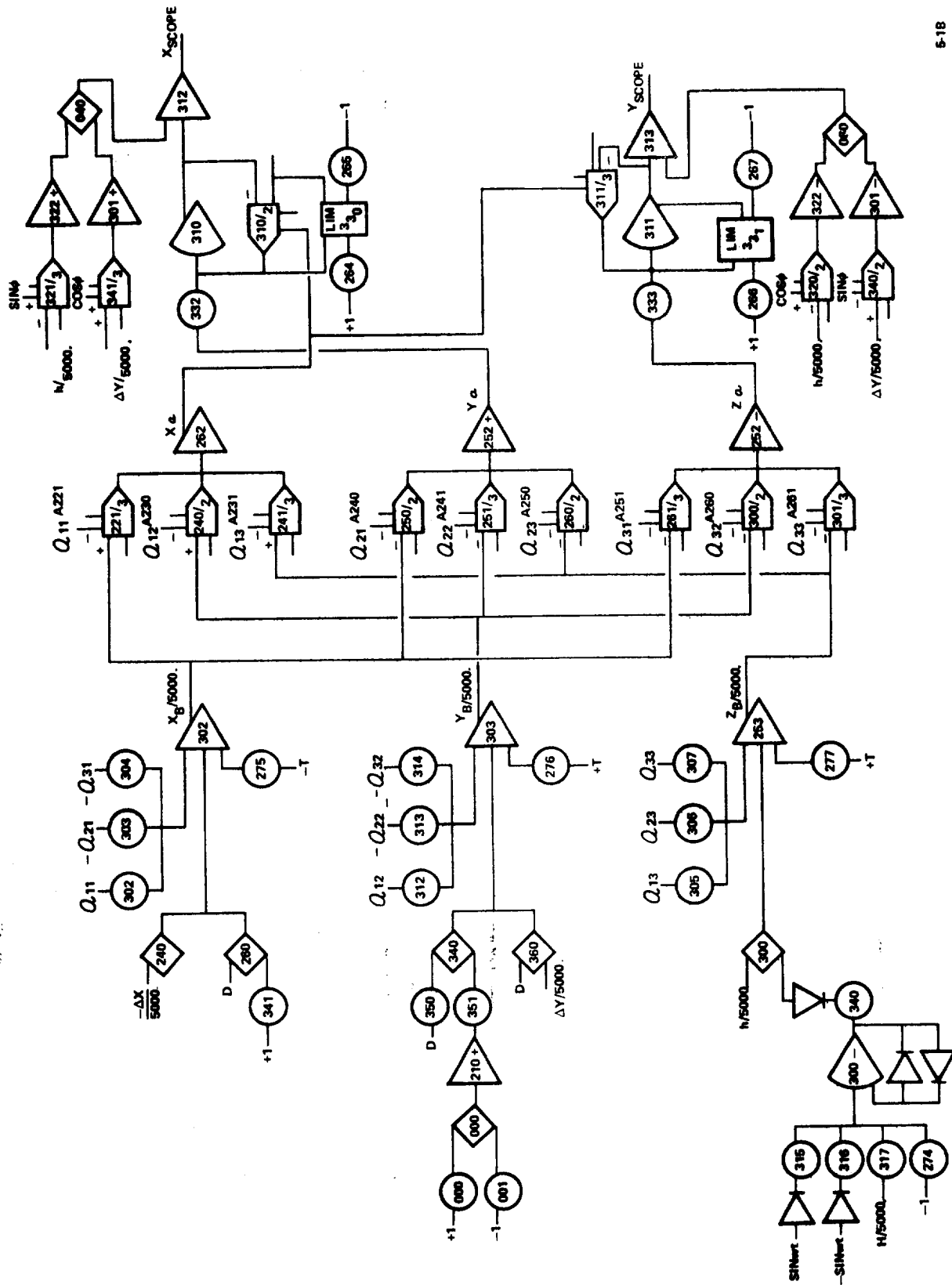


Figure G.8. (Continued)

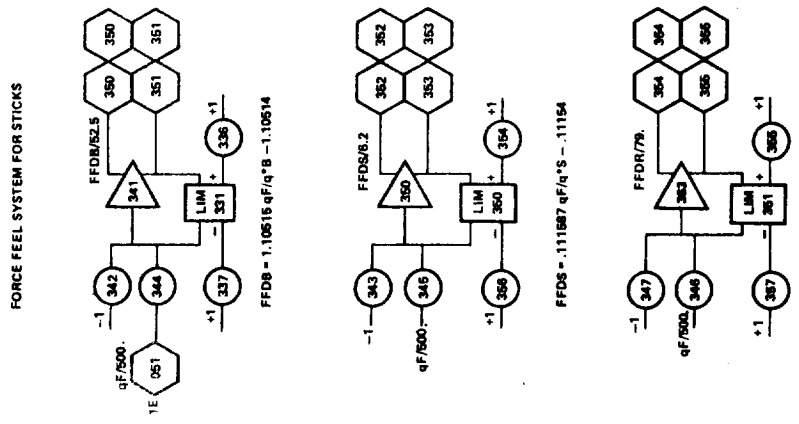
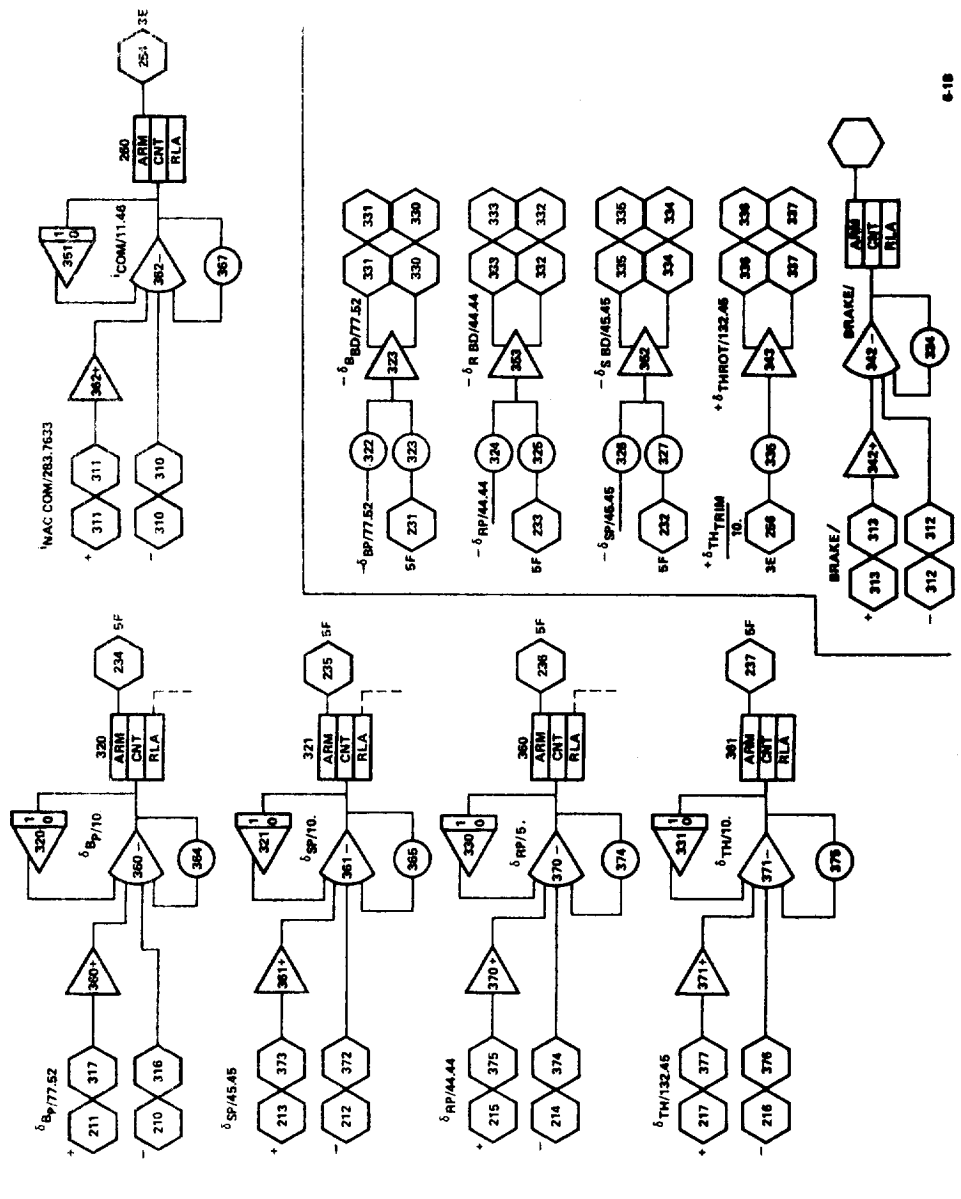


Figure G.8. (Continued)

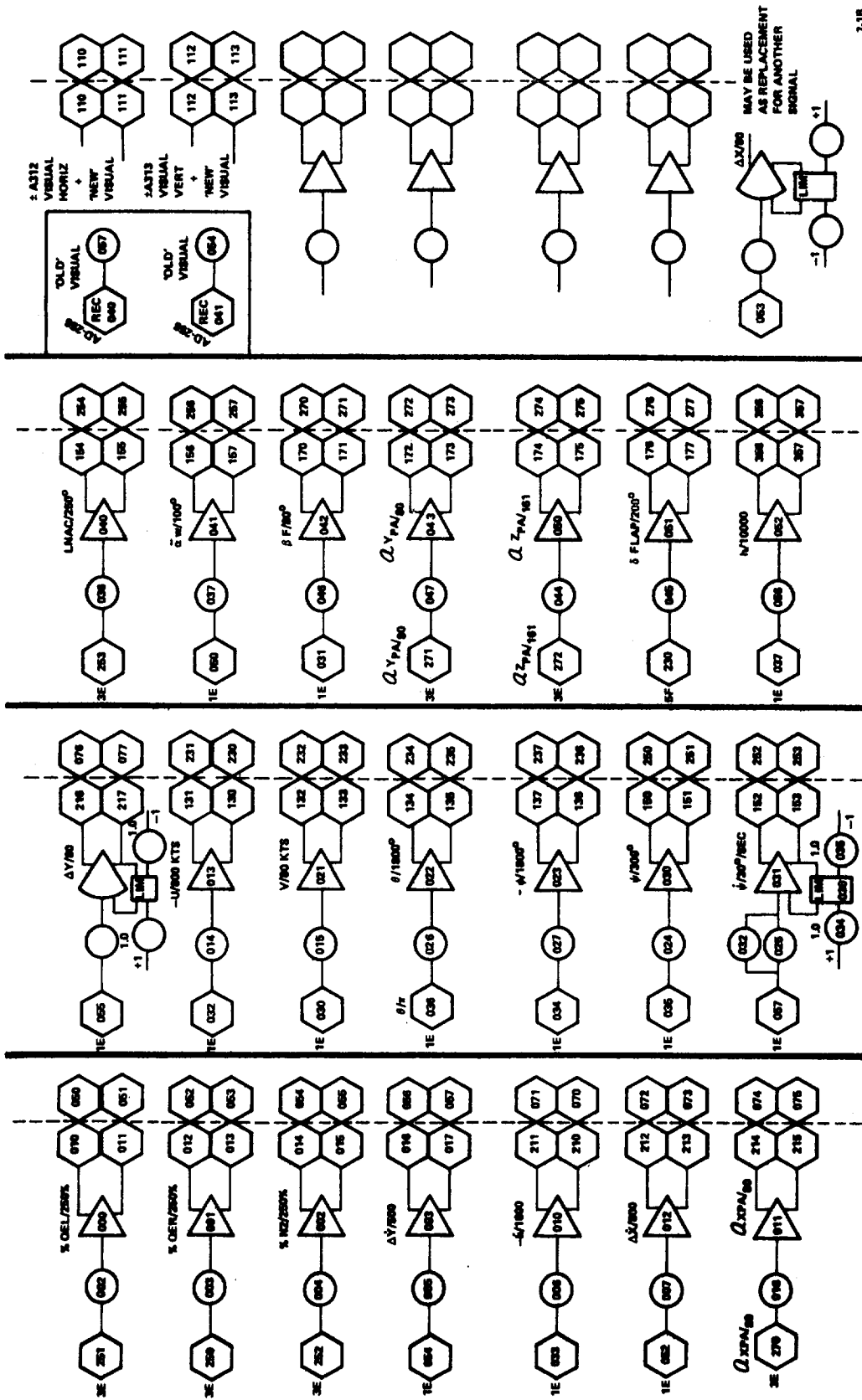


Figure G.8. (Continued)

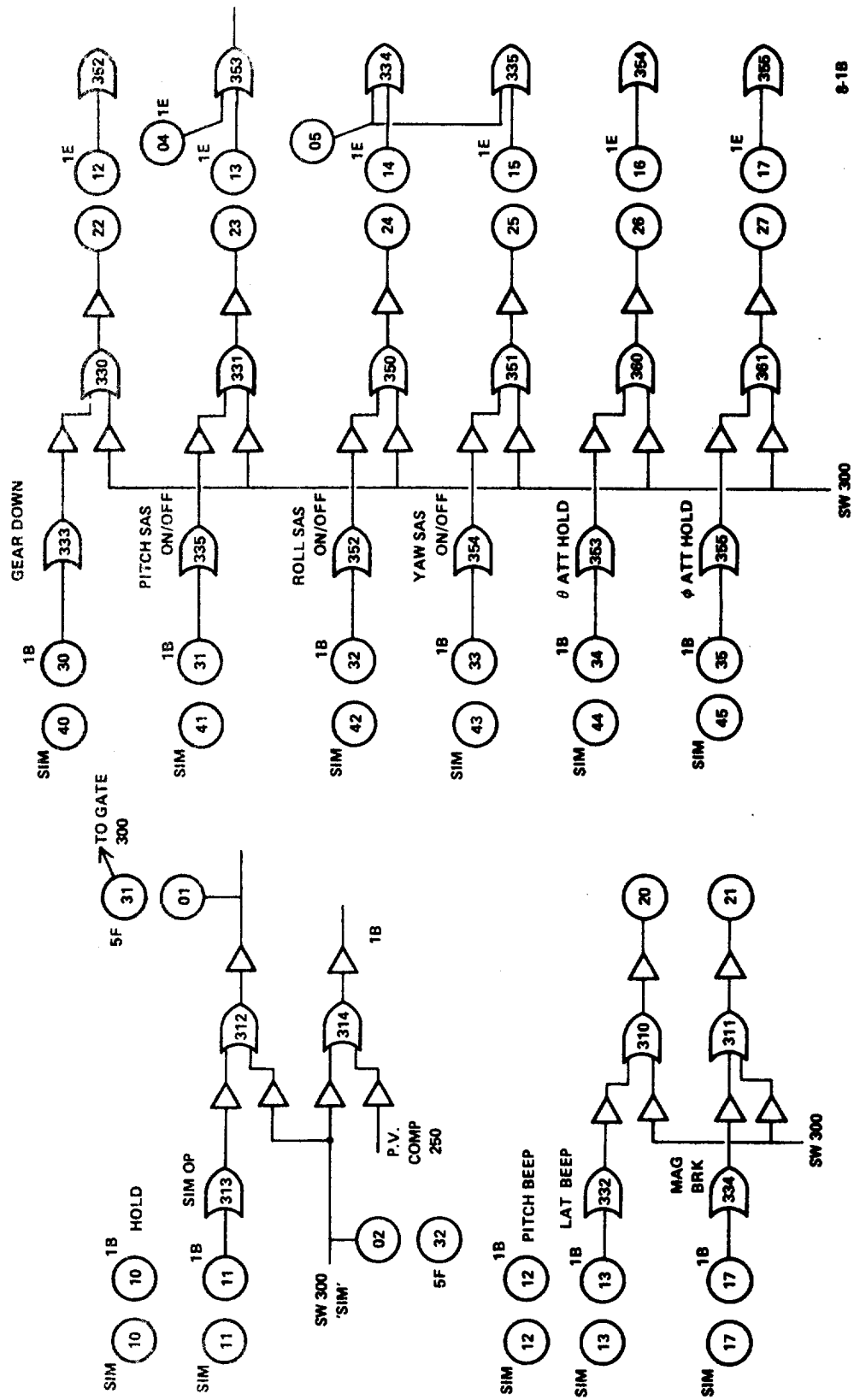


Figure G.8. (Continued)

```

0001 SUBROUTINE STATIC
0002 REAL *8 MATAV(5,5),MATE(5),MVT
0003 REAL *8 MATSAV(5,5),MASESAV(5)
0004 COMMON/COATA/ I(2*5),I(3*5),P3(3*5),P4(4*5),A1P(3*5),A1H(3*5),
* SUT(2*5),TRI(3*5)
0005 COMMON/ELACS/ IWAY,ILC(1),IWAY2(1),ISFAC(2),IAREVT(2),ICOND(2),
1 ITRIM,ITRIM,KTRIM,MOLDI,MPLD2,IHASH,IISLOR,SHLS,SHL5,SHL7,MN,
2 ISTR,ISTR,NDEF,NV5,TRAST
0006 LOGICAL#1 IWARML,IWAR2
0007 COMMON/HYCOM/PRJ ICOND5,NPCS(2),ICHAIN(2),IFRAME(2),NAGCS(2),
* RDNCS(4),NDACS(4),IRCX(4),IFC(4),NCON(4),LETR(4),
* IC(19),ISTIC ,HOLD(19),ISTHO,OPERA(19),
* ISTDG ,DIGAN(19),Istda ,ANDIG(19),Istda,
* ICD(19),ISTIC2 ,HOLD2(19),ISTH2 ,OPERA2(19),
* ISTDG2 ,DIGAN2(19),Istda2 ,ANDIG2(19),Istda2 ,IGU,
* ISTDIT ,IPUNIT,IAD,IUC,IUC2,ICLR,ITSC,IEX,ISETC ,
* WNDIG ,IDUPC(4) ,ISHRC(4) ,ISYNC(4) ,NIOS ,
* THJA ,IFCHAR ,TSRASC(2),TSREQD(2),IRCTS(4),
* TAUL(4) ,TPSNCS(1,2),DTIN(2) ,TRIM(19) ,ISTR5 ,
* TRIM2(19),ISTRM2

```

STK0030

```

C
0008 COMMON/VID/ VIC,GIC,FC,VIC,VIC,THEIC,PHIC,PSIIC,FC,VIC,
1 XIC,PSAS1,PSAS2,PSAS3,PSAS4,PSAS1,PSAS2,PSAS3,PSAS4,PSAS1,
2 YAS1,YSAS2,YSAS3,YSAS4,YSAS5,YSAS6,YSAS7,YSAS8,YSAS1,
3 YS1,YS2,YS3,YS4,YS5,YS6,YS7,YS8,YS9,YS10,
4 YS11,YS12,YS13,YS14,YS15,YS16,YS17,YS18,YS19,YS20,YS21,YS22,YS23,YS24,YS25,YS26,YS27,YS28,YS29,YS30,YS31,YS32,YS33,YS34,YS35,YS36,YS37,YS38,YS39,YS40,YS41,YS42,YS43,YS44,YS45,YS46,YS47,YS48,YS49,YS50,YS51,YS52,YS53,YS54,YS55,YS56,YS57,YS58,YS59,YS60,YS61,YS62,YS63,YS64,YS65,YS66,YS67,YS68,YS69,YS70,YS71,YS72,YS73,YS74,YS75,YS76,YS77,YS78,YS79,YS80,YS81,YS82,YS83,YS84,YS85,YS86,YS87,YS88,YS89,YS90,YS91,YS92,YS93,YS94,YS95,YS96,YS97,YS98,YS99,YS100,
5 AIC1,AIC2,AIC3,AIC4,AIC5,AIC6,AIC7,AIC8,AIC9,AIC10,AIC11,AIC12,AIC13,AIC14,AIC15,AIC16,AIC17,AIC18,AIC19,AIC20,
6 AIC21,AIC22,AIC23,AIC24,AIC25,AIC26,AIC27,AIC28,AIC29,AIC30,AIC31,AIC32,AIC33,AIC34,AIC35,AIC36,AIC37,AIC38,AIC39,AIC40,AIC41,AIC42,AIC43,AIC44,AIC45,AIC46,AIC47,AIC48,AIC49,AIC50,AIC51,AIC52,AIC53,AIC54,AIC55,AIC56,AIC57,AIC58,AIC59,AIC60,AIC61,AIC62,AIC63,AIC64,AIC65,AIC66,AIC67,AIC68,AIC69,AIC70,AIC71,AIC72,AIC73,AIC74,AIC75,AIC76,AIC77,AIC78,AIC79,AIC80,AIC81,AIC82,AIC83,AIC84,AIC85,AIC86,AIC87,AIC88,AIC89,AIC90,AIC91,AIC92,AIC93,AIC94,AIC95,AIC96,AIC97,AIC98,AIC99,AIC100,
7 AAMIC,ZADIC,ZARIC,DCVIC,SMVIC
0009 COMMON/IGCS/ XAERO,XAERD,ZAERP,ZAPP,ALARP,ALARP,AMARP,AMARP,
1 AMERP,QLSP,QLSAR,QLSAL,SMPPR
0010 COMMON/XTE/ DELH,DELS,DELR,DELTH,AI,NCM,UMGSEL,
1 GLATPH,SEOL,GBETPH,GPSTPH,GPRP,GYAN,AINREF,GHPLM,GSCL,
2 GRCYL,GNSCYL,GAIC,GBIC,GBFLP,GBE,GBSP,TPS,DVTAUD,DVTAUF,
3 THATLM,DTHT,RCARLK,TRGVL,TRGVLR,SDQIT,CT,CMCDR,CVMS,
4 CP4,CSF,CMF,CPD,DESL4
0011 COMMON/MDW/ UTRIM,VTIM,ATRIM,MDT,ITHT,RTA,ATTRIM,
1 SKTRIM(13)
0012 COMMON/PMAD/ ENF1 ,ENF2 ,ENF3 ,ENF4 ,ENF1 ,ENF2 ,ENF3 ,
* DNF4 ,DSF1 ,DSF2 ,DSF3 ,DSF4 ,DSF1 ,DSF2 ,
* EP45 ,EPM1 ,EPM2 ,EPM3 ,EPM4 ,EPM5 ,
* DPM5 ,DPM7 ,DPM1 ,DPM2 ,DPM3 ,DPM4 ,DPM5 ,
* DYM5 ,DYM7 ,DYM1 ,DYM2 ,DYM3 ,DYM4 ,DYM5 ,
* DYM6 ,DYM7 ,DYM1 ,DYM2 ,DYM3 ,DYM4 ,DYM5 ,
* DYM6 ,DYM7
0013 COMMON/XMAX/ PDOTMX,QQDTMX,PDOTMX,UPDTMX,VDOTMX,MDOTMX,IMX,VMX,
1 ZARMX,YDUTMX,XDOTMX,ZMX,YMX,VMX,DELSMX,DELSMX,DELRMX,
2 DLDMX,DELMX,DELEMX,DLSPMX,DLTHMX,QLSMX,TPSMX,THATMX,

```

Figure G.9. Analog Static Check Routine (Digital)

3 SHPMX,THOMX,THOMX,OMERX,ITWGX,DCYLX,DCOLMX,DLGNMX,
 4 XMKL,ALCMX,TH7FMX,ALFPMX,AMJPMX,CTMX,CPMX,CAFAX,
 5 CSEMX,COMX,CYMX,CPHOMX,CYMRX,ASFSX,ALDDMX,ALDIX,
 6 AINMX,AINMX,AMACMX,THEMXP,ITMX,PSIMX,PSLGMX,GCYMX,
 7 GSCOMX,GCOCMX,TAJFX,BICIX,AL4GAX,SOFMX,KCOMX,PCIDMX,
 8 DLELX,GUSTX,
 9 PMX,CMX,PMX,THOMX,PHOMX,PSDMX

0014 COMMON/XPARI/ AINM,ALAMDA,ALHST,ALVST,AREAHT,AREA,
 *AREAVT,APVT,AVYAC,AVEYCS,ALS,COOF,COUHT,COOVT,
 *CHORD,CLALHT,CLALPH,CMDF,CMON,CMDF,CMOLN,CMORN,CYALVT,
 3CDDLG,DCMLG,FINPR,DOVT,DSDBET,FFHT,EFFVT,FFIE,FINDEG,
 *FIP,FIIXE,FIIXPR,FIIXH,FIIXE,FIIXPR,FIIXM,FIYF,FIYPR,
 *FIYH,FIZZ,FIZZPR,FIZZMP,OMREE,PC,PI,ROTRAD,
 *SRFR,SRVPR,SG,SHW,SK1,SK2,SK3,
 *SK4,SK5,SK6,SK7,SK8,SK9,SK10,SK20,SK21,
 *SK22,COMMON/1,SK30,SK31,SK32,COMMON/1,SK34,SK35,SK36,
 *SK37,SK38,SK39,SK40,SK41,SK42,SK43,SK44,SK45,
 *SK46,SK47,SK48,SK49,SK50,SL,SLF,SLPA,SLW,
 *SM,SMF,SMN,SMH,SPAN,TAUHT,TAUVT,XFAC,XHT,
 *XMAC,XVT,YN,YPA,YWAC,ZFAC,ZHT,ZPA,ZFAC,
 *ZVT,ZLAL,PHIPH,SK31H1,EN2DF,XWC,ZI1,ZI2,BT3,
 *DKDT,BKDT,PKDT,AKMT,AKMT,AKMT,AKMT,AKMT,AKMT,
 *FEU,CLMAX,ALBAX,AKLSX,BKNSX,SDFPM,DEG2,NGTOPD,HVTKT,
 *PIV,PDGCG,PDTPS,SKPS,VALAX,TAUR1,TAUR2,
 0015 COMMON/XCUTL/ SKDL,SKDL,SKDL,SKDL,SKDL,TH7SLP,TH7SLN,
 1 TAJRL,GLSL,TAUTIC,ICLV,EM,TDASLP,DALM,GTW,OMA,ETIA,
 2 SKDA,GTI,TAUTH,DMG,DSLP,DMLM,DMG,SKGOL,THFILM,THOML,
 3 THOML,SHPL,GTGONV,OMD,ETARD,TTMSLP,TTMSLV,GDRI,GR2,
 4 TAUR,GG,GTHE,TAUQ,TAUQ,TAUHE,GLPJ,GLPSLP,GPOS,TAUPOS,
 5 GP,TAUP,GBFTP,TAURFT,GPFI,TAUPHI,GPISDR,GBETDR,GROR,TAUR,
 6 GPST,TAUPSI,GBETR,TAUR,GPRI,TAUPRI,GR,TAUPL,TAUR2,TAUR3,
 7 RUM,ORUM,DLRLM,DLSLM,DLPL1,
 8 TOMDL,GDLTH,SK41,SK42,SK43,SK44,SK45,
 9 SK46,SK47,SK48,SK49,SK50,GGUST,TAUGST,OMWR,ETAWR,GMDF,
 *MIPF,ETAIF,SKTHW,SCI,SC2,DCMCL,AINRLM,TAURQ1,TAURQ2,
 *TAUFF,TAUCYR,DCYRL1,ASLP,ALTM,TAUSHP,DELALM,
 DLELP

0016 COMMON/SIMMA7/ AXPMX,AYPMX,AZPMX,KJMX,ZDDMX,FBPX,FFSMX,
 1 FPMX,VSTMX,RTSTMX,USTMX,HTSMX,PHISMX,PSISMX,
 2 THSMX,TOISMX,PPMSX,AINSMX,AJDSMX,ALWSMX,DEPSMX,
 3 DRDMX,DRDMX,DRDMX,THDMX,DRPSMX,DRPSMX,DRPSMX,
 4 DTPSMX,XTSMX,YDTSMX,DXSMX,DYSIMX,HSIMX,PSOTX,
 5 BRKMX,PARKSMX,XVISMX,YVISMX,ZVISMX,SCOPMX
 COMMON/SIMPAP/ VISIC,VCAL1,VCAL2,XHAKIZ,YRDA,OSTAR3,OSTAR5,
 1 QSTAR,APB,ABS,APR,HSI,PE,RSI,UPF,
 2 FFLAL,COMJDT,COMDTH,COMYLB,COMDLS,COMDLP,BRAKE,
 3 VISVER,VISHUR,SCDPLM,FRQMT,BIASMT,PKMT1,PKMT2,
 4 GMTSI,GMTS2,SLX,SLY,SLZ,X9IC,X9IC,
 5 Z8IC,XDTESI,YDTEST

0017
 1
 2
 3
 4
 5
 6
 7
 8
 9
 10
 11
 12
 13
 14
 15
 16
 17
 18
 19
 20
 21
 22
 23
 24
 25
 26
 27
 28
 29
 30
 31
 32
 33
 34
 35
 36
 37
 38
 39
 40
 41
 42
 43
 44
 45
 46
 47
 48
 49
 50
 51
 52
 53
 54
 55
 56
 57
 58
 59
 60
 61
 62
 63
 64
 65
 66
 67
 68
 69
 70
 71
 72
 73
 74
 75
 76
 77
 78
 79
 80
 81
 82
 83
 84
 85
 86
 87
 88
 89
 90
 91
 92
 93
 94
 95
 96
 97
 98
 99
 100

Figure G.9. (Continued)

```

0019 CUMMCH/XPAB3/ XP3(91)
      ,SFIL ,SFJL ,SFSEL ,SEPAL ,SEVAL ,SEFL ,SEFL ,SEFL
E      SFTS ,SFNER ,SFCEP ,SEFMS ,SEYMS ,SEFOP ,SEFOS
* DIMENSION A2P(30),A2N(30),S2J(30),TR2(30),A3P(30),A3N(30),
      S3(30),TR3(30)
DIMENSION A4P(30),A4N(30),S4J(30),TR4(30)
EQUIVALENCE (A1P,A2P),(A1N,A2N),(S1J,S2J),(TR1,TR2)
EQUIVALENCE (A1P,A3P),(A1N,A3N),(S1J,S3J),(TR1,TR3)
EQUIVALENCE (A1P,A4P),(A1N,A4N),(S1J,S4J),(TR1,TR4)
DATA E04/15 ,1,1,14/9 ,/
  
```

```

0025 DATA VDE11/55./
0026 DATA THPCTU/0.6/
0027 DATA AINDET/0.25/
0028 DATA QINRF/95.9/ ,ANRATE/2.0/
0029 DATA CBALIS/0.3333/ ,TAUKMN/50./
      DEFINE VALUES TO CERTAIN VARIABLES FOR CHECKPOINT PURPOSES
0030 DATA PCTQ/64./ ,AVEALW/0.4/
0031 DATA RFEU/0.00378/
  
```

COEFFICIENT	ROOT	AINDE	AINDD	EQUATION
1,1	1,2	1,4	1,5	RODT
2,1	2,2	2,4	2,5	QDUT
3,1	3,2	3,4	3,5	RDDT
4,1	4,2	4,4	4,5	AINDDK
5,1	5,2	5,4	5,5	AINDDL

```

0032 P = FIC
0033 Q = QIC
0034 R = RIC
0035 U = UIC
0036 V = VIC
0037 W = WIC
0038 THF = THEIC
0039 PHI = PHIC
0040 PSI = PSIC
0041 HE = ZIC
0042 AIRF = AIRFIC+AINRF
0043 AIRR = AIRRIC
0044 AINL = AINLIC
  
```

Figure G.9. (Continued)

```

0045 AIN0TL = AINLDI
0046 AIN0TR = AINRDI
0047 SMO0JM = XLI*(OMLM,OMGL,DMG)*(UMSELE+JMSLP*AINRF)
0048 IMEGA = IMEGIC+CMG00M
0049 THOM = THOMIC+UIC*THOMMX/UMX*THPCTI+GDTHRT*PLIPI*GDILTH
0050 CPM0J = CPM0R
0051 CVM0R = CVM0P
0052 CPL = CP
0053 CPP = CP
0054 CNEPL = CNE
0055 CNFP2 = CNF0
0056 CSFPL = CSF0
0057 CSFPR = CSF0
0058 CPM0L = CPM0
0059 CVM0R = CVM0
0060 CPM0L = CPM0
0061 CPM0R = CPM00
0062 CVM0L = CVM0
0063 CVM0R = CVM0
0064 CVM0L = CVM0R
0065 CVM0R = CVM0P
0066 PCT0P = PCT0
0067 PCT0L = PCT0
0068 C0M1 = SM+SL*SL*(1.-SM/SM)+ETVDP
0069 CALL SINCOS(PH0L*SG0TRD,SPH0LS,CPH0LS)
0070 CALL SINCOS(TH, SINTHE,COSTHE)
0071 CALL SINCOS(PHI, SINCPI,COSPHI)
0072 CALL SINCOS(PSI, SINCPSI,COSPSI)
0073 CALL SINCOS(AINR, SININR, COSINR)
0074 CALL SINCOS(AINL, SININL, COSINL)
0075 CALL SINCOS(AINR-ALAMDA, SIALMR, CIALMR)
0076 CALL SINCOS(AINL-ALAMDA, SIALML, CIALML)
0077 CALL SINCOS(2.*AINR, S2INR, C2INR)
0078 CALL SINCOS(2.*AINL, S2INL, C2INL)
0079 CALL SINCOS(2.*(AINR-ALAMDA), S200JM, C2LAMR)
0080 CALL SINCOS(2.*(AINL-ALAMDA), S200JL, C2LAML)
0081 S200JR = SININR * SININR
0082 S200JL = SININL * SININL
0083 CALL SINCOS(AINR, SININR, COSTINR)
0084 AVETA = 0.5*(AINR + AINL)
0085 CALL SINCOS(PHIP1, SPHIP1, CPHIP1)
C
C GROUND TRACK
C
C NORTHWARD VELOCITY
0086 VNORTH= U*COSTHE*COSPSI+V*(SINPAI*SINTHE*COSPSI-COSPHI*SINPSI)
* +W*(COSPHI*SINTHE*COSPSI+SINPHI*SINPSI)

```

STK 2482
STK 2490
STK 2500
STK 2510

Figure G.9. (Continued)


```

0087 C EASTWARD VELOCITY
VEAST= U*COSTH+V*SINPT+V*(SINPHI*SINHE+STDPST+COSPHI*(COSPST)
+*(COSPHI*STPH+STPST-SINPHI*(COSPS))
0088 C WESTWARD VELOCITY
VWEST= -U*SINHE+V*SINPHI*(COSTH+V*COSPHI*(COSTH
XDRY= VDRYTH
YDRY= VFAST
ZDRY= VDRYN
HROT= -VDRMPL
HSO= H*H
C CENTER OF GRAVITY CALCULATION
C
C
C COLOCATION W.P.T. PIVOT
XCG = (SME*SLF+S*W*SLW)/S+S*SM/S*W/S*SM*(CILAVL+CILAMP)
ZCG = (SME*SHF+S*W*SHW)/S+S*SM/S*W/S*SM*(SILAVL+SILAMP)
C CG VELOCITY W.P.T. PIVOT (NON-ROTATING AXES)
XTCG = -SLE*SM/S*W*(AIDTLE*SHAMP+AIDTLE*SHAMP)
YTCG = -SLE*SM/S*W*(AIDTLE*CILAVL+AIDTLE*CILAMP)
C DENSITY CALCULATIONS
EQUATION FOR DEL FROM CURVE FIT PROGRAM
DEL = .0995993407 - .3627432044E-7* H
+ .567995171E-09 *HSO - .3727413045E-14 *HSO * H
C
C
C TDEG= TDEG - TDEG**4
THETC = .11927933*(TDEG+459.69)
SQTHC = SQRT(THETC)
UNAVC = 1. / THETC
RPI45= RPI*PI*ROT*PI**5
VTOTAL= SQRT(U*U+V*V+W*W)
VCALTR = VTOTAL*SQRT(ROE/ROO)
C
C CHSELAGE= PIVIT VELOCITY
C
C
C UP = U - Q*ZCG -XDTCC
VP = V + Q*ZCG -P*XCX
WP = W + Q*XCX -ZDTCC
C
C
C FUSELAGE AERODYNAMICS
C
C INPUT EQUATIONS
C
C VALFS= SQRT(U*U+W*W)

```

574415

Figure G.9. (Continued)

```

0111 ALPHF= ATAN2(W*U)
0112 3ETAF= ATAN2(V,VALFS)
0113 SDF= C.5*ONE*VTOTAL*VTOTAL
C LEFT ROTOR HUB VELOCITY - BODY AXES
0114 URLP2 = UP +R*YA -ALS*SINLN*(Q+AIN)TL) + Q*HIL
0115 URLP2 = VP +RLS*(Q+AIN)TL)*SINLN) -P* HIL
0116 URLP2 = WP -P*YN -ALS*(Q+AIN)TL)*COSLN + HIDL
C RIGHT ROTOR HUB VELOCITY - BODY AXES
0117 URLP2 = UP -R*YA -ALS*SINLN*(Q+AIN)TR) +Q* HIL
0118 URLP2 = VP +RLS*(Q+AIN)TR)*SINLN) -P* HIL
0119 URLP2 = WP +P*YN -ALS*(Q+AIN)TR)*COSLN + HILTR
C LEFT ROTOR HUB VELOCITY - SHAFT AXES
0120 URL = URLPR*COSLN -WRLPR*SINLN
0121 VRL = VRLPR
0122 URL = URLPR*SINLN +WRLPR*COSLN
C RIGHT ROTOR HUB VELOCITY - SHAFT AXES
0123 URL = URLPR*COSLN +WRLPR*SINLN
0124 VRL = VRLPR
0125 URL = URLPR*SINLN -WRLPR*COSLN
C ROTOR INPUT EQUATIONS (AF20)
C
C FREE STREAM VELOCITY
0126 VTOTR = SQRT(U**2+V**2+W**2)
0127 VTOTL = SQRT(U**2+V**2+W**2)
0128 URL = WRL*EPWLT*URL
0129 URL = WRL + EPWLT*URL
0130 VZFTL = SQRT(VRL**2+WRTL**2)
0131 VZETR = SQRT(VPR**2+WPTR**2)
C ANGLE OF ATTACK
C
C NOTE ALPHA AND ALPHA ARE DEFINED BETWEEN U AND U* DEGREES
C I.E. 90 +DP- 90 DEGREES
0132 ALPHR = ATAN2(VZFTL,URL) + EPRL
0133 ZETHL = ATAN2(VRL,WRTL)
0134 CALL SINCSIZEHL,SINZHL,COSZHL)
0135 ALPHR = ATAN2(VZETR,URR) + EPILR
0136 ZETHR = ATAN2(VPR,WPTR)
0137 CALL SINCSIZEHR,SINZHR,COSZHR)
C
C ROTOR ANGULAR RATE TRANSFORMS
C
C LEFT ROTOR - WHEEL AXES
0138 PNLN = P*COSLN - P*SINLN
0139 QNLN = Q + AIN)TL
0140 RNLN = P*SINLN + R*COSLN
C LEFT ROTOR - WIND AXES
0141 PNLR = PNLN

```

Figure G.9. (Continued)

```

0142 QNLP = QNLN*COSSZHL -RVLN*SINZHL
0143 RNL = RNLN*COSSZHL +QNLN*SINZHL
C *RIGHT ROTOR - NACELLE AXES
0144 PNP = -P*COSSIR + R*SINIR
0145 QNP = Q + A*INDT
0146 RNP = -P*SINIR -Q*COSSIR
C *RIGHT ROTOR - WIND AXES
0147 PNP = PNP
0148 QNP = QNP*COSSZR +RNP*SINZR
0149 RNP = RNP*COSSZR -QNP*SINZR
C
0150 OMEGAL = OMEGA + PNL
0151 OMEGAN = OMEGA + PNRR
0152 VTIPL = ROTRAD * OMEGAL
0153 VTIPR = ROTRAD * OMEGAR
0154 AMUL = VTOTLR/VTIPL
0155 AMUR = VTOTRR/VTIPR
0156 CMOR = CMOR +CMOR*QNR
0157 CYMR = CYMR +CYMR*RMZ
0158 CMOL = CMOL -CMOL*ONLR
0159 CYML = CYML +CYML*RMRL
C
C *BASIC EQUATIONS OF MOTION -- PRELIMINARY CALCULATIONS
C
C *BUSELAGS
0160 XF = SLF - XCG
0161 YF = SHF - ZCG
C
C *WING
0162 XW = SLW - XCG
0163 YW = SHW - ZCG
C
C *NACELLES
0164 QR = SL * CILQR - XCG
0165 YR = -SL * SILQR - ZCG
C
0166 XL = SL * CILXL - XCG
0167 YL = -SL * SILXL - ZCG
C *MERTIA TERMS
0168 SUMIXX = FIXX + FIXR + 2.*FIXXR
0169 SUMIYY = FIYY + FIYR + 2.*FIYXR
0170 SUMIZZ = FIZZ + FIZR + 2.*FIZXR
0171 SUMIXZ = FIXZ + FIXR + 2.*FIXZR
C
0172 *
FIXX = SUMIXX+(FIZZR-FIXZR)*(SSOIV+SSOIVL)-FIXZR*(SPTNR+SPTIL)
+2.*SMN*YN*YV +S*F*SHF*ZF +SMW*SHW*ZW -SL*SMN*(ZR*SILQR +

```

Figure G.9. (Continued)

```

C
0173      #      ZL* SILAML )
C      FIXX = (SUMI77-SUMIYY)+(FIXXPP-FI7ZPP)*(SS2INR+SS2INL)-FIX7PP*(
*      S2INR+S2INL)+2.*SMN*Y*Y1-(34F*SHF*ZF+SMN*SH*Z#)+
*      SL*SMN*(ZR* SILAME+ZL*SILAML)
C
0174      #      FIXZP = FIXZF+FIXZM+.5*(FIXXPP-FI7ZPP)*(S2INR+S2INL)+FIXZPP*(
*      (C2INR+C2INL)+(SMF*SLF*ZF+SMW*SL*W)+SMN*SL*(70*CI(LAME+
*      ZL* SILAML) )
C
0175      #      FIYY = SUMIYY+SMF*(SLF*XF+SHF*ZF)+SMW*(SLW*XW+SHW*WZ)+SMN*SL*(
*      (XP*GILAMR-ZR*SILAMR)+SMN*SL*(XL*GILAML-ZL*SILAML) )
C
0176      #      FJYY = (FIXXF-FI7ZF)+(FIXXW-FI7Z#)+(FIXXPR-FI7ZPR)*(C2INR+C2INL)
*      -2.*FIXZPR*(S2INR+S2INL)+S4F*(-SLF*XF+SHF*ZF)+SMW*( -CI(W#
*      XW+SHW*WZ)-SMN*SL*(XR*GILAMR+ZR*SILAMR+XL*GILAML+ZL*SILAML) )
C
0177      #      FIXZQ = FIXZF+FIXZM+.5*(FIXXPP-FI7ZPP)*(S2INR+S2INL)+FIXZPP*(
*      (C2INR+C2INL)-SMN*SL*(XP*SILAMP+XL*SILAML) )
C
0179      #      FI7Z = SUMI77+FIXXPR-FI7ZPR)*(SS2INR+SS2INL)+FIXZPP*(S2INR+
*      S2INL)+2.*SMN*Y*Y1+SMF*SLF*ZF+SMW*SLW*XW+SMN*SL*(XP*
*      CILAMR+XL*GILAML)
C
0179      #      FJ77 = SUMIYY-SUMIXX+(FIXXPP-FI7ZPP)*(SS01UP+SS01UL)+FIX7ZPP*(
*      S2INR+S2INL)-2.*SMN*Y*Y1+SMF*SLF*ZF+SMW*SLW*XW+SMN*SL*(
*      (XP*GILAMR+XL*GILAML) )
C
0180      #      FIXX = FIXZF+FIXZM+.5*(FIXXPR-FI7ZPP)*(S2INR+S2INL)+FIXZPP*(
*      (C2INR+C2INL)+SMF*SLF*XF+SMW*SLW*XW+SMN*(XR*SILAMR+
*      XL*SILAML) )
C
0181      #      ALARMN = ALARP+ALARIC*FIXX
0182      #      AMARPN = AMARP+AMARIC*FIYY
0183      #      ZARPW = ZARP+ZARIC*SM
0184      #      ALAERD = ALAERP+ALARWJ
0185      #      AMAERD = AMAERP+AMARWN
0186      #      ZAERD = ZAERP+ZARWN
C
0187      #      ROOT EQUATION: CROSS TERMS
C      TERMP1 = -FJXX*RR*O*P*O*FI7ZP
C
0188      #      ROOT EQUATION: CROSS TERMS
C      TERMD1 = -FJYY*PP*R-FIXZQ*(P*P-R*P)
C
0189      #      ROOT EQUATION: CROSS TERMS
C      TERMR1 = -FJZZ*PP*Q-FIXZR*P*Q

```

Figure G.9. (Continued)

```

C
C
0190 C ROOT EQUATION ROOT COEFFICIENT
      MATA(1,1) = C1XX
C ROOT EQUATION ROOT COEFFICIENT
0191 C MATA(1,2) = C1
C ROOT EQUATION ROOT COEFFICIENT
0192 C MATA(1,3) = -FIXP
C ROOT EQUATION AINDDR COEFFICIENT
0193 C MATA(1,4) = -SL*SM*YN * CILAMR
C ROOT EQUATION AINDDR COEFFICIENT
0194 C MATA(1,5) = SL*SM*YN * CILAML
C ROOT EQUATION FORCING FUNCTION
0195 C MATB(1) = TERMP1 + ALAERO
C
C
C ROOT EQUATION ROOT COEFFICIENT
0196 C MATA(2,1) = C1
C ROOT EQUATION ROOT COEFFICIENT
0197 C MATA(2,2) = C1YV
C ROOT EQUATION ROOT COEFFICIENT
0198 C MATA(2,3) = C1
C ROOT EQUATION AINDDR COEFFICIENT
0199 C MATA(2,4) = E1YVPR+SL*SM*(-ZR*SLAMR +XR*CILAMR )
C ROOT EQUATION AINDDR COEFFICIENT
0200 C MATA(2,5) = E1YVPR+SL*SM*(-ZL*SLAML +XL*CILAML )
C ROOT EQUATION FORCING FUNCTION
0201 C MATR(2) = TERMP1 + ANAERO
C
C
C ROOT EQUATION ROOT COEFFICIENT
0202 C MATA(3,1) = -FIXZP
C ROOT EQUATION ROOT COEFFICIENT
0203 C MATA(3,2) = C1
C ROOT EQUATION ROOT COEFFICIENT
0204 C MATA(3,3) = F1Z7
C ROOT EQUATION AINDDR COEFFICIENT
0205 C MATA(3,4) = SMN*SL*YN* SLAMR
C ROOT EQUATION AINDDR COEFFICIENT
0206 C MATA(3,5) = -SMN*SL*YN*SLAML
C ROOT EQUATION FORCING FUNCTION
0207 C MATB(3) = TERMP1 + ANAERO
C
C
C AINDDR EQUATION ROOT COEFFICIENT
0208 C MATA(4,1) = C1
C AINDDR EQUATION ROOT COEFFICIENT
0209 C MATA(4,2) = C1
C AINDDR EQUATION ROOT COEFFICIENT
0210 C MATA(4,3) = C1
C AINDDR EQUATION AINDDR COEFFICIENT

```

Figure G.9. (Continued)

```

0211      MAT(4,4) = 1.0
           C AINDDF EQUATION AINDDF COEFFICIENT
0212      MAT(4,5) = 0.
           C AINDDF EQUATION FORCING FUNCTION
0213      MAT(4) = 0MIRE**2*(ATAIRF+GINRF*OCYC(-AI*P))-2.*ETAIRF*UMT*CF*AINDTA
           C
           C AINDDL EQUATION POUT COEFFICIENT
0214      MAT(5,1) = 0.
           C AINDDL EQUATION QDOT COEFFICIENT
0215      MAT(5,2) = 0.
           C AINDDL EQUATION POUT COEFFICIENT
0216      MAT(5,3) = 0.
           C AINDDL EQUATION AINDDR COEFFICIENT
0217      MAT(5,4) = 0.
           C AINDDL EQUATION AINDDL COEFFICIENT
0218      MAT(5,5) = 1.0
           C AINDDL EQUATION FORCING FUNCTION
0219      MAT(5) = 0MIRE**2*(ATAIRF+GINRF*OCYC(-AI*P))-2.*ETAIRF*UMT*CF*AINDTA
           C SAVE MATA APRAY
           DO 10 JJ=1,5
0220      MARS(V(JJ)) = MATR(JJ)
           DO 20 KK=1,5
0221      MATSA(V(JJ, KK)) = MATA(JJ, KK)
           CONTINUE
0222      CONTINUE
           CALL MATINV(MATA,5,5, MATR,1,DEFI)
           DO 30 JJ=1,5
0223      ROOT = MATR(JJ)
           DO 40 KK=1,5
0224      MATSA(V(JJ, KK)) = MATSA(V(JJ, KK))
           CONTINUE
           RESTORE MATA APRAY
           DO 30 JJ=1,5
0225      MATR(JJ) = MARS(V(JJ))
           DO 40 KK=1,5
0226      MATA(JJ, KK) = MATSA(V(JJ, KK))
           CONTINUE
           C
           C AIRCRAFT CONDITION CALCULATIONS
           C
           C LINEAR EQUATIONS OF MOTION (PSI, THETA, PHI FULLER SYSTEM)
0227      YDOT = XAERO / SM - SG*SINTHC - Q**4 + R**V
0228      YDOT = YAERO / SM + SG*CSSTHE*SINP4I - R*U + P**H
0229      YDOT = ZAERO / SM + SG*CSSTHE*CSPPHI + Q**U - P**V
           C FULLER ANGLE CALCULATION PSI, THETA, PHI SYSTEM
0230      THEDOT = Q*CSPPHI - R*SINPHI

```

Figure G.9. (Continued)

```

0242 PHDPT = P + (C*SINPHI + P*COSPHI) * SIVTHE / CUSTHE
0243 PSDPT = (C* SINPHI + P* COSPHI) / CUSTHE
C
C C.G. ACCELERATION P.P.T. PIVOT (NON-ROTATING AXES)
0244 XDDCG = -SL*SMN/SM*(AINDDL*SIAML + AINDL*AINDTL*CIAML + AINDR*P*
* SIAMR + AINDTR*AINDTL*CIAMR )
0245 ZDDCG = -SL*SMN/S*(AINDDL*CIAML - AINDL*AINDTL*SIAML + AINDR*
* CIAMR - AINDTR*AINDR*SIAMR )
C
C PILOT STATION ACCELERATIONS (BODY AXES)
C
0246 AVAIL = 12345678.
0247 ACCXA = XAERQ/SM - YDDCG
0248 ACCYA = YAERQ/SM - PDOT*(XCG-SIPA)
0249 ACCZPA = ZAERQ/SM + PDOT*(XCG-SIPA) - ZDDCG + SG
C
C PILOT STATION VELOCITIES (BODY AXES)
C
0250 VPA = UP + D*ZPA - R*YPA
0251 VPA = VP + R*SLPA - P*ZPA
0252 VPA = WP + P*YPA - D*SLPA
C
0253 AMACDP = ( SMN*SL*Y*CIAMR*PDOT - (SM*SL*SL*(1. - SMN/SM)*FIYPR)
* (PDOT + AINDR) - SM*SL*Y*SIAMR*PDOT )
0254 AMACLP = ( -SMN*SL*Y*CIAML*PDOT - (SM*SL*SL*(1. - SMN/SM)*FIYPR)
* (PDOT + AINDL) + SMN*SL*Y*SIAML*PDOT )
0255 AIRFD = XLIM(AINRL, -AINRLM, AINDR)
C
C THROUST MANAGEMENT SYSTEM
C
0256 DLTHPD = GH/TAUTH*DELTH - DLTHP/TAUTH
0257 AEHG = XLIM(ALIM, -1.0, AQ-ASLP*SHPIC)
0258 SHP1 = SHPRR*AEV3
0259 DSHP = SHP1 - SHPIC
0260 DSHPO = SHP1 - SHP2IC
0261 SHP2 = CVTAW*DSHPP
0262 DSHPOP = SHP2IC - SHP3IC
0263 SHP3 = CVTAUF*S2THIC/DEL*DSHPP
0264 SHP4 = SHPRR*SHP3IC - SHP1
0265 SHPD = XLIM(SHPLM, -SHPLM, (SHPA - SHPIC)/TAUSHP)
0266 JAVL = SHPIC/OMEGA
0267 CPPQ = 0.5 * (CPL + CPF)
0268 ARQD = CPRO*OMEGA**2
0269 TMDPT = (590.*QAVL - R*DIERS*ORQD)/EIP
0270 DLTHP = OMEGA - OAGC JM
0271 THRM = XLIM(TCMOLM, -TCMOLM, COM*DLTHM)
0272 DTHRM = XLIM(TOMLM, -TOMLM, TOM*TCMSLP*AINRF)
0273 TMS2 = THDM + DTHDC*COM*DLTHM + GDTHRT*DLTHP + DLTH
0274 TMS10 = XLIM(THRTL, -THRTL, 1./1. = (TMS2 - TMS1 - THDM - GDTHRT)*DLTHP +
DLTH)

```

Figure G.9. (Continued)

```

0275 TMS3= XLIM(THATL4,-THATLM,TMS2-TMS1-T49)*GDTURT*DLTHP*GDLTH)
0276 THTMS = XLIM(TTMSLP,TTMSLN,TMS1+THTM+TMS3*GDTURT*DLTHP*GDLTH)
0277 THTMSR = THTMS*RT46*(V*THGCVR
0278 THTMSI = THTMS*GTHGOV*THGCVL

```

ROLL THRUST

```

0279 CTRPM = RDT1 + CTC*TAURO1/TAUR02*SFTR
0280 RDT10 = CTC/TAUR02*SFTR-CTRPM/TAUR02
0281 CTRPM = RDT2+CTC*TAURO1/TAUR02*SFTR
0282 RDT20 = CTC/TAUR02*SFTR-CTRPM/TAUR02

```

SAS (LATERAL, LINGUITUDINAL)

```

0283 PITCH SAS
0284 PSAS10 = (DELR-PSAS1)/TAUPR
0285 PSAS5 = (GJ*Q-GDB2*PSAS1)/TAUCI
0286 PSAS4 = (GTHE*Q-GDB1*PSAS1)*TAUT4F/TAUT+E
0287 GLONPH = XLIM(1.0,7.0)*GLP2-GLP5LP*V*CALTR)
0288 PSAS20 = PSAS5*GLONPH-PSAS2/TAUCI
0289 PSAS30 = PSAS6*GLONPH-PSAS3/TAUTHE
0290 PSAS7 = PSAS2+PSAS3-PSAS4
0291 DELRS = XLIM(DLRM,-DLRM,PSAS7+DLRBITC)

```

ROLL SAS

```

0292 RSAS10 = (GPOS*DEL5-RSAS1)/TAUPDS
0293 RSAS20 = (GP*P-RSAS2)/TAUP
0294 RSAS40 = (RETAF-RSAS4)/TAURET
0295 RSAS5=GRPHI*P*TAUPHI/TAURHI
0296 RSAS30 = PSAS5*GLATPH-RSAS3/TAUPHI
0297 RSAS6 = PSAS2+PSAS3-RSAS1
0298 DELS3 = XLIM(DLSM,-DLSM,RSAS6*RROLL-PSAS4*CRFTP*3RFTOM)

```

YAW SAS

```

0299 YSAS20 = (DFLR-YASAS2)/TAUDR
0300 YSAS7 = XLIM(RLM,-PLM,R)
0301 YSAS9 = XLIM(DRLM,-DRLM,YASAS2)
0302 YSAS3 = (GSI*YASAS7-GSIOK*YASAS1)*TAJPSI/TAJPSI
0303 YSAS10 = YASAS7*GLATPH-YASAS1/TAUPSI
0304 YSAS10 = XLIM(RELRMX,-DELRMX,-G3ETP*RSAS4-CRFTP*YASAS2)
0305 GLATPR = 1.-GLATPH
0306 YSAS11 = YSAS1+YASAS10*GLATPR
0307 YSAS30 = (P*GPPH-YASAS3)/TAUPR
0308 YSAS12 = G*GR-G*DR*YASAS2-YASAS4
0309 YSAS13 = YSAS12
0310 IF(VGALTR-I*VDFI)*SKFRS) YSAS13 = -YASAS4
0311 YSAS40 = YSAS13/TAURI
0312 YSAS14 = YSAS12*TAUP2/TAUP3+YSAS5
0313 YSAS50 = (YASAS12-YASAS14)/TAUP3

```

Figure G.9. (Continued)


```

0314 YSAS15 = P
0315 IF(VCALTP.LT.VYCTI*(SKEPS)) YSAS15 = .
0316 YSAS16 = YSAS15*GYAW
0317 YSAS17 = (CPH1*YSAS16*TAUPR1-YSAS16)/TAUPP1
0318 YSAS17 = YSAS16-YSAS6
0319 DELRS = XLIM(DCLM)*DELPL1,YSAS11*GDSIPH+YSAS3+YSAS17*GYAW

```

C
C
C

CONTROL EQUATIONS

```

0320 DELRT = DELB
0321 DELST = DELS - DELSS
0322 DELRT = DELR - DELRS
0323 DELRJD = -SKDRD*DELRT
0324 DELLELV = -SKDLP*DELRT + GDF*DELTDZ
0325 DELFLP = GDFLP
0326 DELA12 = -XLIM(D,*)-DELAMX,SKDA*DELST)
0327 DELA12 = XLIM(DELAMX*,*,SKDA*DELST)
0328 DELA1 = XLIM(DELA14,*,*,DELA12*DELRT)
0329 DELA1 = XLIM(DELA14,*,*,DELA12*DELFLP)
0330 DELA1 = DELA1 + DELFLP
0331 DELA1 = DELA1 + DELFLP
0332 DELSPP = XLIM(DLSPLM,*,*,GDSPI)
0333 DELSPL = -XLIM(D,*)-DLSPLM,GDSPI)
0334 DELRT = DELRT*SKDLP*GDSCYL-DELST*SKDLS*GDSCYL
0335 DELST = DELST*SKDLS*GDSCOL
0336 DELRT = DELRT*SKDUR*GDSALON-DELRS
0337 DELRT = XLIM(DCYRLM,*,*,DCYRLM,DCCYL-DCYLC)/TAJCYPI)
0338 GBIIC = XLIM(GICLM,*,*,GICLM,(GAIIC-GAICPI)/TAUGIC)
0339 GAIC = XLIM(GICLM,*,*,GICLM,(GAIIC-GAICPI)/TAUGIC)

```

C

```

0340 GLSAP = GLSB/TAUGLS-GLSBIC/TAUGLS
0341 GLSAPD = GLSAR/TAUGLS-GLSAR/TAUGLS
0342 GLSALD = GLSAL/TAUGLS-GLSAL/TAUGLS
0343 BIRPDD = GMA**2*(GRICP-DCYL-DELON)-2.*ETAAG*OMA*BIICDD
0344 - OMA**2*BIICDD
0345 BIRPDD = GMA**2*(BIICP+DCYL-DELON)-2.*ETAAG*OMA*BIICDD
0346 - OMA**2*BIICDD
0347 BIRPDD = GMA**2*(-GLSAPD-SKDCOL*DCYL+GAICP)-2.*ETAAG*OMA*BIICDD
0348 - OMA**2*BIICDD
0349 BIRPDD = GMA**2*(GLSAIL+SKDCOL*DCYL+GAICP)-2.*ETAAG*OMA*BIICDD
0350 - OMA**2*BIICDD
0351 TH75L = XLIM(TH75L,*,*,TH75LN,TH75LN+DCOL)
0352 TH75L = XLIM(TH75L,*,*,TH75LN,TH75LN+DCOL)

```

C

Figure G.9. (Continued)

```

C
C      WING VERTICAL READING
C353      ALA300 = DMH**2*(ALAPP-ALAPM)/FIX-2.*LTA*DB*DM**AL*AD
C354      AM300 = DMH**2*(AMAPD-AMAPM)/FIY-2.*LTA*DB*DM**AM*AD
C355      ZAP30 = (DMH**2*(ZAPD-ZAPM)/SM-2.*BETA)*DM**ZARDIC
C
CALL ANDA1H(PROJ,RDMS(1),LETP(1),FIC(1),ACON(1),P1(3,3))
CALL ANDA1H(PROJ,RDMS(2),LETP(2),FIC(2),ACON(2),P2(3,3))
CALL ANDA1H(PROJ,RDMS(3),LETP(3),FIC(3),ACON(3),P3(3,3))
CALL ANDA1H(PROJ,RDMS(4),LETP(4),FIC(4),ACON(4),P4(3,3))
C
C      DAC CALCULATION SECTION
C360      P1(2,1) = -ALPH/ZARF*SMX
C361      P1(2,1) = (ALAPR+TERMP1)/FIX/RDRTMX
C362      P1(2,2) = -MATA(1,3)/FIX*RDRTMX/RDRTMX
C363      P1(2,3) = (AMAPR+TERMG1)/FIY/RDRTMX
C364      P1(2,4) = -MATA(1,4)/FIX*ATD*MX/RDRTMX
C365      P1(2,5) = MATA(3) /FI77 / RDRTMX
C366      P1(2,6) = -MATA(1,5)/FIX*ALD*MX/RDRTMX
C367      P1(2,7) = XAPR1 / SV /LDRTMX
C368      P1(2,8) = VTEIM*SKEPS/U4X
C369      P1(2,11) = YAPR0 / SV /VDRTMX
C370      P1(2,12) = VTRIM*SKEPS/VW4X
C371      P1(2,13) = ZAPR0 / SM / ZAP*MX
C372      P1(2,14) = -HTRIM/ZMX
C373      P1(2,15) = VCALTR/HMX
C374      P1(2,16) = -MATA(3,4)/FIY*ALD*MX/RDRTMX
C375      P1(2,17) = VDTLR/SQTRAD/AM*DMX/DM*DMX
C376      P1(2,20) = -MATA(2,5)/FIY*ALD*MX/DM*DMX
C377      P1(2,21) = -ALPHR / ALFRMX
C378      P1(2,22) = THTRIM/TH*MX/RDRTDG
C379      P1(2,23) = VTOTR/PGTRAD/AMUR*MX/DM*SMX
C380      P1(2,24) = -AVEALW / ALW*MX
C381      P1(2,25) = -ALPHR / ALFRMX
C382      P1(2,26) = -MATA(3,1)/FIZZ*RDRTMX/RDRTMX
C383      P1(2,27) = PNLN/DMFG*MX
C384      P1(2,30) = -MATA(3,4)/FIZZ*ALD*MX/RDRTMX
C385      P1(2,31) = PNRN/DMFG*MX
C386      P1(2,32) = -MATA(3,5)/FIZZ*ALD*MX/RDRTMX
C387      P1(2,33) = -VDRTH/RDRTMX
C388      SGN SQF = 1.0
C389      IF(U,LT,C.) SGN SQF = -1.0
C390      P1(2,34) = -SQF*SGNSQF/SQF*MX
C391      P1(2,35) = -VEAST/VDRTMX
C392      P1(2,37) = -BETA / ARF*MX
C393      P2(2,0) = -SMN*SL*VN*CILAMR*RDRTMX/AMAC*MX
C394      P2(2,1) = GLSR/GLSMX
C395      P2(2,2) = (SMN*SL*SL*(1.-SMN/SM)+FIYPRI)*RDRTMX/AMAC*MX
C396      P2(2,3) = -GLSAL/GLSMX
C397      P2(2,4) = SMN*SL*VN*SLILAMR*RDRTMX/AMAC*MX

```

Figure G.9. (Continued)

```

0398 P2(225) = (XCG-SLPA)/XCG1X
0399 P2(226) = HDTP14/VWXX/AC
0400 P2(227) = SHDPP/SUDMX
0401 P2(210) = SMN*SLAYN*CLLAL*POT1X/AMAGX
0402 P2(211) = -SOTATC/DFL*TAUFMX/GROUTN
0403 P2(212) = (SMN*SL*SL*E1L - SMN/SM) + E1YDPI*SDUTMX/AMAGX
0404 P2(214) = -SMN*SL*YN*CLLAL*POT1X/AMAGX
0405 P2(216) = ATTR14/ATMX /POTDGG
0406 P2(217) = ALAPP/FIXX/PDQTMX
0407 P2(222) = WDRIP5/FIP*WEGMX*CMX /ZL/17.
0408 P2(221) = AMARP/FIYY/QDUTMX
0409 P2(223) = ZARP/SM/ZARMY
0410 P2(224) = -QNR / QMX * CPMDMX / CP4MX
0411 P2(225) = GLSAR/GLSMX
0412 P2(226) = -QNL / QMX * CDMYX / CP4MX
0413 P2(230) = RNLR / RMX * CYP4MX / C4MX
0414 P2(232) = RNLR / RMX * CYM2MX / C2MX
0415 P2(237) = PCTOR / PCTDXX

```

C
C
C
BRAPP LE (CONSOLE 1) POT. CALCULATION SECTION

```

0416 P1(330) = ZIC/ZMX
0417 P1(331) = YIC/YMX
0418 P1(333) = VMXX/Z4X/GROUTN
0419 P1(334) = YDUTMX/YMX/GROUTN
0420 P1(335) = XDUTMX/X4X/GROUTN
0421 P1(336) = SKTRIM(31)
0422 P1(337) = SKTRIM(32)
0423 P1(310) = XIC/XMX
0424 P1(312) = 1./TAUR02/GROUTN*SFTF
0425 P1(313) = TAUR01/TAUR02*SFTF
0426 P1(314) = 1./TAUR02/GROUTN
0427 P1(315) = 1./TAUR02/GROUTN*SFTL
0428 P1(316) = TAUR01/TAUR02*SFTL
0429 P1(320) = P7.*SKEPS/UMX
0430 P1(321) = UMX/VWXX/17.
0431 P1(326) = THEMX/PI
0432 P1(327) = PHMX/PI
0433 P1(330) = 141.*SKEPS/UMX
0434 P1(332) = ROT1 / CTMX
0435 P1(333) = POT2 / CTMX
0436 P1(336) = 1./10.
0437 P1(337) = 1./10.
0438 P1(322) = VDF1 *SKEPS / PHX
0439 P1(323) = SKTRIM(33)
0440 P1(324) = SKTRIM(34)
0441 P1(325) = SKTRIM(35)
0442 P1(326) = SKTRIM(36)
0443

```

Figure G.9. (Continued)

0444 P1(240) = PIC/PMX
 0445 P1(241) = QIC/PMX
 0446 P1(242) = PDDTMX/PMX/GRUTON
 0447 P1(243) = QDDTMX/PMX/GRUTON
 0448 P1(244) = RDDTMX/PMX/GRUTON
 0449 P1(245) = RIC/RMX
 0450 P1(246) = VDDTMX/VMMX/GRUTON
 0451 P1(247) = WDDTMX/VMMX/GRUTON
 0452 P1(250) = UDDTMX/UMX/GRUTON*10.
 0453 P1(251) = THDMX/THMXX/GRUTON
 0454 P1(252) = SG*1.0/UDDTMX/10.
 0455 P1(253) = QMXX*VMXX/UDDTMX/10.
 0456 P1(254) = PMXX*VMXX/UDDTMX/10.
 0457 P1(255) = UIC/UMX
 0458 P1(256) = SG*1.0/VDDTMX/10.
 0459 P1(257) = PMXX*UMX/VDDTMX/10.
 0460 P1(264) = PMXX*VMXX/VDDTMX/10.
 0461 P1(265) = ZAPMX/WDDTMX/10.
 0462 P1(266) = SG*1.0/WDDTMX/10.
 0463 P1(267) = QMXX*UMX/WDDTMX/10.
 0464 P1(270) = PHDMX/PHMXX/GRUTON
 0465 P1(271) = PSDMX/PSIMX/GRUTON*10.
 0466 P1(272) = VIC/VMMX
 0467 P1(273) = WIC/VMMX
 0468 P1(274) = THEIC/THMXX
 0469 P1(275) = PHIC/PHMXX
 0470 P1(276) = PMXX*VMXX/WDDTMX/10.
 0471 P1(277) = PSIC/PSIMX
 0472 P1(300) = RSASI/DELSMX
 0473 P1(301) = PSAS2/DELSMX
 0474 P1(302) = GPD\$/TAUPD\$*DELSMX/DELSMX/GRUTON
 0475 P1(303) = 1./TAUPD\$/GRUTON
 0476 P1(304) = GP/TAUP*PMX/DELSMX/GRUTON
 0477 P1(305) = 1./TAUP/GRUTON
 0478 P1(306) = GPHI*PMX/DELSMX/GRUTON
 0479 P1(307) = 1./TAUPHI/GRUTON
 0480 P1(310) = RSAS3/DELSMX
 0481 P1(311) = RSAS4/ARF\$MX
 0482 P1(312) = 1./TAURET/GRUTON
 0483 P1(313) = 1./TAURET/GRUTON
 0484 P1(314) = GBETD*ARF\$MX/DELSMX-1.
 0485 P1(315) = 1./TAUPSI/GRUTON
 0486 P1(316) = DLSLM/DELSMX
 0487 P1(317) = DLSLM/DELSMX
 0488 P1(320) = YSASI/DELRMX
 0489 P1(321) = YSAS2/DELRMX
 0490 P1(322) = GPSI*MX/DELRMX/GRUTON
 0491 P1(323) = GPSIDR/GRUTON
 0492 P1(324) = 1./TAUPD*DELRMX/DELRMX/GRUTON

Figure G.9. (Continued)

```

0493 P1(325) = 1./TAURK/GRUTON
0494 P1(326) = PLM/RMX
0495 P1(327) = PLM/RMX
0496 P1(331) = YSAS2/DELRMX
0497 P1(331) = YSAS6/DELRMX
0498 P1(332) = GRETDP/1.
0499 P1(333) = GRETDP*ABS(MX/DELRMX/1.).
0500 P1(334) = 2./TAURR*DMX/DELRMX/GRUTON
0501 P1(335) = 1./TAURR/GRUTON
0502 P1(335) = DRLM/DELRMX
0503 P1(337) = DRLM/DELRMX
0504 P1(340) = YSAS4/DELRMX
0505 P1(341) = YSAS5/DELRMX
0506 P1(342) = GROR
0507 P1(343) = 1./TAUR3/GRUTON
0508 P1(344) = 1./TAUR3/GRUTON
0509 P1(345) = TAUR2/TAUR3
0510 P1(346) = GR2LRMX/DELRMX/GRUTON
0511 P1(347) = 1./TAURP1/GRUTON
0512 P1(353) = (R*SMX/DELRMX/1.)
0513 P1(351) = 1./TAUR1/GRUTON/0.1
0514 P1(352) = GRETDP*0.41.
0515 P1(354) = 1.0
0516 P1(355) = 1.0
0517 P1(356) = DRLM/DELRMX
0518 P1(357) = DRLM/DELRMX

```

POT. CALCULATION SECTION

```

0519 P2(019) = DLTHP/DLTHMX
0520 P2(021) = SHP2IC/SHPMX
0521 P2(022) = GTH/TAUTH/GRUTON
0522 P2(023) = 1.0/TAUTH/GRUTON
0523 P2(016) = OMLM/OMEGMX
0524 P2(007) = OMG0/OMEGMX
0525 P2(011) = SHP3IC/SHPMX
0526 P2(012) = -OMEGIC/OMEGMX
0527 P2(013) = OMSL*AINMX /OMEGMX
0528 P2(014) = 550./FTR*SHPMX/OMEGMX/145MX
0529 P2(015) = GTHGOV/TTHSMX
0530 P2(015) = THMIC/THOMMX
0531 P2(021) = TMSI/THPMX
0532 P2(021) = THOCU
0533 P2(021) = QTHPE/SOEMX
0534 P2(021) = THOYLP/THOMMX
0535 P2(023) = -THOYLN/THOMMX
0536 P2(024) = THRTLX/THOMMX
0537 P2(024) = THRTLX/THOMMX
0538 P2(025) = THRTLX/THOMMX

```

Figure G.9. (Continued)

0539 P2(076) = THATMX/THOMX
 0540 P2(077) = THATMY/THOMY
 0541 P2(078) = ANRATE/ANRAX*DGTD03
 0542 P2(079) = P4.5*E15*PIR3/AIINMX
 0543 P2(080) = GTHQOV/TIMSX
 0544 P2(081) = THOMY/TIMSX
 0545 P2(082) = THOMX/TIMSX
 0546 P2(083) = GDLTH *DLTHX/THOMX
 0547 P2(084) = SKTRIP(12)
 0548 P2(085) = SKTRIP(13)
 0549 P2(086) = AINDEI*DGTD03/AIINMX
 0550 P2(087) = AINDEI*DGTD03/AIINMX
 0551 P2(088) = GDLTH *DLTHX/THOMX
 0552 P2(089) = GONG*OMEGMX/THOMX
 0553 P2(090) = TOWOLM/TOMMX
 0554 P2(091) = TOWOLM/TOMMX
 0555 P2(092) = GDLTH *DLTHX/THOMX
 0556 P2(093) = TOWOLM/TOMMX
 0557 P2(094) = ALARPI/PDUTX/10.
 0558 P2(095) = ALARPI/PDUTX
 0559 P2(096) = TMSLO/TIMSX
 0560 P2(097) = TMSLO/TIMSX
 0561 P2(098) = L./TAUFF/GRUTON
 0562 P2(099) = L./TAUFF/GRUTON
 0563 P2(100) = L./TAUFF/GRUTON
 0564 P2(101) = L./TAUFF/GRUTON
 0565 P2(102) = AMARDI/PDUTX/10.
 0566 P2(103) = AMARDI/PDUTX
 0567 P2(104) = OMWR**2/10./GRUTON/10.
 0568 P2(105) = 2.*E14*OMWR/GRUTON/10.
 0569 P2(106) = OMWR**2/10./GRUTON/10.
 0570 P2(107) = OMWR**2/10./GRUTON/10.
 0571 P2(108) = 2.*E14*OMWR/GRUTON/10.
 0572 P2(109) = OMWR**2/10./GRUTON/10.
 0573 P2(110) = ZARDIC/ZAPRX/10.
 0574 P2(111) = ZARDIC/ZAPRX
 0575 P2(112) = OMWB**2/10./GRUTON/10.
 0576 P2(113) = 2.*E14*OMWB/GRUTON/10.
 0577 P2(114) = OMWB**2/10./GRUTON/10.
 0578 P2(115) = AINROI/AIINMX
 0579 P2(116) = AINPIC/AIINMX
 0580 P2(117) = AIDOMX/AIINMX/GRUTON
 0581 P2(118) = AINOMX/AIINMX/GRUTON
 0582 P2(119) = OMIRE**2*AIINMX/AIINMX/10.
 0583 P2(120) = 2.*E14*OMIRE*AIINMX/AIINMX/10.
 0584 P2(121) = OMIRE**2*AIINMX/AIINMX/10.
 0585 P2(122) = AINKLM/AIINMX
 0586 P2(123) = AINLOI/AIINMX
 0587 P2(124) = AINLIC/AIINMX

Figure G.9. (Continued)

```

C588 P2(252) = AI00MX/AI00MX /GRUT0N
C589 P2(254) = AI00MX/AI00MX/GRUT0N
C590 P2(254) = (MI0F**2*AI00MX/AI00MX)/I.
C591 P2(255) = 2.*#TAI0F**AI00MX/AI00MX/I.
C592 P2(256) = (MI0F**2*AI00MX/AI00MX)/I.
C593 P2(257) = AI00MX/AI00MX
C594 P2(258) = DELTA /DLTHX
C595 P2(261) = C.
C596 P2(262) = C.
C597 P2(263) = AI00MX/AI00MX
C598 P2(264) = GIMRF#0I0F**2*DCYLMX/AI00MX/I.
C599 P2(265) = GIMRF#0I0F**2*DCYLMX/AI00MX/I.
C600 P2(265) = 1./TAUCYR/I. /GRUT0N
C601 P2(267) = 1./TAUCYR/I. /GRUT0N
C602 P2(270) = CONI*AI00MX/AMACMX /I.
C603 P2(271) = AI00MX/AI00MX
C604 P2(272) = AIRFC/AI00MX
C605 P2(273) = 105.*DGTOP0/AI00MX
C606 P2(274) = 2.*#TAI0F**AI00MX/AI00MX/I.
C607 P2(275) = AMACMX/CONI/AI00MX/I.
C608 P2(274) = SKTEIM(I.7)
C609 P2(277) = SKTEIM(I.3)
C610 P2(300) = CONI*AI00MX/AMACMX /I.
C611 P2(311) = DCYIC/DCYLMX
C612 P2(312) = DCY0LM/DCYLMX/GRUT0N
C613 P2(313) = DCY0LM/DCYLMX/GRUT0N
C614 P2(314) = 2.*#TAI0F**AI00MX/AI00MX/I.
C615 P2(315) = AMACMX/CONI/AI00MX/I.
C616 P2(316) = SHPLN/SHPMX/SRUT0N
C617 P2(317) = SHPLN/SHPMX/GRUT0N
C618 P2(311) = SHPIC/SHPMX
C619 P2(312) = 1./TAUSH0/GRUT0N/I.
C620 P2(313) = 1./TAUSH0/GRUT0N/I.
C621 P2(314) = ASLP*SHPMX
C622 P2(315) = AC
C623 P2(316) = ALIM
C624 P2(317) = L.C
C625 P2(320) = AT0M*CG0MX/TT0SMX/I.
C626 P2(322) = T0M/I.
C627 P2(323) = T0M*CG0MX/AI00MX/I.
C628 P2(324) = T0M/I.
C629 P2(344) = ALAMD*PI
C630 P2(345) = AI00MX/PI
C631 P2(346) = ALAMD*PI
C632 P2(347) = AI00MX/PI
C633 P2(344) = AI00MX**2 /X00MX*SL*SMN/SN -1.
C634 P2(365) = AI00MX**2 /T00MX*SL*SMN/SN
C635 P2(366) = AI00MX/X00MX*SL*SMN/SN
C636 P2(377) = AI00MX/T00MX*SL*SMN/SN

```

Figure G.9. (Continued)

```

0637 P2(372)= VDOTMX/AXPAMX
0638 P2(373)= VDOTMX/AYPAMX
0639 P2(374)= P2(372)*XCCMX/AYPAMX
0640 P2(375)= WDOTMX/AYPAMX
0641 P2(376)= SDOTMX*XCCMX/AYPAMX
0642 P2(377)= SG/AYPAMX
C
C BOARD SF (CIVIL F 3) POT. CALCULATION SECTION
C
0643 P3(02) = OMRD**2/IC./GRUTON/10.
0644 P3(03) = OMRD**2/IC./GRUTON/10.
0645 P3(04) = 2.*F TARD*OMRD/GRUTON/10.
0646 P3(05) = RIGDI/RICMX/10.
0647 P3(06) = RIGDI/RICMX
0648 P3(07) = GRATS
0649 P3(08) = OMRD**2/10./GRUTON/10.
0650 P3(09) = OMRD**2/10./GRUTON/10.
0651 P3(10) = 2.*F TARD*OMRD/GRUTON/10.
0652 P3(11) = RIGDI/RICMX/10.
0653 P3(12) = RIGDI/RICMX
0654 P3(13) = GRATS
0655 P3(14) = OMRD**2/10./GRUTON/10.
0656 P3(15) = OMRD**2/10./GRUTON/10.
0657 P3(16) = 2.*F TARD*OMRD/GRUTON/10.
0658 P3(17) = RIGDI/RICMX/10.
0659 P3(18) = RIGDI/RICMX
0660 P3(19) = GRATS
0661 P3(20) = 1./TAUGMN
0662 P3(21) = OMRD**2/10./GRUTON/10.
0663 P3(22) = OMRD**2/10./GRUTON/10.
0664 P3(23) = 2.*F TARD*OMRD/GRUTON/10.
0665 P3(24) = RIGDI/RICMX/10.
0666 P3(25) = RIGDI/RICMX
0667 P3(26) = GRATS
0668 P3(27) = 1./TAUGMN
0669 P3(28) = OMRD**2/10./GRUTON/10.
0670 P3(29) = OMRD**2/10./GRUTON/10.
0671 P3(30) = 2.*F TARD*OMRD/GRUTON/10.
0672 P3(31) = RIGDI/RICMX/10.
0673 P3(32) = RIGDI/RICMX
0674 P3(33) = GRATS
0675 P3(34) = 1./TAUGMN
0676 P3(35) = OMRD**2/10./GRUTON/10.
0677 P3(36) = OMRD**2/10./GRUTON/10.
0678 P3(37) = 2.*F TARD*OMRD/GRUTON/10.
0679 P3(38) = RIGDI/RICMX/10.
0680 P3(39) = RIGDI/RICMX
0681 P3(40) = GRATS
0682 P3(41) = OMRD**2/10./GRUTON/10.
0683 P3(42) = OMRD**2/10./GRUTON/10.
0684 P3(43) = 2.*F TARD*OMRD/GRUTON/10.
0685 P3(44) = RIGDI/RICMX/10.
0686 P3(45) = RIGDI/RICMX
0687 P3(46) = GRATS
0688 P3(47) = 1./TAUGMN
0689 P3(48) = OMRD**2/10./GRUTON/10.
0690 P3(49) = OMRD**2/10./GRUTON/10.
0691 P3(50) = 2.*F TARD*OMRD/GRUTON/10.
0692 P3(51) = RIGDI/RICMX/10.
0693 P3(52) = RIGDI/RICMX
0694 P3(53) = GRATS
0695 P3(54) = 1./TAUGMN
0696 P3(55) = OMRD**2/10./GRUTON/10.
0697 P3(56) = OMRD**2/10./GRUTON/10.
0698 P3(57) = 2.*F TARD*OMRD/GRUTON/10.
0699 P3(58) = RIGDI/RICMX/10.
0700 P3(59) = RIGDI/RICMX
0701 P3(60) = GRATS
0702 P3(61) = 1./TAUGMN
0703 P3(62) = OMRD**2/10./GRUTON/10.
0704 P3(63) = OMRD**2/10./GRUTON/10.
0705 P3(64) = 2.*F TARD*OMRD/GRUTON/10.
0706 P3(65) = RIGDI/RICMX/10.
0707 P3(66) = RIGDI/RICMX
0708 P3(67) = GRATS
0709 P3(68) = 1./TAUGMN
0710 P3(69) = OMRD**2/10./GRUTON/10.
0711 P3(70) = OMRD**2/10./GRUTON/10.
0712 P3(71) = 2.*F TARD*OMRD/GRUTON/10.
0713 P3(72) = RIGDI/RICMX/10.
0714 P3(73) = RIGDI/RICMX
0715 P3(74) = GRATS
0716 P3(75) = 1./TAUGMN
0717 P3(76) = OMRD**2/10./GRUTON/10.
0718 P3(77) = OMRD**2/10./GRUTON/10.
0719 P3(78) = 2.*F TARD*OMRD/GRUTON/10.
0720 P3(79) = RIGDI/RICMX/10.
0721 P3(80) = RIGDI/RICMX
0722 P3(81) = GRATS
0723 P3(82) = 1./TAUGMN
0724 P3(83) = OMRD**2/10./GRUTON/10.
0725 P3(84) = OMRD**2/10./GRUTON/10.
0726 P3(85) = 2.*F TARD*OMRD/GRUTON/10.
0727 P3(86) = RIGDI/RICMX/10.
0728 P3(87) = RIGDI/RICMX
0729 P3(88) = GRATS
0730 P3(89) = 1./TAUGMN
0731 P3(90) = OMRD**2/10./GRUTON/10.
0732 P3(91) = OMRD**2/10./GRUTON/10.
0733 P3(92) = 2.*F TARD*OMRD/GRUTON/10.
0734 P3(93) = RIGDI/RICMX/10.
0735 P3(94) = RIGDI/RICMX
0736 P3(95) = GRATS
0737 P3(96) = 1./TAUGMN
0738 P3(97) = OMRD**2/10./GRUTON/10.
0739 P3(98) = OMRD**2/10./GRUTON/10.
0740 P3(99) = 2.*F TARD*OMRD/GRUTON/10.
0741 P3(100) = RIGDI/RICMX/10.
0742 P3(101) = RIGDI/RICMX
0743 P3(102) = GRATS
0744 P3(103) = 1./TAUGMN
0745 P3(104) = OMRD**2/10./GRUTON/10.
0746 P3(105) = OMRD**2/10./GRUTON/10.
0747 P3(106) = 2.*F TARD*OMRD/GRUTON/10.
0748 P3(107) = RIGDI/RICMX/10.
0749 P3(108) = RIGDI/RICMX
0750 P3(109) = GRATS
0751 P3(110) = 1./TAUGMN
0752 P3(111) = OMRD**2/10./GRUTON/10.
0753 P3(112) = OMRD**2/10./GRUTON/10.
0754 P3(113) = 2.*F TARD*OMRD/GRUTON/10.
0755 P3(114) = RIGDI/RICMX/10.
0756 P3(115) = RIGDI/RICMX
0757 P3(116) = GRATS
0758 P3(117) = 1./TAUGMN
0759 P3(118) = OMRD**2/10./GRUTON/10.
0760 P3(119) = OMRD**2/10./GRUTON/10.
0761 P3(120) = 2.*F TARD*OMRD/GRUTON/10.
0762 P3(121) = RIGDI/RICMX/10.
0763 P3(122) = RIGDI/RICMX
0764 P3(123) = GRATS
0765 P3(124) = 1./TAUGMN
0766 P3(125) = OMRD**2/10./GRUTON/10.
0767 P3(126) = OMRD**2/10./GRUTON/10.
0768 P3(127) = 2.*F TARD*OMRD/GRUTON/10.
0769 P3(128) = RIGDI/RICMX/10.
0770 P3(129) = RIGDI/RICMX
0771 P3(130) = GRATS
0772 P3(131) = 1./TAUGMN
0773 P3(132) = OMRD**2/10./GRUTON/10.
0774 P3(133) = OMRD**2/10./GRUTON/10.
0775 P3(134) = 2.*F TARD*OMRD/GRUTON/10.
0776 P3(135) = RIGDI/RICMX/10.
0777 P3(136) = RIGDI/RICMX
0778 P3(137) = GRATS
0779 P3(138) = 1./TAUGMN
0780 P3(139) = OMRD**2/10./GRUTON/10.
0781 P3(140) = OMRD**2/10./GRUTON/10.
0782 P3(141) = 2.*F TARD*OMRD/GRUTON/10.
0783 P3(142) = RIGDI/RICMX/10.
0784 P3(143) = RIGDI/RICMX
0785 P3(144) = GRATS
0786 P3(145) = 1./TAUGMN
0787 P3(146) = OMRD**2/10./GRUTON/10.
0788 P3(147) = OMRD**2/10./GRUTON/10.
0789 P3(148) = 2.*F TARD*OMRD/GRUTON/10.
0790 P3(149) = RIGDI/RICMX/10.
0791 P3(150) = RIGDI/RICMX
0792 P3(151) = GRATS
0793 P3(152) = 1./TAUGMN
0794 P3(153) = OMRD**2/10./GRUTON/10.
0795 P3(154) = OMRD**2/10./GRUTON/10.
0796 P3(155) = 2.*F TARD*OMRD/GRUTON/10.
0797 P3(156) = RIGDI/RICMX/10.
0798 P3(157) = RIGDI/RICMX
0799 P3(158) = GRATS
0800 P3(159) = 1./TAUGMN
0801 P3(160) = OMRD**2/10./GRUTON/10.
0802 P3(161) = OMRD**2/10./GRUTON/10.
0803 P3(162) = 2.*F TARD*OMRD/GRUTON/10.
0804 P3(163) = RIGDI/RICMX/10.
0805 P3(164) = RIGDI/RICMX
0806 P3(165) = GRATS
0807 P3(166) = 1./TAUGMN
0808 P3(167) = OMRD**2/10./GRUTON/10.
0809 P3(168) = OMRD**2/10./GRUTON/10.
0810 P3(169) = 2.*F TARD*OMRD/GRUTON/10.
0811 P3(170) = RIGDI/RICMX/10.
0812 P3(171) = RIGDI/RICMX
0813 P3(172) = GRATS
0814 P3(173) = 1./TAUGMN
0815 P3(174) = OMRD**2/10./GRUTON/10.
0816 P3(175) = OMRD**2/10./GRUTON/10.
0817 P3(176) = 2.*F TARD*OMRD/GRUTON/10.
0818 P3(177) = RIGDI/RICMX/10.
0819 P3(178) = RIGDI/RICMX
0820 P3(179) = GRATS
0821 P3(180) = 1./TAUGMN
0822 P3(181) = OMRD**2/10./GRUTON/10.
0823 P3(182) = OMRD**2/10./GRUTON/10.
0824 P3(183) = 2.*F TARD*OMRD/GRUTON/10.
0825 P3(184) = RIGDI/RICMX/10.
0826 P3(185) = RIGDI/RICMX
0827 P3(186) = GRATS
0828 P3(187) = 1./TAUGMN
0829 P3(188) = OMRD**2/10./GRUTON/10.
0830 P3(189) = OMRD**2/10./GRUTON/10.
0831 P3(190) = 2.*F TARD*OMRD/GRUTON/10.
0832 P3(191) = RIGDI/RICMX/10.
0833 P3(192) = RIGDI/RICMX
0834 P3(193) = GRATS
0835 P3(194) = 1./TAUGMN
0836 P3(195) = OMRD**2/10./GRUTON/10.
0837 P3(196) = OMRD**2/10./GRUTON/10.
0838 P3(197) = 2.*F TARD*OMRD/GRUTON/10.
0839 P3(198) = RIGDI/RICMX/10.
0840 P3(199) = RIGDI/RICMX
0841 P3(200) = GRATS
0842 P3(201) = 1./TAUGMN
0843 P3(202) = OMRD**2/10./GRUTON/10.
0844 P3(203) = OMRD**2/10./GRUTON/10.
0845 P3(204) = 2.*F TARD*OMRD/GRUTON/10.
0846 P3(205) = RIGDI/RICMX/10.
0847 P3(206) = RIGDI/RICMX
0848 P3(207) = GRATS
0849 P3(208) = 1./TAUGMN
0850 P3(209) = OMRD**2/10./GRUTON/10.
0851 P3(210) = OMRD**2/10./GRUTON/10.
0852 P3(211) = 2.*F TARD*OMRD/GRUTON/10.
0853 P3(212) = RIGDI/RICMX/10.
0854 P3(213) = RIGDI/RICMX
0855 P3(214) = GRATS
0856 P3(215) = 1./TAUGMN
0857 P3(216) = OMRD**2/10./GRUTON/10.
0858 P3(217) = OMRD**2/10./GRUTON/10.
0859 P3(218) = 2.*F TARD*OMRD/GRUTON/10.
0860 P3(219) = RIGDI/RICMX/10.
0861 P3(220) = RIGDI/RICMX
0862 P3(221) = GRATS
0863 P3(222) = 1./TAUGMN
0864 P3(223) = OMRD**2/10./GRUTON/10.
0865 P3(224) = OMRD**2/10./GRUTON/10.
0866 P3(225) = 2.*F TARD*OMRD/GRUTON/10.
0867 P3(226) = RIGDI/RICMX/10.
0868 P3(227) = RIGDI/RICMX
0869 P3(228) = GRATS
0870 P3(229) = 1./TAUGMN
0871 P3(230) = OMRD**2/10./GRUTON/10.
0872 P3(231) = OMRD**2/10./GRUTON/10.
0873 P3(232) = 2.*F TARD*OMRD/GRUTON/10.
0874 P3(233) = RIGDI/RICMX/10.
0875 P3(234) = RIGDI/RICMX
0876 P3(235) = GRATS
0877 P3(236) = 1./TAUGMN
0878 P3(237) = OMRD**2/10./GRUTON/10.
0879 P3(238) = OMRD**2/10./GRUTON/10.
0880 P3(239) = 2.*F TARD*OMRD/GRUTON/10.
0881 P3(240) = RIGDI/RICMX/10.
0882 P3(241) = RIGDI/RICMX
0883 P3(242) = GRATS
0884 P3(243) = 1./TAUGMN
0885 P3(244) = OMRD**2/10./GRUTON/10.
0886 P3(245) = OMRD**2/10./GRUTON/10.
0887 P3(246) = 2.*F TARD*OMRD/GRUTON/10.
0888 P3(247) = RIGDI/RICMX/10.
0889 P3(248) = RIGDI/RICMX
0890 P3(249) = GRATS
0891 P3(250) = 1./TAUGMN
0892 P3(251) = OMRD**2/10./GRUTON/10.
0893 P3(252) = OMRD**2/10./GRUTON/10.
0894 P3(253) = 2.*F TARD*OMRD/GRUTON/10.
0895 P3(254) = RIGDI/RICMX/10.
0896 P3(255) = RIGDI/RICMX
0897 P3(256) = GRATS
0898 P3(257) = 1./TAUGMN
0899 P3(258) = OMRD**2/10./GRUTON/10.
0900 P3(259) = OMRD**2/10./GRUTON/10.
0901 P3(260) = 2.*F TARD*OMRD/GRUTON/10.
0902 P3(261) = RIGDI/RICMX/10.
0903 P3(262) = RIGDI/RICMX
0904 P3(263) = GRATS
0905 P3(264) = 1./TAUGMN
0906 P3(265) = OMRD**2/10./GRUTON/10.
0907 P3(266) = OMRD**2/10./GRUTON/10.
0908 P3(267) = 2.*F TARD*OMRD/GRUTON/10.
0909 P3(268) = RIGDI/RICMX/10.
0910 P3(269) = RIGDI/RICMX
0911 P3(270) = GRATS
0912 P3(271) = 1./TAUGMN
0913 P3(272) = OMRD**2/10./GRUTON/10.
0914 P3(273) = OMRD**2/10./GRUTON/10.
0915 P3(274) = 2.*F TARD*OMRD/GRUTON/10.
0916 P3(275) = RIGDI/RICMX/10.
0917 P3(276) = RIGDI/RICMX
0918 P3(277) = GRATS
0919 P3(278) = 1./TAUGMN
0920 P3(279) = OMRD**2/10./GRUTON/10.
0921 P3(280) = OMRD**2/10./GRUTON/10.
0922 P3(281) = 2.*F TARD*OMRD/GRUTON/10.
0923 P3(282) = RIGDI/RICMX/10.
0924 P3(283) = RIGDI/RICMX
0925 P3(284) = GRATS
0926 P3(285) = 1./TAUGMN
0927 P3(286) = OMRD**2/10./GRUTON/10.
0928 P3(287) = OMRD**2/10./GRUTON/10.
0929 P3(288) = 2.*F TARD*OMRD/GRUTON/10.
0930 P3(289) = RIGDI/RICMX/10.
0931 P3(290) = RIGDI/RICMX
0932 P3(291) = GRATS
0933 P3(292) = 1./TAUGMN
0934 P3(293) = OMRD**2/10./GRUTON/10.
0935 P3(294) = OMRD**2/10./GRUTON/10.
0936 P3(295) = 2.*F TARD*OMRD/GRUTON/10.
0937 P3(296) = RIGDI/RICMX/10.
0938 P3(297) = RIGDI/RICMX
0939 P3(298) = GRATS
0940 P3(299) = 1./TAUGMN
0941 P3(300) = OMRD**2/10./GRUTON/10.
0942 P3(301) = OMRD**2/10./GRUTON/10.
0943 P3(302) = 2.*F TARD*OMRD/GRUTON/10.
0944 P3(303) = RIGDI/RICMX/10.
0945 P3(304) = RIGDI/RICMX
0946 P3(305) = GRATS
0947 P3(306) = 1./TAUGMN
0948 P3(307) = OMRD**2/10./GRUTON/10.
0949 P3(308) = OMRD**2/10./GRUTON/10.
0950 P3(309) = 2.*F TARD*OMRD/GRUTON/10.
0951 P3(310) = RIGDI/RICMX/10.
0952 P3(311) = RIGDI/RICMX
0953 P3(312) = GRATS
0954 P3(313) = 1./TAUGMN
0955 P3(314) = OMRD**2/10./GRUTON/10.
0956 P3(315) = OMRD**2/10./GRUTON/10.
0957 P3(316) = 2.*F TARD*OMRD/GRUTON/10.
0958 P3(317) = RIGDI/RICMX/10.
0959 P3(318) = RIGDI/RICMX
0960 P3(319) = GRATS
0961 P3(320) = 1./TAUGMN
0962 P3(321) = OMRD**2/10./GRUTON/10.
0963 P3(322) = OMRD**2/10./GRUTON/10.
0964 P3(323) = 2.*F TARD*OMRD/GRUTON/10.
0965 P3(324) = RIGDI/RICMX/10.
0966 P3(325) = RIGDI/RICMX
0967 P3(326) = GRATS
0968 P3(327) = 1./TAUGMN
0969 P3(328) = OMRD**2/10./GRUTON/10.
0970 P3(329) = OMRD**2/10./GRUTON/10.
0971 P3(330) = 2.*F TARD*OMRD/GRUTON/10.
0972 P3(331) = RIGDI/RICMX/10.
0973 P3(332) = RIGDI/RICMX
0974 P3(333) = GRATS
0975 P3(334) = 1./TAUGMN
0976 P3(335) = OMRD**2/10./GRUTON/10.
0977 P3(336) = OMRD**2/10./GRUTON/10.
0978 P3(337) = 2.*F TARD*OMRD/GRUTON/10.
0979 P3(338) = RIGDI/RICMX/10.
0980 P3(339) = RIGDI/RICMX
0981 P3(340) = GRATS
0982 P3(341) = 1./TAUGMN
0983 P3(342) = OMRD**2/10./GRUTON/10.
0984 P3(343) = OMRD**2/10./GRUTON/10.
0985 P3(344) = 2.*F TARD*OMRD/GRUTON/10.
0986 P3(345) = RIGDI/RICMX/10.
0987 P3(346) = RIGDI/RICMX
0988 P3(347) = GRATS
0989 P3(348) = 1./TAUGMN
0990 P3(349) = OMRD**2/10./GRUTON/10.
0991 P3(350) = OMRD**2/10./GRUTON/10.
0992 P3(351) = 2.*F TARD*OMRD/GRUTON/10.
0993 P3(352) = RIGDI/RICMX/10.
0994 P3(353) = RIGDI/RICMX
0995 P3(354) = GRATS
0996 P3(355) = 1./TAUGMN
0997 P3(356) = OMRD**2/10./GRUTON/10.
0998 P3(357) = OMRD**2/10./GRUTON/10.
0999 P3(358) = 2.*F TARD*OMRD/GRUTON/10.
1000 P3(359) = RIGDI/RICMX/10.

```

Figure G.9. (Continued)


```

0683 P3(244) = SKDLS*DELSMX/DCVLYMX*GSCVMX
0684 P3(245) = GLCP/1.
0685 P3(246) = SKDLS*DELSMX/DCVLYMX*GSCVMX
0686 P3(247) = GLSLP*UMX/1.
0687 P3(252) = SKDLR*DFLRMX/DLONMX
0688 P3(253) = SKDLF*DFLRMX/DFLEMX
0689 P3(254) = DELALM/DELAMX
0690 P3(255) = DELALM/DELAMX
0691 P3(257) = 1.
0692 P3(260) = DFLR /DFLRMX
0693 P3(261) = DELS /DELSMX
0694 P3(262) = DELR /DFLRMX
0695 P3(264) = GQ/TAUQI*QMX/DLONMX/GRUTON/1.
0696 P3(265) = GTR*QMX/DLONMX/GRUTON
0697 P3(266) = SKDA*DELSMX/DELAMX
0698 P3(267) = SKDA*DELSMX/DELAMX
0699 P3(272) = OMA**2*GICMX/AICMX/1. /GRUTON/1.
0700 P3(273) = OMA**2*GICMX/BICMX/1. /GRUTON/1.
0701 P3(274) = OMA**2*GICMX/AICMX/1. /GRUTON/1.
0702 P3(275) = OMA**2*GICMX/AICMX/1. /GRUTON/1.
0703 P3(276) = THSMX/TH75MX
0704 P3(277) = THSMX/TH75MX
0705 P3(300) = GLSHIC/GLSMX
0706 P3(301) = GLSAIL/GLSMX
0707 P3(302) = DCOLMX/TH75MX
0708 P3(303) = DCOLMX/TH75MX
0709 P3(304) = TH75LP/TH75MX
0710 P3(305) = TH75LN/TH75MX
0711 P3(306) = TH75LP/TH75MX
0712 P3(307) = TH75LN/TH75MX
0713 P3(310) = RICRPD/AICMX/1.
0714 P3(311) = RICRP /AICMX
0715 P3(312) = 1. /TAUGLS/GRUTON
0716 P3(313) = 1. /TAUGLS/GRUTON
0717 P3(314) = 1. /TAUGLS/GRUTON
0718 P3(315) = 1. /TAUGLS/GRUTON
0719 P3(316) = GLSLM/GLSMX
0720 P3(317) = GLSLM/GLSMX
0721 P3(320) = -GBICP/GICMX
0722 P3(321) = -GBICP/GICMX
0723 P3(322) = OMA**2*DCVLYMX/BICMX/1. /GRUTON/1.
0724 P3(323) = OMA**2*DCVLYMX/BICMX/1. /GRUTON/1.
0725 P3(324) = 2. *EETA*QMA/GRUTON/1.
0726 P3(325) = OMA**2/1. /GRUTON/1.
0727 P3(326) = 1. /TAUGIC/GRUTON/1.
0728 P3(327) = 1. /TAUGIC/GRUTON/1.
0729 P3(330) = PICLPD/BICMX/1.
0730 P3(331) = AICL /BICMX
0731 P3(332) = 1. /TAUGIC/GRUTON/1.

```

Figure G.9. (Continued)

```

0732 P(333) = 1./TAUGC/GRUTON/10.
0733 P(334) = DLFLPC/DLFLMX
0734 P(335) = 1./TAUDH*DELRMX/DLDMX/GRUTON
0735 P(336) = OMA**2*GCLM*/GICMX/10./GRUTON/10.
0736 P(337) = OMA**2*DLDMX*/GICMX/10./GRUTON/10.
0737 P(338) = 1./TAUQ2/GRUTON/10.
0738 P(339) = PSAS2/DLDMX
0739 P(340) = 2.*ETA*OMA/GRUTON/10.
0740 P(341) = OMA**2/10./GRUTON/10.
0741 P(342) = GICLM*/GICMX/GRUTON
0742 P(343) = GICLM*/GICMX/GRUTON
0743 P(344) = GICLM*/GICMX/GRUTON
0744 P(345) = GICLM*/GICMX/GRUTON
0745 P(346) = GICLM*/GICMX/GRUTON
0746 P(347) = GICLM*/GICMX/GRUTON
0747 P(348) = AICRPD/ AICMX/10.
0748 P(349) = AICRPD/ AICMX
0749 P(350) = 1./TAUDR/GRUTON
0750 P(351) = OMA**2*GLSMX*/AICMX/GRUTON/10./10.
0751 P(352) = SKDCOL*OMA**2*DCCLMX*/AICMX/10./GRUTON/10.
0752 P(353) = 2.*ETA*OMA/GRUTON/10.
0753 P(354) = OMA**2/10./GRUTON/10.
0754 P(355) = GLSMX*/DLDMX
0755 P(356) = PSAS1/DLDMX
0756 P(357) = PSAS3/DLDMX
0757 P(358) = PSAS4/DLDMX
0758 P(359) = GDB2*TAUQ1/GRUTON/10.
0759 P(360) = GDB1/GRUTON
0760 P(361) = 1./TAUJ1/GRUTON/10.
0761 P(362) = AICLPP/AICMX/10.
0762 P(363) = AICLP/ AICMX
0763 P(364) = DLRLM*/DLDMX
0764 P(365) = DLRLM*/DLDMX
0765 P(366) = OMA**2*GLSMX*/AICMX/GRUTON/10./10.
0766 P(367) = SKDCOL*OMA**2*DCCLMX*/AICMX/10./GRUTON/10.
0767 P(368) = 2.*ETA*OMA/GRUTON/10.
0768 P(369) = OMA**2/10./GRUTON/10.
0769 XBODY= -XIC+VIC+XHPDIZ+XBIC
0770 YBODY= YPOAD+YPOAD+VIC+YIC+YBIC
0771 ZBODY= M+ZBIC
0771 SA11 = COSTHE * COSPSI
0772 SA12 = SINPHI *SINTHE *COSPSI - COSPHI * SINPSI
0773 SA13 = COSPHI *SINTHE *COSPSI + SINPHI * SINPSI
0774 SA21 = COSTHE * SINPSI
0775 SA22 = SINPHI *SINTHE*SINPSI + COSPHI * COSPSI
0776 SA23 = COSPHI *SINTHE *SINPSI -SINPHI * COSPSI

```

C C C C C

Figure G.9.3(Continued)

```

C
C777 SA31 = - SIN(THC)
C778 SA32 = SIN(PI * COSTHC)
C779 SA33 = COS(PI * COSTHC)
C
C780 XACVIS = -(SA11*XBDY + SA12*YBDY + SA13 *ZBGDY)
C781 YACVIS = -(SA21*XBDY + SA22*YBDY + SA23 *ZBGDY)
C782 ZACVIS = -(SA31*XBDY+SA32*YBDY+SA33*ZBGDY)
C
C783 YSCOPE= ZACVIS/XACVIS*VCAL1*XVIS-H/ZVISMX
C784 XSCOPE= YACVIS/XACVIS*VCAL2*XVISMX/YVISMX
C
C785 FFDR= XLIM(FFB*MX,FFMLD,BLSLOPE*SQF/QSTARR +RDB)
C786 FFDS= XLIM(FFFS*MX,FFMLD,SSLLOPE*SQF/QSTARS + RDS)
C787 FFDR= XLIM(FFB*MX,FFMLD,PSLOPE*SQF/QSTARR + BDR)
C788 FFDS= XLIM(FFFS*MX,FFMLD,PSLOPE*SQF/QSTARS + BDS)
C789 DRKDR= COMDLR-DELR
C790 DRKDR= COMDLR-DELR
C791 DRKDR= COMDLR-DELR
C792 THKDR = -SKTRIM(12)*COMDGT/CMFGX*DELTHK
C793 PSOSIM= XLIM(PSOTSX,-PSDTSX,PSIDDT*ROTANG)
C794 XSIM= XLIM(DXSIMX,-DXSIMX,XIC)
C795 YSIM= XLIM(DYSIMX,-DYSIMX,YIC)
C796 IF(NDLT.EQ.2) GPIC= 975
C797 COMDLR= 0.0
C798 COMDLR= 0.0
C799 COMDLR= 0.0
C800 COMPLETE= 0.0
C801 BRAKE= 0.0
C802 CONTINUE
C
C803 P4(390) = 1.0000
C804 P4(391) = 1.0000
C805 P4(392) = PC1QMX/TQSIMX
C806 P4(393) = PC1QMX/TQSIMX
C807 P4(394) = CAFE*MK/CMPE*100./PDM$AK
C808 P4(395) = YDQTMX/YDTSMX
C809 P4(396) = VMX/HQDTSMX
C810 P4(397) = XDQTMX/XDTSMX
C811 P4(398) = UMX/SKEPS/LSIMX
C812 P4(399) = VMX/SKEPS/VSIMX
C813 P4(400) = AXDPA*VX
C814 P4(401) = PSIM*PDTODG/PDTSIX
C815 P4(402) = PSDMX*ROTODG/PDTSIX/2.0
C816 P4(403) = PI*ROTODG/PHISMX
C817 P4(404) = PSDMX*PDTODG/PDTSIX/2.0
C818 P4(405) = PSDTSX/PDTSIX
C819 P4(406) = PSDTSX/PDTSIX
C820 P4(407) = PSDTSX/PDTSIX

```

975 BOARD IB (CONSOLE 4) SIMULATOR BOARD

Figure G.9. (Continued)

```

0821 P4(036)= AINMX*DDTCGG/ATVSMX
0822 P4(037)= ALRGMX*KTDDG/ALWSMX
0823 P4(034)= AZPAMY/AZPAMY
0824 P4(045)= DFLMX/ZDFPSMX
0825 P4(046)= ABFSMX*DDTCGG/RTSIMX
0826 P4(047)= AYPAMX/AYPAMX
0827 P4(050)= 0.1475
0828 P4(051)= 0.1475
0829 P4(052)= DXSIMX/DXSIMX
0830 P4(053)= DXSIMX/DXSIMX
0831 P4(054)= 1.0000
0832 P4(055)= XMX/DXSIMX/IC.
0833 P4(056)= ZMX/HSEIMX
0834 P4(057)= 1.0000
0835 P4(050)= YMX/YVISMX
0836 P4(051)= ZMX/ZVISMX
0837 P4(247)= XDOTMX / XVISMX / IC.
0838 P4(241)= YDOTMX / YVISMX / IC.
0839 P4(250)= XTEST/XVISMX/IC.
0840 P4(251)= YTEST/YVISMX/IC.
0841 P4(252)= THF / PI
0842 P4(251)= DHI / PI
0843 P4(252)= PSI / PI
0844 P4(243)= FREQMT / IC.
0845 P4(264)= SCORPL
0846 P4(255)= SCORPL
0847 P4(256)= SCORPL
0848 P4(247)= SCORPL
0849 P4(270)= 1.0000
0850 P4(271)= 0.0100
0851 P4(272)= XHRTZ / XVISMX
0852 P4(273)= ZMX / ZVISMX
0853 P4(274)= PIASMT/ZVISMX
0854 P4(275)= YBIC / XVISMX
0855 P4(276)= YRIC / YVISMX
0856 P4(277)= ZBIC / ZVISMX
0857 P4(300)= PSDMX/PI/IC.
0858 P4(301)= 0.1500/PI/IC.
0859 P4(302)= SLX / XVISMX
0860 P4(303)= SLY / YVISMX
0861 P4(304)= SLZ / XVISMX
0862 P4(305)= SLX / ZVISMX
0863 P4(306)= SLY / ZVISMX
0864 P4(307)= SLZ / ZVISMX
0865 P4(310)= 0.5000
0866 P4(311)= 0.6000
0867 P4(312)= SLX / YVISMX
0868 P4(313)= SLY / YVISMX
0869 P4(314)= SLZ / YVISMX

```

Figure G.9. (Continued)

```

0870 P4(315) = PMT1 / ZVISMX
0871 P4(316) = PMT2 / ZVISMX
0872 P4(317) = SZMTSI
0873 P4(320) = 0.6500
0874 P4(321) = 0.6500
0875 P4(322) = DBPSMX/DRRDMX
0876 P4(323) = DELSMX/DRHDMX
0877 P4(324) = DRPSMX/DRBDMX
0878 P4(325) = DELPMX/DRRDMX
0879 P4(326) = DSPSMX/DSBDMX
0880 P4(327) = DELSMX/DSRDMX
0881 P4(330) = 1C.*SKFPS / XDDTMX
0882 P4(332) = VCALL * XVISMX / YVISMX
0883 P4(333) = VCALL2 * XVISMX / ZVISMX
0884 P4(334) = 2.*ARRKMX/ARRKSMX
0885 P4(335) = DLTHMX/THRDMSX
0886 P4(336) = FFRMX/FFRMSX
0887 P4(337) = FFLMLD/FFFLMSX
0888 P4(340) = GZVT32
0889 P4(341) = XHRT17 / XVISMX
0890 P4(342) = -RDS/FFRMSX
0891 P4(343) = -RDS/FFSMX
0892 P4(344) = DSLOPE/STARH*SQF4X/FFR4X
0893 P4(345) = SSLOPE/STAR2*SQF4X/FFS4X
0894 P4(346) = PSLOPE/STARF*SQF4X/FFP4X
0895 P4(347) = -HOR/FFRMSX
0896 P4(350) = YHRTD / YVISMX
0897 P4(351) = YFRAD / YVISMX
0898 P4(354) = FFSMX/FFSMX
0899 P4(355) = FFRMX/FFRMSX
0900 P4(356) = FFLML / FFLMSX
0901 P4(357) = FFLMLD / FFLMSX
0902 P4(358) = XIC / XVISMX
0903 P4(361) = YIC / YVISMX
0904 P4(362) = H/ZMX
0905 P4(364) = 2.*DELBMX/DRPSMX
0906 P4(365) = 2.*DELSMX/DSPSMX
0907 P4(367) = 2.*DRAINSMX/ALDPSMX*BDTJOG
0908 P4(370) = 0.1400
0909 P4(371) = 0.1400
0910 P4(374) = 2.*DFLRMX/DFRPSMX
0911 P4(375) = 2.*DLTHMX/DTPSMX

```

```

RETURN
ENTRY STC741
CALL ANDAIN(PPOJ, BNDJ5(1), LTR(1), IFC(1), NOUN(1), A10, 5, A14, 1, 5,
* SJ1, 4, 5, TRI, 6, 5)

```

```

C
AIP(380) = 7IC/Z4X

```

Figure G.9. (Continued)

```

0916 AIP(071) = YIC/YMX
0917 AIP(072) = UIC*STATHE /UMX
0918 AIP(073) = ZOOT/V*MY
0919 AIP(081) = YDOT/YDOTMX
0920 AIP(083) = XDOT/XDOTMX
0921 AIP(09) = XIC/X*MX
0922 AIP(11) = D.C
0923 AIP(12) = AINGER/AIDDMX
0924 AIP(13) = AINDDL/AIDDMX
0925 AIP(025) = -SKTRIM(03)*VDDT/VDDTMX
0926 AIN(020) = CTC/CTMX
0927 AIP(021) = ROT1/CT*MX
0928 AIP(030) = -CTRPRM/CTMX
0929 AIN(030) = CTC/CTMX
0930 AIP(031) = ROT2/CT*MX
0931 AIP(040) = TH75R/TH75MX
0932 AIN(040) = CPR/CP*MY
0933 AIP(041) = TH75L/TH75MY
0934 AIN(041) = CPL/CP*MX
0935 AIP(050) = -TH75R/TH75MY
0936 AIP(050) = CNFPL/CNFM*MX
0937 AIP(051) = -ALPHA/ALEF*MX
0938 AIP(051) = C*FDR/C*MF*MX
0939 AIP(052) = CTRPRM/CTMX
0940 AIP(053) = C*LRM/C*LM*MX
0941 AIP(060) = -AMID/AMID*MY
0942 AIP(060) = C*SPR/C*SP*MX
0943 AIP(061) = -L
0944 AIN(061) = C*SEPL/C*SEFM*MX
0945 AIP(062) = SKTRIM(01)*UDDT/UDDT*MX
0946 AIP(063) = SKTRIM(05)*WDDT/WDDT*MX
0947 AIP(070) = D.C
0948 AIP(071) = D.C
0949 AIP(073) = PIC/PMY
0950 AIP(081) = QIC/Q*MX
0951 AIP(082) = PDDT/PDDT*MX
0952 AIP(083) = QDDT/QDDT*MX
0953 AIP(090) = RIC/R*MX
0954 AIP(091) = UIC/U*MX
0955 AIP(092) = -PSIDT*PSIDTHE /PSID*MX
0956 AIN(092) = THEDOT/THDMX
0957 AIP(093) = *COSPHI/SMX
0958 AIN(093) = PHIDDT/PHDMX
0959 AIP(095) = VIC/V*MX
0960 AIP(091) = WIC/W*MX
0961 AIP(022) = ROT/ROT*MX
0962 AIP(023) = Q*SIGNPHI/Q*MX
0963 AIN(023) = UDDT/UDDT*MX
0964 AIP(023) = THEIC/THE*MX

```

Figure G.9. (Continued)

```

0965 AIP(231) = PHLIC/PHIMX
0966 AIP(240) = OSIC/OSIMX
0967 AIP(241) = -XAFRO / SM / UOFTAX
0968 AIP(241) = -YAEFO / SM / VDOTAX
0969 AIP(242) = R*SINPHI/RMX
0970 AIN(242) = VDOT/VDOTYX
0971 AIP(243) = -Q*CSPHI/QMX
0972 AIN(243) = WDOT/WDOTYX
0973 AIP(250) = THE/PI
0974 AIP(251) = PHI/PI
0975 AIP(252) = COSTHE*COSPHI
0976 AIP(253) = COSTHE*SINPHI
0977 AIP(260) = BETAF / ABFSMX
0978 AIN(260) = AVFALW / ALWGMX
0979 AIP(261) = SOF / SOFPMX
0980 AIN(261) = -7AERO/SM/ZAPMX
0981 AIP(262) = PSIDOT/PSDMX
0982 AIP(300) = -DELSS/DELSMX
0983 AIN(300) = -RSAS1/DELSMX
0984 AIP(301) = -RSAS2/DELSMX
0985 AIN(301) = -RSAS2/DELSMX
0986 AIP(302) = -YSAS1/DELPWX/SQUOT
0987 AIP(303) = YSAS1/DELPWX
0988 AIP(310) = -YSAS7/RMX
0989 AIN(310) = RSAS3/DELSMX
0990 AIP(311) = RSAS4/ABFSMX
0991 AIP(312) = -RSAS5/DELSMX/SQUOT
0992 AIP(313) = GLATPH/L
0993 AIP(320) = -YSAS11/DELRMX
0994 AIN(320) = YSAS1/DELPWX
0995 AIP(321) = YSAS9/DELPWX
0996 AIP(321) = -YSAS2/DELRMX
0997 AIP(322) = ALPHF/AFPSMX
0998 AIN(322) = VCALTR/UMX
0999 AIP(323) = ALPHK3/ALFRMX
1000 AIN(323) = ALPHL2/ALFRMX
1001 AIP(330) = -YSAS12/DELRMX
1002 AIN(330) = YSAS3/DELRMX
1003 AIP(331) = YSAS16/PMX
1004 AIN(331) = -YSAS6/DELRMX
1005 AIP(340) = YSAS4/DELPWX
1006 AIP(341) = -YSAS5/DELRMX
1007 AIP(342) = AMUP7/AMURMX
1008 AIP(343) = AMUL/AMJPMX
1009 AIN(350) = YSAS14/DELPWX
1010 AIP(350) = -DEIKS/DELPWX
1011 AIP(351) = YSAS13/DELPWX
1012 AIP(352) = -YSAS15/PMX
1013 AIP(353) = GYAW/L

```

Figure G.9. (Continued)

```

1014 A1P(442) = G1A2R/1.
1015 A1P(441) = YSA517/PA/TMX
1016 A1P(442) = OMEGAR/PA/TMX
1017 A1P(443) = OMEGAL/PA/TMX
C
VALUES AT SUMMING JUNCTIONS OF AMPLIFIERS: BOARD 1E (CONSOLE 1)
1018 SJ1(341) = ZD1T/ZMX/GPUTN
1019 SJ1(341) = YD1T/YMX/GPUTN
1020 SJ1(341) = XD1T/XMX/GPUTN
1021 SJ1(341) = SKTR14(0.2)*D1C1/D1C1/TMX
1022 SJ1(321) = 0.0
1023 SJ1(321) = ROT1D/CTMX/GPUTN
1024 SJ1(330) = 0.0
1025 SJ1(331) = ROT2D/CTMX/GPUTN
1026 SJ2(340) = 0.0
1027 SJ2(341) = 0.0
1028 SJ1(351) = 0.0
1029 SJ1(351) = 0.0
1030 SJ1(361) = 0.0
1031 SJ1(361) = 0.0
1032 SJ1(370) = SKT1M(0.4)*V1C1/V1C1/TMX
1033 SJ1(371) = SKT1M(0.4)*W1C1/W1C1/TMX
1034 SJ1(320) = P1C1T/P1MX/GPUTN
1035 SJ1(321) = Q1C1T/Q1MX/GPUTN
1036 SJ1(210) = ZD1T/ZMX/GPUTN
1037 SJ1(211) = UD1T/UMX/GPUTN
1038 SJ1(220) = V1C1T/V1MX/GPUTN
1039 SJ1(221) = R1C1T/R1MX/GPUTN
1040 SJ1(331) = THE1C1T/TH1MX/GPUTN
1041 SJ1(231) = PH1C1T/PH1MX/GPUTN
1042 SJ1(240) = P1C1D1T/P1C1MX/GPUTN
1043 SJ1(331) = P1C1S1D/P1C1MX/GPUTN
1044 SJ1(341) = --R1C1S1D/P1C1MX/GPUTN
1045 SJ1(311) = --R1C1S1D/P1C1MX/GPUTN
1046 SJ1(311) = R1C1S1D/P1C1MX/GPUTN
1047 SJ1(320) = --Y1C1S1D/P1C1MX/GPUTN
1048 SJ1(321) = Y1C1S1D/P1C1MX/GPUTN
1049 SJ1(330) = --Y1C1S1D/P1C1MX/GPUTN
1050 SJ1(331) = Y1C1S1D/P1C1MX/GPUTN
1051 SJ1(340) = --Y1C1S1D/P1C1MX/GPUTN
1052 SJ1(341) = Y1C1S1D/P1C1MX/GPUTN
C
BOARD 1E (CONSOLE 1) VALUES OF TRUNK LINES AND ADCS (FIRST 32 TRS ARE ADCS)
1053 TR1(221) = P/P/MX
1054 TR1(221) = C/C/MX
1055 TR1(222) = P/P/MX
1056 TR1(221) = U/UMX
1057 TR1(260) = V/V/MX
1058 TR1(261) = W/W/MX
1059 TR1(262) = THE/T/H/MX
1060 TR1(263) = PHI/P/H/MX

```

Figure G.9. (Continued)


```

1061 TRI(1320) = PSI/PSIMY
1062 TRI(1321) = WDOT/WDOTX
1063 TRI(1322) = -TIC/TIX
1064 TRI(1363) = ZDOT/VNMX
1065 TRI(1323) = -DELAL/DELAIX
1066 TRI(1321) = DELAR/DELAIX
1067 TRI(1322) = -DELSR/RLSPMX
1068 TRI(1323) = DELSPL/DLSPMX
1069 TRI(136) = CILPDM/CTMX
1070 TRI(1361) = CMEPL/CMFMY
1071 TRI(1362) = CSEPL/CSFMY
1072 TRI(1363) = CPMP/CPMMX
1073 TRI(1370) = $INTHE
1074 TRI(1371) = COSTHE
1075 TRI(1372) = SIMPHI
1076 TRI(1373) = COSPHI
1077 TRI(1374) = SIMPHI*CONSTHE
1078 TRI(1375) = COSPHI*CONSTHE
1079 TRI(120) = CYPDL/CYMY
1080 TRI(121) = CPL/CPMX
1081 TRI(122) = CTRBY/CTMX
1082 TRI(123) = CERP/CFMY
1083 TRI(160) = CSEPP/CSFMY
1084 TRI(161) = CPMPP/CPMMX
1085 TRI(162) = CYPDP/CYMY
1086 TRI(163) = CPE/CPMX

1087 TRI(110) = CPP/CPMX
1088 TRI(111) = CPL/CPMX
1089 TRI(112) = OMEGA/OMEGMX
1090 TRI(113) = SKTDM/CL)*LDOT/UDOTAX
1091 TRI(114) = ALAPM/FIXX/DMTAX
1092 TRI(115) = AMEPM/FY/DMTAX
1093 TRI(116) = ZAPM/SW/TAZAX
1094 TRI(117) = -DELTH/DLTHMX
1095 TRI(111) = -DSHP/SHPMY
1096 TRI(112) = -SHPIC/SHPMX
1097 TRI(113) = -ATPRF/ATPMX
1098 TRI(114) = -YPS/TPSMX
1099 TRI(115) = SHPPD/SHPMY/GULITY
1100 TRI(116) = -DSHPP/SHPMX
1101 TRI(117) = -DVTAUF+SOTMTC/DEL/GRITAX
1102 TRI(118) = SOTHIC/DEL+TAJPMX/GRITAX
1103 TRI(113) = THALM/THATMX
1104 TRI(132) = SOTHTRI/TD/DLTHMX
1105 TRI(133) = -DLTMD/DLTHMX
1106 TRI(134) = DTHDMEDL/CMG/THCMY/1.0.
1107 TRI(135) = DLONG/OMEGMX
1108 TRI(136) = -THGOVL/1.

```

Figure G.9. (Continued)

```

1109 TR1(150) = CMMX/76/MCMX
1110 TR1(151) = CMMX/76/MCMX
1111 TR1(152) = CMMX/76/MCMX
1112 TR1(153) = ATNDEF/76/MCMX
1113 TR1(154) = ACC7PA/76/MCMX
1114 TR1(155) = ACC7PA/76/MCMX
1115 TR1(156) = -XAE76/SM/UDOTMX
1116 TR1(157) = -YAE76/75/VDOTMX
1117 TR1(170) = -ATNB/ATNMX
1118 TR1(171) = -AINL/AINMX
1119 TR1(172) = -T4G0VR/L
1120 TR1(210) = ATNDR/ATDDMX
1121 TR1(211) = ATNDDL/ATDDMX
1122 TR1(212) = PDGT/PODTMX
1123 TR1(213) = PDGT/PODTMX
1124 TR1(214) = PDGT/PODTMX
1125 TR1(215) = -7AEP/SM/VDOTMX
1126 TR1(216) = 7DGT/VMMX
1127 TR1(217) = 7C
1128 TR1(218) = CMMX/76/MCMX
1129 TR1(219) = CMMX/76/MCMX
1130 TR1(222) = CMMX/76/MCMX
1131 TR1(223) = CMMX/76/MCMX
1132 TR1(224) = SKTPT/71#(DDT--STRIN)/VMMX
1133 TR1(225) = DT/76
1134 TR1(252) = 7/GMX
1135 TR1(251) = DELR/DELPMX
1136 TR1(252) = DELS/DELSMX
1137 TR1(253) = DELS/DELSMX
1138 TR1(254) = DELR/DELPMX
1139 TR1(255) = DELS/DELSMX
1140 TR1(256) = -TH75%/TH75MX
1141 TR1(257) = -TH75%/TH75MX
1142 TR1(270) = DELAP/DELAMX
1143 TR1(271) = DELAL/DELLAMX
1144 TR1(272) = -DELSP/DELSPMX
1145 TR1(273) = DELSOL/DELSOLMX
1146 TR1(274) = PDGT/PODTMX
1147 TR1(275) = PDGT/PODTMX
1148 TR1(276) = PDGT/PODTMX
1149 TR1(251) = -DELST/DELSMX
1150 TR1(251) = GORLON/DELST/DELSMX
1151 TR1(253) = -DELRY/DELRYMX
1152 TR1(254) = -DELTY/DELTVMX
1153 TR1(255) = GDSCLADELST/DSCEMX/DELSMX
1154 TR1(256) = GORCYLDELST/DSCEMX/DELSMX
1155 TR1(257) = -GDSCLADELST/DSCEMX/DELSMX
1156 TR1(257) = -GDSCLADELST/DSCEMX/DELSMX
1157 TR1(270) = DELST/DELSMX

```

Figure G.9. (Continued)


```

1203 A2P(23) = THUM/TCOMX
1204 A2P(24) = 0.
1205 A2P(25) = -GDTH/THUM*DELTH/TCOMX
1206 A2P(26) = -SVT/THUM*(12)*COMPT/COMX
1207 A2P(27) = 1.0
1208 A2P(28) = 1.0
1209 A2P(29) = 2*DELTH/COMX/CMFCOMX*DELTH*DELTH
1210 A2P(30) = COMPT/COMX
1211 A2P(31) = COMCOM/COMX
1212 A2P(32) = -THMS/TCOMX
1213 A2P(33) = ALARDI/PCICOMX/1.0
1214 A2P(34) = ALARN/FLXX/PCICOMX
1215 A2P(35) = CPRD/CPMX *2.0
1216 A2P(36) = THATM/THATM
1217 A2P(37) = AMARDI/PCICOMX/1.0
1218 A2P(38) = AMARN/FLXX/PCICOMX
1219 A2P(39) = 9LMS/CMFCOMX
1220 A2P(40) = -TMS2/THUMX
1221 A2P(41) = TMS3/THUMX
1222 A2P(42) = TMS4/THUMX
1223 A2P(43) = 5*THUM/FLXX/COMX/PCICOMX
1224 A2P(44) = ZARDI/FLXX/1.0
1225 A2P(45) = ZARDN/CP/1.0
1226 A2P(46) = ATNR/ATNOMX
1227 A2P(47) = ATNR/ATNOMX
1228 A2P(48) = ATNR/ATNOMX
1229 A2P(49) = ATNR/ATNOMX
1230 A2P(50) = ATNR/ATNOMX
1231 A2P(51) = ATNR/ATNOMX
1232 A2P(52) = PCIC/PCICOMX
1233 A2P(53) = PCIC/PCICOMX
1234 A2P(54) = ATNR/ATNOMX
1235 A2P(55) = CMFCOM/CMFCOMX
1236 A2P(56) = SHPIC/SHPMX
1237 A2P(57) = CMPL/COMX
1238 A2P(58) = CMPL/COMX
1239 A2P(59) = (UMPT-PCICOMX)/COMX
1240 A2P(60) = CMFCOM/COMX
1241 A2P(61) = -SKT/THUM*(12)*COMPT/COMX/COMX
1242 A2P(62) = CMPL/COMX
1243 A2P(63) = PCIC/PCICOMX
1244 A2P(64) = AMARDI/PCICOMX
1245 A2P(65) = PCIC/PCICOMX
1246 A2P(66) = AMARDI/PCICOMX
1247 A2P(67) = 0.0
1248 A2P(68) = PCIC/PCICOMX
1249 A2P(69) = PCIC/PCICOMX
1250 A2P(70) = ATNR/ATNOMX
1251 A2P(71) = PCIC/PCICOMX

```

STK2581

Figure G.9. (Continued)

```

1252 A2N(262) = DCYPO/DCYLX/GBUTON
1253 A2P(263) = THMSP/THSMX
1254 A2N(263) = THMSL/THSMX
1255 A2P(300) = SHPPRR/SHPMX
1256 A2P(301) = SHP1/SHPMX
1257 A2P(302) = ALARP/FIXX/PDGTMX
1258 A2P(303) = AMARP/FIYY/QDQIMX
1259 A2P(310) = SHP4/SHPMX
1260 A2N(310) = SHPO/SHPMX/GRUTON
1261 A2P(311) = SHPIC/SHPMX
1262 A2P(312) = -CMDQR/CPMGX
1263 A2P(320) = AENG
1264 A2P(321) = DTHDOM/L
1265 A2P(322) = ZARP/SM/ARPMX
1266 A2P(323) = AINLOI**2/AINDMX**2
1267 A2P(330) = OLOWG/OMEGMX
1268 A2P(331) = -AINRDI**2/AINDMX**2
1269 A2P(340) = DTHDD**2/ULCMG/OMEGMX
1270 A2P(342) = (AINL-ALAMDA)/PI
1271 A2P(343) = (AINR-ALAMDA)/PI
1272 A2P(352) = -GLSB/GLSMX
1273 A2P(352) = GLSAL/GLSMX
1274 A2P(353) = (XCG-SLPA)/XCGMX
1275 A2P(360) = (AINDDL**SILAML+AINDDR**SILAMD)/AINDMX
1276 A2P(360) = (AINLOI**2*CILAPL+AINRDI**2*CILAMP)/AINDMX**2
1277 A2P(361) = ACCXPA/AXPAMX
1278 A2P(362) = (AINDDL**CILAHL+AINDR**CILAHL)/AINDMX
1279 A2P(362) = (AINLOI**2*SILAML+AINRDI**2*SILAMD)/AINDMX**2
1280 A2P(363) = XCCGG/XDDMX
1281 A2P(363) = ZDDCG/ZDDMX
1282 A2P(370) = RDOT*(XCG-SLPA)/(RDOTMX**XCGMX)
1283 A2P(370) = ACCYPA/AYPAMX
1284 A2P(371) = -QDOT*(XCG-SLPA)/(QDOTMX**XCGMX)
1285 A2P(371) = ACCZPA/AZPAMX

C BOARD 3E (CONSOLE 2) VALUES AT SUMMING JUNCTIONS OF AMPLIFIERS
1286 SJ2(100) = DLTHP/DLTHMX/GBUTON
1287 SJ2(101) = SHPPG/SHPMX/GBUTON
1288 SJ2(110) = SHP30/SHP4X/GBUTON
1289 SJ2(111) = CMDOT/OMEGMX/GBUTON
1290 SJ2(120) = THDMG/THDMX/GBUTON
1291 SJ2(121) = THSID/THSIDX/GBUTON
1292 SJ2(130) = SKTRIM(13)*CMDOT/OMEGMX
1293 SJ2(131) = 0.
1294 SJ2(140) = 0.
1295 SJ2(141) = 0.
1296 SJ2(150) = -ALAPDP/PDGTMX/IC./GBUTON/10.
1297 SJ2(151) = ALAPDI/PDGTMX/GBUTON
1298 SJ2(160) = -AMARPO/QDQIMX/IC./GBUTON/10.
1299 SJ2(161) = AMAROI/QDQIMX/GBUTON

```

Figure G.9. (Continued)

1300 SJ2(070) = ZARDU/CARMX/11/030TON/10.
 1301 SJ2(71) = ZARDU/CARMX/11/030TON/10.
 1302 SJ2(07) = AIN90/AIADMX/GRUTON
 1303 SJ2(71) = AIN90/AIADMX/GRUTON
 1304 SJ2(10) = AIN90/AIADMX/GRUTON
 1305 SJ2(11) = AIN90/AIADMX/GRUTON
 1306 SJ2(12) = AIN90/AIADMX/GRUTON
 1307 SJ2(13) = 0.
 1308 SJ2(14) = 0.
 1309 SJ2(15) = 0.
 1310 SJ2(16) = 0.
 1311 SJ2(17) = -(700+H0T01M)*SKTR1*(R)/VVMX
 1312 SJ2(18) = SKTR1*(R)/VVMX
 1313 SJ2(19) = SKTR1*(R)/VVMX

BOARD 3E (CONSOLE 2) VALUES OF TRUNK LINES AND ADCS (FIRST 32 TR'S ARE ADCS)

1314 TR2(02) = AIN90/AIADMX
 1315 TR2(02) = AIN90/AIADMX
 1316 TR2(22) = AIN90/AIADMX
 1317 TR2(23) = AIN90/AIADMX
 1318 TR2(24) = AIN90/AIADMX
 1319 TR2(25) = AIN90/AIADMX
 1320 TR2(26) = AIN90/AIADMX
 1321 TR2(27) = AIN90/AIADMX
 1322 TR2(28) = AIN90/AIADMX
 1323 TR2(29) = AIN90/AIADMX
 1324 TR2(30) = 0.
 1325 TR2(31) = 0.
 1326 TR2(32) = 0.
 1327 TR2(33) = 0.
 1328 TR2(34) = 0.
 1329 TR2(35) = 0.
 1330 TR2(36) = 0.
 1331 TR2(120) = DM00T/DM00T
 1332 TR2(121) = DM00T/DM00T
 1333 TR2(122) = DM00T/DM00T
 1334 TR2(123) = DM00T/DM00T
 1335 TR2(124) = 1.
 1336 TR2(125) = 1.
 1337 TR2(126) = DM00T/DM00T
 1338 TR2(127) = DM00T/DM00T
 1339 TR2(128) = DM00T/DM00T
 1340 TR2(129) = DM00T/DM00T
 1341 TR2(130) = DM00T/DM00T
 1342 TR2(131) = DM00T/DM00T
 1343 TR2(132) = DM00T/DM00T
 1344 TR2(133) = DM00T/DM00T
 1345 TR2(134) = DM00T/DM00T
 1346 TR2(135) = DM00T/DM00T

Figure G.9. (Continued)

```

1347 TR2(31) = 0.
1348 TR2(32) = 0.
1349 TR2(110) = -DELTH/DLTHMX
1350 TR2(111) = -DSHP/SHPMX
1351 TR2(112) = -SHPTC/SHPMX
1352 TR2(113) = -ATNRF/ATNMX
1353 TR2(114) = -TPS/TPSMX
1354 TR2(115) = SHPPD/SHPPMX/GRUTIN
1355 TR2(116) = -DSHPP/SHPMX
1356 TR2(117) = -QVTAUE*SQTHTC/DEL/GRUTIN
1357 TR2(130) = SQTHTC/DEL*TAUEMX/GRUTIN
1358 TR2(131) = THATLM/THATMX
1359 TR2(132) = GOHRT*DLTHP/DLTHMX
1360 TR2(133) = -DLTHP/DLTHMX
1361 TR2(134) = NTHDOM*DLGCG/THOMMX/LC.
1362 TR2(135) = DLGCG/CHECMX
1363 TR2(136) = -THGOL/I.
1364 TR2(150) = -CWDOR/CPMCMX
1365 TR2(151) = -CYMO/CYPMX
1366 TR2(152) = -CPM/CPPMX
1367 TR2(153) = ATNEEF/ATNMX
1368 TR2(154) = ACC/PA/AZPAMX
1369 TR2(155) = ACC/PA/AZPAMX
1370 TR2(156) = -XAEPO/SW/RODTMX
1371 TR2(157) = -YAEPT/SM/RODTMX
1372 TR2(170) = -ATNP/AINMX
1373 TR2(171) = -AINL/AINMX
1374 TR2(172) = -THGOL/I.
1375 TR2(210) = AINDR/AIDOMX
1376 TR2(211) = AINDL/AIDOMX
1377 TR2(212) = PDOT/PODTMX
1378 TR2(213) = QDOT/QDOTMX
1379 TR2(214) = PDOT/RODTMX
1380 TR2(215) = -ZAEPO/SM/RODTMX
1381 TR2(216) = ZDOT/VMMX
1382 TR2(217) = 0.
1383 TR2(230) = CPMR/CPMCMX
1384 TR2(231) = CPMFL/CPMCMX
1385 TR2(232) = CPMR/CYMMX
1386 TR2(233) = CPMFL/CYMMX
1387 TR2(234) = -SKTRIM(7)*(INDOT-RODTMX)/VMMX
1388 TR2(235) = UIC/UUMX
1389 TR2(310) = TIMSR/TMCMX
1390 TR2(311) = GLSR/GLSMX
1391 TR2(312) = GLSAL/GLSMX
1392 TR2(313) = DCYL/DCYLMX
1393 TR2(314) = GLSAR/GLSMX
1394 TR2(315) = DELRUD/DLRDMX
1395 TR2(316) = -DEFLV/VELEMX

```

Figure G.9. (Continued)

```

1396 TR2(317) = DELLEV/ALFEMX
1397 TR2(320) = RIGLIC/ALFEMX
1398 TR2(331) = RIGLIC/ALFEMX
1399 TR2(332) = AICLIC/ALFEMX
1400 TR2(333) = AICLIC/ALFEMX
1401 TR2(334) = DELLEV/ALFEMX
1402 TR2(337) = TOTR3L/ALFEMX

1403 TR2(252) = POTOL/POTEMX
1404 TR2(251) = POTOL/POTEMX
1405 TR2(252) = OMEGA/OMEGMX
1406 TR2(253) = AINOF / AINMX
1407 TR2(254) = COMIOT/ALFEMX
1408 TR2(255) = COMOTH/ALFEMX
1409 TR2(256) = -SKTR1*(12)*COMOIT/OMEGMX
1410 TR2(257) = AVAIL
1411 TR2(370) = ACCYPA/AYDAMX
1412 TR2(371) = ACCYPA/AYDAMX
1413 TR2(372) = ACCYPA/AYDAMX

C BOARD.5F (CONSOLE 3): AMPLIFIER SCALE FACTOR CALCULATION. P DENOTES POSITIVE OUTPUT
N DENOTES NEGATIVE OUTPUT
GETIUN
ENTRY STOPR
CALL ANDAIN(ORQJ,DOM(SR),LFTY(3),TRC(3),NCR,N(3),ASD,1,5,ABN,1,1,0,
# SJ,4,5,123,4,5)

1414
1415 ENTRY STOPR
1416

1417 AB(380) = RIGLI/RIGMVA/
1418 AB(391) = RIGLI/RIGMVA/
1419 AB(411) = RIGLI/RIGMVA/
1420 AB(421) = RIGLI/RIGMVA/
1421 AB(422) = AICLI/AICMVA/
1422 AB(421) = AICLI/AICMVA/
1423 AB(431) = AICLI/AICMVA/
1424 AB(431) = AICLI/AICMVA/
1425 AB(447) =
1426 AB(441) =
1427 AB(450) =
1428 AB(451) =
1429 AB(461) = GLSAP/RIGMVA
1430 AB(461) =
1431 AB(471) =
1432 AB(471) =
1433 AB(480) =
1434 AB(481) =
1435 AB(481) =
1436 AB(482) = DELSTAB/ALFEMX
1437 AB(483) = DELSTAB/ALFEMX
1438 AB(483) = DELLEV/ALFEMX
1439 AB(491) =
1440 AB(491) =

```

Figure G.9. (Continued)


```

1441 A3P(212) = -DELAR1/DELAMX
1442 A3N(212) = DELAP2/DELAMX
1443 A3P(213) = DELAL1/DELAMX
1444 A3N(213) = -DELAL2/DELAMX
1445 A3P(221) = DELYL/DELAMX
1446 A3P(223) = DEL/DELAMX
1447 A3P(242) = DELR/DELAMX
1448 A3P(243) = DELS/DELAMX
1449 A3P(251) = TH75R/TH75XX
1450 A3P(252) = -DELROD/DELAMX
1451 A3N(252) = -DELSR/DELSPM
1452 A3P(253) = -DELRT/DELRM
1453 A3N(253) = DELSPL/DELSPM
1454 A3P(261) = TH75L/TH75XX
1455 A3P(262) = DELR/DELAMX
1456 A3P(263) = DELFLP/DELAMX
1457 A3N(300) = GLSIC/GLSMX
1458 A3N(301) = -GLSAIL/GLSMX
1459 A3P(302) = DLON/DLONMX
1460 A3P(303) = DELFP/DELFM
1461 A3N(311) = RICKP/RICKX/1.0.
1462 A3P(311) = RICKP /RICKX
1463 A3P(312) = DELAR/DELAMX
1464 A3N(312) = -DELAL/DELAMX
1465 A3P(313) = -VCALIB/IMX
1466 A3P(320) = GRICP/GRICMX
1467 A3P(321) = GRICP/GRICMX
1468 A3N(322) = GRICD/GRICMX/GRUTON
1469 A3N(323) = GRICD/GRICMX/GRUTON
1470 A3N(330) = BICLPD/BICMX/1.
1471 A3P(331) = BICLP /BICMX
1472 A3P(340) = -DELS/DLONMX
1473 A3N(340) = -PSAS1/DLONMX
1474 A3N(341) = PSAS7/DLONMX
1475 A3N(341) = -PSAS2/DLONMX
1476 A3P(350) = AICRPD/AICMX/1.
1477 A3P(351) = AICRP /AICMX
1478 A3P(352) = PSAS5/DLONMX/GRUTON/1.
1479 A3P(353) = PSAS6/DLONMX/GRUTON
1480 A3P(360) = PSAS4/DLONMX
1481 A3N(361) = -PSAS3/DLONMX
1482 A3P(362) = GLONPH/1.
1483 A3N(370) = AICLPD/AICMX/1.
1484 A3P(371) = AICLP /AICMX
1485 A3P(371) = AICLP /AICMX
C BOARD SF (CONSOLE 3) VALUES AT SUMMING JUNCTIONS OF AMPLIFIERS
S13(330) = -BICRPD/BICMX/1. /GRUTON/1.0.
S13(351) = BICRPD/BICMX/GRUTON
S13(360) = -BICLPD/BICMX/1. /GRUTON/1.0.

```

Figure G.9. (Continued)

1489 SJ3(11) = AICD1/AICMX/GRUTN
 1490 SJ3(20) = AICD8/AICMX/GRUTN/1.
 1491 SJ3(21) = AICD1/AICMX/GRUTN
 1492 SJ3(30) = AICD7/AICMX/GRUTN/1.
 1493 SJ3(31) = AICD1/AICMX/GRUTN
 1494 SJ3(40) = GLSAPD/BLSMX/GRUTN
 1495 SJ3(51) = BIRPDD/BICMX/GRUTN/1.
 1496 SJ3(70) = BIRPDD/BICMX/GRUTN/1.
 1497 SJ3(71) = BIRPDD/BICMX/GRUTN/1.
 1498 SJ3(80) = GLSAPD/BLSMX/GRUTN
 1499 SJ3(81) = GLSAPD/BLSMX/GRUTN
 1500 SJ3(81C) = BIRPDD/BICMX/GRUTN/1.
 1501 SJ3(811) = BIRPDD/BICMX/GRUTN
 1502 SJ3(820) = GATCD/GICMX/GRUTN
 1503 SJ3(821) = GATCD/GICMX/GRUTN
 1504 SJ3(830) = BILPDD/BICMX/GRUTN/1.
 1505 SJ3(831) = BILPDD/BICMX/GRUTN
 1506 SJ3(840) = PSAS1D/DLSMX/GRUTN
 1507 SJ3(841) = PSAS2D/DLSMX/GRUTN/1.
 1508 SJ3(850) = BIRPDD/BICMX/GRUTN/1.
 1509 SJ3(851) = AICDPP/AICMX/GRUTN
 1510 SJ3(852) = PSAS4D/DLSMX/GRUTN
 1511 SJ3(853) = PSAS3D/DLSMX/GRUTN
 1512 SJ3(870) = AICLPP/AICMX/GRUTN/1.
 1513 SJ3(871) = AICLPP/AICMX/GRUTN

BOARD 5F (CONSOLE 3) VALUES OF TRUNK LINES AND ADC'S (FIRST 32 TR'S ARE ADC'S)

TR3(121) = DELRT/DELPMX
 TR3(121) = DELST/DELSMX
 TR3(221) = DELST/DELSMX
 TR3(222) = DELRT/DELPMX
 TR3(223) = DELTH/DELTHMX
 TR3(251) = DELPS/DELPMSX
 TR3(261) = DELSS/DELSMX
 TR3(262) = DELPS/DELPMX
 TR3(263) = TH75R/TH75MX
 TR3(320) = TH75L/TH75MX
 TR3(321) = DELAL/DELA
 TR3(31) = C.
 TR3(32) = C.
 TR3(250) = C/CMX
 TR3(251) = DELP/DELPMSX
 TR3(252) = DELS/DELSMX
 TR3(253) = DELSS/DELSMX
 TR3(254) = DELR/DELRMSX
 TR3(255) = DELS/DELSMX
 TR3(256) = TH75R/TH75MX
 TR3(257) = TH75L/TH75MX
 TR3(270) = DELAR/DELA
 TR3(271) = DELAL/DELA
 TR3(272) = C.
 TR3(31) = C.
 TR3(32) = C.
 TR3(250) = C/CMX
 TR3(251) = DELP/DELPMSX
 TR3(252) = DELS/DELSMX
 TR3(253) = DELSS/DELSMX
 TR3(254) = DELR/DELRMSX
 TR3(255) = DELS/DELSMX
 TR3(256) = TH75R/TH75MX
 TR3(257) = TH75L/TH75MX
 TR3(270) = DELAR/DELA
 TR3(271) = DELAL/DELA

Figure G.9. (Continued)

```

1536 TR3(272) = -DELSPK/DLSPMX
1537 TR3(273) = DELSPL/DLSPMX
1538 TR3(274) = PDOT/PODOTMX
1539 TR3(275) = PDOT/PODOTMX
1540 TR3(276) = PDOT/PODOTMX
1541 TR3(317) = THMSL/TTMSMX
1542 TR3(311) = -GLSB/GLSMX
1543 TR3(312) = GLSAL/GLSMX
1544 TR3(313) = -DCYL/DCYLMX
1545 TR3(314) = -GLSAR/GLSMX
1546 TR3(315) = -DELRUD/DLRUMX
1547 TR3(316) = -DEFLV/DELEMX
1548 TR3(317) = DEFLP/DLFMLX
1549 TR3(330) = SICRIG/SICMX
1550 TR3(331) = BICLIC/BICMX
1551 TR3(332) = AICPIC/AICMX
1552 TR3(333) = AICLIC/AICMX
1553 TR3(334) = DFLTH/DLTHMX
1554 TR3(337) = THMSL/TTMSMX
1555 TR3(350) = -DELST/DELSMX
1556 TR3(351) = GORLON*DELRT/DFLPMX
1557 TR3(352) = -DELBT/DELBMX
1558 TR3(353) = -VCALTR/UMX
1559 TR3(354) = -DELRT/DELRMX
1560 TR3(355) = GOSCOL*DELST/GSCOMX/DELS4X
1561 TR3(356) = GORCYL*DELRT/GFCYMX/DEFLPMX
1562 TR3(357) = -GOSCYL*DELST/GSCYMX/DELS4X
1563 TR3(370) = DELST/DELSMX
1564 TR3(371) = -GATC/GTCMX
1565 TR3(372) = -GBTC/GTCMX
1566 TR3(373) = GDFLP/DLFLMX
1567 TR3(374) = GDE/DFLEMX*DGTCRD
1568 TR3(375) = GOSP/DLSPMX

C
1569 TR3(230) = DEFLP/DLFLMX
1570 TR3(231) = DELR / DELBMX
1571 TR3(232) = DELS / DELSMX
1572 TR3(233) = DFLR / DELPMX
1573 TR3(234) = COMDLR / DELRMX
1574 TR3(235) = COMDLS / DELSMX
1575 TR3(236) = COMDLP / DELPMX
1576 TR3(237) = AVAIL

C BOARD 1B (CONSOLE 4) AMPLIFIER SCALE FACTOR CALCULATION. P DENOTES POSITIVE OUTPUT
RETURN N DENOTES NEGATIVE OUTPUT
FMTRY STCOM4
POMOS(4) = HD4
LETR(4) = LT4
CALL ANDAIN(PROJ,IR,14,IEC(1),3,44P,5,5,AN,1,5,3,4,5,IR,4,5,
*5)

```

Figure G.9. (Continued)

1582 A4P(1307) = PCTOL/TQSI*MX
 1583 A4P(1311) = PCTOR/TQSI*MX
 1584 A4P(1322) = PCKP/RPMS*MX
 1585 A4P(1333) = YDOT/YOT*MX
 1586 A4P(1333) = -HDOT/HOTS*MX
 1587 A4P(1311) = ACCXPA/AXPA*MX
 1588 A4P(1312) = XDOT/XETS*MX
 1589 A4P(1313) = -VCALTR/SKFDPS/LSI*MX
 1590 A4P(1321) = V/SKFDPS/VSI*MX
 1591 A4P(1322) = THE*RDJDDG/THE*SMX
 1592 A4P(1333) = -PHI*ROTDDG/PHI*SMX
 1593 A4P(1333) = PSI*ROTDDG/PSI*SMX
 1594 A4P(1333) = PSDSIM/PDSDT*MX
 1595 A4P(1340) = AINRF#PDJDDG/AI*SMX
 1596 A4P(1341) = AVEAL#PDJDDG/AL*SMX
 1597 A4P(1321) = RCTAF*RDJDDG/RTSI*MX
 1598 A4P(1343) = ACCZPA/AZP*MX
 1599 A4P(1351) = DELFLP/DFP*MX
 1600 A4P(1352) = H/H*SI*MX
 1601 A4P(1353) = 0.
 1602 A4P(1353) = 0.
 1603 A4P(1353) = 0.
 1604 A4P(1353) = 1.0000
 1605 A4P(1362) = H/Z*MX
 1606 A4P(1363) = 0.
 1607 A4P(1373) = 0.
 1608 A4P(1371) = 1.0000
 1609 A4P(200) = XIC / YVIS*MX
 1610 A4P(201) = VIC / YVIS*MX
 1611 A4P(202) = SIN*THE
 1612 A4P(203) = COS*THE
 1613 A4P(210) = 1.0000
 1614 A4P(211) = VISIC / XVIS*MX
 1615 A4P(212) = SIN*PHI
 1616 A4P(213) = COS*PHI
 1617 A4P(220) = PSI / PI
 1618 A4P(221) = SA11
 1619 A4P(222) = SIN*PSI
 1620 A4P(223) = COS*PSI
 1621 A4P(230) = SA12
 1622 A4P(231) = SA13
 1623 A4P(240) = SA21
 1624 A4P(241) = SA22
 1625 A4P(242) = SIN*THI = SIN*PHI
 1626 A4P(243) = SIN*THE = COS*PHI
 1627 A4P(250) = SA23
 1628 A4P(251) = SA31
 1629 A4P(252) = YACVIS / YVIS*MX

Figure G.9. (Continued)

```

1630 A4N(252) = ZACVIS / ZVISMX
1631 A4P(253) = ZBODY / ZVISMX
1632 A4P(260) = SA32
1633 A4P(261) = SA33
1634 A4P(262) = YACVIS / YVISMX
1635 A4P(263) = FREQM / LQ.
1636 A4P(300) = (XHPH17-H)/XVISMX
1637 A4N(300) = (R1ASMT-H*GZMTSL)/ZVISMX
1638 A4P(302) = XBODY / XVISMX
1639 A4P(303) = YBODY / YVISMX
1640 A4P(310) = XSCOPE/SCOPMX
1641 A4P(311) = YSCOPE/SCOPMX
1642 A4P(312) = -XSCOPE/SCOPMX-YIC*CDSPH1/XVISMX+H*SINPH1/XVISMX
1643 A4P(313) = YSCOPE/SCOPMX+H*CDSPH1/YVISMX+K*YIC*SINPH1/YVISMX
1644 A4P(320) = C.3000
1645 A4P(321) = C.3000
1646 A4P(323) = -DRKOP/DRDMX
1647 A4P(330) = C.3000
1648 A4P(331) = C.0000
1649 A4P(341) = FFD5 / FFRMX
1650 A4P(342) = -BRAKE/BRKSMX
1651 A4N(342) = BRAKE/BRKMX
1652 A4P(343) = THRKDR/THDDMX
1653 A4P(350) = FFD5 / FFSMX
1654 A4P(351) = C.0
1655 A4P(352) = -DSTKR/CSDMX
1656 A4P(353) = -DRKDR/DRDMX
1657 A4P(362) = -COMPL3/DRPSMX
1658 A4N(360) = COMDL3/DELSMX
1659 A4P(361) = -COMPLS/DRPSMX
1660 A4N(361) = COMPLS/DELSMX
1661 A4P(362) = COMDT/ATDSMX
1662 A4N(362) = COMDT/AINPMX
1663 A4P(363) = FFRX/FFRMX
1664 A4P(370) = -COMDLR/DRPSMX
1665 A4N(370) = COMDLR/DELSMX
1666 A4P(371) = -COMDTH/DTPSMX
1667 A4N(371) = COMDTH/DLTHMX

C BOARD 1B (CONSOLE 4) VALUES OF TRUNK LINES (NO ADC'S ON THIS BOARD)
TR4(010) = PCTQ1 / TQSI4X
TP4(011) = -TR4(010)
TR4(012) = PCTOR/TQSI4X
TR4(013) = -TR4(012)
TR4(014) = PCN2/RPMSMX
TR4(015) = -TR4(014)
TR4(016) = YDRT/YDTS4X
TR4(017) = -TR4(016)
TR4(030) = V / VMX

```

Figure G.9. (Continued)

```

1677 TR4(131) = RTAF / ARFSMX
1678 TR4(132) = -VCALIR / LMX
1679 TR4(133) = -MDUT / VMXX
1680 TR4(134) = -PHI / PI
1681 TR4(135) = PSI / PSIMX
1682 TR4(136) = THE / PI
1683 TR4(137) = H / ZMX
1684 TR4(151) = AVEALW / ALWGMX
1685 TR4(151) = SQE / SQEMX
1686 TR4(152) = XDOT / XDUTMX
1687 TR4(153) = XIC / XMX
1688 TR4(154) = YDOT / YDOTMX
1689 TR4(155) = YIC / YMX
1690 TR4(157) = PSIDOT / PSDMX
1691 TR4(170) = SINTHE
1692 TR4(171) = COSTHE
1693 TR4(172) = SINPHI
1694 TR4(173) = COSPHI
1695 TR4(174) = SINPHI * COSTHE
1696 TR4(175) = COSPHI * COSTHE
1697 TR4(111) = VISHOR
1698 TR4(111) = -TR4(111)
1699 TR4(112) = VISVEP
1700 TR4(112) = -TR4(112)
1701 TR4(130) = VCALIR / SKFPS / LSTMX
1702 TR4(131) = -TR4(130)
1703 TR4(132) = V / SKFPS / VSTMX
1704 TR4(132) = -TR4(132)
1705 TR4(134) = THE * RDTODG / THE SMX
1706 TR4(134) = -TR4(134)
1707 TR4(136) = PHI * RDTODG / PHI SMX
1708 TR4(136) = -TR4(136)
1709 TR4(150) = PSI * RDTODG / PSI SMX
1710 TR4(151) = -TR4(150)
1711 TR4(152) = PSDSY / PSDTSX
1712 TR4(152) = -TR4(152)
1713 TR4(154) = AINDF * RDTODG / AINDSMX
1714 TR4(154) = -TR4(154)
1715 TR4(154) = AVFALW * RDTODG / AVFALWSMX
1716 TR4(157) = -TR4(154)
1717 TR4(170) = 3ETAF * RDTODG / ATSTIMX
1718 TR4(171) = -TR4(170)
1719 TR4(172) = ACCYPA / AYPAMX
1720 TR4(173) = -TR4(172)
1721 TR4(174) = ACCZPA / A7PAMX
1722 TR4(175) = -TR4(174)
1723 TR4(176) = DELFLP / DFPSMX
1724 TR4(177) = -TR4(176)
1725 TR4(210) = HDOT / HDTSMX

```

Figure G.9. (Continued)

1726 TR4(211) = -TR4(212)
 1727 TR4(212) = XDOT/XDOTSMX
 1728 TR4(213) = -TR4(212)
 1729 TR4(214) = ACCXPA/YAPAMX
 1730 TR4(215) = -TR4(214)
 1731 TR4(230) = DELELP/DLEFLMX
 1732 TR4(231) = DELB / DELRMX
 1733 TR4(232) = DELS / DELSMX
 1734 TR4(233) = DELR / DELRMX
 1735 TR4(234) = COMDLR / DELBMX
 1736 TR4(235) = COMDLS / DELSMX
 1737 TR4(236) = COMDLR / DELRMX
 1738 TR4(237) = AVAIL
 1739 TR4(250) = PCTOL/PCTOMX
 1740 TR4(251) = PCTOR/PCTOMX
 1741 TR4(252) = OMEGA / CMEGMX
 1742 TR4(253) = AINRF/AINRMX
 1743 TR4(254) = COMIDT/AINRMX
 1744 TR4(255) = COMDTH / DLTHMX
 1745 TR4(256) = -SKTRIM(12)*XDOT/XDOTSMX
 1746 TR4(257) = AVAIL
 1747 TR4(277) = ACCXPA/YAPAMX
 1748 TR4(278) = ACCYPA/YAPAMX
 1749 TR4(279) = ACCZPA/AZPAMX
 1750 TR4(310) = -COMIDT/AIDSMX
 1751 TR4(311) = -TR4(310)
 1752 TR4(312) = -BRAKE/BARKSMX
 1753 TR4(313) = -TR4(312)
 1754 TR4(330) = DRBKDR/DDBRDMX
 1755 TR4(331) = -TR4(330)
 1756 TR4(332) = DRBKDR/DDBRDMX
 1757 TR4(333) = -TR4(332)
 1758 TR4(334) = DRBKDR/DDBRDMX
 1759 TR4(335) = -TR4(334)
 1760 TR4(336) = THBKDR/THBDMX
 1761 TR4(337) = -TR4(336)
 1762 TR4(357) = FFDR/FFRMX
 1763 TR4(351) = -TR4(350)
 1764 TR4(352) = FFDS/FFSMX
 1765 TR4(353) = -TR4(352)
 1766 TR4(354) = FFDR/FFRMX
 1767 TP4(355) = -TR4(354)
 1768 TR4(356) = H/HSIMX
 1769 TR4(357) = -TR4(356)
 1770 TR4(370) = -COMDLR/DRPSMX
 1771 TR4(371) = -TR4(370)
 1772 TR4(372) = -COMDLS/DSPSMX
 1773 TR4(373) = -TR4(372)
 1774 TR4(374) = -COMDLR/DRPSMX

Figure G.9. (Continued)

DATE 73092

LEVEL 3

VERSION 3

PS

MODEL 44

FORTRAN IV

```
1775 TR4(375)E -TR4(374)  
1776 TR4(376)E -CUMMTH/CTPCMX  
1777 TR4(377)E -TR4(374)  
  
C  
1778 PETIQA  
1779 END
```

Figure G.9. (Continued)

equilibrium. The equations for these feedback loops are shown in Appendix E. Several trim options are available: for a given initial condition of altitude, u and v components of velocity, rotor RPM and initial rates (p,q,r) the aircraft can be trimmed with attitude for specified nacelle angle or with nacelle angle for specified attitude. In addition, the aircraft can be trimmed in backwards or sideways flight. The trim gains used vary with the flight condition. Trim is generally attained in 5-10 seconds for any flight condition using this technique.

G.3 SIMULATION PROGRAM OUTPUT

The primary output of the mathematical model are:

- Trim sheet information
- Dynamic time histories of aircraft response

Figure G.10 shows a typical trim sheet with 180 aircraft parameters printed out and Figure G.11 contains the definitions of all the parameters. Four brush recorders with eight channels of output each are available for recording of the aircraft real time response. Figure G.12 shows a typical example of the output from one recorder. These data are extremely useful in analyzing aircraft responses and in optimizing stability augmentation and control systems.

T I L T R O T O R T R I M D A T A

DATE 03/23/73 TIME 11 HR 2 MIN 40 SEC FLIGHT NO.= RUN NO.= TAPE SEQ. NO.= 0
VTOT= 250.0 KT U = 250.0 KT V = -0.0 KT W = -2.0 KT G.W.= 12320.5 LBS RPH= 385.8 H = 51.5 FT XCS= 9.2 IN ZCG= 21.9 IN

THETA	PHI	PSI	IN REF	TWIST LM	TWIST RM	RCE	THYS L	TH75 R
-C.4400E 00	C.2450E 00	C.0	-0.22918E-01	0.0	0.0	0.23723E-02	0.47136E 02	0.47192E 02
DEL ROT	DELS TOT	DEL TOT	THRUSTLE	DEL SAS	DELS SAS	DELR SAS	AICL	AICR
-C.12590E 01	-C.7500E-02	C.11000E-01	C.20350E 01	0.0	-0.10300E-02	0.10000E-02	0.73893E-02	0.0
ELEVATOR	RUNNER	DEL L	DEL R	DELSPL	DELSPR	FLAP	BICL	BICR
0.23835E 01	0.0	C.63000E-01	C.11700E 00	0.85530E-01	0.90000E-01	0.90000E-01	0.36629E-02	0.0
TPS	OM ENG	SHP AV	SHP RQL	SHP RQR	IXX	IYY	IZZ	D.PRES F
C.18870E 04	C.23582E 04	C.82417E 03	C.85759E 03	0.89021E 03	0.50275E 05	0.14168E 05	0.60628E 05	0.21152E 03
MU L	THRUST L	NORMAL L	SIDE L	M ROT L	M ROT L	L HUB L	M HUB L	N HUB L
0.80349E 00	C.79523E 03	C.62197E 02	-C.22239E 02	-0.13081E 03	0.29939E 03	-0.11038E 05	0.10502E 03	0.43560E 03
MU R	THRUST R	NORMAL R	SIDE R	M ROT R	M ROT R	L HUB R	M HUB R	N HUB R
0.80389E 00	C.82572E 03	C.13206E 03	-0.50044E 02	0.35239E 03	0.66883E 03	0.11352E 05	0.34573E 03	-0.71457E 03
X FUSE	X TAIL	X WING L	X WING R	X NAC L	X NAC R	X TIP L	X TIP R	X/M
-C.32474E 03	-C.16235E 03	-C.54787E 03	-0.54383E 03	-0.47215E 02	-0.47178E 02	0.74795E 03	0.77846E 03	-0.11876E 00
Y FUSE	Y TAIL	Y WING L	Y WING R	Y NAC L	Y NAC R	Y TIP L	Y TIP R	Y/M
0.19445E 01	C.78296E 03	C.30284E-01	C.30555E-01	0.12313E 00	0.12332E 00	0.22726E 02	-0.49107E 02	-0.61603E-01
Z FUSE	Z TAIL	Z WING L	Z WING R	Z NAC L	Z NAC R	Z TIP L	Z TIP R	Z/M
-C.19685E 04	C.52210E 03	-C.55187E 04	-C.56695E 04	0.23069E 02	0.19979E 02	0.82729E 02	0.15328E 03	-0.32217E 02
L FUSE	L TAIL	L WING	M ACT L	L NAC L	L NAC R	L TIP L	L TIP R	L/IXX
-0.35475E 01	C.22225E 01	-C.58618E 03	-0.49072E 04	0.0	0.0	-0.11039E 05	0.11353E 05	0.16997E-01
M FUSE	M TAIL	M WING	M ACT R	M NAC L	M NAC R	M TIP L	M TIP R	M/IVY
-C.17206E 04	C.10696E 05	-C.56448E 04	-C.51483E 04	0.0	0.0	-0.30036E 03	-0.40651E 03	0.10087E-02
N FUSE	N TAIL	N WING	Z WING	N NAC LN	NAC R	N TIP L	N TIP R	N/IZZ
0.17683E 02	-C.14728E 02	C.20164E 02	-0.11128E 05	0.0	0.0	0.57371E 03	-0.90887E 03	-0.13173E-01
ALPH FUS	ALPH HT	ALPHLWSS	ALPHRWS	AL NAC L	AL NAC R	AL ROT L	AL ROT R	H1 L
-0.44233E 00	-0.18752E 01	C.15366E 01	C.15543E 01	-0.49313E 00	-0.48803E 00	0.51441E 00	0.48941E 00	0.0
BETA FUS	ALPH VT	ALPHA LW	ALPHA RW	CY NAC L	CY NAC R	ZETA L	ZETA R	H1 R
-0.54272E-02	C.14400E-02	C.15458E 01	C.15684E 01	0.57043E-05	0.57144E-05	-0.17966E 03	-0.17966E 03	0.0
CL FUSF	CL HT	CL WNG L	CL WNG R	CL NAC L	CL NAC R	CP L	CT L	CMF L
0.46603E-01	-0.41885E-01	C.25928E 00	C.26346E 00	-0.92982E-03	-0.92587E-03	0.25800E-02	0.22860E-02	0.17879E-03
CD FUSE	CD HT	CD WNG L	CD WNG R	CD NAC L	CD NAC R	CSF L	CPM L	CYM L
0.73200E-02	0.86827E-02	C.23336E-01	C.23539E-01	0.22411E-02	0.22392E-02	-0.63930E-04	-0.22291E-04	0.66203E-04
CM FUSF	CY VT	CM WNG L	CM WNG R	CM NAC L	CM NAC R	CP R	CT R	CMF R
-0.56233E-02	0.84995E-04	-0.31167E-01	-0.31720E-01	0.0	0.0	0.26520E-02	0.23760E-02	0.38000E-03
CN FUSE	CD VT	CL(ROLL)	CN WING	CN NAC L	CN NAC R	CSF R	CPM R	CYM R
0.12411E-04	C.78915E-02	-C.41168E-03	C.14161E-04	0.0	0.0	-0.14400E-03	-0.78000E-04	0.14760E-03
EP ZERO	EP TAIL	EP PRR	EP PLR	EP ILR	EP IRL	EP MRR	EP MRL	OMDOT
0.71116E 00	C.14595E 01	C.14267E-01	C.92668E-02	0.42248E-08	0.0	0.0	0.0	-0.11160E 01

Figure G.10. Typical Model 222 Trim Sheet

TOTAL VELOCITY ~ KTS.	"U" COMPONENT OF VELOCITY ~ KTS.	"V" COMPONENT OF VELOCITY ~ KTS.	"W" COMPONENT OF VELOCITY ~ KTS.	GROSS WEIGHT ~ LB ~	ROTOR ARM	ACTITUDE (θ) - DEG.	LONG. LOCATION OF C.G. WITH RESPECT TO PIVOT ~ IN.	VERTICAL LOCATION OF C.G. WITH RESPECT TO PIVOT ~ IN.
PITCH ATTITUDE (θ) - DEG.	ROLL ATTITUDE (ϕ) - DEG.	YAW ANGLE (ψ) - DEG.	PREVAILING WIND ANGLE (α) - DEG.	LEFT WING TWIST AT TIP ($\Delta\theta_{tip}$) - DEG.	RIGHT WING TWIST AT TIP ($\Delta\theta_{tip}$) - DEG.	ATTITUDE (θ) - DEG.	LONG. LOCATION OF C.G. WITH RESPECT TO PIVOT ~ IN.	VERTICAL LOCATION OF C.G. WITH RESPECT TO PIVOT ~ IN.
TOTAL LATERAL STICK POSITION (S_{y}) ~ IN.	TOTAL RUDDER PEDAL POSITION (S_{r}) ~ IN.	TOTAL RUDDER PEDAL POSITION (S_{r}) ~ IN.	THREATLE POSITION (S_{θ}) - IN.	LONG. SAS INPUT (S_{long}) ~ IN.	LATERAL SAS INPUT (S_{lat}) ~ IN.	DIRECTIONAL SAS INPUT (S_{dir}) ~ IN.	CYCLIC PATH (S_{cyc}) - DEG.	RIGHT ROTOR COLL. PITCH AT 75% (S_{75}) - DEG.
ELONGATION DEFLECTOR (S_{e}) - DEG.	LEFT WING DEFLECTOR (S_{l}) - DEG.	RIGHT WING DEFLECTOR (S_{r}) - DEG.	RIGHT WING FLAPING DEFLECTOR (S_{flap}) - DEG.	LEFT WING SIMILAR DEFLECTOR (S_{sim}) - DEG.	RIGHT WING SIMILAR DEFLECTOR (S_{sim}) - DEG.	FLAP DEFLECTOR (S_{flap}) - DEG.	CYCLIC PATH (S_{cyc}) - DEG.	RIGHT ROTOR COLL. PITCH AT 75% (S_{75}) - DEG.
ENGINE THROTTLE INLET TEMPERATURE - DEG.	ENGINE SPARE (S_{e}) - RPT	ENGINE SPARE (S_{e}) - RPT	LEFT ROTOR POWER REQUIRED ($S_{R_{req}}$)	LEFT ROTOR POWER REQUIRED ($S_{R_{req}}$)	TOTAL ROLL INERTIA (J_{roll}) - $lb \cdot in^2$	TOTAL PITCH INERTIA (J_{pitch}) - $lb \cdot in^2$	DYNAMIC PRESSURE (q) - lb/ft^2	RIGHT ROTOR COLL. CYCLIC PATH (S_{cyc}) - DEG.
LEFT ROTOR ANGLE AT $\theta = 10^\circ$	LEFT ROTOR ANGLE (θ_L) ~ IN.	RIGHT ROTOR ANGLE (θ_R) ~ IN.	LEFT ROTOR SIDE FORCE ($S_{L_{side}}$) - LB	LEFT ROTOR SIDE FORCE ($S_{L_{side}}$) - LB	LEFT ROTOR ANGLE AT $\theta = 10^\circ$ (θ_{L10})	TOTAL PITCH MOMENT AT LEFT AND (M_{pitch})	TOTAL YAW MOMENT AT LEFT AND (M_{yaw})	RIGHT ROTOR COLL. CYCLIC PATH (S_{cyc}) - DEG.
RIGHT ROTOR ANGLE RATIO (θ_R)	RIGHT ROTOR ANGLE FORCE ($S_{R_{side}}$) - LB	RIGHT ROTOR ANGLE FORCE ($S_{R_{side}}$) - LB	RIGHT ROTOR SIDE FORCE ($S_{R_{side}}$) - LB	RIGHT ROTOR SIDE FORCE ($S_{R_{side}}$) - LB	RIGHT ROTOR ANGLE AT $\theta = 10^\circ$ (θ_{R10})	TOTAL ROLL MOMENT AT LEFT AND (M_{roll})	TOTAL YAW MOMENT AT LEFT AND (M_{yaw})	RIGHT ROTOR COLL. CYCLIC PATH (S_{cyc}) - DEG.
PUSHING LONG. FORCE (X_{push}) - LB.	LONG. FORCE ON LEFT WING ($X_{L_{long}}$) - LB.	LONG. FORCE ON RIGHT WING ($X_{R_{long}}$) - LB.	LONG. FORCE ON LEFT WING ($X_{L_{long}}$) - LB.	LONG. FORCE ON RIGHT WING ($X_{R_{long}}$) - LB.	RIGHT ANGLE LONG. FORCE (X_{long}) - LB.	LEFT TIP PITCH LONG. FORCE (X_{tip}) - LB.	LONG. ACCELERATION AT CG (\ddot{X}_{cg}) - ft/sec^2	RIGHT ROTOR COLL. CYCLIC PATH (S_{cyc}) - DEG.
PUSHING SIDE FORCE (Y_{push}) - LB.	SIDE FORCE ON LEFT WING ($Y_{L_{side}}$) - LB.	SIDE FORCE ON RIGHT WING ($Y_{R_{side}}$) - LB.	SIDE FORCE ON LEFT WING ($Y_{L_{side}}$) - LB.	SIDE FORCE ON RIGHT WING ($Y_{R_{side}}$) - LB.	RIGHT ANGLE SIDE FORCE (Y_{side}) - LB.	LEFT TIP PITCH SIDE FORCE (Y_{tip}) - LB.	LATERAL ACCELERATION AT CG (\ddot{Y}_{cg}) - ft/sec^2	RIGHT ROTOR COLL. CYCLIC PATH (S_{cyc}) - DEG.
PUSHING VERTICAL FORCE (Z_{push}) - LB.	VERTICAL FORCE ON LEFT WING ($Z_{L_{vert}}$) - LB.	VERTICAL FORCE ON RIGHT WING ($Z_{R_{vert}}$) - LB.	VERTICAL FORCE ON LEFT WING ($Z_{L_{vert}}$) - LB.	VERTICAL FORCE ON RIGHT WING ($Z_{R_{vert}}$) - LB.	RIGHT ANGLE VERTICAL FORCE (Z_{vert}) - LB.	LEFT TIP PITCH VERTICAL FORCE (Z_{tip}) - LB.	VERTICAL ACCELERATION AT CG (\ddot{Z}_{cg}) - ft/sec^2	RIGHT ROTOR COLL. CYCLIC PATH (S_{cyc}) - DEG.
PUSHING ROLLING MOMENT (T_{roll}) - FT-LB.	WING ROLLING MOMENT (T_{roll}) - FT-LB.	WING ROLLING MOMENT (T_{roll}) - FT-LB.	LEFT WING ACTUATOR PITCHING MOMENT (T_{pitch}) - FT-LB.	RIGHT WING ACTUATOR PITCHING MOMENT (T_{pitch}) - FT-LB.	LEFT TIP PITCH ROLLING MOMENT (T_{roll}) - FT-LB.	ROLLING MOMENT AT CG (T_{roll}) - FT-LB.	ROLL ACCELERATION AT CG ($\ddot{\theta}$) - rad/sec^2	RIGHT ROTOR COLL. CYCLIC PATH (S_{cyc}) - DEG.
PUSHING PITCHING MOMENT (T_{pitch}) - FT-LB.	TOTAL WING PITCHING MOMENT (T_{pitch}) - FT-LB.	TOTAL WING PITCHING MOMENT (T_{pitch}) - FT-LB.	RIGHT WING ACTUATOR PITCHING MOMENT (T_{pitch}) - FT-LB.	LEFT WING ACTUATOR PITCHING MOMENT (T_{pitch}) - FT-LB.	LEFT TIP PITCH PITCHING MOMENT (T_{pitch}) - FT-LB.	PITCHING MOMENT AT CG (T_{pitch}) - FT-LB.	PITCH ACCELERATION AT CG ($\ddot{\phi}$) - rad/sec^2	RIGHT ROTOR COLL. CYCLIC PATH (S_{cyc}) - DEG.
PUSHING YAWING MOMENT (T_{yaw}) - FT-LB.	WING YAWING MOMENT (T_{yaw}) - FT-LB.	WING YAWING MOMENT (T_{yaw}) - FT-LB.	TOTAL WING VERTICAL FORCE (Z_{vert}) - LB.	TOTAL WING VERTICAL FORCE (Z_{vert}) - LB.	RIGHT TIP PITCH YAWING MOMENT (T_{yaw}) - FT-LB.	YAWING MOMENT AT CG (T_{yaw}) - FT-LB.	YAW ACCELERATION AT CG ($\ddot{\psi}$) - rad/sec^2	RIGHT ROTOR COLL. CYCLIC PATH (S_{cyc}) - DEG.
PUSHING ANGLE OF ATTACK (OP) - DEG.	HORIZONTAL TAIL ANGLE OF ATTACK (α_{HT}) - DEG.	HORIZONTAL TAIL ANGLE OF ATTACK (α_{HT}) - DEG.	LEFT WING SURSTAY ANGLE OF ATTACK (α_{LWS}) - DEG.	RIGHT WING SURSTAY ANGLE OF ATTACK (α_{RWS}) - DEG.	RIGHT TIP PITCH ANGLE OF ATTACK (α_{tip}) - DEG.	ANGLE OF ATTACK AT CG (α_{cg}) - DEG.	LEFT TIP DEFLECTION (h_{L1}) - IN.	RIGHT ROTOR COLL. CYCLIC PATH (S_{cyc}) - DEG.
PUSHING ATTITUDE (AP) - DEG.	VERTICAL TAIL ANGLE OF ATTACK (α_{VT}) - DEG.	VERTICAL TAIL ANGLE OF ATTACK (α_{VT}) - DEG.	LEFT WING SURSTAY ANGLE OF ATTACK (α_{LWS}) - DEG.	RIGHT WING SURSTAY ANGLE OF ATTACK (α_{RWS}) - DEG.	LEFT TIP PITCH ANGLE OF ATTACK (α_{tip}) - DEG.	ANGLE OF ATTACK AT CG (α_{cg}) - DEG.	RIGHT TIP DEFLECTION (h_{R1}) - IN.	RIGHT ROTOR COLL. CYCLIC PATH (S_{cyc}) - DEG.
PUSHING LIFT COEFF. (C_L)	HORIZONTAL TAIL LIFT COEFF. (C_{L_T})	HORIZONTAL TAIL LIFT COEFF. (C_{L_T})	LEFT WING SURSTAY LIFT COEFF. ($C_{L_{WS}}$)	RIGHT WING SURSTAY LIFT COEFF. ($C_{L_{WS}}$)	LEFT ROTOR THROUST COEFF. (C_{T_R})	LEFT ROTOR THROUST COEFF. (C_{T_R})	LEFT ROTOR LORNET FORCE COEFF.	LEFT ROTOR COLL. CYCLIC PATH (S_{cyc}) - DEG.
PUSHING DRAG COEFF. (C_D)	HORIZONTAL TAIL DRAG COEFF. (C_{D_T})	HORIZONTAL TAIL DRAG COEFF. (C_{D_T})	LEFT WING SURSTAY DRAG COEFF. ($C_{D_{WS}}$)	RIGHT WING SURSTAY DRAG COEFF. ($C_{D_{WS}}$)	LEFT ROTOR THROUST COEFF. (C_{D_R})	LEFT ROTOR THROUST COEFF. (C_{D_R})	LEFT ROTOR YAWING MOMENT COEFF.	LEFT ROTOR COLL. CYCLIC PATH (S_{cyc}) - DEG.
PUSHING PITCHING MOMENT COEFF. (C _{HT})	VERTICAL TAIL LIFT COEFF. (C_{Y_T})	VERTICAL TAIL LIFT COEFF. (C_{Y_T})	LEFT WING SURSTAY PITCHING MOMENT COEFF. ($C_{HT_{WS}}$)	RIGHT WING SURSTAY PITCHING MOMENT COEFF. ($C_{HT_{WS}}$)	RIGHT ROTOR THROUST COEFF. (C_{T_R})	RIGHT ROTOR THROUST COEFF. (C_{T_R})	RIGHT ROTOR LORNET FORCE COEFF.	RIGHT ROTOR COLL. CYCLIC PATH (S_{cyc}) - DEG.
PUSHING YAWING MOMENT COEFF. (C _{HT})	VERTICAL TAIL DRAG COEFF. (C_{DT})	VERTICAL TAIL DRAG COEFF. (C_{DT})	WING SURSTAY PITCHING MOMENT COEFF. (C_{HT})	WING SURSTAY PITCHING MOMENT COEFF. (C_{HT})	RIGHT ROTOR THROUST COEFF. (C_{D_R})	RIGHT ROTOR THROUST COEFF. (C_{D_R})	RIGHT ROTOR YAWING MOMENT COEFF.	RIGHT ROTOR COLL. CYCLIC PATH (S_{cyc}) - DEG.
HOR. TAIL DOWNING AT $\theta = 10^\circ$	HORIZONTAL TAIL DOWNING ANGLE (ϵ) - DEG.	HORIZONTAL TAIL DOWNING ANGLE (ϵ) - DEG.	RIGHT ROTOR DOWNING ANGLE (ϵ_{R10}) - DEG.	LEFT ROTOR DOWNING ANGLE (ϵ_{L10}) - DEG.	RIGHT ROTOR THROUST COEFF. (C_{D_R})	RIGHT ROTOR THROUST COEFF. (C_{D_R})	RIGHT ROTOR YAWING MOMENT COEFF.	RIGHT ROTOR COLL. CYCLIC PATH (S_{cyc}) - DEG.

Figure G.11. Definition of Trim Sheet Parameters

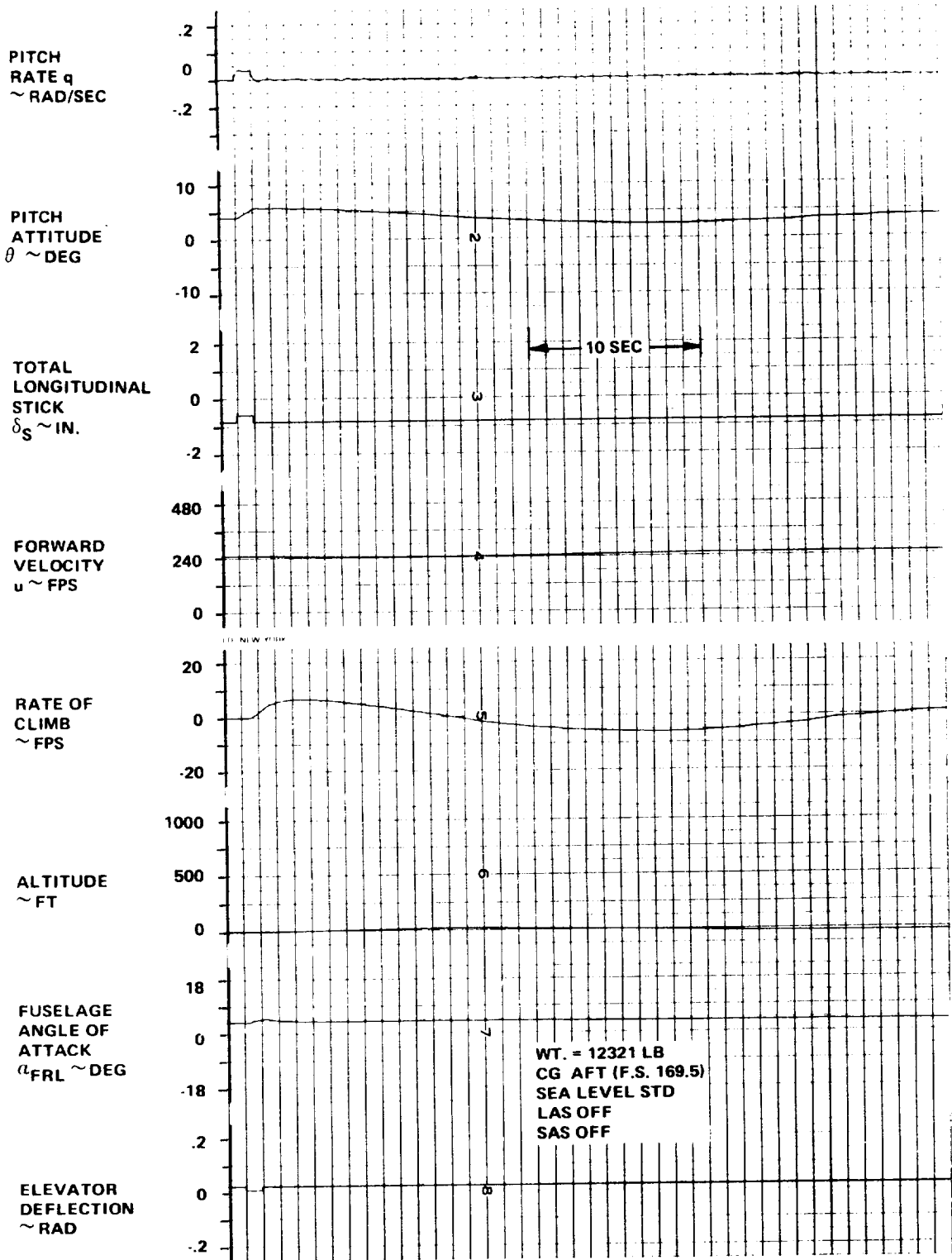


Figure G.12. Typical Time History Response to A .25 Inch Longitudinal Stick Pulse at 150 Knots

APPENDIX H VALIDATION OF THE MODEL 222 SIMULATION AT
 AMES RESEARCH CENTER

This section presents the validation plan which was submitted to NASA prior to the checkout and validation period at the Ames Research Center, and the simulation acceptance and pilot operating instructions and limitations submitted after the checkout period.

H.1 VALIDATION PLAN AND CRITERIA

Validation of large scale hybrid math model is an extremely time consuming and difficult process. The validation plan and criteria to be used by Boeing Vertol personnel in checking out and validating the NASA Model 222 simulation is developed in the following section. The following items will be considered in this validation:

● Trim Checks

- Range of data: 25 kt increments from minimum to maximum speed. (including backward and sideward flight).
- Accuracy (when compared against Boeing Vertol check cases)

<u>Trim Data</u>	<u>Tolerance</u>
Pilot control position	<u>+0.25 in.</u>
Stick and pedal position slope with speed	<u>+10%</u>
Thrust or wing lift	<u>+2 1/2%</u>
Pitch, roll, yaw angles	<u>+1.0°</u>
Collective pitch	<u>+0.5°</u>

These requirements are subject to change pending a detailed selection of the trim conditions.

- Dynamic Responses (Response to control pulses)

- Range of data: An axis by axis check with SAS and LAS systems on and off. Same speeds as for trim data.

- Accuracy (when compared against Boeing Vertol check cases)

Period +10%

Time to double (or half) amplitude +10%

- Stability Derivative Checks

- Range of data: Selected stability and control derivatives will be obtained at no more than five conditions.

- Accuracy when compared against Boeing Vertol check cases)

Selected major stability and control derivatives

($L_V, N_V, L_P, N_P, L_R, N_R, X_U, M_W, M_{\dot{W}}, M_Q, Z_W,$

$L_{\delta_S}, N_{\delta_S}, L_{\delta_R}, N_{\delta_R}, M_{\delta_B}, M_{i_N}, Z_{\delta_{TH}}$) +10%

- Validation of Time Frame

Run selected dynamic response checks at hover and cruise in real time and 1/10 real time i.e. reduced interval of integration. Damping of predominant modes shall not change by more than +10%.

- Transport Lag Checks

The transport lag i.e. aircraft response following control input shall not be greater than one to two time frames (average 1 1/2 time frames)

- Pilot acceptance will be based on a subjective comparison between the results obtained in the Boeing nudge base simulator and those obtained on the FSAA.

H.2 SIMULATION ACCEPTANCE

Following the checkout period at Ames, the following simulation acceptance document was submitted.

The math model, as programmed, is considered acceptable for initial evaluations.

The following differences exist between the math model and the aircraft described in Boeing's proposal for Phase II.

1. The data bank in the math model gives very conservative values of power around the autorotation region. The math model uses data from computer program D-88. Boeing's proposal uses data from wind tunnel model tests which were compared with D-88 predictions. The wind tunnel data showed consistently lower power required in and near autorotation. Revision of the rotor data bank to incorporate the wind tunnel data was not practicable within the time available. The extent of the difference is indicated by a minimum rate of descent at 80 knots from the math model of 2600 feet per minute compared to about 2000 feet per minute from the wind tunnel model data as reported in Volume I, Appendix G.
2. There is no autopilot in the math model. This was not required by the contract Statement of Work.
3. The landing gear dynamics in the model are an existing CSC program and do not represent the Model 222. There is some

indication that the CSC gear causes lateral instability on the ground at less than 25% power.

4. The wing bending and torsion modes were not checked out due to lack of time. Data obtained at Vertol indicate that these have no measurable effect on performance or flying qualities.
5. The representation of the SAS gives proper dynamic characteristics in the SAS on and SAS off modes. Individual component failures are not represented because of mechanization differences between the aircraft and the math model.
6. The actuator dynamics, which were included in the math model used on Boeing's nudge base simulator, were removed from the FSAA simulation in order to keep the time frame to a minimum. Evaluation on the Sigma 8 Computer at NASA showed no measurable difference as a result of removing the actuator dynamics. (The actuators have time constants less than the 50 millisecond time frame of the FSAA simulation.)
7. Boeing's proposed aircraft provides a pilot override for flap position and for rpm selection. These are not included in the math model. The checkout and validation of the tilt rotor math model was accomplished in two phases. These were the math model acceptance and the simulator acceptance.
 - A. Math Model Acceptance:
 1. Trim checks were calculated for a range of speeds from hover to 250 knots in 25 knot intervals. These were checked against previously computed trim conditions.

The results agreed within the tolerances specified in the reference.

2. Due to the limited time available for validation, dynamic responses were not checked over the full range of condition noted in the reference. However, dynamic responses were computed for a representative sample of condition. These compared favorably with those generated at Boeing and were generally within the specified tolerances. Differences could be explained by the different methods which were used to mechanize the equations; e.g., ---in the Boeing hybrid mechanization, rotor data were interpolated parabolically for angle of attack and linearly for advance ratio. In the NASA mechanization, curve fit equations were solved at each angle of attack and linearly interpolated for advance ratio. This tends to produce differences in areas where the data is highly non-linear such as in transition.
3. Stability derivative checks were made at four speeds; 0, 75, 150 and 250 knots. These were generally within the +10% accuracy specified by Boeing. Differences between the results are explainable and primarily due to the different ways the equations were mechanized.
4. Time frame studies and transport lag checks were made. Neither proved to be problem areas even though the NASA

simulation has a frame time in excess of 50 milliseconds. No lags were apparent in the simulation cab due to transport lag.

B. Boeing Pilot Acceptance:

The simulation is considered acceptable for initial evaluation however, Boeing's evaluation pilot made the following comments:

1. Controls:

- . Power lever location not optimum but acceptable for evaluation using seat arm rest for support.
- . Nacelle tilt switch - spring gradient slightly weak, 5° detents appear to be not in center of available travel. Switch occasionally sticks producing uncommanded nacelle actuation. Suitable for evaluation.
- . Stick forces - breakout and damping poor- difficult to achieve positive trim detent. Occasional shift in stick trim from one run to the next. (Simulator equipment problem)

2. Motion:

- . B V pilot considered motion cues unsatisfactory.
- . Lateral motion washouts and/or recentering produced spurious jerks and pulses which were disorienting.

- . Roll angular acceleration cues weak.
- . Pitch, yaw and heave satisfactory.
- . Longitudinal acceleration cues - long period cab tilt ok, short period were jerky and disconcerting with recentering reversals apparent.
- . Summary: There was enough spurious motion that overall the tilt/motion cues were detrimental and the pilot preferred fixed base.

3. Model Flying Qualities:

Generally similar to B V in-house simulation except for:

- . Vertical response slightly overdamped.
- . Unable to cut engine(s) until last day. As a result, not able to properly check out power lever governor override.
- . Pedal fixed turns in prop mode not as well coordinated - 30° banked turns show 1/2 to 3/4 ball slip to T & S indicator, with S/S ind. reading 1° - 2°.

4. Boeing was not able to evaluate the Model 222's response to gusts, since the gust model has not been defined. Response to random turbulence was evaluated.

C. General:

The original time allotted for the checkout and validation of this model was extremely short, particularly in view of the computer software problems and the difficulties encountered in establishing the gains for the FSAA motion drive equations. As a result, the checkout period had to be extended by NASA for two weeks.

H.3 OPERATING INSTRUCTIONS AND LIMITATIONS

As part of the simulation checkout, a set of operating instructions and limitations were prepared. For the most part these refer to the piloted simulation and the mathematical model and do not imply limitations on the Model 222 aircraft.

General:

1. I.C. - Set power lever trim to "0". (suggest using left-hand arm rest)
2. Stick grip has both Mag. brake and vernier "beep" force retrim. If Mag. braking is desired, use only in hover -- advise beep retrimming for transition and prop mode. (In real A/C, Mag. brake will deactivate above 150 KIAS)
3. Flaps and RPM are programmed automatically as a function of nacelle angle. In the Model 222 there will be manual flap and RPM override controls.

4. Nacelle angle has "q" interlock. Nacelles cannot be programmed "up" above 160 KIAS. IF 160 KIAS is exceeded with nacelle angle greater than 0°, they will automatically program to 0° at a rate of 2°/sec.
5. Nacelle angle switch gives nacelle rate proportional to displacement. Switch is spring loaded to center off position and has a detent either side of center, corresponding to approximately $\pm 5^\circ/\text{sec}$ rate. Full displacement will give approximately $\pm 10^\circ/\text{sec}$. For smoothest nacelle operation, use proportional feature; avoid "flick" type beep inputs.
6. Wing leading edge umbrellas automatically open or close at 50 KIAS.
7. Normal power lever travel is 8". This range represents flight idle to maximum power. There is a soft detent at 8 inches of travel which, when exceeded, overrides the governor. In this condition, the power lever controls collective pitch directly. This is provided for use as desired in autorotation and single engine landings.
8. The Model 222 is designed to go through transition at speeds between zero and 160 knots. Typical trimmed nacelle incidences at various speeds are:

i _N - DEG	90	75	60	30	0
Speed - KEAS	0	52	71	95	150

In investigating handling characteristics in the transition mode, it is recommended that these values be used as initial conditions.

In performing normal transitions to and from hover, it is recommended that the nacelle tilt be used as the primary speed control rather than flying at fixed tilt and using the stick for speed control.

Limitations:

1. Observe torque limits:

75% twin engine
100% single engine

2. Autorotation:

Engines must be failed from console to achieve zero torque. Transitions can be made from airplane to helo mode with power lever full back, but some residual torque remains (10% total) and N_R trims out nominally at 70%.

. Autorotative sink rate at $i_N=90^\circ$ approximately 3500 ft/min. Minimum rate of sink is about 2600 ft/min at 80 knots at $i_N=60^\circ$ (70% RPM). Model gives higher descent rates than airplane.

. Power lever has detent at approximately 8". Pushing through detent will override governor (single engine failure or auto collective) and give direct control of collective pitch.

Technique on engine cut in hover - advance power lever to detent, remaining engine will go to 100% torque. Use override as required, but once into direct C.P. control N_R will bleed off in same manner as turbine helo with one engine over-pitched. At topping power, model gross weight is too high for single engine hover. At max single engine power, vertical speed is -300 FPM.

3. At speeds above the normal flight envelope with nacelles tilted, the math model data bank is extrapolated from a curve fit and is not representative of the full scale aircraft. Speed and nacelle incidence limits for valid simulation are shown in the following table:

i_N - DEG	90	60	45	30
Speed - KEAS	100	125	125	140

These speeds should not be exceeded.

4. Aircraft oscillates if power is reduced below approximately 25% on the ground.
5. The math model is not set up to readily perform SAS or governor hardover studies. These may be approximated by setting the appropriate authority limits.
6. The Model 222 autopilot has not been incorporated into the simulation.